COMMUNICATION

ChemComm www.rsc.org/chemcomm

Crystal engineering of the composition of pharmaceutical phases

R. D. Bailey Walsh,[a] M. W. Bradner,[a] S. Fleischman,[a] L. A. Morales,[a] B. Moulton,[a] N. Rodríguez-Hornedo[b] and M. J. Zaworotko*[a]

[a] *Department of Chemistry, University of South Florida, 4202 E Fowler Ave (SCA 400), Tampa, FL 33620-5250, USA. E-mail: xtal@usf.edu; Fax: +1 813-974-3203; Tel: 813-974-4129*

[b] *Department of Pharmaceutical Sciences, College of Pharmacy, University of Michigan, Ann Arbor, MI 48109-1065, USA*

Received (in Columbia, MO, USA) 13th September 2002, Accepted 26th November 2002
First published as an Advance Article on the web 20th December 2002

The carboxylic acid–pyridine supramolecular heterosynthon can be exploited to predictably generate binary crystalline phases involving *rac*-ibuprofen, *rac*-flurbiprofen or aspirin.

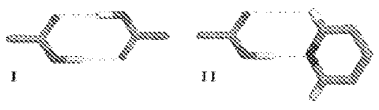
The concept of crystal engineering was originally introduced in the context of stereochemical control of photochemical reactions,[1] but it has subsequently been shown to have wider implications for materials science. In the context of pharmaceuticals, there are important process and intellectual property implications related to control and reproducibility of composition and polymorphism.[2,3] In this contribution, we focus upon how crystal engineering can be applied towards small organic molecules and generation of novel pharmaceutical compositions. This study is premised on the assumption that pharmaceutical molecules are inherently predisposed for such studies since they contain exofunctional supramolecular synthons.[4]

Supramolecular synthons that are based upon hydrogen bonds represent a prototypal tool for crystal engineering[5] and can be readily categorized as illustrated in Scheme 1: 'supramolecular homosynthons' from self-complementary moieties, *e.g.* the dimer formed by carboxylic acids, **I**; 'supramolecular heterosynthons' from two or more components, *e.g.* the dimer formed by pyridines with single or multiple carboxylic acids,[6–10] **II**.

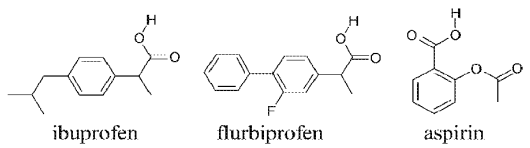
Heterosynthon **II** has previously been exploited for liquid-crystalline materials,[7] two-dimensional beta networks,[7] two-dimensional corrugated sheets[9] and 'ternary supermolecules'[10] and similar heterosynthons have been used as templates for control of solid-state reactions.[11] We herein extend its use to the realm of pharmaceutical molecules by forming novel compositions of ibuprofen,[12] flurbiprofen,[13] and aspirin.[14]

Supramolecular complexes **A–D** form when *rac*-ibuprofen, *rac*-flurbiprofen or aspirin are crystallized in the presence of dipyridyls: (ibuprofen)$_2$(4,4′-bipyridine), **A** (Fig. 1); (flurbiprofen)$_2$(4,4′-bipyridine), **B**, (Fig. 2); (flurbiprofen)$_2$ (trans-1,2-bis(4-pyridyl)ethylene), **C** (Fig. 2); (aspirin)$_2$(4,4′-bipyridine), **D** (Fig. 3); **A–D** were characterized by FT-IR spectroscopy, XRPD, DSC, TGA and single crystal X-ray diffraction† . The crystal structures of **A–D** exhibit the expected 2 : 1 stoichiometries because of heterosynthon **II**. The resulting 3-component adducts are centrosymmetric for **A–C** and exhibit herringbone packing patterns of the type seen in the pure phases.[12,13] All hydrogen bonds in **A–C** are consistent with expected values,[15–18] including the C–H···O interaction[19,20] that affords rigidity to this supramolecular heterosynthon and helps to explain the similarity between the crystal packing of **A–C** and the pure pharmaceutical phases.

The 3-component supramolecular adduct formed between aspirin and 4,4-bipyridine differs from **A–C** in that the 4,4′-bipyridine molecules are twisted with a torsion angle of 39° rather than planar and the planes of the C_6 rings in the aspirin molecules are oriented with a torsion angle of *ca.* 54°. This precludes formation of a centrosymmetric supramolecular adduct and results in dramatically different crystal packing. The crystal packing of adducts of **D** results in a channel inclusion



Scheme 1



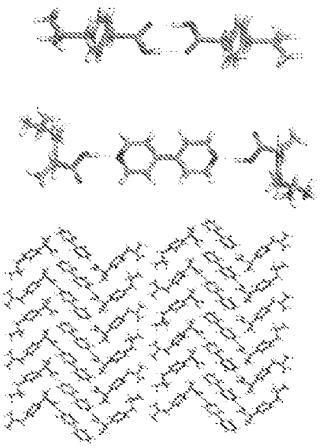


Fig. 1 The 3-component adducts present in pure ibuprofen and **A** (above); the herringbone crystal-packing pattern seen in **A** (below).

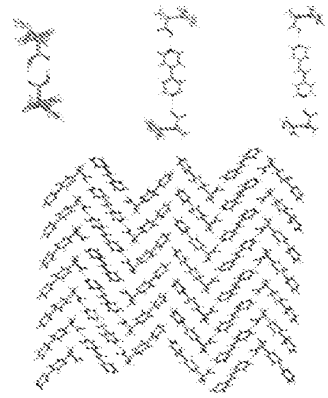


Fig. 2 The 3-component adducts present in pure flurbiprofen, **B** and **C** (above); the herringbone crystal-packing pattern seen in **C**, which is isostructural with **B** (below).

DOI: 10.1039/b208574g

This journal is © The Royal Society of Chemistry 2003

UM00016787
NOVARTIS EXHIBIT 1517
Novartis v. Regents, IPR2023-01347
Page 3769 of 4460

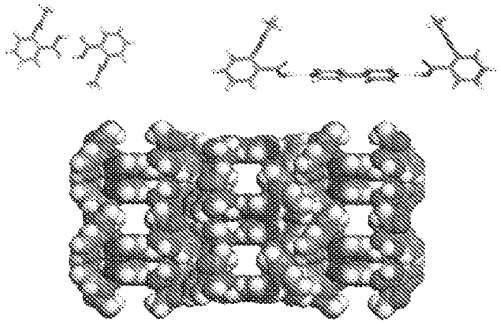


Fig. 3 The 3-component adducts present in pure aspirin and **D** (above); the open framework crystal packing pattern seen in **D** (below). The hourglass channels have effective dimensions as follows: 4.7 Å in height; 2.4 Å wide at the narrowest point (middle); 2.7 Å wide at the widest point (top & bottom).

compound, presumably templated by the presence of hexane during crystallization (Fig. 3). A review of the crystallographic literature revealed that 4,4-bipyridine moieties exhibit torsional flexibility in other circumstances.[15]

In conclusion, supramolecular heterosynthons can be exploited for generation of binary crystals that contain pharmaceutical components and, furthermore, the nature of the non-pharmaceutical component can dramatically affect crystal packing and, therefore, physical properties. For example, the melting points for **A–C** are higher than their pure individual components, and the melting point of **D**, a phase that exhibits dramatically different crystal packing, has a lower melting point than its pure individual components.‡

Whereas **A–D** should only be regarded as model compounds, we believe that the observations reported herein could have broad implications for the formulation of pharmaceuticals since control of composition can in appropriate circumstances now be regarded as being addressable *via* a supramolecular retrosynthetic[21] approach. Further studies will focus upon multiple component crystalline phases that will be designed and optimized for improved pharmaceutical performance and contain components that are generally regarded as safe (GRAS) by the FDA.[22]

M. Z and N. R. H. gratefully acknowledge support from the Vahlteich Research Award from the College of Pharmacy, University of Michigan.

Notes and references

† *Synthesis and data:* A–C were prepared by dissolving the pharmaceutical and bipyridine molecules in a 2 : 1 ratio in acetone and slow evaporation. D was prepared by dissolving aspirin and 4,4′-dipyridyl (2 : 1) in hexane and addition of diethyl ether. FT-IR spectra confirmed that deprotonation did not occur. Single crystal X-ray diffraction data for A–D were collected on a Bruker SMART-APEX CCD Diffractometer. Diffracted data were corrected for absorption using the SADABS[23] program. SHELXTL[24] was used for the structure solution and refinement was based on $|F|^2$. All non-hydrogen atoms were refined anisotropically. Carboxylic acid protons were located and refined with isotropic thermal parameters whereas the remaining hydrogen atoms were fixed in idealized positions and refined isotropically with thermal parameters based upon the corresponding carbon atoms [U (H) = 1.2 Ueq (C)]. In B and C the fluorine atom was disordered between the 2 and 6 positions of the benzene ring with the major component having ~ 70% occupancy. Calculated and experimental XRPD patterns for A–D are consistent with single crystals being representative of the bulk phases.

Crystal data for **A**: $C_{36}H_{44}N_2O_4$, M = 568.73, triclinic, space group $P\bar{1}$; a = 5.759(3), b = 11.683(6), c = 24.705(11) Å, α = 93.674(11), β = 90.880(10), γ = 104.045(7)°, U = 1608.3(13) Å^3, T = 200(2) K, Z = 2, μ(Mo-Kα) = 0.076 mm^{-1}, D_c = 1.174 Mg m^{-3}, λ = 0.71073 Å^3, F(000) = 612, $2\theta_{max}$ = 23.29°. 5208 reflections measured, 3362 unique (R_{int} = 0.0826). Final residuals for 399 parameters were R_1 = 0.0964, wR_2 = 0.2510 for $I > 2\sigma(I)$, and R_1 = 0.1775, wR_2 = 0.2987 for all 3362 data

. *Crystal data* for **B**: $C_{40}H_{34}F_2N_2O_4$, M = 644.69, monoclinic $P2_1/n$; a = 5.860(4), b = 47.49(3), c = 5.928(4) Å, β = 107.382 (8)°, U = 1574.3(19) Å^3, T = 200(2) K, Z = 2, μ(Mo-Kα) = 0.096 mm^{-1}, D_c = 1.360 Mg m^{-3}, λ = 0.71073 Å^3, F(000) = 676, $2\theta_{max}$ = 21.69°. 4246 reflections measured, 1634 unique (R_{int} = 0.0677). Final residuals for 226 parameters were R_1 = 0.0908, wR_2 = 0.2065 for $I > 2\sigma(I)$, and R_1 = 0.1084, wR_2 = 0.2209 for all 1634 data.

Crystal data for **C**: $C_{42}H_{36}F_2N_2O_4$, M = 670.73, monoclinic $P2_1/n$; a = 5.8697(9), b = 47.357(7), c = 6.3587(10) Å, β = 109.492(3)°, U = 1666.2(4) Å^3, T = 200(2) K, Z = 2, μ(Mo-Kα) = 0.093 mm^{-1}, D_c = 1.337 Mg m^{-3}, λ = 0.71073 Å^3, F(000) = 704, $2\theta_{max}$ = 21.69°. 6977 reflections measured, 2383 unique (R_{int} = 0.0383). Final residuals for 238 parameters were R_1 = 0.0686, wR_2 = 0.1395 for $I > 2\sigma(I)$, and R_1 = 0.1403, wR_2 = 0.1709 for all 2383 data.

Crystal data for **D**: $C_{28}H_{24}N_2O_8$, M = 516.49, orthorhombic $Pbcn$; a = 28.831(3), b = 11.3861(12), c = 8.4144(9) Å, U = 2762.2(5) Å^3, T = 173(2) K, Z = 4, μ(Mo-Kα) = 0.092 mm^{-1}, D_c = 1.242 Mg m^{-3}, λ = 0.71073 Å^3, F(000) = 1080, $2\theta_{max}$ = 25.02°. 12431 reflections measured, 2433 unique (R_{int} = 0.0419) Final residuals for 202 parameters were R_1 = 0.0419, wR_2 = 0.1358 for $I > 2\sigma(I)$, and R_1 = 0.0541, wR_2 = 0.1482 for all 2433 data.

CCDC 188913–188916. See http://www.rsc.org/suppdata/cc/b2/b208574g/ for crystallographic files in CIF or other electronic format.

‡ *Melting points* (°C): **A**: 117–120; **B**: 155–160; **C**: 153–158; **D**: 91–96; aspirin: 133–135; ibuprofen: 77–78; flurbiprofen: 113–114; 4,4′-bipyridine: 111–114; trans-1,2-bis(4-pyridyl)ethylene: 150–153.

1 G. M. J. Schmidt, *Pure Appl. Chem.*, 1971, **27**, 647.
2 J. Bernstein, R. J. Davey and J. O. Henck, *Agnew. Chem., Int. Ed. Engl.*, 1999, **38**, 3441.
3 J. D. Dunitz and J. Bernstein. *Acc. Chem. Res.*, 1995, **28**. 193.
4 G. R. Desiraju, *Angew. Chem., Int. Ed. Engl.*, 1995, **34**, 2311.
5 M. C. Etter, *Acc. Chem. Res.*, 1990, **23**, 120.
6 N. Shan, A. D. Bond and W. Jones, *Cryst. Eng.*, 2002, **5**, 9–24.
7 C. M. Palcos and D. Tsiourvas, *Angew. Chem., Int. Ed. Engl.*, 1995, **34**, 1696.
8 J. J. Kane, R. Liao, J. W. Lauher and F. W. Fowler, *J. Am. Chem. Soc.*, 1995, **117**, 12003.
9 C. V. K. Sharma and M. J. Zaworotko, *Chem. Commun.*, 1996, 2655.
10 C. B. Aakeröy, A. M. Beatty and B. A. Helfrich, *Angew. Chem., Int. Ed. Engl.*, 2001, **40**, 3240–3242.
11 L. R. MacGillivray, J. L. Reid and J. A. Ripmeester, *Chem. Commun.*, 2000, 7817–7818.
12 J. F. McConnell, *Cryst. Struct. Comm.*, 3, **73**, 1974; N. Shankland, A. J. Florence, P. J. Cox, D. B. Sheen, S. W. Love, N. S. Stewart and C. C. Wilson, *Chem Commun.*, 1996, 855.
13 J. L. Flippen and R. D. Gilardi, *Acta Crystallogr., Sect B*, 1975, **31**, 926.
14 Y. Kim, K. Machida, T. Taga and K. Osaki, *Chem. Pharm. Bull.*, 1985, **33**, 2641.
15 F. H. Allen and O. Kennard, *Chem. Des. Autom. News*, 1993, **8** , (1)), 31–37. April 2002 release.
16 B. Zaman, M. Tomura and Y. Yamashita, *J. Org. Chem.*, 2001, **66**, 5987–5995.
17 T. L. Nguyen, F. W. Fowler and J. W. Lauher, *J. Am. Chem. Soc.*, 2001, **23**, 11057–11064.
18 B. Yu. Shekunov and P. York, *J. Cryst. Growth*, 2000, **211**, 122–136.
19 P. Vishweshwar, A. Nangia and V. Lynch, *J. Org. Chem.*, 2002, **67**, 556–565.
20 T. Steiner, *Angew.Chem., Int. Ed. Engl.*, 2002, **41**, 48–76.
21 G. R. Desiraju, *Chem. Commun.*, 1997, 1475–1482.
22 FDA/CFSAN/OPA: Inventory of GRAS Notices: Summary of all GRAS Notices. http://vm.cfsan.fda.gov/ ~ dms/eafus.html.
23 G. M. Sheldrick, SADABS; University of Gottingen, 1996.
24 G. M. Sheldrick, SHELXTL, Release 6.10; Bruker AXS: Madison, WI, 2000.

UM00016788
NOVARTIS EXHIBIT 1517
Novartis v. Regents, IPR2023-01347
Page 3770 of 4460

XP-002960386

LEAD ARTICLE

P.D. 19950
p. 115-148 = (34)

Acta Cryst. (1995). B51, 115–148

Understanding and Control of Nucleation, Growth, Habit, Dissolution and Structure of Two- and Three-Dimensional Crystals Using 'Tailor-Made' Auxiliaries

BY ISABELLE WEISSBUCH, RONIT POPOVITZ-BIRO, MEIR LAHAV AND LESLIE LEISEROWITZ

Department of Materials and Interfaces, The Weizmann Institute of Science, Rehovot 76100, Israel

(*Received* 24 *March* 1994, *accepted* 25 *October* 1994)

Abstract

Tailor-made auxiliaries for the control of nucleation and growth of molecular crystals may be classified into two broad categories: inhibitors and promoters. Tailor-made inhibitors of crystal growth can be used for a variety of purposes, which include morphological engineering and etching, reduction of crystal symmetry, assignment of absolute structure of chiral molecules and polar crystals, elucidation of the effect of solvent on crystal growth, and crystallization of a desired polymorph. As for crystal growth promoters, monolayers of amphiphilic molecules on water have been used to induce the growth of a variety of three-dimensional crystals at the monolayer–solution interface by means of structural match, molecular complementarity or electrostatic interaction. A particular focus is made on the induced nucleation of ice by monolayers of water-insoluble aliphatic alcohols. The two-dimensional crystalline structures of such monolayers have been studied by grazing incidence X-ray diffraction. It has become possible to monitor, by this method, the growth, dissolution and structure of self-aggregated crystalline monolayers, and indeed multilayers, affected by the interaction of solvent molecules in the aqueous subphase with the amphiphilic headgroups, and by the use of tailor-made amphiphilic additives.

Leslie Leiserowitz obtained his PhD in 1966, working on thermochromy in the group of the late Gerhard Schmidt at the Weizmann Institute of Science. He then moved to the Organic Chemistry Institute of the University of Heidelberg when he began a systematic investigation of the structural patterns and physical properites of organic crystals. Meir Lahav obtained his PhD in 1967 in solid-state chemistry, also in Gerhard Schmidt's research group. He did postdoctoral research with Paul Bartlett at Harvard. On his return to Israel, he embarked on a program for the design of systems for the generation and amplification of optical activity via crystallization. It was during this period that the Lahav–Leiserowitz collaboration started, with studies of photochemical reactions in solids. This team-work continued with a study of crystal nucleation, growth and dissolution in the presence of tailor-made auxiliaries. Ronit Popovitz-Biro received her PhD in solid-state chemistry in 1979, working in the research group of M. Lahav. After a postdoctoral period at the University of California she returned to the Weizmann Institute. She has since directed her efforts at the oriented growth of crystals via Langmuir monolayers and the design of multilayer films. Isabelle Weissbuch received her PhD in chemistry in 1985 at the Weizmann Institute of Science. She has continued to work at the Weizmann Institute where her main interest has been solid-state chemistry, with emphasis on the design and use of auxiliaries for the control of crystal nucleation, morphology and polymorphism, as well as structure determination of mono- and multilayer films.

1. Introduction

Although crystals and crystallization as a process play an important role in pure and applied science, our ability to design crystals with desired properties, and our control over crystallization based on structural understanding are still limited. Indeed our ignorance of the overall process of crystal growth is brought to the fore by comparison with the controlled crystal growth provided in biomineralization. Organisms can mold crystals of specific morphologies, sizes and orientations in the form of composites of minerals and organic materials with characteristics vastly different from those of their inorganic counterparts (Löwenstam & Weiner, 1989; Addadi & Weiner, 1992). Nevertheless, the technological advances in controlling the microstructure of inorganic materials on the subnanometer scale have led to tremendous success in the preparation of ceramics, synthetic layered microstructures and semiconducting materials. Paradoxically, advances in the field of organic materials have not been as striking, although the techniques for the preparation of films such as Langmuir–Blodgett and self-assembled multilayers on solid support hold promise as pyroelectric, piezoelectric and frequency doubling devices *etc.* The thread that binds these diverse topics involves molecular interactions at interfaces.

The surfaces of a growing crystal can be thought of as composed of 'active sites' which interact stereospecifically with molecules in solution, in a manner similar to enzyme–substrate or antibody–antigen interactions. The repetitive arrangements at crystal surfaces, and the knowledge we have of their structures, offer simpler

© 1995 International Union of Crystallography
Printed in Great Britain - all rights reserved

Acta Crystallographica Section B
ISSN 0108-7681 © 1995

Material may be protected by copyright law (Title 17, U.S. Code)

OCID: <XP__2960386A__I_>

UM00016789
NOVARTIS EXHIBIT 1517
Novartis v. Regents, IPR2023-01347
Page 3771 of 4460

means to pinpoint molecular interactions. It is possible to use the concept of molecular recognition at interfaces to address open questions in the areas of crystal nucleation and growth, crystal polymorphism, and interactions with the growth environment.

Landmark papers for the prediction of crystal morphology were provided by Hartman & Perdok (1955*a*,*b*), Hartman (1973) and Hartman & Bennema (1980), who laid the ground rules for a quantitative determination of crystal morphology, based on the internal crystal structure. Regarding the effect of additives and solvent on crystal growth and morphology, a variety of important experimental studies have been reported in the latter half of this century. For example, Wells (1946) performed elegant experiments particularly on polar crystals to demonstrate the effect of solvent on crystal growth and shape. Changes in habit induced in NaCl crystals by the presence of α-amino acids were reported by Fenimore & Thraikill (1949). Buckley (1951) described a variety of crystal habit modifications, in particular the effect of dyes which led to changes in morphology and to colored inclusions known as hourglass or Maltese cross shapes. Whetstone (1954) explained the nature of such dye adsorption phenomena in inorganic crystals. He invoked a structural match involving Coulomb interactions between the additive and the structure of the crystal surface onto which adsorption occurred. In the case of molecular crystals, the sugar technologists (Smythe, 1967, 1971; van Hook, 1968, 1981; Mantovani, Gilli & Faglioli, 1967) studied the effect of raffinose on the growth of sucrose during extraction of the latter from molasses. By carrying out kinetic studies, they established that raffinose hinders growth along specific directions of sucrose crystals and proved the presence of its selective occlusion. The control, however, on nucleation, growth, dissolution and morphology of molecular crystals remained primarily a matter of 'mix and try'. There was no general approach for the design of additives targeted for binding to particular crystalline phases or preselected faces of any crystal. It was not, and still is not, possible to wield the exquisite control mother nature exerts in the field of biological mineralization.

In recent years a stereochemical approach has been adopted involving the growth and dissolution of molecular crystals in the presence of 'tailor-made' auxiliaries, which interact with specific crystal faces and may be crystal growth inhibitors or nucleation promoters (Addadi *et al.*, 1985; Weissbuch, Addadi, Lahav & Leiserowitz, 1991). With the assistance of such molecular auxiliaries it is possible to examine a variety of processes. We list first those which have involved crystal growth inhibitors. Crystals may be engineered with desired morphologies (Berkovitch-Yellin, Addadi, Idelson, Lahav & Leiserowitz, 1982). A correlation may be made between the chirality of tailor-made additives and the macroscopic properties of affected host crystals. By such means, the absolute configuration of chiral molecules or polar crystals may be assigned (Addadi, Berkovitch-Yellin, Weissbuch, Lahav & Leiserowitz, 1986). With occlusion of the additive into the crystal, the symmetry of the crystal may be reduced, thus making a 'centrosymmetric' crystal emit a second harmonic signal on irradiation with a laser beam (Weissbuch, Lahav, Leiserowitz, Meredith & Vanherzeele, 1989). Molecular crystals can be etched at desired faces on dissolution (Shimon, Lahav & Leiserowitz, 1985, 1986) and the effect of solvent on crystal growth may be elucidated (Wireko *et al.*, 1987; Shimon, Vaida, Addadi, Lahav & Leiserowitz, 1990, 1991). Crystallization of a desired phase may be induced for the resolution of chiral molecules (Addadi, van Mil & Lahav, 1982; Addadi, Weinstein, Gati, Weissbuch & Lahav, 1982), or for the precipitation of a polar crystal polymorph (Staab, Addadi, Leiserowitz & Lahav, 1990).

With tailor-made auxiliaries in the form of crystal nucleation promoters it has proven possible to engineer two-dimensional crystalline monolayers composed of amphiphilic molecules on aqueous solutions to induce, by epitaxy, nucleation of crystals at the monolayer-solution interface (Landau, Popovitz-Biro, Levanon, Leiserowitz & Lahav, 1986; Landau *et al.*, 1989) and, as a corollary, to acquire information relevant to the mechanism of nucleation of crystals in biological environments (Mann, 1988; Mann, Heywood, Rajam & Birchall, 1988). The crystallinity of such Langmuir monolayers on the water surface has been demonstrated by grazing incidence X-ray diffraction measurements, also leading to structure determination almost at the atomic level (Jacquemain *et al.*, 1990). The knowledge acquired from such induced crystallization and diffraction experiments led to the use of alcohol monolayers for induced nucleation of ice (Gavish, Popovitz-Biro, Lahav & Leiserowitz, 1990; Popovitz-Biro, Wang, Majewski, Leiserowitz & Lahav, 1994; Wang *et al.*, 1994). The monolayers on the liquid surface can also be used for studying the effect of solvent on the formation, growth and structure of polymorphic arrangements of two-dimensional crystallites, information not easily deduced from three-dimensional crystals.

Here we present a birds-eye view of all these different, yet connected, topics.

2. Morphological crystal engineering

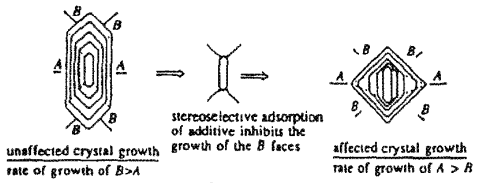
The habit of a crystal is defined by the relative rates of its growth in different directions; the faster the growth in a given direction, the smaller the face developed perpendicular thereto. Consequently, when growth is inhibited in a direction perpendicular to a given face, the area of this face is expected to increase relative to the areas of other faces of the same crystal. Differences in the relative surface areas of the various faces can therefore

Material may be protected by copyright law (Title 17, U.S. Code)

DOCID: <XP___2960386A__I_>

UM00016790
NOVARTIS EXHIBIT 1517
Novartis v. Regents, IPR2023-01347
Page 3772 of 4460

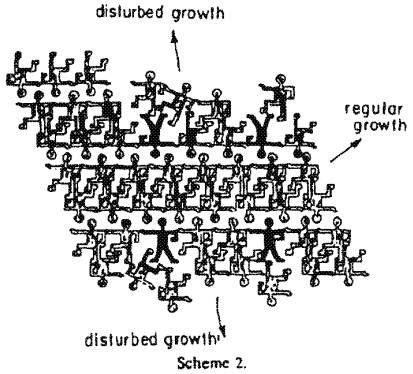
be directly correlated to the inhibition in different growth directions. Dramatic morphological changes observed during the growth of organic crystals in the presence of additives revealed a high degree of specificity in the interaction of the foreign material with the different structures of surfaces of the crystalline matrix. Such a change in crystal morphology is depicted in Scheme 1.



Scheme 1.

As mentioned previously, the role played by impurities on the habit modification of crystals (Kern, 1953) has long attracted the attention of crystal growers. However, such studies did not, in the main, involve morphological change by design. This became possible with the use of 'tailor-made' additives. From a systematic study of a variety of organic compounds crystallized in the presence of additives of molecular structure similar to the structures of the corresponding substrate molecules (Addadi *et al.*, 1985), and so labeled 'tailor-made' additives (or auxiliaries), it was possible to deduce a stereochemical correlation between the structures of the affected crystal surfaces and the molecular structure of the additive. We could infer that the 'tailor-made' additive is adsorbed on the growing crystals, but only at certain surfaces and then with the part of the adsorbate that differs from that of the substrate emerging from the crystal. This selective adsorption of the tailor-made additive at crystal faces and concomitant inhibition of their growth is depicted in Scheme 2. Once this mechanism was established, it became possible to exploit it to systematically modify the morphology of crystals by tailoring additives that bind at preselected faces and thus inhibit growth in a predictable manner.

Benzamide, $C_6H_5CONH_2$, provides an example where the host–additive interactions at the growing solid–liquid interface can be pinpointed and correlated with the change in crystal morphology (Berkovitch-Yellin, Addadi, Idelson, Lahav & Leiserowitz, 1982). This compound crystallizes from ethanol as plates [Fig. 1(*a*)], in the monoclinic space group $P2_1/c$. The molecules in the crystal form hydrogen-bonded cyclic dimers, further interlinked by hydrogen bonds to yield ribbons parallel to the *b*-axis [Fig. 2(*a*)]. The ribbons are stacked along the 5.6 Å *a*-axis to form stable (001) layers. These tightly packed layers juxtapose along the *c*-direction, interacting *via* weak van der Waals interactions between phenyl groups, thus accounting for the {001} plate-like shape of the crystals. Benzoic acid additive, C_6H_5COOH, adopting the stable O=C—OH synplanar conformation, can replace a molecule of benzamide at the end of a ribbon [Fig. 2(*a*)], however, at the site of the additive, an attractive N—H···O bond (-25 kj mol^{-1}) is replaced by repulsion (4–8 kj mol^{-1}) between adjacent oxygen lone-pair electrons of the bound additive molecule and of the oncoming benzamide molecule, leading to an overall loss in energy of 29–33 kj mol^{-1} (Berkovitch-Yellin *et al.*, 1985). As predicted, the presence of benzoic acid in solution inhibits the growth of the benzamide crystals along **b**, transforming the pure plate-like crystals into needles elongated along the *a*-axis [Fig. 1(*b*)]. Inhibition of growth along the *a*-direction was accomplished by adding *o*-toluamide, *o*-$H_3CC_6H_4CONH_2$, to the crystallization solution. The crystals consistently grew as bars elongated in *b* [Fig. 1(*c*)]. The additive *o*-toluamide can easily be adsorbed in the hydrogen-bonding chain without disturbing growth in the *b*-direction. The *o*-methyl group emerges, from the (10$\bar{4}$) side face [Fig. 2(*b*)], and thus interferes with



Scheme 2.

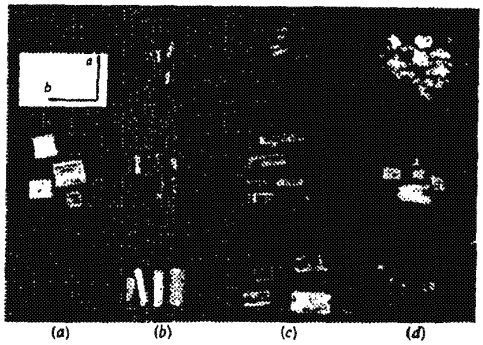


Fig. 1. Crystals of benzamide: (*a*) pure, (*b*)–(*d*) grown in the presence of additives: (*b*) benzoic acid, (*c*) *o*-toluamide and (*d*) *p*-toluamide.

Material may be protected by copyright law (Title 17, U.S. Code)

OCID: <XP___2960386A__I_>

UM00016791
NOVARTIS EXHIBIT 1517
Novartis v. Regents, IPR2023-01347
Page 3773 of 4460

growth in the *a*-direction, along which the dimers are stacked. The relative orientation of benzamide at the {001} faces is shown in Fig. 2(*c*). Thinner and thinner plates [Fig. 1(*d*)] are obtained by adding increasing amounts of *p*-toluamide, *p*-$H_3CC_6H_4CONH_2$, whose *p*-methyl substituent perturbs the already weak van der Waals interactions between the phenyl layers in the *c*-direction [Fig. 2(*c*)].

The present approach which is based upon specific molecular interactions at the solid–liquid interface was applied to a variety of molecular crystals, including α-amino acids, dipeptides, primary and secondary amides, carboxylic acids, sugars, steroids *etc*. It therefore appears to be general and has since been successfully applied to a large class of materials, be they organic (Lewtas, Tack, Beiny & Mullin, 1991; Skoulika, Michaelidis & Aubry, 1991; Antinozzi, Brown & Purich, 1992), inorganic (Black *et al.*, 1991; Cody & Cody, 1991; Ristic, Sherwood & Wojeshowski, 1994) or biological (Markman, Elias, Addadi, Cohen, & Berkovitch-Yellin, 1992).

3. 'Tailor-made' etchants for organic crystals

Growth and dissolution are not reciprocal processes. Growth forms are bound by the slowest growing faces,

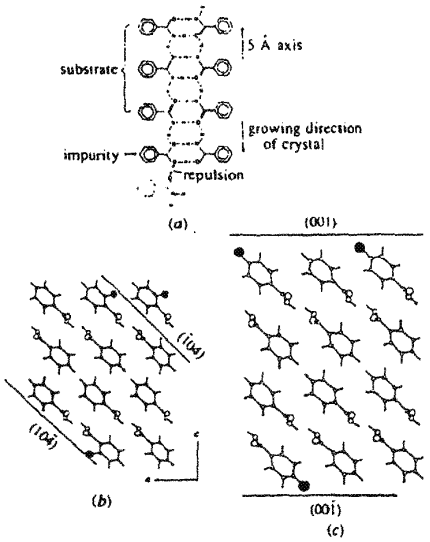


Fig. 2. (*a*) Schematic representation of the ribbon motif of hydrogen-bonded dimers of benzamide molecules interlinked along the 5*b*-axis, showing the effect of benzoic acid inhibiting growth along the *b*-direction. (*b*) Packing arrangement of benzamide, viewed along the *b*-axis, showing the effect of *o*-toluamide inhibiting growth along the *a*-direction. (*c*) Packing arrangement of benzamide, viewed along the *b*-axis, showing the effect of *p*-toluamide inhibiting growth along the *c*-direction.

dissolution forms by the fastest dissolving directions (de Boer, 1993). Nevertheless, we found that a 'tailor-made' inhibitor of growth of a given crystal face affects the rate of dissolution of that same crystal face (Shimon, Lahav & Leiserowitz, 1985, 1986).

It has long been recognized that partial dissolution of crystals in the presence of additives may induce the formation of well shaped etch-pits on particular faces of the crystal. For example, when crystals of calcite were partially dissolved in the presence of D- or L-tartaric, -malic or -lactic acids, etch-pits with enantiomorphous shapes were observed (Honess, 1927). Owing to the complexity of the etching mechanism, no simple model involving a stereochemical correlation between the structure of the etchant, that of the to-be-etched face, and the symmetry and the geometry of the etch-pit, had been evolved, so that selection of etchants was done generally by trial and error.

Crystal dissolution invariably begins at sites of emerging dislocations (Horn, 1952; Gevers, Amelinckx & Dekeyser, 1952). At such sites more than one type of facial surface is exposed to the solvent. When an additive that binds selectively to a given face of the crystal is present in the solution, the crystal dissolves in different directions at rates that differ from those in the pure solution. Subsequently, etch-pits are formed at the dislocation centers on those faces at which the additives are bound. It is also correct to say that there is a difference between etching and dissolution. By inhibiting the latter, the former is made more prominent. The possibility of designing molecules which can interact stereospecifically with a given face of a crystal should, in principle, make those molecules efficient etchants of the face. Therefore, it was anticipated that the same molecules, which act as 'tailor-made' growth inhibitors of a given face, operate as 'tailor-made' etchants of the same face when the crystal is partially dissolved. The generality of this approach was tested on several molecular crystals (Shimon, Lahav & Leiserowitz, 1985, 1986), which we illustrate with one example.

We consider the packing characteristics of the α-form of glycine, $^+H_3NCH_2CO_2^-$, a prochiral molecule containing two H atoms at the central C atom that are enantiotopic, namely, replacing one of these H atoms by a different group yields a chiral molecule. α-Glycine packs in an arrangement [Fig. 3(*a*)] of space-group symmetry $P2_1/n$. Of the four symmetry-related molecules [1, 2, 3 and 4, Fig. 3(*a*)], (1) and (2), related by twofold screw symmetry, have their C—H_{re} bonds pointing in the $+b$-direction and emerging from the (010) face. By symmetry, molecules (3) and (4), related to (1) and (2) by a center of inversion, have their C—H_{si}* bonds pointing toward $-b$ and emerging from the (0$\bar{1}$0) face. Only the (*R*)-amino acid additives

* Note that we have used the Prelog & Helmchen (1982) nomenclature to specify the diastereotopic C—H ligands.

Material may be protected by copyright law (Title 17, U.S. Code)

DOCID: <XP__2960386A__I_>

NOVARTIS EXHIBIT 1517
Novartis v. Regents, IPR2023-01347
Page 3774 of 4460

can substitute a glycine molecule at the (1) and (2) sites, and then only on the (010) face, while only (*S*)-amino acids can be adsorbed at sites (3) and (4) on the (0$\bar{1}$0) face. This constraint arises from the steric requirement that the additive molecule be recognized on the {010} surfaces as a 'host' molecule so that the α-amino acid side chain can replace the H atom of glycine only at the C—H bond emerging from the crystal surface. Otherwise, repulsion would occur between the additive and the surrounding molecules on the crystal surface. α-Glycine crystallizes from water as bipyramids [Fig. 3(*b*)]. Crystallization experiments in the presence of (*R*)-α-amino acid additives led to the formation of pyramids with a (010) basal plane, because growth in the $+b$ direction is inhibited [Fig. 3(*c*)]. (*S*)-α-Amino acid additives induce the enantiomorphous morphology [Fig. 3(*d*)]. Racemic α-amino acid additives cause the formation of {010}* plates [Fig. 3(*e*)], because growth at both the $+b$ and $-b$ sides of the crystal is inhibited (Weissbuch *et al.*, 1983).

The faces relevant to the etching process are of the type {010}, being those inhibited on growth. Plate-like crystals of glycine with such well developed faces were submitted to partial dissolution in an undersaturated solution of glycine containing variable amounts of other α-amino acids. In the presence of racemic additive, the rate of dissolution was much slower than in their absence. Moreover, the inhibition was more pronounced, the bulkier the additive side chain (Shimon, Lahav & Leiserowitz, 1986; Shimon, Zbaida, Addadi, Leiserowitz & Lahav, 1988). When resolved *R*-alanine, $^{+}H_3NCH(CH_3)CO_2^-$, was present in the solution, well developed etch-pits were formed only on the (010) face [Fig. 4(*a*)]. These pits exhibit twofold morphological symmetry with surface edges parallel to the *a*- and *c*-axes of the crystal. The enantiotopic (0$\bar{1}$0) face dissolved smoothly [Fig. 4(*b*)], exactly as it does when the crystal is dissolved in an undersaturated solution of pure glycine. As expected, *S*-alanine induced etch-pits on the (0$\bar{1}$0) face. Racemic alanine etched both opposite {010} faces. The well established role played by dislocations for inducing etch-pit formation was also demonstrated. A pure crystal of glycine was cleaved through its basal plane to expose the (010) and (0$\bar{1}$0) faces. These two

* Note that the symbol {*hkl*} refers to all the symmetry-related faces, whereas (*hkl*) refers to only the face specified by *h,k,l*.

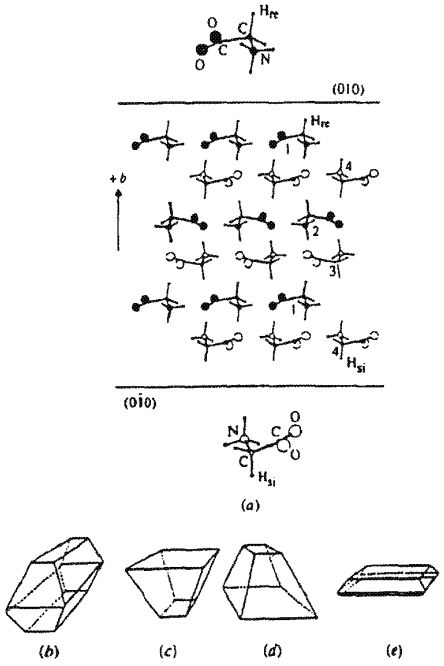


Fig. 3. (*a*) Packing arrangement of α-glycine viewed along the *a*-axis showing the four symmetry-related molecules; the C—H_{re} bonds, almost parallel to *b*, of the molecules point towards the (010) face and the corresponding C—H_{si} bonds towards the (0$\bar{1}$0) face. (*b*)–(*e*) Crystal morphologies of α-glycine when grown in the presence of: (*b*) no additive, (*c*) *R*-α-amino acids, (*d*) *S*-α-amino acids and (*e*) racemic α-amino acid additives.

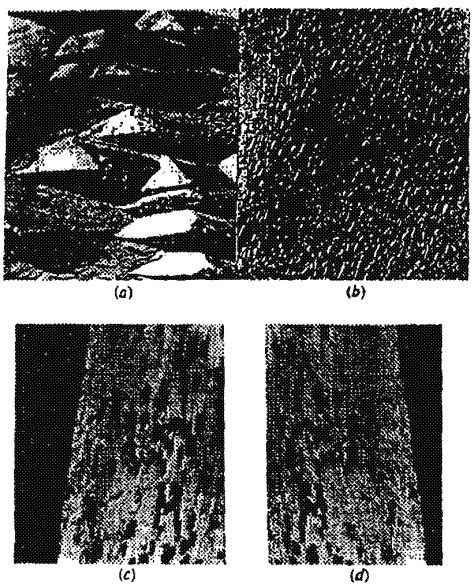


Fig. 4. Optical microscope photographs of the {010} faces of an α-glycine crystal after etching: (*a*) and (*b*) the (010) and (0$\bar{1}$0) faces as etched by *R*-alanine; (*c*) and (*d*) the (010) and (0$\bar{1}$0) faces of a cleaved crystal after etching with racemic alanine.

Material may be protected by copyright law (Title 17, U.S. Code)

OCID: <XP___2960386A__I_>

UM00016793
NOVARTIS EXHIBIT 1517
Novartis v. Regents, IPR2023-01347
Page 3775 of 4460

parts of the crystal, on being etched with racemic alanine additive, displayed etch-pits in equivalent regions of the two cleaved faces [Figs. 4(*c*) and (*d*)].

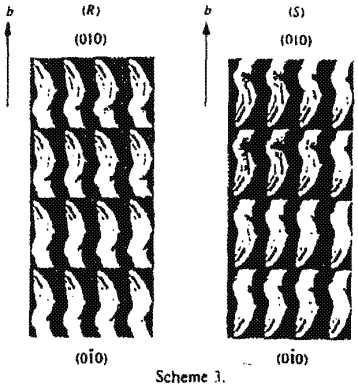
The same type of chiral selectivity holds for an enantiomorphous pair of crystals dissolved in the presence of a chiral-resolved molecule, when only one of the enantiomers is etched. Such enantioselective etching experiments provide a simple method of differentiating between enantiomorphous single crystals which do not express hemihedral faces. The method has been demonstrated for a class of racemic α-amino acids that crystallize as conglomerate mixtures (*i.e.* each enantiomer crystallizes in its own enantiomorphous crystal), such as chiral-resolved glutamic acid.HCl and asparagine.H_2O (Shimon, Lahav & Leiserowitz, 1986). Moreover, it also proved possible to bring about a pronounced separation of enantiomorphs by the enantioselective dissolution of a conglomerate mixture in the presence of 'tailor-made' optically pure polymeric additives (Shimon, Zbaida, Addadi, Leiserowitz & Lahav, 1988).

4. Assignment of absolute configuration of crystals and molecules

4.1. *Polar crystals*

The standard method for the direct assignment of the absolute configuration of polar crystals, composed of chiral, racemic or nonchiral molecules, was introduced by Bijvoet in 1948 with the use of anomalous X-ray scattering. Over the past decade, several independent methods for the assignment of the absolute configuration of polar crystals have been applied, including the effect of tailor-made molecular additives on crystal morphology and structure, as well as gas–solid reactions (Paul & Curtin, 1987) and ferroelectric measurements in liquid crystals (Walba, Razuvi, Clark & Parmer, 1988). The induced change in crystal morphology with tailor-made additives, the anisotropic distribution of the additive inside the host crystal, and the role played by additives for the formation of etch-pits can be taken advantage of for the assignment of the absolute configuration of chiral molecules and polar crystals. In this way it has been possible to assign the absolute molecular structure of a variety of molecular systems, such as α-amino acids, sugars and steroids (Addadi, Berkovitch-Yellin, Weissbuch, Lahav & Leiserowitz, 1986). Although one might argue that these studies have only confirmed what was already known, they demonstrate the interplay between molecular chirality and various macroscopic phenomena, and also satisfy the curiosity of students of stereochemistry with an inadequate knowledge of X-ray scattering. Furthermore, the method has been applied to assign the absolute structures of polar crystals whose constituent molecules are either a racemic mixture or nonchiral, and may be the only viable method if the constituent molecules are hydrocarbons.

To demonstrate the method we first focus on polar crystals composed of chiral-resolved molecules. The method involves the principle of fixing the orientation of the constituent molecules *vis-à-vis* the polar axis, or axes, of the crystal and subsequently determining the absolute configuration of the chiral molecules. This principle is depicted in Scheme 3, which shows two enantiomorphous sets of hands arranged in a lattice, right hands forming an (*R*)* crystal and left hands forming an (*S*)* crystal. The fingers of the hands are exposed at the (010) face of the right-handed 'molecules' and, by symmetry, at the (0$\bar{1}$0) face for the left-handed 'molecules'. Thus, by determining at which face of the crystal specimen the fingers or wrists are exposed, the handedness of the constituent molecules may be assigned. This may be performed by applying the two-step adsorption–inhibition mechanism described above with appropriate tailor-made additives.



Scheme 3.

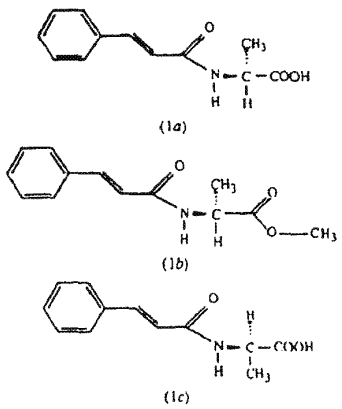
We illustrate this approach with the example of *N*-(*E*-cinnamoyl)alanine (Berkovitch-Yellin, Addadi, Idelson, Leiserowitz & Lahav, 1982). Molecules of *N*-(*E*-cinnamoyl)-*S*-alanine (1*a*) crystallize in space group $P2_1$. The packing arrangement delineated by the crystal faces as grown from methanol solution is shown in Fig. 5. The molecules are arranged such that the carboxyl groups emerge at the two {1$\bar{1}$1} faces and the C(chiral)—H bonds are directed along the +*b* axis. In a study on the effect of tailor-made additives on the morphology of pure *N*-(*E*-cinnamoyl)-(*S*)-alanine [1*a*, Fig. 6(*a*)], it was found, as expected, that the methyl ester (1*b*), of the same absolute configuration as the host molecule (1*a*), induced large {1$\bar{1}$1} faces [Fig. 6(*b*)], since the O—CH_3 group replaces a O—H group emerging from such faces. Tailor-made additive *N*-(*E*-cinnamoyl)-(*R*)-alanine (1*c*) of configuration opposite

*Note that for convenience the parentheses enclosing the chirality of the molecule specifies a crystal; absence thereof, such as *R*, *S* or *R,S*, specifies the molecule only.

DOCID: <XP___2960386A__I_>

UM00016794
NOVARTIS EXHIBIT 1517
Novartis v. Regents, IPR2023-01347
Page 3776 of 4460

) that of the host induced, as expected, a (010) face Fig. 6(*c*)], because of an interchange of CH_3 and H at ıe guest asymmetric carbon so that the C—CH_3 guest ıoiety replaces the emerging host C—H bond.



(1*a*)

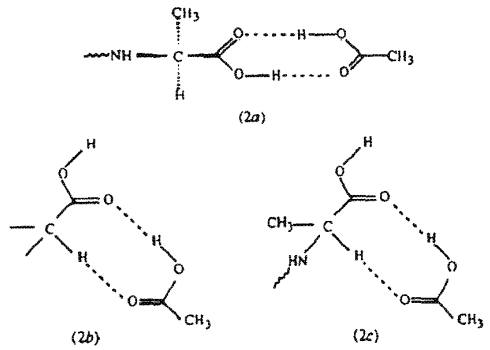
(1*b*)

(1*c*)

It was found that solvent may act in a manner similar to the tailor-made additives, for example, by growing (1*a*) from acetic acid (Shimon, Vaida, Addadi, Lahav & Leiserowitz, 1991) instead of methanol. Acetic acid is a solvent which can selectively bind at the exposed carboxylic acid groups of the two $\{1\bar{1}1\}$ faces, forming a hydrogen-bonded dimer (2*a*). Acetic acid can also bind to the $CHCO_2H$ moiety of cinnamoylalanine *via* a cyclic dimer (2*c*) on the (010) face. The dimer (2*b*) is the motif adopted by acetic acid in its own crystal structure (Jonsson, 1971), forming a C—H···O(carbonyl) interaction. (Taylor & Kennard, 1982; Berkovitch-Yellin & Leiserowitz, 1984). Crystallization of *N*-(*E*-cinnamoyl)alanine (1*a*) from glacial acetic acid yields crystals with the morphology shown in Fig. 6(*d*), in keeping with expectation.

A nice example of how anomers, interconvertible in solution, may be used for the assignment of absolute configuration is provided by the influence on the morphology of α-lactose hydrate crystals by the anomeric β-lactose molecules present in solution (Michaelis & van Kreveld, 1966; Visser & Bennema, 1983).

Direct assignment of the absolute configuration of chiral-resolved molecules by the difference in wetting properties of hydrophobic and hydrophilic crystal faces was made possible (Wang, Lahav & Leiserowitz, 1991) using crystals of the class belonging to chiral-resolved



(2*a*)

(2*b*)

(2*c*)

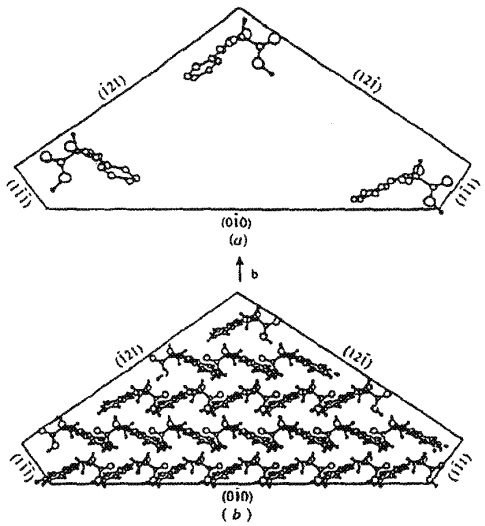


Fig. 5. Packing arrangement of *N*-(*E*-cinnamoyl)-(*S*)-alanine delineated by the faces observed in the pure crystal. To demonstrate the effect of the tailor-made additives, (*a*) shows the orientation of only three host molecules *vis-à-vis* the crystal faces.

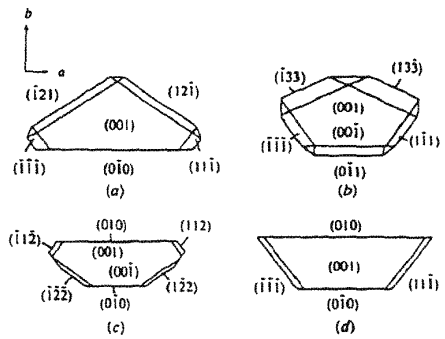


Fig. 6. Morphologies of measured crystals of *N*-(*E*-cinnamoyl)-(*S*)-alanine. (*a*)–(*c*) refer to crystals grown from methanol: (*a*) pure crystal, (*b*) grown in the presence of the methyl ester (1*b*), (*c*) grown in the presence of *E*-cinnamoyl-(*R*)-alanine (1*c*) and (*d*) pure crystal grown from acetic acid.

OCID: <XP___2960386A__I_>

UM00016795
NOVARTIS EXHIBIT 1517
Novartis v. Regents, IPR2023-01347
Page 3777 of 4460

alkyl gluconamides, $C_nH_{2n+1}NHCO(CHOH)_4CHOH$, $n=7$–10. The molecules crystallize as plates in an arrangement akin to that depicted in Scheme 3, namely head-to-tail, as shown in Fig. 7 (Zabel *et al.*, 1986). Thus, one face of the plate crystal is hydrophobic and the opposite hemihedral face is hydrophilic. Contact angle measurements with a variety of polar solvents deposited on the opposite plate-like faces of specimen crystals could establish which face is hydrophobic and which is hydrophilic. This information fixes the orientation of the constituent molecules along the polar *b*-axis of the crystal specimen and consequently their chirality. These wettability experiments also led to crystal growth experiments on these systems to help determine the role of solvent on crystal growth, as discussed in a later section.

The last example involves etching experiments, which have the advantage that they may be performed on pure specimen crystals which had not been grown in the presence of a tailor-made additive. Here we describe the assignment of the absolute structure of racemic (*R*,*S*)-alanine by enantioselective etching (Shimon *et al.*, 1986). This compound crystallizes in the polar space group $Pna2_1$. In the crystal, which is needle-like along the *c*-axis, the *R*- and *S*-molecules are oriented with respect to the polar needle *c*-axis so that the carboxylate CO_2^- groups are exposed at one end of the polar axis and the amino NH_3^+ groups at the opposite end. The crystals exhibit different (hemihedral) faces at opposite ends of the *c*-axis in the sense that one end face is flat and the opposite capped. Conventional X-ray crystallography does not allow one to assign the absolute molecular orientation with respect to the polar axis, and so at which ends are the CO_2^- and the NH_3^+ groups exposed. Etching has been successfully applied for such an assignment by making use of the well developed {210} side faces of the needle. The orientations of the (*R*) and (*S*)-molecules *vis-à-vis* the four symmetry-related {210} side faces for the two possible orientations of the crystal structure with respect to the polar axis are shown in Figs. 8(*a*) and (*b*). Naturally, all four symmetry-related molecules are exposed at each of the four symmetry-related {210} faces, but only one of the four molecules is oriented such that its C—CH_3 group emerges from a particular {210} crystal face, as shown in Fig. 8. Once these orientations in a specimen crystal are determined, the absolute molecular arrangement *vis-à-vis* the polar axis is assigned. Partial dissolution in the presence of *S*-α-amino acids such as serine, $^+H_3NCH(CH_2OH)CO_2^-$, or phenylalanine, $^+H_3NCH(CH_2C_6H_5)CO_2^-$, should replace an (*S*)-alanine substrate molecule at only the $(\bar{2}10)$ and $(2\bar{1}0)$ faces for the orientation shown in Fig. 8(*a*), but would affect the

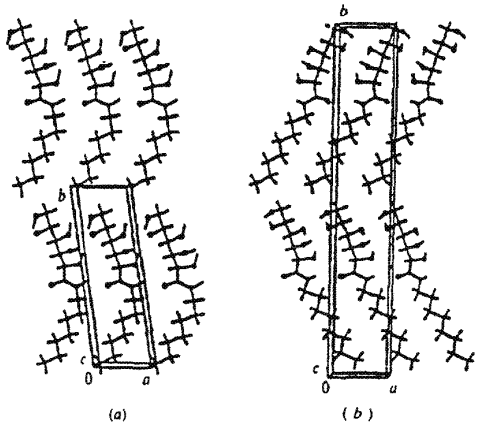


Fig. 7. Head-to-tail packing arrangement of (*a*) *N*-(*n*-heptyl)-D-gluconamide in space group *P*1 and (*b*) *N*-(*n*-octyl)-D-gluconamide in space group $P2_1$.

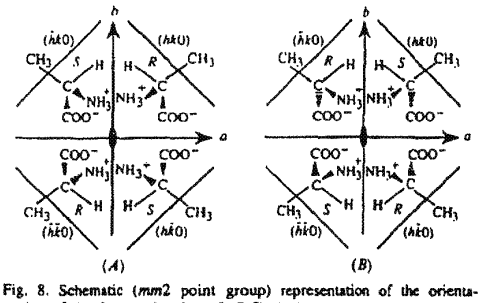


Fig. 8. Schematic (*mm*2 point group) representation of the orientation of the four molecules of (*R*,*S*)-alanine *vis-à-vis* the symmetry-related {210} faces, when viewed along the polar *c*-axis. These four molecules are oriented such that only one has its C—CH_3 group emerging from a given {210} face. (*A*) and (*B*) represent the two alternative orientations of the molecules for the corresponding orientations of the polar crystal structure for a given direction of the *c*-axis.

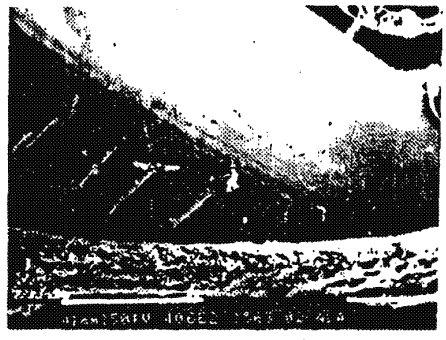


Fig. 9. Scanning electron micrograph of one of the {210} side faces of (*R*,*S*)-alanine etched by (*S*)-threonine; only two adjoining faces are shown, one etched and the other smooth.

DOCID: <XP__2960386A__1_>

UM00016796
NOVARTIS EXHIBIT 1517
Novartis v. Regents, IPR2023-01347
Page 3778 of 4460

(210) and ($\bar{2}\bar{1}0$) pair for the opposite orientation of Fig. 8(*b*). This expectation was demonstrated experimentally, etch-pits being formed on only one pair of {210} side faces (Fig. 9), so fixing the absolute structure of the specimen crystal, and thus of all crystals grown from aqueous solution because the crystals exhibit hemihedral end faces.

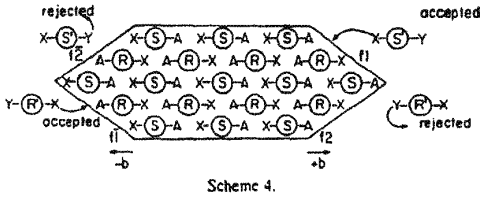
The absolute orientation of specimen polar crystals of (*R,S*)-alanine could also be assigned from growth experiments in the presence of additives designed to affect either of the two polar ends of the crystal. Crystallization experiments in the presence of alanine ethyl ester that would bind at the fast growing CO_2^- end of the crystal yielded much shorter needles. *N*-Methylalanine, which was expected to affect the slow-growing capped end of the crystal, yielded needles as long as from the pure solution, thus fixing the orientation of the molecules in the crystal (Shimon *et al.*, 1986).

Growth experiments in the presence of additives, complemented by surface energy calculations, have also been used for assignment of absolute structure. For example, the absolute orientation of specimen polar crystals of *m*-chloronitrobenzene (*m*-CNB) was determined by crystal growth experiments in the presence of *p*-chloronitrobenzene (*p*-CNB) and *p*-dinitrobenzene (*p*-DNB) additives (Chen, Garside, Davey, Maginn & Matsuoka, 1994). The pure *m*-CNB crystals grown from melt and from acetone solutions do not exhibit hemihedral faces, although the space group is $Pna2_1$. Growth in the presence of *p*-CNB and *p*-DNB yielded asymmetrically shaped crystals affected along the polar *c*-axis. Qualitative calculations of the binding energy of the additives to the crystal were in agreement with the experiment, insofar as the additive could be bound at only one specific end of the polar axis. Docherty, Roberts, Saunders, Black & Davey (1993) calculated a polar morphology of urea (space group $P\bar{4}2_1m$) which was in good agreement with the crystal shape obtained from sublimation. A classical type of energy calculation in which one assumes that the charge distribution of the molecules in the bulk and of those being attached at the surface are the same would not yield a polar morphology. By attaching different atomic charges to the bulk molecules and to those being attached at the surface, through the use of *ab initio* quantum chemical calculations, the polar morphology was computed. However, the assignment of the absolute crystal structure of urea has not yet been confirmed by experimental methods. The crystals of urea grown from benzene or water, discussed in §7.4, do not exhibit polar morphologies.

4.2. *Use of centrosymmetric crystals for assignment of molecular chirality*

In contrast to the situation for chiral crystals, it had not been generally appreciated that in centrosymmetric crystals the orientations of the constituent molecules are unambiguously assigned, with respect to the crystal axes, from a conventional structure determination. Thus, the known orientation of the two enantiomeric molecules in a centrosymmetric crystal can be exploited for the direct assignment of absolute configuration of chiral-resolved molecules, provided the structural information embedded in the racemic crystal is transferred to a chiral additive molecule. The direct assignment of the absolute configuration of such chiral-resolved additives may thus be determined through the morphological changes they induce selectively on one set of enantiotopic faces of centrosymmetric crystals with appropriate packing features.

A prerequisite for application of this method is that within the centrosymmetric racemic crystal a specific functional group *A* attached to an *R*-molecule points towards the faces $f\bar{1}$ and $f\bar{2}$, but not towards the opposite faces *f*1 and *f*2 (Scheme 4). By symmetry, the same functional group attached to an *S*-molecule will emerge at the enantiotopic faces *f*1 and *f*2, but not $f\bar{1}$ and $f\bar{2}$. Crystallization of a centrosymmetric crystal in the presence of a chiral additive *R'*, in which *A* is replaced by *Y*, designed so that it will fit in the site of an *R* molecule on the growing crystal faces $f\bar{1}$ or $f\bar{2}$, but not on the enantiotopic faces *f*1 or *f*2, will hinder growth in the $-b$ direction, but not in the $+b$ direction (Scheme 4). By virtue of symmetry, the enantiomeric additive *S'* will inhibit growth perpendicular to faces *f*1 and *f*2, while racemic additive *R'S'* will inhibit growth in both directions $+b$ and $-b$. This approach is not limited to racemic crystals, but the constituent molecules should at least be prochiral for ease of interpretation. For example, the absolute configuration of all naturally occurring α-amino acids, except proline, may be assigned by their effect on the morphology of the α-form of glycine, a prochiral molecule (Weissbuch *et al.*, 1983). We shall illustrate the above principle making use of centrosymmetric crystals of (*R,S*)-serine to assign the absolute configuration of threonine as an additive (Weissbuch, Shimon *et al.*, 1985).



Scheme 4.

Racemic serine crystallizes in space group $P2_1/a$. Within the structure (Fig. 10), the $C_\beta \rightarrow H_{Si}$ bond vector of the rigid methylene group of the *R*-serine molecule has a major component along $+b$ and, by symmetry, the $C_\beta \rightarrow H_{Re}$ bond vector of the *S*-serine has a major component along $-b$. Thus, their replacement by methyl,

)OCID: <XP___2960386A__I_>

UM00016797
NOVARTIS EXHIBIT 1517
Novartis v. Regents, IPR2023-01347
Page 3779 of 4460

as in threonine, will inhibit growth in the *b*-direction. That is, an *R*-threonine molecule with a side-chain β-carbon of chirality *S* will inhibit growth along $+b$, while the $-CH_3$ group of *S*-threonine will replace the H_{Re} hydrogen of *S*-serine and hence inhibit growth along $-b$. (*R,S*)-serine forms tabular crystals with point symmetry 2/*m* [Fig. 11(*a*)]; the crystals affected by either *R*- or *S*-threonine exhibit reduced morphological point symmetry 2 (the mirror plane is lost) and are enantiomorphous [Figs. 11(*b*) and (*c*)]. When *R,S*-threonine is used as the additive, the morphological point symmetry 2/*m* is left unchanged because the effects induced by each additive separately combine. The crystals turn into rhombs, with a clear increase in the areas of the {011} side faces relative to those of the pure form [Fig. 11(*d*)]. The changes in morphology seen with the additives in Figs. 11(*b*)–(*d*) with respect to that of the pure crystals [Fig. 11(*a*)] can be interpreted only in terms of selective adsorption of the *R*-enantiomer at faces (011) and $(01\bar{1})$, and of *S* at $(0\bar{1}1)$ and $(0\bar{1}\bar{1})$. According to calculated surface binding energies (Weissbuch, Shimon *et al.*, 1985), *R*-threonine may easily be adsorbed only on faces (011) and $(01\bar{1})$ and, by symmetry, *S*-threonine only on $(0\bar{1}1)$ and $(0\bar{1}\bar{1})$. These results fix the absolute chirality of the chiral-resolved threonine additive.

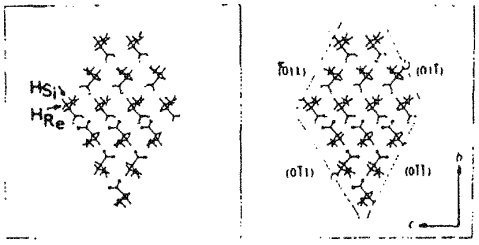


Fig. 10. Stereoscopic view of the packing of the (*R,S*)-serine crystal along the *a*-axis. Each *bc*-layer is composed of *R*- or *S*-molecules only. For clarity, only half of each *R*- (open circles) and *S*- (filled circles) layer is shown. The positions of the four {011} faces are shown with respect to the crystal structure. Threonine additive molecules have been stereospecifically inserted, with the β-methyl groups indicated by large circles.

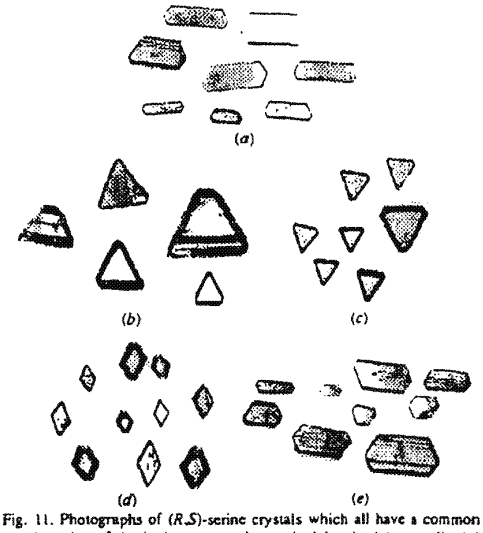


Fig. 11. Photographs of (*R,S*)-serine crystals which all have a common orientation of the lattice axes and a vertical *b*-axis: (*a*) pure; (*b*)–(*e*) grown in the presence of: (*b*) *R*-threonine, (*c*) *S*-threonine, (*d*) *R,S*-threonine and (*e*) *R,S*-allothreonine.

5. Symmetry lowering in crystals following selective occlusion of tailor-made auxiliaries

Crystallization is a commonly used process for purification of inorganic and organic materials, and so the mode of occlusion of impurities or additives inside growing crystals is of paramount technological and theoretical importance. The results presented above, on the interaction of 'tailor-made additives' with the different faces of crystals, have bearing on the general question regarding the distribution and arrangement of occluded 'tailor-made' additives within crystals, indeed on the symmetry and structure of crystalline solid solutions.

A basic concept pertaining to this question is that, in general, the two-dimensional symmetry relating molecules at crystal surfaces is generally lower than the three-dimensional symmetry of the bulk crystal and that the surface structures of nonsymmetry-related faces have different arrangements. For simplicity we illustrate this aspect with a schematic arrangement of space-group symmetry $P2_1/c$, shown in Fig. 12. Note the corresponding symmetry operations of the 2/*m* point group given in the insert. The crystal is delineated by four symmetry-related diagonal faces, labeled {011}. At these four surfaces, the three symmetry relations belonging to space group $P2_1/c$ (*i.e.* center of inversion, twofold screw and glide) are broken, thus their two-dimensional symmetry is limited to translation, plane symmetry *p*1. We now examine the effect of tailor-made additive on these faces. One can easily see that an additive molecule, in black in Fig. 12, bearing an appropriately modified group, will be able to substitute for a substrate molecule at any diagonal face, say (011), but at only one of the four different surface sites, because at that site only the modified group does not disturb the regular pattern of interactions at the crystal surface. Occlusion of such a molecule through the (011) face will lead to a crystal sector of symmetry *P*1, since the occluded molecules therein are related by only translation symmetry. Occlusion of additive through all four diagonal faces {011} will lead to a crystal composed

DOCID: <XP___2960386A__1_>

UM00016798
NOVARTIS EXHIBIT 1517
Novartis v. Regents, IPR2023-01347
Page 3780 of 4460

of four sectors, where these four sectors are related to each other by the 2/*m* point symmetry of the original host crystal.

Consequently, in general, an additive molecule will be anisotropically distributed within the grown crystal, preferentially occluded through different subsets at surface sites on the various faces, leading to a mixed crystal composed of sectors coherently intertwined. The selective occlusion of the additive into a sector will thus lead to a reduction of the crystal symmetry to the symmetry of the face through which it was adsorbed. This principle holds for each crystal sector, although the occluded additive may occupy only a small fraction of the bulk sites. It also holds for the whole crystal, but we note that the different crystal sectors are related to each other by the symmetry elements of the point group of the pure crystal structure. The reduced symmetry of each sector may thus be masked, depending upon the history of crystal growth, whether the sectors are examined separately, and the type of examination. For example, in a crystal containing all sectors, the loss of a glide plane or twofold screw axis should be immediately evident from the lack of the corresponding systematic absences in the X-ray or neutron diffraction pattern (naturally assuming that the crystal is of mosaic texture, which is the general case, and so the different mosaic blocks diffract independently), but not the loss of a rotation axis, mirror plane or center of inversion. Detection of the latter would require at least measurement of the complete set of diffraction data from the individual sector to test for a reduction in Laue diffraction symmetry, generally to be followed by crystal structure refinement. Reduction in crystal symmetry following the above principles was predicted in several host–additive systems and experimentally demonstrated by a variety of methods including changes in crystal morphology, HPLC, frequency doubling of laser light (*i.e.* second harmonic generation SHG), solid-state asymmetric photodimerization and optical birefringence. Symmetry-lowering has also been directly shown by X-ray and neutron diffraction. We now review examples to illustrate the arguments and principles described above.

5.1. *Detection of reduced crystal symmetry by enantiomeric distribution of additives*

The mode of occlusion of additive leading to a reduction in symmetry, depicted schematically in Fig. 12, may be used as an aid to understand the selective occlusion of *R,S*-threonine into the crystals of (*R,S*)-serine (Weissbuch, Shimon *et al.*, 1985). The morphological changes induced in (*R,S*)-serine, as discussed in the previous section (see Fig. 10), imply that *R*-threonine, if occluded, would do so through the (011) and (01$\bar{1}$) faces. By symmetry, *S*-threonine would be occluded through the (0$\bar{1}$1) and (0$\bar{1}\bar{1}$) faces. Thus, the threonine additives, racemic in

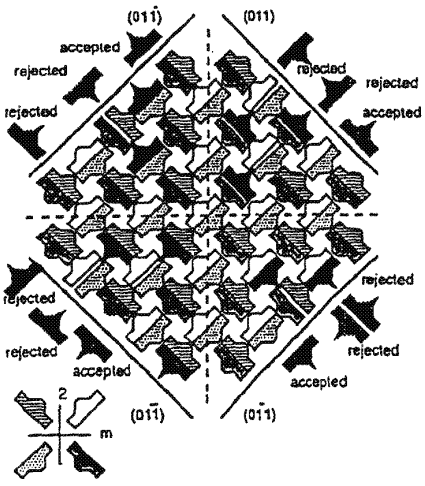


Fig. 12. Schematic representation of adsorption and occlusion of additive molecules (in black) through the four slanted {011} faces in a centrosymmetric crystal space group $P2_1/c$, containing four symmetry-related molecules. Their relative orientations are also depicted in the insert (point symmetry 2/*m*). In each of the four crystal sectors, only one of the symmetry-related molecules can be replaced by the additive on adsorption, which means the loss of all symmetry elements but translation. The crystal symmetry in each sector is thus reduced from $P2_1/c$ to $P1$.

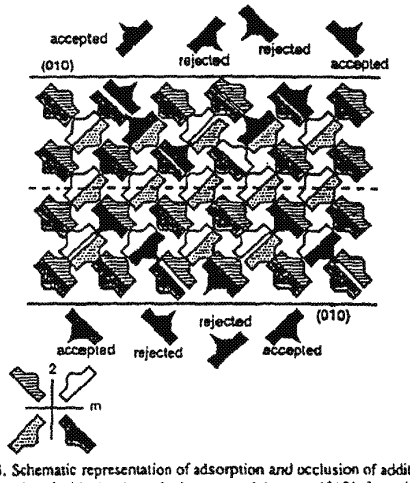


Fig. 13. Schematic representation of adsorption and occlusion of additive molecules (in black) through the top and bottom {010} faces in a crystal of space group $P2_1/c$, resulting in the loss of the glide and inversion symmetry. The crystal symmetry in each half is thus reduced from $P2_1/c$ to $P2_1$.

OCID: <XP___2960386A__i_>

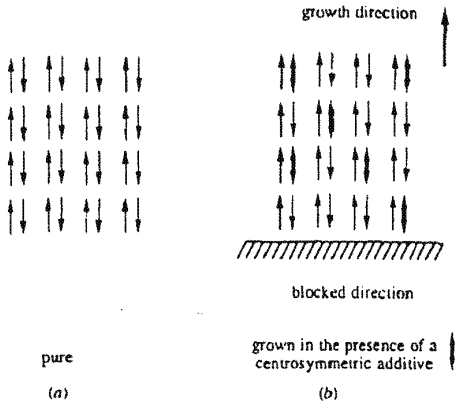
NOVARTIS EXHIBIT 1517
Novartis v. Regents, IPR2023-01347
Page 3781 of 4460

solution, must on occlusion into (*R,S*)-serine crystals be enantiomerically segregated into domains of opposite chirality along the *b*-axis during crystal growth, as was indeed experimentally shown by HPLC methods (Weissbuch, Shimon *et al.*, 1985).

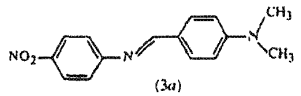
Symmetry lowering of a somewhat similar nature involved the α-form of glycine grown in the presence of α-amino acid additives (Weissbuch *et al.*, 1983). As an aid to understanding we present Fig. 13, which is a model representation of reduction in symmetry from $P2_1/c$ to $P2_1$ when molecules are occluded through the (010) and $(0\bar{1}0)$ faces. The mode of adsorption of α-amino acid additives onto the {010} faces of α-glycine has already been described in §3. In terms of that analysis, only the *R*-α-amino acid additive may be occluded through the (010) face, replacing a glycine molecule at sites (1) and (2) only [Fig. 3(*a*)], yielding a pyramidal morphology [Fig. 3(*c*)]. By symmetry, only the *S*-α-amino acid additives may be occluded into sites (3) and (4) through the $(0\bar{1}0)$ face of α-glycine [Fig. 3(*a*)], yielding an enantiomorphous morphology [Fig. 3(*d*)]. Thus, racemic additives cause the formation of {010} plates [Fig. 3(*e*)], because growth at the $+b$ and $-b$ sides of the crystal is inhibited. These plates were found to contain 0.02–0.2% racemic α-amino acid additive within the crystal bulk with the two enantiomers totally segregated in the two crystal sectors at the $+b$ and $-b$ halves As expected, the *R*-enantiomers populate the $+b$, and the *S*-enantiomers the $-b$ half of the crystal according to HPLC measurements (Weissbuch *et al.*, 1983). In terms of the argument given above, the crystal symmetry of each half of the crystal must be reduced from $P2_1/n$ to $P2_1$, and the two sectors are enantiomorphous. We note that the absolute configuration of the α-amino acid additive can be directly assigned not only from the induced changes in crystal morphology but also from its anisotropic distribution on occlusion within the crystal. Symmetry lowering of a similar nature was also demonstrated in another system, which involved enantiomeric segregation of the dipeptide glycyl–leucine inside growing crystals of glycyl–glycine $^+H_3NCH_2CONHCH_2CO_2^-$ (Weissbuch, Berkovitch-Yellin, Leiserowitz & Lahav, 1985).

5.2. *Detection of reduced crystal symmetry by nonlinear optics*

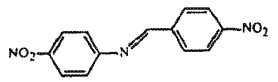
Symmetry lowering in host–additive systems, such as a loss of inversion, glide or twofold screw symmetry, which would introduce (additional) polarity into the crystal, may be probed by nonlinear optical effects, such as second harmonic generation (SHG) which is active in a noncentrosymmetric material. One requirement is that either the host or additive molecule has a large molecular hyperpolarizability tensor β, leading to large optical nonlinearity. Consequently, a centrosymmetric pure crystal structure, which consists of antiparallel pairs of host molecules with high β coefficients [Scheme 5(*a*)], would yield a SHG-active crystal upon site-selective occlusion by a centrosymmetric guest molecule, as shown in Scheme 5(*b*). Because the growth of the crystal is blocked at the bottom face, the additive is adsorbed and occluded through only one of the pair of surface sites at the top exposed face. We demonstrated the potential of this approach with centrosymmetric host crystals of *p*-(*N*-dimethylamino)benzylidene-*p'*-nitroaniline [3*a* (Fig. 14)], which became noncentrosymmetric and SHG-active upon site-selective occlusion of the guest molecule *p,p'*-dinitrobenzylideneaniline (3*b*), which is pseudocentrosymmetic (Weissbuch, Lahav, Leiserowitz, Meredith & Vanherzeele, 1989). In this system the host and guest molecules have large and negligible β-coefficients, respectively.



Scheme 5.



(3*a*)

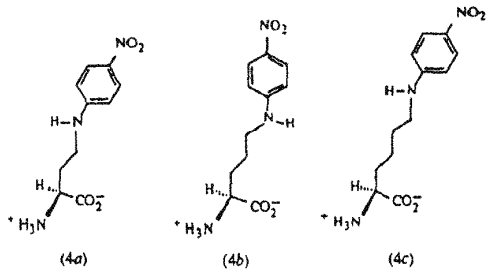


(3*b*)

The reverse situation, where the guest has large hyperpolarizability, is illustated by an α-glycine host crystal containing, as additive, α-amino acids which have a high β coefficient, such as the *p*-nitrophenyl derivatives of α,δ-diamino butyric acid (4*a*), ornithine (4*b*) and lysine (4*c*). The amount of occluded additive was less than 0.2% (wt/wt of glycine), but sufficient to yield colored crystals. In terms of the arguments presented above, {010} plate-like crystals of glycine, grown in the presence of *R,S*-additives, should have their symmetry reduced from $P2_1/n$ to $P2_1$. In fact, the symmetry was

IOCID: <XP___2960366A__1_>

UM00016800
NOVARTIS EXHIBIT 1517
Novartis v. Regents, IPR2023-01347
Page 3782 of 4460



(4a) (4b) (4c)

reduced even further to $P1$ according to the SHG measurements (Weissbuch, Lahav, Leiserowitz, Meredith & Vanherzeele, 1989), providing additional information on the nature of the crystal growth process.

Other systems of interest are the noncentrosymmetric orthorhombic crystals of space-group symmetry $P2_12_12_1$. On symmetry grounds such crystals are nonpolar along the three principal crystallographic axes and therefore frequency doubling is forbidden in these directions. We anticipated that such crystals, when grown in the presence of appropriate additives so as to reduce the crystal symmetry to monoclinic $P2_1$, should become SHG-active along the remaining 2_1 axis but not along those two axes which have lost their twofold screw symmetry. In fact, single crystals of (*S*)-glutamic acid.HCl grown in the presence of appropriate additives were SHG-active along all three axes (Weissbuch, Lahav, Leiserowitz, Meredith & Vanherzeele, 1989), indicating symmetry lowering to $P1$, once again providing information on the nature of the crystal growth process.

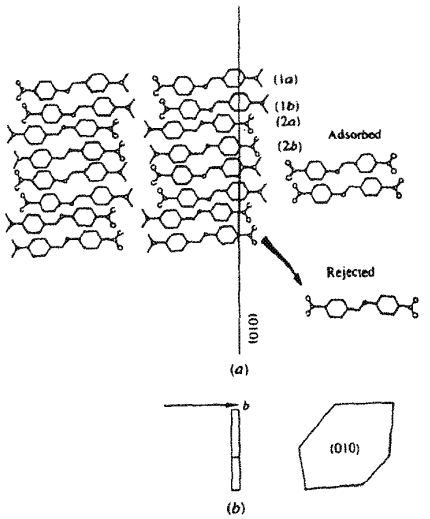
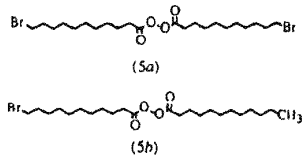


Fig. 14. (*a*) Packing arrangement of a polymorph of the *p*-(*N*-dimethylamino)benzylidene-*p'*-nitroaniline crystal, showing how the dinitro additive may be adsorbed on the (010) face. The additive may be adsorbed only at sites of type (1), but not at type (2) sites. (*b*) Two views of the morphology of the plate-like crystals.

5.3. *Detection of reduced crystal symmetry by optical birefringence*

The properties of optical birefringence in crystals have been used to demonstrate a reduction in crystal class. McBride & Bertman (1989) took advantage of the fact that crystals that belong to a high symmetry class, such as tetragonal, trigonal or hexagonal, are optically uniaxial, whereas crystals that belong to a lower crystal class, such as triclinic, monoclinic or orthorhombic, are optically biaxial. They studied the tetragonal crystals of di(11-bromoundecanoyl) peroxide (*5a*), denoted as Br···Br, in the presence of guest (*5b*) where a Br atom is replaced by CH_3, denoted as Br···CH_3. In the host crystal Br···Br molecules assemble into layers which have Br atoms on both the upper and lower surfaces.



(5a)

(5b)

Successive layers stack Br to Br atoms with a 90° rotation about a fourfold screw axis in the stacking direction. These crystals, which grow as square {001} plates delineated by four {110} side faces, are not birefringent for light travelling along the fourfold screw axis perpendicular to the plate, appearing dark between crossed polarized filters. Crystals of Br···Br containing 15% Br···CH_3 are birefringent, the plate revealing four sectors under crossed polarizers. Birefringence in each sector results from unsymmetrical incorporation of the Br···CH_3 additives during crystal growth. As McBride states in his paper, this method of optical microscopy is convenient for surveying large numbers of crystals, to catalogue their growth patterns, and to identify reduced symmetry domains that may be characterized by diffraction. Such an approach has been followed up by Gopalan, Peterson, Crundwell & Kahr (1993) who have observed reduction in symmetry both by optical birefringence and X-ray crystallographic studies of different sectors in mixed crystals of $NaBrO_3/NaClO_3$ and $NaNO_3/Pb(NO_3)_2$. Garnets where Al^{3+} were replaced by Fe^{3+} ions also show a reduction in lattice symmetry from cubic down to triclinic (Allen & Buseck, 1988).

5.4. *Probing intermolecular forces through reduced crystal symmetry*

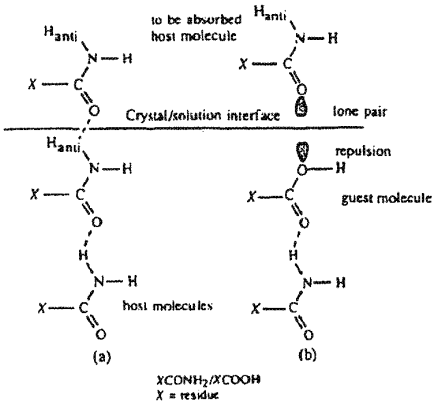
There is interest in investigating the minimal modification of the tailor-made additive with respect to

)OCID: <XP___2960386A__I_>

UM00016801
NOVARTIS EXHIBIT 1517
Novartis v. Regents, IPR2023-01347
Page 3783 of 4460

the host molecule, that would still be recognized and discriminated by the growing crystal surface, and still lead to a reduction in symmetry. Indeed, solid solutions composed of host and additive molecules of similar structure and shape have generally been believed to exhibit the same symmetries as those of the host crystals. A reduction in crystal symmetry involving a structure determination by X-ray or neutron diffraction should allow one to probe fine interactions between host and additive at the crystal surfaces.

We first discuss solid solutions of carboxylic acids (XCO_2H) in primary amides ($XCONH_2$), where an NH_2 group is substituted by an OH moiety (Scheme 6). A strong inhibition of growth develops along the direction of the O=C—N—H_a···O=C hydrogen bond, H_a being the amide H atom in an antiperiplanar conformation to the C=O system. Inhibition arises when a carboxylic acid additive attempts to force the antiperiplanar lone-pair electron lobes of its OH group against a carbonyl oxygen of the underlying molecule, an atom that would normally form a hydrogen bond with the amide's antiperiplanar hydrogen. Incorporation of a carboxylic acid in this orientation would substitute a 8 kj mol^{-1} repulsion for a 25 kj mol^{-1} attraction. The carboxylic acid additive molecule will thus avoid surface sites that require the OH groups to be oriented towards the surface and be preferentially adsorbed at sites where the OH group emerges from the surface (Berkovitch-Yellin *et al.*, 1985).



Scheme 6.

Reduction in crystal symmetry has been demonstrated in two amide–carboxylic acid systems by neutron diffraction and solid-state photodimerization. The former technique was applied to asparagine–aspartic acid (Weissinger-Lewin *et al.*, 1989), where as much as 15% additive was occluded into the crystal by virtue of the numerous hydrogen bonds between guest and host; the dimerization method was applied to the host:additive system *E*-cinnamamide:*E*-cinnamic acid (Vaida *et al.*, 1989) where small amounts (<2%) of cinnamic acid guest were occluded into the host crystal.

(*S*)-Asparagine, $H_2NOCCH_2CH(NH_3^+)CO_2^-$, crystallizes from water as a monohydrate with a tight three-dimensional net of hydrogen bonds in a $P2_12_12_1$ structure [Fig. 15(*a*)]. The morphology is prismatic, with 18 developed faces [Fig. 15(*b*), top]. Crystallization of (*S*)-asparagine in the presence of *S*-aspartic acid, $HO_2CCH_2CH(NH_3^+)CO_2^-$, yields {010} plates [Fig. 15(*b*), bottom]. In terms of the arguments already given for amide–acid systems, the guest aspartic acid molecule should be more easily adsorbed at sites (1) and (3), on the growing (010) surface, than at sites (2) and (4) [Fig. 15(*c*)]; the reverse situation holds for the opposite ($0\bar{1}0$) face. If, on growth of the mixed crystal, the ($0\bar{1}0$) face is blocked so that the amide and acid molecules would only be occluded through the (010) face, the symmetry of the mixed crystal should be reduced to $P12_11$. A low-temperature (18 K) neutron diffraction study with deuterated aspartic acid in protonated asparagine showed the expected reduction in symmetry (Weissinger-Lewin *et al.*, 1989).

Analogously, additive *E*-cinnamic acid, C_6H_5—CH=CH—CO_2H, induces a loss of the center of inversion in the crystal of *E*-cinnamamide, C_6H_5—CH=CH—

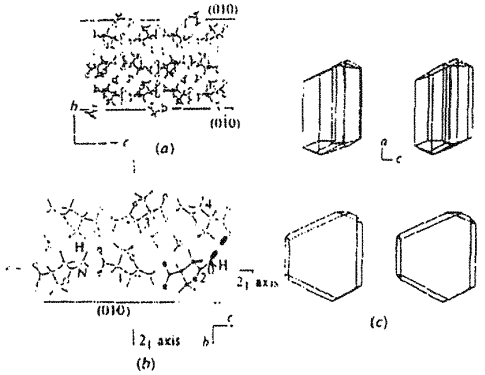


Fig. 15. (*a*) Packing arrangement of (*S*)-asparagine monohydrate viewed along the *a*-axis. Four adsorbed methanol molecules are inserted on the two {010} faces, referring to crystals grown from water–methanol solution. (*b*) Preferential adsorption of aspartic acid on the (010) surface of asparagine (open circles) at sites of type 1 and 3 rather than 2 and 4, as the crystal is growing at the (010) face. Molecules at sites 1 and 3 are shaded, indicating the latter may be occupied by either asparagine or aspartic acid. The probability for aspartic acid to be adsorbed at site 2 (full circles) is less than at site 1 because of O(hydroxyl)···O(carboxylate) lone-pair electron repulsion between 2 and 4. (*c*) Stereoscopic view of morphology of (*S*)-asparagine monohydrate: pure crystals grown from aqueous solution (top), grown in the presence of (*S*)-aspartic acid (bottom), or in water–methanol solution.

IDOCID: <XP___2960386A__I_>

UM00016802
NOVARTIS EXHIBIT 1517
Novartis v. Regents, IPR2023-01347
Page 3784 of 4460

$CONH_2$, which in pure form appears in a centrosymmetric monoclinic arrangement, space group $P2_1/c$. The crystal structure [Fig. 16(*a*)] is composed of hydrogen-bonded dimers interlinked by N—H···O bonds to form a ribbon-like motif which runs parallel to the *b*-axis. *E*-cinnamic acid is preferentially occluded through half the {011} surface sites of the crystal at opposite ends of these ribbons, resulting in a crystal [Fig. 16(*b*)] with two enantiomorphous halves of at most $P2_1$ symmetry. This reduced symmetry was proven photochemically (Vaida *et al.*, 1989). UV irradiation of *E*-cinnamamide yields centrosymmetric photodimers, by virtue of a cyclobutane ring formation involving pairs of close-packed >C=C< bonds across centers of inversion (Fig. 17). Replacement of one such pair by *E*-cinnamic acid results in the formation of asymmetric cinnamamide–cinnamic acid photodimers of opposite chirality at the two enantiomorphous halves of the mixed crystal, with an enantiomeric ratio of 60:40 at each opposite half.

Reduction in crystal symmetry was demonstrated by photodimerization, X-ray and neutron diffraction for the host–guest crystal structure of *E*-cinnamamide–2-*E*-thienylacrylamide (Vaida *et al.*, 1988; Shimon *et al.*, 1993). The host structure [Fig. 16(*a*)] incorporates herringbone contacts between aromatic C—H groups and π-electron clouds of neighboring phenyl rings. In order to induce site-selective adsorption and occlusion, these contacts are replaced in the host–guest system by unfavorable contacts between sulfur lone-pair electrons and the π-electron system [Fig. 18(*a*)]. Thienylacrylamide is occluded through the enantiotopic {011} faces of

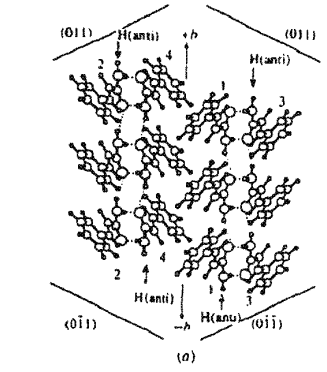


Fig. 16. (*a*) Packing arrangement of *E*-cinnamamide viewed along the *a*-axis delineated by the {011} faces. (*b*) Morphology of *E*-cinnamamide crystals: pure (left) and grown in the presence of cinnamic acid (right).

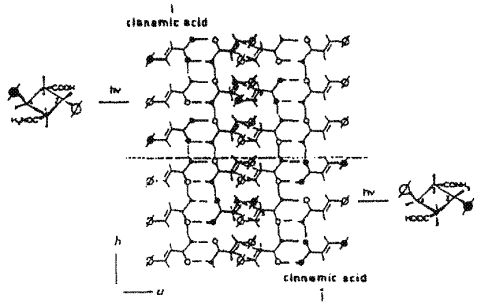


Fig. 17. Ribbons along the *b*-axis of hydrogen-bonded molecules composed of *E*-cinnamamide (open circles) and occluded guest *E*-cinnamic acid molecules (full circles). The latter were adsorbed through site (1) at the $+b$ end and site ($\bar{1}$) at the $-b$ end, leading to two enantiomorphous domains joined at the central dotted line. Also shown are the ribbons related by translation along the *a*-axis, thus depicting the close 4 Å contact between C=C double bonds related by a center of inversion. Two enantiomorphous cyclobutane photodimers between the host and occluded guest from the top and bottom halves of the crystal are also shown.

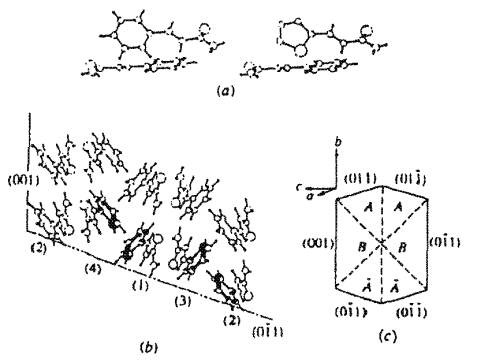


Fig. 18. (*a*) Herringbone contacts involving: (left) two cinnamamide molecules, (right) host cinnamamide and guest thienylacrylamide molecules. (*b*) The four different surfaces sites (1), (2), (3) and (4) of *E*-cinnamamide at the ($0\bar{1}1$) face. S and C atoms of the superimposed 2-thienyl rings in the positions they would assume were they to replace the phenyl rings of cinnamamide molecules at the ($0\bar{1}1$) face are shaded. Site (1) is preferred for guest adsorption on the ($0\bar{1}1$) face since the S atom at that site emerges from the crystal face. By the same argument, (1) and (2) are the preferred sites for guest adsorption on the (001) face. (*c*) Morphological representation of the cinnamamide–thienylacrylamide crystal with six sectors of reduced symmetry.

XOCID: <XP___2960386A__I_>

UM00016803
NOVARTIS EXHIBIT 1517
Novartis v. Regents, IPR2023-01347
Page 3785 of 4460

the crystal [Fig. 18(*b*)]. These faces exhibit *p*1 plane symmetry, since the four different surface sites are not related by symmetry. The guest can easily be adsorbed at only one of these four sites at which the sulfur emerges from the face, leading to *P*1 crystal symmetry upon occlusion of the guest. Thienylacrylamide is also occluded through the {001} faces, which exhibit *pm* plane symmetry. Occlusion through faces of this type should lead to crystal symmetry *Pc*. The mixed crystal should be thus divided into six sectors of reduced symmetry [Fig. 18(*c*)]. The different sectors of the same type, such as *A* and $\bar{A}$ are related to one another by the 2/*m* point symmetry of the host crystal. Low-temperature X-ray and neutron diffraction studies on *A*- and $\bar{A}$-type sectors, cut from a crystal specimen showed symmetry *P*1, in keeping with the photodimerization studies. The proposed reduction in symmetry of the *B*-type sector [Fig. 18(*c*)] was proven to be correct, but only by an X-ray diffraction analysis. We may infer from these results a repulsive intermolecular interaction between the sulfur lone-pair electrons and electron system of neighboring molecules, but we do not have an estimate of the energy.

We have elucidated, by changes in crystal morphology, reduction in crystal symmetry and energy calculations, the molecular conformation of a flexible additive and the effect of diastereomeric chiral additives on crystal morphology and symmetry. For example, for the centrosymmetric crystal of the dipeptide glycyl–glycine when grown in the presence of glycyl–leucine additive, the latter adopts a specific conformation which minimizes unfavorable additive–host molecular interactions at the site of adsorption (Weissbuch, Berkovitch-Yellin, Leiserowitz & Lahav, 1985; Berkovitch-Yellin, Weissbuch & Leiserowitz, 1989).

The pronounced effect threonine exerts on the morphology and structure of racemic serine crystals has been discussed in §4.2 and §5.1. Oddly enough, additive allothreonine, the diastereoisomer of threonine, does not alter very much the morphology of racemic serine crystals [Fig. 11(*e*)], nor is there any enantioselective segregation of allothreonine along the *b*-axis of the crystal. These observations were accounted for in a quantitative way by calculated surface binding energies, according to which, say *S*-allothreonine, is most strongly bound on the {100} faces and somewhat less so on the (011) and (01$\bar{1}$) faces of racemic serine crystals. We note that *R*- and *S*-allothreonine additives are equally well occluded through the {100} faces because of the 2/*m* crystal point symmetry of (*R*,*S*)-serine, thus masking any enantioselective segregation of the additive through the {011} faces (Weissbuch, Shimon *et al.*, 1985).

5.5. *Some general rules on symmetry lowering through additive occlusion*

As a conclusion of this section on crystal symmetry lowering, we may draw some general rules. The local symmetry of a mixed crystal is determined by that of the faces developed. If the symmetry of the crystal face through which an additive is adsorbed is not lower than that of the bulk, there cannot be reduction in symmetry for the crystal sector bound by that face. In other words, the symmetry of a crystal sector cannot be lower than that of the growth sites on the bounding crystal face. This principle is so basic that if a crystal is bound by faces of different plane symmetries, one can, at least in principle, imagine it as formed of different sectors each with bulk symmetry as low as that of its bounding face, the sectors being related to each other by the point symmetry elements of the crystal. Thus, the 'overall' symmetry of the crystal is not reduced. This is a consequence of Curie's principle, as presented in his paper 'Symetrie dans les phenomenes physiques' (Curie, 1894): a physical event cannot have a symmetry lower than that of the event which caused it.

6. Effect of tailor-made additives on crystal texture

Surprisingly, little work has been done to date on the effect of tailor-made additives on mosaicity and coherence length (*i.e.* extent of perfect crystal order) in molecular crystals. Indirect evidence was first brought to light by low-temperature (18 K) neutron diffraction measurements on single crystals of pure asparagine monohydrate and the solid solution of asparagine–aspartic acid monohydrate (Weissinger-Lewin *et al.*, 1989), undertaken to demonstrate symmetry lowering in the latter system (§5.4). The neutron reflections of the specimen crystal of pure asparagine suffered from pronounced extinction effects, whereas the specimen crystal of asparagine–aspartic acid was almost free from extinction. These results were interpreted in terms of much higher mosaicity and smaller mosaic domains in the asparagine–aspartic acid crystals, brought about by the presence of aspartic acid. More direct evidence came from studies on biomineralization (Berman *et al.*, 1990, 1993*a*,*b*), which addressed the fundamental question of whether proteins in calcite mineralized tissue alter the crystal texture in an anisotropic manner. High-resolution synchrotron X-ray diffraction was used to monitor changes in coherence length and angular mosaic spread. It was found that protein extracted from sea urchins and mollusks reduced the coherence lengths of crystals of calcium fumarate and calcium malonate in the directions perpendicular to the planes onto which the proteins were preferentially adsorbed. In contrast, the calcite crystals grown *in vitro* in the presence of the proteins exhibited an increase in angular spread, but no anisotropic effect in coherence length was detected. A biologically produced calcite crystal, on the other hand, showed a preferential reduction in coherence length in the direction of the *c*-axis.

3DOCID: <XP___2960386A__1_>

UM00016804
NOVARTIS EXHIBIT 1517
Novartis v. Regents, IPR2023-01347
Page 3786 of 4460

7. Effect of solvent on crystal growth and morphology

Solvent has a strong influence on the habit of crystalline materials, however, the role played by solvent–surface interactions in enhancing or inhibiting crystal growth is still not completely resolved. To date there have been two different approaches to clarify this point. In one theory, proposed by Bennema and others (Bennema & Gilmer, 1973; Bennema, 1992; Bourne & Davey, 1976; Elwenspoek, Bennema & van Eerden, 1987), favorable interactions between solute and solvent on specific faces leads to reduced interfacial tension, causing a transition from a smooth to a rough interface and a concomitant faster surface growth. Alternatively, it has been proposed that preferential adsorption at specific faces will inhibit their growth as removal of bound solvent poses an additional energy barrier for continued growth. Our studies on the role played by tailor-made additives are in keeping with the latter approach. However, solvent–surface interactions cannot be as clearly analyzed as those between the tailor-made additives and the crystal. In order to help clarify this problem, we describe several approaches that have been adopted.

7.1. *Computational methods*

One of the main difficulties is to disentangle the relative contributions of the internal crystal structure and solvent–surface interactions in determining the crystal morphology. The former may be evaluated by growing the crystal by sublimation, if possible, or by theoretical modeling. The ground rules for a quantitative determination of crystal morphology were laid down by Hartman & Perdok (1955*a*,*b*), Hartman (1973) and Hartman & Bennema (1980). According to their analyses, the crucial relation is between the layer energy, E_L, which is the energy released when a layer is formed, and the attachment energy, E_{att}, which is defined as the energy per molecule released when a new layer is attached to the crystal face. E_{att} controls the growth rate perpendicular to the layer, while E_L measures the stability of the layer. The working hypothesis is that the morphological importance of a crystal face is inversely proportional to its attachment energy. The energies, E_L and E_{att}, may be computed using atom–atom potential energy functions, which are generally made up of van der Waals and electrostatic terms. The latter term is described by an interatomic Coulombic interaction with parameters which depend upon charge distribution and so may be derived by quantum chemical methods, self-consistent force field methods, or from experimental deformation electron-density distributions as determined from low-temperature X-ray diffraction data (Hirshfeld, 1977). By applying such a procedure it became possible to calculate the energy values of E_L and E_{att} for various low-index crystal faces from which the 'theoretical crystal form' may be derived. This method has been applied for a variety of organic (*e.g.* Berkovitch-Yellin, 1985; Berkovitch-Yellin *et al.*, 1985; Boek, Feil, Briels & Bennema, 1991; Docherty, Roberts, Saunders, Black & Davey, 1993) and inorganic (Woensdregt, 1993) crystals.

It is possible to use such information on the theoretical form to help understand the effect of solvent on crystal morphology. For example, the theoretical form of α-glycine (Berkovitch-Yellin, 1985; Boek, Feil, Briels & Bennema, 1991) calculated by this method [Fig. 19(*a*)] is in good agreement with the morphology of α-glycine crystals obtained by sublimation [Fig. 19(*b*)]. This morphology exhibits well developed {010} faces, in keeping with the dominant hydrogen-bonding energy of the molecular bilayer in the *ac*-plane. However, glycine crystals grown from aqueous solution display a distinctly different morphology, which is bipyramidal with large {011} and {110} faces and less well developed {010} faces [Fig. 3(*b*)]. In order to understand these differences, substrate–solvent interactions were taken into account. The large {011} and {110} faces expose CO_2^- and NH_3^+ groups well oriented to have a strong affinity for water. The {010} face exposes alternating layers of C—H or CO_2^- and NH_3^+ groups [Fig. 3(*a*)], and so, on average, is less hydrophilic than the {011} and {110} faces. Moreover, if the solute glycine molecules dock into surface sites primarily as cyclic hydrogen-bonded dimers, the {010} face will essentially expose C—H groups. These observations were expressed by Berkovitch-Yellin in a semi-quantitative form by calculating the Coulomb potential at the various faces, which indicated preferential adsorption of water molecules onto the polar faces. Further support for such arguments comes from the observed crystal morphology of the α-amino acids with hydrophobic chains such as phenylalanine (Weissbuch, Frolow, Addadi, Lahav & Leiserowitz, 1990), valine and isoleucine (Torii & Yitaka, 1970, 1971). Their crystal structures are composed of hydrogen-bonded bilayers as in α-glycine, and their morphologies are plate-like when grown from aqueous solution. Clearly the hydrophobic chains provide in-

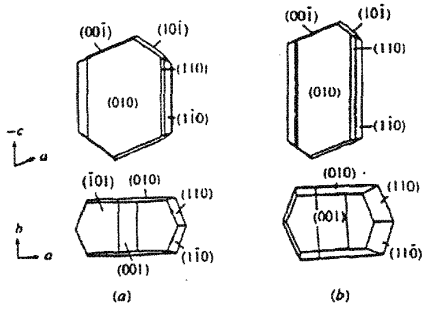


Fig. 19. (*a*) Theoretical crystal form of α-glycine. (*b*) Morphology of α-glycine crystals obtained by sublimation.

OCID: <XP___2960366A__I_>

UM00016805
NOVARTIS EXHIBIT 1517
Novartis v. Regents, IPR2023-01347
Page 3787 of 4460

creased layer energy and a lower binding concentration of water at the sides of such bilayers than in α-glycine, providing a strong propensity for plate formation.

7.2. *Crystalline solvates*

Another approach involved the use of crystalline solvates, where the solvent of crystallization plays the dual role of solvent and crystal solute. Such crystals were grown in the added presence of tailor-made solvent, which is a slightly modified version of the solvate solvent. It was found when crystalline hydrates were grown from aqueous solution in the added presence of methanol (the 'tailor-made' solvent), that the change in morphology was interpretable (Shimon, Vaida, Addadi, Lahav & Leiserowitz, 1990, 1991) in a manner akin to the effect of a tailor-made inhibitor. This approach is illustrated with the crystal of α-rhamnose monohydrate, which contains a polar arrangement [Fig. 20(*a*)] in space group $P2_1$ and, when grown from pure aqueous solution, displays a bipyramidal morphology [Fig. 20(*b*)]. The two O—H bonds of the hydrate water molecules are oriented towards the $+b$ direction, but not towards the $-b$ direction of the crystal. Thus, addition of methanol as a cosolvent changes the morphology of the crystal, completely inhibiting growth along the $+b$ direction and yielding a pyramidal crystal [Fig. 20(*c*)].

A second example is (*S*)-asparagine.H_2O. Crystals grown from pure water are delineated by 18 faces [Fig. 15(*b*), top]. The packing arrangement (Fig. 15*a*), shows that one of the two O—H bonds of each water molecule emerges from the {010} faces, which are poorly expressed. Therefore, methanol molecules can be easily attached at these surface sites [see Fig. 15(*a*)]. The methyl group of each adsorbed methanol protrudes from the two {010} faces, impedes growth in the *b*-direction and thus induces the formation of large {010} crystal faces [Fig. 15(*b*), bottom]. On the {011} faces, only two of the four symmetry-related molecules can be substituted by methanol and so inhibition of {011} should be less dramatic. This reasoning proved to be in keeping with experiment (Shimon, Vaida, Addadi, Lahav & Leiserowitz, 1991); growth in the presence of methanol as additive yielded {010} plates similar in shape to when asparagine is grown in the presence of aspartic acid [Fig. 15(*b*)]. That methanol can indeed be selectively adsorbed on both the {010} and {011} faces was further demonstrated by experiments involving partial dissolution of asparagine.H_2O crystals in methanol solution, revealing etch-pits, although poorly developed, on only these faces (Shimon, Lahav & Leiserowitz, 1986).

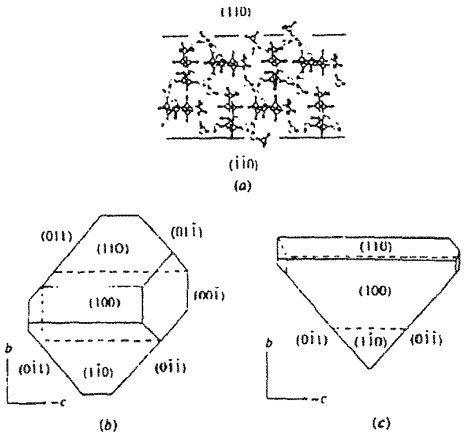


Fig. 20. (*a*) Packing arrangement of α-rhamnose monohydrate crystal viewed along the *a*-axis; the OH bonds of the hydrate water molecules point towards the $+b$, but not the $-b$ direction; replacement of water by methanol on the {110} faces is depicted. (*b*)–(*c*) Crystals viewed along the *a*-axis. Morphologies of α-rhamnose monohydrate crystals grown from: (*b*) aqueous solution and (*c*) 9:1 methanol:water solution.

7.3. *Polar crystals*

In another approach, use was made of the principle that in a polar crystal the attachment energy E_{att} at opposite and hemihedral faces (hkl) and $(\bar{h}\bar{k}\bar{l})$ are the same (neglecting effects such as possible differences in molecular charge density in the bulk and to-be-attached molecules at opposite faces). Although a difference in E_{att} has been invoked to explain the polar morphology of urea obtained by sublimation (Docherty, Roberts, Saunders, Black & Davey, 1993), its effect on morphology must be far less than that of solvent on crystal growth and morphology. Thus, in the absence of a difference in the effect of binding of solvent at the hemihedral faces (hkl) and $(\bar{h}\bar{k}\bar{l})$, these two faces should grow at the same rate (Turner & Lonsdale, 1950). A pronounced difference in growth rate must then be associated with differences in solvent–surface interactions. This principle was exploited in the family of plate-like crystals composed of amphiphilic molecules which pack in layers stacked head-to-tail in a polar arrangement (chain-like amphiphilic molecules normally pack head-to-head and tail-to-tail in the crystalline state). Thus, the polar plate-like crystals are hydrophobic at one plate face and hydrophilic at the opposite face. The idea was to ascertain the relative binding properties of polar solvents to the opposite hemihedral faces from the macroscopic wetting properties, in terms of contact angle measurements, and to correlate this effect with the relative rates of growth of the two crystal faces in the same solvents. In §4.1 we had shown how the absolute configuration of the constituent molecules of chiral-resolved alkylgluconamides, which pack in the desired polar arrangement (Fig. 7), may be assigned from the difference in wetting properties of the hydrophilic and

!DOCID: <XP___2960366A__1_>

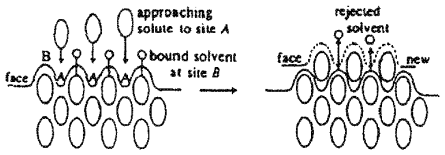
UM00016806
NOVARTIS EXHIBIT 1517
Novartis v. Regents, IPR2023-01347
Page 3788 of 4460

ydrophobic faces. In CH_3OH solution the polar plate-ike crystals of the octyl derivative ($n = 8$) were found o grow almost four times faster at the hydrophobic ide than at the hydrophilic side (Wang, Leiserowitz & Lahav, 1992). This result is completely in keeping vith the observation that water and other polar solvents vet the hydrophilic face more strongly than the opposite ydrophobic face (see §4.1). It is noteworthy that at the ydrophilic face, solvent methanol can form O—H···O ydrogen bonds with the terminal hydroxyl groups of wo neighboring chains, since the translation separation listance between them is *ca* 5 Å.

The theory that strong solvent–surface interactions nhibit crystal growth is also borne out by a compar-son of the effect of tailor-made additives and acetic cid solvent on the morphology of the polar crystals f *N*-(cinnamoyl)alanine, already discussed in §4.1. A enchmark study on the effect of solvent on growth of olar crystals was carried out by Wells (1949). He found hat in aqueous solution, the α-form of resorcinol (1,3-lihydroxybenzene), which crystallizes in space group $^2na2_1$, grows unidirectionally along the polar *c*-axis. The {011} faces at one end of the polar axis have proton donor' properties and the $\{0\bar{1}\bar{1}\}$ faces at the pposite end 'proton acceptor' properties. However, Wells could not fix the absolute direction of growth long the polar axis. This assignment was made with he use of tailor-made additives (Wireko *et al.*, 1987). The unidirectional growth in aqueous solution occurs t the 'proton acceptor' $\{0\bar{1}\bar{1}\}$ faces. This observation vas explained in terms of stronger binding of water to he 'proton acceptor' $\{0\bar{1}\bar{1}\}$ faces (Wireko *et al.*, 1987; Davey, Milisavljevic & Bourne, 1988). However, these nalyses were not completely irrefutable, hinting that ther growth mechanisms might also be responsible. Thus, we describe the next experiments on the polar rystals of γ-glycine and racemic alanine as well as urea, where different mechanisms were invoked to account for heir growth behavior.

1.4. *A 'relay' mechanism of crystal growth as a result of selective solvent binding*

An entirely different approach involved strong elective adsorption of solvent at a subset of molecular urface sites, of say type *B*, and repulsion of solvent t the remaining set of surface sites, of say type *A*, on he crystal face. This is depicted in Scheme 7, where ve emphasize the difference between the two types of ites by assuming a corrugated surface such that the *A*-type site is a cavity and the *B*-type site is on the utside upper surface of the cavity. Scheme 7(*a*) shows he *B*-type sites blocked by solvent *S* and the *A*-type ites unsolvated. Thus, solute molecules can easily fit nto *A*-type sites. However, once docked into position Scheme 7(*b*)], the roles of the *A*- and *B*-type sites are ssentially reversed and the solvent molecules which originally were bound to *B*-type sites would be repelled since they now occupy *A*-type sites. This cyclic process can lead to fast growth by a kind of 'relay' mechanism.



Scheme 7.

In such a situation, where desolvation is rate limiting, we have implicitly made use of the proposal that the free energy of incorporation of a solute molecule helps to displace bound solvent. This relay mechanism may be demonstrated by a crystal with a polar axis and the experiment involves a comparison of the relative rates of growth at the opposite poles for the different solvents, as exemplified by the growth and dissolution of the crystals of (*R,S*)-alanine and the γ-form of glycine in different solvents (Shimon, Vaida, Addadi, Lahav & Leiserowitz, 1990, 1991). These two crystals have similar packing features and so the discussion is confined to (*R,S*)-alanine. As already described in §4.1, the zwitterionic molecules are aligned so as to expose CO_2^- groups at one end of the polar *c*-axis and NH_3^+ groups at the opposite end. The crystal has a polar morphology, with the CO_2^- groups emerging at the flat $-c$ end, as shown in Fig. 21. The $(00\bar{1})$ face at the carboxylate end contains cavities. This face grows and dissolves faster in aqueous solution than the 'smoother' amino face [Fig. 22(*a*)]. We propose that the faster growth at the $(00\bar{1})$ side of the crystal in aqueous solution is due to the relay mechanism of growth, according to the following arguments. The water molecules may be strongly bound by hydrogen bonds to the outermost layer $(00\bar{1})$ of CO_2^- groups. In contrast, the

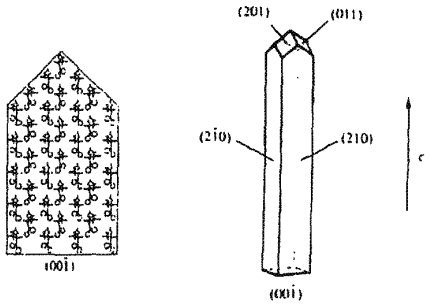


Fig. 21. Packing arrangement of (*R,S*)-alanine delineated by crystal faces, as viewed down the *b*-axis. The capped faces at the +*c* end of the polar axis expose NH_3^+ and $—CH_3$ groups at their surfaces, the opposite $(00\bar{1})$ face exposes carboxylate CO_2^- groups.

OCID: <XP___2960386A__1_>

UM00016807
NOVARTIS EXHIBIT 1517
Novartis v. Regents, IPR2023-01347
Page 3789 of 4460

pockets act as proton acceptors for the NH_3^+ groups of the solute molecules. Replacement of the solute NH_3^+ moiety by solvent water within the pockets yields repulsive or, at best, weakly attractive interactions. The pockets will therefore be weakly hydrated and so relatively easily accessible to approaching solute molecules (Fig. 23). There is, however, an alternative mechanism which may account for the faster growth at the $-c$ end: a higher crystal attachment energy at the $(00\bar{1})$ end of the crystal than at the opposite end. We could demonstrate that the relay mechanism is the more operative on the following basis: we predicted that methanol molecules could bind into the pockets at the $(00\bar{1})$ face. The methyl group of this cosolvent molecule can form attractive, albeit weak, C—H···O interactions within the pocket and the OH group can form a hydrogen bond to the CO_2^- group at the surface of the pocket. In keeping with prediction, crystals of (*R,S*)-alanine in 80% methanol:water mixture grow faster at the $+c$ amino end of the crystal than at the $-c$ carboxylate end [Fig. 22(*b*)], indicating that methanol blocks solute access to the pockets more effectively than water at the $(00\bar{1})$ face.

This work implies that for those crystals which expose at each face set of different surface sites, the average binding energy of solvent to a face may not be a sufficient criterion for establishing the relative morphological importance of the different faces. It may be necessary to assess the ease of replacement of solvent by solute at each of the different surface sites, as well as the different modes of docking the solute molecules at the surface.

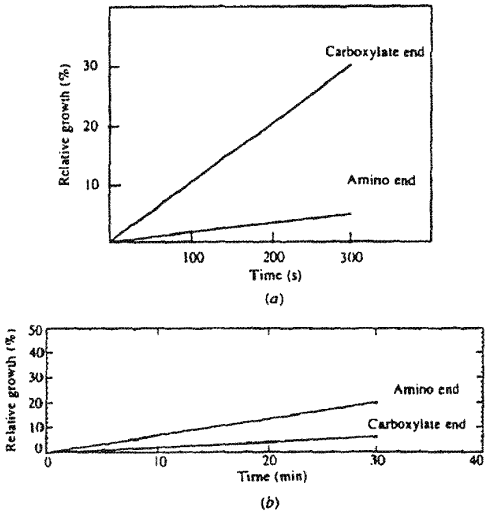


Fig. 22. Graph of the relative growth at opposite poles of the polar axis of (*R,S*)-alanine crystals: (*a*) in water and (*b*) in 4:1 methanol:water mixture.

For example, Boek, Feil, Briels & Bennema (1991) calculated the theoretical growth form of tetragonal urea and found that it is almost cube-like and compares well with those of crystals from ethanol or benzene. However, the theoretical form is very different in shape from the [001] needles obtained from aqueous solution. Boek & Briels (1992) performed molecular dynamics simulations of interfaces between water and crystalline urea. They argued that the observed needle morphology cannot be explained using a simple layer model because of strong adsorption of water to the relevant faces. By examining the interface between a saturated aqueous urea solution and crystalline urea, Boek (1993) explained the [001] needle morphology in terms of wrongly and randomly absorbed urea molecules to the {110} side faces, so providing an increased interfacial entropy. It is noteworthy that oxamide crystals grown from aqueous solution contain *ca* 2% of wrongly oriented oxamide molecules in the lattice (Swaminathan & Craven, 1982).

8. Control of crystal phase formation

Any crystallization process must cross the nucleation barrier. It is generally assumed that as the molecules start to associate in supersaturated solutions, they form embryos with structures resembling those of the to-be-grown crystals. For polymorphic systems embryos of all the observed polymorphs are probably formed. Each type of embryo would structurally resemble the crystal into which it will eventually develop. If this hypothesis is correct, one may use the structural information of the mature crystals to design inhibitors of a particular crystalline phase. The overall consequence of this stereo-

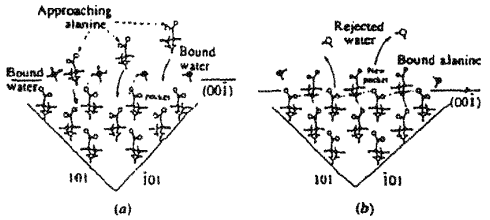


Fig. 23. Schematic representation of the $(00\bar{1})$ face of *R,S*-alanine during crystal growth. (*a*) In this view, approaching solute alanine molecules are depicted as about to be bound within the pockets of the $(00\bar{1})$ face. Also shown are water molecules bound to the outermost CO_2 groups of this face. The pockets remain poorly solvated because lone-pair–lone-pair oxygen–oxygen repulsions inhibit (similar to that described earlier in the asparagine–aspartic acid system, in §5.4) the binding of water within them. (*b*) In this view, the newly adsorbed alanine molecules are each bound *via* three NH···O hydrogen bonds. The previously bound water molecules are shown being rejected by O(water)···O(carboxylate) lone pair–lone pair repulsions. Note the formation of new unsolved pockets.

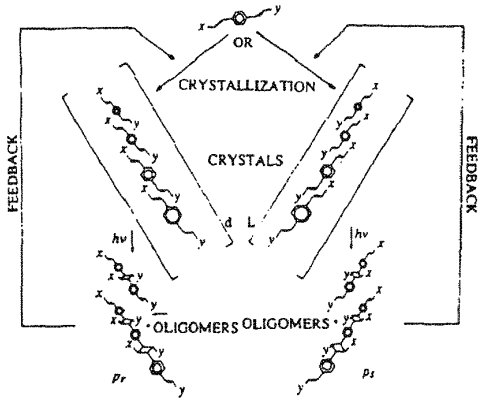
DOCID: <XP___2960386A__1_>

UM00016808
NOVARTIS EXHIBIT 1517
Novartis v. Regents, IPR2023-01347
Page 3790 of 4460

specific inhibition process can be that the unaffected phase, if less stable, will grow by kinetic control. We shall consider several systems where the logic of the above arguments apply. We first discuss the synthesis of chiral enantiomerically pure material from nonchiral reagents. This will be followed by a method for the kinetic resolution of enantiomers and the induced crystallization of a particular polymorph. Finally, the induced nucleation of a particular phase which acts as a template for the nucleation and further growth of the more stable phase into a macroscopic crystal will be discussed.

8.1. *Amplification of chirality by crystallization with chiral additives*

The solid state may be used for the synthesis of chiral enantiomerically pure material from nonchiral reagents by precipitation of nonchiral molecules in appropriately packed chiral crystals, followed by a lattice-controlled reaction (Green, Lahav & Rabinovich, 1979; Addadi *et al.*, 1980). However, crystallization from achiral solvents generally yields {*R*}- and {*S*}-crystals in equal amounts. In order to obtain enantiomerically pure material, it is necessary to inhibit the nucleation of one of the two chiral crystal phases. This was achieved in the following way. Molecular dienes were 'engineered' to pack in chiral crystals (Addadi & Lahav, 1979; Addadi, van Mil & Lahav, 1982; van Mil, Addadi, Gati & Lahav, 1981, 1982), in which the molecules are stacked by translation such that the neighboring C···C double bonds are in appropriate proximity for photodimerization (Scheme 8). UV irradiation of a single crystal yields dimers, trimers and oligomeric products of a single chirality P_r or P_s, dependent upon the chirality of the starting crystal. Thus, the handedness of the molecular stacking arrangement is retained in the structure of the oligomer. A net asymmetric induction of one of the crystalline phases was achieved when crystals were grown in the presence of oligomers of a single chirality (*i.e.* P_r or P_s) obtained from a large single crystal. In all experiments it was observed that a large excess was formed of the phase which was enantiomorphic to that in which the additive itself had been generated: namely, *R*-crystals were obtained from a solution containing P_s additives, and *vice versa*.



Scheme 8.

A natural extension of this work led to the suggestion of a new method for kinetic resolution of a racemic mixture crystallizing in the form of a conglomerate of {*R*}- and {*S*}-crystals (Addadi, van Mil & Lahav, 1981; Addadi *et al.*, 1982), as described below.

8.2. *Resolution of enantiomers*

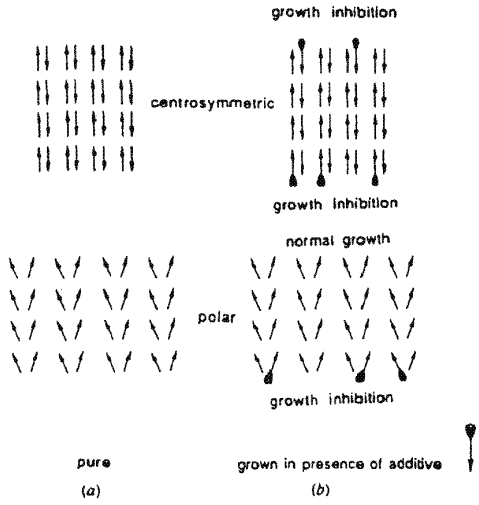
Racemic mixtures of molecules which crystallize as a conglomerate yield two enantiomorphous equienergetic crystalline phases. Kinetic resolution of the conglomerate may be achieved with the assistance of tailor-made chiral-resolved inhibitors which would, in solution, bind enantioselectively and stereoselectively to only one of the enantiomeric crystalline phases and so prevent its eventual growth. This principle has been demonstrated for many systems (Addadi *et al.*, 1982; Addadi, Weinstein, Gati, Weissbuch & Lahav, 1982; Zbaida *et al.*, 1987). There are no particular requirements on molecular packing, although we may state that the higher the point symmetry of the crystal, the more different orientations in the lattice the constituent molecules may occupy, making the inhibition process more pronounced since the additive would be adsorbed on more faces. The kinetic resolution may encompass preferred precipitation from a racemic mixture in solution of one enantiomorph at the expense of the more stable racemic crystal phase. Naturally the energy gap between the racemic crystal and the mixture of resolved enantiomorphs must be relatively small. For example, racemic histidine.HCl precipitates, at 298 K, as a stable racemic dihydrate crystal and a metastable conglomerate of resolved monohydrate crystals. Addition of as little as 1% of the chiral-resolved poly-(*p*-acrylamido-*S*-phenyalanine) additive induced resolution with quantitative yield of the desired enantiomer (Weissbuch, Zbaida, Addadi, Lahav & Leiserowitz, 1987).

8.3. *Induced crystallization of a polar polymorph*

We now consider the preferred precipitation of a crystal containing a polar axis, at the expense of the dimorph which is centrosymmetric and thus nonpolar. The concept is that in crystals with a polar axis all molecules are aligned in the same direction *vis-à-vis* the polar axis. In centrosymmetric crystals neighboring molecules are arranged in an antiparallel manner. These two arrangements are depicted in Scheme 9. Thus, an appropriate tailor-made additive will inhibit growth of the centrosymmetric form at opposite ends of the crystal,

OCID: <XP___2960386A__1_>

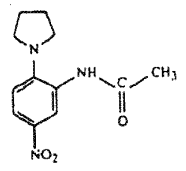
UM00016809
NOVARTIS EXHIBIT 1517
Novartis v. Regents, IPR2023-01347
Page 3791 of 4460



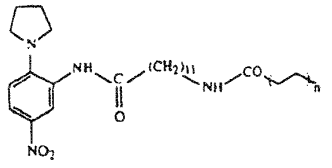
Scheme 9.

and so prevent its appearance, but will only inhibit growth of the polar form at one end of the crystal.

This concept has been demonstrated in two different systems. In *N*-(2-acetamido-4-nitrophenyl)pyrrolidine (PAN; 6*a*), the metastable polar form [Fig. 24(*b*)] displays optical second-harmonic generation. As little as 0.03% of the polymer (6*b*) inhibited precipitation of the pseudo-centrosymmetric stable form of PAN [Fig. (24*a*)], only allowing crystallization of the metastable form (Staab, Addadi, Leiserowitz & Lahav, 1990).

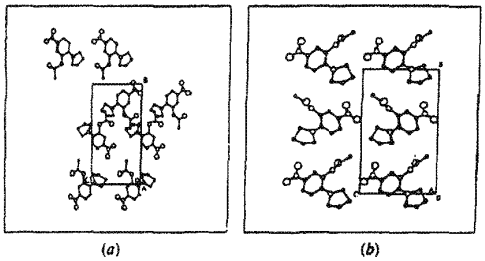


(6*a*)



(6*b*)

The other system involved preferential crystallization from aqueous solution of the γ-form of glycine, when grown in the presence of the additive racemic hexafluorovaline, $(CF_3)_2CHCH(NH_3^+)CO_2^-$ (Weissbuch, Leiserowitz & Lahav, 1994). As already mentioned, glycine usually crystallizes in the centrosymmetric α-form from aqueous solutions, but Iitaka (1961) reported that glycine can precipitate in a polar γ-form from acetic acid or ammonia solutions. Perhaps the crystallization of α-glycine in pure aqueous solution is promoted by the presence in solution of cyclic hydrogen-bonded dimers of glycine (see §7.1), but whose formation is inhibited in acid or base solution, leading to the precipitation of the γ-form. The γ-form appears in space group $P3_1$ (or $P3_2$), arranged in a way similar to (*R*,*S*)-alanine crystal (Fig. 21), so that the molecules expose CO_2^- groups at one end of the polar trigonal axis and NH_3^+ groups at the opposite end [Fig. 25(*a*)]. It was found that racemic hexafluorovaline is an effective inhibitor of growth of α-glycine since it binds to the four {011} faces and so blocks growth along both *b* and the fast *c*-growing directions [Fig. 25(*c*)]. This behavior is in contrast to that of the common α-amino acid additives which bind primarily to the {010} faces and so retard the growth of α-glycine only along the *b*-direction, inducing the formation of the {010} plates, as described earlier in §5.1. The abnormal behavior of hexafluorovaline may be understood in terms of its molecular structure and conformation, as found in its native crystal structure (Weissbuch, Frolow, Addadi, Lahav & Leiserowitz, 1990); steric repulsion imposed by the hexafluoroisopropyl moiety prevents adsorption onto the {010} face, but not at the {011} faces to which it is strongly bound through charge-transfer interactions. Furthermore, hexafluorovaline does not inhibit nucleation and growth of the γ-glycine form because the additive is bound thereto primarily at the NH_3^+ end of its polar axis, the crystal growing unidirectionally along its polar *c*-axis at the CO_2^- end. However, the hexafluorovaline molecules can be also adsorbed on the newly developed {$\bar{1}$51} side faces of the trigonal pyramidal crystals [Fig. 25(*b*)]. The salient lesson to be learnt from these experiments on glycine is that the inhibitor, to be effective, should bind along the fast-growing directions. The antifreeze proteins in fish that inhabit the polar seas act in a similar way; they bind to the fast growing directions of the ice nuclei to inhibit



(*a*) (*b*)

Fig. 24. Crystalline packing arrangements of PAN (6*a*): (*a*) stable form which is pseudocentrosymmetric and (*b*) metastable form where the polar axis is along the vertical direction.

DOCID: <XP___2960386A__I_>

UM00016810
NOVARTIS EXHIBIT 1517
Novartis v. Regents, IPR2023-01347
Page 3792 of 4460

growth (De Vries, 1984; Chakrabartty, Yang & Hew, 1989; Knight, Chang & De Vries, 1991).

8.4. *Information on early stages of nucleation via induced twinning of racemic alanine crystals*

Finally we examine a system in which a chiral-resolved additive induces nucleation of a chiral phase from a racemic mixture in solution, but this step is followed by the eventual precipitation of the thermodynamically stable racemic crystal through an epitaxial structural fit between the two crystalline phases. The constituent molecules are alanine. The racemic (*R,S*)-crystal, already described in §4.1 and §7, crystallizes in the polar space group $Pna2_1$. The molecules form parallel hydrogen-bonded chains along the polar *c*-axis, exposing CO_2^- groups at one end of the polar axis and NH_3^+ groups at the opposite end (Fig. 21). The enantiomorphous crystals of (*R*)- or (*S*)-alanine have very similar cell dimensions, but the hydrogen-bonded chains are arranged antiparallel in space group $P2_12_12_1$, so exposing both CO_2^- and NH_3^+ groups at each end of the *c*-axis. The energy gap between these two phases must be small and their solubilities are very similar. The racemic crystals exhibit a morphology (Fig. 21) of point symmetry *mm*2, in keeping with the space group. Precipitation of alanine from a racemic solution, when grown in the presence of a chiral-resolved α-amino acid additive, such as (*R*)-threonine, yields (*R,S*)-alanine crystals with an affected morphology, propeller-shaped and exhibiting 222 point symmetry [Fig. 26(*a*)]. Growth in the presence of the opposite enantiomeric additive *S*-threonine yields propellers of the mirror image (Weissbuch *et al.*, 1994). The crystals expose CO_2^- groups at each end of the propeller and so would appear to be twinned about the central *ab*-plane, in keeping with observation that the two crystal halves appear to be stitched across this central *ab*-plane. However, the two surfaces in contact across such a twinning plane would each expose NH_3^+ groups, which must be energetically unfavorable. One reasonable explanation for the observed effect is the inhibition of nucleation of both the racemic and the chiral form of alanine homomeric to that of the chiral-resolved additive in solution, leading to nucleation of the opposite enantiomer through the absence of steric interactions with the additive. Indeed this step was done by design. These chiral nuclei then act as templates at their two opposite {001} faces for nucleation sites for epitaxial growth of (*R,S*)-alanine, yielding the 'twinned' crystals. The proposed structural arrangement at the epitaxial interface is shown in Fig. 26(*b*). This arrangement also brings about the point that

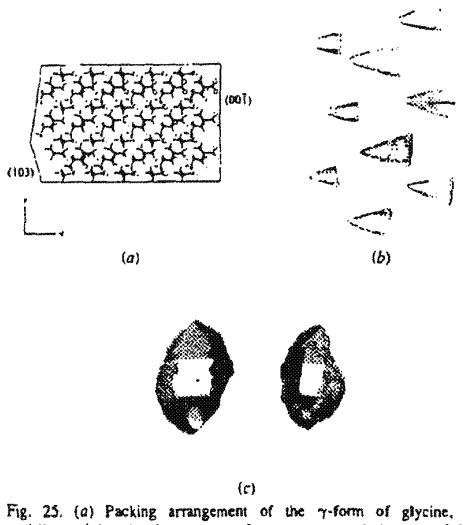


Fig. 25. (*a*) Packing arrangement of the γ-form of glycine, as delineated by the faces grown from aqueous solution containing acetic acid. (*b*) Photograph of γ-glycine crystals grown from aqueous solutions in the presence of hexafluorovaline additive (3% wt). (*c*) Photograph of α-glycine crystals grown from aqueous solution in the presence of a low concentration (1% wt) of hexafluorovaline additive, showing inhibition of the four {011} faces.

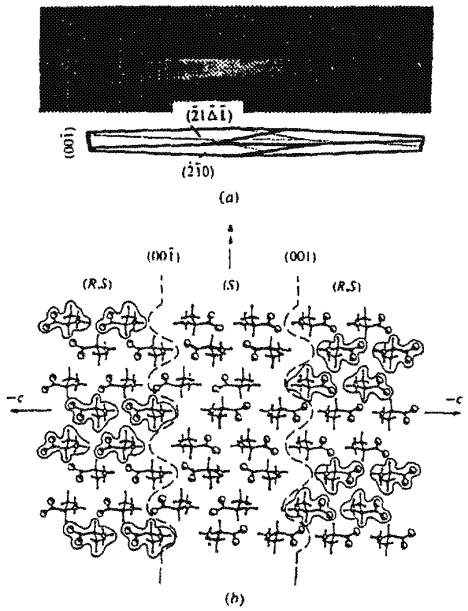


Fig. 26. (*a*) Twinned crystals of (*R,S*)-alanine grown in the presence of 1% *R*-threonine additive. (*b*) Proposed structural arrangement showing the epitaxial growth of (*R,S*)-alanine at the (001) and (00$\bar{1}$) faces of a nucleus of (*S*)-alanine.

IOCID: <XP___2960386A__I_>

UM00016811
NOVARTIS EXHIBIT 1517
Novartis v. Regents, IPR2023-01347
Page 3793 of 4460

each of the two (*R*,*S*) to (*S*) interfaces has half favorable N—H···O hydrogen bonds and half unfavorable, but well-separated, $NH_3^+\cdots{}^+H_3N$ electrostatic interactions, while twinning of the two (*R*,*S*)-domains without an interleaving (*S*)-layer would generate only unfavorable contacts. The tapered arms of the propeller are brought about by the enantioselective adsorption of the chiral additive at two opposite faces of the four {210} side faces. The proposed mechanism of nucleation followed by epitaxial growth was substantiated by the observed growth of (*R*,*S*)-alanine from seeds of chiral-resolved alanine and by growth experiments involving various nonracemic (*R*:*S*) mixtures. Furthermore, X-ray diffraction measurements of a twinned crystal revealed the following: a misalignment between the two halves, and reflections, but only from the crystal center, that are symmetry forbidden for space group $Pna2_1$, and so could arise from a $P2_12_12_1$ crystallite.

9. 'Tailor-made' surfaces composed of amphiphilic monolayers for promotion of crystal nucleation

Crystal nucleation is generally a heterogeneous process. This means that the activation barrier for nucleation is lowered by interaction with template surfaces. This process can happen at different levels of specificity, ranging from nonspecific adsorption to epitaxial growth. One can therefore envisage induced nucleation of desired crystalline structures, even with a specific crystal orientation, by designing appropriate nucleation promoters which match the structure of the crystal on a specific plane.

We described earlier in §3 the changes induced in the α-form of glycine crystals upon growth in the presence of various α-amino acid additives. These changes involved morphology and enantiomeric segregation of the occluded additive molecules. Growth in the presence of hydrophobic α-amino acid additives yielded glycine crystals at the air–solution interface, floating with their {010} faces exposed to air, long before crystals appeared at the bottom of the crystallization vessel (Weissbuch *et al.*, 1984; Weissbuch, Addadi, Leiserowitz & Lahav, 1988). The *R*-α-amino acid additives such as leucine, norleucine, valine and α-amino-octanoic acid induced the formation of pyramidal crystals floating with their (010) faces exposed to air. By symmetry, the *S*-α-amino acid additives induced the enantiomorphous $(0\bar{1}0)$-oriented pyramids. Crystallization experiments in the presence of racemic hydrophobic additives yielded the solution surface covered with {010} plates of both orientations. Crystallization experiments in the presence of optically pure hydrophobic α-amino acid additives (*e.g.* *R*-leucine) and racemic hydrophilic α-amino acids (*e.g.* racemic glutamic acid) yielded only (010)-oriented plates of glycine (Fig. 27). This orienting phenomenon was explained by the spontaneous aggregation of the hydrophobic α-amino acid additives at the solution surface to yield nucleating domains. This proposed mechanism is also in keeping with surface tension measurements, according to which the hydrophobic α-amino acids aggregate at the aqueous solution surface. Moreover, the chiral-resolved hydrophobic α-amino acids, in their own crystal structures form hydrogen-bonded layers akin to that of α-glycine (Benedetti, Pedone & Sirigu, 1973; Weissbuch, Frolow, Addadi, Lahav & Leiserowitz, 1990). The mechanism is also in keeping with HPLC measurements of the floating glycine crystals grown in the presence of the chiral-resolved hydrophobic α-amino acid, which revealed very small amounts, if any, of the additive occluded in the crystals. Thus, it is conceivable that the hydrophobic α-amino acid additives assemble at the solution surface into hydrogen-bonded layers, further stabilized by the binding of glycine solute molecules to form hydrogen-bonded bilayers, and which can induce the oriented nucleation of α-glycine crystals at the solution surface.

These studies led directly to the use of water-insoluble α-amino acid amphiphiles to induce oriented nucleation of α-glycine crystals. Such a design of a synthetic template of a Langmuir monolayer of amphiphilic molecules spread at the air-solution interface and having their polar head groups in contact with the water proved to be a very expedient nucleating system. It has proven possible to induce, by virtue of a designed structural match between nucleator and nucleate, oriented crystallization of α-glycine ($^+H_3NCH_2CO_2^-$) under α-amino acid monolayers such



Fig. 27. A crust of oriented α-glycine plate-like crystals floating on the surface, obtained from a solution containing 1% wt/wt *R*-leucine and racemic glutamic acid. All the floating oriented plates expose their (010) faces to the air due to *R*-leucine, and glutamic acid is added to the solution to induce plate formation. This orientation is recognizable from the crystal shape, since for the majority of the crystals the long edge of each crystal is parallel to the *c*-axis and the short edge is parallel to *a*. For those crystals which appear to be reversed, of which there are approximately five or six in this photograph, the correct (010) orientation was confirmed by X-ray diffraction measurements. For such crystals the long edge was parallel to the *a*-axis and the short edge to *c*.

DOCID: <XP___2960386A__I_>

UM00016812
NOVARTIS EXHIBIT 1517
Novartis v. Regents, IPR2023-01347
Page 3794 of 4460

as palmitoyl lysine, $C_{15}H_{31}CONHC_4H_8CHNH_3^+CO_2^-$ (Landau, Popovitz-Biro, Levanon, Leiserowitz & Lahav, 1986; Landau *et al.*, 1989). Several other types of crystals have since been nucleated at the water surface by Langmuir monolayers through either a (partial) structural fit or an electrostatic attraction. These include *p*-hydroxybenzoic acid (Weissbuch, Berkovic, Leiserowitz & Lahav, 1990), silver propionate (Weissbuch, Majewski *et al.*, 1993), sodium chloride (Landau, Popovitz-Biro, Levanon, Leiserowitz & Lahav, 1986), nanocrystals of PbS (Zhao, Yang, McCormick & Fendler, 1992) and CdS (Fendler, 1993), barium sulphate (Heywood & Mann, 1992*a*,*b*) and the vaterite and calcite form of $CaCO_3$ (Mann, 1988; Mann, Heywood, Rajam & Birchall, 1988). The work on $CaCO_3$ was done as part of model studies on biological mineralization.

We shall make brief mention of the crystalline self-aggregating properties and packing arrangements of the Langmuir monolayers, as established by grazing incidence X-ray diffraction (GID). This will be followed by an outline on the effect of solvent molecules on the growth, dissolution and packing structures of the amphiphilic monolayers. We shall also describe the design of mixed monolayers in order to glean a measure of the critical size of induced nuclei of the three-dimensional crystals at the monolayer–solution interface. Finally, we examine the role played by monolayers of aliphatic alcohols for the induced nucleation of ice.

9.1. *Crystalline self-assembly of amphiphilic monolayers on the water surface*

Structural information on the induced nucleation of the crystals of α-glycine, *p*-hydroxybenzoic acid, silver propionate and ice at the monolayer interface has been independently gleaned by determination of the two-dimensional crystal structures of the monolayers on the liquid surface (Wolf *et al.*, 1987; Jacquemain *et al.*, 1990; Weissbuch, Majewski *et al.*, 1993). This has been achieved by grazing incidence X-ray diffraction (GID) using synchrotron radiation.

Evidence for the formation of self-organized two-dimensional crystalline aggregates (crystallites) composed of water-insoluble amphiphilic molecules, at the air–water interface, has until recently been indirect; it has generally been assumed that the degree of lateral ordering in the uncompressed state is very low, if at all existent. The newly developed method of GID is a powerful tool for exploring this field (Als-Nielsen & Kjaer, 1989; Barton *et al.*, 1988; Als-Nielsen & Mohwald, 1992; Jacquemain *et al.*, 1992) since it allows for the detection of two-dimensional crystalites formed by the amphiphilic molecules and for the determination of their size and structure almost at the atomic level. Using GID, the two-dimensional crystallinity of amphiphilic monolayers in the relaxed state (*i.e.* where the monolayer coverage on the water surface is sufficiently low, *e.g.* <80%, so that the monolayer surface pressure is very low) was shown to be a widespread phenomenon. This was demonstrated for a variety of amphiphiles, such as long fluorocarbon chain α-amino acids (Jacquemain *et al.*, 1990) and carboxylic acids (Dutta *et al.*, 1987; Barton *et al.*, 1988, 1992), hydrocarbon chain alcohols, amides, carboxylic acids (Jacquemain *et al.*, 1991) and their cadmium or calcium salts (Böhm *et al.*, 1994). Indeed the GID spectrum of the cadmium arachidate monolayer (Leveiller *et al.*, 1991) gave direct evidence of an ordered counterionic cadmium layer bound to the carboxylate head group. This result of an ordered counterionic layer is in agreement with induced crystallization of inorganic salts at the Langmuir monolayer interface (Landau, Popovitz-Biro, Levanon, Leiserowitz & Lahav, 1986; Landau *et al.*, 1989; Zhao, Yang, McCormick & Fendler, 1992; Mann, 1988; Mann, Heywood, Rajam & Birchall, 1988). Analysis of the GID data using structure-factor calculations, sometimes complemented by lattice energy calculations yielded two-dimensional crystal structures almost at atomic resolution (Leveiller, Jacquemain, Leiserowitz, Kjaer & Als-Nielson, 1992; Leveiller *et al.*, 1994; Weissbuch, Leveiller *et al.*, 1993; Wang *et al.*, 1994; Böhm *et al.*, 1994).

9.2. *Effect of solvent and tailor-made auxiliaries on growth, dissolution and structure of amphiphilic monolayers*

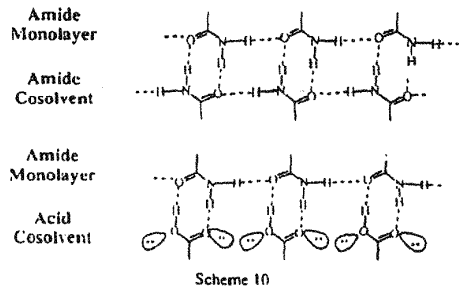
Amphiphilic monolayers on the water surface are an ideal vehicle for study of the effect of solvent on two-dimensional (and by extension, three-dimensional) crystal growth and dissolution. Two-dimensional crystals have an advantage over their three-dimensional counterparts, because solute molecules present in the aqueous subphase only come into contact with the polar head groups of the monolayer on a well characterized interface. Moreover, GID offers the possibility to monitor in real time, changes in two-dimensional crystallinity. We have been able, by GID, to demonstrate that solute can retard, or inhibit, the growth or induce dissolution of monolayer crystallites. For example (Jacquemain *et al.*, 1990), the left part of Fig. 28(*a*) shows that 10 min after the monolayer of perfluorododecyl aspartate (PFA), $C_{10}F_{21}C_2H_4OCOCH_2CH(NH_3^+)CO_2^-$, was deposited over an undersaturated solution of glycine, no diffraction peak was observed and it took around 30 min before crystalline domains could be detected. The inhibition can be understood from the top part of Fig. 28(*b*), which shows how one glycine molecule can bind to two neighboring molecules of the α-amino acid monolayer with strong hydrogen bonds, thus hindering their assembly. The formation of this complex is in kinetic competition with that of the two-dimensional crystalline hydrogen-bonded bilayer, which is composed of quasi-dimers of PFA and glycine [Fig. 28(*b*), top]. Once the PFA monolayer crystallizes, glycine solute molecules together with

)OCID: <XP___2960366A__I_>

UM00016813
NOVARTIS EXHIBIT 1517
Novartis v. Regents, IPR2023-01347
Page 3795 of 4460

PFA form a pseudo-centrosymmetric hydrogen-bonded heterobilayer which provides additional stability to the system. Use of β-alanine, $^{+}H_3NC_2H_4CO_2^-$, as a solute molecule instead of glycine had an entirely different effect on the two-dimensional crystals of uncompressed PFA; it did not strongly inhibit growth as dramatically as glycine, but caused a complete dissolution of the PFA crystals over 2 h, as shown by GID measurements [Fig. 28(*a*), right]. This dissolution was rationalized in terms of a strong interaction of β-alanine with the amino acid head groups of neighboring surfactant molecules leading to a disruption of the two-dimensional crystals [Fig. 28(*b*), bottom], since β-alanine cannot form a hydrogen-bonded heterobilayer with PFA as may glycine.

The second example involves the different hydrogen-bonding properties of the cosolvents formamide ($HCONH_2$) and formic acid (HCO_2H) in aqueous solution, which have a drastic effect on the crystallinity and structure of films of aliphatic amides and carboxylic acids (Weinbach *et al.*, 1993). Arachidamide, $C_{19}H_{39}CONH_2$, on pure water forms a crystalline monolayer according to the Bragg peaks displayed by the GID pattern (Fig. 29). Analysis of the X-ray intensity profiles along the Bragg rods (not shown in Fig. 29) yielded a tilt of the molecular hydrocarbon chains of *ca* 18° *vis-à-vis* the water surface. A 1 M formamide solution as subphase, instead of pure water, did not have a detrimental effect on the monolayer crystallinity, according to the Bragg peak profiles (Fig. 29), but there was a change in structure since the molecular chains were vertically aligned on the subphase, as deduced from the Bragg rod intensity profiles. Replacing formamide by formic acid aqueous subphase did not change the Bragg peak pattern for a 0.3 M solution (Fig. 29), but 1 M formic acid solution inhibited the formation of two-dimensional crystalline $C_{19}H_{39}CONH_2$ monolayers (Fig. 29). The essential difference in binding of formamide and formic acid to the amide groups of the amphiphile is depicted in Scheme 10. It involves the replacement of a $-29\,kJ\,mol^{-1}$ attraction between monolayer-bound formamide molecules by a $8\,kJ\,mol^{-1}$ repulsion between lone-pair electrons of monolayer-bound formic acid molecules. We may deduce that the lone pair–lone pair repulsion between bound formic acid molecules inhibits two-dimensional crystal growth of the $C_{19}H_{39}CONH_2$ monolayer. We note that this inhibition is essentially an extension of the effect of tailor-made carboxylic acid additives on the morphology of primary amide crystals discussed in §2 and §5.4.



Scheme 10

An increase in concentration of the formamide solution to 7 M revealed by GID [Fig. 30(*a*)] the formation of two coexisting crystalline phases of arachidamide, a trilayer and a monolayer (Weinbach *et al.*, 1994). In the monolayer phase [Fig. 31(*a*)], the molecular hydrocarbon chains were aligned vertically with respect to the liquid surface. In the trilayer phase [Fig. 31(*a*)], the chains

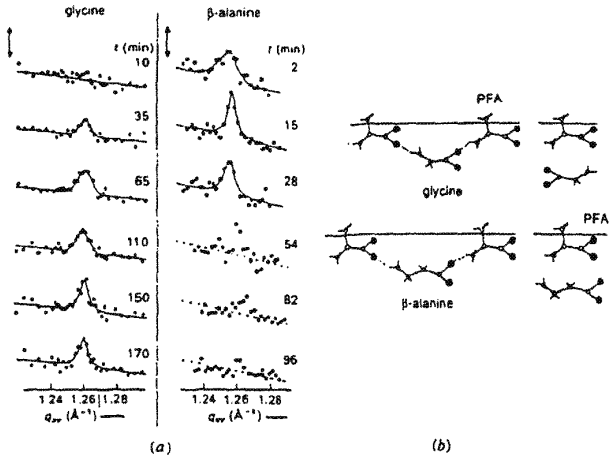


Fig. 28. Uncompressed monolayer of PFA spread at an average molecular area of 45 Å^2 over various solutions. (*a*) GID measurements as a function of time after spreading: over glycine solution (0.015 M; left); over β-alanine solution (0.005 M; right). Note the increase in two-dimensional crystallinity in the former, and the decrease in the latter as indicated by the different time evolution of the peak. q_{xy} ($= 4\pi \sin\theta/\lambda$) is the horizontal scattering vector parallel to the water surface. (*b*) Schematic drawings of 'bridging complexes' between PFA monolayer molecules and the solute molecules for glycine (top) and β-alanine (bottom). A potential quasidimer is illustrated for glycine, while the mismatch is depicted for β-alanine. Key: large stippled circles, O; small empty circles, C; full small circles, N atoms; ···, hydrogen bonds; →, hydrophobic chains.

DOCID: <XP__2960386A__I_>

UM00016814
NOVARTIS EXHIBIT 1517
Novartis v. Regents, IPR2023-01347
Page 3796 of 4460

were tilted *ca* 30° from the normal to the liquid surface. The pure formamide subphase yielded two phases in the trilayer form, the minor one tilted as before and the major phase with the molecular chains vertically aligned. According to the GID pattern [Fig. 30(*b*)], it proved possible to inhibit the trilayer formation, yielding only the monolayer of the phase in which the molecules are vertically aligned [Fig. 31(*b*)], by deposition of the amphiphile together with the tailor-made additive *N*-methylarachidamide. This inhibition process is similar to the behavior of the tailor-made additives on growth of three-dimensional molecular crystals. Spontaneous formation of multilayers of amphiphiles on liquid surfaces may prove not to be a rare phenomenon. It has been found to occur for other amphiphilic systems such as $C_{19}H_{39}CONHCH_2CH_2CONH_2$ on water (Weinbach *et al.*, 1993). Indeed, the bolaamphiphiles $HO—(CH_2)_n—OH$ (n = 22, 23, 30) spontaneously form crystalline multilayers on the water surface (Popovitz-Biro *et al.*, 1994*a*,*b*; Majewski, Edgar *et al.*, 1995).

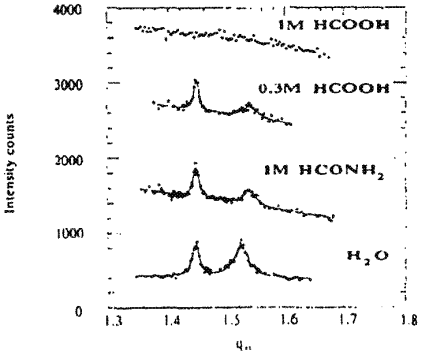


Fig. 29. GID diffraction pattern, showing the Bragg peaks of a monolayer of uncompressed arachidamide spread on various subphases. The horizontal axis $q_{xy} = 4\pi\sin\theta/\lambda$, where θ is the component of the Bragg angle parallel to the monolayer plane.

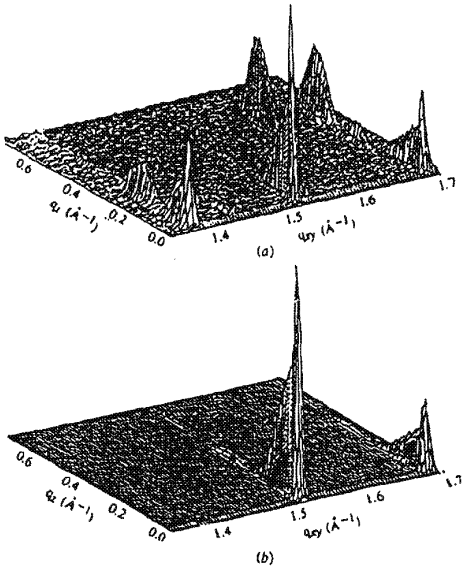


Fig. 30. Two-dimensional intensity plots $I(q_{xy}, q_z)$ of the GID pattern of arachidamide on 70% formamide–water subphase at 278 K. The q_{xy}-axis describes the horizontal X-ray scattering vector $4\pi\sin\theta/\lambda$, where θ is the component of the Bragg angle parallel to the water surface. The q_z-axis describes the vertical X-ray scattering vector. (*a*) Pure arachidamide and (*b*) arachidamide containing 5% *N*-methyl arachidamide.

9.3. *Mixed monolayers as a probe for mimicking the solid–liquid interface*

Although many experiments have been performed in which the crystal morphology can be understood in terms of strong binding of either solvent or additive molecules to specific faces, little work has been reported on the direct determination of the local structure at liquid–crystal interfaces. It is perhaps a consequence of the fact that the structure and dynamics at the solid–liquid interface is not easily amenable to direct study. Nevertheless, *in situ* synchrotron X-ray scattering studies have been recently carried out at the gold–electrolyte (Ocko, Wang, Davenport & Isaacs, 1990; Wang, Davenport, Isaacs & Ocko, 1992) and calcite-water (Chiarello, Wogelins & Sturchio, 1993) interfaces, and the growth and dissolution of ammonium

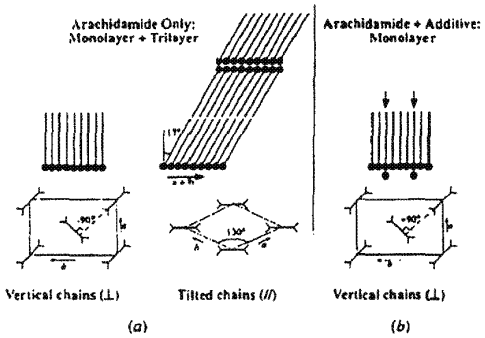


Fig. 31. Schematic representation of the packing arrangements of arachidamide on 70% formamide–water solution, showing side views (top) and views along the hydrocarbon chain axes (bottom). (*a*) Pure arachidamide. Two phases, one a monolayer with chain axes vertically aligned in a herringbone structure and the other a trilayer phase with the chains tilted and parallel. (*b*) Arachidamide plus additive *N*-methyl arachidamide. Monolayer phase with chains vertically aligned in a herringbone arrangement.

OCID: <XP___2960386A__1_>

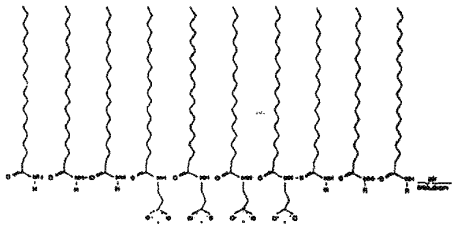
UM00016815
NOVARTIS EXHIBIT 1517
Novartis v. Regents, IPR2023-01347
Page 3797 of 4460

dihydrogen phosphate, $NH_4H_2PO_4$, in aqueous solutions (Cunningham, Gerson, Roberts, Sherwood & Wojciechowski, 1991). A monolayer may be designed so as to partially mimic the solid–liquid structure and so be amenable to study by GID and X-ray reflectivity. Thus, we made use of a 1:1 mixed monolayer of long-chain carboxylic acids and amines to mimic the structure of that crystalline face of β-alanine which exposes the highest concentration of CO_2^- and NH_3^+ groups and which was found to be strongly inhibited on growth in $CdCl_2$ aqueous solution (Gidalevitch, Weissbuch, Kjaer, Als-Nielsen & Leiserowitz, 1994). We had found, both by GID and X-ray reflectivity measurements, an ordered binding of Cd^{2+} and Cl^- ions to the head groups of the mixed monolayer. Moreover, addition of β-alanine to the $CdCl_2$ subphase solution resulted in competitive binding of β-alanine molecules to the head groups of the monolayer.

9.4. *Mixed monolayers for the design of structured surfaces to induce three-dimensional crystallization*

The transfer of structural information from the monolayer to the three-dimensional crystal can provide evidence for a correlation between the size and structure of the monolayer as two-dimensional crystalline 'nuclei' and the tendency for formation of the three-dimensional crystals. The size, or lateral area, of the monolayer inducing nucleation of the three-dimensional crystals may be controlled using mixed monolayer films of type $A + B$, where the pure amphiphile A is an efficient nucleator, whereas pure B amphiphile is not. The oriented growth of three-dimensional crystals may be studied as a function of the molar ratio of the two components in order to establish the threshhold concentration required for efficient nucleation of the crystals (Weissbuch, Majewski *et al.*, 1993).

One approach for the design of mixed monolayers with segregated domains of type A and B involves the use of molecules with a common moiety, structured so as to promote the formation of a homogeneous array of molecular moieties, common to A and B. Molecule A, however, contains additional groups appropriate for the induced three-dimensional crystallization and which would also favor their segregation into domains. As B we used $C_nH_{2n+1}CONH_2$, $n = 19$, and as A $C_nH_{2n+1}CONHCH_2CH_2COOH$, $n = 19$. The hydrogen-bonding amide group provides the driving force for a continous network of hydrocarbon chains. The head group of A, $—CH_2CH_2COOH$, was chosen and indeed found to favor segregation, as shown in Scheme 11, and so induce the crystallization of a variety of layer compounds, for example, metal salts of carboxylic acids. The structural requirement for nucleation is that the crystal be composed of bilayers with the metal ions concentrated at the center of each bilayer. We chose silver propionate, CH_3CH_2COOAg, as an appropriate compound. It was



$A + B$

Scheme 11.

found that mixed monolayers A and B with a molar ratio A:B down to 1:10 induced oriented formation at the air-solution interface of plate-like silver propionate crystals. Only few crystals, and with a different morphology, were obtained for a lower A:B ratio or pure B. A randomly distributed monolayer mixture of two amphiphiles $A' + B'$ did not induce crystallization of silver propionate, as did, for example, stearic acid A' and stearyl alcohol B' in the ratio as high as 1:1. The segregated nature of the $A + B$ domains was demonstrated independently by specular X-ray reflectivity measurements. The presence of cadmium ions bound to neighboring CO_2^- head groups was used as the probe to show the extensive juxtaposition of A-type molecules. The homogeneous and ordered nature of the $A + B$ mixed monolayers was demonstrated by GID for a variety of A:B mixtures (over $CdCl_2$ solution and pure water subphases). The remaining question to be addressed in this analysis is the size of the embedded A-type domains, which will provide information as to the size of the 'nuclei' of silver propionate en route to three-dimensional crystallization. Such information represents one of the principal unknowns in crystallization processes.

9.5. *Induced nucleation of ice by monolayers of long-chain alcohols*

Pure water can be supercooled to temperatures as low as 233–253 K. Therefore, the inhibition or induction of the freezing point of ice, in particular through the role of auxiliaries, has far-reaching ramifications for the living and the non-living world. An intriguing example of inhibition involves the activity of antifreeze proteins in the blood serum of fish in polar seas, these proteins lower the freezing point by no more than 2 K, but this small difference is vital for their survival (De Vries, 1984; Feeney, Burcham & Yeh, 1986; Yang, Sax, Chakrabartty & Hew, 1988). Promotion of ice nucleation, has been exploited in the induced precipitation of rain by silver iodide seeded in clouds (Vonnegut, 1947; Corrin & Nelsen, 1968). On the other hand, it can result in wide-scale damage to nonconiferous plants in temperate climates by frost bacteria (Schnell & Vali, 1972; Maki, Galyan, Chang Chien & Caldwell, 1974; Lindow, Arny

)OCID: <XP___2960386A__1_>

UM00016816
NOVARTIS EXHIBIT 1517
Novartis v. Regents, IPR2023-01347
Page 3798 of 4460

& Upper, 1978; Lindow, 1983), which nucleate ice at temperatures as high as 271 K.

Ice nucleation has been widely studied, yet the role played at the atomic level by auxiliaries involved in the promotion of ice nucleation is still unclear. Several mechanisms have been proposed such as a lattice or structural match between the substrate and the nucleated ice crystal (Fletcher, 1970; Warren, Corotto & Wolber, 1986; Mizuno, 1989; Kajava & Lindow, 1993), or an electric field present in the substrate which orients the water molecules to induce ice nucleation (Prappacher, 1963). To help unravel the complexity of this process, we designed experiments where such mechanisms can be studied in a systematic manner. There is a close expitaxial fit between the *ab*-cell axes of hexagonal ice ($a = b = 4.5$ Å, $\gamma = 120°$) and of the two-dimensional cell of a compressed monolayer of the aliphatic long chain alcohol $C_{21}H_{43}OH$ ($a = b = 4.5$ Å, $\gamma = 113°$) at just above 273 K, as determined from GID measurements (Barton *et al.*, 1988). We found that uncompressed monolayers of aliphatic long chain alcohols were very efficient ice nucleators (Gavish, Popovitz-Biro, Lahav & Leiserowitz, 1990; Popovitz-Biro, Wang, Majewski, Leiserowitz & Lahav, 1994). The induced freezing point of ice for $C_nH_{2n+1}OH$ with n odd reached an asymptotic temperature just below 273 K for an upper value of $n = 31$, the freezing point for n even reached a plateau of 265 K for n in the upper range 22–30. The long-chain carboxylic acids $C_nH_{2n+1}CO_2H$ are, by comparison, poor ice nucleators (Fig. 32).

GID studies of uncompressed monolayers of $C_nH_{2n+1}OH$, $n = 13$–31, on water at 278 K revealed two-dimensional crystalline self-assembly and yielded their packing arrangements to near atomic resolution and information on molecular thermal motion (Wang *et al.*, 1994; Popovitz-Biro, Wang, Majewski, Leiserowitz & Lahav, 1994; Majewski, Popovitz-Biro *et al.*, 1995). The extent of two-dimensional crystalline order (*i.e.* coherence length) and the amount of crystalline material was less for monolayers, with $n = 16$ and 20, than for $n = 23$, 30, 31 according to a GID analysis, the latter property being independently confirmed by FT-IR. The best lattice match to ice was for $n = 30$ and 31, the lattice match to ice being poorer for $n = 13$–20 in terms of area per molecule, so correlating with their less efficient ice nucleation behavior. The packing arrangements of the hydrocarbon chains of monolayers $C_{30}H_{61}OH$ and $C_{31}H_{63}OH$ are very similar, but for the orientation of their $—CH_2OH$ moieties which are different, resulting in different ice nucleation behavior. Fig. 33 shows the packing arrangement of the monolayer of $C_{31}H_{63}OH$. Further evidence for the role played by the orientation of the C—OH group is the ice nucleating properties of alcohols $CH_3(CH_2)_nCOX(CH_2)_mOH$ (X = O, NH). In these systems the freezing point was found to depend on the odd and even value of m, but not on that of n. The two-dimensional crystal structures of two ester-alcohols,

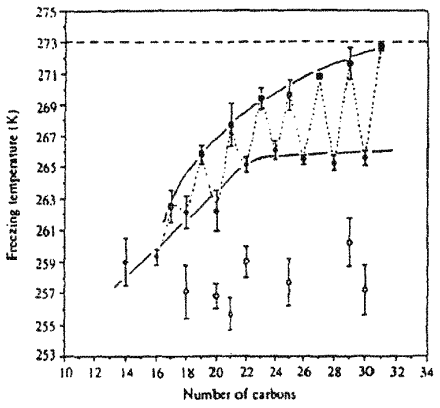


Fig. 32. Freezing points of drops of supercooled water covered by monolayers of alcohol, $C_nH_{2n+1}OH$ (n even, filled diamond; n odd, empty square), and carboxylic acid, $C_nH_{2n+1}CO_2H$ (empty circle). Freezing point curves are drawn separately for alcohols with n odd and n even.

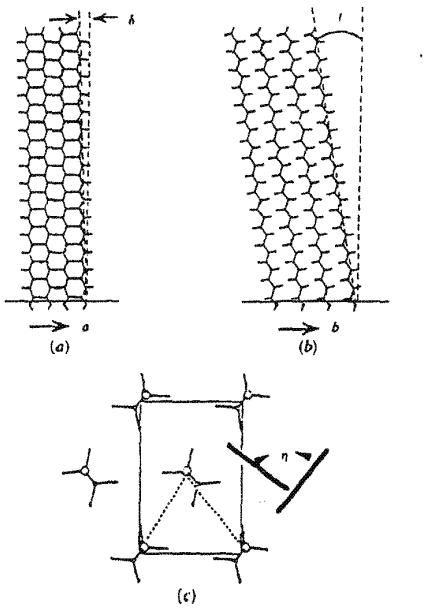


Fig. 33. Two-dimensional crystal structure of the $C_{31}H_{63}OH$ monolayer on water at 278 K, in which the two molecules in the unit cell are essentially related by glide symmetry along the b-axis. (*a*), (*b*) and (*c*) are views along the a-axis, the b-axis and down the molecular axis, respectively.

IOCID: <XP__2960386A__I_>

UM00016817
NOVARTIS EXHIBIT 1517
Novartis v. Regents, IPR2023-01347
Page 3799 of 4460

$n = 19$, $m = 9$, 10, on water were determined by GID and lattice energy calculations yielding distinctly different $-CH_2OH$ orientations. The effect of molecular motion of the alcohol chains on induced ice nucleation was also evident from the GID studies. The atomic displacement parameter (ADP) of $C_nH_{2n+1}OH$ increases with chain shortening from $n = 31$ to 13, which is compatible with the lowering in ice nucleation efficiency. For $n = 31$, the value of ADP parallel to the plane of the monolayer is *ca* 0.12 Å^2, for $n = 19$ a value of 0.25 Å^2, and for $n = 13$ the chain is almost a free rotator according to its large cross-sectional molecular area (Majewski *et al.*, 1995). The epitaxial nature of the induced ice nucleation is obvious from the similarity between the arrangement of O atoms in the (001) layer of ice and in the alcohol monolayer $C_nH_{2n+1}OH$ ($n = 30$, 31) over water, at a temperature of 278 K, as depicted in Figs. 34(*a*) and (*b*). This epitaxial relation was confirmed by the electron diffraction pattern [Figs. 34(*c*) and (*d*)] from an essentially single crystallite of the $C_{31}H_{63}OH$ monolayer on a single crystal of ice, in proper registry (Majewski *et al.*, 1993). Recently we have grown under a $C_{31}H_{63}OH$ monolayer, at a temperature just below 273 K, (001) plates of ice crystals smooth enough that it was possible to detect the presence of the ordered monolayer on ice by GID (Majewski, Popvitz-Biro *et al.*, 1994). Many of these ice crystals had a lateral coherence length as low as 25 Å, probably by virtue of multiple ice nucleation sites. This value of 25 Å provides rather direct information of an estimate on the upper limit of the critical size of ice nuclei as induced by the monolayer just below 273 K, suggesting a cluster of about 100 water molecules.

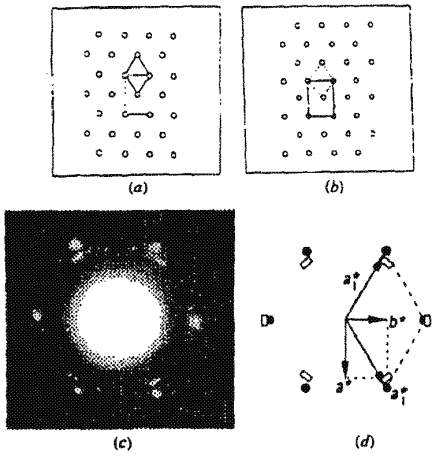


Fig. 34. Layer arrangements of the O atoms in (*a*) an (001) layer of hexagonal ice and (*b*) the alcohol ($C_nH_{2n+1}OH$, $n = 30$, 31) monolayers. The ice lattice is depicted in terms of the regular hexagonal cell (solid line) and a centered rectangular cell (dotted line). The regular rectangular lattice of the alcohol monolayers is drawn as well as a distorted hexagonal net jointing the O atoms. (*c*) Electron diffraction pattern from an essentially single crystallite of the $C_{31}H_{63}OH$ monolayer on a single crystal of hexagonal ice. (*d*) Schematic relation between the reciprocal lattice of ice (filled circles) and of the monolayer (empty rectangles).

10. Induced nucleation of ice on surfaces of α-amino acid crystals and by frost bacteria

There are reports in the literature on induced ice nucleation that indicate mechanisms other than an epitaxial fit. For example, the onset temperature of ice nucleation by crystalline powders of chiral-resolved hydrophobic α-amino acids such as valine, leucine and isoleucine was higher than the temperature induced by their corresponding racemic counterparts (Power & Power, 1962; Barthakur & Maybank, 1963; Parungo & Lodge, 1967). These results were surprising because the chiral and racemic crystal forms of these amino acids resemble each other in molecular packing and crystal morphology. A comparative study of ice nucleation on isostructural faces of single crystals of chiral and racemic α-amino acids showed that crystal polarity plays an important role (Gavish, Wang, Eisenstein, Lahav & Leiserowitz, 1992), as described below.

The hydrophobic α-amino acids pack in hydrogen-bonded layers. In the chiral crystals, molecules within the layer are related by translation and interlinked by N—H···O bonds, as in the α-form of glycine [Fig. 3(*a*)]. In the corresponding racemates, the molecules appear in a similar layer motif. The neighboring layers are interlinked by N—H···O bonds to form bilayers. These bilayers are generated in the chiral crystals by (pseudo-) twofold symmetry and in the racemates by centers of inversion, as in the α-form of glycine [Fig. 3(*a*)]. The chiral crystals are polar as a consequence of the monoclinic (pseudo-) twofold axis parallel to the plane of the bilayer. The racemic crystals are centrosymetric and hence are nonpolar. The plate-like faces of the hydrophobic α-amino acid crystals expose hydrocarbon residues according to water contact angles. Water vapor condensed on these faces at 273 K froze, on cooling, at temperatures higher by 3–5 K on the polar chiral amino acid crystals than on the corresponding centrosymmetric racemates. In a different type of experiment, the substrate crystals were cooled to 258 K before water vapor deposition. Ice crystals hexagonal in shape, and with the *c*-axis tending to be parallel to the face of the substrate, were found to emerge from cracks at their surfaces [Fig. 35(*a*)].

The above results were explained as follows: The structure of the plate faces of the polar and nonpolar α-amino acid crystals are depicted schematically in Figs. 35(*c*) and (*d*). Both faces contain cracks that expose the hydrophobic as well as the hydrophilic CO_2^- and NH_3^+ groups. In a polar crystal the structure of the opposite surfaces within a crack, perpendicular to

DOCID: <XP__2960386A__I_>

UM00016818
NOVARTIS EXHIBIT 1517
Novartis v. Regents, IPR2023-01347
Page 3800 of 4460

the polar axis, are radically different. Were such a surface to carry a net charge, the two opposite faces would carry charges of opposite sign. In contrast, the opposite faces within a crack of a centrosymmetric crystal have similar structures with no net charge on each of the two faces. Therefore, it was deduced that the opposite faces of cracks along the polar axis produced an electric field strong enough for the alignment of water molecules into proton-ordered ice clusters which would be polar along its hexagonal axis [Fig. 35(*b*)]. According to this model it was predicted and shown for alanine and tyrosine, whose racemic crystals have a polar axis and whose chiral counterparts do not, that the racemic crystal induces ice nucleation at temperatures higher by *ca* 5 K. This model is in agreement with calculations of interaction energy between polar and nonpolar hexagonal ice-like clusters contained within the crevice of both (*R*,*S*) and (*S*) of alanine (Lahav, Eisenstein & Leiserowitz, 1993). The ice freezing point results were explained on a more macroscopic level by Wilen (1993), who invoked the role of the difference in dielectric constants of water and ice.

We have already alluded to the fact that several strains of bacterial species, such as *pseudomonas syringae*, can catalyze ice nucleation at temperatures as high as 271 K. The membrane proteins responsible for ice nucleation have been sequenced (Green & Warren, 1985; Warren, Corotto & Wolber, 1986; Warren & Corotto, 1989). It was recognized by Warren and coworkers (1986) that the protein probably consists largely of β-strands. They proposed a schematic arrangement having a triangular shape similar to that of the *ab*-layer of hexagonal ice. Mizuno (1989) proposed a more detailed model. Kajava & Lindow (1993) pointed out some disadvantages of these models: the lack of close packing of the protein structures as well as the inability of the water molecules at the ice-like template to form all necessary hydrogen bonds. They have presented a structural model which consists of a largely planar extended macromolecule with one side interacting with the membrane, and the other side serving as a template for orienting water into an ice lattice. Such ice nuclei would not be formed from an *ab*-layer so that an experimental determination of the oriented ice crystallites could shed light on the validity of the model.

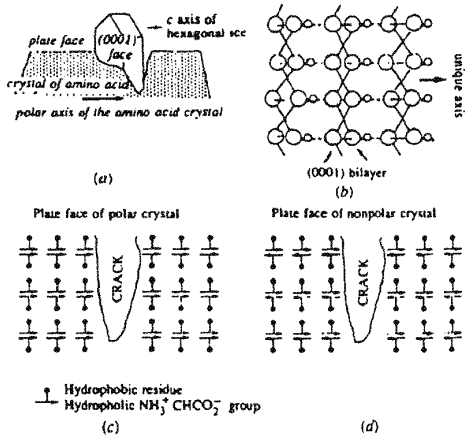


Fig. 35. (*a*) Schematic view of hexagonal ice crystals (exaggerated for clarity) emerging from the plate face of an α-amino acid crystal. (*b*) Molecular packing of a hexagonal ice from which the O—H···O hydrogen bonds along the unique axis are assumed to be proton-ordered and so the structure is polar along this direction. The remaining O—H···O bonds per molecule within each (0001) bilayer are assumed to be proton-disordered. (*c*) Schematic view of a polar α-amino acid crystal composed of hydrogen-bonded bilayers. The polar axis is along the horizontal direction. The opposite faces within the cracks expose different groups. (*d*) Schematic view of the centrosymmetric α-amino acid crystal. The opposite faces within the crack are equivalent.

11. Conclusions

A great variety of crystalline properties can be controlled and modified with the use of tailor-made auxiliaries, including growth and dissolution rates, morphology, crystal texture, etch-pit formation, structure and polymorphism. Surprisingly, such studies also allow one to help elucidate basic scientific questions, such as pinpointing fine molecular interactions at interfaces, the correlation between molecular chirality and macroscopic phenomena in crystals and the role played by solvent on crystal growth and morphology. Control of crystal formation in the very early stages is still primitive and the monitoring of such a process by diffraction methods is still to be done. Very little work has been done with tailor-made additives on liquid crystals or on crystals composed of macromolecules, such as proteins. Indeed one has only to look at the fine control achieved in biomineralization to realize that we still have a long way ahead.

This review describes work carried out over the past decade. We wish to acknowledge the contributions of L. Addadi and Z. Berkovitch-Yellin. We also thank all students and post-doctoral fellows who were engaged in the work and whose names are listed in the references. X-ray diffraction measurements on solid materials were performed together with F. Frolow and neutron diffraction studies with R. K. McMullan of the Brookhaven National Laboratory. The grazing incidence synchrotron X-ray diffraction measurements on the monolayers were carried out at DESY, Hamburg, in a fruitful collaboration with K. Kjaer and J. Als-Nielsen of Riso National Laboratories, Denmark. We thank J. M. McBride and P. Bennema for a critical reading of the manuscript.

OCID: <XP___2960386A__I_>

UM00016819
NOVARTIS EXHIBIT 1517
Novartis v. Regents, IPR2023-01347
Page 3801 of 4460

his work was supported over the years by the Minerva oundation, Münich, the Israel Academy of Sciences, ie US–Israel Binational Science Foundation, The Pe-oleum fund of the American Chemical Society and the ierman–Israeli Foundation.

References

ODADI, L. & LAHAV, M. (1979). *Pure Appl. Chem.* **51**, 1269–1284.

ODADI, L. & WEINER, S. (1992). *Angew. Chem. Int. Ed. Engl.* **31**, 153–169.

ODADI, L., ARIEL, S., LAHAV, M., LEISEROWITZ, L., POPOVITZ-BIRO, R. & TANG, C. P. (1980). In *Chemical Physics of Solids and their Surfaces*, Vol. 8, p. 202. Specialist Periodical Reports.

ODADI, L., BERKOVITCH-YELLIN, Z., DOMB, N., GATI, E., LAHAV, M. & LEISEROWITZ, L. (1982). *Nature*, **296**, 21–26.

ODADI, L., BERKOVITCH-YELLIN, Z., WEISSBUCH, I., LAHAV, M. & LEISEROWITZ, L. (1986). In *Topics in Stereochemistry*, edited by E. L. ELIEL, S. H. WILLEN & N. L. ALLINGER, Vol. 16, pp. 1–85. New York: John Wiley & Sons, Inc.

ODADI, L., BERKOVITCH-YELLIN, Z., WEISSBUCH, I., VAN MIL, J., SHIMON, L. J. W., LAHAV, M. & LEISEROWITZ, L. (1985). *Angew. Chem. Int. Ed. Engl.* **24**, 466–485.

ODADI, L., VAN MIL, J. & LAHAV, M. (1981). *J. Am. Chem. Soc.* **103**, 1249–1251.

ODADI, L., VAN MIL, J. & LAHAV, M. (1982). *J. Am. Chem. Soc.* **104**, 3422–3429.

ODADI, L., WEINSTEIN, S., GATI, E., WEISSBUCH, I. & LAHAV, M. (1982). *J. Am. Chem. Soc.* **104**, 4610–4617.

LLEN, F. M. & BUSECK, P. R. (1988). *Am. Miner.* **73**, 568.

LS-NIELSEN, J. & KJAER, K. (1989). In *The Proceedings of the NATO Advanced Study Institute, Phase Transitions in Soft Condensed Matter*, Series B, Vol. 211, p. 113. New York, London: Plenum Press.

LS-NIELSEN, J. & MOHWALD, H. (1992). In *Handbook of Synchrotron Radiation*, Vol. 4. Amsterdam: North Holland.

NTINOZZI, P. A., BROWN, C. M. & PURICH, D. L. (1992). *J. Cryst. Growth*, **125**, 215–222.

ARTHAKUR, N. & MAYBANK, DR J. (1963). *Nature*, **200**, 866–868.

ARTON, S. W., GOUDOT, A., BOULOUSSA, O., RONDELEZ, F., LIN, B., NOVAK, F., ACERO, A. & RICE, S. (1992). *J. Chem. Phys.* **96**, 1343–1351.

ARTON, S. W., THOMAS, B. N., FLOM, E. B., RICE, S., LIN, B., PENG, J. B., KETTERSON, J. B. & DUTTA, P. (1988). *J. Chem. Phys.* **89**, 2257–2270.

ENEDETTI, E., PEDONE, C. & SIRIGU, A. (1973). *Acta Cryst.* B**29**, 730–733.

ENNEMA, P. (1992). *J. Cryst. Growth*, **122**, 110–119.

ENNEMA, P. & GILMER, G. (1973). In *Crystal Growth, An Introduction*, edited by P. HARTMAN, p. 272. Amsterdam: North-Holland.

ERKOVITCH-YELLIN, Z. (1985). *J. Am. Chem. Soc.* **107**, 8239–8253.

ERKOVITCH-YELLIN, Z. & LEISEROWITZ, L. (1984). *Acta Cryst.* B**40**, 159–165.

ERKOVITCH-YELLIN, Z., ADDADI, L., IDELSON, M., LAHAV, M. & LEISEROWITZ, L. (1982). *Angew. Chem.*, Suppl., pp. 1336-1345.

ERKOVITCH-YELLIN, Z., ADDADI, L., IDELSON, M., LEISEROWITZ, L. & LAHAV, M. (1982). *Nature*, **296**, 27–34.

ERKOVITCH-YELLIN, Z., VAN MIL, J., ADDADI, L., IDELSON, M., LAHAV, M. & LEISEROWITZ, L. (1985). *J. Am. Chem. Soc.* **107**, 3111–3122.

ERKOVITCH-YELLIN, Z., WEISSBUCH, I. & LEISEROWITZ, L. (1989). In *Morphology and Growth Units of Crystals*, p. 247. Tokyo: Terrapub.

ERMAN, A., ADDADI, L., KVICK, A., LEISEROWITZ, L., NELSON, M. & WEINER, S. (1990). *Science*, **250**, 664–667.

ERMAN, A., HANSON, J., LEISEROWITZ, L., KOETZLE, T. F., WEINER, S. & ADDADI, L. (1993*a*). *Science*, **259**, 776–779.

ERMAN, A., HANSON, J., LEISEROWITZ, L., KOETZLE, T. F., WEINER, S. & ADDADI, L. (1993*b*). *J. Phys. Chem.* **97**, 5162–5170.

LACK, S. N., BROMLEY, L. A., COTTIER, D., DAVEY, R. J., DOBBS, B. & ROUT, J. E. (1991). *J. Chem. Soc. Faraday Trans.* **87**, 3409–3414.

OEK, E. S. (1993). Crystal-solution interfaces. PhD Thesis. Univ. of Twente, The Netherlands.

OCK, E. S. & BRIELS, W. J. (1992). *J. Chem. Phys.* **96**, 7010–7018.

BOEK, E. S., FEIL, D., BRIELS, W. J. & BENNEMA, P. (1991). *J. Cryst. Growth*, **114**, 389–410.

BOER, R. C. DE (1993). Morphology related phenomena. PhD Thesis. Catholic Univ. of Nijmegen, The Netherlands.

BOHM, C., LEVEILLER, F., JACQUEMAIN, D., MÖHWALD, H., KJAER, K., ALS-NIELSEN, J., WEISSBUCH, I. & LEISEROWITZ, L. (1994). *Langmuir*, **10**, 830–836.

BOURNE, J. R. & DAVEY, R. J. (1976). *J. Cryst. Growth*, **36**, 278–286.

BUCKLEY, H. E. (1951). *Crystal Growth*. New York: Wiley.

CHAKRABARTTY, A., YANG, D. S. C. & HEW, C. L. (1989). *J. Biol. Chem.* **264**, 11313–11316.

CHEN, B. D., GARSIDE, J., DAVEY, R. J., MAGINN, S. J. & MATSUOKA, M. (1994). *J. Phys. Chem.* **98**, 3215–3221.

CHIARELLO, R. P., WOGELIUS, R. A. & STURCHIO, N. C. (1993). *Geochim. Cosmochim. Acta*, **57**, 4103–4110.

CODY, A. M. & CODY, R. D. (1991). *J. Cryst. Growth*, **113**, 508–519.

CORRIN, M. L. & NELSON, J. A. (1968). *J. Phys. Chem.* **72**, 643–645.

CUNNINGHAM, D. A. H., GERSON, A. R., ROBERTS, K. J., SHERWOOD, J. N. & WOJCIECHOWSKI, K. (1991). In *Advances in Industrial Crystallization*, edited by J. GARSIDE, R. J. DAVEY & A. G. JONES, p. 105. Oxford: Butterworth-Heinemann Ltd.

CURIE, M. P. (1894). *J. Phys.* p. 393.

DAVEY, R. J., MILISAVLJEVIC, B. & BOURNE, J. R. (1988). *J. Phys. Chem.* **92**, 2032–2036.

DE VRIES, A. L. (1984). *Phil. Trans. R. Soc.* **304**, 575–588.

DOCHERTY, R., ROBERTS, K., SAUNDERS, V., BLACK, S. & DAVEY, R. J. (1993). *Faraday Discuss.* **95**, 11–26.

DUTTA, P., PENG, J. B., LIN, B., KETTERSON, J. B., PRAKASH, M., GEOGOPOULOS, P. & ERLICH, S. (1987). *Phys. Rev. Lett.* **58**, 2228–2231.

ELWENSPOEK, M., BENNEMA, P. & VAN EERDEN, J. P. (1987). *J. Cryst. Growth*, **83**, 297–305.

FEENEY, R. E., BURCHAM, T. S. & YEH, Y. (1986). *Ann. Rev. Biophys. Biophys. Chem.* **15**, 59–78.

FENDLER, J. (1993). Private communication.

FENIMORE, C. P. & THRAIKILL, A. (1949). *J. Am. Chem. Soc.* **71**, 2714–2717.

FLETCHER, N. H. (1970). In *The Chemical Physics of Ice*. Cambridge Univ. Press.

GAVISH, M., POPOVITZ-BIRO, R., LAHAV, M. & LEISEROWITZ, L. (1990). *Science*, **250**, 973–975.

GAVISH, M., WANG, J. L., EISENSTEIN, M., LAHAV, M. & LEISEROWITZ, L. (1992). *Science*, **256**, 815–818.

GEVERS, R., AMELINCKX, S. & DEKEYSER, W. (1952). *Naturwissenschaften*, **39**, 448–449.

GIDALEVITCH, D., WEISSBUCH, I., KJAER, K., ALS-NIELSEN, J. & LEISEROWITZ, L. (1994). *J. Am. Chem. Soc.* **116**, 3271–3278.

GOPALAN, P., PETERSON, M. L., CRUNDWELL, G. & KAHR, B. (1993). *J. Am. Chem. Soc.* **115**, 3366–3367.

GREEN, R. L. & WARREN, G. J. (1985). *Nature*, **317**, 645–648.

GREEN, B. S., LAHAV, M. & RABINOVICH, D. (1979). *Acc. Chem. Res.* **12**, 191–197.

HARTMAN, P. (1973). In *Crystal Growth, An Introduction*, p. 367. Amsterdam: North-Holland Publishing Co.

HARTMAN, P. & BENNEMA, P. (1980). *J. Cryst. Growth*, **49**, 145–165.

HARTMAN, P. & PERDOK, W. G. (1955*a*). *Acta Cryst.* **8**, 49–52.

HARTMAN, P. & PERDOK, W. G. (1955*b*). *Acta Cryst.* **8**, 525–529.

HEYWOOD, B. R. & MANN, S. (1992*a*). *Langmuir*, **8**, 1492–1498.

HEYWOOD, B. R. & MANN, S. (1992*b*). *J. Am. Chem. Soc.* **114**, 4681–4686.

HIRSHFELD, F. L. (1977). *Theor. Chem. Acta*, **44**, 129–138.

HONESS, A. P. (1927). *The Nature, Origin and Interpretation of the Etch Figures on Crystals*. New York: Wiley.

HOOK, A. VAN (1968). *Kristal. Acad. Nauk. SSSR Inst. Kristallogr.* **8**, 45.

HOOK, A. VAN (1981). *J. ASSBT*. **21**, 130.

HORN, F. H. (1952). *Philos. Mag.* **43**, 1210–1213.

IITAKA, Y. (1961). *Acta Cryst.* **14**, 1–10.

JACQUEMAIN, D., GRAYER WOLF, S., LEVEILLER, F., DEUTSCH, M., KJAER, K., ALS-NIELSEN, J., LAHAV, M. & LEISEROWITZ, L. (1992). *Angew. Chem. Int. Ed. Engl.* **31**, 130–152.

JACQUEMAIN, D., GRAYER WOLF, S., LEVEILLER, F., LAHAV, M., LEISEROWITZ, L., DEUTSCH, M., KJAER, K. & ALS-NIELSEN, J. (1990). *J. Am. Chem. Soc.* **112**, 7724–7736.

DOCID: <XP___2960386A__I_>

UM00016820
NOVARTIS EXHIBIT 1517
Novartis v. Regents, IPR2023-01347
Page 3802 of 4460

JACQUEMAIN, D., LEVEILLER, F., WEINBACH, S., LAHAV, M., LEISEROWITZ, L., KJAER, K. & ALS-NIELSEN, J. (1991). *J. Am. Chem. Soc.* **113**, 7684–7691.

JONSSON, P. G. (1971). *Acta Cryst.* B**27**, 893–898.

KAJAVA, A. V. & LINDOW, S. E. (1993). *J. Mol. Biol.* **232**, 709–717.

KERN, R. (1953). *Bull. Soc. Fr. Mineral. Cristallogr.* **76**, 391.

KNIGHT, C. A., CHANG, C. C. & DE VRIES, A. L. (1991). *Biophys. J.* **59**, 409–418.

LAHAV, M., EISENSTEIN, M. & LEISEROWITZ, L. (1993). *Science*, **259**, 1469–1470.

LANDAU, E. M., POPOVITZ-BIRO, R., LEVANON, M., LEISEROWITZ, L. & LAHAV, M. (1986). *Mol. Cryst. Liq. Cryst.* **134**, 323–335.

LANDAU, E. M., WOLF, S. G., LEVANON, M., LEISEROWITZ, L., LAHAV, M. & SAGIV, J. (1989). *J. Am. Chem. Soc.* **111**, 1436–1445.

LEVEILLER, F., BOEHM, C., JACQUEMAIN, D., MOHWALD, H., LEISEROWITZ, L., KJAER, K. & ALS-NIELSEN, J. (1994). *Langmuir*, **10**, 819–829.

LEVEILLER, F., JACQUEMAIN, D., LAHAV, M., LEISEROWITZ, L., DEUTSCH, M., KJAER, K. & ALS-NIELSEN, J. (1991). *Science*, **252**, 1532–1536.

LEVEILLER, F., JACQUEMAIN, D., LEISEROWITZ, L., KJAER, K. & ALS-NIELSEN, J. (1992). *J. Phys. Chem.* **96**, 10380–10389.

LEWTAS, K., TACK, R. D., BEINY, D. H. M. & MULLIN, J. W. (1991). *Advances in Industrial Crystallization*, p. 166. Oxford: Butterworth-Heinemann Ltd.

LINDOW, S. E. (1983). *Annu. Rev. Phytopathol.* **21**, 363–384.

LINDOW, S. E., ARNY, D. C. & UPPER, C. D. (1978). *Phytopathology*, **68**, 523–527.

LOWENSTAM, H. A. & WEINER, S. (1989). *On Biomineralization*. New York: Oxford Univ. Press.

MAJEWSKI, J., EDGAR, R., POPOVITZ-BIRO, R., BOUWMAN, W. G., KJAER, K., ALS-NIELSEN, J., LAHAV, M. & LEISEROWITZ, L. (1995). *Angew. Chem.* In the press.

MAJEWSKI, J., MARGULIS, L., JACQUEMAIN, D., LEVEILLER, F., BOHM, C., ARAD, T., TALMON, Y., LAHAV, M. & LEISEROWITZ, L. (1993). *Science*, **261**, 899–902.

MAJEWSKI, J., POPOVITZ-BIRO, R., KJAER, K., ALS-NIELSEN, J., LAHAV, M. & LEISEROWITZ, L. (1994). *J. Phys. Chem.* **98**, 4087–4093.

MAJEWSKI, J., POPOVITZ-BIRO, R., BOUWMAN, W. G., KJAER, K., ALS-NIELSEN, J., LAHAV, M. & LEISEROWITZ, L. (1995). *Chem. Eur. J.* Submitted.

MAKI, L. R., GALYAN, E. L., CHANG CHIEN, M. & CALDWELL, D. R. (1974). *Appl. Microbiol.* **28**, 456–459.

MANTOVANI, G., GILLI, G. & FAGLIOLI, F. (1967). Proc. 13th Conf. CITS, Falsterbo, Sweden, pp. 289–301.

MANN, S. (1988). *Nature*, **332**, 119–124.

MANN, S., HEYWOOD, B. R., RAJAM, S. & BIRCHALL, J. D. (1988). *Nature*, **334**, 692–695.

MARKMAN, O., ELIAS, D., ADDADI, L., COHEN, I. R. & BERKOVITCH-YELLIN, Z. (1992). *J. Cryst. Growth*, **122**, 344–350.

MCBRIDE, J. M. & BERTMAN, S. B. (1989). *Angew. Chem. Int. Engl.* **28**, 330–333.

MICHAELIS, A. S. & VAN KREVELD, X. (1966). *Neth. Milk Dairy J.* **20**, 163–181.

MIL, J. VAN, ADDADI, L., GATI, E. & LAHAV, M. (1981). *J. Am. Chem. Soc.* **103**, 1248–1249.

MIL, J. VAN, ADDADI, L., GATI, E. & LAHAV, M. (1982). *J. Am. Chem. Soc.* **104**, 3429–3434.

MIZUNO, H. (1989). *Proteins: Struct. Funct. Genet.* **5**, 47–65.

OCKO, B. M., WANG, J., DAVENPORT, A. & ISAACS, H. (1990). *Phys. Rev. Lett.* **65**, 1466–1469.

PARUNGO, F. P. & LODGE, J. P. JR. (1967). *J. Atm. Sci.* **24**, 274–277.

PAUL, I. C. & CURTIN, D. Y. (1987). *Organic Solid State Chemistry*, p. 331. Amsterdam: Elsevier.

POPOVITZ-BIRO, R., MAJEWSKI, J., MARGULIS, L., COHEN, S., LEISEROWITZ, L. & LAHAV, M. (1994*a*). *J. Phys. Chem.* **98**, 4970–4972.

POPOVITZ-BIRO, R., MAJEWSKI, J., MARGULIS, L., COHEN, S., LEISEROWITZ, L. & LAHAV, M. (1994*b*). *Adv. Mat.* **6**, 956–959.

POPOVITZ-BIRO, R., WANG, J. L., MAJEWSKI, J., LEISEROWITZ, L. & LAHAV, M. (1994). *J. Am. Chem. Soc.* **116**, 1179–1191.

POWER, B. A. & POWER, F. (1962). *Nature*, **194**, 1170–1171.

PRAPPACHER, H. R. (1963). *Z. Angew. Math. Phys.* **14**, 590–598.

PRELOG, V. & HELMCHEN, G. (1982). *Angew. Chem. Int. Ed. Engl.* **21**, 567–583.

RISTIC, R. I., SHERWOOD, J. M. & WOJESHOWSKI, K. (1994). *J. Phys. Chem.* In the press.

SCHNELL, R. C. & VALI, C. (1972). *Nature*, **236**, 163–165.

SHIMON, L. J. W., LAHAV, M. & LEISEROWITZ, L. (1985). *J. Am. Chem. Soc.* **107**, 3375–3377.

SHIMON, L. J. W., LAHAV, M. & LEISEROWITZ, L. (1986). *Nouv. J. Chem.* **10**, 723–737.

SHIMON, L. J. W., VAIDA, M., ADDADI, L., LAHAV, M. & LEISEROWITZ, L. (1990). *J. Am. Chem. Soc.* **112**, 6215–6220.

SHIMON, L. J. W., VAIDA, M., ADDADI, L., LAHAV, M. & LEISEROWITZ, L. (1991). In *Organic Crystal Chemistry*, p. 74. Oxford Univ. Press.

SHIMON, L. J. W., VAIDA, M., FROLOW, F., LAHAV, M., LEISEROWITZ, L., WEISSINGER-LEWIN, Y. & MCMULLAN, R. K. (1993). *Faraday Discuss.* **95**, 307–327.

SHIMON, L. J. W., WIREKO, F. C., WOLF, J., WEISSBUCH, I., ADDADI, L., BERKOVITCH-YELLIN, Z., LAHAV, M. & LEISEROWITZ, L. (1986). *Mol. Cryst. Liq. Cryst.* **137**, 67–86.

SHIMON, L. J. W., ZBAIDA, D., ADDADI, L., LEISEROWITZ, L. & LAHAV, M. (1988). *Mol. Cryst. Liq. Cryst.* **161**, 199–221.

SKOULIKA, S., MICHAELIDIS, A. & AUBRY, A. (1991). *J. Cryst. Growth*, **108**, 285–289.

SMYTHE, B. M. (1967). *Austr. J. Chem.* **20**, 1115–1131.

SMYTHE, B. M. (1971). *Sugar Technol. Rev.* **1**, 191–231.

STAAB, E., ADDADI, L., LEISEROWITZ, L. & LAHAV, M. (1990). *Adv. Mater.* **2**, 40–43.

SWAMINATHAN, K. S. & CRAVEN, B. M. (1982). *Am. Cryst. Assoc. Ser.* **2**, **10**, 13.

TAYLOR, R. & KENNARD, O. (1982). *J. Am. Chem. Soc.* **104**, 5063–5070.

TORRI, K. & YITAKA, Y. (1970). *Acta Cryst.* B**26**, 1317–1326.

TORRI, K. & YITAKA, Y. (1971). *Acta Cryst.* B**27**, 2237–2246.

TURNER, E. & LONSDALE, K. (1950). *J. Chem. Phys.* **18**, 156.

VAIDA, M., SHIMON, L. J. W., VAN MIL, J., ERNST-CABRERA, K., ADDADI, L., LEISEROWITZ, L. & LAHAV, M. (1989). *J. Am. Chem. Soc.* **111**, 1029–1034.

VAIDA, M., SHIMON, L. J. W., WEISSINGER-LEWIN, Y., FROLOW, F., LAHAV, M., LEISEROWITZ, L. & MCMULLAN, R. K. (1988). *Science*, **241**, 1475–1479.

VISSER, R. A. & BENNEMA, P. (1983). *Neth. Milk Dairy J.* **37**, 109–137.

VONNEGUT, B. (1947). *J. Appl. Phys.* **18**, 593–595.

WALBA, D. M., RAZUVI, H. A., CLARK, N. A. & PARMER, D. S. (1988). *J. Am. Chem. Soc.* **110**, 8686–8691.

WANG, J., DAVENPORT, A., ISAACS, H. & OCKO, B. M. (1992). *Science*, **255**, 1416–1418.

WANG, J.-L., LAHAV, M. & LEISEROWITZ, L. (1991). *Angew. Chem. Int. Ed.* **30**, 696–698.

WANG, J.-L., LEISEROWITZ, L. & LAHAV, M. (1992). *J. Phys. Chem.* **96**, 15–16.

WANG, J.-L., LEVEILLER, F., JACQUEMAIN, D., KJAER, K., ALS-NIELSEN, J., LAHAV, M. & LEISEROWITZ, L. (1994). *J. Am. Chem. Soc.* **116**, 1192–1204.

WARREN, G. J. & COROTTO, L. (1989). *Gene*, **85**, 239–243.

WARREN, G. J., COROTTO, L. & WOLBER, P. (1986). *Nucl. Acids Res.* **14**, 8047–8060.

WEINBACH, S., JACQUEMAIN, D., LEVEILLER, F., KJAER, K., ALS-NIELSEN, J. & LEISEROWITZ, L. (1993). *J. Am. Chem. Soc.* **115**, 11110–11118.

WEINBACH, S., KJAER, K., ALS-NIELSEN, J., GRUBEL, G., LEGRAND, M., LAHAV, M. & LEISEROWITZ, L. (1994). *Science*, **264**, 1556–1570.

WEISSBUCH, I., ADDADI, L., BERKOVITCH-YELLIN, Z., GATI, E., LAHAV, M. & LEISEROWITZ, L. (1984). *Nature*, **310**, 161–164.

WEISSBUCH, I., ADDADI, L., BERKOVITCH-YELLIN, Z., GATI, E., WEINSTEIN, S., LAHAV, M. & LEISEROWITZ, L. (1983). *J. Am. Chem. Soc.* **105**, 6613–6621.

WEISSBUCH, I., ADDADI, L., LAHAV, M. & LEISEROWITZ, L. (1991). *Science*, **253**, 637–645.

WEISSBUCH, I., ADDADI, L., LEISEROWITZ, L. & LAHAV, M. (1988). *J. Am. Chem. Soc.* **11**, 561–567.

WEISSBUCH, I., BERKOVIC, G., LEISEROWITZ, L. & LAHAV, M. (1990). *J. Am. Chem. Soc.* **112**, 5874–5875.

WEISSBUCH, I., BERKOVITCH-YELLIN, Z., LEISEROWITZ, L. & LAHAV, M. (1985). *Isr. J. Chem.* **25**, 362–372.

WEISSBUCH, I., FROLOW, F., ADDADI, L., LAHAV, M. & LEISEROWITZ, L. (1990). *J. Am. Chem. Soc.* **112**, 7718–7724.

DCID: <XP___2960386A__i_>

UM00016821
NOVARTIS EXHIBIT 1517
Novartis v. Regents, IPR2023-01347
Page 3803 of 4460

WEISSBUCH, I., KUZMENKO, I., VAIDA, M., ZAIT, S., LEISEROWITZ, L. & LAHAV, M. (1994). *Chem. Mater.* **6**, 1258–1268.
WEISSBUCH, I., LAHAV, M., LEISEROWITZ, L., MEREDITH, G. R. & VANHERZEELE, H. (1989). *Chem. Mater.* **1**, 114–118.
WEISSBUCH, I., LEISEROWITZ, L. & LAHAV, M. (1994). *Adv. Mat.* **6**, 953–956.
WEISSBUCH, I., LEVEILLER, F., JACQUEMAIN, D., KJAER, K., ALS-NIELSEN, J. & LEISEROWITZ, L. (1993). *J. Phys. Chem.* **97**, 12858–12861.
WEISSBUCH, I., MAJEWSKI, J., KJAER, K., ALS-NIELSEN, J., LAHAV, M. & LEISEROWITZ, L. (1993). *J. Phys. Chem.* **97**, 12848–12857.
WEISSBUCH, I., SHIMON, L. J. W., ADDADI, L., BERKOVITCH-YELLIN, Z., WEINSTEIN, S., LAHAV, M. & LEISEROWITZ, L. (1985). *Isr. J. Chem.* **25**, 353–362.
WEISSBUCH, I., ZBAIDA, D., ADDADI, L., LAHAV, M. & LEISEROWITZ, L. (1987). *J. Am. Chem. Soc.* **109**, 1869–1871.
WEISSINGER-LEWIN, Y., FROLOW, F., MCMULLAN, R. K., KOETZLE, T. F., LAHAV, M. & LEISEROWITZ, L. (1989). *J. Am. Chem. Soc.* **111**, 1035–1040.
WELLS, A. F. (1946). *Philos. Mag.* **37**, 180, 217, 605–629.
WELLS, A. F. (1949). *Discuss. Faraday Soc.* **5**, 197–201.
WHETSTONE, J. (1954). *Faraday Discuss.* pp. 132–140.
WILEN, L. (1993). *Science*, **259**, 1469.
WIREKO, F. C., SHIMON, L. J. W., FROLOW, F., BERKOVITCH-YELLIN, Z., LAHAV, M. & LEISEROWITZ, L. (1987). *J. Phys. Chem.* **91**, 472–481.
WOENSDREGT, C. F. (1993). *Faraday Discuss.* **95**, 97–108.
WOLF, S. G., LEISEROWITZ, L., LAHAV, M., DEUTSCH, M., KJAER, K. & ALS-NIELSEN, J. (1987). *Nature*, **328**, 63–66.
YANG, D. S. C., SAX, M., CHAKRABARTTY, A. & HEW, C. L. (1988). *Nature*, **333**, 232–237.
ZABEL, V., MULLER-FAHRNOW, M., HILGENFELD, R., SAENGER, W., PFANNEMULLER, B., ENKELMANN, V. L. & WELKE, W. (1986). *Chem. Phys. Lipids*, **39**, 313–327.
ZBAIDA, D., WEISSBUCH, I., SHAVIT-GATI, E., ADDADI, L., LEISEROWITZ, L. & LAHAV, M. (1987). *React. Polym.* **6**, 241–253.
ZHAO, X. K., YANG, J., MCCORMICK, L. D. & FENDLER, J. H. (1992). *J. Phys. Chem.* **96**, 9933–9939.

DOCID: <XP___2960386A__I_>

UM00016822
NOVARTIS EXHIBIT 1517
Novartis v. Regents, IPR2023-01347
Page 3804 of 4460

本複製物は、特許庁が著作権法第４２条第２項第１号の規定により複製したものです。
取扱にあたっては、著作権侵害とならないよう十分にご注意ください。

$C_{16}H_{19}IN_4$ (394,3)
Ber.: N 14,21
Gef.: N 13,93

3.3.3. 1-(N-Phenylamidino)pyrazolidin-hydroiodid (3e)

Ausbeute: 52%. Farblose Nadeln. Schmb. 185–187,5 °C (n-C_3H_7OH). UV (CH_3OH, nm(lg ε)): λ_{max} = 222 (4,44). IR (KBr, cm^{-1}): ν = 3380, 3280, 3130, 1630 (C=N), 1580 (NH), 1240 (C–N). ^1H–NMR (DMSO–D_6, ppm): δ = 2,10 (tt, 2H, $-CH_2-$); 2,92 (dt, 2H, $-CH_2-$); 3,48 (t, 2H, $-CH_2-$); 7,17–7,44 (m, 5H, Ar–H); 7,54 (s, 4H, NH).
$C_{10}H_{15}IN_4$ (318,2)
Ber.: N 17,61
Gef.: N 16,64

3.3.4. 1-[N-(4-Methylphenyl)amidino]pyrazolidin-hydroiodid (3f)

Ausbeute: 47%. Farblose Nadeln. Schmb. 152–154 °C (n-C_3H_7OH). UV (CH_3OH, nm(lg ε)): λ_{max} = 231 (4,31). IR (KBr, cm^{-1}): ν = 3370, 3100, 2970, 1620 (C=N), 1585 (NH), 1570, 1230 (C–N). ^1H–NMR (DMSO–D_6, ppm): δ = 2,10 (tt, 2H, $-CH_2-$); 2,29 (s, 3H, $-CH_3$); 2,89 (dt, 2H, $-CH_2-$); 3,43 (t, 2H, $-CH_2-$); 7,05 (d, 2H, Ar–H); 7,20 (d, 2H, Ar–H); 7,41 (s, 4H, NH).
$C_{11}H_{17}IN_4$ (332,2)
Ber.: N 16,87
Gef.: N 17,32

3.3.5. 1-[N-(4-Chlorphenyl)amidino]pyrazolidin-hydroiodid (3g)

Ausbeute: 45%. Farblose Kristalle. Schmb. 169–171,5 °C (n-C_3H_7OH). UV (CH_3OH, nm(lg ε)): λ_{max} = 223 (4,37), 245 (sh 4,17). IR (KBr, cm^{-1}): ν = 3420, 3210, 3100, 1640 (C=N), 1595 (NH), 1560, 1490, 1230 (C–N). ^1H–NMR (DMSO–D_6, ppm): δ = 2,07 (tt, 2H, $-CH_2-$); 2,88 (dt, 2H, $-CH_2-$); 3,41 (t, 2H, $-CH_2-$); 7,15 (d, 2H, Ar–H); 7,42 (d, 2H, Ar–H); 7,55 (s, 4H, NH).
$C_{10}H_{14}ClIN_4$ (352,6)
Ber.: N 15,89
Gef.: N 16,04

3.3.6. 1-[N-(4-Bromphenyl)amidino]pyrazolidin-hydroiodid (3h)

Ausbeute: 51%. Farblose Kristalle. Schmb. 179–182,5 °C (CH_3OH). UV (CH_3OH, nm(lg ε)): λ_{max} = 233 (4,51), 294 (sh 3,85). IR (KBr, cm^{-1}): ν = 3390, 3180, 1630 (C=N), 1585 (NH), 1550, 1470, 1220 (C–N). ^1H–NMR (DMSO–D_6, ppm): δ = 2,11 (tt, 2H, $-CH_2-$); 2,91 (dt, 2H, $-CH_2-$); 3,45 (t, 2H, $-CH_2-$); 7,15 (d, 2H, Ar–H); 7,56 (d, 2H, Ar–H); 7,70 (s, 4H, NH).
$C_{10}H_{14}BrIN_4$ (397,1)
Ber.: N 14,11
Gef.: N 14,24

3.3.7. 1-(N-Naphth-1-ylamidino)pyrazolidin-hydroiodid (3i)

Ausbeute: 48%. Farblose Kristalle. Schmb. 219–223 °C (n-C_3H_7OH). UV (CH_3OH, nm(lg ε)): λ_{max} = 273 (sh 3,87), 283 (3,95), 294 (sh 3,87). IR (KBr, cm^{-1}): ν = 3390, 3300, 3100, 1610 (C=N), 1580 (NH), 1390, 1250 (C–N). ^1H–NMR (DMSO–D_6, ppm): δ = 2,16 (tt, 2H, $-CH_2-$); 2,98 (dt, 2H, $-CH_2-$); 3,52 (t, 2H, $-CH_2-$); 7,30 (s, 4H, NH); 7,35–8,02 (m, 7H, Ar–H).
$C_{14}H_{17}IN_4$ (368,2)
Ber.: N 15,21
Gef.: N 15,23

Wir danken Herrn T. Nagel, Berlin-Chemie, für die Unterstützung bei der Aufnahme und Diskussion der ^1H–NMR-Spektren.

Literatur

1 Morgenstern, O.; Richter, P. H.; Klemann, A.: Pharmazie 46 418 (1991); 1. Mitteilung
2 Buhle, E. L.; Moore, A. M.; Wiselogle, F. Y.: J. Am. Chem. Soc. 65, 29 (1943)
3 Kunze, F.; Godfrey, L. E. A.: Angew. Chem. 75, 1157 (1963)

Eingegangen am 25. Juli 1990

Dr. O. Morgenstern
Friedrich-Ludwig-Jahn-Str. 17
O-2200 Greifswald

記事連番0004

Arzneimittelwerk Dresden GmbH, Geschäftsbereich Forschung und Entwicklung

Untersuchungen über Additionsverbindungen von Carbamazepin

H. WUNDERLICH, L. ZENKER, H. USBECK, A. STARK, D. LOHMANN und W. THIEL

Es werden Additionsverbindungen von Carbamazepin mit Ammoniumchlorid, Ammoniumbromid und Formamid dargestellt und charakterisiert (IR-Spektren, Verhalten gegenüber Wasser, Löslichkeit).

Derivatives of carbamazepine with ammonium halogenides and formamide

The reaction of carmamazepine with ammonium chloride, ammonium bromide, and formamide is described. The products were characterized by means of IR spectra, the reaction with water and their solubility.

1. Einleitung

Das Antiepileptikum Carbamazepin (Finlepsin® AWD; 1) bildet Additionsverbindungen, die in der Literatur schon mehrfach Erwähnung fanden. So beschrieben Föhlmann et al. [1] die Anlagerung von Wasser unter Bildung von Carbamazepindihydrat. Von japanischen Autoren wurde über ein Monoaceton-Addukt ausführlich berichtet [2]. In einer DDR-Patentschrift [3] sind Additionsverbindungen aus 1 und anorganischen oder organischen Säuren mitgeteilt worden.
Im Rahmen unserer Arbeiten zur technischen Herstellung und Reinigung von 1 konnten wir feststellen, daß dieses auch mit Ammoniumhalogeniden und Formamid Addukte bildet.

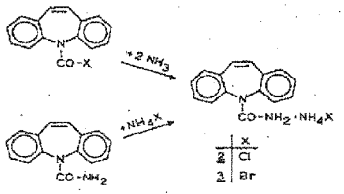
2. Untersuchungen und Ergebnisse

2.1. Additionsverbindungen aus Carbamazepin und Ammoniumhalogeniden

2.1.1. Herstellung

Bei der Reaktion von 5-Chlorcarbonyl-5H-dibenz[b, f]azepin (4, X=Cl) mit gasförmigem Ammoniak in siedendem Chloroform wird ein farbloses, in Chloroform schwer lösliches Kristallisat erhalten, dessen Schmelzverhalten von dem des 1 verschieden ist. In gleicher Weise verläuft die Reaktion in Alkoholen, Butylacetat, Benzen oder Toluen. Aus der Elementaranalyse folgt, daß die Substanz stöchiometrisch aus 1 und Ammoniumchlorid im Verhältnis 1:1 zusammengesetzt ist. Geht man von 1 aus, so lassen sich in geeigneten organischen Lösungsmitteln durch Zusatz von Ammoniumhalogeniden ebenfalls die bislang nicht bekannten Addukte isolieren (vgl. 3.1.). Die Bildungsweise der Addukte ist im Schema 1 dargestellt.

Schema 1



UM00016823
NOVARTIS EXHIBIT 1517
Novartis v. Regents, IPR2023-01347
Page 3805 of 4460

本複製物は、特許庁が著作権法第４２条第２項第１号の規定により複製したものです。
取扱にあたっては、著作権侵害とならないよう十分にご注意ください。

Die Additionsverbindungen 2 und 3 sind an der Luft stabil und lassen sich in niederen Alkoholen unzersetzt umkristallisieren. Um die neuen Verbindungen genauer zu charakterisieren, wurden neben spektroskopischen und Löslichkeitsuntersuchungen auch umfassende elektrochemische und röntgenstrukturanalytische Untersuchungen eingeleitet, über deren Ergebnisse gesondert berichtet wird [4, 5].

2.1.2. IR-Spektren

Die IR-Spektren (in KBr) der beiden Addukte 2 und 3 sind einander sehr ähnlich (Tabelle 1). Unterschiede gegenüber 1 zeigen sich an einer doppelt auftretenden Carbonylbande bei 1650 und 1660 cm^{-1}, an der verschobenen Bandengruppe für νNH-Schwingungen und an der breiten, intensiven Bande bei 1435 cm^{-1}, die wir einer verschobenen δNH-Schwingung zuordnen. Daraus läßt sich ein stärkerer Einfluß des ionischen Partners im Kristallgitter auf die Carbamoylgruppe ableiten. Das NH_4^+-Kation in 2 und 3 zeigt eine sehr intensive, breite Bande bei 2960 cm^{-1}.

Tabelle 1 IR-Absorptionsbanden [cm^{-1}] der Ammoniumhalogenid-Addukte im Vergleich zu repräsentativen Kristallmodifikationen des Carbamazepins ($I_α$, $I_β$)

2	3	$I_β$	$I_α$	Schwingung
770	765	750		γCH (out-of-plane)
1435	1435	1375	1385	δNH
1480	1480	1480		νC=C
1575	1575	1585		(aro-
1595	1595	1595		matisch)
1650	1650	1665	1685	νC=O
1660	1660	—	—	
3245	3250	3270		νNH
3310	3315	3335		
3400	3395	3460	3475	

Die IR-Spektren berechtigen zu der Annahme, daß es sich um definierte Additionsverbindungen und nicht nur um Gemische handelt.

2.1.3. Verhalten gegenüber Wasser

Die Zerlegung der 1-NH_4X-Addukte in Wasser läuft vor allem bei nicht ausreichender Wassermenge unvollständig ab. Ein bloßes Auswaschen des Reaktionsproduktes mit Wasser führt nicht zu reinem 1. Offenbar war Schindler [6] bei der Erstbeschreibung der Synthese von 1 aus 5-Chlorcarbonyl-5H-dibenz[b, f]azepin und Ammoniak diesem Irrtum unterlegen, als er nach wiederholtem Umkristallisieren den Schmb. mit 204–206 °C anstatt mit dem zutreffenden von 190–192 °C angab.

Die Herstellung von 1-NH_4X-Addukten ist nach Schema 1 in organischen Lösungsmitteln auch in Gegenwart von begrenzten Mengen Wasser möglich und gestattet z. B. die Anwendung von konz. Ammoniaklösung. So liefert die Reaktion zwischen 4 (X = Cl) und 25% wäßriger Ammoniaklösung in Butylacetat als Finalprodukt das 1-NH_4Cl-Addukt in guter Ausbeute [7]. Dies ist bei der technischen Herstellung von 1 und für die weiteren Reinigungsoperationen von Bedeutung, denn 10-Bromcarbamazepin oder 10,11-Dihydrocarbamazepin bilden mit Ammoniumchlorid unter vergleichbaren Bedingungen keine Addukte.

Zur Ermittlung der Löslichkeit wurden 20 mg Substanz (Variante A) bzw. 100 mg Substanz (Variante B) mit einem Zusatz von 25,0 ml Wasser im verschlossenen Erlenmeyer-Kolben mittels Thermovibrator bei 25 °C geschüttelt. Zum Vergleich wurde eine äquimolare Mischung von 23,6 mg Carbamazepin-β-modifikation ($I_β$) und 5,3 mg Ammoniumchlorid mit einem Zusatz von 25 ml destilliertem Wasser untersucht.

Nach der in Tabelle 2 angegebenen Zeit wurden Proben der klaren wäßrigen Lösung genommen und ihr Gehalt an Carbamazepin UV-spektroskopisch bestimmt. Die Ergebnisse sind in Tabelle 3 zusammengestellt.

Tabelle 2 Löslichkeiten (mg 1/100 ml Lösung) von 2, 3, $1_β$ und einem äquimolaren Gemisch $1_β$ + NH_4Cl bei 25 °C

Zeit [h]	2 A	2 B	3 A	$1_β$ A	$1_β$ + NH_4Cl
1	14,6	29,3	11,8	14,3	14,4	14,1
3	14,1	27,9	12,1	13,4	13,2	
7	13,9	23,8	12,2	12,9	12,9	13,0
24	15,2	17,2	13,6	12,8	12,8	12,0
48	—	15,6	14,6	12,6	12,3	

Unter vergleichbaren Bedingungen zeigen alle Substanzen ähnliche Löslichkeitswerte. Geringfügige Unterschiede lassen sich durch Abweichungen in den Korngrößen- und Phasenverteilungen erklären. Der Einfluß des anwesenden Ammoniumhalogenids auf die Löslichkeit ist unerheblich.

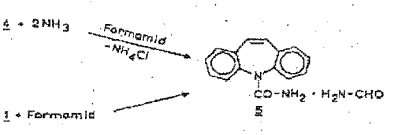
Eine nach 1 h zusätzlich vorgenommene argentometrische Chloridbestimmung in der wäßrigen Lösung der Probe 2 (B) ergab bereits den auf die Einwaage berechneten vollen Chloridwert. Diese Ergebnisse zeigen, daß nach 1 h nur noch 1 (heterogen) neben freiem Ammoniumchlorid in homogener Lösung vorliegt. Die beträchtlich erhöhte Anfangslöslichkeit bestätigt das Vorliegen eines Adduktthabitus. Der schnell fortschreitende Übergang in einen anderen Habitus ist begleitet von einer Übersättigung der wäßrigen Phase, die sich langsam zum normalen Löslichkeitsgleichgewicht von 1 hin abbaut (Tabelle 2, Spalte 2). Die IR-Spektren der luftgetrockneten Adduktrückstände und von $I_β$ aus den Ansätzen der Löslichkeitsbestimmungen enthalten die charakteristischen Banden des Einsatzstoffes nicht mehr. Es liegen Mischphasen von $1_α$ und $1 \cdot 2\,H_2O$ vor.

Das Löslichkeitsverhalten deutet auf eine nur lockere Bindung des Ammoniumchlorids im Kristallgefüge.

2.2. Additionsverbindung aus Carbamazepin und Formamid

Verwendet man zur Beschleunigung der Reaktion von 4 (X = Cl) mit konz. wäßrigem Ammoniak als zusätzliche Lösungskomponente Formamid, so erhält man überraschenderweise anstelle von 1 ein im verwendeten Lösungsmittelgemisch schwer lösliches Addukt aus 1 und Formamid. Die Bildung dieses Adduktes 5 ist in Chloroform ebenfalls direkt aus 1 und Formamid möglich (Schema 2).

Schema 2



Die elementaranalytische Untersuchung ergab für 5 wiederum eine Zusammensetzung im Molverhältnis 1:1. Durch Wasser und wäßrige alkalische Lösungen wird es in seine Komponenten zerlegt.

UM00016824
NOVARTIS EXHIBIT 1517
Novartis v. Regents, IPR2023-01347
Page 3806 of 4460

整理番号:　　発送番号:667855　発送日:平成21年10月 8日　　4/E

本複製物は、特許庁が著作権法第４２条第２項第１号の規定により複製したものです。
取扱にあたっては、著作権侵害とならないよう十分にご注意ください。

5 ist aus wasserfreien Alkoholen (Methanol, Ethanol) in Gegenwart von 1 bis 5% Formamid unzerlegt umkristallisierbar. Bei Anwendung von wäßrigen Alkoholen erfolgt eine vollständige Zerlegung des Adduktes. Aus der warmen Mutterlauge kristallisiert reines 1 aus, das bei Raumtemperatur völlig klar in Chloroform löslich ist. Das Addukt ist im Unterschied dazu in Chloroform schwer löslich.
Formamid verdrängt offenbar auf Grund seiner stärkeren Affinität zu 1 Ammoniumchlorid. Bei Anwendung von Methyl- oder Dimethylformamid anstelle von Formamid ist dies nicht der Fall, vielmehr wird hierbei 2 isoliert.

3. Experimenteller Teil

Die IR-Spektren wurden mit einem Spektralphotometer Specord 75 IR (Carl Zeiss JENA) aufgenommen, die Schmb. werden mit einem Heiztischgerät nach Boëtius sowie dem Thermosystem FP5 (Mettler) bestimmt, wobei Übereinstimmung erzielt wurde.

3.1. 5-Carbamoyl-5H-dibenz[b, f]azepin (1)-NH_4Cl-Addukt (2)

3.1.1. 47,2 g (0,2 mol) 1 werden unter Erwärmen in 500 ml 96%

C_2H_5OH gelöst. Dann wird eine filtrierte Lösung von 10,7 g (0,2 mol) NH_4Cl in 5 ml H_2O zugesetzt. Man erwärmt die Mischung 15 min zum Sieden, kühlt sie auf 15 °C und saugt den entstandenen Niederschlag nach 24 h ab. Dieser wird mit wenig C_2H_5OH gewaschen und bei 100 °C getrocknet. Nach Umkristallisation aus der 20fachen Menge C_2H_5OH erhält man Nadeln. Schmb. 195,5–199 °C.
$C_{15}H_{16}ClN_3O$ (289,8)

Ber.:	C	62,17	H	5,57	N	14,50	Cl	12,24
Gef.:	C	61,93	H	5,54	N	14,40	Cl	12,02
		62,21		5,63		14,43		12,17

3.1.2. 12,8 g (0,05 mol) 5-Chlorcarbonyl-5H-dibenz[b, f]azepin

werden in 45 ml Butylacetat verrührt. Man erwärmt auf 80 °C, tropft in die entstehende Lösung 15 ml einer 25%ig wäßrigen NH_3-Lösung und rührt 1 h bei 80 °C. Anschließend werden über einen Wasserabscheider ca. 10 ml H_2O abdestilliert. Der Ansatz wird dann auf 12 °C gekühlt, das Kristallisat über eine Filternutsche abgesaugt und zweimal mit je 10 ml Butylacetat gewaschen. Es wird bei 100 °C getrocknet und aus 90%ig wäßrigem i-C_3H_7OH umkristallisiert.

3.2. 1-NH_4Br-Addukt (3)

47,2 g (0,2 mol) 1 werden im siedenden Wasserbad in 200 ml Butylacetat gelöst. Man tropft eine Lösung von 20 g (0,224 mol) NH_4Br in 10 ml H_2O zu, erhitzt 0,5 h, kühlt die Mischung auf 15 °C und filtriert den ausgefallenen Niederschlag ab. Dieser wird mit Butylacetat gewaschen und bei 100 °C getrocknet. Durch Umkristallisation aus C_2H_5OH erhält man das 1:1-Addukt als farblose, verfilzte Nadeln.
Schmb. 119–201 °C.
$C_{15}H_{16}BrN_3O$ (334,2)

Ber.:	C	53,89	H	4,82	N	12,56	Br	23,93
Gef.:	C	52,69	H	4,84	N	12,50	Br	25,10
		52,46		4,86		12,50		25,11

3.3. 1-Formamid-Addukt (5)

23,6 g (0,1 mol) 1 werden bei Raumtemperatur in 100 ml $CHCl_3$ unter Rühren gelöst. In die klare Lösung werden unter Rühren 5,6 g (0,125 mol) NH_3 – CHO zugegeben. Die Lösung beginnt sich einzutrüben und in wenigen min erfolgt die Kristallisation. Nach 2–3 h Kühlen im fließenden Wasserbad wird das Kristallisat abgesaugt und mit gekühltem $CHCl_3$, das 1% NH_3 – CHO enthält, gewaschen. Der farblose Filterkuchen wird im Trockenschrank bei ca. 70 °C getrocknet. Man erhält 23 g (81,7%) 5. Schmb. 189–192 °C (bei 142–145 °C erfolgt eine deutliche Kristallumwandlung).
$C_{16}H_{13}N_3O_2$ (281,3)

Ber.:	C	68,31	H	5,37	N	14,94		
Gef.:	C	68,55	H	5,36	N	15,10		

3.4. Bestimmung der Löslichkeit von 1, 2 und 3

Substanzeinwaagen von ca. 20 mg und 25 ml dest. H_2O (A) bzw. 100 mg und 25 ml dest. H_2O (B) werden in je einem 100 ml-Schliff-Erlenmeyer gegeben. Die verschlossenen Kolben werden bei 25 °C 125 rotierenden Schüttelbewegungen je min ausgesetzt. Das Klarfiltrat einer Probenahme wird 1:10 mit dest. H_2O verdünnt und die UV-Absorption in einer 10 mm Küvette bei 286 nm gegen dest. H_2O gemessen. Für die analog auszuführende Eichmessung werden ca. 8 mg Einwaage 1 in 100 ml dest. H_2O durch leichtes Erwärmen und ggf. mit Ultraschall klar gelöst.

Literatur

1 Pöhlmann, H.; Gulde, Ch.; Jahn, R.; Pfeifer, S.: Pharmazie 30, 709 (1975)
2 Kaneniwa, N.; Yamaguchi, T.; Watari, N.; Otsuka, M.: Yakugaku Zasshi 104 2, 184 (1984)
3 Arzneimittelwerk Dresden: DD 133 053 (8. 9. 77., 29. 11. 78.)
4 Dännbier, U.; Jugelt, W.: Pharmazie 46, 512 (1991)
5 Reck, G.; Thiel, W.: ibid. 46, 509 (1991)
6 Geigy, Ag.: DAS 1 136 707 (19. 2. 58, 20. 9. 62)
7 Arzneimittelwerk Dresden, DD 260 696 (25. 5. 87., 5. 10. 88.)

Eingegangen am 25. Juli 1990

Dr. H. Wunderlich
Wilhelm-Pieck-Str. 35,
Radebeul 1,
O-8122

Analytisches Zentrum Berlin-Adlershof[1] und Arzneimittelwerk Dresden GmbH[2]

記事番号0005

Kristallstrukturen der Addukte Carbamazepin-Ammoniumchlorid und Carbamazepin-Ammoniumbromid sowie deren Umwandlung in Carbamazepin-Dihydrat

G. RECK[1] und W. THIEL[2]

Die Addukte Carbamazepin-Ammoniumchlorid und Carbamazepin-Ammoniumbromid haben isomorphe Kristallstrukturen. In ihnen gibt es stabile Schichten, in denen die Wirkstoffmoleküle, Ammonium- und Chlorid- bzw. Bromidionen über 6 symmetrieunabhängige Wasserstoffbrücken miteinander verknüpft sind. In Wasser werden die Addukte durch eine topotaktische Reaktion vollständig in Carbamazepin-Dihydrat umgewandelt.

Crystal structures of the adducts carbamazepine-ammonium chloride and carbamazepine-ammonium bromide and their transformation in carbamazepine dihydrate

The adducts carbamazepine ammonium chloride and carbamazepin ammonium bromide have isomorphous crystal structures. Drug molecules, ammonium, and chloride (bromide) ions are connected by 6 symmetry independent hydrogen bonds forming stable layers in the crystal. In water the adducts are transformed completely to carbamazepine dihydrate by a topotactic reaction.

1. Einleitung

Der antiepileptische Wirkstoff 5H-Dibenz[b, f]-azepin-5-carboxamid (Carbamazepin, 1) bildet mit Ammoniumchlorid beim Umkristallisieren in Ethanol ein Addukt (2), das über 200 °C schmilzt und damit eine wesentlich höhere Schmelztemperatur als der reine Wirkstoff (189–193 °C) besitzt. Das IR-Spektrum zeigt eine deutliche Veränderung einiger Banden [1].

UM00016825

NOVARTIS EXHIBIT 1517
Novartis v. Regents, IPR2023-01347
Page 3807 of 4460

Cited Document //

整理番号: 発送番号:667861 発送日:平成21年10月 8日 2

本複製物は、特許庁が著作権法第４２条第２項第１号の規定により複製したものです。
取扱にあたっては、著作権侵害とならないよう十分にご注意ください。

Crystal Engineering Using Anilic Acids and Dipyridyl Compounds through a New Supramolecular Synthon

Md. Badruz Zaman,[†,‡] Masaaki Tomura,*[,†] and Yoshiro Yamashita*[,§]

Institute for Molecular Science, Myodaiji, Okazaki 444-8585, Japan, and Department of Electronic Chemistry, Interdisciplinary Graduate School of Science and Engineering, Tokyo Institute of Technology, 4259 Nagatsuta, Midori-ku, Yokohama 226-8502, Japan

yoshiro@echem.titech.ac.jp

Received December 14, 2000

The anilic acids, 2,5-dihydroxy-1,4-benzoquinone (**1a**), 2,5-dibromo-3,6-dihydroxy-1,4-benzoquinone (bromanilic acid; **1b**), 2,5-dichloro-3,6-dihydroxy-1,4-benzoquinone (chloranilic acid; **1c**), and 2,5-dicyano-3,6-dihydroxy-1,4-benzoquinone (cyananilic acid; **1d**), were cocrystallized with rigid organic ligands containing two pyridine rings, 2,4-bipyridine (**2a**), 4,4′-bipyridine (**2b**), 1,2-bis(2-pyridyl)-ethylene (**3a**), 1,2-bis(4-pyridyl)ethylene (**3b**), 2,2′-dipyridylacetylene (**4a**), 3,3′-dipyridylacetylene (**4b**), and 4,4′-dipyridylacetylene (**4c**). Fourteen complexes **5**−**18** were obtained as single crystals, and their crystal structures were successfully determined by X-ray analysis. All complexes except those with **2a** are 1:1 and are composed of an infinite linear or zigzag tape structure, the formation of which is ascribed to intermolecular O−H···N, N^+−H···O, or N^+−H···O^- hydrogen bonds or a combination of these between the anilic acids and the dipyridyl compounds. In the complexes **5** and **6**, no infinite tape structure is observed although the molecular units connected by a similar hydrogen-bonding pattern are formed. For the 1:1 complexes, we have found two types of stacking arrangements, segregated stacks (**7**, **9**, **12**−**15**, **18**) and alternated ones (**8**, **10**, **11**, **16**, **17**). In the complexes of **1c** with the series of dipyridylacetylenes **4** (**14**, **15**, **17**), the neutral, dication, and monocaction states are formed depending on the nitrogen positions, which can be attributed to the different basicity of the pyridyl groups.

Introduction

Organic solid materials based on hydrogen-bonded donor and acceptor molecules have been the objects of recent intensive studies[1] aimed at building a new class of compounds which are interesting from viewpoints of basic science as well as of applications such as biological sensors and catalysis.[2−5] Hydrogen bonding is expected to regulate electronic properties of solids and work as switching units for molecular devices. Rational design based on crystal engineering[2−4] including supramolecular chemistry[5] is particularly important for the progress of this field. This is considered to be accomplished by fundamental studies on weak intermolecular interactions which govern orientation, recognition, and assembly of components in the solid state. Specific noncovalent interactions between different functionalities seem to control single and multicomponent crystallization.

Our work has focused on the development of new organic donor−acceptor (DA) interactions as supramo-

* To whom correspondence should be addressed. Phone: +81-45-924-5571. Fax: +81-45-924-5489.
† Institute for Molecular Science.
‡ Permanent address: Department of Applied Chemistry and Chemical Technology, University of Dhaka, Dhaka-1000, Bangladesh.
§ Tokyo Institute of Technology.

(1) Some reviews for hydrogen-bond donor and acceptor molecules: (a) Kyogoku, Y.; Lord, R. C.; Rich, A. *Proc. Natl. Acad. Sci. U.S.A.* **1967**, *57*, 250. (b) Martin, T. W.; Derewenda, Z. S. *Nat. Struct. Biol.* **1999**, *6*, 403. (c) Melandez, R. E.; Carr, A. J.; Linton, B. R.; Hamilton, A. W. In *Molecular Self-Assembly Organic Versus Inorganic Approaches*; Fujita, M., Ed.; Structure and Bonding, Vol. 96; Springer-Verlag: Berlin and Heidelberg, Germany, 2000; p 31. (d) Zimmerman, S. C.; Corbin, P. S. In *Molecular Self-Assembly Organic Versus Inorganic Approaches*; Fujita, M., Ed.; Structure and Bonding, Vol. 96; Springer-Verlag: Berlin and Heidelberg, Germany, 2000; p 63. (e) Jeffrey, G. A. *An Introduction to Hydrogen Bonding*; Oxford University Press: Oxford, U.K., 1997.

(2) (a) Mitani, T. *Mol. Cryst. Liq. Cryst.* **1989**, *171*, 343. (b) Gokel, G. W. *Chem. Soc. Rev.* **1992**, *21*, 39. (c) Izatt, R. M.; Bruening, R. L.; Tarbet, B. J.; Griffin, L. D.; Bruening, M. L.; Karkowiak, K. E.; Bradshaw, J. S. *Pure Appl. Chem.* **1990**, *62*, 1115. (d) McGrady, J. E.; Stranger, R. *J. Am. Chem. Soc.* **1997**, *119*, 8512. (e) Casades, I.; Fornes, V.; Gigante, B.; Garcia, H. *Chem. Phys. Lett.* **1999**, *305*, 365. (f) Chenthamarakshan, C. R.; Eldo, J.; Ajayaghosh, A. *Macromolecules* **1998**, *32*, 251. (g) Hulliger, J.; Langley, P. J.; Quintel, A.; Rechsteiner, P. Roth, S. W. In *Supramolecular Engineering of Synthetic Metallic Materials*; Veciana, J., Rovira, C., Amabilino, D. B., Eds.; NATO ASI Series C; Kluwer: London, 1999; p 67.

(3) For an overview of recent crystal engineering, see the following volumes: (a) *Comprehensive Supramolecular Chemistry*; Atwood, J. L., Davies, J. E. D., MacNicol, D. D., Vogtle, F., Lehn, J.-M., Eds.; Pergamon: Oxford, U.K., 1996; Vol 6. (b) *Crystal Engineering: The Design and Applications of Functional Solids*; Seddon, K. R., Zaworotko, M. J., Eds.; NATO ASI Series; Kluwer Academic: Dordrecht, The Netherlands, 1998. (c) *Design of Organic Solids*; Weber, E., Ed.; Topics in Current Chemistry; Springer-Verlag: Berlin and Heidelberg, Germany, 1998; Vol. 198. (d) *Crystal Engineering: From Molecules and Crystals to Materials*; Braga, D.; Grepioni, F.; Orpen, A. G., Eds.; NATO ASI Series C; Kluwer Academic: Dordrecht, The Netherlands, 1999. (e) *Molecular Self-Assembly Organic Versus Inorganic Approaches*; Fujita, M., Ed.; Structure and Bonding; Springer-Verlag: Berlin and Heidelberg, Germany, 2000; Vol. 96.

(4) Some crystal engineering reviews are: (a) Desiraju, *G. R. Crystal Engineering: The Design of Organic Solids*; Elsevier: Amsterdam, 1989. (b) Etter, M. C. *Acc. Chem. Res.* **1990**, *23*, 120. (c) Etter, M. C.; Urbanczyk-Lipkowska, Z.; Zia-Ebrahimi, M.; Panunto, T. W. *J. Am. Chem. Soc.* **1990**, *112*, 8415. (d) Zhao, X.; Chang, Y.-L.; Fowler, F. W.; Lauher, J. W. *J. Am. Chem. Soc.* **1990**, *112*, 6627. (e) Aakeroy, C. B.; Seddon, K. R. *Chem. Soc. Rev.* **1993**, 397. (f) Chang, Y.-L.; West, M.-A.; Fowler, F. W.; Lauher, J. W. *J. Am. Chem. Soc.* **1993**, *115*, 5991. (g) MacDonald, J. C.; Whitesides, G. M. *Chem. Rev.* **1994**, *94*, 2383. (h) Subramanian, S.; Zaworotko, M. *Coord. Chem. Rev.* **1994**, *137*, 354. (i) Russel, V. A.; Ward, M. D. *Chem. Mater.* **1996**, *8*, 1654. (j) Aakeroy, C. B. *Acta Crystallogr., Sect. B* **1997**, *53*, 569. (k) Desiraju, G. R. *Angew. Chem., Int. Ed. Engl.* **1995**, *34*, 2311. (l) Hosseini, M. W.; Andre, D. C. *Chem. Commun.* **1998**, 727. (m) Brammer, L.; Zhao, D.; Ladipo, F. T.; Braddock-Wilking, J. *Acta Crystallogr., Sect. B* **1995**, *51*, 632.

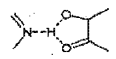
10.1021/jo001746i CCC: $20.00 © 2001 American Chemical Society
Published on Web 08/09/2001

UM00016826
NOVARTIS EXHIBIT 1517
Novartis v. Regents, IPR2023-01347
Page 3808 of 4460

本複製物は、特許庁が著作権法第４２条第２項第１号の規定により複製したものです。
取扱にあたっては、著作権侵害とならないよう十分にご注意ください。

lecular synthons for the preparation of ordered solid phases.[6] Our strategy is to investigate geometrically and stoichiometrically matched donor and acceptor molecules which can be used to propagate oriented patterns in the crystal engineering. We are concerned with the use of organic component molecules which can form a variety of structures and mediate electron−proton transfer. Employing organic molecules to form crystalline architectures seems an attractive idea for a crystal engineering approach. Simple association of two complementary compounds through noncovalent interactions can be used to create organic materials with new remarkable physical properties and potential applications in optical and electronic devices, which are not possessed by either of the components alone.[2c−e,13]

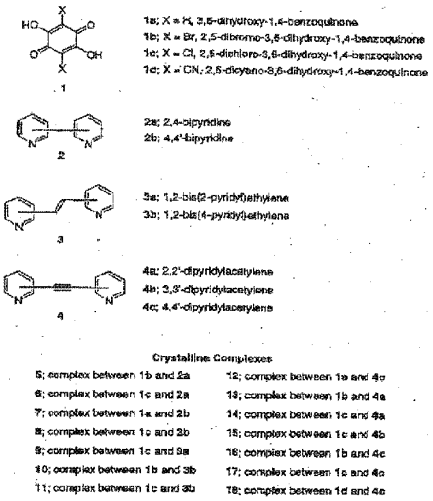
Our attempt is to develop a new tool for crystal engineering that is associated with a great variety of hydrogen-bonded DA-type compounds in which donor and acceptor molecules can be combined within robust hydrogen-bonded architectures. Development of new supramolecular synthons with specific bonding features is important to design materials with interesting features. We have chosen benzoquinone-type molecules with dihydroxy groups, anilic acids, which have excellent proton-donating properties and can undergo multistage deprotonation and protonation processes. These acids can be associated with a variety of proton acceptors as counterpart to give predictable supramolecular architectures. In the course of this work, we have prepared cyananilic acid (**1d**)[7] as a poor electron acceptor molecule and studied it as a hydrogen-bonded counterion in conducting charge-transfer complexes with a variety of organic sulfur-containing donors.[8,9] The monoanion and dianion of **1d** were assembled into supramolecular structures through the one- and two-dimensional hydrogen-bonded network.[10] In our preliminary communication, we have used dipyridyl-type bases as proton acceptors and constructed a new supramolecular synthon (**I**) motif.[11] We have also



I

prepared three rigid organic ligands containing pyridine rings separated by an acetylene spacer (**4a**−**c**) that formed crystalline complexes with a common organic acid (**1c**).[12] These complexes have infinite one-dimensional tapelike structures that lead to supramolecular polymeric systems. As a continuation of these works, we have attempted to combine a variety of proton donor and acceptor molecules to obtain novel supramolecular structures. In this paper, we will present the preparation of supramolecular complexes by complementary combination of proton donors (D) (anilic acids, **1**) and proton acceptors (A) (bidentate nitrogen ligands, **2**−**4**) via hydrogen-bonded interactions (Scheme 1).

Scheme 1



Results

Preparation of Cocrystals. Generally, the formation of cocrystals of proton donors (D) and acceptors (A) requires the following conditions: (i) D and A molecules matched geometrically and stoichiometrically, (ii) facile acid−base reactions between D and A molecules, (iii) good solubility of the D and A molecules in solvents, and (iv) precipitation of the formed complexes from the solution. Considering the above conditions, we have successfully obtained single crystals of complexes **5**−**18** composed of anilic acids and dipyridyl compounds. The following three simple procedures were used to obtain the above single crystals suitable for X-ray analysis: (i) slow diffusion using an H-shaped tube, (ii) mixing of two components in hot solutions, and (iii) slow evaporation technique. Methanol, ethanol, acetone, acetonitrile, and their mixture in various ratios were used as solvents for the preparation of these cocrystals. Details of the synthesis are explained in the Experimental Section.

Structural Analyses. The cocrystals of anilic acids with dipyridyl compounds obtained here take various

(5) (a) Lehn, J.-M. *Supramolecular Chemistry*; VCH: Weinheim, Germany, 1995. (b) *Comprehensive Supramolecular Chemistry*; Atwood, J. L., Davies, J. E. D., MacNicol, D. D., Vogtle, F., Lehn, J.-M., Eds.; Pergamon: Oxford, U.K., 1996; Vols. 1−11.

(6) (a) Greer, M. L.; Blackstock, S. C. *J. Org. Chem.* **1996**, *61*, 7895. (b) Blackstock, S. C.; Poehling, K.; Greer, M. L. *J. Am. Chem. Soc.* **1995**, *117*, 6617. (c) Greer, M. L.; McGee, B. J.; Rogers, R. D.; Blackstock, S. C. *Angew. Chem., Int. Ed. Engl.* **1997**, *36*, 1864. (d) McGee, B. J.; Sherwood, L. J.; Greer, M. L.; Blackstock, S. C. *Org. Lett.* **2000**, *2*, 1180.

(7) (a) Wallenfels, K.; Bachmann, G.; Hofmann, D.; Kern, R. *Tetrahedron* **1965**, *21*, 2239. (b) Zaman, M. B.; Morita, Y.; Toyoda, J.; Yamochi, H.; Sekizaki, S.; Nakasuji, K. *Mol. Cryst. Liq. Cryst.* **1996**, *287*, 249.

(8) Zaman, M. B.; Morita, Y.; Toyoda, J.; Yamochi, H.; Saito, G.; Yoneyama, N.; Enoki, T.; Nakasuji, K.; *Chem. Lett.* **1997**, 729.

(9) Zaman, M. B.; Toyoda, J.; Morita, Y.; Yamochi, H.; Saito G.; Nakasuji, K. *Synth. Met.* **1999**, *102*, 1691.

(10) Yamochi, H.; Nakamura, S.; Saito, G.; Zaman, M. B.; Toyoda, J.; Morita, Y.; Nakasuji, K.; Yamashita, Y. *Synth. Met.* **1999**, *102*, 1725.

(11) Zaman, M. B.; Tomura, M.; Yamashita, Y. *Chem. Commun.* **1999**, 999.

(12) Zaman, M. B.; Tomura, M.; Yamashita, Y. *Org. Lett.* **2000**, *2*, 273.

(13) (a) MacGillivray, L. R.; Spinney, H. A.; Reid, J. L.; Ripmeester, J. A. *Chem. Commun.* **2000**, 517. (b) Batchelor, E.; Klinowski, J.; Jones, W. *J. Mater. Chem.* **2000**, *10*, 839.

UM00016827
NOVARTIS EXHIBIT 1517
Novartis v. Regents, IPR2023-01347
Page 3809 of 4460

整理番号:　　発送番号:667861　発送日:平成21年10月 8日　　4

本複製物は、特許庁が著作権法第４２条第２項第１号の規定により複製したものです。
取扱にあたっては、著作権侵害とならないよう十分にご注意ください。

structures which were clarified by X-ray analysis. To rationally control the structures, we have examined the effects of the spacers and nitrogen positions in the dipyridyl compounds and substituents (H, Br, Cl, CN) of the anilic acid that influence the solubility, hydrogen-bonding ability, ionicity, geometry, and stacking arrangements of the molecules. The structures of the 14 complexes are discussed below. The geometry of the intermolecular hydrogen bonds for the complexes for which X-ray structures are first determined in this paper is summarized in Table 1.

Complexes 5 and 6. The complexes are isomorphous and crystallize in the monoclinic $P2_1/n$ space group, and the molecules **1b** in **5** and **1c** in **6** are located on the inversion center. The complexes have a 1:2 (D/A) stoichiometric ratio with the transfer of the two acidic protons of the donors to the nitrogen atoms of the acceptors to give a monoprotonated cation. The hydrogen atom positions in these cocrystals were identified on different Fourier maps and further confirmed by careful observation of C−O bond lengths and concerned hydrogen-bonding distances. The nitrogen atoms at the 4-position of the pyridine rings form a bifurcated interionic N^+−H···O^- (1.71 Å for **5** and 1.74 Å for **6**) and N^+−H···O (2.29 Å for **5** and **6**) hydrogen-bonded network (see Table 1). Thus, the robust synthon **I** generated at the 4-position forms molecular A···D···A-type pairs. The views of such crystalline architecture and their synthon **I** are shown in Figure 1. There is no hydrogen-bonding interaction in the nitrogen atom at the 2-position of the pyridine ring, and as a consequence, no infinite $(D\cdots A)_n$ linkage was observed, in contrast to the structures of 1:1 complexes described below. Moreover, the pyridine rings are twisted at the central C−C bond with a dihedral angle of 16.4° for **5** and 15.4° for **6** between the ring planes. Therefore, the nitrogen atom at the 2-position of the pyridine ring is diverted much closer to the adjacent hydrogen-bonded A···D···A pairs, where the distances between the planes of **1b,c** and **2a** within the DA pair are 3.42 Å for **5** and 3.40 Å for **6**. The distances between the planes of the 2-pyridine rings (3.43 Å for **5** and 3.40 Å for **6**) suggest closer AA interactions in the adjacent hydrogen-bonded A···D···A pairs. Thus, a pair of A···D···A aggregation is close-packed in alternated stacking arrangements with other pairs from the DA- or AA-type connectivity (Figure 2).

Complex 7. The complex crystallizes in the monoclinic $C2/c$ space group, and both **1a** and **2b** are located on the inversion center. The geometry and the C=O, C−OH, and C−C bond distances are consistent with those of the typical neutral anilic acids.[14] In this complex, no proton is transferred from the acid to the base molecule. However, intermolecular hydrogen-bonded H−O···N and =O···N distances of 2.63 and 3.08 Å are observed (Figure 3), which create the robust supramolecular synthon **I**. The **1a** and **2b** units are linked by O−H···N hydrogen bonds (1.55 Å) into a one-dimensional infinite molecular tape along the [1 0 2] direction. The angle between the two pyridine rings in **2b** is 29.2°, and two molecules of **1a** in the tapes tilt toward the pyridine rings with the angles of 19.6° and 48.6°. Each molecule in the tapes forms a segregated stacking along the [0 1 1] direction (Figure 4).

Complex 8. The complex crystallizes in the monoclinic $P2_1/n$ space group, and both **1c** and **2b** are located on the inversion center. In this complex, both of the hydroxyl protons are transferred from **1c** to the nitrogen atoms of the pyridine rings of **2b**, and attractive one-dimensional infinite molecular tape structures are formed through the robust supramolecular synthon **I**. Details of the crystalline architecture are described in our preliminary communication.[11] The C−O bond distances are shorter than those found in other dianion structures. The ring C−C bond distances are also consistent with those of the dianion with an aromatic ring.[14]

Complex 9. The complex crystallizes in the triclinic $P\bar{1}$ space group, and both **1c** and **3a** are located on the inversion center. In the complex **9**, the dianion of **1c** is observed and the dianion has similar C−O and C−C bond distances to those in the complex **8**.[11,14] The central C=C bond length [1.313(5) Å] of **3a** is a typical value of a double bond, and the configuration around the double bond is trans. The crystal architecture, stacking arrangement, and hydrogen-bonded linkage through the supramolecular synthon **I** are previously described and will not be discussed again.[11]

Complexes 10 and 11. The complexes are isomorphous and crystallize in the monoclinic $P2_1/c$ space group, and **1b,c** and **3b** are located on the inversion center. Both of the acids **1b**[15] and **1c**[14,15] are fully deprotonated to produce the dianions. These structures also involve bifurcated N^+−H···O hydrogen bonds (2.64 and 3.08 Å for **10**, 2.64 and 3.04 Å for **11**) between the nitrogen atoms of **3b** and the two oxygen atoms of **1b,c**, thus

Table 1. Geometry of the Intermolecular Hydrogen Bonds between the Anilic Acids and the Dipyridyl Compounds in the Complexes 5−7, 10−13, 16, and 18

		distance[a] (Å)				angle[b] (deg)
complex	D−H···A	D−H	H···A	D···A	D−H···A
5[c]	N2−H2A···O2^{i}	0.99(4)	1.71(4)	2.685(3)	155(3)
	N2−H2A···O1^{ii}	0.99(4)	2.29(4)	2.951(3)	123(3)
6[c]	N2−H2···O2^{iii}	0.96(3)	1.74(3)	2.621(2)	161(3)
	N2−H2···O2^{iii}	0.96(3)	2.23(3)	2.969(3)	127(2)
7	O1−H1···N1	1.15(6)	1.55(6)	2.641(6)	157(5)
10[c]	N1−H1···O1^{iv}	0.95(3)	1.71(3)	2.644(4)	167(3)
	N1−H1···O2^{iv}	0.95(3)	2.53(3)	3.077(4)	117(3)
11	N1−H1···O1	1.01(6)	1.68(6)	2.641(4)	164(5)
	N1−H1···O2	1.01(6)	2.49(6)	3.044(5)	114(4)
12	O1−H1···N1	1.07(5)	1.70(4)	2.654(3)	146(4)
13[c]	O2−H2A···N1^{v}	1.15(10)	1.59(10)	2.642(3)	145(8)
16[c]	N1−H1···O4^{vi}	1.04(6)	1.58(6)	2.577(4)	158(5)
	N1−H1···O8^{vi}	1.04(6)	2.34(5)	2.971(5)	118(4)
	O2−H2A···N2^{vii}	1.21(9)	1.45(9)	2.617(4)	164(7)
18[c]	N1−H1···O1^{viii}	0.86(2)	2.01(5)	2.738(3)	142(6)
	N1−H1···O2	0.86(2)	2.22(6)	2.927(9)	140(6)

[a] A hydrogen bond for which the H···A distance is below the sum of the covalent radius of A and 2.0 Å is listed. [b] A hydrogen bond for which D−H···A angle is above 110° is listed. [c] Symmetry code *i*: $x + 3/_{2}, -y + 3/_{2}, z - 1/_{2}$. *ii*: $-x + 3/_{2}, y - 1/_{2}, -z + 3/_{2}$. *iii*: $x + 3/_{2}, -y + 1/_{2}, z - 1/_{2}$. *iv*: $-x + 2, y + 1/_{2}, -z + 3/_{2}$. *v*: $x, y + 1, z - 1$. *vi*: $x - 1/_{2}, -y + 1/_{2}, z - 1/_{2}$. *vii*: $x + 1/_{2}, -y + 1/_{2}, z - 1/_{2}$. *viii*: $-x + 1, -y + 1, -z$.

(14) (a) Andersen, E. K. *Acta Crystallogr.* **1967**, *22*, 188. (b) Andersen, E. K. *Acta Crystallogr.* **1967**, *22*, 191. (c) Andersen, E. K. *Acta Crystallogr.* **1967**, *22*, 196. (d) Banchekrour, R.; Savariault, J.-M. *Acta Crystallogr., Sect. C* **1995**, *51*, 186. (e) Kanters, J. A.; Schouten, A.; Duisenberg, A. J. M.; Glowiak, T.; Malarski, Z.; Sobczyk, L.; Grech, E. *Acta Crystallogr., Sect. C* **1991**, *47*, 2143. (f) Zaman, M. B.; Tomura, M.; Yamashita, Y.; Sayaduzzaman, M.; Chowdhury, A. M. S. *CrystEngComm.* **1999**, 9.

(15) (a) Rohl, C. *Mater. Res. Bull.* **1987**, *22*, 1483. (b) Rohl, C.; Weiss, A. *Mater. Res. Bull.* **1987**, *22*, 497. (c) Aliev, A. G.; Kandrat'ev, S. I.; Atovmyan, L. O.; Karpov, V. V. *Bull. Acad. Sci. USSR* **1981**, *30*, 339.

UM00016828
NOVARTIS EXHIBIT 1517
Novartis v. Regents, IPR2023-01347
Page 3810 of 4460

本複製物は、特許庁が著作権法第４２条第２項第１号の規定により複製したものです。
取扱にあたっては、著作権侵害とならないよう十分にご注意ください。

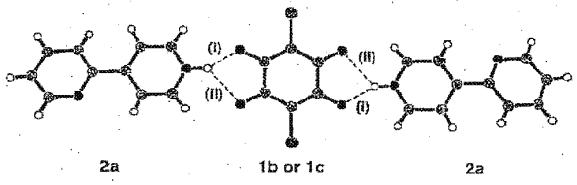


Figure 1. Hydrogen-bonded A···D···A pair of **5** and **6**. Dotted lines show the intermolecular N–H···O hydrogen bonds: (i) 1.71 Å for **5** and 1.74 Å for **6**; (ii) 2.29 Å for **5** and **6**.

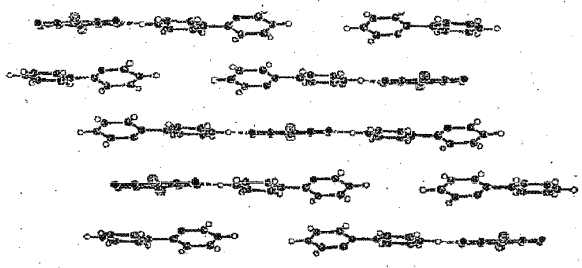


Figure 2. Alternated stacking arrangements of **6**, which contain pyridine rings–bromanilate rings and pyridine rings–pyridine rings overlaps. Dotted lines show the intermolecular N–H···O hydrogen bonds.

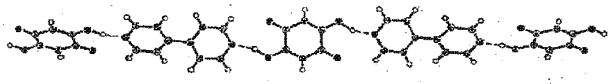


Figure 3. One-dimensional molecular tape of **7**. Dotted lines show the intermolecular O–H···N hydrogen bonds (1.55 Å).

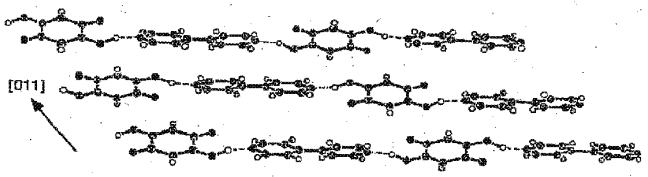


Figure 4. Segregated stacking arrangements along the [0 1 1] direction of **7**. Dotted lines show the intermolecular O–H···N hydrogen bonds.

creating the robust supramolecular synthon I. In both **10** and **11**, one-dimensional molecular tape structures are observed toward the two cross diagonal lines within the *ab* plane. The crossed tape structures are shown in Figure 5. Within the tape structures, the dihedral angles between the planes of **1b,c** and the pyridine rings are 24.2° and 23.5° for **10** and **11**, respectively. The molecular tapes in **10** and **11** run in a mild zigzag fashion because of the trans configuration of **3b**. Moreover, the molecules **1b,c** and **3b** in **10** and **11** compose alternated stacks along the [1 1 0] and [−1 1 0] directions (Figure 6). The DA pair in the alternated stacking involves close contacts between the adjacent tapes, where the distances between the planes of **1b,c** and **3b** are 3.55 and 3.53 Å for **10** and **11**, respectively.

Complex 12. The complex crystallizes in the monoclinic $P2_1/n$ space group, and both **1a** and **4c** are located on the inversion center. The bond distances and the angles of **1a** in **12** are similar to those in the complex **7**. Two molecules, **1a** and **4c**, connect with an intermolecular O–H···N hydrogen bonding (2.65 Å), and the dihedral angle between the planes of the pyridine ring of **4c** and **1a** is 4.5°. No proton transfer from **1a** to **4c** is observed. An infinite one-dimensional tape structure with an intertape distance of 3.4 Å is formed along the [2 0 1] direction. In addition, each component molecule forms a segregated stacking along the *a* axis (Figure 7).

Complexes 13 and 14. The complexes are isomorphous and crystallize in the triclinic $P\bar{1}$ space group, and both **4a** and **1b,c** are located on the inversion center. The

UM00016829
NOVARTIS EXHIBIT 1517
Novartis v. Regents, IPR2023-01347
Page 3811 of 4460

本複製物は、特許庁が著作権法第４２条第２項第１号の規定により複製したものです。
取扱にあたっては、著作権侵害とならないよう十分にご注意ください。

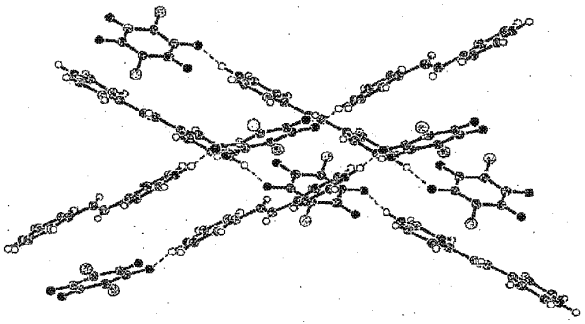


Figure 5. Two crossed one-dimensional molecular tapes of **16**. Dotted lines show the intermolecular N−H···O hydrogen bonds.

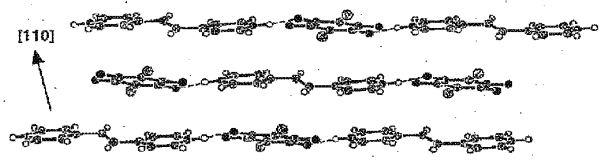


Figure 6. Alternated stacking arrangements along the [1 1 0] direction of **16**. Dotted lines show the intermolecular N−H···O hydrogen bonds.

molecular structure and stacking arrangements of the complex **13** are similar to those of the complex **14**, which was previously reported.[12] No proton transfer from **1b,c** to **4a** is observed. These complexes contain a zigzag one-dimensional tape structure with an infinite linkage of **1b,c** and **4a** through the supramolecular synthon I and have segregated stackings with DD- and AA-type pairs.

Complex 15. The complex crystallizes in the triclinic $P\bar{1}$ space group, and both **1c** and **4b** are located on the inversion center. The complex **15** contains 3.3 molecules of water. Both of the protons transfer from the hydroxyl groups of **1c** to the nitrogen atoms of **4b**. Thus, the two molecules, **1c** and **4b**, connect with interionic N^+−H···O^- (2.65 Å) and N^+−H···O= (2.87 Å) hydrogen bonds and form the supramolecular synthon I. The molecular architecture displays a zigzag tape structure, which is viewed as a square grid-type network along the *c* axis (Figure 8). Within the network, cavities are formed, which are occupied by the water molecules. Each component molecule forms a segregated stacking along the *c* axis. Details of this interesting structure are described in our preliminary communication.[12]

Complexes 16 and 17. The complexes are isomorphous and crystallize in the monoclinic $P2_1/n$ space group, and both **1b,c** and **4c** are located on a general position. The molecular structure and stacking arrangements of the complex **16** are similar to those of the complex **17**, which was previously reported.[12] In the crystal structure of **16**, one pyridine ring of **4c** is protonated and combines with **1b** via bifurcated N^+−H···O^- (2.58 Å) and N^+−H···O= (2.97 Å) hydrogen bonds, while the other pyridine ring is not protonated and forms H−O···N (2.62 Å) and =O···N (2.98 Å) hydrogen-bonding interactions (see Table 1). Thus, an infinite one-dimensional molecular tape structure is observed along the *c* axis (Figure 9). Two pyridine rings of **4c** in **16** are twisted with dihedral angles of 78.0°. In this work, **16** and **17** are the only examples of complexes containing a dipyridyl compound with two perpendicular pyridine rings. The dihedral angles between the planes of **1b** and the pyridine rings of **4c** are 73.5° and 4.5° for the nonprotonated and protonated side, respectively. The component molecule **1b** is partially overlapped with the protonated pyridine ring of **4c** and forms an alternated DA-type stacking along the *b* axis with **4c**.

Complex 18. The complex crystallizes in the triclinic $P\bar{1}$ space group, and both **1d** and **4c** are located on the inversion center. The geometry of **1d** has similar C−O and C−C bond distances to those of our previously described complexes of **1d**.[9,16] The component molecules **1d** and **4c** connect via the bifurcated N^+−H···O^- and N^+−H···O hydrogen bonds (N···O distances, 2.74 and 2.93 Å) and form the robust supramolecular synthon I. This is the first example of the supramolecular synthon I with **1d**. Thus, an infinite one-dimensional tape structure along the [1 1 0] direction is observed. The intertape distances, which are 3.22 and 3.42 Å for the distances between **1d**−**1d** and **4c**−**4c** planes, respectively, are very close. The dihedral angle between the plane of **1d** and the pyridine ring of **4c** is 59.6°. The most remarkable feature of the molecular tape in **18** is its bent structure with the angle of 121° at the hydrogen-bonding coupling part of the tape. This value is unusual compared to the

(16) Andersen, E. K.; Andersen, I. G. K. *Acta Crystallogr., Sect. B* **1975**, *31*, 379.

UM00016830
NOVARTIS EXHIBIT 1517
Novartis v. Regents, IPR2023-01347
Page 3812 of 4460

本複製物は、特許庁が著作権法第４２条第２項第１号の規定により複製したものです。
取扱にあたっては、著作権侵害とならないよう十分にご注意ください。

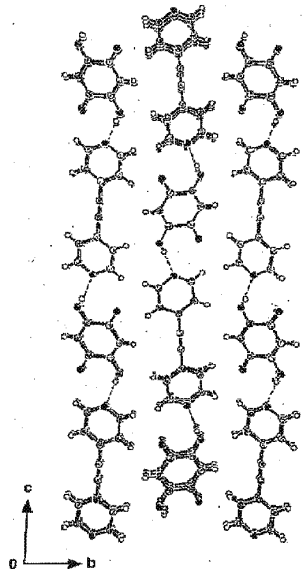


Figure 7. Packing diagram of **12** viewed along the *a* axis. One-dimensional molecular tape is formed along the [2 0 1] direction. Dotted lines show the intermolecular O−H···N hydrogen bonds (2.65 Å), and the C=O···N interaction is 3.04 Å.

other molecular tape structures described in this work (the corresponding angles for the tape structures of the complexes **7**, **10**−**14**, and **16** are 155°−178° with an average of 170°). Such features of the tape structure in **18** are illustrated in Figure 10. Each component molecule forms a segregated DD- and AA-type stacking along the *c* axis (Figure 11).

Discussion

We discuss here the factors determining the crystal structures described above. The structures of these complexes are related to the following factors: (i) the positions of the nitrogen atoms of the dipyridyl compounds, (ii) the proton-donating abilities of the acidic acids which are determined by the substituents, and (iii) the geometry of the one-dimensional molecular tape structures.

The donor−acceptor ratios of the complexes **5** and **6** are 1:2, while the other complexes **7**−**18** have 1:1 composition. The 1:2 complexes are obtained from only 2,4-bipyridine, while the 1:1 complexes are derived from the symmetrical dipyridyl compounds. In the 1:2 complexes, the hydrogen bond is formed at the 4-pyridyl ring and the nitrogen of the 2-pyridyl ring is not involved in the hydrogen bonding. This fact can be explained by the difference in the basicity of the pyridine rings depending on the nitrogen positions. The PM3 calculations[17] show that the net atomic charges of the nitrogen atoms of 4- and 2-pyridyl rings in 2,4-bipyridine are −0.0719 and −0.0668, respectively, suggesting that the basicity is higher at the 4-position than it is at the 2-position.

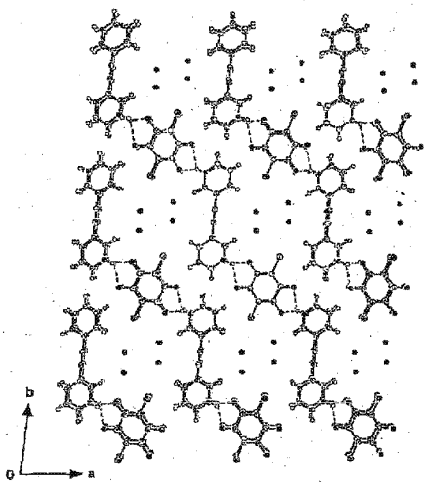


Figure 8. Square grid-type network of **15** viewed along the *c* axis. The cavities are occupied by the water molecules. Dotted lines show the intermolecular N−H···O hydrogen bonds.

In the 1:1 complexes, linear and zigzag molecular tape structures are observed. The linear tape structures are obtained only from the 4,4′-dipyridyl derivatives. On the other hand, the 2,2′- and 3,3′-isomers bring the zigzag tape structures. The 3,3′-isomer particularly gives a unique grid-like structure with a void. In the case of the complex **18**, the zigzag tape structure is produced despite the 4,4′-isomer **4c** in **18**. Compared with other zigzag tape structures, the zigzag tape in **18** bends at the coupling part via intermolecular hydrogen bonds or at the supramolecular synthon **I**. Such a conformation of the tape causes close packing of the tapes and stabilizes the crystal structure. It is noteworthy that the linear tape structures appear in the monoclinic crystal system and the triclinic crystal system affords zigzag tapes.

The positions of nitrogen atoms of the pyridyl groups also affect the ionicity of the complexes. In the complexes of **1c** with dipyridylacetylene **4** (complexes **14**, **15**, and **17**), the neutral (from the 2,2′-derivative **4a**), dication (from the 3,3′-derivative **4b**), and monocaction (from the 4,4′-derivative **4c**) states are observed. Although molecular packing and morphology in the solid state may affect the proton transfer to the nitrogen atoms of the pyridyl groups, the major reasons for these phenomena can be attributed to the differences in the basicity of the pyridyl groups depending on the nitrogen positions.[12] This is

(17) (a) Stewart, J. J. P. *J. Comput. Chem.* **1989**, *10*, 209. (b) Stewart, J. J. P. *J. Comput. Chem.* **1989**, *10*, 221.

UM00016831
NOVARTIS EXHIBIT 1517
Novartis v. Regents, IPR2023-01347
Page 3813 of 4460

本線製物は、特許庁が著作権法第４２条第２項第１号の規定により複製したものです。
取扱にあたっては、著作権侵害とならないよう十分にご注意ください。

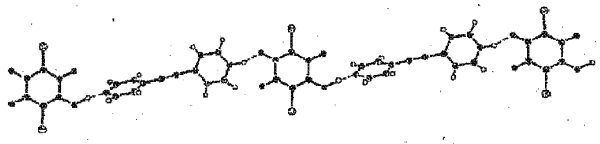


Figure 9. One-dimensional molecular tape of **16**. Dotted lines show two types of the intermolecular hydrogen bonds, N^+—H···O (1.58 Å) and O—H···N (1.42 Å).

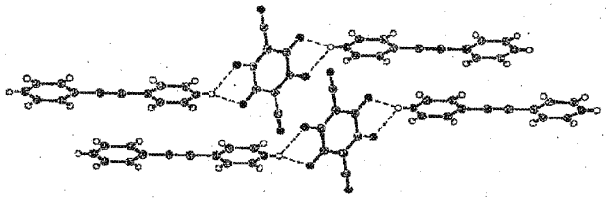


Figure 10. Two one-dimensional molecular tapes of **18**. Dotted lines show the intermolecular N^+—H···O hydrogen bonds (2.01 and 2.22 Å).

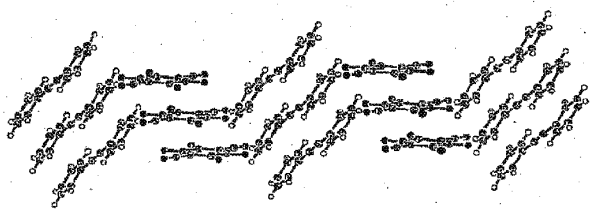


Figure 11. Segregated stacking arrangements along the c axis of **18**. The interstack distances are 3.22 and 3.42 Å for the stacks of **1d** and **4c**, respectively.

supported by the PM3 calculations of the net atomic charge of the nitrogen atoms of **4** (**4a**, −0.0607; **4b**, −0.0771; **4c**, −0.0742).

Among the four anilic acids used in this work, **1a** has the lowest proton-donating property, and the crystalline complexes **7** and **12** obtained from **1a** are neutral. Acids **1b** and **1c** with moderate proton-donating ability afford monoprotonated or deprotonated complexes with dipyridyl compounds containing nitrogen atoms at the 4- or 3-position of the pyridine rings. These acids form neutral complexes **13** and **14** with the weakest proton-accepting base **4a** containing nitrogen atoms at the 2-position of the pyridine rings. Only the crystalline complex **18** obtained from the strongest proton donor **1d** with **4c** is fully deprotonated and involves relatively short contacts between the neighboring donor and acceptor molecules. The acid **1d** rapidly produces colored powders with other dipyridyl compounds **2**—**4**, even if polar solvents are used for the preparation of complexes. The rapid complexation of **1d** is attributed to its strong proton-donating ability.

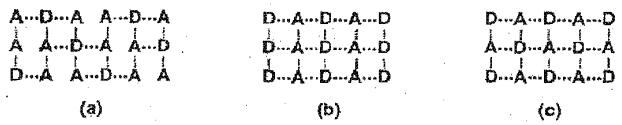
For the rational design of supramolecular architectures, strategies with structural predictability can be used in the construction of one-, two-, or three-dimensional patterns. A primary one-dimensional tape motif can be designed and obtained by using strong intermolecular interactions such as hydrogen bonding. The addition of functional groups or weaker intermolecular interactions to the tapes can expand the one-dimensional networks into two-dimensional layers or sheets. A three-dimensional supramolecular architecture can be achieved by the same process to connect the two-dimensional layers. In this study, we have found three types of stacking arrangements, the patterns of which are illustrated in Scheme 2. In the complexes **5** and **6**, the A···D···A units overlap two-dimensionally to form a cross-linked layer network (Scheme 2a). For the 1:1 complexes, the segregated stacks (Scheme 2b) are obtained in **7**, **9**, **12**—**15**, and **18** and the alternated ones (Scheme 2c) are realized in **8**, **10**, **11**, **16**, and **17**. The molecular tapes in the complexes which gave the segregated stacks are roughly planar, and the dihedral angles between the rings are small. Thus, the favorable overlapping of the tapes causes the segregated stacks. In contrast, the molecular tapes in **8**, **10**, **11**, **16**, and **17** have larger dihedral angles between the rings such as a chain. This steric effect and the favorable charge-transfer interactions between the anilic acids and the dipyridyl compounds might bring the alternated stacks.

UM00016832
NOVARTIS EXHIBIT 1517
Novartis v. Regents, IPR2023-01347
Page 3814 of 4460

整理番号: 発送番号:667861 発送日:平成21年10月 8日 9

本複製物は、特許庁が著作権法第４２条第２項第１号の規定により複製したものです。
取扱にあたっては、著作権侵害とならないよう十分にご注意ください。

Scheme 2



(a) (b) (c)

Conclusions

In this study, we have shown that the simple combination of anilic acids and dipyridyl compounds can create a variety of supramolecular architectures by self-assembly. The crystalline architectures described here are composed of an infinite one-dimensional molecular tape structure via the supramolecular synthon I with three types of intermolecular hydrogen bonds (N^+–H···O^-, N^+–H···O, and O–H···N). Strong resemblances between the crystal structures of the segregated stacking type (**7**, **9**, **12**–**15**, and **18**) or the alternated stacking type (**8**, **10**, **11**, **16**, and **17**) suggest the robustness and reproducing ability of the supramolecular synthon I. Charge-assistance effect[18] enhances the robustness of the synthon I in this system. The positions of the nitrogen atoms of the dipyridyl compounds strongly affect the crystalline architecture and ionicity of the component molecules which can be determined by proton transfer.

Although the anilic acids are well-known to form coordination bonds with a variety of metals,[14d,15a,b,19] they have not been well exploited for the rational design of organic solids.[20] This is the first example in which the anilic acids were used to create the supramolecular synthon I for crystal engineering purposes. The combination of two-component systems reported here may be a fundamental example for the design of low-dimensional structures. As an extension of our results, combination of other bidentate nitrogen ligands with proton donors would lead to an interesting crystalline architecture through a supramolecular synthon like I. Unusual physical properties such as conductivities may arise from charge-transfer interactions between component molecules.

Experimental Section

Starting Materials. Compounds **1d**,[7b] **4a**,[21] **4b**,[22] and **4c**[23] were prepared according to the literature methods. Other compounds, **1a**–**c**, **2**, and **3**, were commercially available and purified by usual methods. All the solvents were distilled before the use for the reactions.

General Procedures for the Preparation of Single Crystals. Method I. An equivalent molar amount (0.03–0.10 mmol) of the anilic acid and the dipyridyl compound was placed at the bottom of the H-shaped tube, and the tube was filled with solvents (10–25 mL). After 3–30 days, crystals grew at room temperature.

Method II. A solution of the anilic acid (0.05–0.10 mmol) in a freshly distilled hot solvent (5–15 mL) was mixed with a solution of the dipyridyl compound (0.05–0.10 mmol) in a distilled hot solvent (5–10 mL). Within a week, the crystals suitable for single-crystal X-ray diffraction appeared in the flask.

Method III. A solution of the anilic acid (0.05–0.10 mmol) in 10–20 mL of a dry solvent was added to a solution of the dipyridyl compound (0.05–0.10 mmol) in 10–15 mL of a dry solvent. Slow evaporation at room temperature for 1–3 days afforded the colored solution. The single crystals suitable for single-crystal X-ray diffraction were grown from this solution by complete or partial evaporation of the solvent from the reaction mixture. The crystals were characterized by IR, elemental analysis, and X-ray crystallographic analysis.

Complex 5. Red prismatic crystals were prepared from the mixture of acetone–methanol by method I in 96% yield; mp 201–202 °C; IR (KBr) 2350–2800, 2176 (broad), 1630 (sharp), 1517, 1470 cm^{-1}. Anal. Calcd for $C_{28}H_{12}N_6O_4Br_2$ (1:2): C, 51.17; H, 2.97; N, 9.13. Found: C, 51.09; H, 3.02; N, 8.98.

Complex 6. Red prismatic crystals were prepared from methanol and acetone by method I in 98% yield; mp 214–215 °C; IR (KBr) 2350–2800, 2176 (broad), 1630 (sharp), 1519, 1476 cm^{-1}. Anal. Calcd for $C_{28}H_{12}N_6O_4Cl_2$ (1:2): C, 59.90; H, 3.48; N, 10.75. Found: C, 59.86; H, 3.43; N, 10.70.

Complex 7. Orange plate crystals were prepared from acetone by method II in 90% yield; mp 164–165 °C; IR (KBr) 2360 (broad), 1637, 1601 cm^{-1}. Anal. Calcd for $C_{16}H_{12}N_2O_4$ (1:1): C, 64.86; H, 4.08; N, 9.46. Found: C, 64.67; H, 4.17; N, 9.28.

Complex 8. Brown needle crystals were prepared from acetone by method I in 98% yield; mp 228 °C dec; IR (KBr) 2400–2800, 2170 (broad), 1632 (sharp), 1504, 1488 cm^{-1}. Elemental analysis was previously described.[11]

Complex 9. Brown plate crystals were prepared from acetone–methanol by method I in 95% yield; mp 215–218 °C dec; IR (KBr) 2400–2800, 2124 (broad), 1640 (sharp), 1548, 1523 cm^{-1}. Elemental analysis was previously described.[11]

Complex 10. Brown rod crystals were prepared from acetone–methanol (2:1) by method I; yield 92%; mp 252–255 °C dec; IR (KBr) 2250–2700, 2132 (broad), 1625 (sharp), 1506 cm^{-1}. Anal. Calcd for $C_{16}H_{12}N_2O_4Br_2$ (1:1): C, 45.03; H, 2.52; N, 5.83. Found: C, 44.99; H, 2.54; N, 5.58.

Complex 11. Reddish brown prismatic crystals were prepared from acetone–methanol (1:1) by method II in 90% yield; mp 280–282 °C dec; IR (KBr) 2250–2700, 2152 (broad), 1624 (sharp), 1494 cm^{-1}. Anal. Calcd for $C_{16}H_{12}N_2O_4Cl_2$ (1:1): C, 55.26; H, 3.09; N, 7.16. Found: C, 55.18; H, 3.08; N, 7.05.

Complex 12. Orange rod crystals were prepared from acetonitrile–ethanol by method III in 84% yield; mp 195–196 °C; IR (KBr) 2354 (broad), 1648, 1618, 1607 cm^{-1}. Anal. Calcd for $C_{18}H_{12}N_2O_4$ (1:1): C, 67.50; H, 3.78; N, 8.75. Found: C, 67.04; H, 3.84; N, 8.68.

Complex 13. Brown needle crystals were prepared from acetone by method I in 92% yield; mp 190–192 °C; IR (KBr) 2473 (broad), 1660, 1601 cm^{-1}. Anal. Calcd for $C_{18}H_{10}N_2O_4Br_2$ (1:1): C, 42.22; H, 2.11; N, 5.86. Found: C, 44.86; H, 1.92; N, 5.77.

Complex 14. Brown needle crystals were prepared from methanol–acetone (1:1) by method I in 83% yield; mp 194–

(18) Braga, D.; Grepioni, F. *Acc. Chem. Res.* **2000**, *33*, 601.
(19) (a) Calvo, M. A.; Lanfredi, A. M. M.; Oro, L. A.; Pinillos, M. T.; Tejel, C.; Tiripicchio, A.; Ugozzoli, F. *Inorg. Chem.* **1993**, *32*, 1147. (b) Kawata, S.; Kitagawa, S.; Furuichi, I.; Munakata, M. *Angew. Chem., Int. Ed. Engl.* **1994**, *33*, 1759. (c) Kawata, S.; Kitagawa, S.; Kondo, M.; Kataka, M. *Synth. Met.* **1995**, *71*, 1917. (d) Decurtins, S.; Schmalle, H. W.; Zheng, L.-M.; Ensling, J. *Inorg. Chim. Acta* **1996**, *224*, 165. (e) Cueto, S.; Straumanu, H.-P.; Eys, P.; Petter, W.; Gramlich, V.; Rys, F. *Z. Acta Crystallogr., Sect. C* **1992**, *48*, 458.
(20) (a) Tomura, M.; Yamashita, Y. *CrystEngComm* **2000**, 16. (b) Ishida, H.; Kashino, S. *Acta Crystallogr., Sect. C* **1999**, *55*, 1149. (c) Ishida, H.; Kashino, S. *Acta Crystallogr., Sect. C* **1999**, *55*, 1714.
(21) Teitei, T.; Collin, P. J.; Sasse, W. H. F. *Aust. J. Chem.* **1972**, *25*, 171.
(22) Teitei, T.; Wells, D.; Sasse, W. H. F. *Aust. J. Chem.* **1978**, *26*, 2129.
(23) Tanner, M.; Ludi, A. *Chimica* **1980**, *34*, 23.

UM00016833
NOVARTIS EXHIBIT 1517
Novartis v. Regents, IPR2023-01347
Page 3815 of 4460

整理番号:　　発送番号:667861　発送日:平成21年10月 8日　　10/E

本複製物は、特許庁が著作権法第４２条第２項第１号の規定により複製したものです。
取扱にあたっては、著作権侵害とならないよう十分にご注意ください。

195 °C; IR (KBr) 2484 (broad), 1660, 1607 cm^{-1}. Elemental analysis was previously described.[12]

Complex 15. Brown plate crystals were prepared from acetone by method I in 93% yield; mp 176–178 °C; IR (KBr) 2454 (broad), 1660, 1607 cm^{-1}. Elemental analysis was previously described.[12]

Complex 16. Brown plate crystals were prepared from acetonitrile–acetone (1:4) by method I in 98% yield; mp 216–220 °C; IR (KBr) 2280–2650, 2164, 2081, 1630, 1601, 1520 cm^{-1}. Anal. Calcd for $C_{18}H_{10}N_2O_4Br_2$ (1:1): C, 45.22; H, 2.11; N, 5.86. Found: C, 45.11; H, 2.11; N, 5.42.

Complex 17. Brown needle crystals were prepared from acetonitrile–acetone (1:1) by method I in 90% yield; mp 230–231 °C; IR (KBr) 2280–2650, 2156, 2062, 1625, 1500 cm^{-1}. Elemantal analysis was previously described.[12]

Complex 18. Yellow needle crystals were prepared from acetonitrile by method II in 82% yield; mp >330 °C; IR (KBr) 2350–2880, 2203 (strong), 1632, 1543 cm^{-1}. Anal. Calcd for $C_{20}H_{10}N_4O_4$ (1:1): C, 63.69; H, 2.82; N, 15.84. Found: C, 64.01; H, 2.89; N, 15.42.

X-ray Crystallography. Reflection data were collected on a Rigaku AFC-7R diffractometer using Mo Kα radiation (λ = 0.710 69 Å) and Enraf-Nonius CAD4 diffractometer using Cu Kα radiation (λ = 1.541 78 Å) at 296 K. No absorption correction was applied for all crystals except the complexes **13** and **16**. Absorption correction was applied to **13** and **16** using empirical procedures based on azimuthal ψ scans of seven reflections having an Eulerian angle, χ, near 90°. All structures were solved by direct methods and refined by full-matrix least-squares on F^2 with SHELX-97.[24] All non-hydrogen atoms were refined anisotropically. All hydrogen atoms were localized in the Fourier maps and refined isotropically.

Crystal data for 5: $C_{28}H_{18}Br_2N_4O_4$, fw = 610.26, monoclinic, space group $P2_1/n$, a = 8.827(1) Å, b = 11.838(1) Å, c = 11.191(1) Å, β = 92.62(3)°, V = 1168.1(2) Å^3, Z = 2, D_c = 1.735 g cm^{-3}, $F(000)$ = 608, μ(Cu Kα) = 4.770 mm^{-1}, crystal dimensions = 0.20 × 0.20 × 0.20 mm^3, 2545 reflections collected, 2391 independent (R_{int} = 0.0356), R1 = 0.0349, wR2 = 0.0956 for $I > 2\sigma(I)$, R1 = 0.0389, wR2 = 0.0990, S = 1.069 for all data.

Crystal data for 6: $C_{26}H_{18}Cl_2N_4O_4$, fw = 521.34, monoclinic, space group $P2_1/n$, a = 8.6979(5) Å, b = 11.5877(6) Å, c = 11.2992(6) Å, β = 91.274(4)°, V = 1138.6(1) Å^3, Z = 2, D_c = 1.527 g cm^{-3}, $F(000)$ = 536, μ(Cu Kα) = 2.953 mm^{-1}, crystal dimensions = 0.25 × 0.10 × 0.10 mm^3, 2456 reflections collected, 2302 independent (R_{int} = 0.0222), R1 = 0.0358, wR2 = 0.0869 for $I > 2\sigma(I)$, R1 = 0.0701, wR2 = 0.1004, S = 0.998 for all data.

Crystal data for 7: $C_{16}H_{12}N_2O_4$, fw = 296.28, monoclinic, space group $C2/c$, a = 20.773(3) Å, b = 7.1001(7) Å, c = 9.157(1) Å, β = 93.855(7)°, V = 1348.3(3) Å^3, Z = 4, D_c = 1.460 g cm^{-3}, $F(000)$ = 616, μ(Cu Kα) = 0.892 mm^{-1}, crystal dimensions = 0.25 × 0.10 × 0.02 mm^3, 1184 reflections collected, 1150 independent (R_{int} = 0.1124), R1 = 0.0612, wR2 = 0.1267 for $I > 2\sigma(I)$, R1 = 0.2182, wR2 = 0.1859, S = 0.962 for all data.

Crystal data for 10: $C_{18}H_{12}Br_2N_2O_6$, fw = 480.12, monoclinic, space group $P2_1/c$, a = 8.3546(5) Å, b = 8.0001(6) Å, c = 13.261(1) Å, β = 104.495(6)°, V = 856.1(1) Å^3, Z = 2, D_c = 1.858 g cm^{-3}, $F(000)$ = 472, μ(Cu Kα) = 1.858 mm^{-1}, crystal dimensions = 0.10 × 0.10 × 0.10 mm^3, 1868 reflections collected, 1750 independent (R_{int} = 0.0202), R1 = 0.0341, wR2 = 0.0903 for $I > 2\sigma(I)$, R1 = 0.0523, wR2 = 0.1034, S = 0.870 for all data.

Crystal data for 11: $C_{18}H_{12}Cl_2N_2O_6$, fw = 391.20, monoclinic, space group $P2_1/c$, a = 8.3843(5) Å, b = 7.8904(6) Å, c = 12.926(3) Å, β = 105.053(7)°, V = 825.8(2) Å^3, Z = 2, D_c = 1.573 g cm^{-3}, $F(000)$ = 400, μ(Cu Kα) = 3.794 mm^{-1}, crystal dimensions = 0.10 × 0.10 × 0.02 mm^3, 1762 reflections collected, 1683 independent (R_{int} = 0.0492), R1 = 0.0468, wR2 = 0.1236 for $I > 2\sigma(I)$, R1 = 0.1204, wR2 = 0.1589, S = 0.818 for all data.

Crystal data for 12: $C_{18}H_{12}N_2O_4$, fw = 320.30, monoclinic, space group $P2_1/n$, a = 3.815(2) Å, b = 10.594(2) Å, c = 18.393(1) Å, β = 95.49(2)°, V = 740.0(4) Å^3, Z = 2, D_c = 1.438 g cm^{-3}, $F(000)$ = 332, μ(Mo Kα) = 0.104 mm^{-1}, crystal dimensions = 0.20 × 0.10 × 0.03 mm^3, 1529 reflections collected, 1352 independent (R_{int} = 0.0255), R1 = 0.0472, wR2 = 0.1088 for $I > 2\sigma(I)$, R1 = 0.1238, wR2 = 0.1280, S = 0.924 for all data.

Crystal data for 13: $C_{18}H_{10}Br_2N_2O_4$, fw = 478.10, triclinic, space group $P\bar{1}$, a = 8.9452(2) Å, b = 11.0548(4) Å, c = 11.0525(3) Å, α = 60.946(2)°, β = 95.49(2)°, γ = 84.022(3)°, V = 413.04(3) Å^3, Z = 1, D_c = 1.895 g cm^{-3}, $F(000)$ = 234, μ(Cu Kα) = 1.895 mm^{-1}, crystal dimensions = 0.35 × 0.10 × 0.02 mm^3, 1781 reflections collected, 1691 independent (R_{int} = 0.0141), R1 = 0.0320, wR2 = 0.0869 for $I > 2\sigma(I)$, R1 = 0.0350, wR2 = 0.0892, S = 1.015 for all data.

Crystal data for 16: $C_{18}H_{10}Br_2N_2O_4$, fw = 478.10, monoclinic, space group $P2_1/n$, a = 13.211(1) Å, b = 6.8099(8) Å, c = 18.895(2) Å, β = 95.49(2)°, V = 1696.5(3) Å^3, Z = 4, D_c = 1.872 g cm^{-3}, $F(000)$ = 936, μ(Cu Kα) = 6.316 mm^{-1}, crystal dimensions = 0.20 × 0.15 × 0.05 mm^3, 3505 reflections collected, 3459 independent (R_{int} = 0.0183), R1 = 0.0368, wR2 = 0.0986 for $I > 2\sigma(I)$, R1 = 0.0587, wR2 = 0.1113, S = 0.931 for all data.

Crystal data for 18: $C_{20}H_{10}N_4O_4$, fw = 370.32, triclinic, space group $P\bar{1}$, a = 8.910(7) Å, b = 9.827(14) Å, c = 5.323(6) Å, α = 102.71(14)°, β = 104.88(9)°, γ = 104.66(12)°, V = 415.0(8) Å^3, Z = 1, D_c = 1.482 g cm^{-3}, $F(000)$ = 190, μ(Mo Kα) = 0.107 mm^{-1}, crystal dimensions = 0.30 × 0.20 × 0.02 mm^3, 1620 reflections collected, 1516 independent (R_{int} = 0.1135), R1 = 0.0584, wR2 = 0.1150 for $I > 2\sigma(I)$, R1 = 0.3899, wR2 = 0.1880, S = 0.890 for all data.

Acknowledgment. We thank Professor K. Nakasuji, Dr. J. Toyoda, and Dr. Y. Morita of Osaka University for their continuous encouragement and advice for this work. M.B.Z. thanks the Institute for Molecular Science for postdoctoral fellowships. This work was supported by a Grant-in-Aid for Scientific Research from the Ministry of Education, Culture, Sports, Science and Technology, Japan.

Supporting Information Available: The X-ray crystallographic data (ORTEP drawings and tables of the crystal data, bond lengths and angles, atomic coordinates, and anisotropic thermal parameters) for **5**–**7**, **10**–**13**, **16**, and **18**. This material is available via the Internet at http://pubs.acs.org.

JO001746I

(24) Sheldrick, G. M., *SHELX-97. Program for the Solution and the Refinement of Crystal Structures*; University of Göttingen: Göttingen, Germany, 1997.

UM00016834
NOVARTIS EXHIBIT 1517
Novartis v. Regents, IPR2023-01347
Page 3816 of 4460

Steric Control of Secondary, Solid-State Architecture in 1:1 Complexes of Melamines and Barbiturates That Crystallize as Crinkled Tapes

Jonathan A. Zerkowski and George M. Whitesides*

Contribution from the Department of Chemistry, Harvard University, Cambridge, Massachusetts 02138

*Received August 28, 1992. Revised Manuscript Received March 2, 1994**

Abstract: This paper describes the single-crystal X-ray structures of four 1:1 complexes between *N,N'*-di(*tert*-butyl)-melamine and 5,5-disubstituted barbituric acids (substituents = CH_2CH_3, CH_2CF_3, CH_3, and C_6H_5). These complexes crystallize as infinite "crinkled" tapes having components joined by a triad of hydrogen bonds. The tapes are prevented from adopting a linear motif due to steric repulsion between *tert*-butyl groups on adjacent melamines; the crinkled motif avoids such repulsion. The tape backbones deviate from planarity to permit close packing of the crinkled tapes. Crystals of these complexes of a size and shape suitable for single-crystal X-ray diffraction analysis are readily grown; this system therefore seems well-suited for systematic study of the relationships between molecular and crystalline structure.

Introduction

We are studying the solid-state structures of 1:1 cocrystals of derivatives of melamine and of barbituric acid.[1-3] These cocrystals consist of crystallographically infinite hydrogen-bonded tapes that pack with their long axes parallel. By varying the steric properties of the substituents on the melamine component, we have prepared examples of linear tapes[3] and crinkled tapes.[2,4] We have also obtained one cyclic pseudo-C_3 structure (a "rosette").[2] These three structural motifs are the simplest ones that can be derived from the complex between cyanuric acid and melamine (CA·M).

Our previous work has kept the barbiturate component constant (as barbital, **Bar(Et)$_2$**), and varied the structure of the melamine. In the research reported in this paper, by contrast, we held the melamine component constant (as *N,N'*-di(*tert*-butyl)melamine, **Mel(tBu)$_2$**) and varied the barbiturate. One goal of this work was to test the hypothesis that sterically hindered substituents on the melamine would yield crinkled tapes. We chose **Mel(tBu)$_2$** because it is a truncated version of the melamine—*N,N'*-bis(4-*tert*-butylphenyl)melamine—that produced a rosette; we have rationalized the formation of the cyclic structure on the basis of the steric demands of the *tert*-butyl group.[2] We also wished simply to explore the influence of the substituents on the barbiturate on the solid-state structure: we are still surveying the range of solid-state structures accessible through manipulation of variants of CA·M, and we expect these data to complement those obtained in other studies.

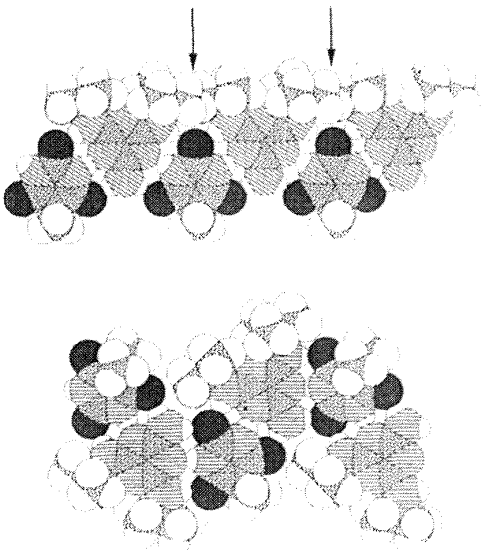
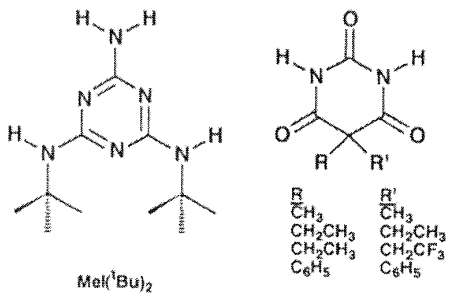


Figure 1. Top: Hypothetical linear tape of the **Mel(tBu)$_2$·Bar(CH$_3$)$_2$** complex, with regions of steric repulsion indicated by arrows. Bottom: The observed crinkled format of this complex, which relieves the steric hindrance.



Results

Formation and Features of Crinkled Tapes. The bulky *tert*-butyl substituent makes formation of linear tapes impossible for steric reasons. Figure 1 (top) shows regions of steric repulsion between the *tert*-butyl groups of adjacent melamines in a hypothetical linear tape incorporating **Mel(tBu)$_2$**. The bottom of the figure shows that the crinkled format avoids such steric repulsion: the *tert*-butyl groups are separated and are disposed on opposite sides of the tape.[5] One crystallographic axis (underlined in Table 1) is the repeat distance in a crinkled tape.

* Abstract published in *Advance ACS Abstracts*, April 1, 1994.

(1) Zerkowski, J. A.; Seto, C. T.; Wierda, D. A.; Whitesides, G. M. *J. Am. Chem. Soc.* **1990**, *112*, 9025.

(2) Zerkowski, J. A.; Seto, C. T.; Whitesides, G. M. *J. Am. Chem. Soc.* **1992**, *114*, 5473.

(3) Zerkowski, J. A.; MacDonald, J. C.; Seto, C. T.; Wierda, D. A.; Whitesides, G. M. *J. Am. Chem. Soc.* **1994**, *116*, 2382.

(4) Zerkowski, J. A.; Mathias, J. P.; Whitesides, G. M. *J. Am. Chem. Soc.*, following paper in this issue.

0002-7863/94/1516-4298$04.50/0 © 1994 American Chemical Society

UM00016835
NOVARTIS EXHIBIT 1517
Novartis v. Regents, IPR2023-01347
Page 3817 of 4460

Table 1. Crystallographic Data for **Mel(ᵗBu)₂·Bar(R)(R′)** Complexes

R,R′	space group	*a* (Å)	*b* (Å)	*c* (Å)	β[a] (deg)	*R*[b]	C_k*[c]	ρ[d] (g/cm³)	solvent[e] of crystallization	deviation from planarity[f] (Å)
Et, Et	$Pna2_1$	13.634	11.708	15.739[g]		0.037	0.62	1.149	MeOH	0.54
Et, CH_2CF_3	$P2_12_12_1$	12.975	15.709	12.796		0.089	0.61	1.214	EtOH	0.78
Me, Me	$P2_1/c$	11.451	16.285	11.665	98.23	0.052	0.66	1.217	MeOH	0.29
Ph, Ph	$P2_1/c$	15.103	15.829	12.642	114.65	0.060	0.68	1.254	MeOH	0.58

[a] A blank indicates that the angle is constrained to be 90°. [b] $R = \sum|F_o - F_c|/\sum F_o$. [c] This value is the packing coefficient based on molecular volumes calculated with MacroModel (see the Results section for the definition of C_k and ref 3 for a discussion of the relationship between C_k and C_k*). [d] This value is the calculated density. [e] No solvent is included in the crystal lattice in any of these complexes. [f] This value is the average deviation of the atoms in the tape backbone from the mean plane of the backbone. [g] The underlined cell dimensions represent the repeat distance in a tape (see the Results section).

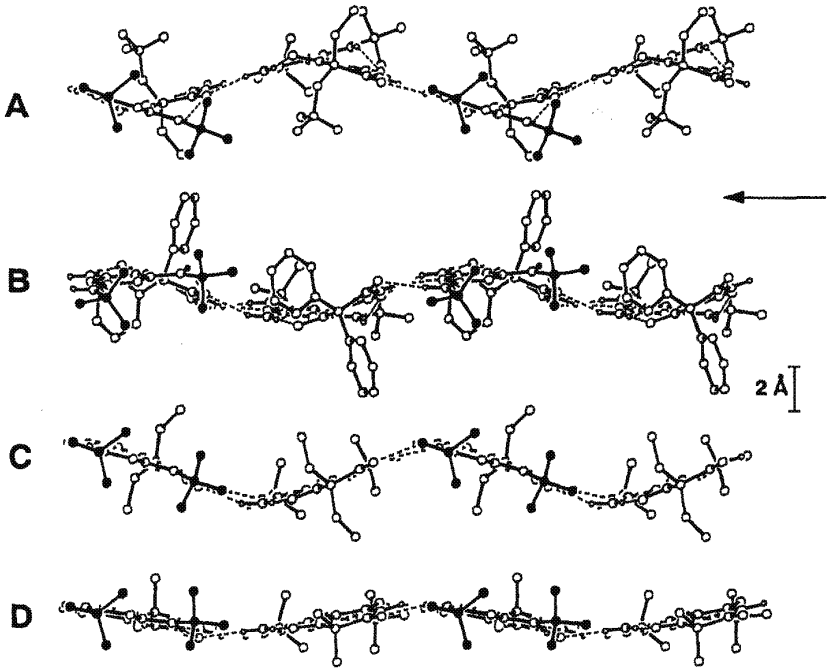


Figure 2. Side views of crinkled tapes of **Mel(ᵗBu)₂** complexes showing their deviation from planarity: (A) **Bar(Et)(CH_2CF_3)** complex; (B) **Bar(Ph)₂** complex; (C) **Bar(Et)₂** complex; (D) **Bar(CH_3)₂** complex. The deviation decreases from A to D (see Table 1). The arrow indicates the direction of a view down the long tape axes. The filled-in *tert*-butyl groups are on the edges of the tapes that are nearer to the viewer.

This distance is the length of a screw-related pair of Mel·Bar dimers along the tape axis, illustrated, for example, by the distance between symmetry-equivalent filled-in *tert*-butyl groups in Figure 2. Figure 2 also shows that the crinkled tapes deviate from planarity in a direction perpendicular to the infinite hydrogen-bonded axis. This deformation, or "waviness", turns the crinkled tapes into quasi-three-dimensional structures. To a first approximation, there is a rough trend between the degree of waviness and the size of the axis underlined in Table 1. The tape with the greatest deviation from planarity (the complex with **Bar(Et)-(CH_2CF_3)**) has the shortest unit projection (15.709 Å) along the tape axis.

At the macroscopic level, crystals of these crinkled tapes are blocky chunks or plates. Crystals of linear tapes, by contrast, were most frequently obtained as fine needles, a morphology that reflected the parallel packing of the linear tapes.[3] In addition, crystals of crinkled tapes were on average larger than crystals of linear tapes. A fixed-tube X-ray source, rather than a rotating anode generator, could therefore have been used for single-crystal X-ray analysis. Equally importantly, the crystals of these **Mel-(ᵗBu)₂** complexes were easier to grow than crystals of complexes of *para*-substituted diphenylmelamines and barbital.[3,6]

Solid-State Structures of Complexes of Mel(ᵗBu)₂·Bar(R)(R′). To convey the important points of intermolecular orientation, we have constructed conglomerate pictures (Figures 3–6) showing several views of tape packing at once. The deviation from planarity of these crinkled tapes makes them appear "thicker" than linear tapes in an end-on view. Nonetheless, such a view (looking down the crystallographically infinite hydrogen-bonded axis) is still useful in showing the relative orientation, or the tertiary architecture, of tapes. Table 1 lists crystallographic data and some geometric parameters of tape packing.

***N,N′*-Di(*tert*-butyl)melamine/Barbital, Mel(ᵗBu)₂·Bar(Et)₂ (Figure 3).** This complex was investigated to provide a comparison to our previous work on systems that contained **Bar(Et)₂** and substituted diphenylmelamines. The only variable structural unit in these cocrystals is thus the melamine, and crinkling can be attributed to its characteristics. The backbone of this tape is wavy (Table 1 and Figures 2 and 3): the average displacement of the atoms in the tape backbone from their own mean plane is

(5) Steric repulsion was also responsible for crinkling in the complex between *N,N′*-bis(4-methoxycarbonylphenyl)melamine and barbital that we reported previously.[2]

(6) This ready crystallization is attested to by the fact that the single crystals of **Mel(ᵗBu)₂·Bar(Et)₂** and **Mel(ᵗBu)₂·Bar(Et)(CH_2CF_3)** used for diffraction were obtained from the very first crystallization attempts made on these complexes.

UM00016836
NOVARTIS EXHIBIT 1517
Novartis v. Regents, IPR2023-01347
Page 3818 of 4460

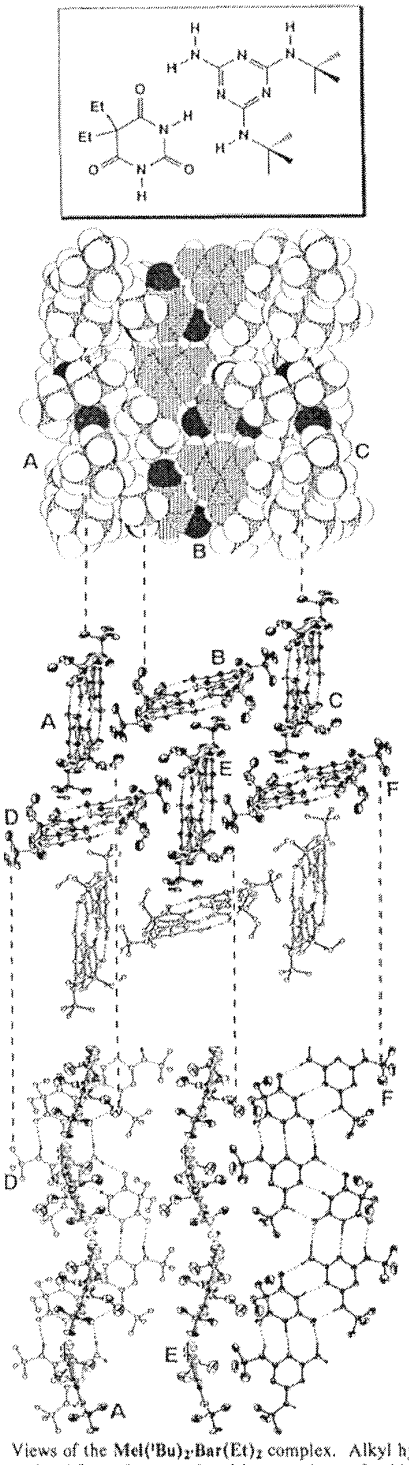


Figure 3. Views of the $Mel(^tBu)_2Bar(Et)_2$ complex. Alkyl hydrogens have been omitted from the central and bottom views. In this and the following figures, tapes that appear in more than one view are drawn with thermal ellipsoids in the central, end-on view and are connected with vertical dotted lines. In the bottom view, the highlighted tapes are nearer to the viewer.

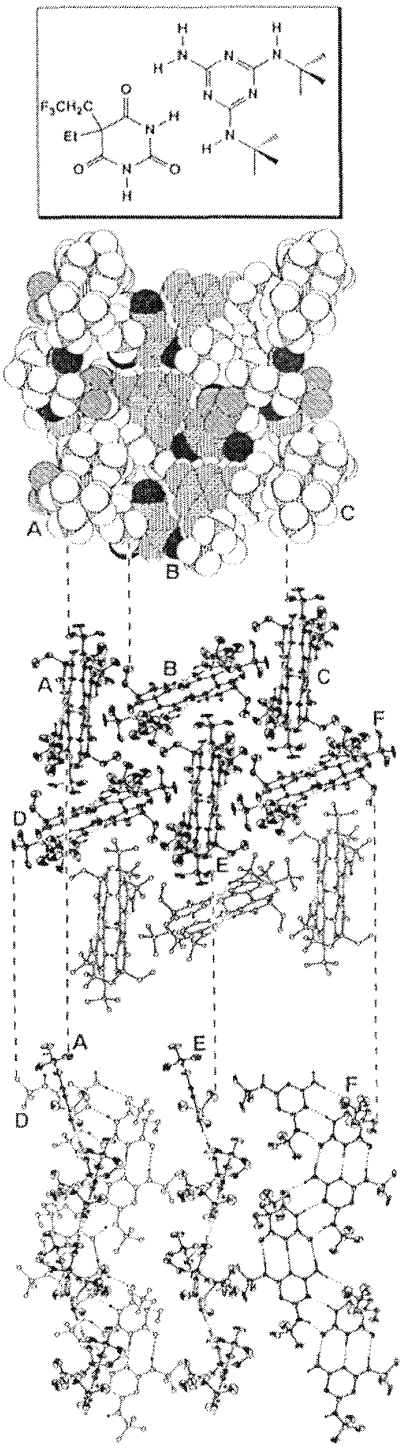


Figure 4. Views of the $Mel(^tBu)_2Bar(Et)(CH_2CF_3)$ complex. Alkyl hydrogens have been omitted from the central and bottom views.

0.54 Å.[7] By contrast, the seven linear tapes of complexes of *para*-substituted diphenylmelamines with barbital that we reported previously are less wavy, with an average deviation from planarity of 0.13 Å.[3]

(7) We define the mean plane of a tape as the six ring atoms of each heterocycle plus the three hydrogen-bonding exocyclic heteroatoms, three nitrogens for the melamine and three oxygens for the barbiturate.

UM00016837
NOVARTIS EXHIBIT 1517
Novartis v. Regents, IPR2023-01347
Page 3819 of 4460

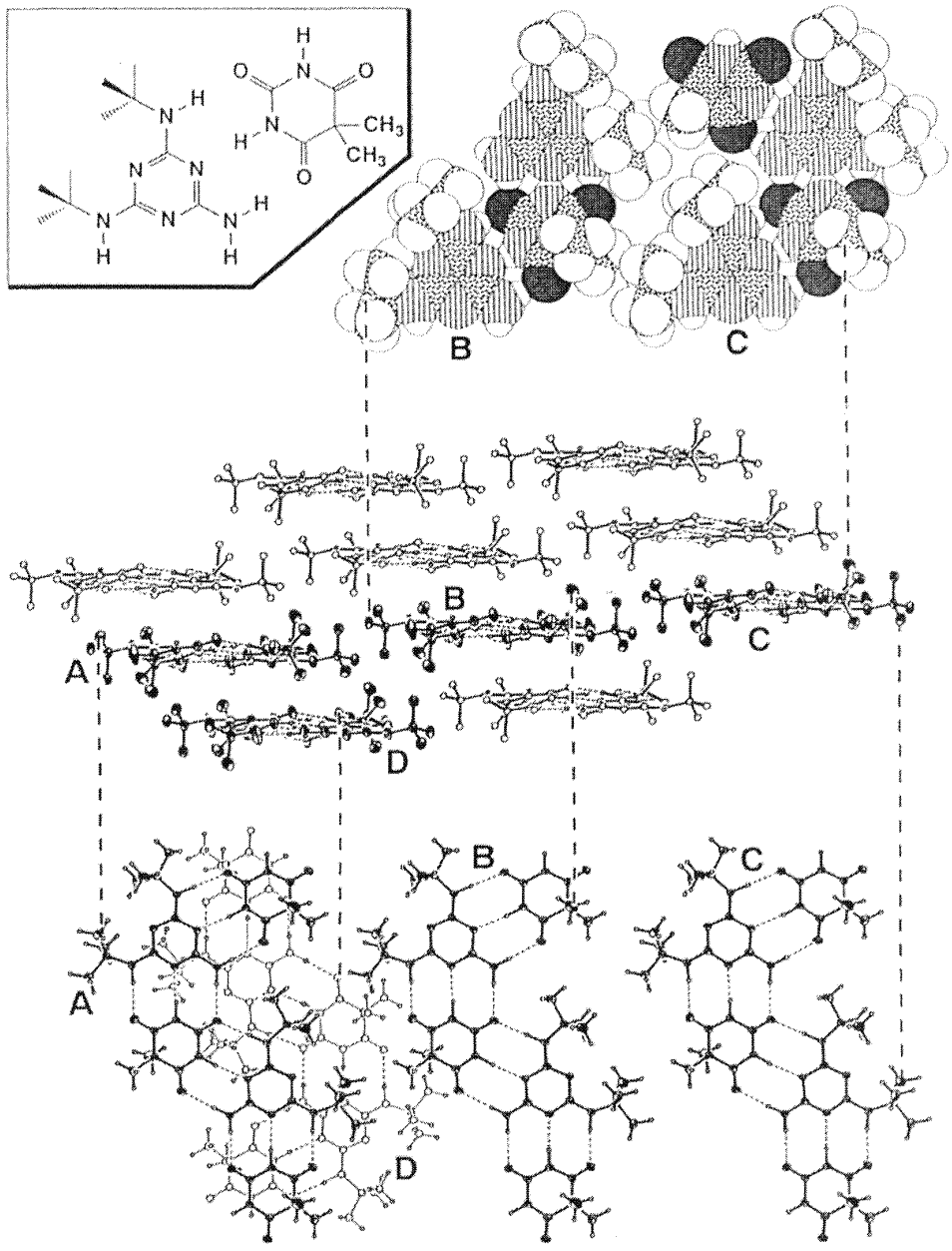


Figure 5. Views of the **Mel(ᵗBu)₂·Bar(CH₃)₂** complex. Alkyl hydrogens have been omitted from the central view.

***N,N'*-Di(*tert*-butyl)melamine/5-Ethyl-5-(2,2,2-trifluoroethyl)-barbituric Acid, Mel(ᵗBu)₂/Bar(Et)(CH₂CF₃) (Figure 4).** This complex represents a minimal steric perturbation on the **Bar(Et)₂** complex. We are also interested in studying the packing of compounds containing fluorocarbon units, to see if the fluorines segregate away from hydrocarbon regions or exhibit other patterns of behavior that might be used to control solid-state structure. The stacking of the **Mel(ᵗBu)₂·Bar(Et)(CH₂CF₃)** crinkled tapes is similar to that of the **Mel(ᵗBu)₂·Bar(Et)₂** tapes. In this solid-state structure, there are also no fluorine-rich regions and no contacts under the sums of van der Waals radii involving fluorines.

***N,N'*-Di(*tert*-butyl)melamine/5,5-Dimethylbarbituric Acid, Mel-(ᵗBu)₂·Bar(CH₃)₂ (Figure 5).** We investigated this complex because it is an abbreviated analogue of the **Bar(Et)₂** complex: that is, the size of the barbiturate substituent has been decreased. The tape backbones are less wavy than in the structures incorporating **Bar(Et)₂** and **Bar(Et)(CH₂CF₃)** (Table 1).

***N,N'*-Di(*tert*-butyl)melamine/5,5-Diphenylbarbituric Acid, Mel-(ᵗBu)₂·Bar(Ph)₂ (Figure 6).** In this complex, the steric perturbation of the barbiturate substituent is in the opposite direction from **Bar(CH₃)₂**: the phenyl groups are larger and more rigid than the ethyl groups. The phenyl rings are not packed in either edge-to-face or face-to-face orientations. There is, however, a CH···O contact (2.5 Å, $\sum_{vdW} \sim 2.7$ Å) between a barbiturate oxygen on one tape and an *o*-phenyl proton in an overlapping tape (e.g. tapes A and D in Figure 6).[8]

Packing Fractions (Table 1). The packing fraction C_k is a

UM00016838
NOVARTIS EXHIBIT 1517
Novartis v. Regents, IPR2023-01347
Page 3820 of 4460

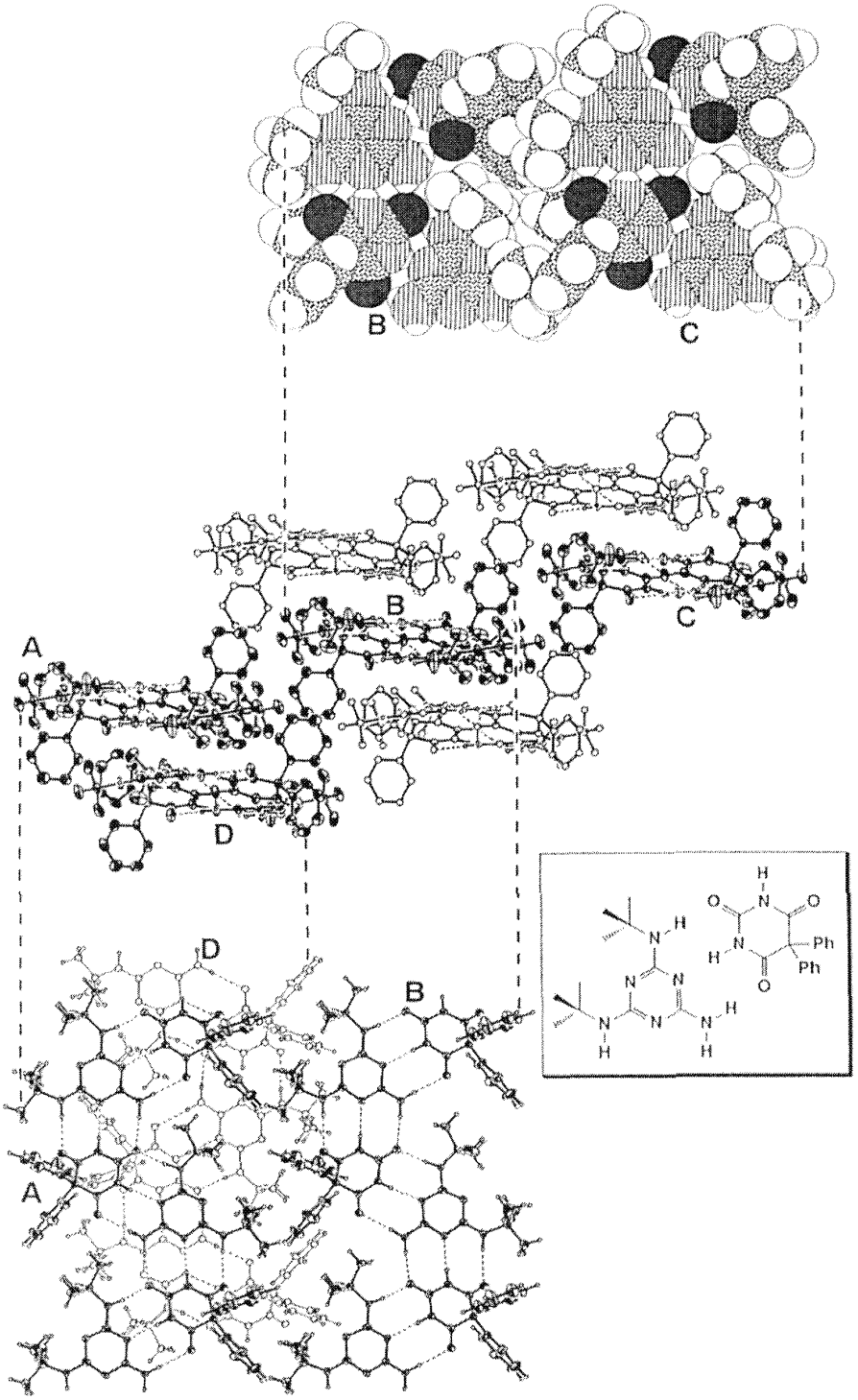


Figure 6. Views of the **MeI(ᵗBu)₂·Bar(Ph)₂** complex. Alkyl and aryl hydrogens have been omitted from the central view.

measure of the completeness with which the molecules of a crystal fill space;[9] our modified value C_k* is based on molecular volumes calculated using MacroModel.[10] The C_k* values for the two herringbone complexes, **MeI(ᵗBu)₂·Bar(Et)₂** and **MeI(ᵗBu)₂·Bar(Et)(CH₂CF₃)**, are at the lower end of the normal range.[11] Nonetheless, there are no discrete cavities large enough to allow inclusion of solvent molecules. The mean value for these four crinkled tape complexes, 0.64, is lower than that (0.69) for the

(8) We do not know if this contact is attractive or repulsive. For a discussion of CH···O contacts, see: Desiraju, G. R. *Acc. Chem. Res.* **1991**, *24*, 290.

UM00016839
NOVARTIS EXHIBIT 1517
Novartis v. Regents, IPR2023-01347
Page 3821 of 4460

linear tape complexes of *para*-substituted diphenylmelamines with barbital.[3]

Discussion

The results presented here confirm our hypothesis that steric hindrance involving the *tert*-butyl substituents of the melamine would force hydrogen-bonded tapes to pack in a crinkled motif rather than in a linear motif. The most important result of this work, therefore, is that the *secondary* crystalline architecture (the tape motif: *linear*, *crinkled*, or *cyclic*) of complexes of melamines and barbiturates can be predicted and controlled using steric effects. We have not yet searched for polymorphism in these complexes, but we do believe that **Mel(^{t}Bu)$_2$** will reliably yield crinkled tapes.

At the level of tertiary architecture (the stacking of tapes in the crystal), we propose that the deviation of crinkled tapes from planarity to produce a wavy shape (Figure 2) occurs to maximize packing efficiency. This observation is consistent with the broad guideline that, in crystals in general, intermolecular contact of van der Waals surfaces tends toward a maximum.[9,11] In these crystals of crinkled tapes, regions of space that would otherwise be voids are filled by the deformation of the hydrogen-bonded backbone of tapes from planarity. The views at the bottoms of Figures 3 and 4 illustrate this increased packing efficiency for the two complexes (those with **Bar(Et)$_2$** and **Bar(Et)(CH$_2$CF$_3$)**) that adopt the herringbone pattern. Two adjacent, perpendicular tapes fit together compactly, by matching the crinkling of one and the waviness of the other. Figure 7 presents a closeup view of these relationships.

In wavy tapes, the hydrogen bonds are bent from linearity. For the N–H···O bonds, the angles at hydrogen are 167°, 145°, 175°, and 157°, and for the N–H···N bonds, the angles are 174° and 173°. The hydrogen atoms involved in these hydrogen bonds were located crystallographically from electron density maps. Bent hydrogen bonds are frequently observed in crystal structures and do not appear to be energetically unfavorable (although there must be a level of deformation beyond which the tapes would not hold together).[12,13]

Conclusions

The four crystal structures of complexes of **Mel(^{t}Bu)$_2$** with barbiturates show that the triad of hydrogen bonds that holds together crystallographically infinite tapes is robust to substitutions that cause unfavorable intratape steric interactions. The formation of crinkled tapes can be rationalized using steric arguments: bulky substituents on the melamines (here, *tert*-butyl groups) prevent adoption of a linear format and force tapes to crinkle. In terms of designing organic solids, we expect to be able to use this effect to obtain crystals built from the crinkled structural motif. In fact, the ease of crystallization of these crinkled tapes recommends their use in systematic physical–organic studies of the solid state. Another result instructive for future work is that tapes are tolerant of different classes of substituents (alkyl and aryl groups) on both melamine and barbiturate components. Systematic variation on either component is a valid approach to crystal engineering.

(9) $C_k = N \cdot V_{mol}/V_{cell}$, where N is the number of molecules in a unit cell, V_{mol} is the molecular volume, and V_{cell} is the volume of the unit cell. Kitaigorodsky, A. I. *Organic Chemical Crystallography*; Consultants Bureau: New York, 1961.

(10) See ref 3 for a discussion of the relationship of C_k^* to C_k.

(11) Values of C_k usually range from roughly 0.65 to 0.77. Desiraju, G. R. *Crystal Engineering: The Design of Organic Solids*; Elsevier: New York, 1989.

(12) Taylor, R.; Kennard, O. *Acc. Chem. Res.* **1984**, *17*, 320.

(13) Gas-phase studies have shown that linear hydrogen bonds are the most stable (Legon, A. C.; Miller, D. J. *Acc. Chem. Res.* **1987**, *20*, 39). Crystals, however, need to balance a number of intermolecular forces, and hydrogen bonds seem to be able to deform to some extent to permit close packing between other parts of molecules.[11,12]

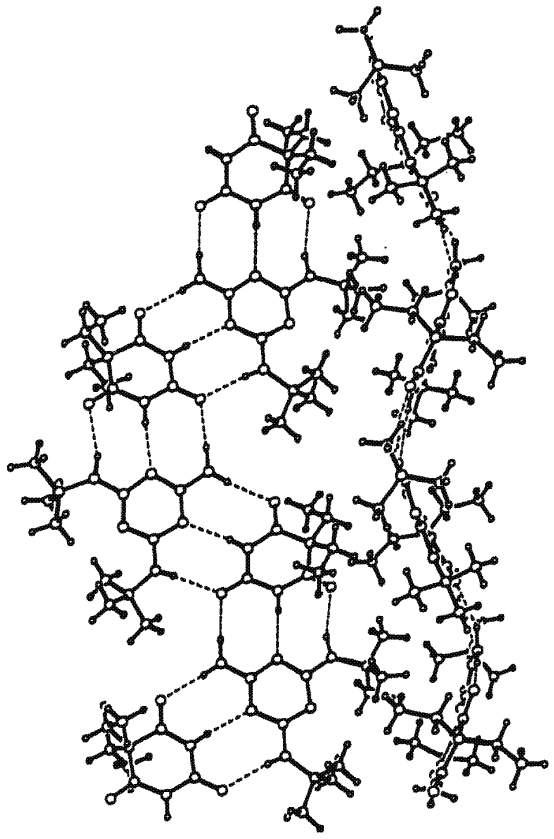


Figure 7. View of two adjacent, roughly perpendicular tapes of **Mel(^{t}Bu)$_2$·Bar(Et)$_2$** showing the steric complementarity of their fit. The tape on the right is viewed from the side; the tape on the left is tilted approximately 25° out of the plane of the page (see Figure 3). The deviations from planarity of the tape viewed perpendicularly to the mean plane of its hydrogen bond network (right) clearly are complementary to the protuberances and indentations of the quasiperpendicular tape (left).

While we still have no clear rationalization of intertape packing, we note that it is possible to relate the waviness of a tape—that is, the deviation of its hydrogen-bonded backbone from planarity—to the minimization of voids (and the maximization of the packing fraction, C_k) in the crystal. Crinkled tapes appear to deviate from planarity in order to pack as closely as possible to neighboring tapes. Since our system of tapes appears to be robust enough to tolerate a range of substitutional modifications, we believe that experiments designed to examine the consequences of steric perturbations on packing can be performed in a controlled and consistent fashion.

This system provides another model with which to study the physical–organic chemistry of the solid state. It should provide a consistent molecular framework—parallel, crinkled tapes—with which to probe relations between molecular and crystalline structure.

Experimental Section

General. *tert*-Butylamine was obtained from Aldrich Chemicals. Both 5,5-dimethylbarbituric acid[14] and 5,5-diphenylbarbituric acid[15] were prepared by literature procedures. General techniques were as previously published.[3]

(14) (a) *Organic Syntheses*; Blatt, A. H., Ed.; Wiley and Sons: New York, 1943; Collect. Vol. II, p 60. (b) Thorne, J. T. *J. Chem. Soc.* **1881**, *39*, 543.

(15) McElvain, S. M. *J. Am. Chem. Soc.* **1935**, *57*, 1303.

UM00016840
NOVARTIS EXHIBIT 1517
Novartis v. Regents, IPR2023-01347
Page 3822 of 4460

2-Amino-4,6-bis(*tert*-butylamino)-1,3,5-triazine (Mel(^{t}Bu)$_2$). A solution of cyanuric chloride (2.0 g, 10.8 mmol) was prepared in 100 mL of freshly distilled THF in a round-bottomed flask and cooled in an ice-water bath. A solution of *tert*-butylamine (1.14 mL, 10.8 mmol) and diisopropylethylamine (1.88 mL, 10.8 mmol) in 20 mL of THF was added from a dropping funnel over the course of 15 min with magnetic stirring. When addition was complete, the ice-water bath was removed and stirring was continued for another hour. The mixture was heated to reflux in an oil bath and another equivalent each of *tert*-butylamine and diisopropylethylamine (in 20 mL of THF) was added. Since the boiling point of *tert*-butylamine is 46 °C, some of this compound was lost to the atmosphere, even with a water-cooled condenser affixed to the reaction flask. Over the course of another 3 h, additional portions of a *tert*-butylamine solution in THF were added to the reaction, amounting to an additional 0.4 equiv. This amount was sufficient to produce primarily one product (2-chloro-4,6-bis(*tert*-butylamino)-1,3,5-triazine) as determined by TLC. The reaction was cooled to room temperature, and solvent was removed by rotary evaporation at aspirator pressure. The residue was slurried in 100 mL of diethyl ether and solids were removed by filtration at aspirator pressure through a short plug of silica gel, which was then washed with more diethyl ether (3 × 30 mL). The ether solutions were combined, and solvent was removed by rotary evaporation at aspirator pressure.

The 2-chloro-4,6-bis(*tert*-butylamino)-1,3,5-triazine was placed in a 15-mL pressure bottle along with a magnetic stirring bar, approximately 8 mL of 2:1 1,4-dioxane/H_2O, and 3 mL of 30% NH_4OH. The pressure bottle was capped and heated in an oil bath to 100–105 °C (**CAUTION: behind a safety shield**). Heating was continued for 5 h, after which the pressure bottle was cooled to room temperature and opened. TLC indicated that some starting material remained, but the most intense spot was the product di(*tert*-butyl)melamine. The reaction mixture was poured into 150 mL of H_2O and stirred well. The precipitated product was collected by vacuum filtration, washed with H_2O (2 × 25 mL), and dried on a vacuum line at 0.1 Torr for several hours. It was then purified by chromatography on silica gel with ethyl acetate as eluant (R_f = 0.3). The product, after rotary evaporation of solvent, was a white solid (1.57 g, 61%): melting point 166–7 °C; ^{1}H NMR (300 MHz, $CDCl_3$) δ 4.85 (br s, 2 H), 4.5 (br s, 2 H), 1.4 (s, 18 H); HRMS-EI (M^+) calcd for $C_{11}H_{22}N_6$ 238.1906, found 238.1913.

5-Ethyl-5-(2,2,2-trifluoroethyl)barbituric acid. The precursor 2,2,2-trifluoroethyl trifluoromethanesulfonate was prepared by a literature procedure from 2,2,2-trifluoroethanol, $(CF_3SO_2)_2O$, and pyridine in $CFCl_3$.[16] A solution of this trifluoromethanesulfonate (2.46 g, 10.6 mmol) in 10 mL of freshly distilled diethyl ether was added over the course of 30 min from a dropping funnel to a refluxing solution of diethyl malonate (1.52 mL, 10 mmol) and NaH (80% by weight, 0.30 g, 10 mmol) in 100 mL of EtOH. Reflux was continued for 3 h, at which point an aliquot was removed, concentrated by rotary evaporation at aspirator pressure, and dried on a vacuum line at 0.1 Torr. The desired diethyl 2,2,2-trifluoroethylmalonate had been formed, as determined by ^{1}H NMR spectroscopy and comparison to literature chemical shifts.[17] Refluxing was continued for another 2 h, after which ethyl iodide (1.2 mL, 15 mmol) and powdered anhydrous K_2CO_3 (1.66 g, 12 mmol) were added to the mixture. Reflux was continued for 3 days. The reaction mixture was cooled to room temperature and solids were removed by filtration at aspirator pressure. Solvent and excess ethyl iodide were removed from the filtrate by rotary evaporation at aspirator pressure. The resulting colorless oil was judged by ^{1}H NMR spectroscopy to be sufficiently pure diethyl ethyl(2,2,2-trifluoroethyl)malonate to proceed to the next step.

A solution of the malonate (1.5 g, 5.6 mmol) in 20 mL of dry EtOH was added in one portion to a gently refluxing homogeneous solution of urea (0.53 g, 8.8 mmol) and sodium (0.37 g, 16 mmol) in 100 mL of dry EtOH in a round-bottomed flask in an oil bath. The temperature of the bath was increased to 105 °C, and reflux was continued overnight. The reaction was then cooled to room temperature and solvent was removed by rotary evaporation at aspirator pressure. The yellow residue thus obtained was dissolved in 50 mL of H_2O and washed with Et_2O (3 × 50 mL). The aqueous layer was neutralized by dropwise addition of concentrated HCl. The resulting white precipitate was collected by vacuum filtration at aspirator pressure and was recrystallized from hot water, giving 0.73 g (55%) of the barbituric acid. Chemical shifts of the ^{1}H NMR spectrum (300 MHz, acetone-d_6) agreed with literature values.[17]

Preparation of Complexes. Equimolar amounts of **Mel(^{t}Bu)$_2$** and the barbiturate were dissolved together (in one flask) in THF. The solvent was removed by rotary evaporation at aspirator pressure, and the composition of the complex was checked by ^{1}H NMR spectroscopy. If integration of peaks indicated that one component was present in excess, the other component was added to bring their ratio to 1:1. The melting points of the complexes were the following: **Mel(^{t}Bu)$_2$·Bar(Et)$_2$**, 236–8 °C; **Mel(^{t}Bu)$_2$·Bar(Et)(CH$_2$CF$_3$)**, 245–7 °C; **Mel(^{t}Bu)$_2$·Bar(CH$_3$)$_2$**, 248–50 °C; **Mel(^{t}Bu)$_2$·Bar(Ph)$_2$**, 264–6 °C dec.

Crystallization of Complexes. Mel(^{t}Bu)$_2$·Bar(Et)$_2$ and **Mel(^{t}Bu)$_2$·Bar(Ph)$_2$**: Crystals were grown by room-temperature evaporation of a solution of the complex in MeOH in a 5-mL screw-top vial with the lid resting loosely on top of the vial.

Mel(^{t}Bu)$_2$·Bar(Et)(CH$_2$CF$_3$) and **Mel(^{t}Bu)$_2$·Bar(CH$_3$)$_2$**: Crystals were grown by allowing a solution of the complex in boiling EtOH or MeOH, respectively, to cool to room temperature by enclosing a round-bottomed flask containing the solution in a corked Dewar flask. The Dewar flask was allowed to rest undisturbed for 24 h before opening it to check on the progress of crystal growth.

X-ray Crystallography. For details of X-ray data collection, structure solution, and refinement, see the supplementary material. Data were collected on **Mel(^{t}Bu)$_2$·Bar(CH$_3$)$_2$**, **Mel(^{t}Bu)$_2$·Bar(Et)(CH$_2$CF$_3$)**, and **Mel(^{t}Bu)$_2$·Bar(Ph)$_2$** by Molecular Structure Corp., The Woodlands, TX, on a Rigaku AFC5R diffractometer equipped with a rotating anode generator. These structures were solved and refined at Harvard using the Siemens SHELXTL-PLUS package of programs. Data collection, structure solution, and refinement for **Mel(^{t}Bu)$_2$·Bar(Et)$_2$** were performed by Crystalytics Co., Lincoln, NE.

Acknowledgment. We acknowledge the support of the National Science Foundation through Grants CHE-91-22331 to G.M.W. and CHE-80-00670 to the Department of Chemistry for the purchase of the Siemens X-ray diffractometer.

Supplementary Material Available: Crystallographic details including tables of atomic positional parameters and bond lengths and angles (65 pages); tables of observed and calculated structure factors (44 pages). This material is contained in many libraries on microfiche, immediately follows this article in the microfilm version of the journal, and can be ordered from the ACS; see any current masthead page for ordering information.

(16) Gassman, P. G.; Harrington, C. K. *J. Org. Chem.* **1984**, *49*, 2765.
(17) Muller, N. *J. Org. Chem.* **1986**, *51*, 263.

UM00016841
NOVARTIS EXHIBIT 1517
Novartis v. Regents, IPR2023-01347
Page 3823 of 4460

The C–H···O Hydrogen Bond in Crystals: What Is It?

GAUTAM R. DESIRAJU

School of Chemistry, University of Hyderabad, Hyderabad 500 134, India

Received May 28, 1991 (Revised Manuscript Received September 17, 1991)

The concept of a C–H···O hydrogen bond, which is becoming increasingly important for our understanding of how molecules align themselves in crystals, dates back to Pauling's observation that the boiling point of acetyl chloride (51 °C) is substantially higher than that of trifluoroacetyl chloride (<0 °C). He ascribed this discrepancy to hydrogen-bond formation even though the expected hydrogen-bonding groups are not present.[1] In other early studies, Glasstone suggested that complexes of haloforms with ketones (X_3C—H···O═C<) have a definite existence,[2] while Jeffrey correlated the relatively high melting point of dimethyl oxalate (54 °C) with methyl···carbonyl interactions in the crystal.[3] The ever-growing literature on C–H···O bonds, the increasing interest in molecular and crystal engineering,[4] and the work carried out in our laboratories during the last three years has prompted the writing of the present Account.

Posing the question in the title of this Account in a provocative article,[5] Donohue gave a derisive answer: "It isn't". His remark proved to be the nemesis of structural chemists, who for more than a decade thereafter shunned the idea of a C–H group forming a hydrogen bond with electronegative atoms. Donohue's comment was a rebuttal to Sutor, who assumed a van der Waals distance of 2.6 Å for the H···O contact and claimed that C–H···O hydrogen bonds exist in caffeine (H···O, 2.07 Å), theophylline (2.25 Å), and other compounds.[6,7] Donohue, however, argued that the 2.6-Å value was inappropriate. Quoting Ramachandran's values for "normally allowed" (2.4 Å) and "outer limit" (2.2 Å) O···H distances,[8] he claimed that no special bonding effects are needed to explain Sutor's C–H···O geometries. In retrospect, it is interesting to note that Ramachandran always believed that C–H···O hydrogen bonds exist and that they contribute significantly to the stability of biomolecules![9] The distance ranges were apparently mentioned by him merely to alert crystallographers about different types of O···H contacts. In the hiatus that followed, a solitary article by Cohen on the structural chemistry of quinones is noteworthy[10] because it hints that C–H···O bond strengths need not be well-correlated with O···H distances and because it identifies C–H···O interactions as "lateral" in crystal structures of planar molecules.

A landmark study by Taylor and Kennard in 1982 provided conclusive evidence of the existence of C–H···O hydrogen bonds in crystals.[11] These authors showed that C–H···O contacts are electrostatic and that they occur within certain distance (C···O, 3.0–4.0 Å) and angle (C–H···O, 90–180°) ranges. We identified these directional preferences in several crystal structures of planar oxygenated compounds,[12] and an Account published in 1986 delineates the role of these C–H···O interactions in crystal engineering.[13] The choice between several competing packing arrangements of these planar compounds may be understood *only* by a consideration of the directional properties of weak C–H···O bonds present in these structures.

Today, there is a consensus that C–H···O bonds have significant implications in many diverse areas of structural chemistry. These interactions are no longer considered an esoteric phenomenon with little practical importance or as a mere hunting ground for crystallographic disputes. Owing to the frequent occurrence of oxygen in organic compounds (68% of 1991 Cambridge Database[14] entries), thousands of crystal structures must contain short C···O distances, many of which could arise from C–H···O bonds. The significance of these C–H···O interactions in a particular structure increases with their number relative to the stronger O–H···O and N–H···O interactions. Further, the energy of the C–H···O bond (1–2 kcal/mol) is just in the range where it can compete with conformational forces in small molecules and with forces responsible for the tertiary structure of macromolecules. Accordingly, a preferred molecular conformation in an organic solvent may yield to an "unfavorable" conformation in aqueous media because of additional C–H···O stabilization, while an appropriate C–H···O bond may clinch the site of protein folding. C–H···O interactions seem to determine the ordering of CO and alkylidyne molecules in a mixed adsorbate on a clean Pt(111) surface,[15] and to specify the stereochemistry of CH_3OH inclusion within ZSM-5 zeolite channels.[16]

In this Account, an attempt has been made to understand the significance of C–H···O hydrogen bonds in organic crystals and to evaluate them more rigorously

Gautam R. Desiraju was born in Madras in 1952, obtained his Ph.D. in 1976 at the University of Illinois at Urbana–Champaign, and is now a Professor of Chemistry at the Central University of Hyderabad. His research interests are in the area of crystal engineering, molecular recognition, and materials chemistry.

(1) Pauling, L. *The Nature of the Chemical Bond*; 3rd ed.; Cornell University Press: Ithaca, 1960; p 459.
(2) Glasstone, S. *Trans. Faraday Soc.* **1937**, *33*, 200.
(3) Dougill, M. W.; Jeffrey, G. A. *Acta Crystallogr.* **1953**, *6*, 831.
(4) Desiraju, G. R. *Crystal Engineering: The Design of Organic Solids*; Elsevier: Amsterdam, 1989.
(5) Donohue, J. In *Structural Chemistry and Molecular Biology*; Rich, A., Davidson, N., Eds.; W. H. Freeman: San Francisco, 1968; pp 459–463.
(6) Sutor, D. J. *Nature* **1962**, *68*, 195.
(7) Sutor, D. J. *J. Chem. Soc.* **1963**, 1105.
(8) Ramachandran, G. N.; Ramakrishnan, C.; Sasisekharan, V. *J. Mol. Biol.* **1963**, *7*, 95.
(9) Ramakrishnan, C., personal communication, 1988.
(10) Bernstein, J.; Cohen, M. D.; Leiserowitz, L. In *The Chemistry of Quinonoid Compounds*; Patai, S., Ed.; Interscience: New York, 1974; p 37.
(11) Taylor, R.; Kennard, O. *J. Am. Chem. Soc.* **1982**, *104*, 5063.
(12) Sarma, J. A. R. P.; Desiraju, G. R. *J. Chem. Soc., Perkin Trans. 2* **1987**, 1195.
(13) Sarma, J. A. R. P.; Desiraju, G. R. *Acc. Chem. Res.* **1986**, *19*, 222.
(14) Allen, F. H.; Bellard, S.; Price, M. D.; Cartwright, B. A.; Doubleday, A.; Higgs, H.; Hummelink, T.; Hummelink-Peters, B. G.; Kennard, O.; Motherwell, W. D. S.; Rodgers, J. R.; Watson, D. G. *Acta Crystallogr.* **1979**, *B35*, 2331.
(15) Blackman, G. S.; Kao, C. T.; Bent, B. E.; Mate, C. M.; van Howe, M. A.; Somorjai, G. A. *Surf. Sci.* **1988**, *66*, 207.
(16) Catlow, C. R. A., personal communication, 1990.

0001-4842/91/0124-0290$02.50/0 © 1991 American Chemical Society

UM00016842
NOVARTIS EXHIBIT 1517
Novartis v. Regents, IPR2023-01347
Page 3824 of 4460

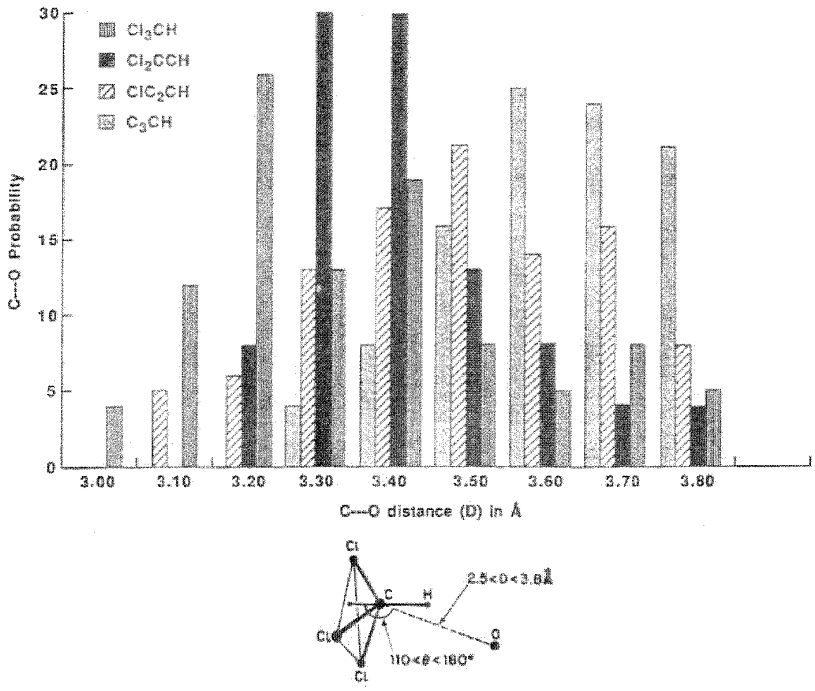
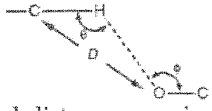


Figure 1. Schematic view of a C–H···O interaction in the compounds $(Cl_{3-n}R_n)CH$ showing chosen limits for distances (D) and angles (θ) along with histograms of C···O distances for the four compound categories (n = 0, 1, 2, 3). Note that the histograms are offset according to C–H acidity. C, C_2, and C_3 refer to any alkyl or aryl groups R which are not electron-withdrawing.

using criteria which are customary for the stronger N–H···O and O–H···O hydrogen bonds: lengths, angles, and effects on physical, spectroscopic, and crystallographic properties. One may ask: (a) Are certain intermolecular C–H···O lengths and angles characteristic of certain donor and acceptor groups? (b) Do C–H···O interactions resemble van der Waals forces or O–H···O and N–H···O hydrogen bonds? (c) Are some organic crystal structures defined and controlled by C–H···O interactions, or do structures merely accommodate the C–H···O geometry within the overall framework of van der Waals forces and strong hydrogen bonds?

C–H···O Lengths

The length, D, of a hydrogen bond is one of its most characteristic attributes. For strong bonds, O···O and N···O distances are centered around 2.75 and 2.85 Å, respectively, and cluster within a narrow range (0.2 Å).



These nonbonded distances are significantly shorter than the conventional van der Waals separations.[17] The value of D is more sensitive to the nature of the H atom than to the nature of the basic acceptor: the more acidic the hydrogen, the shorter the bond. For C–H···O bonds, the situation is far less clear-cut. Because of the very weakness of the interaction, C–H···O bonds can be distorted by other crystal forces and C···O distances with $3.0 < D < 4.0$ Å are common. Here, van der Waals radii are not so helpful.

At this point, it should be emphasized that such radii are empirical quantities that permit only an approximate rationalization of nonbonded distances in crystals. Deviations are marked for weaker interactions. The Sutor–Donohue–Ramachandran controversy arose largely because of the erroneous assumption that a particular set of van der Waals radii are constants of fundamental importance and that interactions may be termed "short" or "long" on this basis. Even anisotropic radii, advocated in recent times,[18,19] appear to be overparametrized quantities, allowing for good agreement with experiment but offering little by way of chemical insight. In general, the use of any one consistent set of isotropic radii is probably adequate. What is of *chemical* importance is a statistically significant shift toward shorter or longer intermolecular distances within a group of compounds.

The basic problem in evaluating the geometrical attributes of a weak interaction such as the C–H···O hydrogen bond is a high noise-to-information ratio. Since the interaction is so easily deformed, the variation in bond geometry is considerable and even careful crystallographic studies may not lead to sensible conclusions *if the number of structures sampled is small.* If a large number of structures are examined, however, systematic trends in the data may lead to a meaningful chemical result. Chemistry emerges from crystallography. A statistical approach, greatly facilitated by the availa-

(17) For instance, see: (a) Ramachandran, G. N.; Venkatachalam, C. M.; Krimm, S. *Biophys. J.* **1966**, *6*, 849. (b) Ramakrishnan, C.; Prasad, N. *Int. J. Protein Res.* **1971**, *III*, 209. (c) Mitra, G.; Ramakrishnan, C. *Int. J. Pept. Protein Res.* **1977**, *9*, 27. (d) Taylor, R.; Kennard, O.; Versichel, W. *J. Am. Chem. Soc.* **1983**, *105*, 5761.

(18) Nyburg, S. C.; Faerman, C.; Prasad, L. *Acta Crystallogr.* **1985**, *B46*, 592.

(19) Ishikawa, M.; Ikuta, S.; Katada, M.; Sano, H. *Acta Crystallogr.* **1990**, *B46*, 592.

UM00016843
NOVARTIS EXHIBIT 1517
Novartis v. Regents, IPR2023-01347
Page 3825 of 4460

bility of crystallographic databases, is therefore invaluable in the study of weak intermolecular interactions.

Accordingly, let us consider Figure 1, which is a histogram of C···O distances in chloroalkanes ($Cl_{3-n}R_n$)–C–H···O with $0 \leq n \leq 3$. The Cambridge Database was used to retrieve all ordered structures of chloroform solvates which have nonbonded contacts from the C–H group of $CHCl_3$ to an O atom.[20] The mean C···O length for the 100 retrieved contacts with $D < 3.90$ Å is 3.32 (2) Å. When contacts from C–H groups in compounds of the types $RCHCl_2$, R_2CHCl, and R_3CH to intermolecular O were also retrieved (excluding cases with strongly electron withdrawing substituents, R), the mean C···O lengths obtained for 23, 87, and 868 contacts respectively are 3.40 (3), 3.46 (2), and 3.59 (1) Å. The histograms for these four groups of compounds are offset regularly, showing that, in general, *shorter C–H···O contacts are obtained for more acidic C–H groups*. One must appreciate that this kind of information could not have been obtained from a few structures, since the histograms overlap in almost the entire range 3.00–4.00 Å and, in particular, in the region 3.30–3.80 Å.

A similar analysis was performed for C–H···O bonds involving alkyne (—C≡C—H···O) and alkene (>C═C(R)—H···O) groups.[21] The mean C···O distance for 105 alkyne geometries is 3.46 (2) Å while that for 622 alkene geometries is 3.64 (1) Å. This large difference cannot be rationalized on the basis of C–H bond length differences but must result from carbon acidity differences between alkyne and alkene C–H groups.

Are C–H···O distances greater than the van der Waals limit significant? The above results show that systematic gradations in C···O distances for different types of very weakly acidic C–H groups extend well beyond the "conventional" van der Waals limit. This means that the C–H···O contact is not really a van der Waals interaction but is primarily electrostatic, falling off much more slowly with distance. Now, electrostatic forces between approaching molecules prior to crystallization (r^{-1} dependence) are effective at distances longer than those at which dispersion forces (r^{-6}) are important. So, even long C···O separations (3.50–4.00 Å) may have to be considered seriously, and C–H···O bonds may have an orienting effect on molecules before the influence is felt of van der Waals forces which will eventually determine the packing of hydrocarbon residues in the crystal. If this is the case, the surprising constancy of the C–H···O angular geometry is readily explained.

C–H•••O Angles

The relatively fixed angular geometries of C–H···O bonds are striking because intermolecular angles are usually deformed more easily than lengths. The important angular attributes of the C–H···O bond are the C–H···O bending angle (θ) and the H···O–C angle (ϕ). While observed θ values cluster in the range 150–160°, Ramachandran and others have shown that, purely from geometrical considerations and excluding energy factors, the number of A–H···B bonds whose bending angle lies in the range θ to $\theta + d\theta$ is proportional to $2\pi \sin\theta\, d\theta$.[11,22,23] This geometrical correction leads to a distribution that is clearly indicative of a linear interaction.

Curiously, this tendency toward linearity is shared by both strong and weak C–H···O bonds. In the study of 622 alkene and 105 alkyne C–H···O bonds discussed above, there is a 50% (alkyne) and 60% (alkene) probability that θ lies in the range 165–180°. It is interesting that the longer alkene contacts are as linear as (or even more linear than?) the shorter alkyne contacts. In contrast, it appears that, for O–H···O and N–H···O hydrogen bonds, O···O and N···O nonbonded repulsions tend to straighten out the shorter bonds; in other words, the stronger the bond, the more linear it is likely to be.[24] That both strong and weak C–H···O bonds are linear would suggest that analogous C···O repulsion is not a major factor in determining bond linearity. Perhaps the C···O distances are too long for such repulsions to exert a significant effect on angle geometry. Alternatively, alkyl–oxygen repulsion (R···O), which is a possibility in alkenes (>C═C(R)—H···O) but not in alkynes (—C≡C—H···O), may result in the alkene contacts being more linear.

That the C–H···O bond is electrostatic in character is evidenced by the fact that the H atom tends to point toward the lone pairs of the O atom rather than be repelled by them, an illustration of the so-called Legon–Millen rules.[25] There is general agreement that, for carbonyl acceptors, the H···O═C angle ϕ is distributed around 120° and that the C–H group lies in the plane defined by the O lone pairs. For ethereal acceptors, the C–H bond tends to be in the plane of the O lone pairs, but the directional preferences within this plane, say toward the conventional lone pair directions, are far less apparent. These preferences or lack thereof have been justified theoretically.[26]

Spectroscopic Studies

If the C–H···O interaction is to be termed a hydrogen bond, appropriate spectroscopic measurements should reveal the effects of such bonding.[27] The C–H stretch in 1,3,5-trichlorobenzene is depressed by 35 cm^{-1} in the presence of pyridine, the result of a C–H···N bond.[28] Sim attempted to correlate IR spectral shifts of the C(sp)–H bond between dilute solution and the solid state with the corresponding C···O length in the crystal.[29] However, this work was inconclusive because C–H···O bonds with more or less identical geometrical properties (D, θ, ϕ) were found to have significantly different spectral shifts.[30] For example, in propargyl 2-bromo-3-nitrobenzoate (C···O, 3.39 Å), the spectral shift between the solid state and dilute CCl_4 solution is 47 cm^{-1}, but in triethylprop-2-ynylammonium *p*-bromobenzenesulfonate (C···O, 3.36 Å), the corresponding shift is 69 cm^{-1}. However, an increase from two to nine in the number of compounds studied sufficed to reveal clear chemical information. When we

(20) Desiraju, G. R. *J. Chem. Soc., Chem. Commun.* **1989**, 179.
(21) Desiraju, G. R. *J. Chem. Soc., Chem. Commun.* **1990**, 454.
(22) Balasubramanian, R.; Chidambaram, R.; Ramachandran, G. N. *Biochim. Biophys. Acta* **1970**, *221*, 196.
(23) Kroon, J.; Kanters, J. A.; van Duijneveldt-van de Rijdt, J. G. C. M.; Vliegenhardt, J. *J. Mol. Struct.* **1975**, *24*, 109.
(24) Taylor, R.; Kennard, O. *Acc. Chem. Res.* **1984**, *17*, 320.
(25) Legon, A. C.; Millen, D. J. *Acc. Chem. Res.* **1987**, *20*, 39.
(26) Legon, A. C.; Millen, D. J. *Chem. Soc. Rev.* **1987**, *16*, 467.
(27) Green, R. D. *Hydrogen Bonding by C–H Groups*; Wiley: New York, 1974.
(28) Allerhand, A.; Schleyer, P. v. R. *J. Am. Chem. Soc.* **1963**, *85*, 1715.
(29) Calabrese, J. C.; McPhail, A. T.; Sim, G. A. *J. Chem. Soc. B* **1966**, 1235.
(30) Calabrese, J. C.; McPhail, A. T.; Sim, G. A. *J. Chem. Soc. B* **1979**, 282.

UM00016844
NOVARTIS EXHIBIT 1517
Novartis v. Regents, IPR2023-01347
Page 3826 of 4460

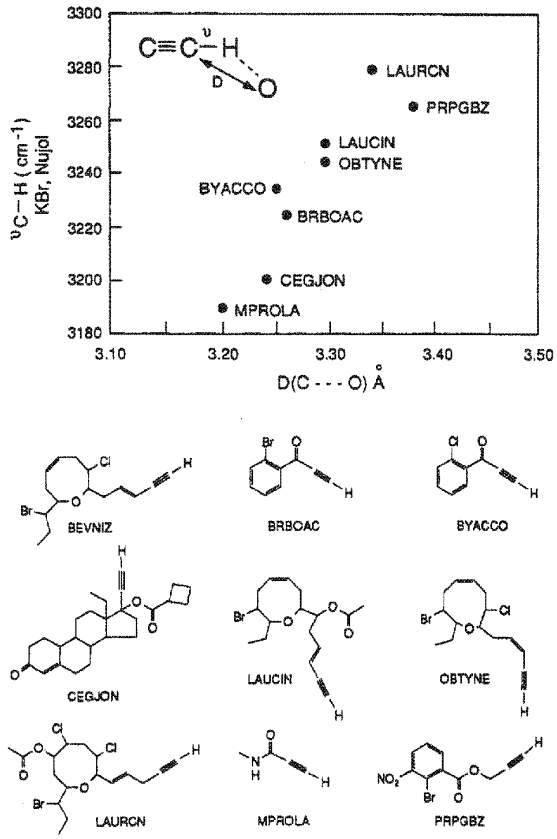


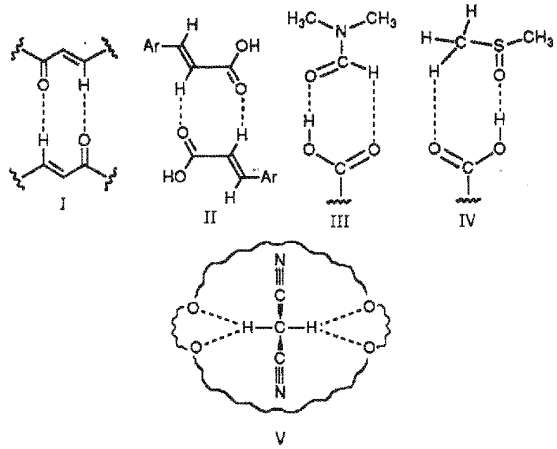
Figure 2. A correlation between crystallographic and spectroscopic (IR) properties of some C–H···O bonded terminal acetylenes. Structural formulas and Cambridge Database refcodes are given. In the compound BEVNIZ, the acetylenic H atom does not make a close approach to an intermolecular O atom and the C–H stretching frequency in the solid state and solution are identical.

redid Sim's work with nine terminal acetylenes, we noted a good correlation between the solid-state C(sp)–H stretching frequencies and intermolecular C···O distances (Figure 2).[31] The bromobenzenesulfonate studied by Sim now appears to be an outlier. We found that a closer approach of the oxygen atom progressively weakens the acetylenic C–H bond, suggesting that the C–H···O contact *is* a bonding interaction. Figure 2 also shows that the formation of a typical C–H···O bond with $D \sim 3.2$ Å releases an amount of energy equivalent to 100 cm^{-1}, that is, ca. 0.3 kcal/mol. Undoubtedly there is considerable scatter in C–H···O distances, and in retrospect, the early literature on C–H···O interactions appears confusing because a statistically significant number of compounds were not studied.

In general, a sufficiently activated C–H group seems to be required to observe consistent spectral shifts, and there exist a number of related studies involving acetylenes. The forbidden C≡C stretch in unsubstituted acetylene appears in the IR spectrum in the presence of donor solvents like acetone, indicating the removal of symmetry by intermolecular association.[27] Complexes of acetylene with water and other oxygen-containing bases have been isolated in inert matrices at low temperatures, and IR evidence of C–H···O bonding has been obtained.[32,33] The two activated methylene H atoms in the $\overset{O}{O}>CH_2$ group in 3,4-(methylenedioxy)-β-nitrostyrene form two C–H···O bonds (C···O, 3.15, 3.21 Å), and an IR spectral shift of 55 cm^{-1} between the solid state and $C_6H_5NO_2$ solution is obtained.[34] Activated C–H groups in quinones have been studied by solid-state ^{13}C NMR spectroscopy, and the chemical shifts of carbonyl C atoms that participate in >C=O···H—C hydrogen bonding are shifted downfield by 1–3 ppm from the corresponding solution values.[35] In comparison, the solid-state solution shift in a conventional >C=O···H—O hydrogen-bond situation is 8 ppm. The lack of proper spectroscopic evidence for C–H···O bonds formed by less activated C–H groups could stem from the fact that the spectral shifts are just not large enough. Alternatively, C–H···O interactions of weakly and strongly acidic C–H groups may be fundamentally different. However, not enough definitive work has been done to distinguish between these possibilities.

C–H • • • O Bonds and Crystal Engineering

The long-range, electrostatic and "orienting" nature of the C–H···O interaction determines its important role in crystal engineering. Common patterns such as I–V among others illustrate that the more acidic hydrogen atoms in organic molecules (alkyne > quinone > alkene > aromatic > aliphatic) tend to form C–H···O bonds more consistently and that, as far as possible, these bonds are adjusted within the framework of stronger interactions such as O–H···O and N–H···O hydrogen bonds.



A number of quinones and quinone complexes form C–H···O mediated layered crystal structures;[10] acetic acid forms a C–H···O stabilized catemer rather than a dimer; and the syn–anti conformational preference of crystalline α,β-unsaturated acids is strongly dependent on C–H···O bonding.[36] In general, a full understanding of the packing arrangement in an oxygen-containing organic crystal structure is possible only when the C–H···O bonds are considered. However, it is not easy to predict *any* arbitrary oxygenated crystal structure just

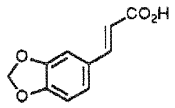
(31) Desiraju, G. R.; Murty, B. N. *Chem. Phys. Lett.* **1987**, *139*, 360.
(32) Peterson, K. J.; Klemperer, W. *J. Chem. Phys.* **1984**, *81*, 3842.
(33) De Laat, A. M.; Ault, B. S. *J. Am. Chem. Soc.* **1987**, *109*, 4232.
(34) Pedireddi, V. R.; Sarma, J. A. R. P.; Desiraju, G. R. *J. Chem. Soc., Perkin Trans. 2*, in press.
(35) Scheffer, J. R.; Wong, Y. F.; Patil, A. O.; Curtin, D. Y.; Paul, I. C. *J. Am. Chem. Soc.* **1985**, *107*, 4898.
(36) Berkovitch-Yellin, Z.; Leiserowitz, L. *Acta Crystallogr.* **1984**, *B40*, 159.

UM00016845
NOVARTIS EXHIBIT 1517
Novartis v. Regents, IPR2023-01347
Page 3827 of 4460

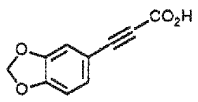
on the basis of C–H···O interactions.

Progress has been made in designing crystal structures of planar oxygenated aromatics that are determined by an interplay of herringbone-steering C···H interactions[37,38] and lateral C–H···O bonds which steer to stacked (or β) structures with short axes of 3.8–4.2 Å.[12,13] The inclined herringbone pattern may be stabilized by C(δ–)···H(δ+) interactions whereas the C···C stabilized stack structures are characterized by parallel, overlapped molecules. Planar aromatic hydrocarbons generally adopt the herringbone structure (or its variants) because C···H interactions predominate. Their oxygenated derivatives show a pronounced tendency to adopt the stack structure because the lateral nature of the C–H···O contacts, which arise from the O atoms, assists in the formation of two-dimensional motifs such as sheets or ribbons. The numbers of O and H atoms seem to determine if a herringbone or stack structure will be formed for a particular molecule. To summarize, the stack structure is favored by higher C:H ratios, and these ratios are effectively raised by an increasing number of O atoms.

These ideas have been applied in the design of crystal structures that permit an intermolecular solid-state Diels–Alder reaction.[39] The strategy involved identification of substances that may act as either diene or dienophile and will crystallize in a structure that permits a topochemical 4 + 2 conversion. Accordingly, substituted phenylpropiolic acids were considered; not only are they used in self-Diels–Alder reactions in lignan synthesis but the crystallographically related *trans*-cinnamic acids have been extensively investigated. The starting point in this crystal engineering exercise, the 4-Å stack structure of 3,4-(methylenedioxy)cinnamic acid (VI), was therefore chosen deliberately. The



VI



VII

crystal structure is layered, the layers being constructed by linking O–H···O bonded centrosymmetric dimers with C–H···O bonds. As described above, other factors being constant, a planar aromatic having a higher C:H ratio prefers the stack structure. Accordingly, one may extrapolate from the stack structure of VI, $C_{10}H_8O_4$, that of [3,4-(methylenedioxy)phenyl]propiolic acid (VII), $C_{10}H_6O_4$. Both VI and VII are planar molecules with similar volumes, shapes, and functionalities. The smaller number of H atoms in VII was expected therefore to enhance the tendency for stack structure adoption.

This prediction was confirmed; acids VI and VII are isomorphous, and Figure 3 shows that VII molecules form a compact sheet characterized by O–H···O (O···O, 2.63 Å) and C–H···O (C···O, 3.36, 3.39 Å) bonds. These bonds stabilize the sheet motif and with it the stacked β-structure. Analogously, (3,4-dimethoxyphenyl)- and (3,4,5-trimethoxyphenyl)propiolic acids, both of which are efficiently C–H···O bonded, also form layered 4-Å structures.[40] Almost predictably, phenylpropiolic acid

(37) Desiraju, G. R.; Gavezzotti, A. *J. Chem. Soc., Chem. Commun.* **1989**, 621.
(38) Desiraju, G. R.; Gavezzotti, A. *Acta Crystallogr.* **1989**, *B45*, 473.
(39) Kishan, K. V. R.; Desiraju, G. R. *J. Org. Chem.* **1987**, *52*, 4640.

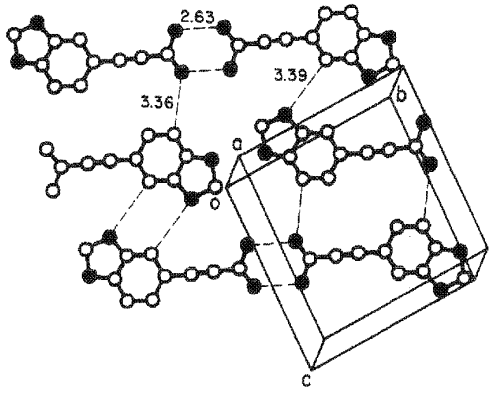


Figure 3. View of the crystal structure of [3,4-(methylenedioxy)phenyl]propiolic acid (VII) down the 4-Å short axis. Oxygen atoms are shaded. C–H···O and O–H···O bonds are shown.

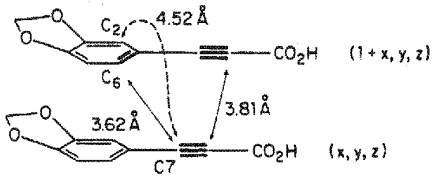


Figure 4. Schematic view of a topochemical Diels–Alder reaction for acid VII.

($C_6H_5C{\equiv}CCO_2H$) forms O–H···O hydrogen-bonded dimers which pack in a herringbone fashion since a paucity of O atoms results in a dovetailing of terminal phenyl groups so as to optimize C···H interactions. The theme conveyed is that a *critical number of oxygen atoms will permit a planar aromatic molecule to cross the structural threshold from a C···H stabilized herringbone structure to a C–H···O stabilized layer structure.*

Our model for a solid-state intermolecular Diels–Alder reaction draws from the early work of Haworth,[41] who found that when phenylpropiolic acids (such as VII) are refluxed with acetic anhydride, the symmetrical anhydrides $(ArC{\equiv}CCO)_2O$ so formed are converted quantitatively into anhydrides of the corresponding 1-phenylnaphthalene-2,3-dicarboxylic acids. The chemical expedient of forming the symmetrical anhydride in situ brings diene and dienophile components together for a Diels–Alder reaction. By construction of a 4-Å short axis, the identical 4 + 2 cycloaddition is achieved in the solid at temperatures below 80 °C and the molecular arrangement in the crystal parallels Haworth's original lignan synthesis very closely (Figure 4). In contrast, the unsubstituted acid which does not have a 4-Å stack structure is heat stable below its melting point.

C–H • • • O Bonds as Crystal Structure Directors

Typically, the directional preferences of C–H···O bonds are satisfied within the geometrical constraints of stronger forces such as O–H···O and N–H···O hydrogen bonding, $\pi\pi$ stacking, and donor–acceptor interactions. However, C–H···O bonds need not be passive

(40) Desiraju, G. R.; Kishan, K. V. R. *J. Am. Chem. Soc.* **1989**, *111*, 4838.
(41) Haworth, R. D.; Kelly, W. *J. Chem. Soc.* **1936**, 745.

UM00016846
NOVARTIS EXHIBIT 1517
Novartis v. Regents, IPR2023-01347
Page 3828 of 4460

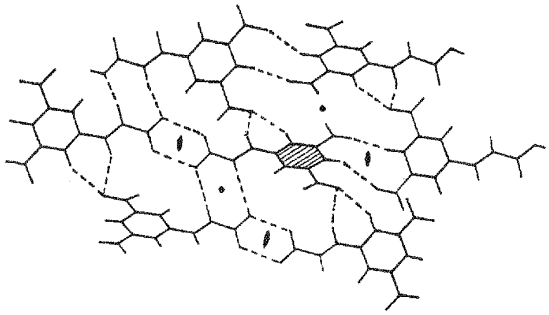


Figure 5. Crystal structure of 3,5-dinitrocinnamic acid (VIII) to show O–H···O and C–H···O hydrogen bonds. The reference molecule is shaded and linked to one of its 2-fold related neighbors by O–H···O bonds.

bystanders in a crystal; in fact they may be able to discriminate between alternative O–H···O (or other) networks which, though geometrically reasonable, are structurally quite distinct. In such cases, C–H···O bonds may be termed "steering" or "tugboat" interactions which, though small in energy, are sufficient to select a particular crystallization pathway from among several possibilities. The energy of an individual C–H···O interaction may be small, but if their number crosses a critical threshold, the structure may focus into an unconventional packing.

An arresting example is provided by 3,5-dinitrocinnamic acid (VIII), a molecule that contains several activated H and acceptor O atoms. Acid VIII crystallizes as an O–H···O dimer wherein the hydrogen-bonded molecules are related, not by an inversion center, as is usual, but by a 2-fold rotation axis.[42] Both inversion and 2-fold dimers are equienergetic, and in principle, both are reasonable possibilities. However, Figure 5 shows an extensive C–H···O bond network (seven contacts with C···O < 3.75 Å) in the crystal. These C–H···O bonds dominate the structure, and their combined directional requirements appear to be incompatible with an O–H···O inversion dimer.

In other carboxylic acids such as *trans*-cinnamic acid (II), a smaller number of C–H···O bonds stabilize the inversion dimer. In the extreme, there are cases such as (4-chlorophenyl)propiolic acid (IX) where the complete absence of C–H···O interactions leads to an unexpected hydrogen-bonded catemer motif rather than the dimer (Figure 6).[43] The O–H···O catemer is intrinsically more stable than the dimer. Therefore, if the dimer is to be formed, it must be stabilized additionally by C–H···O bonds or in some other manner. Conversely, if the C–H···O bond forming ability is reduced, the catemer is favored. Failure of IX, $C_9H_5ClO_2$, to form C–H···O bonds could arise from adverse C:H:O ratios because the crystal structures of 4-chlorobenzoic and 4-chlorocinnamic acids, with higher relative O stoichiometries, contain C–H···O bonds and the molecules crystallize as dimers.

Such studies show that C–H···O bonds, which are probably far more ubiquitous than has been generally recognized, need to be considered as important contributors in the formation of hydrogen-bond patterns

(42) Desiraju, G. R.; Sharma, C. V. K. M. *J. Chem. Soc., Chem. Commun.*, in press.
(43) Desiraju, G. R.; Murty, B. N.; Kishan, K. V. R. *Chem. Mater.* **1990**, *2*, 447.

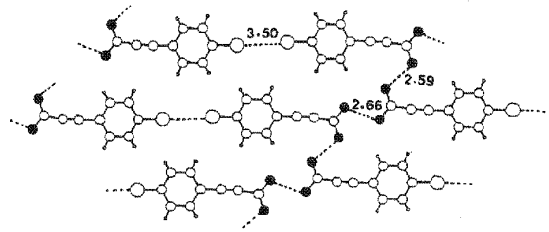


Figure 6. Crystal structure of (4-chlorophenyl)propiolic acid (IX) down the short axis to show O–H···O and Cl···Cl interactions. Oxygen atoms are shaded. Molecular layers such as shown here are stacked along the short axis. Notice the catemer O–H···O network and the absence of C–H···O interactions.

in organic crystals and that their presence or absence could well determine the manner of networking of stronger O–H···O hydrogen bonds. Consequently, an ability to predict hydrogen-bond patterns could be improved by a better understanding of C–H···O interactions.

The C–H • • •O Hydrogen Bond in Crystals: What Is It?

The evidence in hand suggests that the C–H···O bond is, like the O–H···O and N–H···O hydrogen bonds, a largely electrostatic, attractive interaction with a long-range distance character. The length of the bond is variable but depends on C–H acidity. The angular approaches of the C–H and O–C groups which form the bond are largely predictable. Considering also the spectroscopic data on C–H···O bonds, especially of the more acidic C–H groups, it seems that the terminology C–H···O *hydrogen bond* is fully justified.

The attractive and non van der Waals character of the C–H···O interaction is also indicated since the addition of specific hydrogen-bonding terms of the $-D\exp(-Fr)$ or the Morse type[44,45] improves the optimization of oxohydrocarbon crystals with (exp–6–1) or 12–6–1) potentials. A heavier theoretical treatment is difficult, among other reasons, because of basis set superposition errors. However, ab initio calculations show that while $H_2O\cdots CH_3NO_2$ does not form a hydrogen bond, $H_2O\cdots CH_2(CN)_2$ forms a hydrogen bond of ca. 5 kcal/mol energy.[46] Other calculations indicate that an activated C–H group is polarized C($\delta-$)--H($\delta+$) and can hence form an electrostatic interaction with an O atom. A less activated C–H bond dipole, however, has the sense C($\delta+$)--H($\delta-$) that is reversed by O atom polarization in a C–H···O bond.[47] These results corroborate our own findings that strongly acidic groups form better C–H···O bonds, but more needs to be done before we can determine if C–H···O interactions of weakly and strongly acidic C–H groups are similar or fundamentally different. All these studies show that the C–H···O bond is an attractive interaction, but it must be emphasized that neither a geometrical–statistical nor a theoretical approach reveals the degree of covalent bonding between the C–H and O moieties. Spectroscopy is probably a better tool to resolve this question.

(44) Cox, S. R.; Hsu, L. Y.; Williams, D. E. *Acta Crystallogr.* **1981**, *A31*, 293.
(45) Gavezzotti, A. *J. Phys. Chem.*, in press.
(46) Kumpf, R. A.; Damewood, J. R. *J. Chem. Soc., Chem. Commun.* **1988**, 621.
(47) Wiberg, K. B.; Waldron, R. F.; Schulte, G.; Saunders, M. *J. Am. Chem. Soc.* **1991**, *113*, 971.

UM00016847
NOVARTIS EXHIBIT 1517
Novartis v. Regents, IPR2023-01347
Page 3829 of 4460

"What is a C–H···O hydrogen bond?" In the same vein one might well ask, "What is an O–H···O or an N–H···O hydrogen bond?" At a practical level, structural chemists have not been used to thinking in terms of C–H···O bonds, and it is in order to reexamine older ideas about crystal packing in this new light. For example, there is every indication that phenomena such as three-center bonding (bifurcation) and cooperative and resonance-assisted hydrogen bonding exist for C–H···O networks, and hence chemists will find it worthwhile to consider *all* interactions, weak (C–H···O, O–H···C) and strong (O–H···O, N–H···O), while attempting to understand hydrogen-bond arrangements and indeed crystal packing, in general. References to C–H···O bonds in the physical organic literature are even more sparse, but here again, these forces have been invoked to explain some surprising observations.[47,48] In conclusion, it seems appropriate to state (with due apologies to Donohue) that a better answer to the question in the title of this Account and this section is: "*It certainly is.*"

Warm thanks are due to the following students, past and present, who have worked with me on the topic of C–H···O hydrogen bonding in organic crystals: J. A. R. P. Sarma, K. V. Radha Kishan, V. R. Pedireddi, C. V. K. M. Sharma, and B. N. Murty. I thank J. P. Glusker and A. Gavezzotti for their valuable comments on this manuscript. It is impossible to list all the colleagues with whom I have had spirited discussions on this controversial subject, but I must mention C. Ramakrishnan and R. Parthasarathy, who filled me in on the early days of C–H···O bonds, especially in the G. N. Ramachandran group in Madras.

Registry No. C, 7440-44-0; O, 17778-80-2.

(48) Shultz, G.; Hargittai, I.; Doerner, T.; Gleiter, R. *Chem. Ber.*, in press.

Acyclic Stereochemical Control in Free-Radical Reactions

NED A. PORTER,*,† BERND GIESE,*,‡ and DENNIS P. CURRAN*,§

Department of Chemistry, Duke University, Durham, North Carolina 27706, Institute of Organic Chemistry, University of Basel, CH-4056 Basel, Switzerland, and Department of Chemistry, University of Pittsburgh, Pittsburgh, Pennsylvania 15260

Received June 17, 1991 (Revised Manuscript Received September 5, 1991)

Since Gomberg's discovery of the persistent triphenylmethyl radical over 90 years ago,[1] there has been a steady increase in interest in free radicals. Recent years have seen the emergence of new free-radical synthetic methods that are efficient and convenient,[2,3] and new chain-propagation schemes have been reported that are based on tin hydride–alkyl halide or borohydride–mercurial reductions, halogen atom transfer reactions,[3] thiohydroxamate[4] or allylstannane addition–fragmentation processes,[5,6] and manganese(III) oxidations.[7]

Ring construction by free-radical cyclization has proved to be particularly useful, and five-membered rings are readily produced by this approach. The fundamental work of Walling, Beckwith, and Ingold[8] provided information about the regiochemistry, absolute rate, and stereochemistry of cyclizations. Synthetic efforts have benefited tremendously from this body of mechanistic work, and the cyclization reaction has been put to good synthetic use.[9,10] Intermolecular free-radical addition reactions have also received renewed interest. Systematic studies have shown that polar and steric effects are most important in controlling the rate of addition of radicals to carbon–carbon double bonds, and there are many examples of the useful incorporation of intermolecular radical additions into synthetic sequences.[2,3]

Despite major advances in the past 10 years, a significant barrier for the application of free-radical methodology in organic synthesis remains: there is no general approach to the control of acyclic stereochem-

Ned Porter graduated from Princeton in 1965 with a B.S. in chemical engineering and accepted a position as Assistant Professor at Duke University in 1969, after receiving his Ph.D. with Paul D. Bartlett at Harvard. He is now a James B. Duke Professor of Chemistry at Duke. His major research interests have involved studies of free radicals and radical pairs, lipids and bilayer membranes, and more recently, radical macrocyclization, hydrophobic stereoenforcement, and enzyme photoactivation.

Bernd Giese studied in Heidelberg, Hamburg, and Munich, where he received his Dr. Rer. Nat. (1969) working in the group of Rolf Huisgen. After two years at BASF/Ludwigshafen, he carried out his habilitation in Münster and Freiburg (1976). He has been Professor at TH Darmstadt (1978–1988) and has held the chair of organic chemistry at the University of Basel since 1989. His primary research interests are the structure, selectivity, synthetic applications, and biochemical importance of radicals.

Dennis P. Curran received his B.S. from Boston College in 1975 and his Ph.D. from the University of Rochester in 1979, where he worked under Professor Andrew S. Kende. After a postdoctoral stay with Professor Barry M. Trost at the University of Wisconsin as a National Institutes of Health Postdoctoral Fellow, he joined the faculty of the Chemistry Department at the University of Pittsburgh in September 1981. He was promoted to the rank of Associate Professor in 1986 and Professor in 1988. His research interests lie in the area of natural products synthesis and the development of new synthetic methods.

† Duke University.
‡ University of Basel.
§ University of Pittsburgh.

(1) Gomberg, M. *J. Am. Chem. Soc.* **1900**, *22*, 757.
(2) Giese, B. *Radicals in Organic Synthesis: Formation of Carbon-Carbon Bonds*, Pergamon Press: New York, 1986.
(3) (a) Curran, D. P. *Synthesis* **1988**, 417–439, 489–513. (b) Curran, D. P. In *Comprehensive Organic Chemistry: Selectivity, Strategy and Efficiency in Modern Organic Chemistry*; Trost, B., Fleming, I., Eds.; Pergamon: New York; Vol. 4, Chapters 4.1 and 4.2, in press. (c) Jasperse, C. P.; Curran, D. P.; Fevig, T. L. *Chem. Rev.*, in press.
(4) (a) Barton, D. H. R.; Crich, D.; Motherwell, W. B. *Tetrahedron* **1985**, *41*, 3901. (b) Crich, D. *Aldrichimica Acta* **1987**, *20*, 35.
(5) (a) Keck, G. E.; Yates, J. B. *J. Am. Chem. Soc.* **1982**, *104*, 5829. (b) Grignon, J.; Servens, C.; Pereyre, M. *J. Organomet. Chem.* **1975**, *96*, 225.
(6) Baldwin, J. E.; Kelly, D. R. *J. Chem. Soc., Chem. Commun.* **1985**, 682.
(7) (a) Snider, B. B.; Mohan, R.; Kates, S. A. *J. Org. Chem.* **1985**, *50*, 3559. (b) Heiba, E. I.; Dessau, R. M.; Rodewald, P. G. *J. Am. Chem. Soc.* **1974**, *96*, 7977.
(8) See, for example: Beckwith, A. L. J.; Ingold, K. U. *Rearrangements in Ground and Excited States*; deMayo, P., Ed.; Academic Press: New York, 1980; Vol. 1, p 162.
(9) Hart, D. J. *Science* **1984**, *223*, 883.
(10) Stork, G. *Selectivity—A Goal For Synthetic Efficiency*; Bartman, W. T. B., Trost, B., Eds.; VCH: Weinheim, 1984.

0001-4842/91/0124-0296$02.50/0 © 1991 American Chemical Society

UM00016848
NOVARTIS EXHIBIT 1517
Novartis v. Regents, IPR2023-01347
Page 3830 of 4460

Electronic Acknowledgement Receipt

EFS ID:	8731678
Application Number:	10378956
International Application Number:	
Confirmation Number:	4742
Title of Invention:	Multiple-component solid phases containing at least one active pharmaceutical ingredient
First Named Inventor/Applicant Name:	Michael J. Zaworotko
Customer Number:	23557
Filer:	Glenn Ladwig/J'Nese Williams
Filer Authorized By:	Glenn Ladwig
Attorney Docket Number:	USF.106XC1
Receipt Date:	29-OCT-2010
Filing Date:	03-MAR-2003
Time Stamp:	13:59:28
Application Type:	Utility under 35 USC 111(a)

Payment information:

Submitted with Payment	no

File Listing:

Document Number	Document Description	File Name	File Size(Bytes)/ Message Digest	Multi Part /.zip	Pages (if appl.)
1	NPL Documents	PDR_2590.pdf	2355309 4f6d0255e9e4deac0b22f09f51173892c103c76a	no	6
Warnings:					
Information:					

2	NPL Documents	PressRelease_2002.pdf	102813 940884781e87b5c11cc300c06f153716e5db74fd	no	2
Warnings:					
Information:					
3	NPL Documents	Privitera.pdf	70988 95979fd2266478fa9df6ea492b039df1ac1094f3	no	1
Warnings:					
Information:					
4	NPL Documents	Reynolds.pdf	455374 03ba34284b75ebb06bb9af0ab780c00d750ed33e	no	5
Warnings:					
Information:					
5	NPL Documents	Rosenfeld.pdf	713326 9cbcce04d0bc70dd8fa962ddef2d181ee799bb86	no	15
Warnings:					
Information:					
6	NPL Documents	Rubino.pdf	303274 be96cd6199b7b5f5f07f1bdd054e43d3ef96238f	no	5
Warnings:					
Information:					
7	NPL Documents	Sachdeo.pdf	108732 ed6805d69493a2c3b105b508b8a747859528d8e6	no	1
Warnings:					
Information:					
8	NPL Documents	Salem.pdf	203051 8f6b4fe5d57cc2935a456f91b2ce22901d264864	no	3
Warnings:					
Information:					
9	NPL Documents	Thayer.pdf	884286 ada2fcaadc8756a12aca46a60ea65c4266029f35	no	8
Warnings:					
Information:					
10	NPL Documents	USPharmacopia-23.pdf	169868 bf9ddfe44aa1526f6e7ac6b2f015c65fe41f3bec	no	1
Warnings:					
Information:					

11	NPL Documents	Walsh.pdf	423668 cfae3740ee3aa67a1e4104af0b8adbb510b5b0db	no	2
Warnings:					
Information:					
12	NPL Documents	Weissbuch-1995.pdf	2958902 376b66d794356b47c2f571940f101c820b918a95	no	34
Warnings:					
Information:					
13	NPL Documents	Wunderlich.pdf	481775 d8b50945bea2f36832273e4992d56e1ab6cbbe51	no	3
Warnings:					
Information:					
14	NPL Documents	Zaman-2.pdf	1408428 13abc64a3721523ab3658f87dbece24d0c8761d2	no	9
Warnings:					
Information:					
15	NPL Documents	Zerkowski-StericControl.pdf	1050800 265fd2d7381d5789c34e61c0635367d1709bbede	no	7
Warnings:					
Information:					
16	NPL Documents	desiraju_1991_CHbonding_acc chemres.pdf	2007027 2c6f24c2f0b9ee66020eace389045074c5a800e9	no	7
Warnings:					
Information:					
		Total Files Size (in bytes):	13697621		

This Acknowledgement Receipt evidences receipt on the noted date by the USPTO of the indicated documents, characterized by the applicant, and including page counts, where applicable. It serves as evidence of receipt similar to a Post Card, as described in MPEP 503.

New Applications Under 35 U.S.C. 111
If a new application is being filed and the application includes the necessary components for a filing date (see 37 CFR 1.53(b)-(d) and MPEP 506), a Filing Receipt (37 CFR 1.54) will be issued in due course and the date shown on this Acknowledgement Receipt will establish the filing date of the application.

National Stage of an International Application under 35 U.S.C. 371
If a timely submission to enter the national stage of an international application is compliant with the conditions of 35 U.S.C. 371 and other applicable requirements a Form PCT/DO/EO/903 indicating acceptance of the application as a national stage submission under 35 U.S.C. 371 will be issued in addition to the Filing Receipt, in due course.

New International Application Filed with the USPTO as a Receiving Office
If a new international application is being filed and the international application includes the necessary components for an international filing date (see PCT Article 11 and MPEP 1810), a Notification of the International Application Number and of the International Filing Date (Form PCT/RO/105) will be issued in due course, subject to prescriptions concerning national security, and the date shown on this Acknowledgement Receipt will establish the international filing date of the application.

Substitute for form 1449B/PTO

INFORMATION DISCLOSURE STATEMENT BY APPLICANT

(use as many sheets as necessary)

Sheet 1 of 1

Complete if Known	
Application Number	10/378,956
Filing Date	March 3, 2003
First Named Inventor	Michael J. Zaworotko
Group Art Unit	1627
Examiner Name	Sahar Javanmard
Attorney Docket Number	USF.106XC1

NON PATENT LITERATURE DOCUMENTS

Examiner Initials*	Cite No. [1]	Include name of the author (in CAPITAL LETTERS), title of the article, (when appropriate), title of the item (book, magazine, journal, serial, symposium, catalog, etc.), date, page(s), volume-issue number(s), publisher, city and/or country where published.	T[2]
	R1	STAHL, P.H. *The Practice of Medicinal Chemistry;* "Chapter 35: Preparation of water-soluble compounds through salt formation" 1 January 2003, Elsevier, NL, pp. 601-615, XP002566271.	
	R2	RASENACK, N. *et al.* "Dissolution Rate Enhancement by *in Situ* Micronization of Poorly Water-Soluble Drugs" *Pharmaceutical Research,* December 2002, 19(12):1894-1900.	
	R3		
	R4		
	R5		
	R6		
	R7		
	R8		
	R9		
	R10		
	R11		
	R12		
	R13		

Examiner Signature		Date Considered	

*EXAMINER: Initial if reference considered, whether or not citation is in conformance with MPEP 609. Draw line through citation if not in conformance and not considered. Include copy of this form with next communication to applicant.

[1] Applicant's unique citation designation number (optional). [2] Applicant is to place a check mark here if English language Translation is attached.

This collection of information is required by 37 CFR 1.98. The information is required to obtain or retain a benefit by the public which is to file (and by the USPTO to process) an application. Confidentiality is governed by 35 U.S.C. 122 and 37 CFR 1.14. This collection is estimated to take 2 hours to complete, including gathering, preparing, and submitting the completed application form to the USPTO. Time will vary depending upon the individual case. Any comments on the amount of time you require to complete this form and/or suggestions for reducing this burden, should be sent to the Chief Information Officer, U.S. Patent and Trademark Office, P.O. Box 1450, Alexandria, VA 22313-1450. DO NOT SEND FEES OR COMPLETED FORMS TO THIS ADDRESS. **SEND TO: Commissioner for Patents, P.O. Box 1450, Alexandria, VA 22313-1450.**

If you need assistance in completing the form, call 1-800-PTO-9199 (1-800-786-9199) and select option 2.

J:\USF\106XC1\PTO\SIDS8-form.doc/DNB/jnw

Pharmaceutical Research, Vol. 19, No. 12, December 2002 (© 2002) *Research Paper*

Dissolution Rate Enhancement by *in Situ* Micronization of Poorly Water-Soluble Drugs

Norbert Rasenack[1] and Bernd W. Müller[1,2]

Received August 21, 2002; accepted September 6, 2002

Purpose. The purpose of this study was to evaluate a novel *in situ* micronization method avoiding any milling techniques to produce nano- or microsized drug particles by controlled crystallization to enhance the dissolution rate of poorly water-soluble drugs.

Methods. Ibuprofen, itraconazole, and ketoconazole microcrystals were prepared by the association of the previously molecularly dispersed drug using a rapid solvent change process. The drug was precipitated in the presence of stabilizing agents, such as hydrocolloids. The obtained dispersion was spray-dried. Particle size, morphology, dissolution rate, specific surface area, and wettability were analyzed. Physicochemical properties were characterized using differential scanning calorimetry and X-ray diffractometry.

Results. The obtained dispersions showed a homogeneous particle size distribution. Drugs are obtained in a mean particle size of approximately 2 μm and below. A high specific surface area was created and *in situ* stabilized. Different stabilizers showed differences in protecting the precipitated drug from crystal growth. The surface was hydrophilized because of the adsorbed stabilizer. Thus, a drug powder with markedly enhanced dissolution rate was obtained.

Conclusions. *In situ* micronization is a suitable method for the production of micro-sized drugs. This technique can be performed continuously or discontinuously and uses only common technical equipment. Compared to milled products drug properties are optimized as all particle surfaces are naturally grown, the particle size is more uniformly distributed and the powder is less cohesive.

KEY WORDS: micronization; inhibition of crystal growth; dissolution rate enhancement; poorly water-soluble drug; controlled crystallization.

INTRODUCTION

The poor water solubility of many drugs—especially several newly developed substances—is a challenge in pharmaceutical research. Because of their low bioavailability, several potential drugs have to be delayed or abandoned in pharmacological screenings because of their lipophilicity (1). Their dissolution rate is the limiting factor in most case because drugs with high lipophilicity can permeate biomembranes quickly. Thus, the research on strategies for drug dissolution enhancement is of high interest. According to the Noyes-Whitney equation, the administration of a drug in a reduced particle size is a very promising way to improve drug bioavailability of poorly soluble substances (2). The common way for reducing the particle size is the disruption of previously formed larger particles by milling techniques such as jet-milling, milling in a pearl-ball-mill, or high-pressure homogenization. However, these methods have several disadvantages resulting from the mechanical disruption process. The micronization process using mills is extremely inefficient (3) because of the high-energy input that can alter the surface properties as a thermodynamically activated surface is created (4,5). Even a small amount of activated material at the surface affects the drug substance properties, such as the blending characteristics (6) or flow properties (7). When the partially amorphous surface recrystallizes, the physical properties of the drug change. The conversion of crystalline solid surfaces into partially amorphous solid surfaces leads to a "dynamic nature" of the micronized drug (8). The newly created surfaces are not naturally grown because the cleavage plane is the crystal face with the smallest attachment energy (9). Thus, this surface will dominate the size-reduced particles and the milled powder is characterized by their surface properties. In most cases the surface shows poor wetting properties; therefore, because of agglomeration, the increase in the dissolution rate is not as high as calculated from the increase in surface area. Nanosuspensions (DissoCubes®) are milled by high-pressure homogenizers (10,11). The high pressures used cause changes in the crystal structure, and as a result, the amorphous fraction in the particle increases (12). Thus milling affects several physical properties of the drug, such as powder flow, agglomeration behavior, or electrostatic behavior. Beside these effects, the chemical reactivity or degradation also can be affected by milling (13,14). Even the particle size can change during storage after micronization because of stress relaxation processes (15). Beside these problematic properties, a further disadvantage especially of jet-milling processes, is a broad size distribution (16). Because of abrasion, the product can be afflicted with metallic impurities that can affect the chemical stability as a result of catalytic activity.

Because of the disadvantages of milling processes, techniques were developed that produce the drug directly in the optimal particle size. However, the preparation and stabilization of small particles is not easy because of their tendency to grow. Thus, several examples of inorganic clusters prepared for example in electrochemical cells exist, but stable dispersions of organic substances (beside polymer-lattices) are scarce. Because of the high surface that must be created, the established methods need high amounts of stabilizing excipients leading to amorphous products. The most important examples are the so-called hydrosols developed by Gaßmann *et al.* (17). Hydrosols are colloidal aqueous suspensions containing drug nanoparticles of poorly water-soluble drugs for intravenous administration. They are prepared by a precipitation process as the drug solution is mixed with a relatively high volume of water (96–98% water after mixing) in the presence of stabilizing agents such as poloxamer and modified gelatins, which act as "short term stabilizers" (17). After precipitation, the amorphous hydrosol is stable for approximately 60 min because of the stabilizers and the high amount of nonsolvent. After this time, the drug crystallizes. Because the clouding correlates with the particle size, crystallization and particle growth can be observed by a steep increase of absorbance at a wavelength where the drug substance does not absorb. Thus, for durable stabilizing the amorphous nanosized drug, the hydrosol is immediately spray-dried with ex-

[1] Department of Pharmaceutics and Biopharmaceutics, Christian Albrecht University Kiel, Gutenbergstr. 76, 24118 Kiel, Germany.
[2] To whom correspondence should be addressed. (e-mail: bwmueller@pharmazie.uni-kiel.de)

0724-8741/02/1200-1894/0 © 2002 Plenum Publishing Corporation

UM00016854
NOVARTIS EXHIBIT 1517
Novartis v. Regents, IPR2023-01347
Page 3836 of 4460

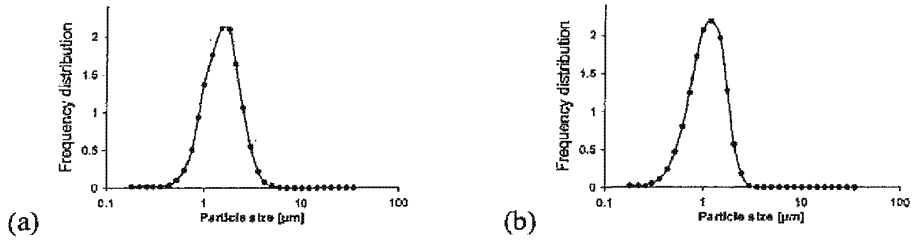


Fig. 1. Particle size distribution in dispersion 60 min after precipitation (HPMC solution). (a) ibuprofen; (b) ketoconazole.

cipients such as lactose or mannitol before crystallization occurs. Before use, the preparations are reconstituted with water. Hydrosols contain the drug in a particle size of approximately 200 nm and are thus suitable for parenteral application. An example is cyclosporin, which can be formed as a hydrosol (ratio drug: gelatin = 1: 20). According to this principle, colloidal dispersions of β-carotene are produced. Amorphous carotenoid nanoparticles contain high amounts of stabilizing agents, such as gelatin, and softening agents, such as sugar. Because the amount of β-carotene is approximately 10–15% (18,19), these preparations can be called embeddings. Because of the high amount of stabilizer and the immediately spray-drying, the product is amorphous. Micronized drugs can also be prepared using supercritical carbon dioxide (20,21). The drug is precipitated in the supercritical fluid. A disadvantage of this technique is the high machine expenditure.

The aim of this study was to prepare crystalline micro sized drug particles of poorly water-soluble drugs use in oral administration forms to enhance the dissolution rate. Because the drug powders are prepared directly in the micronized state during the particle formation without any further size-reduction, this technique can be described as an *in situ* micronization technique. The molecularly dispersed drug is transformed to particles in the desired size and stabilized in the formed dispersion. Because they are model drugs with a poor solubility in water, ibuprofen, itraconazole, and ketoconazole were used. The first aim was to find a stabilizing agent that was able to stabilize the associated drug in small particle size against crystal growth. Furthermore, the use of an effective stabilizer is important to obtain a drug powder with a drug load as high as possible. By the use of a suitable stabilizer, the crystal germs can be stabilized. To find a stabilizer with high affinity to the newly created high surface, several potential stabilizing agents were compared. The resulting product showed a high drug load and contained the drug in crystalline form.

MATERIALS AND METHODS

Materials

Ibuprofen 50 was provided by BASF AG (Ludwigshafen, Germany), and itraconazole and ketoconazole were supplied by Janssen Pharmaceutica (Beerse, Belgium). For comparison of the analytical data, drugs were used as obtained and called "common crystals." Acetone and isopropyl alcohol (Merck KG, Darmstadt, Germany) were of analytical grade. Water was used in double-distilled quality. The stabilizing agents used were agar (Merck KG), calcium caseinate (Lactonat®EC, Lactoprot, Kaltenkirchen, Germany), dextran 200 (Sigma, Deisenhofen, Germany), gelatin A (Merck KG), hydroxyethylcellulose HEC (Natrosol®Pharm G, Natrosol®HHX, Hercules, Wilmington, DE, USA), hydroxyethylstarch (HES 130, HES 450, Fresenius Kabi, Bad Homburg, Germany), hydroxypropylcellulose HPC (Klucel® GF, Klucel® LF, Herculesmethylcellulose MC (Tylose® M 4000, Clariant, Frankfurt, Germany), methylhydroxyethylcellulose MHEC (Tylopur® MH 50, Tylopur® MH 4000, Clariant), hydroxypropylmethylcellulose (HPMC; Metolose® 60 SH 15, 4000, 10,000, Shin Etsu, Tokyo, Japan), sodium carboxymethylcellulose NaCMC (Tylopur® C 30), sodium alginate (Sigma), pectin (pectin Classic AU 204, low viscosity, Herstreith & Fox KG, Neuenburg, Germany), polyvinylalcohol (average molecular weight 30,000–70,000; Sigma), and polyvinylpyrrolidone (Kollidon®30, BASF AG).

Crystallization Procedure

Crystallization was conducted using the solvent change method by instantaneously mixing two liquids in the presence of a stabilizing agent as described by Rasenack and Müller (22). In the first step, the drug was dissolved in an organic solvent that is miscible with water. The chosen concentration depends on the solubility of the drug (ibuprofen: 5 g/100 mL isopropyl alcohol; itraconazole: 0.75 g/500 mL acetone; ketoconazole: 0.5 g/100 mL acetone). The stabilizing agents were dissolved in water. By batch-wise mixing the two liquids (20

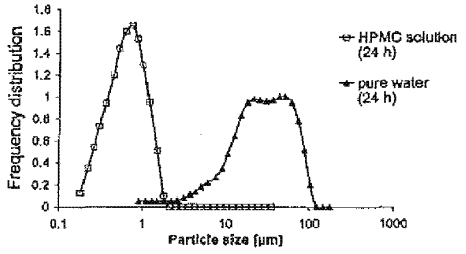


Fig. 2. Particle size distribution of itraconazole 24 h after precipitation with pure water respectively. HPMC solution.

UM00016855
NOVARTIS EXHIBIT 1517
Novartis v. Regents, IPR2023-01347
Page 3837 of 4460

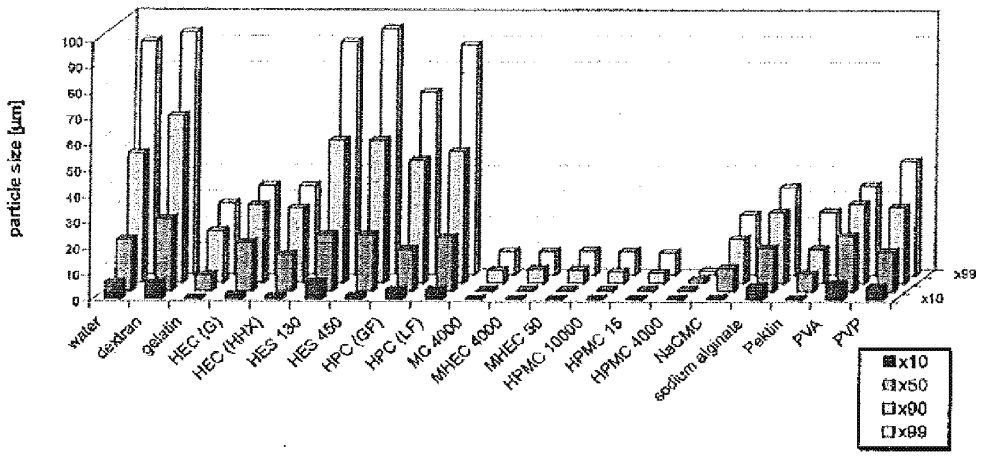


Fig. 3. Particle size of itraconazole (dispersion 24 h after precipitation) [concentration of stabilizer in water = 0.025% (m/m)].

mL of drug solution + 80 mL of nonsolvent in the case of ibuprofen and ketoconazole, respectively, 50 mL of drug solution + 80 mL of nonsolvent in the case of itraconazole) a dispersion is formed. The nonsolvent was poured rapidly from a beaker into the drug solution under stirring conditions using a magnetic stirrer. The stability of the dispersion depends on the stabilizer that is used. For each drug, several stabilizers and different concentrations were tested by measuring the particle size at different times after precipitation. A solution of HPMC (ibuprofen: 0.1%; itraconazole: 0.025%; ketoconazole: 0.05%) was used for preparing the micronized drugs. After spray-drying the prepared dispersion during its stability (Büchi 190 Mini Spray-dryer, Büchi Labortechnik AG, Flawil, Switzerland; $temperature_{inlet}$: 128°C; $temperature_{outlet}$: 55°C; air flow 600 Nl/h; 0.5-mm noozle; aspirator stream 40 m^3/h) a micro- respectively nanosized drug powder was obtained (drug content: ibuprofen 92.6%; itraconazole 79.0%; ketoconazole 71.4%). In this study, the spray-drying process was not used to form particles as if solutions are spray-dried but only to dry previously formed particles. Because of the small particles, a high stream of volume was used to obtain a higher yield. Furthermore, a cone was inserted between the bottom of the cyclone and the collecting vessel. Passing through the gap of approximately 1.5 mm, the powder can deposit in the collecting vessel. Swirling up and swirling out of the collecting vessel is reduced.

Product Characterization

Particle Size

The volume particle size distribution was measured using a laser diffractometer (HIelos, Sympatec GmbH, Clausthal Zellerfeld, Germany). The dispersions were diluted with water and measured in a cuvette. The spray-dried drug powder was previously suspended in water. Particle size distribution is characterized by the X10 (10% below this size), the X50, X90, and the X99-value.

Powder Dissolution

Dissolution studies were performed assuring sink-conditions according to the paddle method (USP) using an Erweka DT6 dissolution apparatus (Erweka, Heusenstamm, Germany). The stirring speed used was 100 rpm, and the temperature was maintained at 37°C ± 0.5°C. The dissolution medium (900 mL) was phosphate buffer pH 7.4 (USP 25) in the case of ibuprofen and simulated intestinal fluid in the case

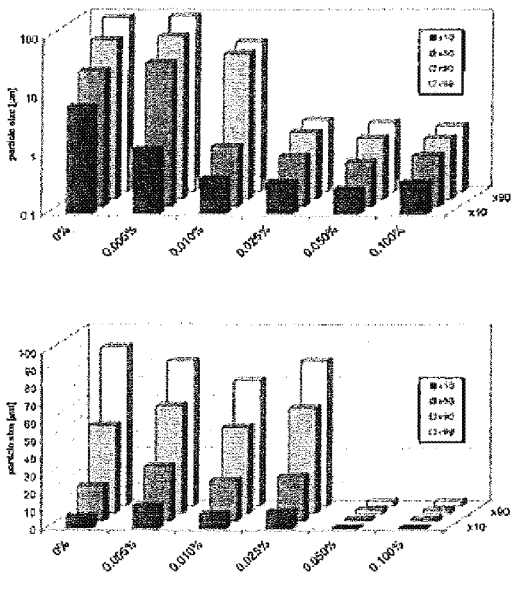


Fig. 4. Influence of different concentrations of HPMC4000 on particle size in dispersion. (a) itraconazole 24 h after precipitation; (b) ketoconazole 120 min after precipitation [concentration in precipitating liquid in & (m/m)].

UM00016856
NOVARTIS EXHIBIT 1517
Novartis v. Regents, IPR2023-01347
Page 3838 of 4460



Fig. 5. Scanning electron micrograph of ibuprofen. (a) common crystals; (b) micronized drug.

of itraconazole and ketoconazole. This dissolution medium consisted of 0.25% sodium dodecyl sulfate and 0.2% sodium chloride (all Merck KG). Surface tension was lowered by sodium dodecyl sulphate in an attempt to mimic *in vivo* conditions as described by Pedersen *et al.* (23). Because of their physiologic relevance for dissolution testing of poorly water-soluble drugs the addition of a surfactant is generally to be preferred to e.g., hydroalcoholic mediums (24). Quantification of the dissolved amount of drug was conducted spectrophotometrically at 221 nm (ibuprofen), 262 nm (itraconazole), 226 nm (ketoconazole) (Lambda40 UV VIS Spectrometer, Perkin Elmer, Wilten, CT, USA). All samples were analyzed in triplicate.

Scanning Electron Microscopy

Scanning electron micrographs were taken using a Philips XL 20 (Philips, Eindhoven, Netherlands). Samples were fixed on an aluminium stub with conductive double-sided adhesive tape (Leit-Tabs, Plano GmbH, Wetzlar, Germany) and coated with gold in an argon atmosphere (50 Pa) at 50 mA for 50 s (Sputter Coater, Bal-Tec AG, Liechtenstein).

Specific Surface Area

The specific surface area was determined using the gas adsorption method. Calculation is based on the BET equation. A Surface Area Analyzer Gemini-2360 (Micromeritics Instrument Corporation, Norcross, GA, USA) was used.

Contact Angle

The contact angle was measured by the sessile drop technique using a goniometer (G1, Krüss GmbH, Hamburg, Germany). A compressed disc of the powder (200 mg) was made at 30 kN for 90 s under vacuum. The contact angle between the disc and a single drop of water (25 μL) was determined 10 s and 180 s after the droplet was put onto the disc. Determination was repeated 20 times.

Differential Scanning Calorimetry (DSC)

A differential scanning calorimeter (DSC7, Perkin Elmer, Connecticut, USA) was used. The equipment was calibrated using indium and zinc. Samples were heated at 10°C/min in aluminium pans under nitrogen atmosphere. The onsets of the melting points and enthalpies of fusion were calculated by the software (Pyris, Perkin Elmer, CT, USA).

X-Ray Diffractometry

Powder X-ray diffraction patterns were collected in transmission using an X-ray diffractometer with a rotating anode (Stoe and Cie GmbH, Darmstadt, Germany) with Cu Kα1 radiation (monochromator: graphite) generated at 200 mA and 40 kV. Powder was packed into the rotating sample holder between two films (PETP).

RESULTS AND DISCUSSION

When a hydrophobic substance is precipitated, a hydrophobic surface is formed. The energy of the system increases. Thus a stabilizing agent—provided that it has any affinity to



Fig. 6. Scanning electron micrograph of itraconazole. (a) common crystals; (b) micronized drug.

UM00016857
NOVARTIS EXHIBIT 1517
Novartis v. Regents, IPR2023-01347
Page 3839 of 4460

(a) (b)

Fig. 7. Scanning electron micrograph of ketoconazole. (a) common crystals; (b) micronized drug.

the surface—covers the newly formed surface spontaneously. Thereby, the surface energy and consequently the enthalpy of the system is lowered. The small particles that normally would agglomerate because of their hydrophobic surface are sterically stabilized against crystal growth by a layer of protective polymer (25).

Characterizing the Precipitated Dispersion

The analgesic drug ibuprofen and the antifungal drugs itraconazole and ketoconazole show a mean particle size of approximately 2 μm and below if precipitated in the presence of a stabilizing agent. The particle size distributions of the formed dispersions are shown in Figs. 1 and 2. In all cases a tight particle size distribution is received. The effect of the stabilizing agent (HPMC) on the particle size of itraconazole is obvious (Fig. 2): 24 h after precipitation itraconazole with pure water, a broad particle size distribution with a mean particle size (X50) of 30 μm is formed. In contrast, a tight particle size distribution with a mean particle size (X50) of 600 nm is formed if the drug is precipitated in the presence of HPMC. Thus, HPMC can stop the molecular association and the crystal growth by forming a protective layer around the nucleation germs. The stability of the dispersion depends on the stabilizer that is used. When comparing the particle size distribution obtained in the presence of different stabilizing agents, differences are detected (Fig. 3); particularly, cellulose ethers with alkyl-substituents (MC, MHEC, HPMC) are able to protect a particle growth. Additives with a mainly hydrophilic molecule structure, such as dextran, hydroxyethylstarch, or polar substituted cellulose ethers, do not stabilize the formed drug particles in that way. This shows that the additive must be able to interact with the newly formed surface. As e.g., HPMC shows surface activity (26), it can be adsorbed onto the newly created surface of the precipitated drug to lower the interfacial tension; particularly, cellulose ethers containing methoxyl or hydroxypropyl groups are adsorbed onto hydrophobic solid surfaces as described for hydrophobic silicon dioxide (27). A dependency of the resulting particle size on the viscosity of the precipitating liquid (determined using an Ubbelohde-viscometer) cannot be found. The effect of different concentrations on the resulting particle size of precipitated itraconazole (dispersion 24 h after precipitation) is shown in Fig. 4a. A minimum necessary amount of stabilizer (0.025% in the precipitating liquid) was found. Below this concentration, a particle growth occurs. However, the use of a higher amount of HPMC does not result in smaller itraconazole particles. A protective layer around the particles seems to be important. A similar relationship can be observed in the case of ketoconazole (Fig. 4b). Here two groups of particle size distributions can be observed: Below a minimal concentration of the stabilizer, large crystals with a mean particle size (X50) of 25 μm are obtained. If the minimum effective amount is used, a tight particle size distribution with a mean particle size of 1.2 μm is obtained. Because of the higher solubility of ketoconazole compared with itraconazole, the particle growth of ketoconazole is more rapid and thus the two groups of preparations can be sharply distinguished. Itraconazole that is not stabilized effectively grows slowly, thus different particle sizes (Fig. 4a) are observed in the case of using different amounts of stabilizer as a result of the fact that particle growth has not yet finished.

Characterizing the Spray-Dried Drug Powders

After spray-drying the prepared dispersions, drug powders are obtained (Fig. 5b, Fig. 6b, and Fig. 7b). The precipitated drugs are isomorphic with the common crystals, as X-ray and DSC analysis showed. The particle size distribution of the dispersions is fixed by the drying process. However, because of the fact that a suspension is spray-dried, the particle size is not affected by the spray-drying process. The common crystals of ibuprofen (Fig. 5a) are prepared by crystallization and show a relatively homogeneous particle size. However, the milled drugs itraconazole and ketoconazole show very heterogeneous particle sizes (Fig. 6a and Fig. 7a). The drug powders prepared in this study consist of uniform particles. Because of the small particle size, the drug is agglomerated. After redispersing the drug powder in water, the particle size

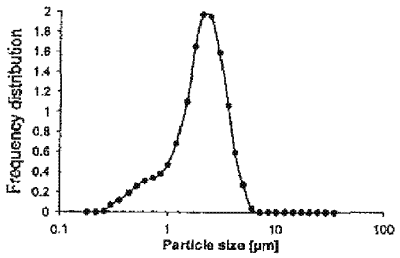


Fig. 8. Particle size distribution of micronized ketoconazole (dispersed in water).

UM00016858
NOVARTIS EXHIBIT 1517
Novartis v. Regents, IPR2023-01347
Page 3840 of 4460

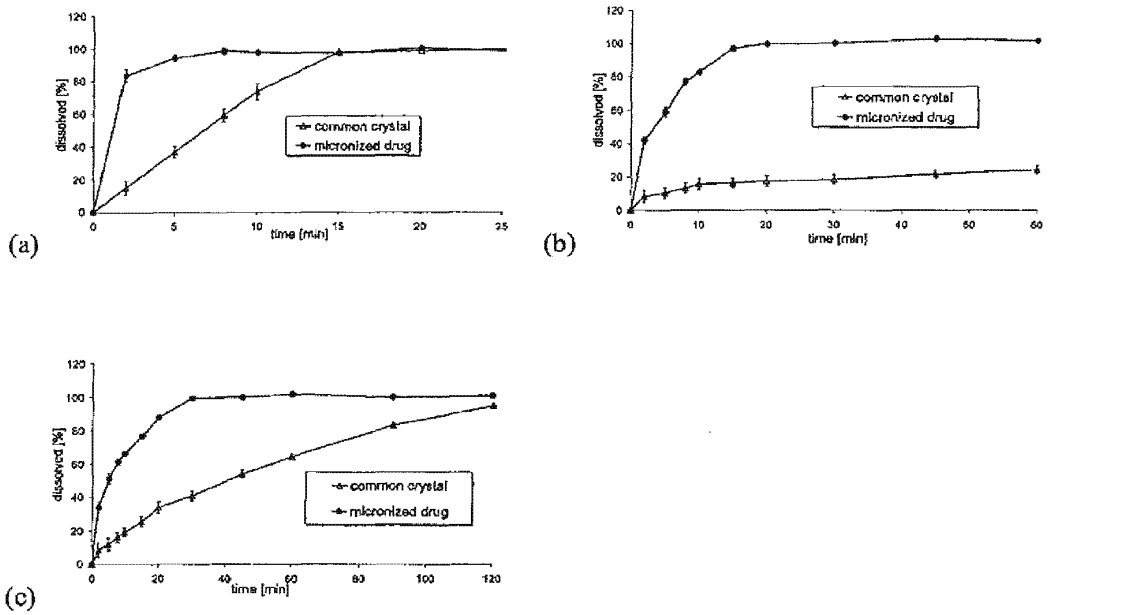


Fig. 9. Powder dissolution. (a) ibuprofen; (b) itraconazole; (c) ketoconazole.

distribution (Fig. 8) is nearly the same as in the dispersion that is spray-dried. Thus, the agglomerated crystals are deagglomerated. No electrostatic effects occur; thus, the powder flow is increased compared with milled itraconazole or ketoconazole. The dissolution rate of the micronized drugs is significantly increased compared with the common crystals (Fig. 9). Particularly, the common crystals of itraconazole only show a very slow dissolution because of the effect of aerophilization, which is often observed with milled drugs. Thus, the dissolution rate of a milled drug is lower than would be expected from the Noyes-Whitney equation. The crystals are not wettable (not even by the used simulated gastric juice containing a surfactant). Thus, they are agglomerated on the surface of the dissolution medium. The dramatic increase in drug dissolution rate can be explained by an increased specific surface area (Table I). This high surface area is hydrophilized, the contact angle is decreased because of adsorbed hydrophilic HPMC (Table II). The contact angles of the micronized drugs are nearly the same for ibuprofen, itraconazole, and ketoconazole and also nearly the same as for the pure cellulose ether. The adsorbed HPMC determines the surface properties of the resulting product. Thus by precipitating microcrystals in the presence of stabilizing protective additives, a high and hydrophilized surface area can be formed in a one process step without using any milling techniques.

CONCLUSIONS

By the method used in this study, small drug particles are prepared without size-reduction techniques. Micronized poorly water-soluble drugs can be prepared by controlled crystallization of primary molecularly dispersed substances. The precipitation technique in the presence of protective hydrophilic polymers followed by spray-drying results in a drug powder with a markedly enhanced drug dissolution rate. A high and hydrophilized surface area is created. To form a protective layer on the crystal surface, the polymer must have an affinity to the hydrophobic crystal surface. Compared with, e.g., solid dispersions or cyclodextrin encapsulations, the amount of drug in the preparation is relatively high. The production process can be conducted discontinuously or continuously using a static mixer and is possible as a one-process step and needs only common equipment. This technique offers a relatively easy way for production of micronized drugs that are characterized by a homogeneous particle size distribution. Critical effects resulting from milling processes are avoided.

Table I. Specific Surface Area [m^2/g] (±S.D.)

	Common crystal	Micronized drug
Ibuprofen	0.11 ± 0.01	2.00 ± 0.09
Itraconazole	0.21 ± 0.02	4.03 ± 0.10
Ketoconazole	0.18 ± 0.02	3.01 ± 0.09

Results: mean of three measurements; S.D. = standard deviation

Table II. Contact Angle [°] (±S.D.)

	Common crystal		Micronized drug	
	t_1 = 0 s	t_2 = 180 s	t_1 = 0 s	t_2 = 180 s
Ibuprofen	63.9 ± 1.5	62.3 ± 1.4	42.3 ± 1.6	33.0 ± 1.5
Itraconazole	48.2 ± 1.3	47.2 ± 1.0	39.1 ± 1.4	30.1 ± 1.3
Ketoconazole	44.6 ± 1.1	42.8 ± 1.3	38.2 ± 1.3	29.8 ± 1.1

Results: mean of 20 measurements; S.D. = standard deviation.

UM00016859
NOVARTIS EXHIBIT 1517
Novartis v. Regents, IPR2023-01347
Page 3841 of 4460

ACKNOWLEDGMENT

We would like to thank Janssen Pharmaceutica and BASF AG for the supply of the drugs.

REFERENCES

1. J. R. Robinson. Recent advantages in formulation of poorly absorbed Drugs. In *Current Status on Targeted Drug Delivery to the gastrointestinal tract*, Capsugel Library, 1993 pp. 59–63.
2. Y. Kawashima. Nanoparticulate systems for improved drug delivery. *Adv. Drug Deliv. Rev.* **47**:1–2 (2001).
3. E. L. Parrott. Comminution. In J. Swarbrick, J. C. Boylan (eds.), *Encyclopedia of Pharmaceutical Technology*, Vol. 3., Marcel Decker Inc., New York, 1990 pp. 101–121.
4. L. Mackin, R. Zanon, J. M. Park, K. Foster, H. Opalenik, and M. Demonte. Quantification of low levels (< 10%) of amorphous content in micronised active batches using dynamic vapour sorption and isothermal microcalorimetry. *Int. J. Pharm.* **231**:227–236 (2002).
5. M. D. Ticehurst, P. A. Basford, C. J. Dallinan, T. M. Lukas, P. V. Marshall, G. Nichols, and D. Smith. Characterisation of the influence of micronisation on the crystallinity and physical stability of revatropate hydrobromide. *Int. J. Pharm.* **193**:247–259 (2000).
6. L. Mackin, S. Sartnurak, I. Thomas, and S. Moore. The impact of low levels of amorphous material (< 5%) on the blending characteristics of a direct compression formulation. *Int. J. Pharm.* **231**:213–226 (2002).
7. J. C. Feeley, P. York, B. S. Sumby, and H. Dicks. Determination of surface properties and flow characteristics of salbutamol sulphate, before and after micronisation. *Int. J. Pharm.* **172**:89–96 (1998).
8. G. H. Ward and R. K. Schultz. Process-induced crystallinity changes in albuterol sulfate and its effect on powder physical stability. *Pharm. Res.* **12**:773–779 (1995).
9. R. J. Roberts, R. C. Rowe, and P. York. The relationship between indentation hardness of organic solids and their molecular structure. *J. Mater. Sci.* **29**:2289–2296 (1994).
10. C. Jacobs, O. Kayser, and R. H. Müller. Nanosuspensions as a new approach for the formulation for the poorly soluble drug tarazepide. *Int. J. Pharm.* **196**:161–164 (2000).
11. R. H. Müller, C. Jacobs, and O. Kayser. Nanosuspensions as Particulate Drug Formulations in Therapy. Rationale for Development and what We Can Expect for the Future. *Adv. Drug Deliv. Rev.* **47**:2–19 (2001).
12. R. H. Müller, H. L. Böhm, and M. J. Grau. Nanosuspensionen—Formulierungen für schwerlösliche Arzneistoffe mit geringer Bioverfügbarkeit; 1. Herstellung und Eigenschaften. *Pharm. Ind.* **61**:74–78 (1999).
13. E. Shalaev, M. Shalaeva, and G. Zografi. The effect of disorder on the chemical reactivity of an organic solid, tetraglycine methyl ester: change of the reaction mechanism. *J. Pharm. Sci.* **91**:584–593 (2002).
14. J.-O. Waltersson and P. Lundgren. The effect of mechanical comminution on drug stability. *Acta Pharm. Suec.* **22**:291–300 (1985).
15. V. Joshi, S. Dwivedi, and G. H. Ward. Increase in the specific surface area of budesonide during storage postmicronization. *Pharm. Res.* **19**:7–12 (2002).
16. R. H. Müller, K. Peters, R. Becker, and B. Kruss. Nanosuspensions for the i.v. administration of poorly sofuble drugs—stability during sterilization and long-term storage. *Proc. Intern. Symp. Control. Rel. Bioact. Mater.* **22**:574-575 (1996).
17. P. Gaßmann, M. List, A. Schweitzer, and H. Sucker. Hydrosols—Alternatives for the parenteral application of poorly watersoluble drugs. *Eur. J. Pharm. Biopharm.* **40**:64–72 (1994).
18. D. Horn. Preparation and characterisation of microdisperse bioavailable carotenoid hydrosols. *Angew. Makrom. Chem.* **166**:139–153 (1989).
19. H. Auweter, H. Bohn, H. Haberkorn, D. Horn, E. Luddecke, and V. Rauschenberger. Production of carotenoid preparations in the form of coldwater-dispersible powders, and the use of the novel carotenoid preparations, US patent no. 5,968,251, October 19, 1999.
20. H. Steckel, J. Thies, and B. W. Müller. Micronizing of steroids for pulmonary delivery by supercritical carbon dioxide. *Int. J. Pharm.* **152**:99–110 (1997).
21. J. Kerc, S. Srcic, Z. Knez, and P. Sencar-Bozic. Micronization of drugs using supercritical carbon dioxide. *Int. J. Pharm.* **182**:33–39 (1999).
22. N. Rasenack, and B. W. Müller. Verfahren zur Herstellung und Anwendung von Mikro- und Nanoteilchen durch aufbauende Mikronisation, German Patent Application No. 102 14 031.6 (2002).
23. B. L. Pedersen, A. Müllertz, H. Brondsted, and H. G. Kristensen. A comparison of the solubility of danazol in human and simulated gastrointestinal fluids. *Pharm. Res.* **17**:891–894 (2000).
24. V. P. Shah, J. J. Konecny, R. L. Everett, B. McCullough, A. C. Noorizadeh, and J. P. Skelly. In vitro dissolution profile of water-insoluble drug dosage forms in the presence of surfactants. *Pharm. Res.* 6:612–618 (1989).
25. H. Schott. Colloidal Dispersions—Gennaro A.R., Chase G.D., Gibson, M.R., Granberg, C.B., Harvey, S.C., King, R.E., Martin, A.N., Medwick, T., Swinyard, E.A., and Zink, G.L. (eds.). In: *Remington's Pharmaceutical Sciences*; The Philadelphia College of Pharmacy and Science, 1985, pp. 286–289 Philadelphia, Pennsylvania.
26. S. A. Chang and D. G. Gray. The surface tension of aqueous hydroxypropyl cellulose solutions. *J. Colloid. Interface Sci.* **67**: 255–265 (1978).
27. R. Daniels and A. Barta. Pharmacopoeial cellulose ethers as oil-in-water emulsifiers. I. Interfacial Properties. *Eur. J. Pharm. Biopharm.* **40**:128–133 (1994).

UM00016860
NOVARTIS EXHIBIT 1517
Novartis v. Regents, IPR2023-01347
Page 3842 of 4460

XP-002566271

DG

35

PREPARATION OF WATER-SOLUBLE COMPOUNDS THROUGH SALT FORMATION

P. Heinrich Stahl

There is nothing in the universe but alkali and acid, from which nature composes all things.
Ott. Tachenius (1671)

I	Introduction	601
II	The solubility of compounds in water	602
	A Prediction of solubility	602
	B Ionization of weak electrolytes	602
	C Solubility of electrolytes	603
III	Acids and bases for salt formation	606
	A Selection of salt formers	608
IV	Obtaining solid salts	610
	A Some principles and practical considerations of preparation	610
	B Solid-state properties	612
V	Criteria for salt selection	613
	A Essential parameters and properties	613
References		614

I INTRODUCTION

An optimal drug candidate is not only a highly potent ligand, selective to the receptor species to which it has been designed to bind, has more favourable kinetics of binding than its naturally competing ligands, and has adequate chemical and metabolic stability. Moreover, it should satisfy a series of requirements set by areas remote from the immediate environment of the receptors. Most important, there is the need for substantial transport from outside the organism to the sites of action. Biopharmaceutically relevant substance properties can enable or limit the crossing of absorption barriers and for administering a drug in dosed amounts or suitable concentration. Preparations need to be designed and developed for timely and quantitative delivery of the active substance. Although pharmaceutical formulation techniques offer numerous possibilities, there are limitations in mastering problems incurred by substances with suboptimal inherent properties, and the least of the consequences is that they slow down the drug development process.

An NCE (new chemical entity) rarely meets all the requirements of an ideal drug substance. As lead optimization concentrates towards improvement of biological activity as evaluated by *in vitro* tests, other desirable properties often fall behind, although the awareness is increasing that acceptable pharmacokinetic properties should be built into a drug molecule as well.

Functional groups that turn a molecule into an electrolyte provide the opportunity for the formation of salts. Salt formation is a means to change the properties while the chemical structure of the active entity is left intact. Yet, a new chemical entity is created by salt formation with all the consequences.

About half of all present-day drugs are used as salts, and for the chemist it is obvious to try improving the properties of a drug candidate by the formation of a suitable salt, in particular with the intention to enhance solubility and in consequence, the rate of dissolution as prerequisite parameters for absorption. However, one should be aware, that high solubility alone does not guarantee good absorption.

In this chapter not only the topic of water-soluble salts but also some general points to consider when the final form of a drug substances will be decided upon. Although it is generally accepted that solubility in aqueous media is the most crucial physicochemical property of a drug substance, it is not appropriate that only a single parameter should dominate such an important decision. Since here only

The Practice of Medicinal Chemistry
ISBN 0-12-744481-5

Copyright © 2003 Elsevier
All rights of reproduction in any form reserved.

BNSDOCID: <XP_____2566271A__I_>

UM00016861
NOVARTIS EXHIBIT 1517
Novartis v. Regents, IPR2023-01347
Page 3843 of 4460

the essentials of the complex field of salt formation and selection can be dealt with, the reader may refer to a recent monograph on the subject.[1]

II THE SOLUBILITY OF COMPOUNDS IN WATER

A Prediction of solubility

Solubility is understood as the concentration in a solution found in equilibrium with an excess of the solid solute at a given temperature. It is generally accepted that solubility in aqueous media is the most crucial physicochemical property of a drug substance. In order to get an estimate of the solubility of a nonelectrolyte at a very early stage, many computational approaches have been made. Among them, a surprisingly simple and yet effective tool is available, the General Solubility Equation (GSE) as developed and refined during the last two decades by Yalkowsky and his coworkers[2,3] using a thermodynamically sound approach for establishing a semi-empirical correlation:

$$\log S = 0.5 - 0.01(Mp - 25) - \log K_{ow} \qquad (1)$$

where S is the molar solubility of the solute, K_{ow} the octanol/water partition coefficient, which can be calculated from the structural formula (ClogP),[4] and Mp is the melting point (in centigrade, °C) as the only experimental data, representing the easiest accessible descriptor of the strength of a solid's crystal lattice. Based on the assumption, that the nonionized form of an electrolyte may be regarded as a nonelectrolyte, an extension of the GSE has recently been proposed. By simply combining equation (1) with the solubility–ionization relationships (equations in Table 35.2), it is possible to construct pH solubility profiles for acids, bases and zwitterions.[5]

B Ionization of weak electrolytes

In physicochemical terms, about two-thirds of all existing drug entities belong to the class of weak electrolytes, i.e. substances which in aqueous solution are at least partly present as ions. They are formed by releasing protons (acids) into, or by accepting protons (bases) from, an aqueous environment. Ionized species are easily hydrated and hence are generally more soluble in an aqueous phase than their nonionized source. The aqueous solubility of weak electrolytes is influenced and can be controlled by adjusting the pH of the solution via the equilibrium between the nonionized and the ionized species.

The dissociation of a monoprotic acid HA is described by the equilibrium between the concentrations of the nonionized acid molecule (= [HA]) and of its anion (= $[A^-]$):

$$[HA] \overset{K_a}{\rightleftarrows} [H^+] + [A^-] \qquad (2)$$

The equilibrium constant K_a of this reaction is the ionization constant, which is defined by

$$K_a = \frac{[H^+]\cdot[A^-]}{[HA]} \qquad (3)$$

Because ionization constants are small and inconvenient figures, they are expressed as their negative decadic logarithms:

$$pK_a = -\left({}^{10}\log K_a\right) \qquad (4)$$

As an example, the K_a of acetic acid converts from 1.738×10^{-5} to $pK_a = 4.76$. Similarly, for a monobasic compound the dissociation equilibrium is expressed as follows:

$$[BH^+] \overset{K_a}{\rightleftarrows} [B + H^+] \qquad (5)$$

with the dissociation constant

$$K_a = \frac{[H^+]\cdot[B]}{[HB^+]} \qquad (6)$$

Since the protonated base can be considered as an acid corresponding to the free base, it is possible to characterize both, acids and bases with the same parameter, i.e. the acid ionization constant. The K_a or the pK_a, respectively, is the key parameter indicating the strength of an electrolyte (Table 35.1).

Table 35.1 *Examples of acids and bases aligned according to strength*

	pK_a	Acids	Bases	pk_a	
Strong	1.3	Oxalic acid, $pK_{a,1}$	Caffeine	0.6	Weak
↑	1.6	Saccharin	Quinine, $pK_{a,2}$	4.1	↓
	2.8	Benzylpenicillin	Pyridine	5.2	
	3.0	Salicylic acid, $pK_{a,1}$	Papaverine	5.9	
	4.1	Diclofenac	Apomorphine	7.0	
	6.5	Sulfadiazine	Benzoctamine	7.6	
	7.1	Sulfathiazole	Quinine, $pK_{a,1}$	8.0	
	7.4	Phenobarbital, $pK_{a,1}$	Cocaine	8.4	
	8.4	Phenytoin	Imipramine	9.5	
	8.8	Theophyllin	Atropine	9.7	
	10.0	Phenol	Amantadine	10.3	
	11.8	Phenobarbital, $pK_{a,2}$	Piperidine	11.2	
Weak	13.8	Salicylic acid, $pK_{a,2}$	Arginine, $pK_{a,1}$	13.2	Strong

BNSDOCID: <XP_____2566271A__I_>

UM00016862
NOVARTIS EXHIBIT 1517
Novartis v. Regents, IPR2023-01347
Page 3844 of 4460

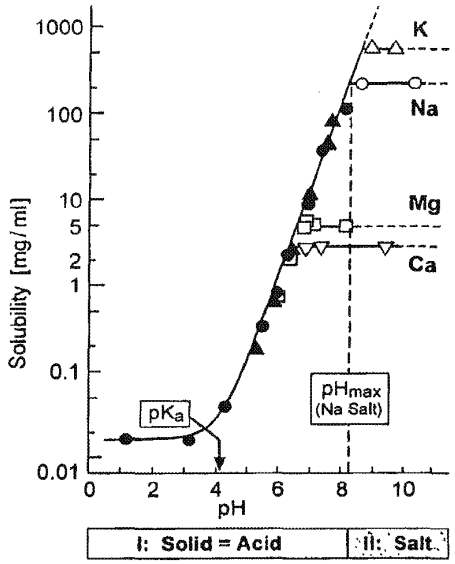
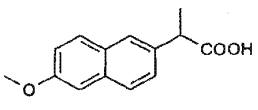


Fig. 35.1 pH solubility profiles of four salts of *naproxen* (pK_a = 4.15) in water at 25°C. Starting material was naproxen acid (full symbols) or the respective salt (open symbols). (Redrawn from Cowhan.[6])

C Solubility of electrolytes

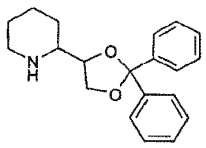
General features of pH solubility profiles

Monoprotic acids and bases. An ideal pH solubility profile for a weakly monoprotic acidic compound is exemplified by *naproxen* **1**, as shown in Fig. 35.1. It is obtained by increasing the pH, e.g. by stepwise adding amounts of a base, for example sodium hydroxide, to a suspension of the acid and determining the concentration of dissolved acid after equilibration. The pH range of the diagram is divided into two regions marked as region I and II, respectively, according to the nature of the excess solid phase in equilibrium with the saturated solution. In region I (pH < 8.3 in Fig. 35.1) the excess solid phase is the free acid, whereas in region II (pH > 8.3), it is the sodium salt. In region I, the total solubility is described by the sum of concentrations of the neutral and the dissociated fractions of the acid:



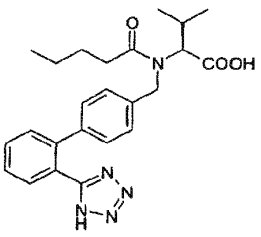
Naproxen

1



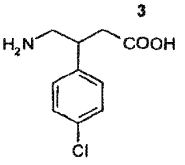
Dexoxadrol

2



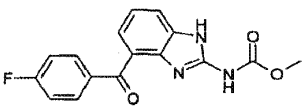
Valsartan

3



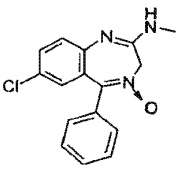
Baclofen

4



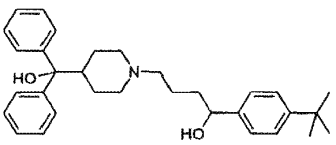
Flubendazole

5



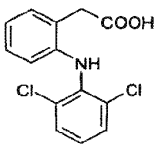
Chlordiazepoxide

6



Terfenadine

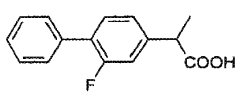
7



Diclofenac

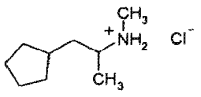
8

BNSDOCID: <XP_____2566271A__I_>



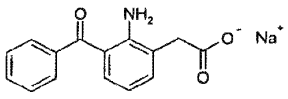
Flurbiprofen

9



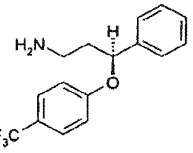
Cyclopentamine hydrochloride

10



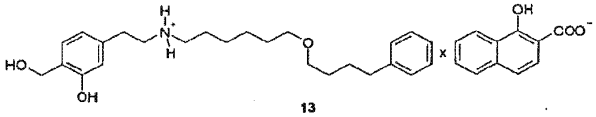
Amfenac sodium

11



Seproxetine

12



13

Salmeterol xinafoate

$$S = [HA] + [A^-] \quad (7)$$

$$S = S_0\left(1 + \frac{K_a}{[H^+]}\right) \quad (8)$$

where S is the total solubility at any given pH, S_0 is the intrinsic solubility of the free acid, [HA] and $[A^-]$ represent concentrations in solution of the undissociated and dissociated forms, respectively, and K_a is the acid dissociation constant defined in equation (3).

Region I may be further subdivided into a range where the solubility is essentially independent of the pH (pH $<$ ca.3) and the range adjacent to region II, between pH approximately 3 and 7.3 characterized by an exponential dependence of solubility on pH.

The total solubility in region II is described by:

$$S = \left(1 + \frac{[H^+]}{K_a}\right)\sqrt{K_{sp}} \quad (9)$$

$$K_{sp} = [Na^+]\cdot[A^-] \quad (10)$$

where K_{sp} is the solubility product of the salt, and $\sqrt{K_{sp}} = S_s$ is the intrinsic solubility of the salt.

Thus, the two equations (8) and (9) are sufficient to describe the entire pH solubility profile of a monoprotic acid, and the point of intersection is defined by equation (11):

$$pH_{max} = pK_a + \log\frac{S_0}{\sqrt{K_{sp}}} = pK_a + \log S_0 - \tfrac{1}{2}\log K_{sp} \quad (11)$$

For a weak base, the pH solubility profile is essentially the mirror image of that of a weak acid along a vertical axis, as illustrated in Fig. 35.2 by the central stimulant and analgesic *dexoxadrol* **2**.

As in the case of the acid, there is a region in equilibrium with excess undissolved free base, here at high pH values and a region with high and constant solubility at low pH values. An analogous set of equations applies for the two legs of the theoretical pH solubility profile (equations (11) and (12)), whereas for the position of pH_{max}, equation (10) is equally valid for bases.

$$\text{High pH region (II)} : S = [B] + [BH^+] = S_0\left(1 + \frac{[H^+]}{K_a}\right) \quad (12)$$

$$\text{Low pH region (I)} : \quad S = \left(1 + \frac{K_a}{[H^+]}\right)\sqrt{K_{sp}} \quad (13)$$

pH_{max}. At pH_{max}, both the nonionized species and the respective salt coexist in the undissolved solid. Bogardus

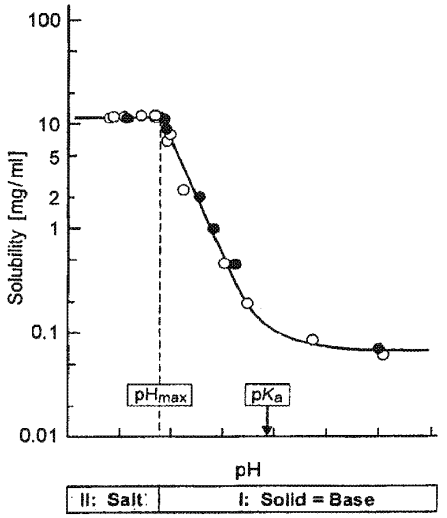


Fig. 35.2 pH solubility profile of *dexoxadrol* in water at approximately 23°C. Open and full circles indicate different analytical methods. (Redrawn from Kramer and Flynn.[7])

BNSDOCID: <XP_____2566271A__I_>

UM00016864
NOVARTIS EXHIBIT 1517
Novartis v. Regents, IPR2023-01347
Page 3846 of 4460

et al.[8] reported that indeed the excess solid in equilibrium with the saturated solution of doxycycline at pH_{max} contained both the free base and the hydrochloride salt phases.

pH_{max} constitutes a further descriptor of the solubility profile specific for the particular salt, as may be recognized from the profiles of the four salts of naproxen presented in Fig. 35.1. The different counterions limit the solubility at different levels, resulting in differences as high as two orders of magnitude. A counterion can gain influence on solubility only at pH values where the drug substance is ionized, and salt formation cannot improve solubility in pH regions where the nonionized species prevails. It should be noted that the solubilization capacity by pH control for weak electrolytes is limited by the solubility product K_{sp} of the salt formed. Once the solubility of the salt is reached, pH control cannot further solubilize the compound.

Diprotic acids and bases. Many drug substances bear more than one ionizable function: acidic or basic functional groups or, in case of amphoteric substances, even both types in the same molecule. In order to evaluate their influence on solubility, the key parameter is again the pK_a. In Table 35.2, the equations describing the pH profiles for mono- and diprotic acids and bases are given in their exponential form. As an example, the graph in Fig. 35.3 shows the profile of a diprotic base with pK_a values relatively close to each other. As upon addition of an acid to a suspension of the base the pH decreases, the solubility starts to increase by one order of magnitude as the pH decreases by one unit once it gets below the first protonation step, $pK_{a,1}$. However, as the pH drops below the second ionization step, $pK_{a,2}$, the solubility increases by two orders of magnitude per one pH unit. Similar relationships apply for diprotic acids. A further aspect of diprotic electrolytes may be illustrated by the speciation diagram (Fig. 35.4) of the diprotic acid *valsartan* **3** ($pK_{a,1} = 3.90$, carboxylic acid; $pK_{a,2} = 4.73$, tetrazole). This graph shows the relative abundance of the ionic and

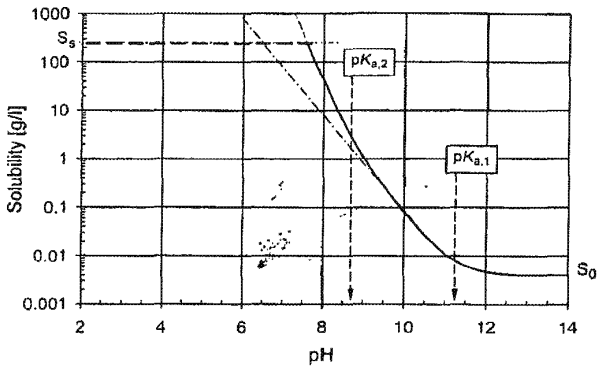


Fig. 35.3 Theoretical pH solubility profile of a diprotic base with the pK_a values $pK_{a,1} = 11.25$ and $pK_{a,2} = 8.7$; $S_0 = 0.004$. The point-dashed line shows the course of solubility if there were only the first basic function.

Table 35.2 *Solubility equations for mono- and diprotic acids and bases*

$pH \leq pH_{max}$		$pH \geq pH_{max}$	
Monoprotic acid			
$S = S_0 \cdot \left(1 + 10^{pH-pK_a}\right)$	(17)	$S = S_S \cdot \left(1 + 10^{pK_a-pH}\right)$	(18)
Diprotic acid			
$S = S_0 \cdot \left(1 + 10^{pH-pK_{a,1}}\right) \cdot \left(1 + 10^{pH-pK_{a,2}}\right)$	(19)	$S = S_{S,2} \cdot \left(1 + 10^{pK_{a,2}-pH}\right)$	(20)
Monoprotic base			
$S = S_S \cdot \left(1 + 10^{pH-pK_a}\right)$	(21)	$S = S_0 \cdot \left(1 + 10^{pK_a-pH}\right)$	(22)
Diprotic base			
$S = S_{S,2} \cdot \left(1 + 10^{pH-pK_a}\right)$	(23)	$S = S_0 \cdot \left(1 + 10^{pK_{a,1}-pH}\right) \cdot \left(1 + 10^{pK_{a,2}-pH}\right)$	(24)

$S_{S,2}$ is the solubility of the neutral salt of the diprotic acid or base, respectively. Other symbols are as used in the text.

BNSDOCID: <XP_____2566271A__I_>

UM00016865
NOVARTIS EXHIBIT 1517
Novartis v. Regents, IPR2023-01347
Page 3847 of 4460

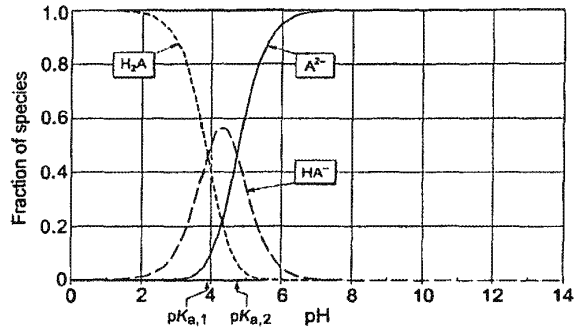


Fig. 35.4 pH species distribution diagram of *valsartan* (see text).

nonionic species of the acid in solution as a function of pH. The maximum fraction that the mono-anion can reach is at pH 4.2, and amounts to a percentage of 56% of the dissolved acid, while at the same time 22% each of the nonionized acid and the di-anion are simultaneously present. A consequence from such relations is that it will depend on the relative solubilities of the respective ion pairs, which of them would form the excess solid in equilibrium with a saturated aqueous solution in the intermediate pH range, and it is possible that from aqueous solutions a pure acidic salt cannot be isolated.

Special types of amphoteric substances are the zwitterionic compounds. Every molecule that has an acidic pK_a lower than the pK_a of its basic function is a zwitterion, because such a substance has acidic and basic groups strong enough to neutralize one another; hence, they are 'inner salts'. As shown in Fig. 35.5 the solubility profile of *baclofen* **4** ($pK_{a,1} = 3.85$, proton gained; $pK_{a,2} = 9.25$, proton lost), a typical example of this class, exhibits a solubility minimum in the pH range where the zwitterion is the predominant species.

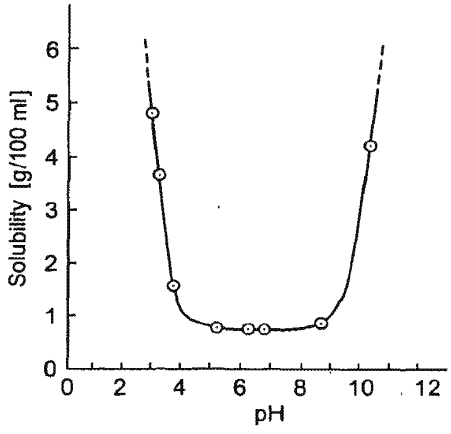


Fig. 35.5 Solubility pH profile of *baclofen* at 25°C in aqueous buffers.

Practical evaluation of solubility

The principle of solubility determination was already briefly described above. The suspension system should be held at a constant and controlled temperature. Before sampling it should be given sufficient time for equilibration, which is accelerated by using finely ground material. Ideally, equilibrium is assured by repeated sampling. The concentration in the filtered samples is determined by a suitable analytical method, most frequently by direct UV or by HPLC assay; the latter would help to detect any degradation during the equilibration process. The frequently applied 'quick' method of heating a sample in water to achieve complete dissolution and cooling to room temperature leads more often than not to erroneous results due to supersaturation effects and also due to changes of the excess solid like polymorphic transformation or change of the state of hydration induced by higher temperature. Sometimes solid samples are obtained by lyophilization and are therefore amorphous. An amorphous substance is both, much more soluble and more hygroscopic, than the same material is in a crystalline state.

It is important to note all relevant parameters of the data points in a solubility experiment: temperature, pH, concentration, nature of the excess solid, i.e. whether salt or free acid (base) is present, and whether changes with reference to the initial sample material concerning the polymorphic state or the degree of hydration have taken place. While such careful studies are appropriate at a later stage, i.e. prior to the final candidate selection, other techniques are applied for screening large numbers of compounds at an earlier stage. As for screening the biological activity, high throughput techniques are also applied for solubility screening. A typical non-specific microtechnique is based on the turbidimetric indication of the transition between complete and incomplete dissolution when stock solutions of substances in DMSO are diluted with water or aqueous buffers.[9] This technique can be performed on 96-well microtiter plates and adapted for a first screening of salt formers and establishing pH solubility profiles.

III ACIDS AND BASES FOR SALT FORMATION

Numerous acids and bases are in use for providing the counterions to form salts. Figures 35.6 and 35.7 show acids and bases, indicating the frequency of their use in drug salts of prescription drug products. However, salt forming agents are material, which are not expressively approved by the health authorities for that particular use, and hence there are

BNSDOCID: <XP_____2566271A__I_>

UM00016866
NOVARTIS EXHIBIT 1517
Novartis v. Regents, IPR2023-01347
Page 3848 of 4460

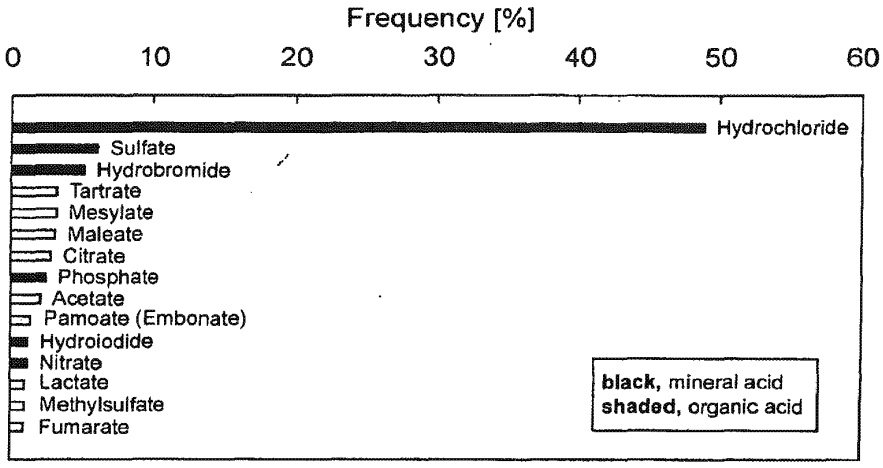


Fig. 35.6 Percentage of the 15 most frequently used acids for salt formation, resulting from a survey of the 1998 edition of *Index Nominum.*

no official lists. A drug is approved not as an isolated active entity but only in the context of the drug product as a whole, i.e. as the dosage form intended for the market, containing the active ingredient in its complete chemical form. The counter-ion is not a separate item of application. The use of such 'inactive' moieties is rather justified by their prior occurrence as salt formers in established drugs, and their further use as safe 'inactive' moiety in drug salts can be largely derived from their presence in marketed drug products. A periodically updated register of approved drug products is the *Orange Book*[10] which lists drug products whose safety and efficacy has been evaluated, so it may be searched also for salt forms of drug substances.

The high frequency of hydrochlorides and sodium salts has not only the background of convenience but can be derived from the fact that both ions are the most abundant electrolytes in the body and hence are expected to cause no alterations of physiological functions. Other salt-forming acids are naturally occurring components of food or natural substrates of the intermediary metabolism. The number of organic bases usable as salt formers is much smaller, because generally, amines and other nitrogen bases have

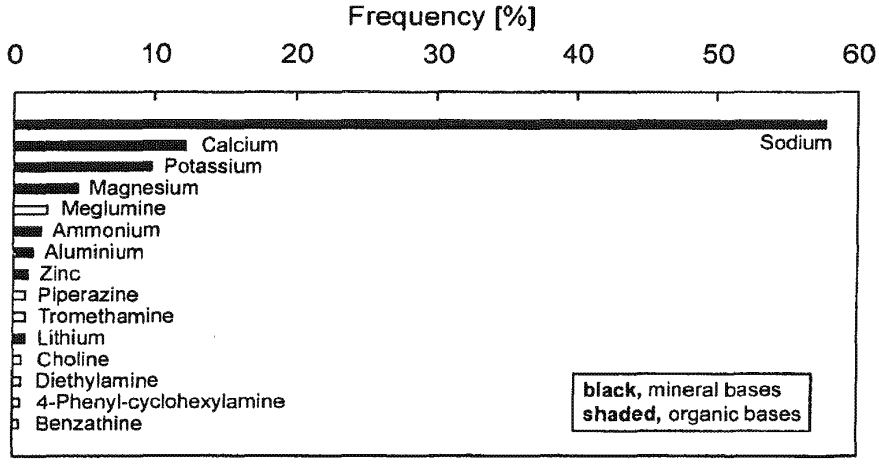


Fig. 35.7 Percentage of the 15 most frequently used bases for salt formation resulting from a survey of the 1998 edition of *Index Nominum.*

BNSDOCID: <XP_____2566271A__L>

their own pharmacodynamic activity, unless they are very rapidly metabolized. Exceptions are the essential basic amino acids, e.g. arginine and lysine.

A Selection of salt formers

pK_a

Which acids or bases should be considered for forming salts with a drug substance? This must chiefly be decided with regard of physicochemical parameters, in the first place based on the pK_a values involved. When forming a salt the acid transfers a proton to the conjugate base, which in turn must be selected to be ready for accepting the proton. This is generally the case if the pK_a of the acid is at least two units lower than the pK_a of the base. This corresponds to a situation where in water both components are ionized to a degree of at least 99%. Strong mineral acids such as HCl ($pK_a = -6$) or H_2SO_4 ($pK_a = -3$) could form solid salts with the anthelmintic *flubendazole* **5** having a pK_a value as low as 4.1, whereas with acetic acid or with benzoic acid ($pK_a = 4.2$) an attempt to prepare a salt would not be successful with such a very weak base. For basic drugs, Gould[11] has published detailed physicochemical relationships along a decision analysis procedure including useful tables of salt-forming acids.

Resulting pH

The next parameter to consider is the pH resulting in the aqueous solution of a salt. The pH may be estimated even before the salt has been prepared, since equations (14)–(16) for the three general cases of salt types of weak electrolytes sallow a theoretical approach:

$$\text{weak acid} \times \text{strong base: pH} = \tfrac{1}{2}(pK_{a,acid} + pK_w + \log c) \quad (14)$$

$$\text{weak base} \times \text{strong acid: pH} = \tfrac{1}{2}(pK_{a,base} - \log c) \quad (15)$$

$$\text{weak acid} \times \text{weak base: pH} = \tfrac{1}{2}(pK_{a,acid} + pK_{a,base}) \quad (16)$$

where, pK_w is the negative ionization exponent of water with the value of 14 at 25°C, and c is the concentration of the salt. How the solubility and pH can be estimated, using equations (12) and (15), respectively, is demonstrated for the weakly basic tranquillizer *chlordiazepoxide* **6** ($pK_a = 4.6$). For a solution containing 50 mg ml^{-1} (0.167 M) as the hydrochloride salt, the calculated pH is 2.7. With the known solubility of the nonionized base (2 mg ml^{-1}), equation (12) predicts a solubility of 200 mg ml^{-1} at this pH (in fact, the solubility of the hydrochloride in water is 100 mg ml^{-1} = 0.33 M). Trying to prepare an acetate of chlordiazepoxide would make little sense for three reasons: (1) the pK_a of acetic acid is just about the same as that of the drug base; (2) an equimolar solution of base and acetic acid would have a calculated pH of 4.78, at which pH in 1 ml a mere 4 mg of the base are soluble, a solubility value not really worthwhile for a salt; (3) if a solid acetate were feasible it would, on contact with water or humid air, release the volatile acetic acid, and the solid drug base would be left behind.

The common-ion effect

While the preference for preparing hydrochlorides and sodium salts is favoured by the physiological abundance of Cl^- and Na^+ ions, these can also bring about negative effects. One of them is the suppression of solubility, which becomes particularly apparent with hydrochlorides and sodium salts of moderate to low intrinsic solubility. The presence of additional ions of the same kind, e.g. in physiological saline, in the stomach and in blood, causes a reduction of solubility by the law of mass action. This 'common-ion effect' depresses the solubility of *terfenadine* (7) hydrochloride in water (2 mg ml^{-1} at pH of approximately 5) down to a tenth when 0.05 M NaCl is added. The solubility of *diclofenac* **8** sodium in water (25°C) is 21.3 mg ml^{-1}, but 6.7 mg ml^{-1} in physiological saline. Under the same conditions, the corresponding figures for 4-(5,6-dimethyl-2-benzofuranyl)-piperidine hydrochloride, an experimental antidepressant, are 3.8 and 0.44 mg ml^{-1}, respectively. While hydrochlorides of aliphatic amines are highly soluble (oxprenolol: 720 mg g^{-1} solution at 25°C), those of cycloaliphatic and heteroaromatic nitrogen bases are often sparingly soluble. Numerous examples have been reported where hydrochloride salts exhibited lower solubility than other salts.[12–16] Solubility and dissolution rate of hydrochlorides administered orally may be further suppressed by the common-ion effect,[17–19] since the chloride ion is present at concentrations between 100 and 140 mval l^{-1} in gastric fluid.[20] There are examples of pyrimidine derivatives whose hydrochlorides are even less soluble than the free bases. Bogardus and Blackwood[8,21] compared the intrinsic dissolution rates of doxycycline monohydrate and hydrochloride dihydrate in 0.1 M HCl. Although the hydrochloride is better soluble in water, it dissolved six times slower than the free base form due to the common-ion effect.

Due to their strength, mineral acids (and the alkali hydroxides) are appreciated for forming stable salts with very weak bases (and acids, respectively), they will be considered in first place, provided the above pH estimations would not exclude them in individual cases. Once several alternative salt formers have been selected, experimental screening will identify those rendering high solubility.

BNSDOCID: <XP_____2566271A__I_>

UM00016868

NOVARTIS EXHIBIT 1517
Novartis v. Regents, IPR2023-01347
Page 3850 of 4460

Tong and Whitesell[22] have described a substance-sparing procedure. Using less than 50 mg of investigational material, they exemplified their *in situ* salt screening method with GW1818X, a basic drug candidate (a piperidine base, $pK_a = 8.02$; relative molar mass 571.60) having a solubility of 4.4 mg l^{-1} in water. They investigated the solubilities of six salts using 0.1 M aqueous solutions of HCl, methanesulfonic, phosphoric, citric, succinic and tartaric acids and simultaneously characterized the excess materials that were crystalline except for the oily citrate and tartrate residues. The rank order of solubility in water (mg ml^{-1}) found with the salt samples subsequently prepared in gram amounts, was as follows: mesylate (9.2) > phosphate (6.8) > succinate (2.9) > hydrochloride (1.2). However, the initial screening had already shown that the intrinsic solubility of the phosphate salt, which was reached at a lower pH (i.e. in region II), had indeed the highest solubility (13.5 mg ml^{-1}) in the series, as was already found by *in situ* screening.

Predictability of salt solubility

Given an acidic or basic drug, the straightforward determination of the salt forming partner leading to a salt with the desired water solubility would be highly desirable. However, so far the predictive tools for estimating solubility based on the structure of the constituting ions are not at hand. Although some empirical structure–solubility relationships have been studied within closely related drug series, or with the salts of a given drug with a series of salt-forming ions, the pharmaceutical scientist is left with empirical tendencies or rank orders. So often, the highest solubilities are achieved with mesylates, lactates and salts of polyhydroxy acids of basic drugs, and with the potassium, tromethamine, meglumine and arginine salts of acidic drugs. Figure 35.1 reflects a typical rank order. As an additional observation, the series of *diclofenac* salts presented in Table 35.3 demonstrates the nonuniform temperature dependence of solubility even in a series of closely related members. In Fig. 35.8, linear solubility profiles of *terfenadine* 7 are shown, obtained with four different acids; the few experimental points are supplemented with theoretical curves. The frequently encountered rank order: lactate > methanesulfonate > hydrochloride > phosphate is found in this example. Here also the common-ion effect becomes dominant towards the low pH end of the profile because (1) for reaching the low pH values, the acid concentration of the respective acid has to be increased, which also raises the concentration of the respective anion; and (2) the overall level of solubility of this drug is rather low. Nevertheless, sometimes surprising changes of rank orders may be found, as in the example of GW1818X mentioned above with the highly soluble phosphate salt, whereas most phosphates are rather sparingly soluble.

Table 35.3 *Solubility of diclofenac salts in water*

Salt	25°C	pH	37°C	pH
Diclofenac (acid)	0.0071	5.8	0.0120	6.9
Calcium	0.58	6.8	0.62	6.8
Sodium	19.08	7.8	22.5	7.8
Potassium	47.05	7.8	120.5	8.2
Ethylenediamine	1.76	7.2	2.86	7.2
Diethylamine	13.95	7.6	18.3	7.6
Meglumine[a]	14.5	8.0	15.9	7.6
HEP[b]	44.7	8.3	484	7.8

Solubility (mg ml^{-1}) is expressed as the free acid; the pH of the saturated solution is given.
[a]1-deoxy-1-(methylamino)-D-glucitol.
[b]2-pyrrolidino-2-ethanol.

The solubility of salts is determined by (1) the interactions of the drug ions among themselves; and (2) between themselves and their counter-ions in the crystal lattice of the solid salt, represented by the lattice energy $\Delta G_{lattice}$; (3) between each sort of ions and water, expressed as the solvation energies of the cation ΔG_{cation}, and of the anion, ΔG_{anion}. The molar free energy of solution, $\Delta G_{solution}$, is the balance between those interactions:

$$\Delta G_{solution} = \Delta G_{cation} + \Delta G_{anion} - \Delta G_{lattice} \quad (17)$$

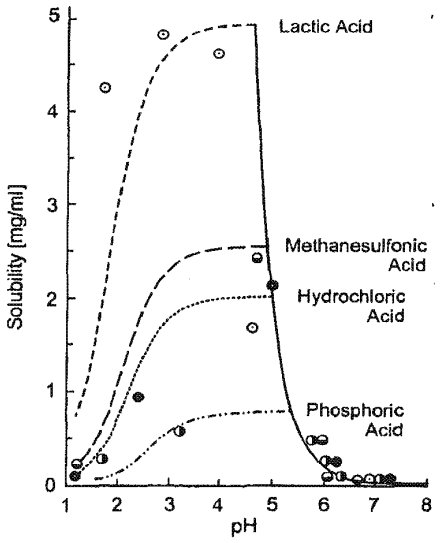


Fig. 35.8 pH profiles of the solubility of *terfenadine* with different acids. (Redrawn from Streng *et al.*[15])

BNSDOCID: <XP_____2566271A__I_>

UM00016869
NOVARTIS EXHIBIT 1517
Novartis v. Regents, IPR2023-01347
Page 3851 of 4460

In principle both the lattice energy and the hydration energies increase with an increase in cation or anion charge and decrease with an increase in ionic radius. They are also expected to increase with the polarity or with the hydrogen-bonding nature of the counterion. The overall effect of a given structural change on water solubility will depend on which terms, the lattice energy or the hydration energies, are more sensitive to the change in structure. Due to the complexity of drug molecules and in consequence, the multitude of the number and nature of interactions, the contribution of each term cannot yet be reliably estimated.

Anderson and Conradi[23] studied the effect of six ammonium salts of *flurbiprofen* **9**, differing in the hydrophobicity of the cation, on the water solubility. The solubility correlated well with the melting point of the salts, but the tromethamine salt with the most hydrophilic cation ranked only third in solubility. Chowhan[6] in his investigation of the sodium, potassium, magnesium and calcium salts of four carboxylic acids found that even the rank order of the salts of this cation series is not uniform. The result of a study on the sodium salts of 11 drugs, Rubino[24] confirms the correlation of melting point and salt solubility. How the melting point and other characteristics can be used to guide the process leading towards a salt of desired properties is presented in Table 35.4.

Other criteria

Not only physicochemical but also safety aspects can play a role when the decision is made as to which salt formers to include in a search for the optimum salt. Acids and bases that are traditionally in use for preparing salts are regarded as biologically 'inert'. However, not all of them are entirely indifferent. Some of them are indeed inert, such as the chloride, phosphate, or sodium ions. As an example, sodium ions are well tolerated, whereas elevated concentrations of potassium ions can cause local necrosis of the mucosa of the gastrointestinal tract. Salicylic acid, though formerly sometimes used as counter-ion, has its own pharmacological activity and can therefore not be regarded as an inert salt former. The route of administration, the prospective doses or concentrations, the therapeutic area of the drug candidate and the expected treatment regimen (acute or chronic) need to be taken into account even at this early stage. A comprehensive compilation of salt-forming acids and bases and their characteristics is found in Stahl and Wermuth.[1]

IV OBTAINING SOLID SALTS

A Some principles and practical considerations of preparation

Based on pH profiles of solubility, aqueous solutions can be prepared by adjusting the pH with a suitable acid or base in concentrations just necessary to achieve a solution, be it for immediate use for tests by the biologist, as well as for developing injectable formulations by the pharmacist. This is even done in production scale in pharmaceutical manufacturing if solutions are the final product, or if for some reason it is preferred to produce, isolate and store the free drug acid (or base). However, while in solubility screening experiments certain salt-forming acids or bases, respectively, may prove suitable for increasing solubility in water by pH adjustment, this is not the only requirement to be met for salt formation. In addition, conditions must be found for preparing and isolating a salt. After all the resulting solid is expected to be a physically stable and stoichiometrically reproducible product.

To this end, the process of salt formation is performed preferably in nonaqueous media. No drug salt can be isolated under conditions where it is fully ionized. Ion pairs constituting the salt need an environment that suppresses dissociation as much as possible. Drug substance and salt-forming agent are dissolved separately in solvents of moderate polarity, e.g. alcohols, esters, ethers and ketones. If one of the components is available in aqueous solution only (e.g. phosphorous acid), the other solvent should be water-miscible. While the solutions of the components are gradually mixed, the salt frequently starts to precipitate. If not, crystallization may be induced by raising the degree of supersaturation, which can be effected by cooling, by evaporating the solvent or by slow addition of a miscible anti-solvent (nonsolvent), or by a combination of these measures.

The preparation of salts is illustrated by two example procedures for a hydrochloride salt and for a sodium salt.

Cyclopentamine hydrochloride **10**: 141 g (1 mol) 1-cyclopentyl-2-methylaminopropane (= *cyclopentamine*) are dissolved in 500 ml of dry ether. Dry hydrogen chloride is passed into the solution until the weight of the mixture has increased by 36 g. During the addition of the hydrogen chloride, the hydrochloride salt of cyclopentamine precipitates as a white powder. The salt is filtered off and washed with dry ether. Cyclopentamine hydrochloride thus prepared melts at about 113–115°C. The yield is practically quantitative.

Amfenac sodium **11**: A stirred solution of 111 g (0.43 mol) of 2-amino-3-benzoyl-phenylacetic acid (= *amfenac*) in 777 ml of tetrahydrofuran is treated with 31.3 g (0.39 mol) of 50% NaOH. After cooling the solution at 0°C for 3 h, the solid which precipitates is collected by filtration to yield 64 g (56%) of the expected sodium salt, m.p. 245–252°C. An analytical sample is obtained by dissolving 1.0 g of the crude salt in 10 ml of 95% EtOH and treating the solution with 5 ml of isopropyl ether. The pure sodium salt precipitates slowly to yield 0.9 g of yellow solid, m.p. 254–255.5°C.

BNSDOCID: <XP_____2566271A__L>

UM00016870
NOVARTIS EXHIBIT 1517
Novartis v. Regents, IPR2023-01347
Page 3852 of 4460

Table 35.4 Manipulating characteristics of basic drugs by change of salt form

Characteristic	Direction of change	Direction of change
Melting point	*Decrease*	*Increase*
Action to achieve change	1 Use more flexible aliphatic acids with aromatic bases 2 Move to more highly substituted acids that destroy crystal symmetry	1 Use small counter ions, e.g. Cl^- 2 If aromatic base use aromatic anions 3 If base has hydrogen bonding properties use small hydroxy carboxylic acids
Consequences of change	1 Increases solubility 2 May form noncrystallizing liquid (rarely possible, rarely desired!)	1 Decreases solubility 2 Reduces processing problems
Solubility, dissolution rate	*Increase*	*Decrease*
Action to achieve change	1 Decrease melting point 2 Decrease pK_a and increase soly. of acid 3 Increase hydroxylation of acid 4 Move to small organic acid in case of common ion effect	1 Increase melting point 2 Increase hydrophobicity of acid
Consequences of change	1 Increases bioavailability 2 Enables possibly liquid formulation	1 Suspensions physically more stable (reduced rate of particle growth) 2 Solid dosage forms: retarded release
Stability	*Decrease*	*Increase*
Action to achieve change	—	1 Increase hydrophobicity of acid 2 Use carboxylic rather than sulfonic or mineral acids 3 (in case of acid-labile a.s. base:) Use acid of higher pK_a to reduce pH of adsorbed water 4 Decrease solubility 5 Increase crystallinity
Consequences of change	—	1 Reduces hygroscopicity 2 Improves resistance to attack by environmental agents
Wettability	*Decrease*	*Increase*
Action to achieve change	1 Increase hydrophobicity of acid	1 Increase polarity of counterion 2 Use acid with high degree of hydroxylation 3 Use acid of lower pK_a 4 Attempt recrystallization from different solvents to alter crystal habit
Consequences of change	1 Reduces degree of hygroscopicity/deliquescence	1 Improves dissolution and bioavailability

Adapted from Gould.[11]

In the crystallization of salts, water may assume different roles. At times, the presence of traces up to stoichiometrical amounts may favour crystallization, in particular if preferably a hydrated salt form has a strong tendency to crystallize. In other cases, strictly anhydrous conditions may be mandatory which should be observed with highly water-soluble salts. Also, if salt formation of very weakly acidic (basic) substances with strong bases (acids) is intended the presence of water would cause partly protolytic disproportionation of the salt, then the result would be a salt contaminated with the free acid (base) form of the drug substance.

A series of typical preparative procedures for salt formation can be found in Wermuth and Stahl.[25]

BNSDOCID: <XP_____2566271A__I_>

UM00016871

NOVARTIS EXHIBIT 1517
Novartis v. Regents, IPR2023-01347
Page 3853 of 4460

B Solid-state properties

Polymorphism and hydrate formation

A salt, once isolated, may maintain its physical properties for long periods of storage, and repeated observations would render the same characteristics, e.g. melting point, or solubility. However, many salts are not only able to crystallize in different crystal forms but also may transform from one form to a different one even in the solid state: they exhibit the phenomenon of polymorphism. In addition, more frequently than with nonelectrolytes, pseudopolymorphism is encountered: the stoichiometric inclusion of solvent molecules in the crystal lattice producing solvates, and in particular hydrates, if the solvent is water. Such variations of a drug's solid state are highly important for the manufacturing of solid and semisolid dosage forms since the different forms differ in all their substance parameters and properties, including solubility and dissolution. Once they are encountered, both, polymorphs and hydrates, can become disturbing, especially if one form transforms to a different one during production. A consequence may then be that the final drug substance or salt cannot be delivered reproducibly in the same form. Transformation of polymorphs can also take place during storage of the substance, or during processing, manufacturing or storage of dosage forms. Therefore, the thermodynamically most stable form is preferred. This also includes stable hydrates or stable anhydrates, where 'stable' means that within acceptable ranges of storage and processing temperatures and humidity, no change will take place with respect to the crystal polymorphic state or the degree of hydration. Anhydrous material can form hydrates on contact with water or when exposed to humid air. Generally, hydrates are less soluble in water than the corresponding anhydrates. (One of the very rare exceptions to this rule is reported in Kristl *et al.*[26]) Although salt hydrates usually form rapidly, the rate of their formation can vary widely, taking from minutes to months. Thus, the solubility and dissolution rate of an anhydrous salt can be initially high, leading to supersaturation with respect to a hydrate which might appear with delay, whereupon the concentration in a solution drops as the hydrate crystallizes, or a dissolution process would slow down due to the transformation of the undissolved anhydrous solid to a hydrate. Equilibria of hydrate formation in humid air are graphically presented as water sorption isotherms as shown in Fig. 35.9 for the potassium salt of *diclofenac* **8**. When exposed to stepwise increasing humidity, this salt takes up 4 mol of water, once 60% relative humidity is exceeded. Whereas in other cases, a hydrate would revert to the anhydrate if the humidity drops below the same minimum value when it has been formed (in this case, below 60%), this sorption isotherm exhibits hysteresis: the salt hydrate retains water even at lower humidity. Only below 40% is the hydrate water lost completely. The question must be asked

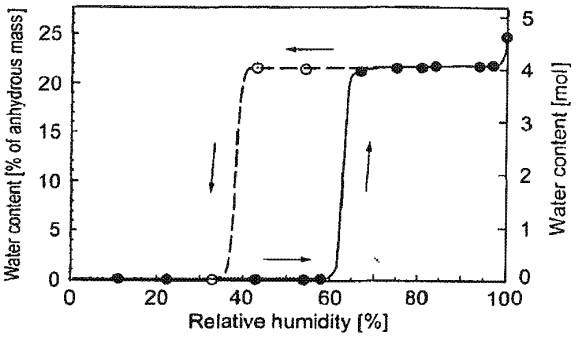


Fig. 35.9 Water sorption isotherm (23°C) of diclofenac potassium at atmospheric pressure. Full circles, adsorption; empty circles, desorption.

whether the propensity to form a hydrate might interfere with, for example, tablet production. For this particular case the following consideration leads to the conclusion that no interference would occur. If a wet granulation process is applied to form a homogeneous granular mass for producing tablets, an aqueous binder solution is worked into the powder mixture consisting of the drug salt and excipients. Clearly, the tetrahydrate is intermediatedly formed during this procedure. Checking the sorption isotherm against the temperature and humidity conditions of the subsequent drying of the wet granulation at a temperature above 60°C it can be concluded that the drying process not only removes the excess water introduced by the binder solution, but also the hydrate water completely. However, when the intermediate tablet mass is further processed, care must be taken that the humidity in the manufacturing facility is controlled to values below 60% so that the anhydrous state will be maintained, and the final tablet product will be sealed in blister packs. This example can make clear that hydrates are not generally prohibitive in drug product development and manufacture, if the climatic stability ranges of the different forms of the particular substance are sufficiently known and such climatic conditions are applied as to avoid transformations.

Chemical stability

The salt form can have an effect on the chemical stability of the drug. If a potentially reactive salt-forming agent has been chosen unwittingly the resulting salt may decompose under certain conditions. Such cases have been reported for fumarate and maleate salts. A pH-dependent adduct formation with maximum reactivity at pH ≈ 5 took place with the dimaleate of the development compound PGE-7762928 (two basic nitrogens; $pK_{a,1} = 4.3$; $pK_{a,2} = 10.6$).[27] Further.

BNSDOCID: <XP_____2566271A__I_>

UM00016872
NOVARTIS EXHIBIT 1517
Novartis v. Regents, IPR2023-01347
Page 3854 of 4460

with the selective serotonin reuptake inhibitor *seproxetine* (= *S*-norfluoxetine; **12**) maleate hemihydrate, the interaction of the primary amine group with the anion in aqueous solution (optimum pH range 5.5–8.5) resulted in adduct formation.[28]

The stability in the solid state of the free acid and three salts of a prostaglandin derivative were compared on samples stored at 33°C, protected from light. After 2 months, > 10% of the acid, > 50% of the sodium salt, < 2% of the potassium salt and 2–3% of the Tris (= tromethamine) salt were decomposed. The surprisingly large differences could be correlated neither with the water solubility nor with the melting point.[29]

Powell[30] found a dramatic difference in stability between the phosphate and the sulfate salts of codeine in solution at room temperature. Whereas the phosphate solution had a shelf life of 1.1 years, the extrapolated shelf life of the sulfate was 44 years. The low stability of the former was ascribed to a catalytic effect of the phosphate anion on the degradation of codeine.

These few examples underline the importance of the stability aspect of salt selection.

V CRITERIA FOR SALT SELECTION

The selection of the final salt form must take into account that each one of the different salts of a drug candidate has its own profile of properties, and an ideal profile would match the biopharmaceutical and technological requirements for a particular dosage form and route of administration. Rarely high solubility can be the only criterion of decision. In addition, the requirements of the envisaged dosage form need to be respected. For example, a salt with the highest solubility, but a pH of 2.8 for the saturated solution in water, might be corrosive to tableting machinery,[31] which would preclude manufacturing of a 200-mg tablet product. So the decision could vote for a less soluble, but also less aggressive salt. In contrast, for preparing an injectable solution such a low pH could be tolerated if the solution is designed for administration by addition to an intravenous infusion. A step-wise route to salt selection has been proposed by Morris and coworkers.[32] Often the result of the decision process is a compromise between several competing property profiles, or if one salt form is intended to be used in different dosage forms.

A Essential parameters and properties

Here are summarized the essential factors that constitute the pharmaceutically relevant profile of a drug candidate and hence for any salt in consideration.

The *solubility* (pH profile) should be as high as possible for injectables, moderate for peroral dosage forms.

Hygroscopicity, the adsorptive uptake and release of water or the deliquescence of highly soluble salts, can be decisive for technical problems. As an example, sodium valproate, used as an anticonvulsive, deliquesces at humidity ≥43% relative humidity and therefore requires special precautions during processing for solid dosage forms.

The propensity to form hydrates in water or in humid air must be known. If hydrates form, the conditions of formation and the climatic range (temperature, humidity) of stability must be known, and the compatibility of both for the form to be chosen must be assessed.

Morphic state: It must be clear whether the salt is monomorphic or polymorphic. If it is polymorphic, the relationship between the polymorphic forms (monotropic, enantiotropic), their relative thermodynamic stability (stable or metastable at room temperature) and the temperature range of their physical stability need to be clarified.

Crystallinity: The degree of crystallinity must be known. Amorphous materials are thermodynamically not stable, and stabilization is likely to take place under a broad range of conditions and half-life times. The morphology and crystal habit is of interest for mechanical processing procedures such as milling, mixing, powder flow and compression.

Melting point: A melting point lower than approximately 100°C can cause problems during mechanical handling and processing. In particular, melting or lumping can occur when comminution by milling is attempted.

Chemical stability under a variety of macro- and microenvironmental conditions is a highly critical property determining the expected shelf life of products. The stability of the bulk solid and in solution must be studied, whereby the influence of environmental factors (pH, temperature, humidity, oxygen, light) and including the presence of various excipients on drug stability must be established.

Corrosiveness: salts of weak bases with strong acids need to be tested whether or not they are corrosive on tableting tools.

Such profiles are studied in preformulation programs,[33] but some of the properties must already be known before the decision for the final salt form is made. A change of the salt form of a drug substance at later stages of product development must be avoided. Otherwise, many essential studies would then have to be repeated with the new salt at a cost of additional time and resources. Besides the essential parameters and properties of immediate pharmaceutical-technological and biopharmaceutical interest mentioned above, further issues may have to be considered in the final decision concerning other areas: (1) chemical processing, handling and economy: the yield and quality of

BNSDOCID: <XP_____2566271A__I_>

UM00016873

NOVARTIS EXHIBIT 1517
Novartis v. Regents, IPR2023-01347
Page 3855 of 4460

crystallization, of milling; in addition, the equivalent mass ratio *active entity:salt* can play a role, if a drug is likely to be used in high doses, because a large counter-ion could cause unwieldy large doses to be administered; (2) patent aspects: physical and chemical variations of a drug substance can be employed for extending the proprietary substance protection by a suitable strategy of patent application for salt forms or crystal modifications that are characterized by particularly advantageous (pharmaceutical, biopharmaceutical, medical or technical) properties and can open up new areas of application. It should be mentioned that salt formation is not only used to improve solubility, but also for reducing solubility. Thus, sparingly soluble salts can be used for developing peroral slow-release drug products. Typical applications are the pamoates (= embonates) of imipramine, pyrantel, pyrvinium and others; also the resinates, in which the drug substance is loaded on an ion exchanger.[34,35] *Salmeterol xinafoate* **13** (= 1-hydroxy-2-naphthoate) is an example of tailoring the properties of a bronchodilating beta-stimulant by means of salt formation to an optimum performance in inhalation. The sparingly soluble xinafoate salt dissolves slowly thereby contributing to the long-acting properties of the drug substance. At the same time, mucosal irritation by osmotic effects is avoided.

REFERENCES

1. Stahl, P.H. and Wermuth, C.G., (eds) (2002) *Handbook of Pharmaceutical Salts — Preparation, Selection and Use*. Verlag Helvetica Chimica Acta, Zürich.
2. Yalkowsky, S.H. (1985) Solubility and solubilization of nonelectrolytes. In Yalkowsky, S.H. (ed.). *Techniques of Solubilization of Drugs*, pp. 1–14. Marcel Dekker, New York.
3. Jain, N. and Yalkowsky, S.H. (2001) Estimation of the aqueous solubility. I: Application to organic nonelectrolytes. *J. Pharm. Sci.* **90**: 234–252.
4. CLOGP (2001) BioByte Corp. and Pomona College: Claremont, CA, USA.
5. Yang, G., Jain, N. and Yalkowsky, S.H. (2001) Estimation of the aqueous solubility. III: Application to weak-electrolyte drugs in buffered solutions. *AAPS: 2001 Annual Meeting & Exposition*. Denver, CO, USA, *AAPS PharmSci.* 3 Number 3 (Suppl.), poster No. W4446.
6. Chowhan, Z.T. (1978) pH-Solubility profiles of organic carboxylic acids and their salts. *J. Pharm. Sci.* **67**: 1257–1260.
7. Kramer, S.F. and Flynn, G.L. (1972) Solubility of organic hydrochlorides. *J. Pharm. Sci.* **61**: 1896–1904.
8. Bogardus, J.B. and Blackwood, R. K. J. (1979) Dissolution rates of doxycycline free base and hydrochloride salts. *J. Pharm. Sci.* **68**: 1183–1184.
9. Bevan, C.D. and Lloyd. R.S. (2000) A high-throughput screening method for the determination of aqueous drug solubility using laser nephelometry in microtiter plates. *Anal. Chem.* **72**: 1781–1787.
10. *The Electronic Orange Book: Approved Drug Products with Therapeutic Equivalence Evaluations (Internet version of the Orange Book)*. US Department of Health and Human Services, Public Health Service, Food and Drug Administration, Center for Drug Evaluation and Research (CDER), Office of Information Technology, Division of Data Management and Services. http://www.fda.gov/cder/ob/default.htm.
11. Gould, P.L. (1986) Salt selection for basic drugs. *Int. J. Pharm.* **33**: 201–217.
12. Senior, N. (1973) Some observations on the formulation and properties of chlorhexidine. *J. Soc. Cosmet. Chem.* **24**: 259–278.
13. Nudelman, A., McCaully, R.J. and Bell, S.C. (1974) Water-soluble derivatives of 3-oxy-substituted 1,4-benzodiazepines. *J. Pharm. Sci.* **63**: 1880–1885.
14. Agharkar, S., Lindenbaum, S. and Higuchi, T. (1976) Enhancement of solubility of drug salts by hydrophilic counterions: properties of organic salts of an antimalarial drug. *J. Pharm. Sci.* **65**: 747–749.
15. Streng, W.H., Hsi, S.K., Helms, P.E. and Tan, H. G. H. (1984) General treatment of pH-solubility profiles of weak acids and bases and the effects of different acids on the solubility of a weak base. *J. Pharm. Sci.* **73**: 1679–1684.
16. Hussain, M.A., Wu, L.S., Koval, C. and Hurwitz, A.R. (1992) Parenteral formulation of the *kappa* agonist analgesic, DuP 747, via micellar solubilization. *Pharm. Res.* **9**: 750–752.
17. Miyazaki, S., Nakano, M. and Arita, T. (1975) A comparison of solubility characteristics of free bases and hydrochloride salts of tetracycline antibiotics in hydrochloric acid solutions. *Chem. Pharm. Bull.* **23**: 1197–1204.
18. Miyazaki, S., Oshiba, M. and Nadai, T. (1980) Unusual solubility and dissolution behaviour of pharmaceutical hydrochloride salts in chloride-containing media. *Int. J. Pharm.* **6**: 77–85.
19. Miyazaki, S., Oshiba, M. and Nadai, T. (1981) Precaution on use of hydrochloride salts in pharmaceutical formulation. *J. Pharm. Sci.* **70**: 594–596.
20. Lentner, C. (ed.). (1981) *Geigy Scientific Tables*, 8th edn. vol. 1, p. 145. Ciba-Geigy AG, Basel.
21. Bogardus, J.B. and Blackwood, R.K.J. (1979) Solubility of doxycycline in aqueous solution. *J. Pharm. Sci.* **68**: 188–194.
22. Tong, W.Q. and Whitesell, G. (1998) *In situ* salt screening — a useful technique for discovery support and preformulation studies. *Pharm. Dev. Technol.* **3**: 215–223.
23. Anderson, B.D. and Conradi, R.A. (1985) Predictive relationships in the water solubility of salts of a nonsteroidal anti-inflammatory drug. *J. Pharm. Sci.* 74: 815–820.
24. Rubino, J.T. (1989) Solubilities and solid state properties of the sodium salts of drugs. *J. Pharm. Sci.* **78**: 485–489.
25. Wermuth, C.G. and Stahl, P.H. (2002) Selected procedures for the preparation of pharmaceutically acceptable salts. In Stahl, P.H. and Wermuth, C.G. (eds). *Handbook of Pharmaceutical Salts — Preparation, Selection and Use*, pp. 249–263. Verlag Helvetica Chimica Acta, Zürich.
26. Kristl, A., Srčič, S., Vrečer, F., Šuštar, B. and Vojnovic, D. (1996) Polymorphism and pseudopolymorphism: influencing the dissolution properties of the guanine derivative acyclovir. *Int. J. Pharm.* **139**: 231–235.
27. Gazda, M., Dansereau, R.J., Crail, D.J., Sakkab, D.H. and Virgin, M.M. (1998) Maleate adduct formation during solid-oral dose form screening of PGE-7762928. *Pharm. Sci.* **1**: S403.
28. Schildcrout, S.A., Risley, D.S. and Kleemann, R.L. (1993) Drug–excipient interactions of seproxetine maleate hemihydrate: Isothermal stress methods. *Drug Dev. Ind. Pharm.* **19**: 1113–1130.
29. Anderson, B.D. (1985) Prodrugs for improved formulation properties. In Bundgaard, H. (ed.). *Design of Prodrugs*, pp. 243–269. Elsevier Science, Biomedical Division, Amsterdam.

BNSDOCID: <XP_____2566271A__I_>

UM00016874

NOVARTIS EXHIBIT 1517
Novartis v. Regents, IPR2023-01347
Page 3856 of 4460

30. Powell, M.F. (1986) Enhanced stability of codeine sulfate: effect of pH, buffer, and temperature on the degradation of codeine in aqueous solution. *J. Pharm. Sci.* **75**: 901–903.
31. Stahl, P.H. (1993) Characterization and improvement of the stability behaviour of drug substances. In Grimm, W. and Krummen, K. (eds). *Stability Testing in the EC, Japan and the USA*. pp. 15–32. Wissenschaftliche Verlagsgesellschaft, Stuttgart.
32. Morris, K.R., Fakes, M.G., Thakur, A.B., *et al.* (1994) An integrated approach to the selection of optimal salt form for a new drug candidate. *Int. J. Pharm.* **105**: 209–217.
33. Wells, J.I. (1988) *Pharmaceutical Preformulation*. Ellis Horwood, Chichester.
34. Borodkin, S.S. (1993) Ion exchange resins and sustained release. In Swarbrick, J. and Boylan, J.C. (eds). *Encyclopedia of Pharmaceutical Technology*, pp. 203–216. Marcel Dekker, New York.
35. Borodkin, S.S. (1991) Ion-exchange resin delivery systems. In Tarcha, P.J. (ed.). *Polymers for Controlled Drug Delivery*, pp. 215–230. CRC Press, Boca Raton.

BNSDOCID: <XP_____2566271A_I_>

UM00016875

NOVARTIS EXHIBIT 1517
Novartis v. Regents, IPR2023-01347
Page 3857 of 4460

Electronic Acknowledgement Receipt

EFS ID:	9182697
Application Number:	10378956
International Application Number:	
Confirmation Number:	4742
Title of Invention:	Multiple-component solid phases containing at least one active pharmaceutical ingredient
First Named Inventor/Applicant Name:	Michael J. Zaworotko
Customer Number:	23557
Filer:	Glenn Ladwig/J'Nese Williams
Filer Authorized By:	Glenn Ladwig
Attorney Docket Number:	USF.106XC1
Receipt Date:	06-JAN-2011
Filing Date:	03-MAR-2003
Time Stamp:	18:36:17
Application Type:	Utility under 35 USC 111(a)

Payment information:

Submitted with Payment	no

File Listing:

Document Number	Document Description	File Name	File Size(Bytes)/ Message Digest	Multi Part /.zip	Pages (if appl.)
1		SIDS8.pdf	272627 6fb0ab225ae1732d52784cc43804ae12359b55b9	yes	3

	Multipart Description/PDF files in .zip description				
	Document Description		Start	End	
	Transmittal Letter		1	2	
	Information Disclosure Statement (IDS) Filed (SB/08)		3	3	
Warnings:					
Information:					
2	NPL Documents	RasenackNorbert_et_al.pdf	205307 3b1d10c32860e14a46bf5637e578c8ece731c29a	no	7
Warnings:					
Information:					
3	NPL Documents	Stahl2003.pdf	377751 bbe1ad93da0bb9a59b0e5198cd385a592db4f52a	no	15
Warnings:					
Information:					
		Total Files Size (in bytes):	855685		

This Acknowledgement Receipt evidences receipt on the noted date by the USPTO of the indicated documents, characterized by the applicant, and including page counts, where applicable. It serves as evidence of receipt similar to a Post Card, as described in MPEP 503.

New Applications Under 35 U.S.C. 111
If a new application is being filed and the application includes the necessary components for a filing date (see 37 CFR 1.53(b)-(d) and MPEP 506), a Filing Receipt (37 CFR 1.54) will be issued in due course and the date shown on this Acknowledgement Receipt will establish the filing date of the application.

National Stage of an International Application under 35 U.S.C. 371
If a timely submission to enter the national stage of an international application is compliant with the conditions of 35 U.S.C. 371 and other applicable requirements a Form PCT/DO/EO/903 indicating acceptance of the application as a national stage submission under 35 U.S.C. 371 will be issued in addition to the Filing Receipt, in due course.

New International Application Filed with the USPTO as a Receiving Office
If a new international application is being filed and the international application includes the necessary components for an international filing date (see PCT Article 11 and MPEP 1810), a Notification of the International Application Number and of the International Filing Date (Form PCT/RO/105) will be issued in due course, subject to prescriptions concerning national security, and the date shown on this Acknowledgement Receipt will establish the international filing date of the application.

I hereby certify that this correspondence is being electronically filed in the United States Patent and Trademark Office on January 6, 2011.

Glenn P. Ladwig, Patent Attorney, Reg. # 46,853

SUPPLEMENTAL INFORMATION DISCLOSURE STATEMENT
Patent Application
Docket No. USF.106XC1
Serial No. 10/378,956

IN THE UNITED STATES PATENT AND TRADEMARK OFFICE

Examiner	:	Sahar Javanmard
Art Unit	:	1627
Applicants	:	Michael J. Zaworotko, Brian Moulton, Nair Rodriguez-Hornedo
Serial No.	:	10/378,956
Filed	:	March 3, 2003
Conf. No.	:	4742
For	:	Multiple-Component Solid Phases Containing at Least One Active Pharmaceutical Ingredient

Mail Stop Amendment
Commissioner for Patents
P.O. Box 1450
Alexandria, VA 22313

SUPPLEMENTAL INFORMATION DISCLOSURE STATEMENT
UNDER 37 C.F.R. §§ 1.97 AND 1.98

Sir:

In accordance with 37 C.F.R. § 1.56, the references listed on the attached form PTO/SB/08 are being brought to the attention of the Examiner for consideration in connection with the examination of the above-identified patent application. A copy of each cited reference is enclosed.

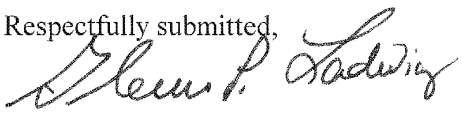
It is respectfully requested that the references cited on the attached form PTO/SB/08 be considered in the examination of the subject application and that their consideration be made of record.

J:\USF\106XC1\PTO\SIDS8.doc/DNB/jnw

This information is being submitted subsequent to the filing of a Request for Continued Examination, but before the mailing of an Office Action on the merits. If any fee is required please use Deposit Account No. 19-0065.

Applicants respectfully assert that the substantive provisions of 37 C.F.R. §§ 1.97 and 1.98 are met by the foregoing statement.

Respectfully submitted,



Glenn P. Ladwig
Patent Attorney
Registration No. 46,853
Phone No.: 352-375-8100
Fax No.: 352-372-5800
Address: P.O. Box 142950
Gainesville, FL 32614-2950

GPL/jnw
Attachments: Form PTO/SB/08; copies of references cited therein.

J:\USF\106XC1\PTO\SIDS8.doc/DNB/jnw

Substitute for form 1449A/PTO

INFORMATION DISCLOSURE STATEMENT BY APPLICANT

(use as many sheets as necessary)

Sheet 1 of 2

Complete if Known	
Application Number	10/378,956
Filing Date	March 3, 2003
First Named Inventor	Michael J. Zaworotko
Art Unit	1627
Examiner Name	Sahar Javanmard
Attorney Docket Number	USF.106XC1

U.S. PATENT DOCUMENTS

Examiner Initials*	Cite No. [1]	Document Number Number - Kind Code [2] (if known)	Publication Date MM-DD-YYYY	Name of Patentee or Applicant of Cited Document	Pages, Columns, Lines, Where Relevant Passages or Relevant Figures Appear
	U1				
	U2				
	U3				
	U4				
	U5				
	U6				
	U7				
	U8				
	U9				

FOREIGN PATENT DOCUMENTS

Examiner Initials*	Cite No. [1]	Foreign Patent Document Country Code [3] - Number [4] - Kind Code [5] (if known)	Publication Date MM-DD-YYYY	Name of Patentee or Applicant of Cited Document	Pages, Columns, Lines, Where Relevant Passages or Relevant Figures Appear	T [6]
	F1	EP 0 731 795 B1	12-22-1999	G.D. Searle & Co.	All	
	F2	WO 2000/42021 A1	07-20-2000	Merck Frosst Canada & Co.	All	
	F3					
	F4					
	F5					
	F6					

Examiner Signature		Date Considered	

*EXAMINER: Initial if reference considered, whether or not citation is in conformance with MPEP 609. Draw line through citation if not in conformance and not considered. Include copy of this form with next communication to applicant. [1] Applicant's unique citation designation number (optional). [2] See Kind Codes of USPTO Patent Documents at www.uspto.gov or MPEP901.04. [3] Enter Office that issued the document, by the two-letter code (WIPO Standard T.3). [4] For Japanese patent documents, the indication of the year of the reign of the Emperor must precede the serial number of the patent document. [5] Kind of document by the appropriate symbols as indicated on the document under WIPO Standard ST. 16 if possible. [6] Applicant is to place a check mark here if English language Translation is attached.

This collection of information is required by 37 CFR 1.97 and 1.98. The information is required to obtain or retain a benefit by the public which is to file (and by the USPTO to process) an application. Confidentiality is governed by 35 U.S.C. 122 and 37 CFR 1.14. This collection is estimated to take 2 hours to complete, including gathering, preparing, and submitting the completed application form to the USPTO. Time will vary depending upon the individual case. Any comments on the amount of time you require to complete this form and/or suggestions for reducing this burden, should be sent to the Chief Information Officer, U.S. Patent and Trademark Office, P.O. Box 1450, Alexandria, VA 22313-1450. DO NOT SEND FEES OR COMPLETED FORMS TO THIS ADDRESS. **SEND TO: Commissioner for Patents, P.O. Box 1450, Alexandria, VA 22313-1450.**

If you need assistance in completing the form, call 1-800-PTO-9199 (1-800-786-9199) and select option 2.

J:\USF\106XC1\PTO\SIDS9-form.doc/DNB/jnw

Substitute for form 1449B/PTO

INFORMATION DISCLOSURE STATEMENT BY APPLICANT

(use as many sheets as necessary)

Sheet 2 of 2

Complete if Known	
Application Number	10/378,956
Filing Date	March 3, 2003
First Named Inventor	Michael J. Zaworotko
Group Art Unit	1627
Examiner Name	Sahar Javanmard
Attorney Docket Number	USF.106XC1

NON PATENT LITERATURE DOCUMENTS

Examiner Initials*	Cite No.[1]	Include name of the author (in CAPITAL LETTERS), title of the article, (when appropriate), title of the item (book, magazine, journal, serial, symposium, catalog, etc.), date, page(s), volume-issue number(s), publisher, city and/or country where published.	T[2]
	R1	STAHLY, G. P. "A Survey of Cocrystals Reported prior to 2000" *Crystal Growth & Design,* 2009, 9:4212-4229.	
	R2		
	R3		
	R4		
	R5		
	R6		
	R7		
	R8		
	R9		
	R10		
	R11		
	R12		
	R13		

Examiner Signature		Date Considered	

*EXAMINER: Initial if reference considered, whether or not citation is in conformance with MPEP 609. Draw line through citation if not in conformance and not considered. Include copy of this form with next communication to applicant.

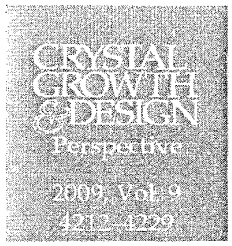
[1] Applicant's unique citation designation number (optional). [2] Applicant is to place a check mark here if English language Translation is attached.

This collection of information is required by 37 CFR 1.98. The information is required to obtain or retain a benefit by the public which is to file (and by the USPTO to process) an application. Confidentiality is governed by 35 U.S.C. 122 and 37 CFR 1.14. This collection is estimated to take 2 hours to complete, including gathering, preparing, and submitting the completed application form to the USPTO. Time will vary depending upon the individual case. Any comments on the amount of time you require to complete this form and/or suggestions for reducing this burden, should be sent to the Chief Information Officer, U.S. Patent and Trademark Office, P.O. Box 1450, Alexandria, VA 22313-1450. DO NOT SEND FEES OR COMPLETED FORMS TO THIS ADDRESS. **SEND TO: Commissioner for Patents, P.O. Box 1450, Alexandria, VA 22313-1450.**

If you need assistance in completing the form, call 1-800-PTO-9199 (1-800-786-9199) and select option 2.

J:\USF\106XC1\PTO\SIDS9-form.doc/DNB/jnw

DOI: 10.1021/cg900873t



A Survey of Cocrystals Reported Prior to 2000

G. Patrick Stahly*

Chemfocus LLC, 3908 Summycroft Place, West Lafayette, Indiana 47906, and Triclinic Labs Inc., 1201 Cumberland Avenue, Suite S, West Lafayette, Indiana 47906

Received July 25, 2009; Revised Manuscript Received August 16, 2009

ABSTRACT: A history of cocrystals reported in the literature prior to the year 2000 is presented. Concentration is on cocrystals that contain only organic components, not including species commonly referred to as solvates and clathrates. However, brief mention is made of some cocrystals containing both organic and inorganic components. The discovery and early history of cocrystals are discussed, with emphasis on centers of activity. Numerous examples are then utilized to illustrate the structural variety and utility of cocrystals described in the literature.

Introduction

There is a vast amount of information in the chemical literature related to cocrystals. It is, however, widely dispersed. In addition, there have always been, and remain, multiple terms used to describe multicomponent crystals. For those reasons, a comprehensive history of cocrystals would be an undertaking beyond the scope of this article. Instead, only work published prior to 2000 is reviewed herein. Emphasis will be on early history, centers of activity, and examples selected to illustrate various types of cocrystals and their uses.

I will define a cocrystal as I have in the past, as a crystalline structure with unique properties that is made up of two or more components. A component may be an atom, ionic compound, or molecule.[1] A better, more precise description of a component is the one utilized in Gibbs theory, stated by Kitaigorodsky as "...a constituent part of a system, such that its composition, at least in one state of aggregation, does not depend on the concentration of the other parts."[2] Using that broad definition, species such as hydrates, solvates, and clathrates are cocrystals. Hydrates and solvates are multicomponent crystals in which one component is water or an organic compound used as a solvent, respectively. The term clathrate, introduced by Powell in 1948,[3] refers to cocrystals in which one component is contained in spaces within the crystal structure of the second component. The crystallizing substance is commonly called the host and the substance contained in the spaces is commonly called the guest. A well-known host molecule is urea, which crystallizes in helices in order to maximize hydrogen bonding. The helices are hollow, and many structurally diverse molecules can reside in the voids. It should be noted that urea also is known to form nonclathrate, stoichiometric cocrystals.

It is important to realize, however, that the cocrystal definition I have adopted for this Perspective represents my opinion. Different views have been expressed regarding nomenclature and classification of crystals containing multiple components. Kitaigorodsky, in the preface to his 1986 book, *Mixed Crystals*, noted that the title would denote different things to different people, and that it could be applied to both "...crystals composed of different molecules and also to solids that are a mixture of crystals with different structures."[4] Where I use the term "cocrystal", others have advocated the use of "co-crystal",[5] "molecular complex",[6] or "multi-component molecular crystal".[7] Some prefer to define cocrystals as structures made up of components which are themselves crystalline solids at room temperature.[8] Using that classification scheme, cocrystals (both components are solid at room temperature) and solvates (one component is liquid at room temperature) become subsets of the broader class of multicomponent crystals.

Historically, one finds variations on the terms "compound" or "complex" frequently used in the literature to describe cocrystals, but other names are also employed. Quinhydrone was described as a compound containing molecular proportions of quinone and quinol by its discoverer.[9] It was later called a molecular compound,[10] as were related substances containing halogenated species.[11] Cocrystals containing two different benzoins in equimolar amounts were found to form readily and were called addition compounds.[12] The structure of a crystal containing 1-methylthymine and 9-methyladenine in a 1:1 molar ratio was determined from X-ray diffraction measurements and was described in the report as a hydrogen-bonded complex.[13] Wenner, in studying the reactions of ascorbic acids with weak amine bases, found that L-ascorbic acid and D-isoascorbic acid combine with nicotinamide to form definite compounds, and concluded that "...we think it incorrect to name the new compounds "salts", and hence refer to the combination of L-ascorbic acid and nicotinamide as "nicotinamide-L-ascorbic acid complex" rather than calling it "nicotinamide L-ascorbate".[14] A cocrystal containing a 2:1 ratio of pyrene and pyromellitic dianhydride was called a molecular complex,[15] and one containing a 2:1 ratio of hexamethylbenzene and tetracyanoethylene was called a solid-state complex.[16] Kitaigorodsky used the term "mixed molecular crystals" to describe both solid solutions and what he called molecular compounds.[17] Recently, cocrystals of fullerenes and cubane were called heteromolecular crystals.[18]

Terms used to describe the components in a multicomponent crystal have also varied in the literature. Often in the case of cocrystals there is a central molecule of interest that is cocrystallized with various other components. In those cases, the secondary component has been referred to as the cocrystal former (coformer for short), ligand, or guest (as in clathrates as described above). I will use the term coformer herein.

*To whom correspondence should be addressed. E-mail: pstahly@triclinicabs.com.

Published on Web 08/27/2009

© 2009 American Chemical Society

UM00016995
NOVARTIS EXHIBIT 1517
Novartis v. Regents, IPR2023-01347
Page 3864 of 4460

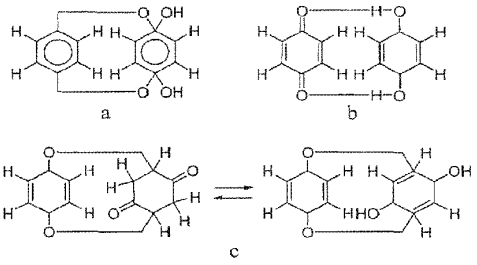


Figure 1. Quinhydrone (3) structures proposed by Jackson and Oenslager (a),[22] Willstatter and Piccard (b),[23] and Posner (c).[24]

Thus, it is recognized that the issues of nomenclature and classification of cocrystals are not settled. Neither a comprehensive review of those issues nor discussion of the merits of proposals that have appeared in the literature are undertaken in this Perspective. Instead, the focus is on the structural variety of molecules that have been found to form cocrystals and how cocrystals have been used. Selected examples are presented; a comprehensive listing of cocrystals known prior to 2000 is not intended. My hope is that the Perspective will cause researchers that are currently active in the field of cocrystals to pause and look back at literature that may be easily forgotten in the race to new technologies.

The cocrystals that are the primary subject of this Perspective are those containing only organic components, though brief mention will be made of some cocrystals containing both organic and inorganic components. However, hydrates, solvates, clathrates, and cocrystals containing components such as mineral acids, halogens, and inorganic molecules such as hydrogen peroxide, as well as compounds best described as metal coordination complexes, are not included. The criterion used to identify solvates for exclusion is that one component is an organic compound commonly used as a solvent. That is, of course, a subjective criterion, and is based only on my experience and opinion.

Cocrystals Containing All Organic Components

The first organic:organic cocrystal was reported by Wohler in 1844 during studies on quinone.[9] He found that by mixing solutions of quinone (**1**) and "colorless" hydroquinone (also called quinol, **2**), a crystalline substance was formed that he called "green hydroquinone". That he described as one of the finest materials known to organic chemistry, similar to murexide (the ammonium salt of purpuric acid) but even surpassing it in splendor and beauty of color.[19] On the basis of chemical behaviors and elemental analyses, Wohler concluded that green hydroquinone was made up of a 1:1 molar combination of **1** and **2**.

Following the initial publication, there appeared in the literature a series of papers describing analyses of the new material, and for a while a controversy about its makeup existed. Most data supported Wohler's view that quinone and hydroquinone were present in a 1:1 molar ratio, but Wichelhaus believed the ratio to be 2:1. Ultimately, the 1:1 stoichiometry was found to be correct. Ling and Baker published a short history of the dispute as well as their own work in which several related cocrystals were made from halogenated quinones.[10] They referred to green hydroquinone as quinhydrone (**3**), a name which apparently originated prior to publication of their paper, and described it as "a molecular compound of quinone and quinol".

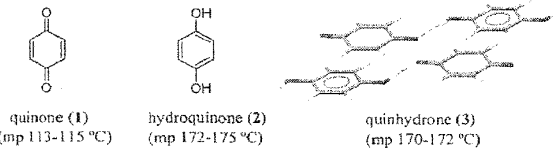


Figure 2. The structures of quinone, hydroquinone, and quinhydrone.

Remember that X-ray diffraction analysis was unavailable at that time. X-rays were discovered by Rontgen in 1895, and were used to solve the first crystal structure, of sodium chloride, in 1914.[20] It was not until 1923 that the first full X-ray structure solution of an organic molecule, hexamethyltetramine, was published.[21] Therefore, chemists were unsure of the types of intermolecular chemical bonds holding quinhydrone together, not knowing if they were covalent, ionic, or dipole in nature. Some of the structures proposed are shown in Figure 1.

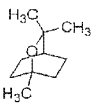
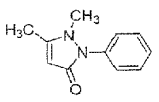
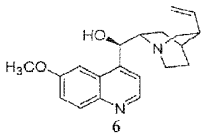
Early X-ray diffraction studies of **3** conducted in the 1930s and 1940s confirmed the existence of discrete quinone and hydroquinone moieties.[25] On the basis of the unit cell information obtained, π-stacking of the rings was deduced. It was not until 1958 that the full structure of a monoclinic quinhydrone crystal was published.[26] Quinone and hydroquinone molecules were found to alternate in zigzag chains held together by O−H···O hydrogen bonds. The planar molecules pack parallel to one another, with an intermolecular distance considerably shorter than those found in many other crystals of aromatic compounds. That π-stacking interaction was suggested to be responsible for the high density of **3** (1.40 g/cm^3) compared to **1** (1.32 g/cm^3) and **2** (1.33 g/cm^3), as well as its color. The monoclinic structure was redetermined in 1965[27] and the crystal structure of a polymorphic, triclinic form of quinhydrone was published in 1968.[28] Figure 2 shows the chemical structures of **1** and **2**, as well as the packing diagram of the monoclinic form of **3**.[29]

After the discovery of quinhydrone, researchers began to seek other types of organic cocrystals. In the late 1800s and early 1900s, many were discovered. One of the more prolific researchers during that time was German chemist Paul Pfeiffer, who in 1922 published his book *Organische Molekulverbindungen* (Organic Molecular Compounds).[30] Most of that book is made up of two sections, one covering cocrystals containing a mixture of inorganic and organic components (Anorganisch-organische Molekulverbindungen) and a second covering cocrystals containing all organic components (Rein organische Molekulverbindungen). A part of each section is a listing of the cocrystals that had been reported prior to the book's publication. Most of the inorganic:organic cocrystals listed fall outside the scope of this paper, as they are best classified as solvates or metal coordination complexes. However, some of those fall into classes that will be briefly discussed later, namely, carboxylic acids cocrystallized with alkali metal carboxylate salts and organic molecules cocrystallized with simple alkali metal or ammonium salts.

The Rein organische Molekulverbindungen section lists just over 300 cocrystals. Almost all contain aromatic compounds, and well over half contain di- or trinitro aromatic compounds. 1,3,5-Trinitrobenzene, picric acid (1-hydroxy-2,4,6-trinitrobenzene), and picryl chloride (1-chloro-2,4,6-trinitrobenzene) readily cocrystallize with both functionalized and unfunctionalized aromatics, including polycyclic

UM00016996
NOVARTIS EXHIBIT 1517
Novartis v. Regents, IPR2023-01347
Page 3865 of 4460

Chart 1. Some Cocrystals Containing Commercially Important Compounds Reported by Pfeiffer in 1922

Component 1	Component 2
 **4**	phenol, 2-methylphenol, 3-methylphenol, 4-methylphenol, 2-propylphenol, 2-methoxyphenol, pyrocatechol, resorcinol, hydroquinone, 1-naphthol, 2-naphthol, 1,2,3-benzenetriol, 1-hydroxybenzoic acid, methyl 2-hydroxybenzoate
 **5**	2-methylphenol, 3-methylphenol, 4-methylphenol, 2-hydroxymethylphenol, 2-methoxyphenol, pyrocatechol, resorcinol, hydroquinone, 5-methylresorcinol, 1,2,3-benzenetriol, 1,3,5-benzenetriol, methyl 3-amino-4-hydroxybenzoate
 **6**	phenol, 2-methoxy-4-allylphenol, 2,4,6-tribromophenol, pyrocatechol, resorcinol

aromatic hydrocarbons, aromatic amines, aromatic alcohols, halogenated aromatics, aromatic heterocyclic compounds containing nitrogen or oxygen, aromatic ketones, aromatic aldehydes, and aromatic acids. About 80 cocrystals in which one component was benzoquinone or a related compound were listed. Coformers in those cases were mostly aromatic alcohols or amines.

Another class of molecules that readily form cocrystals are aromatic alcohols such as phenols and naphthols. Coformers include aromatic amines, nitrogen-containing heterocyclic aromatics, ureas, and acetamide. Some interesting examples of cocrystals containing aromatic alcohols are those containing commercially important compounds as one of the components. Eucalyptol (**4**), isolated from the blue gum tree (*Eucalyptus globulus*), is used in flavorings, fragrances, and cosmetics because of its aroma and taste. Fourteen eucalyptol-containing cocrystals were listed by Pfeiffer (Chart 1). The fact that eucalyptol has no aromatic moieties is noteworthy. The finding of such cocrystals taught that π-stacking interactions between components is not necessary for cocrystal formation. Also listed were 12 cocrystals containing the analgesic antipyrine (**5**) and five cocrystals containing the antimalaria compound quinine (**6**) (Chart 1).

It is interesting that a number of cocrystals of **5** are included in the 1895 pharmaceutical text *Modern Materia Medica* (4th edition). Two **5**·resorcinol cocrystals, one called resopyrine and the other called resorcylalgin, are mentioned, but no discussion of the structural difference between them is given.[31] The **5**·1,2,3-benzentriol (pyrogallol) cocrystal is called pyrogallopyrine.[32] A cocrystal of **5** and 2-naphthol, which had been described in the literature[33] but apparently was not included in Pfeiffer's book, was given the name naphthopyrin and described as one of several phenol compounds of **5**.[34] Although it appears that the 2-naphthol-containing cocrystal was not administered to humans, at least prior to publication of the fourth edition of *Modern Materia Medica*, it was not because of concern about the pharmaceutical acceptability of 2-naphthol. The description of naphthols in that book includes the following: "Internally doses of 5 to 8 grains, several times a day, have been recommended for intestinal disinfection, especially in typhus (Robin and others). In chronic diarroea very good results have followed its administration (Ewald)." A cocrystal of **5** and chloral, called hypnal, was described as tasteless and odorless needles melting at 58–60 °C, and was reported to alleviate pain and produce quiet sleep when given to patients with troublesome coughs.[35] The related cocrystal containing **5** and butylchloral, called butylhypnal, was reported to exist as colorless needles melting at 70 °C.[35] Migranine was described as a preparation containing four components in fixed proportions, 89.4% **5**, 8.2% caffeine, 0.56% citric acid, and 1.84% water.[36] It was stated, however, that whether the preparation was a simple mixture or a chemical compound was unknown. Migranine was used for treatment of migraine headaches, and "never failed to ward off attacks even in the most severe cases during five years' experience".[36]

Just after Pfeiffer's book was published, Ludwig Kofler was appointed professor in the Institute of Pharmacognosy at the University of Innsbruck. From that time (1926) until his death in 1951, Kofler pioneered and improved the art of thermal microscopy. Kofler, his wife Adelheid Kofler, and their colleague, Maria Kuhnert-Brandstatter (nee Brandstatter), investigated hundreds of organic molecules using that technique, and authored nearly 250 publications describing their work. Some of those publications describe use of the "contact method" to determine phase diagrams of binary or ternary mixtures of organic compounds.[37] In the contact method, two small portions of different crystalline substances are sequentially melted and resolidified on a microscope slide so that a set of two thin crystalline films having a zone of contact is created. By slow heating of that preparation under the microscope, melting of various portions can be observed and the binary phase diagram is revealed. For example, two substances which do not interact exhibit a low-melting zone at a specific

UM00016997
NOVARTIS EXHIBIT 1517
Novartis v. Regents, IPR2023-01347
Page 3866 of 4460

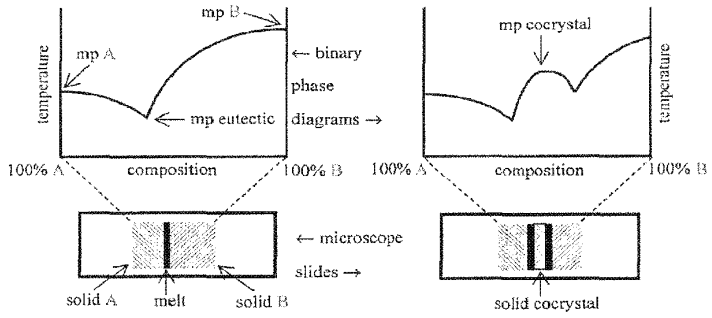
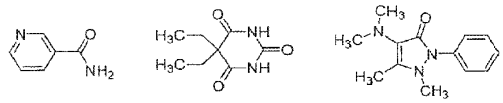


Figure 3. The relationship between contact preparation melting behaviors, shown in the bottom pictures, to melting point binary phase diagrams, shown in the top pictures.

composition, called the eutectic. That is illustrated in the left side of Figure 2. On heating a contact preparation of hypothetical compounds A and B under the hot-stage microscope, the first region to melt will be the low melting eutectic composition. When a single eutectic melt is observed, as depicted in the bottom left illustration, it indicates that A and B do not interact to form a cocrystal. On the other hand, substances that form a cocrystal exhibit two eutectics, between which resides the cocrystal, as shown on the bottom right side of Figure 3. The observance of two melting zones separated by solid indicates that a cocrystal of A and B has formed. By continuing to heat the preparation, the melting point of that cocrystal can be determined. The appearance of melting zones under the hot-stage microscope constitutes a direct representation of the binary melting point diagram of the two compounds. Binary melting point phase diagrams are constructed by plotting A and B composition on the X axis and temperature on the Y axis. Those diagrams for hypothetical compounds A and B are shown in the top pictures in Figure 3. Note that phase behaviors of binary mixtures can be quite a bit more complex than the simple examples depicted in Figure 3.

Using the contact method, known cocrystals were studied and new cocrystals were discovered. For example, the phase diagram for anthracene and picric acid was constructed,[38] and the cocrystal that had first been reported in 1867 was observed.[39] New cocrystals of similar types reported include 1-methyl-2,4,6-trinitrobenzene-carbozole[40] and 1-naphthol-2-naphthylamine.[41] Cocrystals of urea and long-chain aliphatic acids were studied, but those are actually clathrates in which a urea cage can be occupied by varying amounts of the coformer.[42] It was found that nicotinamide (**7**), which is part of the vitamin B group, forms cocrystals with carboxylic acids and a few other types of compounds. Two-component cocrystals were reported containing nicotinamide and adipic acid, azelaic acid, glutaric acid, palmitic acid, sebacic acid, stearic acid, suberic acid, decanedicarboxylic acid, hexadecanedicarboxylic acid, diallylbarbituric acid, ethyl 4-hydroxybenzoate, pyrocatechol, 2,4-dinitrophenol, 2,5-dinitrophenol, and 2,6-dinitrophenol.[43] Particularly interesting was the report that barbital (**8**), which was marketed as a sleeping aid from 1903 until the 1950s under the brand name Veronal, forms a cocrystal with pyramidone (**9**).[44] Pyramidone has been used commercially as an analgesic and an antipyretic. Apparently, the cocrystal was tested in vivo, as it is stated in the publication that there was no difference in therapeutic activity when either the cocrystal or a physical mixture of the components was prescribed.



7 **8** **9**

Not surprisingly, cocrystals can be polymorphic. As discussed above, quinhydrone (**3**) exists in monoclinic and triclinic forms. Kofler studied the interactions between 1,3,5-trinitrobenzene or picric acid and the aromatic hydrocarbons fluorene, naphthalene, phenanthrene, anthracene, 1-naphthylamine, and 2-naphthalamine.[45] Of the 12 combinations, all form cocrystals, eight of which are dimorphic and one of which is tetramorphic. Also interesting is that cocrystals may contain more than two components. An example is the structure containing 3 mol of 4-aminobenzoic acid, 1 mol of 2,4,6-trinitrobenzoic acid, and 1 mol of 1,3,5-trinitrobenzene, which was called a triheteromolecular adduct.[46]

During the time Pfeiffer, Kofler, Kofler, and Kuhnert-Brandstatter were at least partially focused on cocrystals and phase behavior, other researchers were finding cocrystals serendipitously. Cloez reported an attempt to dibrominate cholesterol by adding 1 equiv of bromine in carbon disulfide to a solution of cholesterol in the same solvent.[47] When half of the bromine had been added, needles crystallized from solution, and then redissolved during addition of the reminder of the bromine. The white needles were isolated and found to be a 1:1 cocrystal of cholesterol and dibromocholesterol. One of the keys in understanding the structure was that the cocrystal could be prepared by crystallization from a solution containing equimolar amounts of the pure components. Von Narwall reported a study of the reduction of cinchonine with metals.[48] Treatment of the compound with sodium or sodium amalgam afforded the expected hydrogenated derivatives. However, when he added metallic tin to a hydrochloric acid solution of cinchonine the product was a 1:1 cocrystal of cinchonine and cinchonine hydrochloride. Schroeter attempted to prepare benzoic acid using the relatively new Gringnard reagent.[49] It had been reported previously that treatment of phenyl magnesium iodide with carbon dioxide gave benzoic acid. But the reaction behaved somewhat differently when phenyl magnesium bromide was used. Treatment of that reagent with carbon dioxide, followed by acidic hydrolysis, gave a crystal-

UM00016998
NOVARTIS EXHIBIT 1517
Novartis v. Regents, IPR2023-01347
Page 3867 of 4460

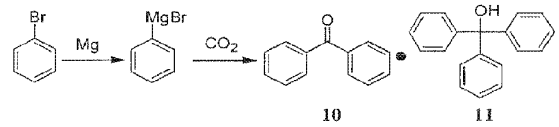
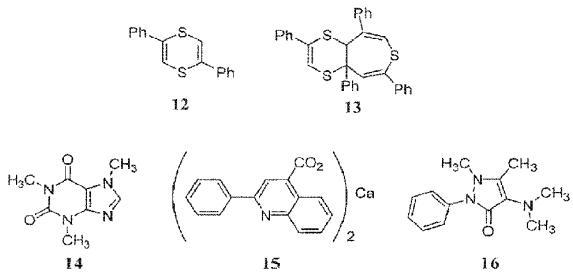


Figure 4. The addition of carbon dioxide to phenyl magnesium bromide resulted in the isolation of a 1:1 cocrystal of benzophenone and triphenylcarbinol.

line powder in about 6% yield. That material turned out to be a 1:1 cocrystal of benzophenone (**10**) and triphenylcarbinol (**11**) which melts at 165 °C (Figure 4), apparently formed by continued addition of the Grignard reagent to the initially formed product. Szmant et al. treated 2,5-diphenyl-[1,4]-dithiine (**12**) with peracetic acid and isolated a product to which he tentatively assigned the structure **13**.[50] That assignment was based on previous reports of Diels–Alder reactions occurring during oxidation of thiophenes. However, results from additional analyses of the product were inconsistent with structure **13**.[51] Identification of the product as a 1:1 cocrystal of **12** and **13** was confirmed by separation of the two components using column chromatography, as well as crystallization of the cocrystal by addition of 2-propanol to a benzene solution containing equimolar proportions of **12** and **13**.



The potential utility of cocrystals was recognized early and continuously explored during the 20th century. Some cocrystals considered for pharmaceutical applications were discussed earlier. A few additional examples are presented here. The observation that the aqueous solubility of caffeine (**14**) is increased in the presence of sodium salicylate was investigated by Regenbogen and Schoorl, who identified what they believed to be a cocrystal of **14** and salicylic acid.[52] Ultimately, Schoorl isolated a hydrated cocrystal composed of one molecule of **14**, one sodium salicylate molecule, and five water molecules.[53] That cocrystal is particularly interesting in that it contains an un-ionized organic molecule and an organic salt, bearing some resemblance to the acid/acid salt class of cocrystals discussed later. Similar cocrystals were patented by Czechoslovakians Oscar and Rudolf Adler, who are better known for patenting the use of activated carbon for water dechlorination. They were granted a U.S. patent for cocrystals containing salts of phenylquinoline carboxylic acids and substituted pyrazolones.[54] For example, by heating to 110 °C, with stirring, an equimolar mixture of calcium 2-phenyl-4-quinoline carboxylate (**15**) and 1-phenyl-2,3-dimethyl-4-dimethylamino-5-pyrazolone (**16**) with a little water, a clear melt was obtained. Cooling of the melt gave the 1:1 cocrystal, which they called a molecular compound. The claimed cocrystals were described as "...particularly suitable in cases of true gout with inflammatory joint manifestations, uratic diathesis, chronic joint disorders, or chronic arthritis when administered through the mouth with 3–4 doses of 0.5–0.6 g per day." Another example of a cocrystal containing an organic salt and an organic molecule was patented by Zellner.[55] He found that caffeine (**14**) and theophylline cocrystallized with sodium 2-naphthylacetic acid, and claimed that "The new molecular compounds have the advantage over caffeine and theophylline that they are much better soluble in water than the purines as such. For instance, the molecular compound with caffeine permits the preparation of aqueous solutions containing 80% of the molecular compound." Apparently, complexation occurs in solution as well since the cocrystal structure is lost on dissolution.

A cocrystal of nicotinamide (**7**) and L-ascorbic acid (vitamin C) was found and patented by chemists working for the Gelatin Products Corporation. Bailey et al. established the existence of the 1:1 cocrystal by generating the melting point phase diagram in 1945.[56] Fox patented the cocrystal in 1947, generating pure samples by mixing equimolar amounts of the components in the dry state.[57] Leading to discovery of the cocrystal was an investigation of unwanted thickening of oil-based multivitamin preparations containing nicotinamide and L-ascorbic acid. The patent claimed that preparations of reduced viscosity were obtained when the cocrystal was incorporated instead of the individual components. Buu-Hoi et al. reported testing the cocrystal, which was called Nicastubine, in guinea pigs.[58] It showed antiscorbutic (prevention of scurvy) activity and offered some protection against tuberculosis.

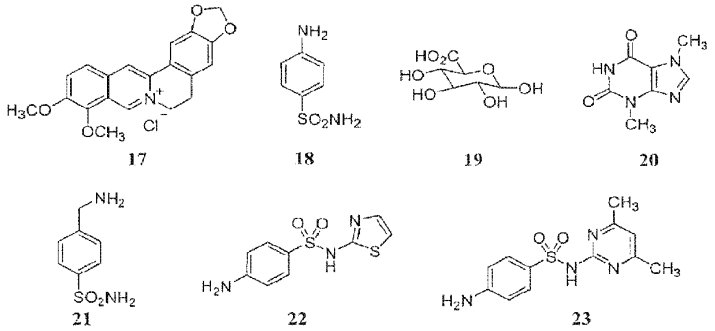
Kranz et al. found that a cocrystal containing equimolar amounts of sodium theophyllinate and glycine increased the water solubility of theophylline.[59] A clinical study showed that the cocrystal was tolerated in "unusually large amounts in man" and elicited the "typical theophylline response."

Higuchi studied complex formation in solution using solubility measurements. He found that caffeine forms complexes in solution with a number of pharmaceutically active or acceptable compounds such as benzoic acid, benzoate ion,[60] aspirin, 4-hydroxybenzoic acid, 3-hydroxybenzoic acid, salicylic acid, salicylate ion, butyl paraben,[61] sulfathiazole, sulfadiazine, 4-aminobenzoic acid, benzocaine, phenobarbital, and barbital.[62] He ultimately isolated cocrystals of caffeine and gentisic acid that had stoichiometries of 1:1 and 1:2 caffeine:gentisic acid.[63] Those cocrystals reduced the dissolution rate of caffeine and therefore, according to Higuchi "...present a potentially useful way of formulating caffeine in dosage forms such as chewable tablets that are intended to linger in the mouth. Such dosage forms would only release caffeine slowly and should, consequently, have an improved taste factor over ones containing pure caffeine."

Several Japanese groups studied the potential pharmaceutical use of cocrystals in the 1950s. Among those reported are cocrystals of penicillins with amino-4-toluenesulfonamide,[64] aminopyrine with glycerol monophenyl ether derivatives,[65] 5,5-diphenylhydantoin with antipyrine,[66] aminopyridine with barbituric acid derivatives,[67] and berberine chloride (**17**) with sulfa drugs such as sulfanilamide (**18**).[68] Japanese researchers recognized that cocrystals could increase the dissolution rate of active pharmaceutical ingredients (APIs). Glucuronic acid (**19**) cocrystals of caffeine (**14**) and theobromine (**20**) were reported to have higher solubility than **14** and **20** themselves.[69] It may be reasonably assumed that the high water solubility of

UM00016999
NOVARTIS EXHIBIT 1517
Novartis v. Regents, IPR2023-01347
Page 3868 of 4460

component **19** is responsible for enhanced dissolution rates of the APIs, but the distinction between solubility and dissolution rate was not addressed in the publications. Similarly, homosulfamine (**21**) cocrystals of sulfa drugs were said to increase the solubility of the sulfa drugs.[70] That effect probably does not result from individual component solubilities, as **21** is structurally very similar to sulfa drugs such as **18**. Perhaps enhanced dissolution rates of sulfa drugs from homosulfamine-containing cocrystals results from weaker intermolecular interactions in the cocrystals compared to those in the single-component sulfa drug crystals. In any case, those results portend one of the important properties of cocrystals under scrutiny today, that of increasing the aqueous dissolution rate of poorly water-soluble APIs.[71]



The number of reports of cocrystals having pharmaceutical utility grew somewhat in the late 1900s. Most of those studied contained known classes of compounds such as the sulfa drugs, barbiturates, and xanthine alkaloids such as caffeine (**14**), theophylline, and theobromine (**20**). Sakiguchi compared the aqueous dissolution behavior of a 1:1 cocrystal of **18** and sulfathiazole (**22**) to that of a physical mixture of the compounds.[72] At equilibrium the system consists of both components in solution and a solid phase containing a mixture of **22** and the cocrystal, but the equilibrium arises by much different kinetic pathways depending on the starting solid. The components of the physical mixture initially dissolve rapidly, then the rates decrease as undissolved particles become coated with precipitating cocrystal. The rates of component dissolutions were considerably different starting with the cocrystal. At about 1 h, the concentration of **18** was over five times higher when starting with the physical mixture compared to starting with the cocrystal. Also interesting is the fact that with the cocrystal as starting material, a metastable equilibrium was observed, its duration ranging from 6 h at 35 °C to >24 h at 15 °C, wherein the solid phase consisted only of the cocrystal. After that, equilibrium was slowly attained. The result is that the aqueous dissolution rate of the more water-soluble component (**18**) is reduced and that of the less water-soluble component (**21**) is increased when the cocrystal is used compared to when a physical mixture is used. Idealized solubility curves are shown in Figure 5. Note that the preceding example illustrates the broad concept that cocrystals can potentially increase or decrease the dissolution rate of a molecule of interest.

The dissolution and pharmacokinetic behavior of a cocrystal of **20** and phenobarbital was studied.[73] Theophylline (**20**) is more water-soluble (about 8 mg/mL) than phenobarbital (about 1 mg/mL), and consequently the dissolution rate of **20** is slower from the cocrystal than from crystalline **20** itself. It was found that the powder dissolution profile correlated with the graph of the serum level of **20** plotted against time, meaning that administration of the cocrystal provided peak blood levels at longer times than did administration of **20** alone. The authors concluded that "Bioavailability may be influenced by complexation or interaction of 2 drugs in a tablet." In addition to illustrating the ability of cocrystals to affect bioavailability, that study suggests that cocrystals could be useful for combination therapies. In fact, a commercial product that contains **20** and phenobarbital, as well as ephedrine, is known (Tedrol), but the cocrystal was not used therein.

Sulfadimidine (**23**) readily forms 1:1 cocrystals with a variety of carboxylic acids. The first X-ray structure of such, the acid component being salicylic (2-hydroxybenzoic) acid, was reported in 1988.[74] Subsequently, Caira et al. found similar cocrystals containing 2-aminobenzoic acid,[75] 4-aminobenzoic (anthranilic) acid,[75] 4-aminosalicylic acid,[76] acetylsalicylic acid,[76] benzoic acid,[77] 4-chlorobenzoic acid,[77] and ortho-phthalic acid.[77] Those cocrystals could be prepared from solution or by grinding equimolar proportions of the solid components in a ball mill.[77] Competitive experiments were carried out, in which **23** and two acids were ground together. When anthranilic acid was one of the pair its cocrystal always resulted. Also, when the cocrystal containing **23** and salicylic acid was ground with 1 equiv of anthranilic acid, the major product was the cocrystal containing **23** and anthranilic acid. A similar reaction did not take place when benzoic acid was used in place of anthranilic acid. Evaluation of the crystal structures of the components led Caira to hypothesize that the driving force for formation of the anthranilic acid cocrystal in the competition and substitution reactions involves the relative thermodynamic stabilities of the cocrystals compared to the homomeric crystals. Carboxylic acids often exist as hydrogen-bonded acid dimers in their crystals. Anthranilic acid is an exception, however, having one un-ionized molecule and one zwitterion in the asymmetric unit of the crystal. The lack of stable hydrogen-bonded dimers was thought to reduce the stability of the homomeric anthranilic acid crystal to less than that of the **23**: anthranilic acid cocrystal, providing the driving force for formation of the latter.

The potential utility of cocrystals to solve pharmaceutical development problems, such as poor dissolution rate, has apparently been broadly recognized only recently. Although

UM00017000
NOVARTIS EXHIBIT 1517
Novartis v. Regents, IPR2023-01347
Page 3869 of 4460

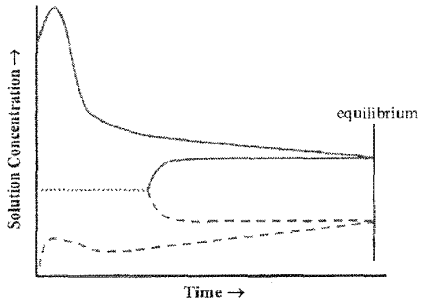


Figure 5. Idealized aqueous solubility curves for sulfanilamide (**18**), sulfathiazole (**22**), and the 1:1 **18**:**22** cocrystal. The red lines represent concentrations attained when starting with a physical mixture (solid is **18** and dashed is **22**). The blue lines represent concentrations attained when starting with the cocrystal (solid is **18** and dashed is **22**). The purple dotted line represents the concentration attained when starting with the cocrystal, during the metastable equilibrium phase (where the solid remains pure cocrystal). Adapted from ref 73.

presaged by the types of studies discussed above, it was not until about 2000 that the idea seemed to take hold. Since then the number of publications in the area has grown explosively. The slow acceptance of cocrystals as potential APIs is at least partially due to the understandably conservative approach taken by most drug companies toward meeting regulatory requirements. It is hard enough to get a drug approved and on the market without offering something perceived to be new to regulatory agencies. However, I note in that context that a couple of cocrystals have been approved for human consumption. The nicotinamide · ascorbic acid cocrystal discussed above is listed in the U.S. Code of Federal Regulations section 172, which is entitled Food Additives Permitted for Direct Addition to Food for Human Consumption.[78] It is described as "...the product of the controlled reaction between ascorbic acid and nicotinamide, melting in the range 141 °C to 145 °C." and useful "...as a source of ascorbic acid and nicotinamide in multivitamin preparations." Although it is administered in solution, a cocrystal containing un-ionized caffeine and citric acid, first reported in 1926,[79] was approved by the U.S. Food and Drug Administration in 1999.[80] The trade name is CAFCIT and it is prescribed for the short-term treatment of sleep apnea in infants. In any case, the reluctance to risk regulatory disapproval has likely been overshadowed by the fast-growing cost of drug development as well as the increasing loss of active molecules in development because of their poor water solubility or other suboptimal physical properties. Cocrystals are another possible crystalline form of an API that, if containing pharmaceutically acceptable components, should be thought of as salts from a regulatory point of view. As such, they can sometimes be used to "rescue" poor development candidates. Since this article only covers research reported prior to 2000, the more recent work of those studying pharmaceutical applications of cocrystals are not covered.[81]

Because of the considerable attention currently given pharmaceutical applications of cocrystals, it might be easy to overlook the many nonpharmaceutical applications that have been reported. Some examples follow.

Pfeiffer et al. understood that the forces responsible for intermolecular binding of molecules into cocrystals were the same as those that function in biological construction, such as

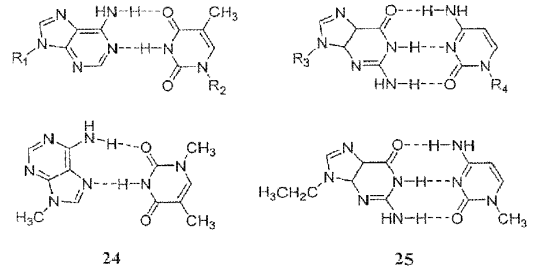


Figure 6. Structures of the adenine:thymine (top left) and guanine:cytosine (top right) base pairs in DNA (R_1, R_2, R_3, R_4 = attachment to phosphate-deoxyribose backbone), and the 1:1 cocrystals of 9-methyladenine:1-methylthymine (**24**) and 9-ethylguanine:1-methylcytosine (**25**).

the building of proteins.[82] Thus, biological structures have inspired small molecule cocrystal research. In the structure of DNA, first proposed in 1953,[83] the planar adenine:thymine base pair is held together by two hydrogen bonds and the planar guanine:cytosine base pair is held together by three. Cocrystals of those free nucleotide bases containing alkyl groups at positions where they are attached to the phosphate-deoxyribose backbone in DNA were made (Figure 6, **24** and **25**). Cocrystal **24** was obtained by crystallization of an equimolar solution of the components from water.[84] It is noteworthy that the hydrogen bonding pattern between the components is different in DNA than it is in the cocrystal. Although the adenine amino group hydrogen bonds to a thymine carbonyl oxygen atom in both structures, the thymine NH group hydrogen bonds to a nitrogen atom in the 6-membered ring of adenine in DNA but to a nitrogen atom in the 5-membered ring of adenine in the cocrystal. On the other hand, the hydrogen bonding pattern between the components in cocrystal **25**, prepared by crystallization from dimethylsulfoxide solution, is the same as that found in the guanine:cytosine base pair of DNA.[85] Interestingly, Etter et al. reported that **24** can be prepared by grinding the components in the solid state, but **25** cannot.[86] A series of similar cocrystals, containing variously substituted nucleotide bases, were reported. Wilson summarized those found in the literature prior to 1988, listing 12 homobase-pairs and 25 heterobase pairs.[87]

Nucleotide base cocrystals were used in the study of the mechanism of radiation damage to DNA. Ionizing radiation leads to free radicals, which can reside on the base pairs. Schmidt obtained electron spin resonance spectra of gamma-irradiated **24** and found that the resulting free radical is more long-lived in that cocrystal than it is in the crystal of 1-methylthymine alone.[88] Similar work was carried out by Kar et al.[89]

Related is the use of cocrystals as protection against sun exposure damage to the skin. Ultraviolet (UV) radiation causes dimerization of adjacent nucleotide bases in DNA, but studies showed that the reaction is wavelength-dependent, and that dimerization caused by 280-nm radiation can actually be reversed by 240-nm radiation. Cocrystals composed of nucleotides (phosphoric acid esters of N-glycosides of nucleotide bases) and aminocarboxylic acids were patented as topically applied sun screens.[90] They contain 1 mol of the nucleotide and 1−4 mol of the acid. Either component can be present in un-ionized form or as a salt. An example is the

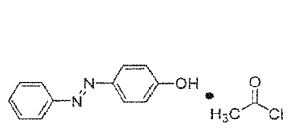
UM00017001
NOVARTIS EXHIBIT 1517
Novartis v. Regents, IPR2023-01347
Page 3870 of 4460

cocrystal containing 1 mol of adenosine-5′-monophosphoric acid and 2 mol of sodium 4-aminobenzoate. The nucleotide portions provide skin compatibility and water solubility, the latter allowing incorporation in aqueous skin protective compositions. The cocrystals show strong absorption of radiation between 320 and 280 nm, but minimum absorption of 240-nm radiation.

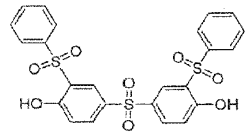
Pfeiffer et al. published reviews of articles describing cocrystals of amino acids and polypeptides with various types of organic compounds.[91] He concluded that, since those molecules are loosely related to more complex molecules such as proteins, tannins, and dyes, the processes of tanning and dyeing involve cocrystal formation at the surface of solid materials. Somewhat related was the use of colored cocrystals as hair dyes, such as those containing polyhydric phenols and aromatic diamines.[92] A specific example is the yellow, 2:1 cocrystal of 1,3-diaminobenzene and 1,3,5-trihydroxybenzene (phloroglucinol).

Quehl patented cocrystals useful for finishing operations in the textile industry.[93] Textile finishing involves treatment of fabric to improve its look, performance, or feel. Quehl found that cocrystals of urea and sugars were advantageous in finishing, even though they are applied in solution. By mixing approximately equimolar amounts of urea and glucose in water, a syrup was obtained which "...normally does not tend to crystallize." Further, "Only when the syrup is left standing for some time and subjected to occasional rubbing with a glass rod, small needles will separate therefrom, whereupon the largest portion of the mass soon solidifies from the center of crystallization and forms a crystal-magma." The cocrystal obtained in that way melts at 117 °C; urea melts at 132 °C and glucose at 85 °C. The difficulty encountered in finishing operations in which the solutions of the components were used separately or in nonequimolar mixtures was that crystallization occurred on the fabric. By generating the cocrystal, then dissolving it for application, crystallization on the fabric was avoided. An interesting use of slow-growing cocrystals to prevent crystallization!

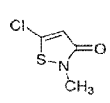
Cocrystals were used to impart stability to inherently unstable compounds. Fischer et al. reported that inorganic and organic acid halides cocrystallize with hydroxyazo compounds.[94] He made more than 30 such cocrystals containing about fifteen different acid chlorides and bromides. Those were prepared in nearly quantitative yield by crystallization from solution or simply shaking the components together in the absence of solvent. An example is the dark red cocrystal containing acetyl chloride and 4-(phenylazo)phenol (**26**). Cocrystal **26**, which melts at 172 °C, was kept in an open vessel for days without decomposing. Normally, acid chlorides are readily hydrolyzed when exposed to atmospheric conditions. It should be noted that mixing of a hydroxyazo compound with an acid chloride might be expected to lead to an esterification reaction with liberation of hydrogen halide. If that occurred, could the cocrystals described by Fischer actually be simply esters, or cocrystals of esters with hydrogen halides? Those possibilities seem unlikely, as molecular weight determinations showed that the cocrystals dissociate almost completely in benzene solution. In addition, alkyl- and acyl-substituted hydroxyazo compounds fail to produce the cocrystals, even though they contain the potentially reactive hydroxyl group. Aoki et al. found that some disinfectants form cocrystals with specific phenol derivatives, providing the ability to stabilize, reduce the volatility of, and control the release rate of the disinfectants.[95] An example is the cocrystal containing 1 mol of **27**, the phenol derivative, and 2 mol of **28**, the disinfectant. Compound **28** is an easily decomposed liquid, but the cocrystal renders it a thermally stable powder.



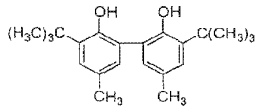
26



27



28

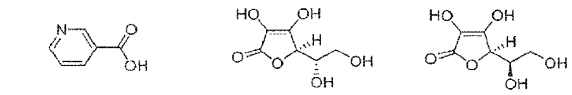


29

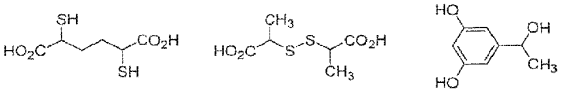
Purification processes enabled by cocrystals were described. Christiani et al. reported the purification of cholesterol via its cocrystal with digitonin, which is a glycoside of molecular weight 1229.[96] Fatty acids were purified by crystallization of their cocrystals with acetamide.[97] Commercial fatty acids, such as stearic, palmitic, myristic, and lauric acids, of about 90% purity were mixed with an equimolar amount of acetamide and an organic solvent and warmed to effect solution. Cooling gave cocrystals which were separated from the viscous mother liquors by centrifugation. From the recovered cocrystals, purified fatty acids, free of homologues, could be obtained. Bis-phenols, such as **29**, are used as antioxidants. They can be recovered in pure form from crude reaction product mixtures by treating solutions of the mixtures with amines and recovering the cocrystals formed between bisphenols and amines.[98] A wide variety of amines were used, including hydrazine, alkylamines such as methylamine and ethylamine, aromatic amines such as pyridine and 2,6-lutidine, and hydroxyamines such as ethanolamine and triethanolamine. Cocrystals allowed recovery of expensive cephalosporins from dilute solutions such as mother liquors remaining from direct crystallizations. Cocrystallization of cefaclor, cephalexin, cepfradine, or loracarbef with parabens (para-hydroxybenzoate esters), followed by pH-mediated precipitation, provided the purified cephalosporins as solids and left the parabens in solution.[99]

Examples of chiral selectivity during cocrystallizations were reported. Cocrystals of nicotinamide (**7**) and L-ascorbic acid were discussed in earlier sections of this manuscript. Wenner studied cocrystal formation between nicotinic acid (**30**) and ascorbic acids, with a surprising result.[14] L-Ascorbic acid (**31**) readily cocrystallized with **30**, but its diastereomer, D-isoascorbic acid (**32**), did not. Wenner stated "This difference in the formation of a complex cannot be explained by differences in acidity between L-ascorbic and D-isoascorbic acid, because both show practically the same pH in solutions. It seems logical to ascribe the difference in behavior to the difference in structure of both acids. Obviously the stearic arrangement of the particular ascorbic acid is instrumental in bringing about the combination with nicotinic acid." On the basis of melting point curves, Fredga discovered an example of enantiomeric selectivity.[100] The levo isomer of dimercaptoadipic acid (**33**) formed a 1:1 cocrystal with the levo isomer of dithiodilactic acid (**34**), but not with the dextro isomer of **34**.

UM00017002
NOVARTIS EXHIBIT 1517
Novartis v. Regents, IPR2023-01347
Page 3871 of 4460



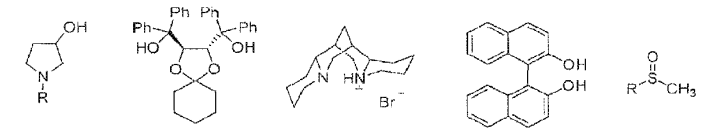
30 31 32



33 34 35

The natural extension of such chiral selectivity is to utilize optically pure cocrystal components as resolution agents, much the same way that optically pure acids (bases) are used to resolve racemic bases (acids) via diastereomeric salt crystallization. Indeed, resolutions by diastereomeric cocrystal crystallizations were reported. Brucine was used to resolve racemic resorcylmethylcarbinol (**35**), a compound that is not acidic enough to form a salt with brucine.[101] Treatment of racemic **35** with brucine in an organic solvent resulted in crystallization of a cocrystal containing dextro-**35** and brucine. The diastereomeric cocrystal, containing levo-**35** and brucine, could not be obtained. Successive recrystallizations of the cocrystal and liberation of **35** by extraction of brucine into acidic water afforded optically enriched dextro-**35**. However, resolution ceased at a specific enrichment level, and a cocrystal containing optically pure dextro-**35** could not be obtained. In order to complete the resolution, the dextro isomer from the cocrystal crops and the levo isomer from the mother liquors were separated from brucine and each was dissolved in solvent. Concentration of each solution induced crystallization of racemic **35**, which exists as a racemic compound, leaving optically pure dextro- and levo-**35** in the mother liquors.

A more efficient resolution was carried out of 3-hydroxypyrrolidinines (**36**) via their cocrystals with the optically active diol (**37**).[102] Two recrystallizations of each initially formed cocrystal sufficed to provide optically pure **36**. 1,2-Dibromohexafluoropropane contains no functional groups that allow salt formation, but was resolved as a cocrystal with (−)-sparteine hydrobromide (**39**).[103] In that case only one recrystallization was required. A case of mutual optical resolution of components of a cocrystal was found by Toda et al.[104] When a solution of (+)-bis-β-naphthol ((+)-**39**) and racemic sulfoxide **40a** in benzene was allowed to stand at room temperature for 12 hours, a 1:1 cocrystal containing (+)-**39** and (+)-**40a** separated as colorless prisms. One recrystallization from benzene followed by decomposition of the cocrystal afforded 100% optically pure (+)-**40a** in 77% yield. The reverse resolution, of racemic **40a** by chiral **39**, occurred similarly. The success of the resolution procedure depended on apparently minor changes in the R group of **40**. While (+)-**39** efficiently resolved **40a**, it poorly resolved the related compounds **40b** and **40c**, and failed to form a cocrystal with **40d**.



36 R = H; R = benzyl; R = ethyl **37** **38** **39** **40** a) R = *m*-tolyl; b) R = phenyl; c) R = *o*-tolyl; d) R = *p*-tolyl

Some interesting solid-state reactions which occur in cocrystals were observed. Etter et al. reported an unexpected nucleophilic aromatic substitution reaction which apparently occurs because of molecular orientation in a cocrystal.[105] Cocrystal **41** was prepared from solution or by grinding together 4-chloro-3,5-dinitrobenzoic acid and 4-aminobenzoic acid (Figure 7). Analysis of **41** by differential scanning calorimetry revealed an irreversible exothermic event which occurred at 180 °C. A drop of aqueous silver nitrate solution suspended over a sample of **41** during heating developed a precipitate of silver chloride, showing that hydrochloric acid was being evolved. The product of the exothermic reaction was identified as **42**, and it could be obtained in quantitative yield simply by heating **41**. Although a crystal structure of **41** was not obtained, the suspicion is that a hetero acid dimer results in alternation of the components in the structure and that serendipitous proximity of the amino and C−Cl moieties leads to the solid-state reaction. Toda reported that cocrystals containing two different alcohols, when treated with *para*-toluenesulfonic acid in the solid state, afforded unsymmetrical ethers.[106] A series of such reactions was studied, the starting cocrystals being produced either from solution or by grinding the solid components. In one example, cocrystal **43** afforded ether **44** in 78% yield. When the components of **43** were treated with *para*-toluenesulfonic acid in solution, both symmetrical ethers and the unsymmetrical ether **44** were obtained in statistical ratios. The conclusion was that the components of **43** exist as hydrogen-bonded pairs in the crystal, which leads to selective formation of unsymmetrical **44** from the cocrystal.

A rather unusual type of cocrystal was discovered by Hirata et al. during studies of viscoelastic systems. Addition of aromatic compounds to aqueous solutions of cationic surfactants afforded solutions having remarkable viscoelasticities. Examination of such solutions by electron microscopy revealed the presence of large rod-like micelles mixed with a few single crystals.[107] A solution of hexadecyltrimethylammonium bromide and 2-iodophenol that was allowed to stand deposited crystals, which were recovered by centrifugation and found to be a 1:1 cocrystal of the two components.[108] Approximately 140 similar cocrystals were made, containing cationic alkyltrimethylammonium bromides or anionic sodium alkyl sulfates along with aromatic components encompassing a wide variety of structures.[109] While the

UM00017003
NOVARTIS EXHIBIT 1517
Novartis v. Regents, IPR2023-01347
Page 3872 of 4460

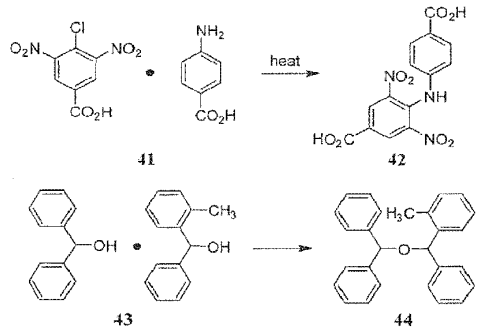


Figure 7. Examples of solid-state reactions of cocrystals.

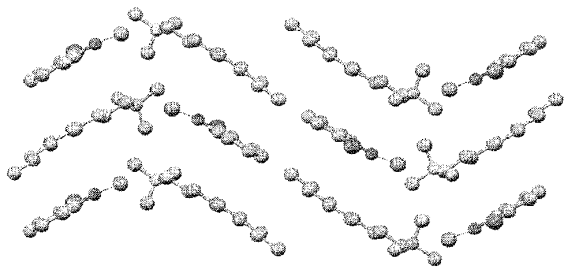


Figure 8. A packing diagram from the crystal structure of the 1:1 cocrystal of decytrimethylammonium bromide and 2-iodophenol.[113] Carbon atoms are gray, nitrogen atoms are blue, oxygen atoms are red, iodine atoms are purple, bromine atoms are brown, and hydrogen bonds are dotted lines. Hydrogen atoms are omitted for clarity.

structures of the cocrystals containing cationic surfactants differ from those containing anionic surfactants, in each the aromatic molecules reside in contact with the hydrophobic portions of the surfactants. A typical structure of a cationic surfactant cocrystal is shown in Figure 8. The aromatic molecules lie between the hydrophobic tails of the surfactant molecules, but near their ionic ends. The aromatic alcohol groups are hydrogen bonded to the bromide ions. Similar structures exist for cocrystals containing cationic surfactants and aromatic molecules devoid of donor groups. In those, the aromatics reside at the ionic end of the surfactants even though hydrogen bonding to bromide is not possible. The pharmaceutical utility of such cocrystals was not lost on Hirata. He found that aromatic, water-insoluble APIs cocrystallize with cationic surfactants. Flopropione (1-(2,4,6-trihydroxyphenyl)-1-propanone), an antispasmodic marketed in Japan, and 4-chloro-meta-cresol, which has been used as a topical antiseptic, cocrystallize with hexadecyltrimethylammonium bromide.[110] The flopropione cocrystal was found to dissolve considerably faster in water than either a physical mixture of the components or flopropione itself, and the 4-chloro-meta-cresol cocrystal was found to be more thermally stable (less loss from vaporization) compared to 4-chloro-meta-cresol itself.

Numerous cocrystals containing heterocyclic nitrogen bases and carboxylic acids were reported in the 1990s. A list of selected examples, which is not intended to be comprehensive, is shown in Table 1. A disproportionally high number of cocrystals of that particular class seem to have been studied, leading to the question "Why is this relatively narrow structural class of cocrystals of particular interest?" The answer is crystal engineering. That field of study, which emerged in the last half of the 20th century, was defined by Desiraju in 1989 as "the understanding of intermolecular interactions in the context of crystal packing and in the utilisation of such understanding in the design of new solids with desired physical and chemical properties".[111] Such supramolecular syntheses have been approached retrosynthetically, where common intermolecular interactions observed in crystal structures are used to devise what are called supramolecular heterosynthons. Those are noncovalently bound, multicomponent assemblies that can pack to give long-range structural order.[112]

Typically, hydrogen bonds play an important role in binding functionalized organic molecules into crystals, and are relatively easily recognized in crystal structures based on shortened contact distances and specific directionalities. Thus, searches for hydrogen bonding patterns that could be used to build supramolecular heterosynthons leading to new crystal structures were undertaken by several research groups. Many of the cocrystals in Table 1 were generated during studies of that type. The work of Margaret C. Etter, one of the more prolific researchers of the era, led to a set of empirically derived rules that correlate functional groups and hydrogen bonding patterns.[114] By understanding the crystal structures of individual molecules and applying the hydrogen-bonding rules, Etter et al. designed cocrystals containing 2-aminopyrimidine and carboxylic acids (Table 1).[115] Knowing that 2-aminopyrimidine and, often, carboxylic acids exist as hydrogen-bonded dimers in their homomeric crystal structures, she reasoned that they might form heteromeric dimers which would be supramolecular heterosynthons for new structures (Figure 9). That proved to be the case, leading to the discovery of new, 2-aminopyrimidine-containing cocrystals in her laboratories[115] as well as by other research groups (Table 1).[116−119] Similarly, carboxylic acids were found to form supramolecular heterosynthons with other functionalized heterocyclic bases such as 2-amino-5-nitropyridine[121] and 2-pyridone.[128] Cocrystals containing other hydrogen bonding patterns were constructed by similar analyses of homomeric structures, examples being the cocrystals containing 2-aminopyrimidones and dicarboxylic acids.[120]

It must be mentioned that consideration of one type of hydrogen-bonding pattern alone is a rather narrow view into the interactions that might lead to rationally designed cocrystals. For example, it was stated above that carboxylic acids often exist as hydrogen-bonded dimers in the crystalline state. Quantitatively, of the over 4000 entries in the 2004 version of the Cambridge Structural Database of crystal structures in which at least one carboxylic acid moiety is present, about 29% were found to have that dimer structure.[130] More commonly, the acid moieties are associated with other functional groups to form supramolecular heterosynthons. The success realized using the relatively simple dimer analysis discussed above suggests that once a better understanding of factors leading to supramolecular heterosynthons is achieved, cocrystal design will be more readily accomplished.

Some of the cocrystals in Table 1 are interesting for a different reason. For example, consider the 1:1 cocrystal of 2,4,6-trimethylpyridine and benzoic acid, the structure of which was determined at 150 K.[129] The single hydrogen bond in the structure is between the carboxylic acid group of

UM00017004
NOVARTIS EXHIBIT 1517
Novartis v. Regents, IPR2023-01347
Page 3873 of 4460

Table 1. Selected Cocrystals Containing Heterocyclic Nitrogen Bases and Carboxylic Acids

base component	acid component	reference
2-aminopyrimidine	benzoic, 3-bromobenzoic, 4-methylbenzoic, 3-nitrobenzoic, isophthalic, malonic, succinic	115
	2-aminobenzoic, 3-aminobenzoic, 2-nitrobenzoic, *o*-phthalic	116
	2,4,6-trinitrobenzoic	117
	p-phenylenediacetic	118
	terephthalic	119
2-amino-6-ethyl-4(3H)-pyrimidone	adipic, succinic	120
2-amino-6-methyl-4(3H)-pyrimidone	adipic, glutaric	120
2-amino-5-nitropyridine	chloroacetic	121
2-amino-6-phenyl-4(3H)-pyrimidone	adipic	120
3-amino-1,2,4-triazole	4-nitrobenzoic	117
4,4′-bipyridine	maleic, fumaric	122
	adipic, glutaric, malonic	123
(*R*)-4-(4-chlorophenyl)pyrrol-2-one	(−)-tartaric	124
3,5-dimethylpyrazole	2,4,6-trimethylbenzoic	125
3-hydroxypyridine	2,4-dichloro-5-fluorophenoxyacetic, 2,4-dichlorophenoxyacetic, 3,5-dinitrobenzoic, phenoxyacetic, 2,4,5-trichlorophenoxyacetic	117
phenazine	malonic	126
phthalazine	phthalic	127
2-pyridone	adipic, oxalic, sebacic, suberic, succinic	128
2,4,6-triaminopyrimidine	adipic, glutaric, malonic, succinic	123
2,4,6-trimethylpyridine	benzoic	129

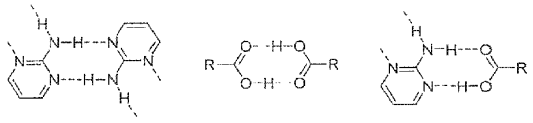


Figure 9. Hydrogen-bonded dimers in the 2-aminopyrimidine crystal (left), carboxylic acid crystals (center), and cocrystals (right).

benzoic acid and the nitrogen atom of the pyridine, as expected since they are the best proton donors and acceptors in the system. Note, however, that the pair does not form a salt; the proton is not transferred from the acid to the base. On the other hand, the analogous crystals containing 1,4,6-trimethylpyridine and 2-nitrobenzoic acid or 3,5-dinitrobenzoic acid are salts, with the protons residing on the pyridine nitrogen atoms. Since the nitro-containing benzoic acids are more acidic than benzoic acid itself, it is likely that the structural differences are due to differences in the pK_a separation between the acid and the base. However, for acids and bases having a ΔpK_a of about two or less, the crystalline environment is critical in determining whether a cocrystal or salt results.[131] That situation, which has been called the salt−cocrystal continuum, was recently discussed in detail.[132]

Cocrystal engineering is especially important in the field of nonlinear optics (NLOs). An NLO material is one in which certain responses to radiation are not linearly proportional to properties of the radiation. For example, certain crystals exhibit the property of second harmonic generation, also called frequency doubling. One is monopotassium phosphate. When the output of a Nd:YAG laser, which is near-infrared radiation at a wavelength of 1064 nm, is passed through a crystal of monopotassium phosphate at a specific angle, green laser light at a wavelength of 532 nm results. The frequency is doubled, halving the wavelength. Such behavior results when polarization of the crystal is not linearly proportional to the electric field of the impinging radiation.

Organic materials offer potential advantages over inorganic materials in NLO applications, including higher hyperpolarizabilities and faster response times. Inherently, molecules which contain suitably disposed electron withdrawing and electron donating groups are highly polarizable. In order for that polarizability to persist in the crystalline state, the molecules must pack parallel to each other in a noncentrosymmetric fashion (having no center of symmetry). Noncentrosymmetric packing of organics is infrequent, occurring in about only 10% of the crystal structures of achiral, organic molecules. The result is that many compounds possessing favorable NLO properties at the molecular level do not maintain those properties at the crystalline level. Crystal engineers sought to overcome that problem using cocrystals, wherein expected hydrogen-bonding patterns could be used to overcome centrosymmetric packing of highly polarizable molecules.

An example is the merocyanine dye **45**, which is called Brooker's merocyanine.[133] The electronic structure of **45** depends on the relative contribution of its two resonance forms, the quininoid form being favored in nonpolar media and the zwitterionic form being favored in polar media. It is an outstanding NLO candidate, exhibiting a very high molecular hyperpolarizability as well as good thermal and photo stabilities. However, compound **45** packs centrosymmetrically in its crystal, and in addition forms poor quality single crystals that are unsuitable for NLO applications. By cooling methanol or ethanol solutions containing equimolar amounts of **45** and either compound **47** or **48**, cocrystals were obtained.[134] The packing in each cocrystal differed, but the presence of the nitrophenols altered the structures in a positive way, from an NLO point of view, relative to the structure of **45** alone. A study of those structures led to development of a cocrystal containing compounds **46** and **49**.[135] That exhibited strong second-harmonic signal generation, suggesting noncentrosymmetric packing of **46**. The structure of that monohydrated cocrystal is quite interesting (Figure 10). A proton is transferred from the weakly acidic **49** to the oxygen anion of the zwitterionic form of **46**. That generates hydrogen bonded, oppositely charged pairs of molecules, a cationic **46**-H-**46** pair and an anionic **49**-H-**49** pair. Note that in the **46**-H-**46** pair the hydrogen bond is between the hydroxyl group of the protonated zwitterionic form and the carbonyl

UM00017005
NOVARTIS EXHIBIT 1517
Novartis v. Regents, IPR2023-01347
Page 3874 of 4460

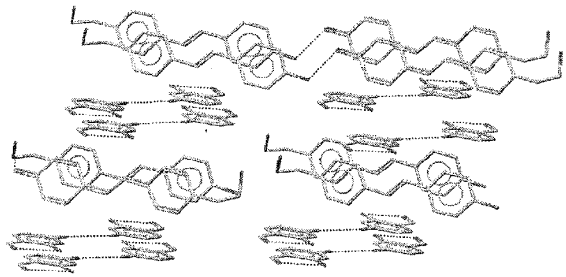
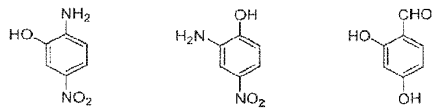


Figure 10. The structure of the 1:1 cocrystal of compound **46** and **49**.[136] Carbon atoms are gray, hydrogen atoms are white, nitrogen atoms are blue, oxygen atoms are red, and hydrogen bonds are dotted lines. Water molecules are omitted for clarity.

oxygen atom of the quininoid form, rendering the pair noncentrosymmetric.



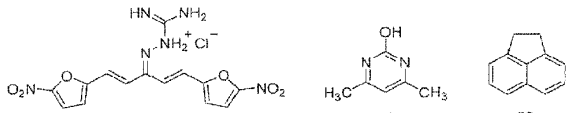
45 (R = CH_3), **46** (R = CH_2CH_2OH)



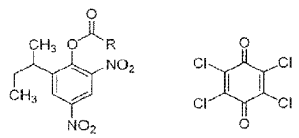
47 **48** **49**

A related approach was taken with the highly polarizable 4-nitrophenols. Huang et al. reported generation of twenty-two cocrystals containing phenol-pyridine pairs, including two cyanophenols, four nitrophenols, and five pyridines.[137] Many of those are salts, apparently depending on the ΔpK_a between the constituents. However, the salts tend to hydrogen bond to a third molecule, forming either 2:1 cocrystals or hydrates. For example, one of the cocrystals is composed of one 2-methoxy-4-nitrophenoxy anion, one 4-(dimethylamino)pyridinium cation, and one un-ionized 2-methoxy-4-nitrophenol molecule. That cocrystal, and three others like it, packed noncentrosymmetrically and thus exhibited second harmonic generation activity. It was postulated that ionic cocrystals of that type might have a greater chance of forming noncentrosymmetric structures than do achiral organic molecules in general.

A few isolated examples of cocrystal uses are worth mentioning. Cocrystals containing nitrovin hydrochloride (**50**) and amines such as 2-hydroxy-4,6-dimethylpyrimidine (**51**) were patented as animal feed additives.[138] A Romanian patent was issued for cocrystals containing acenaphthene (**52**) and the fungicides dinobuton (**53**), binapacryl (**54**), and chloranil (**55**).[139] The known bis-phenol:amine cocrystals[98] were used as components of heat responsive marking sheets, wherein heating of areas containing the cocrystals releases the contained amines to react with other sheet components, creating colored compounds.[140] Cocrystals of fluorinated bis-phenols and quaternary phosphonium chlorides are useful as fluoroelastomer vulcanization promoters.[141] Hydroquinones, used as auxiliary developers in self-developing photographic film, make film production difficult because of their poor water dispersibility, and tend to migrate in the film layers to undesirable locations. Both of those problems can be overcome by the use of cocrystals containing the hydroquinones and tetrasubstituted paradiamides such as *N*,*N*,*N*′,*N*′-tetraalkylterephthalamides.[142] Etter et al. found that triphenylphosphine oxide forms cocrystals with aromatic compounds containing hydrogen bond donor groups, providing large, blocky crystals of higher quality than crystals of the aromatic compounds alone.[143]



50 **51** **52**



53 R = $OCH(CH_3)_2$
54 R = $C{\equiv}C(CH_3)_2$ **55**

The survey presented above represents an extensive body of work on cocrystals. There are, however, other types of cocrystals that were not discussed. I will mention two of those types briefly. The first are cocrystals that contain a carboxylic acid cocrystallized with an organic or inorganic salt of the same acid. The second are cocrystals that contain an organic molecule and a simple alkali metal or ammonium, inorganic salt.

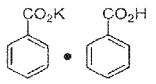
Cocrystals Containing Carboxylic Acids and Their Salts

Examination of crystal structures reveals that certain functional groups favor specific hydrogen-bonding patterns. That is true for carboxylic acids, which, as mentioned above, often exist as hydrogen-bonded dimers when in the crystalline state (Figure 9). Those dimers cannot, of course, be formed between carboxylic salt molecules. So, is there some arrangement of the carboxylate groups that will occur repeatedly in crystalline carboxylate salts? The answer is a qualified yes. Salts crystallize in a number of ways, one of which creates a cocrystal that contains 1 mol of carboxylate salt and 1 mol of un-ionized carboxylic acid. The qualification is how one would define repeatedly. Although there are quite a few structures of that type reported, not all salts form them, and the frequency of their existence seems to be less that the frequency of free acids forming hydrogen-bonded dimers.

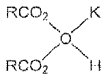
Examples of such cocrystals were reported in the mid 1800s, although their structures were not immediately understood. An example is potassium hydrogen benzoate (**56**), which was first isolated in 1852 from the residue left after distillation of a mixture of potassium acetate and benzoyl chloride.[144] Farmer later made it, and a series of similar cocrystals, by crystallization from ethanol solutions containing the theoretical amounts of acid and base (2 equiv of benzoic acid and 1 equiv of potassium hydroxide to give **56**).[144] At that time, interactions between the components of such cocrystals were investigated in solution, where it was found that the species were largely uncomplexed. The

UM00017006
NOVARTIS EXHIBIT 1517
Novartis v. Regents, IPR2023-01347
Page 3875 of 4460

nature of the interaction was a matter for speculation only, one theory being that oxygen was quadrivalent (**57**).[144]

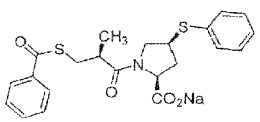


56

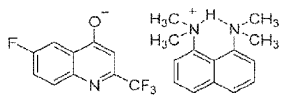


57

Over the years, cocrystals containing an acid and acid salt in a 1:1 ratio were found for a wide variety of acids and salts. A representative list of some of those reported for common acids and their salts is in Table 2. Note the structural variety of acids included. More complex acid salts are also known to form cocrystals containing a mole of the parent acid; the sodium salt of the pharmaceutically important zofenopril (**58**) is an example.[145] Even some noncarboxylic acid salts exist as 1:1 acid:acid salt cocrystals, as does the proton sponge salt of an acidic quinolinol (**59**).[146]



58



59

Not all known acid:acid salt cocrystals have a simple 1:1 ratio of components. For example, oxalic acid and pyridine form a cocrystal containing 1 mol of the mono salt and 1 mol of the free acid (Table 2),[178] as well as a cocrystal containing 2 mol of the mono salt and 1 mol of the free acid.[201] In fact, organic acid salts can exist as solids having a variety of component ratios. Barry et al. studied alkylammonium salts of simple dicarboxylic acids and classified their structures as "normal" or "anomalous".[184] For a dicarboxylic acid AH_2 and a monobasic amine B, they called salts having stoichiometries AHB and AB_2 normal and those having stoichiometries A_2H_3B and $A_3H_4B_2$ anomalous. Their anomalous salts are cocrystals by the definition given at the beginning of this review. A solid of stoichiometry A_2H_3B contains one mono salt (AHB) and one free acid (AH_2), while a solid of stoichiometry $A_3H_4B_2$ contains either one free acid (AH_2) and two mono salts (AHB) or two free acids (AH_2) and one di salt (AB_2).

As with all crystal forms, formation of the various salt types is unpredictable. Barry et al. found that reaction of maleic acid with one equivalent of tetramethylammonium hydroxide gave the mono salt (AHB) and with one-half equivalent gave the 1:1 cocrystal (A_2H_3B).[184] On the other hand, reaction of fumaric acid with either one, one-half, or two-thirds equivalent of tetramethylammonium hydroxide gave only the 1:1 salt (AHB). Reaction of fumaric acid with one-half or one-third equivalent of tetraethylammonium hydroxide (note ethyl instead of methyl) gave the cocrystal of type $A_3H_4B_2$. That cocrystal could be recrystallized from methanol-ether mixtures without change, but when recrystallized from 2-propanol afforded the mono salt (AHB).

The structural feature that favors formation of cocrystals as opposed to simple salts seems to be hydrogen bonding between the COOH group of a free acid molecule and the COO^- group of a carboxylate salt molecule. As usual, however, overall packing and other molecular interactions dictate the actual hydrogen bonding network and whether cocrystals will form at all. Speakman determined the structures of a number of acid:acid salt cocrystals and classified them as either containing crystallographically distinct acid and acid salt groups, or, more commonly, containing crystallographically indistinct, symmetrically related acid molecules.[191] In phenolic acid:acid salt cocrystals a related hydrogen bond is present between the un-ionized OH group and the ionized O^- group.[202]

There appears to be little in the literature concerning utility of acid:acid salt cocrystals. It is noteworthy that one of the oldest examples, sodium hydrogen diacetate, is listed in the U.S. Code of Federal Regulations as a substance that can be directly added to food.[203] Its use in foods has been as an antimicrobial, flavoring, or pH control agent.

Cocrystals Containing an Organic Component and a Simple Alkali Metal or Ammonium Salt

There are many cocrystals described that contain an organic and an inorganic component. The section in Pfeiffer's book *Organische Molekulverbindungen* covering cocrystals containing a mixture of inorganic and organic components is longer than the section covering cocrystals containing all organic components.[30] Alkali and alkaline earth salts, as well as mineral acids, halogens, and many other types of inorganic compounds, can cocrystallize with organic molecules. Rather than attempting to cover all types of organic:inorganic cocrystals in this manuscript, a few examples will be presented of cocrystals containing organic components and simple alkali metal or ammonium inorganic salts. The examples should be viewed as the tip of the iceberg of organic:inorganic cocrystals, but are particularly interesting, in my view, because of the potential for changing the physical properties of organic molecules using innocuous, inexpensive salts.

Sodium chloride will cocrystallize with some organic molecules, particularly those bearing multiple hydroxyl groups. Gill published a paper in 1871 in which he described preparation of a cane sugar/salt (sucrose·NaCl) cocrystal.[204] He began his work to sort out a controversy in the literature over the reality of such compounds. French chemists had reported producing a crystalline compound containing a 1:1 ratio of sucrose and sodium chloride, but other chemists, both French and German, were unable to obtain it. Gill produced a cocrystal having that ratio of components as well as two waters of crystallization ($C_{12}H_{22}O_{11}\cdot NaCl\cdot 2H_2O$, **60**), but did so only once. As part of a series of crystallizations from aqueous solutions containing various ratios of sucrose and NaCl, he obtained crystalline sucrose by concentrating a solution in which sucrose and NaCl were present in equimolar amounts. On further concentration of the mother liquor, cocrystal **60** was deposited. Recrystallization of **60** from aqueous alcohol led to crystals containing varying ratios of sucrose and NaCl, and recrystallization of those products of indefinite compositions led to crystalline sucrose. However, addition of ether to an aqueous alcohol solution of **60** deposited an oily layer, in which **60** appeared again after a period of 8 or 10 months. Gill was unable to find conditions allowing production of **60** at will, noting "I have only once succeeded in preparing that compound since the first lot of accidentally formed crystals, and on this solitary occasion there had been a continuance of very cold weather during the whole period of crystallisation." As part of that same study, Gill found a 2:3 sucrose:NaCl cocrystal, another slow-growing substance that required several months to appear. He also found a cocrystal of sucrose with NaI, but could not isolate

UM00017007
NOVARTIS EXHIBIT 1517
Novartis v. Regents, IPR2023-01347
Page 3876 of 4460

Table 2. Cocrystals Containing Carboxylic Acid Salts and Carboxylic Acids in a 1:1 Ratio

acid	cations
formic	Li,[147] Na,[147] K,[147−149] Rb,[150] Cs,[150] Ba[151]
acetic	Na,[152] K,[153] Cs,[154] NH_4[155]
glycolic	K,[156] Rb[157]
chloroacetic	NH_4,[158] adeninium[159]
dichloroacetic	K[160]
trichloroacetic	NH_4[161]
dibromoacetic	K[162]
trifluoroacetic	K,[163,164] Rb,[164] Cs[164]
phenylacetic	Na,[165] K,[166] Rb[166]
(*S*)-mandelic	(*S*)-1-phenylethylammonium[167]
propionic	K[149]
butanoic	K[149,166]
crotonic	K[168]
valeric	K[149]
caproic	K[149]
caprylic	K[149]
undecylic	K[149]
lauric	K,[149] 4-hydroxy-2,2,6,6-tetramethylpiperidinium[169]
myristic	K[149,170]
palmitic	Na,[171] K[149]
stearic	Na,[171] K[149]
oleic	K[149]
erucatic	K[149]
tricosanoic	K[172]
cinnamic	K,[173] NH_4[173]
oxalic	K,[174] Rb,[175] Cs,[176] Ba,[177] pyridinium[178]
malonic	Na,[179] K,[180] pryidinium[178]
succinic	K,[181] pyridinium,[178] D,L-lysinium,[182] L-lysinium,[182] L-argininium[183]
glutaric	tri-*n*-propylammonium[184]
maleic	Li,[185] tetramethylammonium,[184]
fumaric	K,[186] pyridinium,[178] 2-aminopyridinium,[187] tetramethylammonium,[184]
tartaric	3-hydroxyquinuclidine[188]
benzoic	K,[144] NH_4,[144,189] trimethoprim[190]
3-toluic	K[144]
4-toluic	K,[144] NH_4[144]
2-bromobenzoic	K,[144] NH_4[144]
3-bromobenzoic	K,[144] NH_4[144]
4-bromobenzoic	K,[144] NH_4[144]
2-nitrobenzoic	K,[144] Rb,[191] pyridinium[178]
3-nitrobenzoic	K,[144] NH_4,[144] pyridinium[178]
4-nitrobenzoic	K,[144,191] NH_4,[144] pyridinium,[178,192] 2-vinylpyridinium[192]
salicylic	Li,[193] Na,[193] K,[193,144] Rb,[194] NH_4,[194] pyridinium,[178] 8-hydroxyquinolinium[195]
acetylsalicylic	K,[196] Rb[197]
4-hydroxybenzoic	K,[144,198] Rb,[144] NH_4,[144] pyridinium[178]
4-methoxybenzoic	K,[199] Rb[199]
2,4-dinitrobenzoic	pyridinium[178]
3,5-dinitrobenzoic	pyridinium,[178] 2-vinylpyridinium[192]
2-chloro-5-nitrobenzoic	pyridinium[178]
phthalic acid	pyridinium,[178] tetramethylammonium,[184] tetraethylammonium[184]
homophthalic	K[200]
isophthalic	pyridinium[178]

crystals having definite proportions of components using the salts LiCl, LiBr, LiI, NaBr, NaOAc, $NaNO_2$, $NaIO_3$, KCl, KBr, KI, NH_4Cl, NH_4Br, or NH_4I. In some cases crystallization did not occur at all, and in others crystals containing variable amounts of salts were formed. For example, crystals obtained from solutions of sucrose and NH_4Cl contained anywhere from 0.78% to 7.2% NH_4Cl. It is interesting to note, however, that those crystals, while indistinguishable in habit from sucrose itself, were described as follows. "That the crystals are not simply sugar with adhering ammonic chloride is, I think, shown by their individual perfection, and by the fact that they are deliquescent, whereas neither constituent is so." Perhaps a solid solution had been found. I was unable to locate references to any other studies of sucrose · NH_4Cl crystals in the literature, other than a Japanese patent that claims addition of sucrose to aqueous NH_4Cl solutions allows production of NH_4Cl crystals that are 4−5 times normal size.[205]

Crystal structures were ultimately determined for two of the cocrystals reported by Gill, ($C_{12}H_{22}O_{11}\cdot NaCl\cdot 2H_2O$, **60**)[206] and ($2C_{12}H_{22}O_{11}\cdot 3NaI\cdot 3H_2O$).[207] Although Gill was unable to synthesize it, a sucrose · NaBr cocrystal was later obtained and its crystal structure was determined.[208] A couple other sugars were found to cocrystallize with alkali metal salts, including 2,5-*O*-methylene-D-mannitol with NaCl[209] and α-D-glucose with NaCl,[210] NaBr,[211] and NaI.[211] A paper by Fenton describing cocrystals of 2-(hydroxymethyl)-5-phenacyloxy-4H-pyran-4-one (see below) mentioned, during a discussion of the application of infrared spectroscopy to characterization of the cocrystals, an interesting observation.[212] Apparently, sodium present in the KBr discs commonly used to hold samples for infrared analysis causes "alterations" in the spectrum of D-glucose, and that was attributed to the formation of a glucose · NaBr cocrystal.

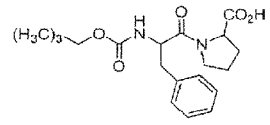
Note that a few cocrystals of sugars with alkaline earth metal salts have been reported. Examples are sucrose·$CaCl_2$,[213] galactose·$CaBr_2$,[214] and fructose·$CaCl_2$.[215] The last cocrystal was used to purify fructose.

Aside from sugars, organic molecules containing various types of hydrogen bond donor groups can cocrystallize with

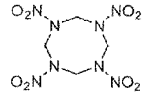
UM00017008
NOVARTIS EXHIBIT 1517
Novartis v. Regents, IPR2023-01347
Page 3877 of 4460

alkali metal salts. Examples include dihydroxyacetone·1/2NaCl,[216] 4,4′-diaminodiphenylmethane·NaCl,[217] 4,4′-diamino-2,3-diphenylbutane·NaCl,[218] ethylenediamine·LiCl,[219] *tert*-butoxycarbonyl-phenylalanyl-proline (**61**)·NaCl,[220] succinic acid·KF,[221] succinic acid·CsF,[222] and malonic acid·KF.[223]

Particularly interesting is the cocrystal containing the high-energy compound cyclotetramethylenetetranitramine (HMX, **62**) and ammonium perchlorate (NH_4ClO_4).[224] Ammonium perchlorate is widely used as an oxidant in solid rocket propellant systems, usually as a dispersion in the finely divided metallic fuel. However, its high degree of water solubility results in degradation to perchloric acid in the presence of ambient moisture. That necessitates the use of desiccants and hermetic motor seals. The cocrystal, on the other hand, is insoluble in water, and is stable when dispersed in solid fuel without protection from ambient moisture.

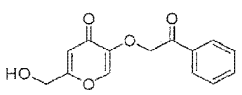


61

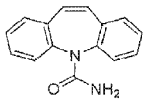


62

2-(Hydroxymethyl)-5-phenacyloxy-4H-pyran-4-one (**63**), a derivative of the antibiotic kojic acid, cocrystallizes with a surprisingly wide variety of salts.[212] Cocrystals of 1:1 (**63**:salt) stoichiometry were found containing CsBr, NH_4Br, RbI, CsI, NH_4I, NaNCS, KNCS, RbNCS, and CsNCS. Cocrystals of 2:1 (**63**:salt) stoichiometry were found containing NaCl, KCl, RbCl, CsCl, NH_4Cl, NaBr, KBr, RbBr, NaI, and KI. The structures of **63**·NaCl,[225] **63**·NaI·H_2O,[226] and **63**·KI[227] were determined by X-ray analysis. Important intermolecular interactions consist of multiple donations of oxygen atom lone pairs to the salt cations (chelation), as well as hydrogen bonding between the hydroxyl group and the salt anions. While in some systems the ability of an organic molecule to form cocrystals with salts seems to depend on the lattice energy of the salt itself or the radii of the salt atoms, those factors do not correlate with the cocrystals obtained from **63**. As usual, a complex interplay of intermolecular interactions, which is difficult to predict, leads to stable cocrystals of **63** and inorganic salts.



63



64

Even molecules that appear to contain little functionality that would be expected to interact with an inorganic molecule can form cocrystals with simple salts. For example, the drug carbamazepine (**64**) cocrystallizes in a 1:1 ratio with either ammonium chloride or ammonium bromide.[228] Those cocrystal structures are interesting. Carbamazepine exists as hydrogen-bonded dimers, which are linked by pairs of ammonium halide molecules into a three-dimensional organic:inorganic network (Figure 11).

Conclusion

An explosion of interest in the pharmaceutical use of cocrystals took place in the past decade. However, it is important to understand that cocrystals have been the subject of research for the past 165 years. They have been used in many industries, including pharmaceutical, textile, paper, chemical processing, photographic, propellant, and electronic. A wide variety of organic molecules have been reported to cocrystallize, both with other organic molecules and with inorganic compounds.

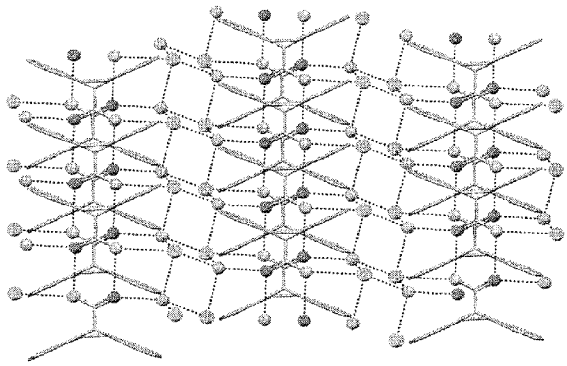


Figure 11. The structure of the 1:1 cocrystal of carbamazepine (**64**) and ammonium chloride.[229] Carbon atoms are gray, nitrogen atoms are blue, oxygen atoms are red, chlorine atoms are green, and hydrogen bonds are dotted lines. Hydrogen atoms are omitted for clarity.

Even though cocrystals have been around for a long time, there is still a lot to be discovered. The current focus on pharmaceuticals has shown that empirically searching for cocrystals of APIs, even using a limited set of coformers, will yield them about 60% of the time.[1] The variety of known types suggests that there are likely many commercially important molecules that will cocrystallize; one just has to select a relevant set of coformers and start looking.

References

(1) Stahly, G. P. *Cryst. Growth Des.* **2007**, *7*, 1007–1026.
(2) Kitaigorodsky, A. I. *Mixed Crystals*; Springer-Verlag: Berlin, 1984; p 17.
(3) Powell, H. M. *J. Chem. Soc.* **1948**, 61.
(4) Kitaigorodsky, A. I. *Mixed Crystals*; Springer-Verlag: Berlin, 1984; p V.
(5) Dunitz, J. D. *CrystEngComm* **2003**, *4*, 506.
(6) Desiraju, G. R. *CrystEngComm* **2003**, *5*, 466–467.
(7) Bond, A. D. *CrystEngComm* **2007**, *9*, 833–834.
(8) (a) Almarsson, Ö.; Zaworotko, M. *Chem. Commun.* **2004**, 1889–1896. (b) Aakeroy, C. B.; Salmon, D. J. *CrystEngComm* **2005**, *7*, 439–448.
(9) Wohler, F. *Annalen Chem. Pharm.* **1844**, *51*, 145–163.
(10) Ling, A. R.; Baker, J. L. *J. Chem. Soc.* **1893**, *63*, 1314–1327.
(11) Anderson, J. S. *Nature* **1937**, *140*, 583–584.
(12) Buck, J. S.; Ide, W. S. *J. Am. Chem. Soc.* **1931**, *53*, 2784–2787.
(13) Hoogsteen, K. *Acta Crystallogr.* **1963**, *16*, 907–916.
(14) Wenner, W. *J. Org. Chem.* **1949**, *14*, 22–26.
(15) Ilmet, I.; Kopp, L. *J. Phys. Chem.* **1966**, *70*, 3371–3372.
(16) Hall, B.; Devlin, J. P. *J. Phys. Chem.* **1967**, *71*, 465–466.
(17) Kitaigorodsky, A. I. *Mixed Crystals*; Springer-Verlag: Berlin, 1984; p 11.
(18) Pekker, S.; Kovats, E.; Oszlanyi, G.; Benyei, G.; Klupp, G.; Bortel, G.; Jalsovszky, I.; Jakab, E.; Borondics, F.; Kamaras, K.; Bokor, M.; Kriza, G.; Tompa, K.; Faigel, G. *Nat. Mater.* **2005**, *4*, 764–767.
(19) "Das grune Hydrochinon ist einer der schonsten Stoffe, welche die organische Chemie aufzuweisen hat. Es ist dem Murexid sehr ahnlich, ubertrifft es aber noch an Glanz und Schonheit der Farbe." from ref 9.

UM00017009
NOVARTIS EXHIBIT 1517
Novartis v. Regents, IPR2023-01347
Page 3878 of 4460

(20) Bragg, W. L. *Proc. R. Soc. (London)* **1914**, *A89*, 248.
(21) Dickinson, R. G.; Raymond, A. L *J. Am. Chem. Soc.* **1923**, *45*, 22.
(22) Jackson, C L.; Oenslager, G. *Ber. Dtsch. Chem. Ges.* **1895**, *28*, 1614–1617.
(23) Willstatter, R.; Piccard, J. *Ber. Dtsch. Chem. Ges.* **1908**, *41*, 1458–1475.
(24) Posner, T. *Justus Lieb. Annal. Chem.* **1904**, *336*, 85–167.
(25) Anderson, J. S. *Nature* **1937**, *140*, 850.
(26) Matsuda, H.; Osaki, K; Nitta, I. *Bull. Chem. Soc. Jpn.* **1958**, *31*, 611–620.
(27) Sakurai, T. *Acta Crystallogr.* **1965**, *19*, 320–330.
(28) Sakurai, T. *Acta Crystallogr.* **1968**, *B24*, 403–412.
(29) The diagram was generated from structure QUIDON01 in the Cambridge Structural Database.
(30) Pfeiffer, P. *Organische Molekulverbindungen*; Verlag von Ferdinand Enke: Stuttgart, 1922.
(31) Helbing, H. *Modern Materia Medica*, 4th ed.; Lehn & Fink: New York, 1895; p 148.
(32) Helbing, H. *Modern Materia Medica*, 4th ed.; Lehn & Fink: New York, 1895; p 18.
(33) Springer, E. *Pharm. Ztg.* **1901**, *46*, 430–431.
(34) Helbing, H. *Modern Materia Medica*, 4th ed.; Lehn & Fink: New York, 1895; p 122.
(35) Helbing, H. *Modern Materia Medica*, 4th ed.; Lehn & Fink: New York, 1895; p 19.
(36) Helbing, H. *Modern Materia Medica*, 4th ed.; Lehn & Fink: New York, 1895; p 22.
(37) See, for example Kofler, L.; Kofler, A.; Brandstatter, M. *Thermo-Mikro-Methoden*; Verlag Chemie: Weinheim/Bergstrasse, 1954, pp 151–171 andKuhnert-Brandstatter, M. *Thermomicroscopy in the Analysis of Pharmaceuticals; International Series of Monographs in Analytical Chemistry*; Pergamon Press: Oxford; 1971; Vol. 45, Chapter 11.
(38) Kofler, A. *Z. Phys. Chem.* **1942**, *A190*, 287–306.
(39) Berthelot *Bull. Soc. Chim. France* **1892**, *7*, 34. (b) *Jahresberichte Fortschr. Chem.* **1867**, 604.
(40) Kofler, A. *Z. Phys. Chem.* **1942**, *A190*, 287–306.
(41) Kofler, A.; Brandstatter, M. *Z. Phys. Chem.* **1943**, *192*, 229–259.
(42) Kuhnert-Brandstatter, M; Burger, A. *J. Therm. Anal.* **1997**, *50*, 559–567.
(43) Kofler, L.; Kofler, A. *Ber. Dtsch. Chem. Ges. B: Abhandlungen* **1943**, *76B*, 718–722.
(44) Kofler, A.; Fischer, R. *Arch. Pharm. Ber. Dtsch. Pharm. Ges.* **1932**, *270*, 441–449.
(45) Kofler, A. *Z. Elektrochem. Angew. Phys. Chem.* **1944**, *50*, 200–207.
(46) Lynch, D. E.; Smith, G.; Byriel, K. A.; Kennard, C. H. L. *J. Chem. Soc., Chem. Commun.* **1992**, 300–301.
(47) Cloez, Ch. *C. R. Hebdomadaires Seances de l'Acad. Sci.* **1897**, *124*, 864–6.
(48) von Norwall, F. K. E. *Monatshefte fuer Chem.* **1895**, *16*, 321–332.
(49) Schroeter, G. *Ber. Dtsch. Chem. Ges.* **1903**, *36*, 3005–300.
(50) Szmant, H. H.; Dixon, J. *J. Am. Chem. Soc.* **1953**, *75*, 4354.
(51) Szmant, H. H.; Alfonso, L. M. *J. Am. Chem. Soc.* **1956**, *78*, 1064–1066.
(52) Regenbogen, A.; Schoorl, N. *Pharm. Weekblad* **1924**, *61*, 34–36.
(53) Schoorl, N. *Pharm. Weekblad* **1929**, *66*, 357–358.
(54) Adler, O.; Alder, R. U.S. Patent 1,954,909, **1934**.
(55) Zellner, H. U.S. Patent 2,994,640, **1961**.
(56) Bailey, C. W.; Bright, J. R.; Jasper, J. J. *J. Am. Chem. Soc.* **1945**, *67*, 1184–1186.
(57) Fox, S. H.; Paterson, L. U.S. Patent 2,433,688, **1947**.
(58) Buu-Hoi, N. P.; Ratsimamanga, A. R.; Xuong, N. D.; Nigeon-Dureuil, M. *Bull. Soc. Chim. Biol.* **1953**, *35*, 326–33.
(59) Krantz, J. C. Jr.; Holbert, J. M.; Iwamoto, H. K.; Carr, C. J. *J. Am. Pharm. Assoc.* **1947**, *36*, 248–250.
(60) (a) Higuchi, T.; Zuck, D. A. *J. Am. Pharm. Assoc.* **1952**, *41*, 10–13. (b) Higuchi, T.; Zuck, D. A. *J. Am. Pharm. Assoc.* **1953**, *42*, 132–138.
(61) Higuchi, T.; Zuck, D. A. *J. Am. Pharm. Assoc.* **1953**, *42*, 138–145.
(62) Higuchi, T.; Lach, J. L. *J. Am. Pharm. Assoc.* **1954**, *43*, 340–354.
(63) Higuchi, T.; Pitman, I. H. *J. Pharm. Sci.* **1973**, *62*, 55–58.
(64) Ide, K. Japanese patent 26004646, **1951**.
(65) Okamoto, K.; Kadowaki, H. Japanese patent 33008099, **1958**.
(66) Fujinaga, Z. Japanese patent 29008048, **1954**.
(67) Kuroyanagi, S. Japanese patents 27001947 and 27001948, **1952**.
(68) Watanabe, H.; Sasaki, M. *Yakugaku Zasshi* **1960**, *80*, 119–122.
(69) Sano, H.; Inabe, K. Japanese patents 33000195, 33000196, and 33000197, **1958**.
(70) Naito, Y.; Shirai, H.; Oda, N. *Yakugaku Zasshi* **1953**, *73*, 663–665.
(71) See, for example (a) Childs, S. L.; Chyall, L. J.; Dunlap, J. T.; Smolenskaya, V. N.; Stahly, B. C.; Stahly, G. P. *J. Am. Chem. Soc.* **2004**, *126*, 13335–13342. (b) McNamara, D. P.; Childs, S. L.; Giordano, J.; Iarriccio, A.; Cassidy, J.; Shet, M. S.; Mannion, R.; O'Donnell, E.; Park, A. *Pharm. Res.* **2006**, *23*, 1888–1897.
(72) Sekiguchi, K.; Ito, K. *Chem. Pharm. Bull.* **1965**, *13*, 405–413.
(73) Bettis, J. W.; Lach, J. L.; Hood, J. *Am. J. Hospital Pharm.* **1973**, *30*, 240–243.
(74) Patel, U.; Haridas, M.; Singh, T. P. *Acta Crystallogr., Sect. C* **1988**, *44*, 1264–1267.
(75) Caira, M. R. *J. Crystallogr. Spectrosc. Res.* **1991**, *21*, 641–648.
(76) Caira, M. R. *J. Crystallogr. Spectrosc. Res.* **1992**, *22*, 193–200.
(77) Caira, M. R.; Nassimbeni, L. R.; Wildervanck, A. F. *J. Chem. Soc., Perkin Trans. 2* **1995**, 2213–2216.
(78) 21 CFR 172.315.
(79) Wietz, R. *J. Pharm. Chim.* **1926**, *4*, 439–45.
(80) http://www.fda.gov/cder/da/da0999.htm
(81) For readers who are interested, good entry points to the literature may be found in publications authored by Drs. Scott L. Childs (Renovo Research), William Jones (University of Cambridge), Nair Rodriguez-Hornedo (University of Michigan), and Michael J. Zaworotko (University of South Florida).
(82) Pfeiffer, P.; Angern, O. *Z. Physiol. Chem.* **1925**, *143*, 265–271.
(83) Watson, J. D.; Crick, F. H. C. *Nature* **1953**, *171*, 737–738.
(84) Hoogsteen, K. *Acta Crystallogr.* **1963**, *16*, 907–91.
(85) O'Brien, E. J. *Acta Crystallogr.* **1967**, *23*, 92–106.
(86) Etter, M. C.; Reutzel, S. M.; Choo, C. G. *J. Am. Chem. Soc.* **1993**, *115*, 4411–4412.
(87) Wilson, C. C. *Nucleic Acids Res.* **1988**, *16*, 385–393.
(88) Schmidt, J.; Snipes, W. *Int. J. Radiat. Biol. Relat. Studies Phys., Chem., Med.* **1967**, *13*, 101–109.
(89) Kar, L.; Bernhard, W. A. *Radiat. Res.* **1983**, *93*, 232–253.
(90) Jacobi, O. K. U.S. Patent 3,937,809, **1976**.
(91) (a) Pfeiffer, P. *Gerber* **1926**, *52*, 204–205. (b) Pfeiffer, P. *Collegium (Darmstadt)* **1926**, 479–487.
(92) Naegeli, C.; Kaltman, H. *Helv. Chim. Acta* **1933**, *16*, 980–988.
(93) Quehl, K. U.S. Patent 2,116,640, **1938**.
(94) Fischer, W. M.; Taurinsch, A. *Ber. Dtsch. Chem. Ges. B: Abhandlungen* **1931**, *64B*, 236–239.
(95) Aoki, I.; Sato, T.; Masato, A.; Hiroshi, S. World Patent Application WO99/11609 A1.
(96) von Christiani, A.; Pailer, M. *Microchim. Acta* **1937**, *1*, 26–29.
(97) Magne, F. C.; Mod, R. R.; Skau, E. L. *J. Am. Oil Chem. Soc.* **1957**, *34*, 127–129.
(98) Bowman, R. S.; Dubbs, A. C.; Hedenburg, J. F. U.S. Patent 2,829,175, **1958**.
(99) Amos, J. G.; Indelicato, J. M.; Pasini, C. E.; Reutzel, S. M. U.S. Patent 6,001,996, **1999**.
(100) Fredga, A. *Arkiv Kemi, Mineral. Geol.* **1940**, *14B*.
(101) Eisenlohr, F.; Meier, G. *Ber. Dtsch. Chem. Ges.* [*Abteilung*] *B: Abhandlungen* **1938**, *71B*, 1005–1013.
(102) Nishikawa, K.; Tsukada, H.; Abe, S.; Kishimoto, M.; Yasuoka, M. *Chirality* **1999**, *11*, 166–171.
(103) Farina, A.; Meille, S. V.; Messina, P. M.; Metrangolo, P.; Resnati, G.; Vecchio, G. *Angew. Chem., Int. Ed.* **1999**, *38*, 2433–2436.
(104) Toda, F.; Tanaka, K.; Mak, T. C. W. *Chem. Lett.* **1984**, 2085–2088.
(105) Etter, M. C.; Frankenbach, G. M.; Bernstein, J. *Tetrahedron Lett.* **1989**, *30*, 3617–3620.
(106) Toda, F.; Okuda, K. *J. Chem. Soc., Chem. Commun.* **1991**, 1212–1214.
(107) Hirata, H.; Sakaiguchi, Y. *Bull. Chem. Soc. Jpn.* **1989**, *62*, 581–582.
(108) Hirata, H.; Kanda, Y.; Sakaiguchi, Y. *Bull. Chem. Soc. Jpn.* **1989**, *62*, 2461–2464.
(109) (a) Sawada, K.; Kitamura, T.; Ohashi, Y.; Iimura, N.; Hirata, H. *Bull. Chem. Soc. Jpn.* **1998**, *71*, 2109–2118. (b) Hirata, H.; Iimura, N. *J. Colloid Interface Sci.* **1998**, *199*, 111–122.
(110) Iimura, N.; Sawada, K.; Ohashi, Y.; Hirata, H. *Bull. Chem. Soc., Jpn.* **1999**, *72*, 2417–2422.
(111) Desiraju, G. R. Crystal Engineering. *The Design of Organic Solids*; Elsevier: Amsterdam, 1989.
(112) Desiraju, G. M. *Angew. Chem., Int. Ed.* **2007**, *46*, 8342–8356.
(113) The diagram was generated from structure CACBOX in the Cambridge Structural Database.
(114) Etter, M. C. *Acc. Chem. Res.* **1990**, *23*, 120–126.
(115) Etter, M. C.; Adsmond, D. A. *Chem. Commun.* **1990**, 589–591.

UM00017010
NOVARTIS EXHIBIT 1517
Novartis v. Regents, IPR2023-01347
Page 3879 of 4460

(116) Smith, G.; Genter, J. M.; Lynch, D. E.; Byriel, K. A.; Kennard, C. H. L. *Aust. J. Chem.* **1995**, *48*, 1151–1166.
(117) Byriel, K. A.; Kennard, C. H. L.; Lynch, D. E.; Smith, G.; Thompson, J. G. *Aust. J. Chem.* **1992**, *45*, 969–981.
(118) Chinnakali, K.; Fun, H.-K.; Goswami, S.; Mahapatra, A. K.; Nigam, G. D. *Acta Crystallogr., Section C: Cryst. Struct.* **1999**, *C55*, 399–401.
(119) Goswami, S.; Mahapatra, A. K.; Ghosh, K.; Nigam, G. D.; Chinnakali, K.; Fun, H.-K. *Acta Crystallogr., Section C: Cryst. Struct. Commun.* **1999**, *C55*, 87–89.
(120) Liao, R.-F.; Lauher, J. W.; Fowler, F. W. *Tetrahedron* **1996**, *52*, 3153–3162.
(121) Le Fur, Y.; Bagieu-Beucher, M.; Masse, R.; Nicoud, J.-F.; Lévy, J.-P. *Chem. Mater.* **1996**, *8*, 68–75.
(122) Chatterjee, S.; Pedireddi, V. R.; Rao, C. N. R. *Tetrahedron Lett.* **1998**, *39*, 2843–2846.
(123) Pedireddi, V. R.; Chatterjee, S.; Ranganathan, A.; Rao, C. N. R. *Tetrahedron* **1998**, *54*, 9457–9474.
(124) Caira, M. R.; Nassimbeni, L. R.; Scott, J. L.; Wildervanck, A. F. *J. Chem. Crystallogr.* **1996**, *26*, 117–122.
(125) Foces-Foces, C.; Infantes, L.; Aguilar-Parrilla, F.; Golubev, N. S.; Limbach, H.-H.; Elguero, J. *J. Chem. Soc., Perkin Trans. 2* **1996**, 349–353.
(126) Pedireddi, V. R.; Jones, W.; Chorlton, A. P.; Docherty, R. *Chem. Commun.* **1996**, 997–998.
(127) Rogers, R. D.; Sharma, C. V. K.; Whitcomb, D. R. *Cryst. Eng.* **1998**, *1*, 255–262.
(128) Aakeroy, C. B.; Beatty, A. M.; Zou, M. *Cryst. Eng.* **1998**, *1*, 225–241.
(129) Foces-Foces, C.; Llamas-Saiz, A. L.; Lorente, P.; Golubev, N. S.; Limbach, H.-H. *Acta Crystallogr., Section C: Cryst. Struct. Commun.* **1999**, *C55*, 377–381.
(130) Almarsson, Ö.; Zaworotko, M. J. *Chem. Commun.* **2004**, 1889–1896.
(131) Steiner, T.; Majerz, I.; Wilson, C. C. *Angew. Chem., Int. Ed.* **2001**, *40*, 2651–2654.
(132) Childs, S. L.; Stahly, G. P.; Park, A. *Mol. Pharmaceutics* **2007**, *4*, 323–338.
(133) Brooker, L. G. S.; Keyes, G. H.; Sprauge, R. H.; VanDyke, R. H.; VanLare, E.; VanZandt, G.; White, F. L. *J. Am. Chem. Soc.* **1951**, *73*, 5326–5332.
(134) Pan, F.; Wong, M. S.; Gramlich, G.; Bosshard, C.; Gunter, P. *Chem. Commun.* **1996**, 1557–1558.
(135) (a) Pan, F.; Wong, M. S.; Gramlich, G.; Bosshard, C.; Gunter, P. *J. Am. Chem. Soc.* **1996**, *118*, 6315–6316. (b) Wong, M. S.; Pan, F.; Bosch, M.; Spreiter, R.; Bosshard, C.; Gunter, P. *J. Opt. Soc. Am. B* **1998**, *15*, 426–431.
(136) The diagram was generated from structure TETQAK in the Cambridge Structural Database.
(137) Huang, K-S; Britton, D.; Etter, M. C.; Byrn, S. R. *J. Mater. Chem.* **1997**, *7*, 713–720.
(138) Nooi, J. U.S. Patent 3,778,435, **1973**.
(139) Baicu, T.; Radu, V.; Ileana, N.; Nicolae, I. Romanian Patent 67434, **1979**.
(140) Baumann, M. F.; Lawton, W. R. U.S. Patents 3,185,583, 3.185,584, and 3,185,585. **1965**.
(141) Japanese Patents 55108884, 1980; 58049394, 1983; 59023577, 1984; and 62037040, 1987.
(142) Taylor, L. D.; Warner, J. C. U.S. Patent 5,338,644, **1994**.
(143) Etter, M. C.; Baures, P. W. *J. Am. Chem. Soc.* **1988**, *110*, 639–640.
(144) Farmer, R. C. *J. Chem. Soc.* **1903**, *83*, 1440–1449.
(145) Anderson, N. G.; Lust, D. A.; Colapret, K. A.; Simpson, J. H.; Malley, M. F.; Gougoutas, J. Z. *J. Org. Chem.* **1996**, *61*, 7955–7958.
(146) Vergeer, P.; Kooijman, H.; Schreurs, A. M. M.; Kroon, J.; Grech, E. *Acta Crystallogr., Sect. C.* **1999**, *55*, 1822–1824.
(147) Groschuff, E. *Ber. Dtsch. Chem. Ges.* **1903**, *36*, 1783–1795.
(148) Larsson, G.; Nahringbauer, I. *Acta Crystallogr., Sect. B* **1968**, *24*, 666–672.
(149) Levi, T. G. *Gazz. Chim. Ital.* **1932**, *62*, 709–716.
(150) Trunov, V. K.; Velikodni, Y. A.; Chubinidze, A. D.; Sas, T. M. *Koord. Khim.* **1982**, *8*, 94–97.
(151) Chubinidze, A. D.; Velikodni, Y. A.; Trunov, V. K. *Koord. Khim.* **1983**, *9*, 259–261.
(152) (a) Villiers, A. *Compt. Rend.* **1877**, *84*, 774. (b) Villiers, A. *Compt. Rend.* **1877**, *85*, 755. Lescoeur, H. *Compt. Rend.* **1877**, *84*, 1029. (c) Lescoeur, H. *Ann. Chim. Phys.* **1893**, *28*, 237. (d) Wyckoff, R. W. G. On the Symmetry and Crystal Structure of Sodium Hydrogen Acetate, $NaH(C_2H_3O_2)_2$. In *The American Journal of Science*; 5th Series, Volume IV; Dana, E. S., Ed.; The Tuttle; Morehouse & Taylor Co.: New Haven, CT, 1922; pp 193–198, (e) Speakman, J. C.; Mills, H. H. *J. Chem. Soc.* **1961**, 1164–1175.
(153) Currie, M. *J. Chem. Soc., Perkin Trans. 2* **1971**, 832–835.
(154) Trunov, V. K.; Endeladze, N. O. *Zh. Strukt. Khim.* **1986**, *27*, 153–155.
(155) Nahringbauer, I. *Acta Chem. Scand.* **1969**, *23*, 1653–1666.
(156) Mayers, R. F.; Keve, E. T.; Skapski, A. C. *J. Chem. Soc. (A)* **1968**, 2258–2262.
(157) Golič, L.; Speakman, J. C. *J. Chem. Soc.* **1965**, 2521–2530.
(158) Ichikawa, I. *Acta Crystallogr., Sect. B* **1972**, *28*, 755–760.
(159) Maixner, J.; Zachova, J.; Huml, K. *Collect. Czech. Chem. Commun.* **1993**, *58*, 861–868.
(160) Leban, I. *Cryst. Struct. Commun.* **1974**, *3*, 245–248.
(161) Golič, L.; Lazarini, F. *Cryst. Struct. Commun.* **1975**, *4*, 487–490.
(162) Baran, J.; Videnova, V.; Glowiak, T.; Ratajczak, H. *Acta Crystallogr., Sect. B* **1979**, *35*, 2722–2723.
(163) Hara, R.; Cady, G. *J. Am. Chem. Soc.* **1964**, *76*, 4285–4287.
(164) Golič, L.; Speakman, J. C. *J. Chem. Soc.* **1965**, 2530–2542.
(165) Crawford, M. *J. Chem. Soc.* **1941**, 259–63.
(166) Bakunin, M.; Vitale, E. *Gazz. Chim. Ital.* **1935**, *65*, 593–616.
(167) Lopez de Diego, H. *Acta Crystallogr., Sect. C* **1995**, *51*, 253–256.
(168) McGregor, D. R.; Speakman, J. C.; Lehmann, M. S. *J. Chem. Soc., Perk. Trans. 2* **1977**, 1740–1745.
(169) Kettmann, V.; Kello, E.; Vrabel, V.; Garaj, J.; Karvas, M.; Goghova, M.; Durmis, J. *Acta Crystallogr., Sect. C* **1989**, *45*, 787–791.
(170) Dumbleton, J. H. *Acta Crystallogr.* **1965**, *19*, 279–280.
(171) Buerger, M. J. *Am. Mineral.* **1945**, *30*, 551–571.
(172) Crowfoot, D. M. *J. Chem. Soc.* **1936**, 716–718.
(173) Bryan, R. F.; Mills, H. H.; Speakman, J. C. *J. Chem. Soc.* **1963**, 4350–4355.
(174) Haas, D. J. *Acta Crystallogr.* **1964**, *17*, 1511–1516.
(175) Trunov, V. K.; Efremov, V. A.; Tskhelashvili, N. B. *Zh. Strukt. Khim.* **1990**, *31*, 19–25.
(176) Follner, H. *Z. Anorg. Allg. Chem.* **1969**, *370*, 235–237.
(177) (a) Mutin, J.-C.; Huard, C.; Thrierr-Sorel, A. *C. R. Acad. Sci., Ser. C* **1968**, *267*, 1783–1788. (b) Huard, C.; Favre-Brun, Y.; Bertrand, G.; Thrierr-Sore, A. *C. R. Acad. Sci., Ser. C* **1969**, *269*, 1517–1520.
(178) Pfeiffer, P.; Birenoweig, G.; Hofmann, A.; Windheuser, C. *Ber. Dtsch. Chem. Ges.* **1914**, *47*, 1580–1596.
(179) Kalsbeek, N. *Acta Crystallogr., Sect. C* **1992**, *48*, 878–883.
(180) Currie, M. *Chem. Commun.* **1972**, 972–973.
(181) Dunlop, R. S.; Speakman, J. C. *Z. Kristallogr.* **1973**, *138*, 100–112.
(182) Prasad, G. S.; Vijayan, M. *Acta Crystallogr., Sect. B* **1991**, *47*, 927–935.
(183) Prasad, G. S.; Vijayan, M. *Int. J. Pept. Protein Res.* **1990**, *35*, 357–364.
(184) Barry, J. E.; Finkelstein, M.; Ross, S. D. *J. Org. Chem.* **1982**, *47*, 64–68.
(185) Kirfel, A.; Will, G.; Recker, K.; Wallrafen, F.; Gao, Z. S. *Z. Kristallogr.* **1983**, *165*, 117–125.
(186) Gupta, M. P.; Prasad, N. *Acta Crystallogr., Sect. B* **1972**, *26*, 2628–2630.
(187) Goswami, S.; Mahapatra, A. K.; Nigam, G. D.; Chinnakali, K.; Fun, H.-K.; Razak, I. A. *Acta Crystallogr., Sect. C* **1999**, *55*, 583–585.
(188) Erman, L. Y.; Mindrul, V. F.; Mikhaleva, I. L.; Pankov, D. I.; Kurochkin, V. K. *Zh. Strukt. Khim.* **1994**, *35*, 161–163.
(189) Oxton, I. A.; Cameron, E. S.; Knop, O.; McCulloch, A. W. *Can. J. Chem.* **1977**, *55*, 3831–3837.
(190) Bettinetti, G. P.; Caramella, C.; Giordano, F.; La Manna, A.; Margheritis, C.; Sinistri, C. *J. Therm. Anal.* **1983**, *28*, 285–294.
(191) Shrivastava, H. N.; Speakman, J. C. *J. Chem. Soc.* **1961**, 1151–1163.
(192) Carrow, C. J.; Wheeler, K. A. *Cryst. Eng.* **1998**, *1*, 263–275.
(193) (a) Hoffmann, E. *Arch. Pharm.* **1878**, *57*, 226. (b) Hoffmann, E. *Jahresber.* **1878**, 759.
(194) Downie, T. C.; Speakman, J. C. *J. Chem. Soc.* **1954**, 787–793.
(195) Jebamony, J. R.; Muthiah, P. T. *Acta Crystallogr., Sect. C.* **1988**, *54*, 539–540.
(196) Manojlovic, L.; Speakman, J. C. *J. Chem. Soc. A* **1967**, 971–979.
(197) Grimvall, S.; Wengelin, R. F. *J. Chem. Soc. A* **1967**, 968–970.
(198) Manojlovic, L. *Acta Crystallogr., Sect. B* **1968**, *24*, 326–330.
(199) McGregor, D. R; Speakman, J. C. *J. Chem. Soc. A* **1968**, 2106–2108.

UM00017011
NOVARTIS EXHIBIT 1517
Novartis v. Regents, IPR2023-01347
Page 3880 of 4460

(200) Gupta, M. P.; Dubey, D. S. *Indian J. Phys.* **1969**, *43*, 777–779.
(201) Newkome, G. R.; Theriot, K. J.; Fronczek, F. R. *Acta Crystallogr., Sect. C* **1985**, *41*, 1642–1644.
(202) See, for example Kanters, J. A.; ter Horst, E. H.; Kroon, J.; Grech, E. *Acta Crystallogr., Sect. C* **1992**, *48*, 328–332.
(203) 21 CFR 184.**1754**.
(204) Gill, C. H. *J. Chem. Soc.* **1871**, *24*, 269–275.
(205) Misumi, S.; Ishikawa, Y.; Tanaka, S. Japanese patent 29006870, **1954**.
(206) Beevers, C. A.; Cochran, W. *Nature* **1946**, *157*, 872.
(207) Cochran, W. *Nature* **1946**, *157*, 231.
(208) Beevers, C. A.; Cochran, W. *Proc. R. Soc. London, Ser. A* **1947**, *190*, 257–272.
(209) Wood, R. A.; James, V. J.; Mills, J. A. *Cryst. Struct. Commun.* **1976**, *5*, 207–210.
(210) Ferguson, G.; Kaitner, B.; Connett, B. E.; Rendle, D. F. *Acta Crystallogr., Sect. B* **1991**, *47*, 479–484.
(211) Rendle, D. F.; Glazier, E. J. *Powder Diffr.* **1992**, *7*, 38–41.
(212) Fenton, D. E. *J. Chem. Soc., Dalton Trans.* **1973**, 1380–1383.
(213) Jones *Microscope* **1963**, *13*, 346.
(214) Cook, W. J.; Bugg, C. E. *J. Am. Chem. Soc.* **1973**, *95*, 6442–6446.
(215) GB patent 1357399, **1974**.
(216) Utkin, L. M. *Biokhimiya* **1939**, *4*, 600–606.
(217) Jarvis, J. A. J.; Owston, P. G. *Chem. Commun.* **1971**, 1403–1404.
(218) Marullo, N. P.; Lloyd, R. A. *J. Am. Chem. Soc.* **1966**, *88*, 1076–1077.
(219) Jamet-Delcroix, S. *J. Chimie Phys.* **1967**, *64*, 601–607.
(220) Milne, P. J.; Oliver, D. W.; Van Rooyen, P. H.; Roos, H. M. *J. Chem. Crystallogr.* **1997**, *27*, 167–175.
(221) Emsley, J.; Jones, D. J.; Osborn, R. S. *J. Chem. Soc., Chem. Commun.* **1980**, 703–704.
(222) Emsley, J.; Jones, D. J.; Kuroda, R. *Acta Crystallogr., Sect. C* **1983**, *39*, 729–730.
(223) Emsley, J.; Jones, D. J.; Kuroda, R. *J. Chem. Soc., Dalton Trans.* **1982**, 1179–1184.
(224) Levinthal, M. L. U.S. Patent 4,086,110, **1978**.
(225) Phillips, S. E. V; Trotter, J. *Can. J. Chem.* **1976**, *54*, 2723–2732.
(226) Phillips, S. E. V.; Truter, M. R. *J. Chem. Soc., Dalton Trans.* **1975**, 1066–1070.
(227) Hughes, D. L.; Phillips, S. E. V.; Truter, M. R. *J. Chem. Soc., Dalton Trans.* **1974**, 907–911.
(228) Reck, G.; Thiel, W. *Pharmazie* **1991**, *46*, 509–512.
(229) The diagram was generated from structure VUBCAW in the Cambridge Structural Database.

UM00017012
NOVARTIS EXHIBIT 1517
Novartis v. Regents, IPR2023-01347
Page 3881 of 4460

Electronic Acknowledgement Receipt	
EFS ID:	9357133
Application Number:	10378956
International Application Number:	
Confirmation Number:	4742
Title of Invention:	Multiple-component solid phases containing at least one active pharmaceutical ingredient
First Named Inventor/Applicant Name:	Michael J. Zaworotko
Customer Number:	23557
Filer:	Glenn Ladwig/J'Nese Williams
Filer Authorized By:	Glenn Ladwig
Attorney Docket Number:	USF.106XC1
Receipt Date:	01-FEB-2011
Filing Date:	03-MAR-2003
Time Stamp:	18:42:05
Application Type:	Utility under 35 USC 111(a)

Payment information:

Submitted with Payment	no

File Listing:

Document Number	Document Description	File Name	File Size(Bytes)/ Message Digest	Multi Part /.zip	Pages (if appl.)
1		SIDS9.pdf	470943 f7d7ac42e11043c89667c90a967b6d5da9682e33	yes	4

	Multipart Description/PDF files in .zip description		
	Document Description	**Start**	**End**
	Transmittal Letter	1	2
	Information Disclosure Statement (IDS) Filed (SB/08)	3	4

Warnings:					
Information:					
2	Foreign Reference	EP0731795.pdf	3611479 9d6986e5430fd7692c121b1776dc25a2e1543c3b	no	93
Warnings:					
Information:					
3	Foreign Reference	WO00-042021.pdf	625503 e3ff7545df6e6a50a52f962be92168fe3e53a468	no	20
Warnings:					
Information:					
4	NPL Documents	Stahly.pdf	2998498 a410ec8be5df3ae99ad0f4efb57c28be728b1673	no	18
Warnings:					
Information:					
		Total Files Size (in bytes):	7706423		

This Acknowledgement Receipt evidences receipt on the noted date by the USPTO of the indicated documents, characterized by the applicant, and including page counts, where applicable. It serves as evidence of receipt similar to a Post Card, as described in MPEP 503.

<u>New Applications Under 35 U.S.C. 111</u>
If a new application is being filed and the application includes the necessary components for a filing date (see 37 CFR 1.53(b)-(d) and MPEP 506), a Filing Receipt (37 CFR 1.54) will be issued in due course and the date shown on this Acknowledgement Receipt will establish the filing date of the application.

<u>National Stage of an International Application under 35 U.S.C. 371</u>
If a timely submission to enter the national stage of an international application is compliant with the conditions of 35 U.S.C. 371 and other applicable requirements a Form PCT/DO/EO/903 indicating acceptance of the application as a national stage submission under 35 U.S.C. 371 will be issued in addition to the Filing Receipt, in due course.

<u>New International Application Filed with the USPTO as a Receiving Office</u>
If a new international application is being filed and the international application includes the necessary components for an international filing date (see PCT Article 11 and MPEP 1810), a Notification of the International Application Number and of the International Filing Date (Form PCT/RO/105) will be issued in due course, subject to prescriptions concerning national security, and the date shown on this Acknowledgement Receipt will establish the international filing date of the application.

I hereby certify that this correspondence is being electronically filed in the United States Patent and Trademark Office on February 1, 2011.

/Glenn P. Ladwig/

Glenn P. Ladwig, Patent Attorney, Reg. # 46,853

SUPPLEMENTAL INFORMATION DISCLOSURE STATEMENT
Patent Application
Docket No. USF.106XC1
Serial No. 10/378,956

IN THE UNITED STATES PATENT AND TRADEMARK OFFICE

Examiner	:	Sahar Javanmard
Art Unit	:	1627
Applicants	:	Michael J. Zaworotko, Brian Moulton, Nair Rodriguez-Hornedo
Serial No.	:	10/378,956
Filed	:	March 3, 2003
Conf. No.	:	4742
For	:	Multiple-Component Solid Phases Containing at Least One Active Pharmaceutical Ingredient

Mail Stop Amendment
Commissioner for Patents
P.O. Box 1450
Alexandria, VA 22313

SUPPLEMENTAL INFORMATION DISCLOSURE STATEMENT
UNDER 37 C.F.R. §§ 1.97 AND 1.98

Sir:

In accordance with 37 C.F.R. § 1.56, the references listed on the attached form PTO/SB/08 are being brought to the attention of the Examiner for consideration in connection with the examination of the above-identified patent application. Copies of the cited references are enclosed.

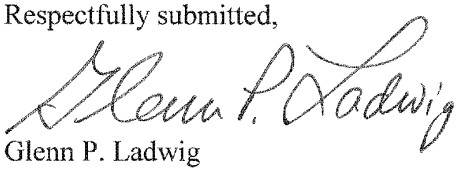
It is respectfully requested that the references cited on the attached form PTO/SB/08 be considered in the examination of the subject application and that their consideration be made of record.

J:\USF\106XC1\PTO\SIDS9.doc/DNB/jnw

This information is being submitted subsequent to the filing of a Request for Continued Examination, but before the mailing of an Office Action on the merits. If any fee is required please use Deposit Account No. 19-0065.

Applicants respectfully assert that the substantive provisions of 37 C.F.R. §§ 1.97 and 1.98 are met by the foregoing statement.

Respectfully submitted,



Glenn P. Ladwig
Patent Attorney
Registration No. 46,853
Phone No.: 352-375-8100
Fax No.: 352-372-5800
Address: P.O. Box 142950
Gainesville, FL 32614-2950

GPL/jnw
Attachments: Form PTO/SB/08; copies of references cited therein

J:\USF\106XC1\PTO\SIDS9.doc/DNB/jnw

Substitute for form 1449A/PTO

INFORMATION DISCLOSURE STATEMENT BY APPLICANT

(use as many sheets as necessary)

Sheet 1 of 2

Complete if Known	
Application Number	10/378,956
Filing Date	March 3, 2003
First Named Inventor	Michael J. Zaworotko
Art Unit	1627
Examiner Name	Sahar Javanmard
Attorney Docket Number	USF.106XC1

U.S. PATENT DOCUMENTS

Examiner Initials*	Cite No.[1]	Document Number Number - Kind Code[2] (if known)	Publication Date MM-DD-YYYY	Name of Patentee or Applicant of Cited Document	Pages, Columns, Lines, Where Relevant Passages or Relevant Figures Appear
	U1	US- 2010/0331285 A1	12-30-2010	Almarsson *et al.*	All
	U2				
	U3				
	U4				
	U5				
	U6				
	U7				
	U8				
	U9				

FOREIGN PATENT DOCUMENTS

Examiner Initials*	Cite No.[1]	Foreign Patent Document Country Code[3] - Number[4] - Kind Code[5] (if known)	Publication Date MM-DD-YYYY	Name of Patentee or Applicant of Cited Document	Pages, Columns, Lines, Where Relevant Passages or Relevant Figures Appear	T[6]
	F1					
	F2					
	F3					
	F4					
	F5					
	F6					

Examiner Signature		Date Considered	

*EXAMINER: Initial if reference considered, whether or not citation is in conformance with MPEP 609. Draw line through citation if not in conformance and not considered. Include copy of this form with next communication to applicant. [1] Applicant's unique citation designation number (optional). [2] See Kind Codes of USPTO Patent Documents at www.uspto.gov or MPEP901.04. [3] Enter Office that issued the document, by the two-letter code (WIPO Standard T.3). [4] For Japanese patent documents, the indication of the year of the reign of the Emperor must precede the serial number of the patent document. [5] Kind of document by the appropriate symbols as indicated on the document under WIPO Standard ST. 16 if possible. [6] Applicant is to place a check mark here if English language Translation is attached.

Substitute for form 1449B/PTO

INFORMATION DISCLOSURE STATEMENT BY APPLICANT

(use as many sheets as necessary)

Sheet 2 of 2

Complete if Known	
Application Number	10/378,956
Filing Date	March 3, 2003
First Named Inventor	Michael J. Zaworotko
Group Art Unit	1627
Examiner Name	Sahar Javanmard
Attorney Docket Number	USF.106XC1

NON PATENT LITERATURE DOCUMENTS

Examiner Initials*	Cite No. [1]	Include name of the author (in CAPITAL LETTERS), title of the article, (when appropriate), title of the item (book, magazine, journal, serial, symposium, catalog, etc.), date, page(s), volume-issue number(s), publisher, city and/or country where published.	T[2]
	R1	BOND, A.D. *et al.* "On the Polymorphism of Aspirin" *Angew. Chem. Int. Ed.*, 2007, 46:615-617.	
	R2	BOND, A.D. *et al.* "On the Polymorphism of Aspirin: Crystalline Aspirin as Intergrowths of Two "Polymorphic" Domains" *Angew. Chem. Int. Ed.*, 2007, 46:618-622.	
	R3	SUMMERS, M.P. *et al.* "The polymorphism of aspirin" *J. Pharm. Pharmac.*, 1970, 22:615-616.	
	R4	WHEATLEY, P.J. "The Crystal and Molecular Structure of Aspirin" *J. Chem. Soc.*, 1964, 6036-6048.	
	R5	Office Action dated April 13, 2011 in U.S. Application Serial No. 12/861,203, filed August 23, 2010.	
	R6		
	R7		
	R8		
	R9		
	R10		
	R11		
	R12		
	R13		

Examiner Signature		Date Considered	

*EXAMINER: Initial if reference considered, whether or not citation is in conformance with MPEP 609. Draw line through citation if not in conformance and not considered. Include copy of this form with next communication to applicant. [1] Applicant's unique citation designation number (optional). [2] See Kind Codes of USPTO Patent Documents at www.uspto.gov or MPEP901.04. [3] Enter Office that issued the document, by the two-letter code (WIPO Standard T.3). [4] For Japanese patent documents, the indication of the year of the reign of the Emperor must precede the serial number of the patent document. [5] Kind of document by the appropriate symbols as indicated on the document under WIPO Standard ST. 16 if possible. [6] Applicant is to place a check mark here if English language Translation is attached.

UM00017018
NOVARTIS EXHIBIT 1517
Novartis v. Regents, IPR2023-01347
Page 3887 of 4460

DOI: 10.1002/anie.200602378

Aspirin

On the Polymorphism of Aspirin**

Andrew D. Bond, Roland Boese, and Gautam R. Desiraju**

A second polymorph of aspirin, *o*-acetylsalicylic acid, (form II), was recently reported by Peterson, Zaworotko, and co-workers (hereafter referred to as PZ).[1] This new form was obtained by crystallization of pure aspirin in the presence of either levetiracetam or acetamide from MeCN, and it was characterized by single-crystal X-ray diffraction. Form II was *"also characterized by melting point, IR, DSC, and HPLC"*. It was stated that *"there are clear differences between the unit-cell parameters"* of form I and form II, and also that *"the molecular geometry of aspirin molecules in form II is slightly different in terms of the torsion angle defined by the carboxylic acid and acetyl groups, although the centrosymmetric carboxylic acid dimer remains intact"*. The crystal packing of the new polymorph proposed by PZ is different from that of form I. Notably, *"methyl groups form catemeric C–H···O hydrogen bonds with the carbonyl oxygen of the acetyl group versus centrosymmetric dimers in form I"*.

While new polymorphs of older compounds are constantly being discovered[2] and there is much interest in this phenomenon in the pharmaceutical industry because of the legal implications of finding new polymorphs and pseudo-polymorphs of active pharmaceutical ingredients (APIs),[3] we wish to clarify in this communication that the form II of aspirin as reported by PZ may just as easily be derived, to the accuracy and precision reported by these workers, from experimental diffraction data collected from what is undoubtedly a single crystal of the well-known form I. While the reasons for this unusual occurrence are still being explored by us, we have deemed our initial result to be of sufficient importance to warrant a preliminary communication, not least because of the peculiar chemico-legal significance of polymorphism in the pharmaceutical industry today, and the ubiquitous nature of the molecule in question.

The first crystal structure determination of aspirin (form I) was performed by Wheatley,[4] who stated in his 1964 paper that *"a number of attempts"* had been made prior to his work. The space group is $P2_1/c$, and the conventional R-factor was 0.108. Somewhat high R-factors such as these were not uncommon in those times. In 1984, Kim et al. reported the same structure with an R-factor of 0.046.[5] In 2002, Wilson redetermined the same crystal structure from neutron diffraction data collected at seven temperatures between 20 K and 300 K,[6] and the R-factors (on F) in these determinations are in the range 0.080 to 0.090. We felt these R-factors to be definitely high and accordingly redetermined the crystal structure. For this purpose we selected a well-formed crystal from a commercial sample (Merck Art. 85, DAB 7). The unit cell [$a = 11.2776(2)$, $b = 6.5517(1)$, $c = 11.2741(2)$ Å, $\beta = 95.837(1)°$, $V = 828.70(2)$ Å^3] corresponds to that reported by Wheatley,[4] Kim,[5] and Wilson.[6] The refinement on data to $2\theta = 56°$ ($Mo_{K\alpha}$ radiation) is acceptable ($R1[I>2\sigma(I)] = 0.033$); indeed, this is the best structure determination on aspirin form I to date,[7] and we use it as a benchmark in this paper.

At the outset, we noted several anomalous indicators in the PZ structure: 1) The data are truncated to $2\theta = 40°$ ($Mo_{K\alpha}$); 2) The R-factors are unacceptably large ($R1[I>2\sigma(I)] = 0.162$, $wR2$(all data) $= 0.308$; 3) All atoms are refined isotropically, implying that anisotropic refinement was not possible; 4) Several of the refined U_{iso} values are zero or disturbingly close to zero. Most revealingly, we noted that the unit cell reported by PZ [$a = 12.095(7)$, $b = 6.491(4)$, $c = 11.323(6)$ Å, $\beta = 111.509(9)°$, $V = 827.1(8)$ Å^3] can be transformed to the cell obtained by us for form I with the metric transformation [1 0 ½ 0 −1 0 0 0 −1]. Likewise, our experimental form I cell can be transformed to a cell having $a = 12.084$, $b = 6.552$, $c = 11.274$ Å, $\beta = 111.81°$, $V = 828.7$ Å^3. This is depicted schematically in Figure 1.

We next returned to our experimental diffraction data and applied this relationship so that our data were indexed on the basis of the PZ unit cell.[8] Subsequent integration and data reduction was followed by a straightforward structure solution with direct methods,[9] using default settings in the space group $P2_1/c$ obtained automatically by the software. The result (Figure 1) was completely superimposable on the PZ structure! Isotropic refinement on data to $2\theta = 50°$ proceeded to $R1 = 0.081$ with reasonable molecular and intermolecular geometries and U_{iso} values in the range 0.019(1)–0.027(1) Å^2. However, anisotropic refinement failed completely. In short,

[*] Prof. Dr. R. Boese
Institut für Anorganische Chemie
Universität Duisburg-Essen
Universitätstrasse 5, Essen 45117 (Germany)
Fax: (+49) 201-183-2535
E-mail: roland.boese@uni-essen.de
Prof. Dr. G. R. Desiraju
School of Chemistry
University of Hyderabad
Hyderabad 500 046 (India)
Fax: (+91) 402-313-4828
E-mail: gautam_desiraju@yahoo.com
Dr. A. D. Bond
Department of Physics and Chemistry
University of Southern Denmark
5230 Odense (Denmark)

[**] We acknowledge financial support from the DST and the DAAD in the form of a joint Indo-German research project.

Supporting information for this article is available on the WWW under http://www.angewandte.org or from the author. These include: a detailed comparison of the form I and form II structures, a description of the transformation between the two structures/lattices in real and reciprocal space, full details of the procedure for producing the form II structure from simulated data and from our experimental data, and electronic files (CIF, HKL, RES) to accompany the discussion.

© 2007 Wiley-VCH Verlag GmbH & Co. KGaA, Weinheim

UM00017019
NOVARTIS EXHIBIT 1517
Novartis v. Regents, IPR2023-01347
Page 3888 of 4460

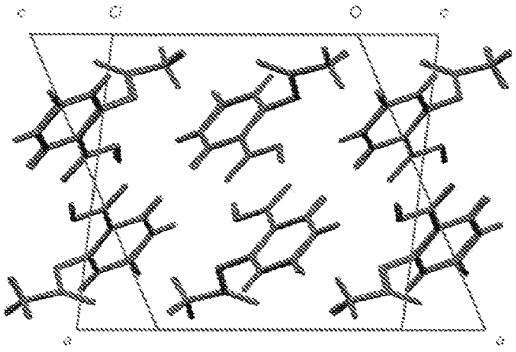


Figure 1. Superposition of the form I structure (red) and the PZ structure (blue), showing the metric relationship between the unit cells. For the form I cell, the *b* direction points into the page. For the PZ cell, the *b* direction points out of the page.

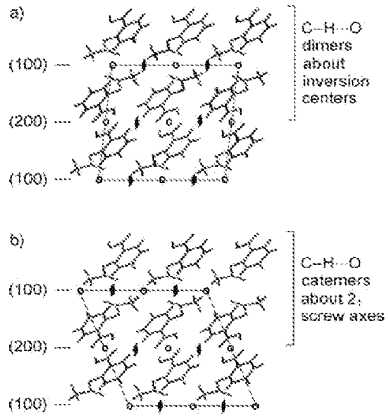


Figure 2. Positions of the symmetry elements in the form I (a, red) and form II (b, blue) crystal structures of aspirin. In both cases, centrosymmetric O–H···O dimers are formed about inversion centers in the (200) plane of the unit cell. In form I (a), centrosymmetric C–H···O dimers are formed about inversion centers in the (100) planes. In form II (b), the symmetry elements in the (100) planes are translated by $^1/_4c$, such that C–H···O catemers are formed about 2_1 screw axes running along *b*.

the same single-crystal data set may be reduced on the basis of two different unit cells, and both can be solved to obtain crystal structures that are ostensibly different yet chemically reasonable. However, while one of the structures (form I) refines satisfactorily, the other structure (form II) resists complete refinement. It is obvious that the first structure is correct. Is the second structure incorrect?

It is instructive to consider how and why this situation could have arisen. Since our refinement has an *R*-factor of 0.033, we clearly examined a crystal of form I. It is not evident at the present time and with the data given by PZ in their paper[1] whether 1) they examined a crystal of form II and could not proceed with the refinement beyond a reasonable point because of reasons not yet known or 2) they examined a crystal of form I, from the data of which the form II structure emerged, as we have shown is possible. In any case, it is difficult for us now to be sure of the indexing procedure employed by PZ and to understand how they obtained their particular unit cell. Incorrect unit cells usually get eliminated either because they do not lead to a sensible space group, the structure does not solve, or if it does solve, the refinement leads to absurd molecular and/or intermolecular geometries. None of these situations occurred for the PZ crystal.

Inspection of Figure 1 shows that the consequences of proceeding with the PZ unit cell on a form crystal are subtle.[10] The principal distinction between the form I and form II structures is the positioning of the symmetry elements with respect to the molecules. In each unit cell, two distinct sets of inversion centers can be envisaged, one set lying in the (100) planes, and one set lying in the (200) planes (Figure 2). If the origin is chosen in both structures so that the carboxylic acid dimers are formed about the (200) inversion centers, the (100) inversion centers in the form I structure are consistent with C–H···O dimers. For the form II structure, however, the unit cell is skewed along the [001] direction, shifting the (100) inversion centers with respect to the molecules. Now, 2_1 screw axes that lie half-way between the inversion centers in space group $P2_1/c$ generate C–H···O catemers in the *b* direction. Ordinarily, such a situation would produce physically unreasonable intermolecular contacts. In this case, however, the metric features have conspired to ensure that the new positions for the symmetry elements are suitable to generate seemingly normal catemers. In summary, we have here an apparently bizarre occurrence,[11] wherein an "incorrect" crystal structure does not suffer from unacceptable intermolecular contacts. Indeed, PZ have described the packing of form II in terms of perfectly acceptable current paradigms of weak hydrogen bonding,[12] and the lattice energies of the two forms, one certainly real and the other not identified satisfactorily, are within 0.45 kJ mol^{-1} of each other; according to Dreiding force field calculations form II is the more stable form.

Numerous sources of potential error exist in crystal structure determinations. These can arise, for example, from poor crystallinity, solvent loss, presence of impurities, disorder, and subtle twinning. Our principal point is that there can be no substitute for a fully acceptable and properly rigorous X-ray structural analysis accompanied by a correct modeling of the structure in difficult and ambiguous cases. This is painfully true in the present situation where so much store is set by the discovery of a new polymorph of an API. The present example sounds a cautionary note, and we wish to make the plea that structural chemists apply proper evaluation to the crystallographic results that are obtained with increasingly automated methods.[13] Too often, the crystallographic analyses that underpin structural studies are taken lightly and deemed to be a more or less routine exercise. At the present time, what is sure is that data collected on an authentic sample of form I of aspirin can be treated to produce the form II structure reported by PZ to their level of accuracy and precision. Since the main experimental evidence that they provided for the existence of form II of aspirin was their single-crystal X-ray structure determination, all of their claims must be re-evaluated with appropriate and additional

 © 2007 Wiley-VCH Verlag GmbH & Co. KGaA, Weinheim

UM00017020
NOVARTIS EXHIBIT 1517
Novartis v. Regents, IPR2023-01347
Page 3889 of 4460

experimental evidence before one is able to conclude that a new polymorph of aspirin has indeed been discovered. In the end, it is not clear if their form II structure is an artifact of improper handling of data or a poor crystallographic result on a suboptimal crystal. Nothing in their paper[1] helps one to select between these possibilities.

We are aware of two possible caveats in the argument in this paper: 1) We have chosen to measure and analyze data collected from a commercial sample rather than from one crystallized in the presence of levetiracetam or acetamide and acetonitrile, that is, under the conditions chosen by PZ. Whether this is an important issue can only be revealed by experimentation. 2) Our calculations do not simulate entirely the data interpretation of PZ in that our simulation is based on 437 reflections, all with l even, none with l odd. PZ used 748 reflections, with the same maximal 2θ value of 40°; among their 648 reflections with $I > 2\sigma(I)$, there must be some with l odd.[10] We are currently investigating both these issues.

In conclusion, we wish to state that at the present time, and with the information given by PZ in their paper,[1] it is not possible to determine if there is a second form of aspirin in the samples obtained by PZ, or whether levetiracetam or acetamide would be needed to produce any such form. We would not like to express any opinion as to whether co-crystallization of a compound with another compound is likely to increase the chances of obtaining polymorphs. These are matters that need to be resolved with further experimentation and/or modeling. We are currently examining these issues with the aim of obtaining a larger and more complete "structural landscape" of the aspirin system.

Received: June 13, 2006

Keywords: aspirin · polymorphism · structure determination · X-ray diffraction

[1] P. Vishweshwar, J. A. McMahon, M. Oliveira, M. L. Peterson, M. J. Zaworotko, *J. Am. Chem. Soc.* **2005**, *127*, 16802.

[2] a) R. K. R. Jetti, P. K. Thallapally, A. K. Katz, H. L. Carrell, K. Singh, K. Lahiri, S. Kotha, R. Boese, G. R. Desiraju, *Angew. Chem.* **2004**, *116*, 1169; *Angew. Chem. Int. Ed.* **2004**, *43*, 1149; b) K. Shankland, W. I. F. David, C. R. Pulham, N. Blagden, R. J. Davey, M. Song, *Angew. Chem.* **2005**, *117*, 7194; *Angew. Chem. Int. Ed.* **2005**, *44*, 7032; c) A. V. Trask, G. M. Day, W. D. S. Motherwell, W. Jones, *Chem. Commun.* **2006**, 54.

[3] a) *Polymorphism in Pharmaceutical Solids* (Ed.: H. G. Brittain), Marcel Dekker, New York, **1999**; b) A. Nangia, *Cryst. Growth Des.* **2006**, *6*, 1 and references therein.

[4] P. J. Wheatley, *J. Chem. Soc.* **1964**, 6036.

[5] Y. Kim, K. Machida, T. Taga, K. Osaki, *Chem. Pharm. Bull.* **1985**, 33, 2641.

[6] C. C. Wilson, *New J. Chem.* **2002**, *26*, 1733.

[7] Crystal data on form I of aspirin: $C_9H_8O_4$, $M_r = 180.15$, monoclinic, space group $P2_1/c$, $a = 11.2776(2)$, $b = 6.5517(1)$, $c = 11.2741(2)$ Å, $\beta = 95.837(1)°$, $V = 828.70(2)$ Å^3 $T = 123(2)$ K, $\mu(Mo_{K\alpha}) = 0.115$ mm^{-1}, 24706 reflections measured, 2043 unique reflections ($R_{int} = 0.0255$), 1756 observed reflections, $R1[I > 2\sigma(I)] = 0.0330$, $wR2$(all data) $= 0.0925$, $S = 1.08$. CCDC 610952 contains the supplementary crystallographic data for this paper. These data can be obtained free of charge from The Cambridge Crystallographic Data Centre via www.ccdc.cam.ac.uk/data_request/cif.

[8] Full details of our experimental procedures are available in the Supporting Information. To put aside any question of experimental issues, crystal quality, etc. we note that the PZ result can be obtained purely by manipulation of data simulated from the form I structure. If the simulated single-crystal data set is subjected to the transformation [1 0 ½ 0 1 0 0 0 1], the form II structure can be refined against the transformed data to emulate the PZ result.

[9] G. M. Sheldrick, *SHELXS*-97. University of Göttingen, Germany, **1997**.

[10] Comprehensive details of the relationship between the structures are available in the Supporting Information. The appearance of the form II structure from the form I data set is not a case of a false solution from direct methods. It is the wrong choice of unit cell (and indeed the wrong crystal lattice) that results in a false arrangement of symmetry elements. We further add that since the transformation [1 0 ½ 0 −1 0 0 0 −1] is not a genuine crystallographic one, the resulting form II unit cell does not account for all reflections in the form I diffraction pattern. Specifically, all reflections hkl with odd l are omitted and therefore the simulated transformed data set is only 50% complete. For the experimental data, all reflections with odd l appear unobserved. Remarkably, even this does not prohibit stable (isotropic) refinement of the form II structure: standard F^2 refinement against all data produces a model with reasonable geometry and U_{iso} values. Of course, the R-factors are high. Acceptable R-factors can be obtained by application of a $2\sigma(I)$ cut-off. The fact that PZ did not report this issue suggests that some of their odd l reflections were non-zero at the $2\sigma(I)$ level.

[11] It is very difficult to assess just how unusual this is. We note only that in our combined experience of many crystal-structure analyses, this is the first such example that we have identified.

[12] G. R. Desiraju, *Chem. Commun.* **2005**, 2995.

[13] The problems in the PZ structure are manifested in the high R-factors, the erratic U_{iso} values, and the (supposed) necessity for an unacceptable 2θ cutoff. All these indicators are flagged as suspicious within an automated checking system such as checkCIF/PLATON.

 © 2007 Wiley-VCH Verlag GmbH & Co. KGaA, Weinheim

UM00017021
NOVARTIS EXHIBIT 1517
Novartis v. Regents, IPR2023-01347
Page 3890 of 4460

Polymorphism

DOI: 10.1002/anie.200603373

On the Polymorphism of Aspirin: Crystalline Aspirin as Intergrowths of Two "Polymorphic" Domains**

Andrew D. Bond, Roland Boese,* and Gautam R. Desiraju**

In the preceding paper, we highlighted the ambiguity that exists in the literature concerning the nature of crystalline aspirin.[1] In 2004, Ouvrard and Price demonstrated computationally that the long-established aspirin crystal structure[2–4] was amongst those predicted to be most stable, but they identified a slightly more stable structure as the thermodynamic minimum.[5] At the time, it was unclear whether the predicted minimum-energy structure was a remnant of inadequate energy assessment,[6] or whether it was a plausible structure that awaited discovery. This issue appeared to be resolved in 2005, when Peterson, Zaworotko, and co-workers (hereafter referred to as PZ) claimed to have obtained the predicted second polymorph,[7] following X-ray analysis of aspirin crystals obtained from hot acetonitrile solution in the presence of either levetiracetam or acetamide. The proposed new polymorph was labelled aspirin "form II", and the long-established aspirin crystal structure was thereby designated "form I".

The distinction between the proposed aspirin polymorphs is subtle. They contain identical arrangements of O–H···O hydrogen-bonded dimers lying in layers, but these layers are arranged differently with respect to each other in the two forms (Figure 1). In form I, the layers are arranged so that C–H···O interactions form centrosymmetric dimers (arrangement **A**, Figure 1). In the proposed form II, adjacent layers

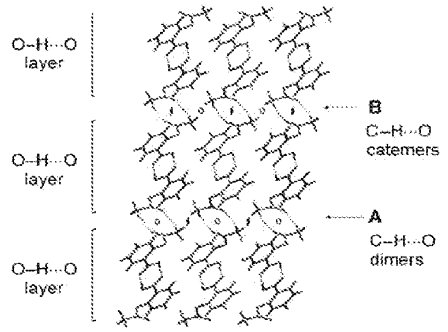


Figure 1. Illustration of the two interlayer arrangements within a representative aspirin crystal. Arrangement **A**, comprising centrosymmetric C–H···O dimers, exists between the layers that are colored red. Arrangement **B**, comprising C–H···O catemers extending along 2_1 screw axes, exists between the layers that are colored blue. The change in color within the central layer is for illustration only; all O–H···O hydrogen-bonded layers are identical.

are arranged so that C–H···O interactions generate catemers (arrangement **B**, Figure 1). Both interlayer arrangements are reasonable and acceptable in terms of the C–H···O interactions. Taken with the accord between the experimental and computational findings,[5] the PZ description of aspirin polymorphism appeared superficially to be plausible.[7] However, there are serious problems with their structure refinement. For the proposed form II, their crystallographic *R*-factors are unacceptable ($R1 = 0.162$, $wR2 = 0.327$), and several refined displacement parameters are close to or equal to zero, with anisotropic refinement being impossible. Combined with very close metric similarity between the unit cells of the form I and form II structures, this caused us to raise the question of whether the proposed form II might actually be an experimental artifact originating from erroneous handling of diffraction data collected from a form I crystal.[1] Indeed, we showed that form II of aspirin as reported by PZ may be derived, to the accuracy and precision reported by those workers, from experimental diffraction data collected on an aspirin crystal that was most certainly form I. Thus, we stressed that the PZ report did not establish the existence of aspirin form II to any acceptable level of scientific rigor.[1] In this report, we are able to resolve the issue fully. Aspirin exhibits a tendency to crystallize with an

[*] Dr. A. D. Bond
Department of Physics and Chemistry
University of Southern Denmark
5230 Odense (Denmark)
Fax: (+45) 6615-8780
E-mail: adb@chem.sdu.dk
Prof. Dr. R. Boese
Institut für Anorganische Chemie
Universität Duisburg-Essen
Universitätstrasse 5, 45117 Essen (Germany)
Fax: (+49) 201-183-2535
E-mail: roland.boese@uni-due.de
Prof. Dr. G. R. Desiraju
School of Chemistry
University of Hyderabad
Hyderabad 500 046 (India)
Fax: (+91) 40-2301-0567
E-mail: gautam_desiraju@yahoo.com

[**] G.R.D. and R.B. acknowledge financial support from the DST and the DAAD in the form of a joint Indo-German research project. A.D.B. is grateful to the Danish Natural Science Research Council and the Carlsberg Foundation (Denmark) for funding and for provision of the X-ray diffraction equipment in Odense. R.B. thanks Dr. Carsten Schauerte and Anika Szesni for their assistance. We are grateful to Prof. H.-B. Bürgi (University of Berne) for contributing to the qualitative description of the diffraction data during the refereeing process, and for kindly identifying himself at the penultimate stage of this process.

Supporting information for this article is available on the WWW under http://www.angewandte.org or from the author.

InterScience
© 2007 Wiley-VCH Verlag GmbH & Co. KGaA, Weinheim

UM00017022
NOVARTIS EXHIBIT 1517
Novartis v. Regents, IPR2023-01347
Page 3891 of 4460

intergrowth structure, in which layers of O–H···O hydrogen-bonded dimers form domains with arrangement **A** and domains with arrangement **B**, within the same single crystal. The distribution and total ratio of the domains is variable but appears to be limited. Aspirin form I, which comprises 100% arrangement **A**, is commonplace, but pure form II, which would comprise 100% arrangement **B**, has not been realized.

The crucial experimental result was first obtained after we freshly synthesized aspirin from salicylic acid (see the Supporting Information) and prepared single crystals by rapidly cooling a solution in hot acetonitrile (Table 1). Single-crystal X-ray diffraction analysis of these crystals (denoted **1a**, laths of typical dimension $0.20 \times 0.10 \times 0.05$ mm) proceeded apparently routinely to provide the form II structure, with $R1 = 0.071$ and $wR2 = 0.197$, against data measured to $2\theta = 50°$ ($Mo_{K\alpha}$).[8] Unlike the PZ report, our refinement was anisotropic and entirely satisfactory, although we noted that our R-factors were a little higher than expected. These crystals were obtained without addition of levetiracetam or acetamide, demonstrating that the additive is not a significant factor. We obtained similar results by slow evaporation of an acetonitrile solution, indicating that the rapid cooling procedure also is not important. Powder X-ray diffraction seemed to confirm that the single crystal **1a** was representative of the bulk sample,[9] and the polymorphism of aspirin might therefore appear to be clear-cut. However, reconstruction of precession photographs in the a^*c^* planes of our experimental data (Figure 2a) revealed numerous additional reflections lying halfway between those of the principal form II lattice in the odd l rows, together with diffuse streaks along a^* between the Bragg reflections. In physical terms, the diffraction pattern demonstrates that aspirin crystals contain layers of O–H···O hydrogen-bonded dimers that are consistent (Figure 1), but that these layers form domains in which they adopt arrangement **A** (form I) and domains in which they adopt arrangement **B** (form II). The existence of the form I and form II domains is shown by the two sets of Bragg reflections, while the streaks indicate some degree of stacking disorder.

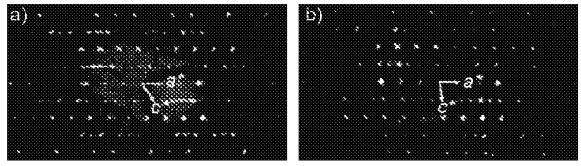


Figure 2. Reconstructed (h –1 l) precession photographs for crystals **1a** and **2**. a) Crystal **1a** exhibits sharp Bragg reflections corresponding to the form II lattice (reciprocal lattice vectors shown), broader maxima halfway between these reflections in the odd l rows, and diffuse streaks along a^*. This indicates extended form II domains, smaller domains of form I, and regions in which there is a disordered distribution. b) For crystal **2**, the most intense Bragg reflections correspond to the form I lattice (reciprocal lattice vectors shown), and Bragg reflections of comparable profile exist for the form II lattice. This indicates a relatively more ordered structure than in **1a** (a) with extended form I and form II domains.

From analyses of numerous crystals obtained under various experimental conditions, including crystallization in the presence of acetamide[10] (Table 1), we find that both the relative intensities of the two sets of Bragg reflections and the extent of the streaking are variable. In crystal **2** (Figure 2b), for example, all Bragg reflections are relatively sharp, and there are no obvious streaks, consistent with extended well-ordered domains of form I and form II. In crystals **1a** and **1b**, sharp Bragg reflections for the form II lattice indicate extended form II domains, while the broader Bragg reflections between these lattice points indicate smaller domains of form I. The diffuse streaks also indicate regions with a less ordered pattern of interlayer arrangements **A** and **B**. Thus, both the sizes and distribution of the form I and form II domains are variable.

The interpretation of one-dimensionally diffuse diffraction data has a long history[11] and has been summarized

Table 1: Summary of crystallization conditions and single-crystal refinements.

Crystallization conditions	No.	Conventional refinement of single-crystal data[b]			Single-crystal refinement with batch scaling factors			Refined batch scaling factors[c]
		form	$R1$	$wR2$	form	$R1$	$wR2$	
rapid cooling of solution in hot MeCN	**1a**[a]	I	0.344	0.658	I	0.075	0.202	0.132(1)
		II	0.071	0.197	II	0.054	0.132	0.747(2)
	1b[a]	I	0.544	0.846	I	0.076	0.220	0.038(1)
		II	0.041	0.116	II	0.034	0.080	0.858(2)
rapid cooling of solution in hot MeCN in the presence of 1 equiv acetamide	**2**	I	0.059	0.175	I	0.056	0.140	0.803(3)
		II	0.305	0.631	II	0.076	0.288	0.146(1)
as synthesized (see the Supporting Information)	**3**[d]	I	0.033	0.089	I	0.033	0.089	0.982(4)
		II	unstable		II	0.076	0.141	0.003(1)

[a] Crystals **1a** and **1b** are different single crystals from the same crystallization batch. [b] Based on data sets obtained from two separate standard integrations of the CCD frames, considering only Bragg peaks. Refinements are performed against all F^2 data to $2\theta_{max} = 50°$ ($Mo_{K\alpha}$). $R1$ is quoted for data with $I > 2\sigma(I)$, $wR2$ is quoted for all data. [c] The high precision refers to that obtained from the least-squares refinement. See the text for discussion of the approximations and limitations of the approach. [d] A pure form I crystal. For form I refinement, the batch scale factor refines to be essentially unity. Conventional form II refinement against all F^2 data is unstable. For batch refinement, the scale factor refines to zero, effectively omitting all odd l reflections, thereby emulating a data set that contains only the even l reflections. This is exactly the situation that we noted in our previous manuscript.[1]

 © 2007 Wiley-VCH Verlag GmbH & Co. KGaA, Weinheim

UM00017023
NOVARTIS EXHIBIT 1517
Novartis v. Regents, IPR2023-01347
Page 3892 of 4460

recently for molecular crystals.[12] The literature includes examples in which layered structures exhibit only one kind of interlayer arrangement, that is, structures for which there are alternative positions of adjacent layers that have exactly equivalent interatomic/intermolecular contacts (as for the close packing of spheres, for example).[13] The aspirin case is apparently the first of its kind in that it exhibits two distinctly different interlayer arrangements (**A** and **B**), both of which are physically and chemically reasonable. The accidental energetic degeneracy of the two possibilities,[5,6] combined with the specific metric relation between the form I and form II lattices, is the reason for the unusual crystallographic observations, since it allows aspirin diffraction patterns to be processed in two different ways to provide two different structures, both of which are physically reasonable. The metric transformation [1 0 ½ 0 −1 0 0 0 −1] that relates the form I and form II unit cells causes all Bragg reflections *hkl* with even *l* to overlay but places the odd *l* reflections of form II halfway between those of form I.[14] Thus, the Bragg reflections arising from the two types of domain appear to a first approximation as a weighted overlay of the form I and form II diffraction patterns, with the distribution dependent on the relative domain ratio. If such a diffraction pattern is indexed in the usual way to one or other of the form I or form II unit cells, standard integration (that is, considering only Bragg reflections, and discounting any other features),[15] will provide a data set in which the even *l* reflections are of the correct intensity, but the odd *l* reflections are systematically weak. This is the path that was followed by PZ.[7] The extent to which the odd *l* reflections are in error reflects the ratio of the form I and form II domains.

On the basis of our description, a practical procedure to obtain an estimate of the total domain ratio is to introduce a batch scale factor into the crystallographic refinements, applied only to reflections with odd *l*. The refined value of this scale factor gives the relative weights of the form I and form II reciprocal lattices and therefore a direct estimate of the crystal composition. This estimate will be good for crystals that exhibit only sharp Bragg peaks and no diffuse streaks, while it will be more approximate when the streaking is more significant. Thus, the approach would be exact for two perfectly ordered domains with a single domain boundary, but it becomes progressively more approximate for real aspirin crystals as the extent of the domain disorder increases. The procedure gives a total composition estimate but no direct information concerning the sizes of the form I and form II domains or their distribution. For crystal **1a**, such a refinement against the form II data set[16] gives $R1 = 0.054$ and $wR2 = 0.132$, a significant improvement on the standard refinement, and the refined batch scale factor indicates that roughly 75% of the crystal comprises form II domains. The practical effectiveness of the process is illustrated more dramatically by batch refinement of the form I data set obtained from the same crystal. While standard treatment of the form I structure gives $R1 = 0.344$, $wR2 = 0.658$ and does not permit anisotropic refinement, introduction of the batch scale factor allows routine refinement with all non-H atoms anisotropic to give $R1 = 0.075$, $wR2 = 0.202$. In this instance, the refined batch scale factor indicates approximately 15% form I domains. The discrepancy between the two indications of the crystal composition (in other words, that they do not sum to 100%) reflects principally the failure to account for the diffuse features of the diffraction pattern.[17] With this procedure, the refined crystal structure will be either pure form I (100% arrangement **A**) or pure form II (100% arrangement **B**) if the batch scale factor should refine to unity. This is the case for crystal **3** (Table 1), which is pure form I. In all other cases, the intergrowth structure is present, and a more complex analysis of the entire diffraction pattern, including diffuse features, is necessary to extract further information regarding domain size and distribution.[12]

Using our straightforward approach, a general correlation can be derived between approximate domain ratio and the expected crystallographic *R*-values for a conventional treatment of the X-ray data.[18] Figure 3 provides a guide for assessment of the total domain ratio in any aspirin crystal using the *R*-values obtained from F^2 refinement on the basis of either the pure form I or the (hypothetical) pure form II structure if standard data reduction and refinement procedures should be followed. Using the correlation shown in Figure 3, the *R*-factors reported by PZ[7] show that their crystal actually comprised approximately equal proportions of domains with interlayer arrangement **A** and domains with interlayer arrangement **B**.

Chemically speaking, it is reasonable (albeit realized in hindsight) that aspirin crystals should provide intergrowth

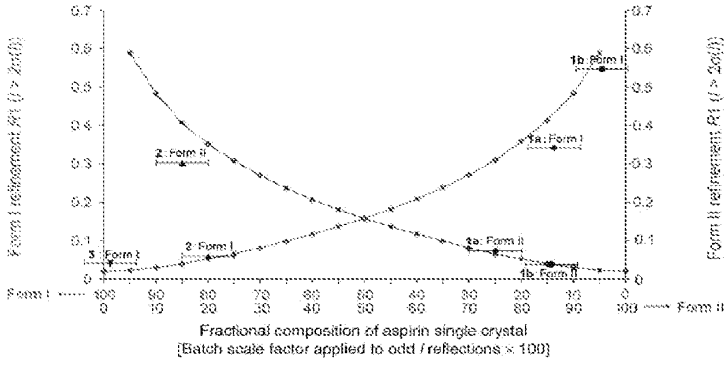


Figure 3. Correlation between total domain ratio and expected crystallographic *R*1 value, obtained for conventional refinement against all F^2 data. The correlation is derived from experimental data for crystal **3** (see the Supporting Information for full details). The red and blue curves refer to standard data reduction and refinement on the basis of the form I and form II structures, respectively, for an aspirin crystal with domain ratio indicated by the horizontal axis. The experimental points correspond to the *R* values obtained for the crystals listed in Table 1. For these, the composition estimate is taken from the batch scale factor refinement, with error bars indicating ±5% composition. For example, conventional refinement of crystal **1a** as form II gives $R1 = 0.071$. The separate batch scale factor refinement indicates 75% form II domains. The same crystal **1a** refined conventionally as form I gives $R1 = 0.344$, with the separate batch scale factor refinement indicating 15% form I domains.

 © 2007 Wiley-VCH Verlag GmbH & Co. KGaA, Weinheim

UM00017024
NOVARTIS EXHIBIT 1517
Novartis v. Regents, IPR2023-01347
Page 3893 of 4460

structures in this way. The strongest interactions (O–H···O, herringbone) occur within the layers parallel to the (100) planes, which constitute the persistent building blocks within aspirin crystals. These are presumably the most robust growth units[19] in the system. Shearing of these layers relative to each other along [001], which is in effect the movement that transforms arrangement **A** into arrangement **B**, involves rupture and creation of weak C–H···O interactions. The energy difference between the **A** and **B** arrangements is clearly very small,[5,6] and together with the consistent layer surface at (100), this permits facile turnover between the two possibilities in the composite crystal. If the energy difference were significantly greater, individual crystals of one pure polymorph (either form I or form II) would be accordingly more stable. Ouvrard and Price[5] noted that form II should have "a low shear elastic constant, implying that it is so readily deformed that there may be problems in its growth". In the course of our present study, we have frequently observed crystals of pure form I (at least to the limits of detection possible for single-crystal and powder X-ray diffraction[20]), but the maximum proportion of form II domains that we have observed is approximately 85%. Thus, aspirin form II has not been documented in a pure form so far. Whether this means that arrangement **A** is inherently more stable than arrangement **B**, contrary to the calculations,[5] is a matter that remains to be firmly established. If it were, form II might be a metastable kinetic product[21] which could still potentially be observed, but which might transform to the more stable form I. However, we have not observed any such transformation, at least for single crystals standing in air over a period of two months.[22] It is also possible that arrangement **B** is indeed more stable than arrangement **A**,[5] but that the growth problems associated with arrangement **B** prevent the isolation of a pure aspirin form II. In this case, approximately 85% arrangement **B** may be the most that we can expect. Clearly, much future work remains to clarify completely the thermodynamic and kinetic aspects of crystalline aspirin.

Finally, the case of aspirin raises issues with regard to nomenclature. As for any evolving scientific area, crystal engineering is presently subject to lively and ongoing debate pertaining to the naming of concepts and phenomena. Terms such as "co-crystal" and "pseudopolymorph" have been discussed recently in this context.[23] The term "polymorph" has so far stayed above such controversies and is used to signify a situation where the same substance exhibits different crystal packing arrangements.[24] For crystallographers, this definition might be considered to encompass only crystals for which long-range translational order is dominant; in other words, it is appropriate only at one end of a continuum that ranges from perfect crystals to systems without long-range translational order. To chemists, the accepted distinction is rather more clear. Polymorphism implies that a molecule may adopt one or other type of packing arrangement in the crystalline state, and different polymorphs are distinct entities that display different physical and chemical properties. A single crystal of a given chemical substance is either one polymorph or another. In this context, one might ask how many polymorphs of aspirin actually exist. The domains with interlayer arrangements **A** (form I) and **B** (form II) certainly represent two different crystal structures that serve as reference points. However, considering that aspirin crystals display both arrangements within a single crystal, should aspirin really be described as polymorphic? What is certain is that the PZ description of their crystal as a polymorph distinct from form I is not justifiable. The PZ crystal, like several other aspirin crystals described in this paper, is an intergrowth of two "polymorphic" domains. We emphasize that the intergrowth crystals are exactly that: they are not simply mixtures of form I and form II, and they are not twins. Each aspirin crystal is an integral whole in which the domains are intimately connected with each other, with possibly many turnovers of domain within a single crystal. Further, it seems that the ratio of the domains in aspirin crystals is likely to be constant in any particular batch prepared under the same conditions.

This issue has implications beyond nomenclature. Should individual form I/form II compositions qualify for separate patent protection? Should patents be granted only for ranges of form I and form II domain ratios and not for specific compositions?[25] Is (pure) form II entitled to patent protection considering that it has not been realized as yet? Could this problem be solved by calling these crystals "polytypes", considering the voluminous literature on this topic in inorganic solid-state chemistry?[26] If so, would different polytypes then be entitled to patent protection? These and other issues suggest that one keeps an open mind with regard to definitions in crystal engineering, including that of the term "polymorph".[27] In an evolving subject, no definition should be carved in stone.

The Supporting Information includes details of the synthesis and crystallization procedures, powder X-ray diffraction data, reconstructed precession photographs for single crystals **1a**, **1b**, **2**, and **3**, a description of the geometry and intensities of the Bragg reflections in aspirin diffraction patterns, and details regarding the correlation between *R*-factors and the total domain ratio. The results of all refinements referred to in Table 1 are available in CIF format, with the corresponding *hkl* data available in SHELXL HKLF-4 format. All CCD frames (Bruker APEX2 format) can be obtained from the authors on request.

Received: August 17, 2006
Revised: October 3, 2006
Published online: December 1, 2006

Keywords: aspirin · polymorphism · polytypism · stacking fault · X-ray crystallography

[1] A. D. Bond, R. Boese, G. R. Desiraju, *Angew. Chem. Int. Ed.* **2006**, DOI: 10.1002/ange.200602378; *Angew Chem.* **2006**, DOI: 10.1002/anie.200602378.
[2] P. J. Wheatley, *J. Chem. Soc.* **1964**, 6036.
[3] Y. Kim, K. Machida, T. Taga, K. Osaki, *Chem. Pharm. Bull.* **1985**, *33*, 2641.
[4] C. C. Wilson, *New J. Chem.* **2002**, *26*, 1733.
[5] C. Ouvrard, S. L. Price, *Cryst. Growth Des.* **2004**, *4*, 1119.

 © 2007 Wiley-VCH Verlag GmbH & Co. KGaA, Weinheim

UM00017025
NOVARTIS EXHIBIT 1517
Novartis v. Regents, IPR2023-01347
Page 3894 of 4460

[6] The minimum-energy structure was just 0.2 kJ mol^{-1} lower in energy than the established crystal structure, and in our opinion this value is so small that the order of energies might just as easily have been reversed.

[7] P. Vishweshwar, J. A. McMahon, M. Oliveira, M. L. Peterson, M. J. Zaworotko, *J. Am. Chem. Soc.* **2005**, *127*, 16802.

[8] The highest form II domain ratio observed from 15 single-crystal data collections is in crystal **1b**. For this crystal, conventional refinement of the form II structure gives: $C_9H_8O_4$, $M_r = 180.15$, monoclinic, space group $P2_1/c$, $a = 12.1515(10)$, $b = 6.5064(5)$, $c = 11.3677(9)$ Å, $\beta = 111.574(3)°$, $V = 835.79(12)$ Å^3, $T = 180(2)$ K, $\mu(Mo_{K\alpha}) = 0.114$ mm^{-1}, $2\theta_{max} = 50°$, 9778 reflections measured, 1474 unique reflections ($R_{int} = 0.029$), 1149 observed reflections, $R1(I > 2\sigma(I)) = 0.041$, $wR2$(all data) = 0.116, $S = 1.02$. CCDC-617840 contains the supplementary crystallographic data for this paper. These data can be obtained free of charge from The Cambridge Crystallographic Data Centre via www.ccdc.cam.ac.uk/data_request/cif.

[9] Compared to the powder X-ray diffraction pattern of pure form I, the principal features that reveal the presence of form II domains are peaks at $2\theta \approx 20.9$ and 26.0° (at 295 K, see the Supporting Information).

[10] With extremely rapid cooling of a hot equimolar solution of aspirin and acetamide in acetonitrile (that is, by plunging the flask directly into liquid N_2 or dry ice/2-propanol), we obtained a 1:1 molecular complex of aspirin and acetamide, which contains the expected acid–amide heterosynthon. This would argue in favor of acetamide acting as a growth inhibitor at the (200) faces of aspirin, leading to platelike crystals that cannot grow easily along [100]. It is likely that levetiracetam would behave in a similar way, and this is the morphology reported by PZ for their aspirin crystal. Crystal data for the aspirin/acetamide (1:1) co-crystal: $(C_9H_8O_4)(C_2H_5NO)$, $M_r = 239.22$, orthorhombic, space group *Pbca*, $a = 9.5268(4)$, $b = 8.7495(3)$, $c = 28.4520(11)$ Å, $V = 2371.61(16)$ Å^3, $T = 203(2)$ K, $\mu(Mo_{K\alpha}) = 0.107$ mm^{-1}, 68487 reflections measured, 3074 unique reflections ($R_{int} = 0.059$), 2586 observed reflections, $R1(I > 2\sigma(I)) = 0.042$, $wR2$(all data) = 0.119, $S = 1.04$. CCDC-618012 contains the supplementary crystallographic data for this paper. These data can be obtained free of charge from The Cambridge Crystallographic Data Centre via www.ccdc.cam.ac.uk/data_request/cif.

[11] a) H. Jagodzinski, *Acta Crystallogr.* **1949**, *2*, 201; b) H. Jagodzinski, *Acta Crystallogr.* **1949**, *2*, 208; c) "Disorder Diffuse Scattering of X-rays and Neutrons": H. Jagodzinski, F. Frey in *International Tables for Crystallography, Vol. B* (Ed.: U. Shmueli), International Union of Crystallography and Kluwer Academic Publishers, Dordrecht, **2001**.

[12] H.-B. Bürgi, M. Hostettler, H. Birkedal, D. Schwarzenbach, *Z. Kristallogr.* **2005**, *220*, 1066.

[13] a) K. Dornberger-Schiff, H. Grell-Niemann, *Acta Crystallogr.* **1961**, *14*, 167; b) K. Dornberger-Schiff, J. D. Dunitz, *Acta Crystallogr.* **1965**, *19*, 471; c) K. Dornberger-Schiff, *Acta Crystallogr. Sect. A* **1982**, *38*, 483; d) D. Schwarzenbach, K. Kirschbaum, A. A. Pinkerton, *Acta Crystallogr. Sect. B* **2006**, *62*, 944.

[14] In crystallographic parlance, the Bragg reflections with even l are referred to as "family reflections" and are common to both the form I and form II structures. The family reflections alone define a "superposition structure", which in the case of aspirin comprises two O–H···O dimers overlaid in a unit cell with c dimension half that of the true c dimension. The distribution of the intensities along the odd l rows contains the information to decompose the superposition structure into chemically reasonable arrangements, that is, the information regarding the particular sequence of the O–H···O layers. See Ref. [12].

[15] Neglecting any diffuse scattering is clearly a simplification. However, the procedures that we describe have the advantage that they are standard (that is, they are based only on procedures used for routine crystallographic analyses), require no specialist knowledge, and can be applied in any crystallographic laboratory.

[16] The term "form II data set" refers to the list of intensities (the *hkl* file) that is obtained when the diffraction data are indexed on the basis of the form II unit cell and integrated using standard procedures. The additional Bragg reflections that could be described on the basis of the form I unit cell and any diffuse features are ignored. The term "form I data set" refers to the opposite situation.

[17] In particular, there may be problems associated with assessment of the background intensity in the presence of diffuse streaks in the vicinity of the Bragg reflections.

[18] The correlation is derived from the experimental form I data set (crystal **3**), with a suitable fractional scale factor applied to the odd l reflections (see the Supporting Information for full details). The batch refinement must be based on all F^2 data. The Figure provides an immediate approximate guide, based on standard refinement procedures. Application of the batch refinement procedure will provide an improved estimate.

[19] R. J. Davey, K. Allen, N. Blagden, W. I. Cross, H. F. Lieberman, M. J. Quayle, S. Righini, L. Seton, G. J. T. Tiddy, *CrystEngComm* **2002**, *4*, 257.

[20] Since interlayer arrangements **A** and **B** are structurally and energetically so finely balanced, disorder is thermodynamically inherent in the aspirin system. All aspirin crystals should contain some of arrangements **A** and **B** at real temperatures. They are detectable by X-ray diffraction only when their number becomes significant.

[21] In general, for any system of hydrogen bonds (O–H···O or C–H···O) wherein the dimer and catemer alternatives are well matched, there is a consensus that the catemer is kinetically favored since it is a higher dimensional pattern than the dimer. See: D. Das, G. R. Desiraju, *Chem. Asian J.* **2006**, *1*, 231.

[22] PZ have reported that "form II" transforms into form I at 100 K. Our assessment of the stability of the form II domains is based on re-collection of single-crystal data for **1b** after the crystal had stood in air for two months.

[23] Co-crystal: a) G. R. Desiraju, *CrystEngComm* **2003**, *5*, 466; b) J. D. Dunitz, *CrystEngComm* **2003**, *5*, 468. Pseudopolymorph: c) K. R. Seddon, *Cryst. Growth Des.* **2004**, *4*, 1088; d) G. R. Desiraju, *Cryst. Growth Des.* **2004**, *4*, 1089; e) J. Bernstein, *Cryst. Growth Des.* **2005**, *5*, 1661; f) A. Nangia, *Cryst. Growth Des.* **2006**, *6*, 1.

[24] However, one of us has argued (in Ref. [23d]) that difficulties in the use of the word "pseudopolymorph" might have arisen because the definition of the term "polymorph" is too rigid with respect to identity of chemical composition among substances that are deemed to qualify for the polymorph epithet.

[25] To some extent, this situation parallels that of isomorphous crystalline solvates, for which patents have been granted for ranges of solvent content. However, while variable solvent content is a common occurrence, it is not clear how common the aspirin situation will be.

[26] A. R. Verma, P. Krishna, *Polymorphism and Polytypism in Crystals*, Wiley, New York, **1966**.

[27] G. Coquerel *Chem. Eng. Proc.* **2006**, *45*, 857

 © 2007 Wiley-VCH Verlag GmbH & Co. KGaA, Weinheim

UM00017026
NOVARTIS EXHIBIT 1517
Novartis v. Regents, IPR2023-01347
Page 3895 of 4460

80/15707

J. Pharm. Pharmac., 1970, 22, 615

LETTERS TO THE EDITOR

The polymorphism of aspirin

Mitchell & Saville (1967) demonstrated that various samples of commercial aspirin have different rates of dissolution. Subsequently, Tawashi (1968, 1969) has reported the existence of aspirin in two polymorphic forms (designated Forms I and II). During the course of present work concerned with the tabletting characteristics of various polymorphic forms of drugs, we have been able to identify several aspirin polymorphs in addition to those already reported. Table 1 shows the conditions under which the polymorphs were obtained.

Confirmatory evidence that all the samples examined were aspirin and differed only in crystalline form is afforded by the fact that no differences could be detected in their ultraviolet spectra when dissolved in ethanol (determined using a Unicam SP800 recording spectrophotometer).

A Perkin-Elmer Differential Scanning Calorimeter DSC-1 equipped with an effluent analyser was used for the thermal analysis of the polymorphs. Samples weighing between 2 and 10 mg were analysed using a scanning rate of 8° min^{-1}. No traces of solvent of crystallization were detected by the effluent analyser when any of the aspirin samples were fused. This therefore excludes the possibility that the samples were solvated forms of aspirin. The DSC traces for the six polymorphs are shown in Fig. 1.

A Kofler hot stage microscope was used to confirm the melting points of the polymorphs. The results are shown in Table 1. The instrument was also used to observe solution phase transformations of pairs of polymorphs. The solvent for this work was n-pentanol saturated with one component of the particular polymorph pair under study. Some of the phase transformations are summarized in Table 2.

Since different polymorphs have different crystal packing conditions, it is to be expected that they will have different true densities. Density determinations were made at 20° using a specific gravity bottle with a displacement medium of light liquid paraffin. Table 1 contains the results of this work.

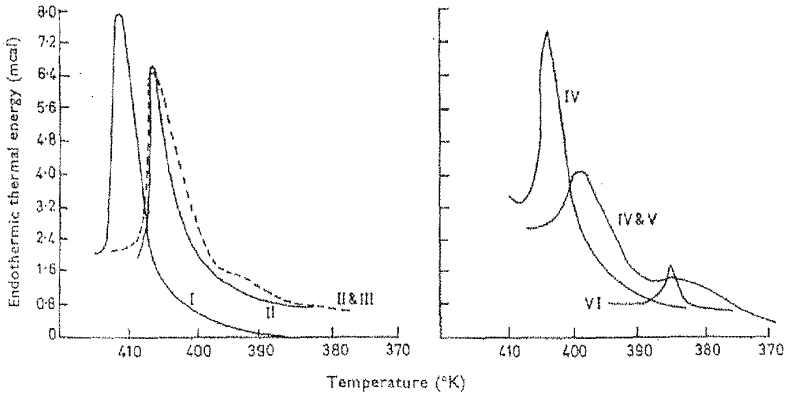


FIG. 1. DSC traces of the six polymorphs of aspirin.

UM00017027

NOVARTIS EXHIBIT 1517
Novartis v. Regents, IPR2023-01347
Page 3896 of 4460

Table 1. *Methods of preparation and physical characteristics of aspirin polymorphs*

Method of preparation	Form nomenclature	Melting point (°C) DSC	Melting point (°C) Hot stage microscope	Density at 20° C (g ml^{-1})
Slow recrystallization from 96% ethanol at 20°	Form I	135	133	1·40
Slow recrystallization from n-hexane at 0°	Form II	129	128	1·50
Slow recrystallization from n-hexane at 20°	Form II & Form III	123 & 114	124 & 115	*
Slow recrystallization from n-octane at 20°	Form IV	123	121	1·36
Slow recrystallization from n-octane at 0°	Form IV & Form V	119 & 100	118 & 100	*
Sublimation of aspirin vapour under vacuum	Form VI	108	110	1·29

* Not possible to isolate polymorphs and make density determinations.
The melting points of polymorphs prepared by Tawashi (1968) were Form I 143° and Form II 125°.

Table 2. *Solution phase transformations of polymorph pairs at 20° C in n-pentanol*

Pair of polymorphs examined	Transformation observed
Form I + Form II	Form II ⟶ Form I
Form II + Form III	No transformation
Form I + Form IV	Form IV ⟶ Form I
Form II + Form IV	Form II ⟶ Form IV

X-ray powder diffraction (Phillips PW 1009/30) using nickel-filtered copper radiation was also performed on the polymorphs. However, only minor differences in the number and intensity of the lines in the diffraction patterns were observed.

The aspirin polymorphs were stable in the presence of moisture and upon storage. Grinding of the polymorphs in a Glen Creston micro-ball mill had no effect with the exception of Form III that was transformed to Form II.

Further work is continuing on the characterization of the polymorphs using dissolution techniques.

The authors would like to thank Dr. J. D. Donaldson for helpful discussions concerning the X-ray powder diffraction studies.

One of us (M.P.S.) would like to thank the Science Research Council for the award of a Research Studentship.

Department of Pharmacy,
Chelsea College of Science and Technology,
University of London,
Manresa Road, London, S.W.3, U.K.

M. P. SUMMERS
J. E. CARLESS
R. P. ENEVER

April 27, 1970

REFERENCES

MITCHELL, A. G. & SAVILLE, D. J. (1967). *J. Pharm. Pharmac.*, **19**, 729–734.
TAWASHI, R. (1968). *Science, N.Y.*, **160**, 76.
TAWASHI, R. (1969). *J. Pharm. Pharmac.*, **21**, 701–702.

UM00017028
NOVARTIS EXHIBIT 1517
Novartis v. Regents, IPR2023-01347
Page 3897 of 4460

View Online

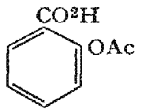
Published on 01 January 1964 on http://pubs.rsc.org | doi:10.1039/JR9640006036
Downloaded by US Patent & Trademark Office on 19 October 2010

1163. *The Crystal and Molecular Structure of Aspirin.*

By P. J. Wheatley.

The crystal structure of aspirin (acetylsalicylic acid) has been determined by three-dimensional *X*-ray diffraction methods. The crystals are monoclinic, space group $P2_1/c$, with $a = 11{\cdot}446$, $b = 6{\cdot}596$, $c = 11{\cdot}388$ Å, $\beta = 95°\ 33'$. The final parameters were obtained by a least-squares refinement of 2055 intensities collected with a Hilger–Watts linear diffractometer. The eight hydrogen atoms were located from a three-dimensional difference synthesis and included in the refinement. The final *R* factor, including 267 planes of zero intensity, was 10·8%.

The crystal structure of aspirin (I) has not previously been determined, although it is known that a number of attempts have been made.[1] This investigation was undertaken to provide



(I)

adequate structural knowledge which might form a basis for an interpretation of the mode of operation of this remarkable drug.

Experimental.—$C_9H_8O_4$. $M = 180{\cdot}2$. Monoclinic. $a = 11{\cdot}446 \pm 0{\cdot}013$, $b = 6{\cdot}596 \pm 0{\cdot}006$, $c = 11{\cdot}388 \pm 0{\cdot}009$ Å, $\beta = 95°\ 33' \pm 2'$. $U = 855{\cdot}7$ Å^3. $D_m = 1{\cdot}40$. $Z = 4$. $D_c = 1{\cdot}398$. $F(000) = 376$. Space group $P2_1/c$ (C_{2h}^5, No. 14).

Excellent crystals (m. p. 143°) can be obtained from many common organic solvents with [*b*] as the axis of elongation. Those used in the present analysis were grown from benzene. The cell dimensions, obtained from oscillation photographs (Cu-K_α, $\lambda = 1{\cdot}5418$ Å), yield the axial ratio: $a:b:c :: 1{\cdot}7533:1:1{\cdot}7265$, $\beta = 95°\ 33'$. They may be compared with the optical results of Niini:[2] $a:b:c :: 1{\cdot}7322:1:1{\cdot}7322$, $\beta = 95°\ 42{\cdot}5'$, and with those of Nitta and Watanabe obtained by *X*-rays:[3] $a = 11{\cdot}37$, $b = 6{\cdot}54$, $c = 11{\cdot}37$ kX, $a:b:c :: 1{\cdot}7385:1:1{\cdot}7385$, $\beta = 95°\ 27'$.

The intensities were collected round [*b*] with Mo-K_α radiation on a Hilger–Watts linear diffracto-

[1] Private communication from Dr. J. H. Robertson.
[2] R. Niini, *Z. Krist.*, 1931, **79**, 532.
[3] I. Nitta and T. Watanabe, *Sci. Papers Inst. Phys. Chem. Res.* (*Tokyo*), 1937, **31**, 125.

UM00017029
NOVARTIS EXHIBIT 1517
Novartis v. Regents, IPR2023-01347
Page 3898 of 4460

View Online

meter equipped with SrO–ZrO_2 balanced filters.[4] On the *h*0*l*–*h*2*l* layers, each reflexion was measured three times, and on *h*3*l*–*h*9*l* five times, with each filter. The *h*0*l*–*h*5*l* intensities were collected with a 3°, and the *h*6*l*–*h*9*l* with a 4° oscillation angle. About thirty reflexions had to be hand-measured. For these, a 4° oscillation was used. The maximum recording angle was $\theta = 30°$. A half-minute motor was used. The scale of the intensities so obtained was such that, when corrected for Lorentz and polarization factors, the resulting observed structure factors were on a scale slightly greater than absolute. In these circumstances it was felt justified to include all planes with the actual corrected count obtained, except when such a count was negative, in which case the reflexion was allotted zero intensity. In this manner 2055 independent reflexions (excluding 0*k*0) were obtained, of which 267 (13%) were zero. The analysis is based on these 2055 planes, and all values of R and R' include the zero reflexions.

The structure was solved from a sharpened three-dimensional Patterson synthesis. The

Downloaded by US Patent & Trademark Office on 19 October 2010
Published on 01 January 1964 on http://pubs.rsc.org | doi:10.1039/JR9640006036

TABLE 1.

Final atomic co-ordinates in Å. Standard deviations are given as units in the last place.

Atom	*X*	*Y*	*Z*
O(1)	0·1209 (27)	1·2377 (28)	1·1004 (28)
O(2)	1·3764 (26)	0·9148 (28)	−0·5786 (27)
O(3)	3·2639 (23)	2·7176 (26)	−1·0070 (23)
O(4)	4·6127 (29)	1·4508 (33)	0·3906 (27)
C(1)	1·7513 (31)	2·8796 (34)	0·7679 (33)
C(2)	2·8180 (33)	3·3762 (34)	0·1047 (33)
C(3)	3·4249 (36)	4·5825 (39)	0·4774 (40)
C(4)	2·9845 (39)	5·3062 (40)	1·5338 (43)
C(5)	1·9428 (39)	4·8260 (40)	2·2077 (40)
C(6)	1·3357 (34)	3·6315 (37)	1·8242 (36)
C(7)	1·0279 (32)	1·5944 (34)	0·4241 (33)
C(8)	4·1795 (33)	1·7226 (39)	−0·7189 (36)
C(9)	4·5424 (45)	1·0675 (52)	−1·9791 (42)
H(1)	0·8160 (690)	−0·0133 (794)	−0·9209 (687)
H(3)	4·1336 (446)	4·8674 (491)	0·0158 (447)
H(4)	3·4349 (446)	6·1985 (501)	1·8538 (446)
H(5)	1·6477 (446)	5·3156 (498)	2·9276 (446)
H(6)	0·6357 (444)	3·3448 (494)	2·2671 (443)
H(7)	3·5432 (572)	0·7956 (657)	−2·6885 (574)
H(8)	4·9306 (572)	0·2440 (646)	−1·9332 (573)
H(9)	4·9193 (566)	1·5189 (643)	−2·4623 (573)

TABLE 2.

Thermal parameters in Å². Standard deviations are given as units in the last place.

Atom	U_{11}	U_{22}	U_{33}	$2U_{12}$	$2U_{23}$	$2U_{13}$
O(1)	0·0501 (15)	0·0458 (15)	0·0562 (16)	−0·0372 (25)	−0·0190 (26)	0·0416 (25)
O(2)	0·0465 (14)	0·0480 (15)	0·0518 (15)	−0·0169 (25)	−0·0285 (26)	0·0253 (24)
O(3)	0·0392 (12)	0·0416 (13)	0·0359 (12)	0·0016 (21)	0·0094 (21)	0·0136 (19)
O(4)	0·0589 (17)	0·0729 (21)	0·0413 (14)	0·0562 (32)	0·0125 (29)	0·0040 (25)
C(1)	0·0292 (15)	0·0332 (16)	0·0384 (16)	0·0005 (25)	0·0082 (27)	0·0032 (25)
C(2)	0·0366 (16)	0·0322 (16)	0·0375 (17)	0·0127 (27)	0·0084 (27)	0·0020 (26)
C(3)	0·0398 (18)	0·0394 (19)	0·0547 (22)	−0·0131 (31)	0·0127 (34)	0·0119 (32)
C(4)	0·0471 (20)	0·0380 (19)	0·0609 (24)	−0·0040 (33)	−0·0036 (36)	0·0058 (35)
C(5)	0·0483 (21)	0·0403 (19)	0·0510 (21)	0·0080 (33)	−0·0164 (34)	0·0124 (33)
C(6)	0·0341 (16)	0·0396 (18)	0·0436 (18)	−0·0022 (29)	−0·0030 (30)	0·0128 (28)
C(7)	0·0335 (16)	0·0339 (16)	0·0366 (16)	0·0057 (26)	0·0078 (27)	0·0027 (26)
C(8)	0·0309 (16)	0·0476 (20)	0·0431 (19)	−0·0029 (30)	0·0057 (32)	0·0112 (27)
C(9)	0·0582 (25)	0·0721 (30)	0·0481 (22)	0·0157 (45)	−0·0199 (43)	0·0236 (38)
H(1)	0·12 (6)	0·12 (7)	0·12 (6)	0·0 (1)	0·0 (1)	0·023 (99)
H(3)	0·04 (3)	0·04 (3)	0·04 (3)	0·0 (5)	0·0 (5)	0·008 (50)
H(4)	0·04 (3)	0·04 (3)	0·04 (3)	0·0 (5)	0·0 (5)	0·008 (50)
H(5)	0·04 (3)	0·04 (3)	0·04 (3)	0·0 (5)	0·0 (5)	0·008 (50)
H(6)	0·04 (3)	0·04 (3)	0·04 (3)	0·0 (5)	0·0 (5)	0·008 (50)
H(7)	0·08 (5)	0·08 (5)	0·08 (5)	0·0 (8)	0·0 (8)	0·015 (75)
H(8)	0·08 (5)	0·08 (5)	0·08 (5)	0·0 (8)	0·0 (8)	0·015 (75)
H(9)	0·08 (5)	0·08 (5)	0·08 (5)	0·0 (8)	0·0 (8)	0·015 (75)

[4] U. Arndt and D. C. Phillips, *Acta Cryst.*, 1961, **14**, 807.

UM00017030
NOVARTIS EXHIBIT 1517
Novartis v. Regents, IPR2023-01347
Page 3899 of 4460

View Online

Downloaded by US Patent & Trademark Office on 19 October 2010
Published on 01 January 1964 on http://pubs.rsc.org | doi:10.1039/JR9640006036

TABLE 3.

h	*k*	*l*	F_o	F_c	Δ	*h*	*k*	*l*	F_o	F_c	Δ	*h*	*k*	*l*	F_o	F_c	Δ
5	0	14	-285	-259	-26	6	0	10	-375	-295	-84	1	1	-2	-1306	-1270	-38
0	0	12	125	66	59	6	0	8	0	11	-11	1	1	-3	2502	2438	64
0	0	10	-753	-721	-32	6	0	6	-469	-490	21	1	1	-4	461	495	-34
0	0	8	-2592	-2585	-7	6	0	4	-1237	-1308	71	1	1	-5	-2371	-2362	11
0	0	6	-597	-627	30	6	0	2	749	777	-28	1	1	-6	1114	988	126
0	0	4	-324	-141	-183	6	0	0	3109	3003	106	1	1	-7	-2904	-2738	-166
0	0	2	9561	10804	-1243	6	0	-2	2222	2091	131	1	1	-8	165	172	13
1	0	14	249	156	93	6	0	-4	387	362	25	1	1	-9	0	-61	61
1	0	12	-354	-218	-136	6	0	-6	659	642	17	1	1	-10	-110	-153	43
1	0	10	-1096	-1135	39	6	0	-8	0	58	-58	1	1	-11	170	168	2
1	0	8	-2568	-2470	-98	6	0	-10	-318	-88	-230	1	1	-12	-203	-160	-43
1	0	6	-2578	-2519	-59	6	0	-12	0	109	-109	1	1	-13	-191	-118	-73
1	0	4	-319	-297	-22	8	0	-14	-153	-299	146	1	1	-14	225	261	-36
1	0	2	-1661	-1621	-60	9	0	12	-219	-49	-170	1	1	-15	0	49	-49
1	0	0	3917	3628	89	9	0	10	0	68	-68	2	1	14	0	-43	43
1	0	-2	3242	3151	91	9	0	8	977	1035	-58	2	1	13	135	119	16
1	0	-4	-3033	-3164	131	9	0	6	1451	1595	-144	2	1	12	0	65	-65
1	0	-6	-279	-237	-42	9	0	4	1059	1061	-2	2	1	11	174	189	-15
1	0	-8	1521	1991	-70	9	0	2	-187	-226	39	2	1	10	114	77	37
1	0	-10	1467	1428	39	9	0	0	-894	-909	15	2	1	9	132	284	-152
1	0	-12	88	204	-116	9	0	-2	554	545	9	2	1	8	-299	-355	56
2	0	14	-172	-98	-74	9	0	-4	-1033	-1100	67	2	1	-7	151	75	76
2	0	12	0	-145	145	9	0	-6	-1545	-1538	-7	2	1	6	530	576	-46
2	0	10	1224	1263	-39	9	0	-8	-403	-392	-11	2	1	5	805	714	91
2	0	8	611	666	-55	9	0	-10	-623	-670	47	2	1	4	-3263	-3120	-143
2	0	6	0	142	-142	10	0	8	0	8	-8	2	1	3	5361	5374	-13
2	0	4	2654	2506	148	10	0	6	398	493	-95	2	1	2	-8846	-9211	365
2	0	2	-6704	-6850	146	10	0	4	-385	-280	-105	2	1	1	7444	7653	-209
2	0	0	-4631	-4609	-22	10	0	2	-141	-27	-114	2	1	0	2834	2841	-7
2	0	-2	4023	3913	110	10	0	0	979	1046	-67	2	1	-1	2975	2840	135
2	0	-4	-3897	-3723	-174	10	0	-2	946	965	-19	2	1	-2	2753	2655	98
2	0	-6	-1000	-942	-58	10	0	-4	114	70	44	2	1	-3	-1494	-1510	16
2	0	-8	-1153	-1218	65	10	0	-6	-819	-793	-26	2	1	-4	2628	2539	89
2	0	-10	-1940	-1942	2	10	0	-8	-904	-894	-10	2	1	-5	-2422	-2257	-165
2	0	-12	-301	-377	76	10	0	-10	-761	-663	-98	2	1	-6	1322	1305	17
3	0	14	-225	-256	31	11	0	8	-288	-361	73	2	1	-7	-1386	-1367	-19
3	0	12	-266	-168	-98	11	0	6	-191	-180	-11	2	1	-8	-742	-780	38
3	0	10	325	317	8	11	0	4	0	-32	32	2	1	-9	592	641	-49
3	0	8	875	887	-12	11	0	2	747	683	64	2	1	-10	813	869	-56
3	0	6	-1883	-1727	-156	11	0	0	628	659	-31	2	1	-11	1264	1294	-30
3	0	4	-3222	-3172	-50	11	0	-2	-417	-411	-6	2	1	-12	777	831	-54
3	0	2	2934	2908	26	11	0	-4	-1026	-1026	0	2	1	-13	429	438	-9
3	0	0	2644	2573	71	11	0	-6	-1177	-1170	-7	3	1	14	405	353	52
3	0	-2	2671	2586	85	11	0	-8	0	167	-167	3	1	13	0	150	-150
3	0	-4	-203	-41	-162	11	0	-10	603	599	4	3	1	12	365	342	23
3	0	-6	-1892	-1834	-58	12	0	8	102	172	-70	3	1	11	-620	-600	-20
3	0	-8	189	178	11	12	0	6	767	892	-125	3	1	10	964	933	31
3	0	-10	700	728	-28	12	0	4	1260	1324	-64	3	1	9	-792	-835	43
3	0	-12	646	635	11	12	0	2	129	60	69	3	1	8	1208	1223	-15
3	0	-14	321	202	119	12	0	0	0	93	-93	3	1	7	312	286	26
4	0	12	271	445	-174	12	0	-2	0	24	-24	3	1	6	-515	-569	54
4	0	10	1144	1194	-50	12	0	-4	-677	-812	135	3	1	5	-499	-566	67
4	0	8	1371	1413	-42	12	0	-6	0	-272	272	3	1	4	0	-133	133
4	0	6	-233	-345	112	12	0	-8	632	543	89	3	1	3	554	437	117
4	0	4	-839	-780	-59	12	0	-10	517	552	-35	3	1	2	-5101	-4913	-188
4	0	2	0	-218	218	13	0	4	-362	-348	-14	3	1	1	4017	3970	47
4	0	0	-4148	-4057	-91	13	0	2	-390	-403	13	3	1	0	-8607	-9138	531
4	0	-2	-1731	-1694	-37	13	0	0	233	250	-17	3	1	-1	-2927	-2884	-43
4	0	-4	-4293	-4058	-235	13	0	-2	1241	1335	-94	3	1	-2	-3931	-3899	-32
4	0	-6	-1822	-1807	-15	13	0	-4	1116	1205	-89	3	1	-3	-3749	-3590	-159
4	0	-8	4096	4185	-89	13	0	-6	0	95	-95	3	1	-4	-2866	-2685	-181
4	0	-10	2862	2759	103	14	0	4	-540	-674	134	3	1	-5	1008	980	28
4	0	-12	640	543	97	14	0	2	177	48	129	3	1	-6	-1084	-1070	-14
4	0	-14	339	229	110	14	0	0	-141	-34	-107	3	1	-7	211	246	-35
5	0	12	196	74	122	14	0	-2	570	610	-40	3	1	-8	492	505	-13
5	0	10	-121	-121	0	14	0	-4	499	316	183	3	1	-9	503	486	17
5	0	8	-653	-724	71	14	0	-6	-432	-442	10	3	1	-10	1459	1461	-2
5	0	6	332	308	24	15	0	4	-495	-617	122	3	1	-11	933	903	30
5	0	4	-1215	-1198	-17	15	0	2	-215	-273	58	3	1	-12	1464	1411	53
5	0	2	-1589	-1885	-104	15	0	0	-281	-335	54	3	1	-13	235	221	14
5	0	0	-1114	-1045	-69	15	0	-2	-350	-306	-44	4	1	12	0	59	-59
5	0	-2	-1051	-996	-55	15	0	-4	354	239	115	4	1	11	0	76	-76
5	0	-4	1696	1780	116	16	0	0	0	-29	29	4	1	10	386	450	-64
5	0	-6	901	820	81	16	0	-2	0	119	-119	4	1	9	198	236	-38
5	0	-8	1114	1115	-1	16	0	-4	403	535	-132	4	1	8	997	972	25
5	0	-10	1676	1887	-11	0	1	15	-261	-180	-81	4	1	-7	507	446	61
5	0	-12	162	173	-11	0	1	14	-267	-294	27	4	1	6	-769	696	-73
5	0	-14	-273	-200	-73	0	1	13	-765	-716	-49	4	1	5	-1302	-1160	-142
6	0	12	-334	-277	-57	0	1	12	-530	-502	-28	4	1	4	1060	1005	75
6	0	10	0	115	-115	0	1	11	-682	-726	44	4	1	3	-4340	-4159	-181
6	0	8	0	114	-114	0	1	10	-1076	-1105	29	4	1	2	-288	-447	159
6	0	6	-1813	-1600	-213	0	1	9	-129	-212	83	4	1	1	-2924	-2899	-25
6	0	4	-2459	-2514	15	0	1	8	185	57	128	4	1	0	-77	-134	57
6	0	2	-1605	-1450	-155	0	1	7	267	261	6	4	1	-1	-459	-531	72
6	0	0	-1734	-1764	30	0	1	6	490	538	-48	4	1	-2	2648	2670	-178
6	0	-2	-2025	-1719	-306	0	1	5	132	84	48	4	1	-3	-1050	-1116	26
6	0	-4	340	536	-198	0	1	4	-2792	-2696	-96	4	1	-4	263	290	-27
6	0	-6	-2358	-2330	-28	0	1	3	-1059	-1069	10	4	1	-5	-1148	-983	-165
6	0	-8	-2262	-2200	-62	0	1	2	4627	4977	-350	4	1	-6	1116	1155	-39
6	0	-10	1009	999	10	0	1	1	-3028	-3119	91	4	1	-7	-632	-518	-114
6	0	-12	702	720	-18	1	1	15	0	-80	80	4	1	-8	-662	-705	43
6	0	-14	406	413	-7	1	1	14	0	8	-8	4	1	-9	-1142	-1132	-10
7	0	12	310	355	-45	1	1	13	-256	-332	76	4	1	-10	-1929	-1930	1
7	0	10	339	356	-17	1	1	12	-182	-213	31	4	1	-11	-446	-451	5
7	0	8	385	547	-162	1	1	11	-244	-313	69	4	1	-12	-244	-231	-13
7	0	6	-1325	-1376	51	1	1	10	687	869	18	4	1	-13	93	276	-183
7	0	4	-1309	-1300	-9	1	1	9	1135	1097	38	5	1	12	-278	-58	-220
7	0	2	404	292	112	1	1	8	2172	2124	48	5	1	11	890	903	-13
7	0	0	4343	4261	82	1	1	7	1295	1305	-10	5	1	10	-877	-523	46
7	0	-2	1895	1779	116	1	1	6	2637	2768	69	5	1	9	266	345	-79
7	0	-4	-1308	-1206	-102	1	1	5	-723	-711	-12	5	1	8	0	-127	127
7	0	-6	-513	-491	-22	1	1	4	-1837	-1991	154	5	1	7	167	73	94
7	0	-8	-1622	-1660	38	1	1	3	2269	2159	110	5	1	6	-514	-456	-58
7	0	-10	-787	-774	-13	1	1	2	-7345	-7613	268	5	1	5	-959	-882	-77
7	0	-12	193	249	-56	1	1	1	1573	1650	-77	5	1	4	-3336	-3317	-19
7	0	-14	-511	-506	-5	1	1	0	-2693	-2664	-29	5	1	3	-3157	-3155	-2
8	0	12	523	534	-11	1	1	-1	-1092	-1097	5	5	1	2	-1092	-969	-124

UM00017031
NOVARTIS EXHIBIT 1517
Novartis v. Regents, IPR2023-01347
Page 3900 of 4460

View Online

Downloaded by US Patent & Trademark Office on 19 October 2010
Published on 01 January 1964 on http://pubs.rsc.org | doi:10.1039/JR9640006036

TABLE 3—*continued.*

h	*k*	*l*	F_o	F_c	Δ	*h*	*k*	*l*	F_o	F_c	Δ	*h*	*k*	*l*	F_o	F_c	Δ
5	1	1	0	54	−54	9	1	−6	582	540	42	1	2	9	983	1012	−29
5	1	0	614	540	74	9	1	−7	−1439	−1448	9	1	2	8	−237	−245	8
5	1	−1	3358	3296	62	9	1	−8	−174	−54	−120	1	2	7	114	156	−42
5	1	−2	4136	3995	141	9	1	−9	0	178	−178	1	2	6	1339	1324	15
5	1	−3	688	564	104	9	1	−10	−162	−253	91	1	2	5	0	−22	22
5	1	−4	3274	3158	116	9	1	−11	196	222	−26	1	2	4	1229	1128	101
5	1	−5	−505	−362	−143	10	1	10	−435	−482	47	1	2	3	187	201	−14
5	1	−6	−491	−411	−80	10	1	9	0	94	−94	1	2	2	2104	2081	23
5	1	−7	0	−125	125	10	1	8	−193	−305	112	1	2	1	−2258	−2246	−10
5	1	−8	−435	−430	−5	10	1	7	0	124	−124	1	2	0	1541	1436	105
5	1	−9	−536	−561	25	10	1	6	−342	−311	−31	1	2	−1	781	822	−41
5	1	−10	−485	−501	16	10	1	5	376	383	−7	1	2	−2	−656	−577	−79
5	1	−11	0	40	−40	10	1	4	−310	−296	−14	1	2	−3	−2359	−2367	28
5	1	−12	0	−67	67	10	1	3	1090	1079	11	1	2	−4	630	404	226
5	1	−13	196	49	147	10	1	2	0	−11	11	1	2	−5	−5702	−5494	−208
6	1	12	285	316	−31	10	1	1	1061	1068	−7	1	2	−6	534	533	1
6	1	11	461	562	−101	10	1	0	−290	−258	−32	1	2	−7	−1295	−1243	−52
6	1	10	601	790	11	10	1	−1	240	112	128	1	2	−8	−617	−560	−57
6	1	9	83	165	−82	10	1	−2	564	651	−87	1	2	−9	261	369	−108
6	1	8	875	867	12	10	1	−3	0	−13	13	1	2	−10	−1429	−1475	46
6	1	7	−235	−250	15	10	1	−4	509	523	−14	1	2	−11	524	539	−15
6	1	6	1434	1376	58	10	1	−5	325	243	82	1	2	−12	−437	−342	−95
6	1	5	0	−151	151	10	1	−6	−227	−178	−49	1	2	−13	859	801	58
6	1	4	516	550	−34	10	1	−7	−281	−382	101	1	2	−14	286	326	−40
6	1	3	−156	−41	−115	10	1	−8	−156	−140	−16	1	2	−15	370	264	106
6	1	2	−976	−1020	44	10	1	−9	0	−111	111	2	2	14	−327	−262	−65
6	1	1	−148	−211	63	10	1	−10	156	149	7	2	2	13	138	156	−18
6	1	0	−1379	−1389	10	10	1	−11	227	319	−92	2	2	12	−294	−260	−34
6	1	−1	461	475	−14	11	1	8	0	−159	159	2	2	11	233	70	163
6	1	−2	1225	1038	187	11	1	7	342	392	−50	2	2	10	−634	−679	45
6	1	−3	1027	952	75	11	1	6	0	44	−44	2	2	9	−362	−376	−4
6	1	−4	0	−193	193	11	1	5	−407	−424	17	2	2	8	−720	−765	45
6	1	−5	850	809	41	11	1	4	407	322	85	2	2	7	617	756	61
6	1	−6	−2851	−2952	61	11	1	3	−321	−398	77	2	2	6	833	878	−45
6	1	−7	1802	1758	44	11	1	2	276	251	−15	2	2	5	1706	1675	31
6	1	−8	−1068	−1058	−10	11	1	1	0	66	−66	2	2	4	−1942	−1893	−49
6	1	−9	1498	1436	62	11	1	0	−604	−633	29	2	2	3	114	162	−48
6	1	−10	−322	−246	−76	11	1	−1	−170	−62	−88	2	2	2	−4210	−3811	−399
6	1	−11	0	209	−209	11	1	−2	−118	−164	46	2	2	1	−1524	−1459	−65
6	1	−12	0	−113	113	11	1	−3	473	494	−21	2	2	0	−2716	−2535	−181
6	1	−13	−196	−136	−62	11	1	−4	405	343	66	2	2	−1	−924	−764	−160
7	1	12	−207	−193	−14	11	1	−5	526	651	−125	2	2	−2	−2766	−2680	−86
7	1	11	−198	−117	−81	11	1	−6	180	78	102	2	2	−3	97	24	73
7	1	10	−162	−51	−111	11	1	−7	−360	−316	−44	2	2	−4	586	555	31
7	1	9	0	−74	−74	11	1	−8	213	227	−14	2	2	−5	0	21	−21
7	1	8	−574	−581	7	11	1	−9	−407	−365	−42	2	2	−6	507	521	−14
7	1	7	200	143	57	11	1	−10	0	−178	178	2	2	−7	−110	−103	−7
7	1	6	585	582	3	11	1	−11	0	−123	123	2	2	−8	256	311	−55
7	1	5	1043	1001	42	12	1	6	0	−167	167	2	2	−9	322	369	−47
7	1	4	1057	1051	6	12	1	5	−529	−574	45	2	2	−10	−474	−535	61
7	1	3	0	−93	93	12	1	4	−1122	−1217	95	2	2	−11	227	200	27
7	1	2	1560	1559	1	12	1	3	−874	−988	114	2	2	−12	−697	−772	75
7	1	1	−1469	−1470	1	12	1	2	−999	−1060	61	2	2	−13	−215	−215	0
7	1	0	2447	2438	5	12	1	1	−288	−299	11	3	2	14	0	1	−1
7	1	−1	−223	−134	−89	12	1	0	−180	−138	−42	3	2	13	0	19	−19
7	1	−2	1197	1192	5	12	1	−1	221	145	76	3	2	12	414	474	−60
7	1	−3	412	377	35	12	1	−2	200	282	−82	3	2	11	−253	−30	−223
7	1	−4	2313	2292	21	12	1	−3	0	−171	171	3	2	10	1641	1641	0
7	1	−5	319	264	55	12	1	−4	1323	1381	−58	3	2	9	−784	−738	46
7	1	−6	180	16	164	12	1	−5	0	−131	131	3	2	8	1060	1082	−22
7	1	−7	1120	1174	−54	12	1	−6	1209	1258	−49	3	2	7	208	307	−99
7	1	−8	−2092	−2088	−4	12	1	−7	−167	−171	4	3	2	6	1993	1963	30
7	1	−9	450	401	49	12	1	−8	360	325	35	3	2	5	−1956	−1942	−14
7	1	−10	−793	−804	11	12	1	−9	−423	−323	−100	3	2	4	2031	1949	82
7	1	−11	−336	−394	58	13	1	6	0	−184	184	3	2	3	−2819	−2641	−178
7	1	−12	−716	−600	−118	13	1	5	229	114	115	3	2	2	−5253	−4796	−457
7	1	−13	0	25	−25	13	1	4	−378	−565	187	3	2	1	−5345	−4999	−346
8	1	10	−219	−316	97	13	1	3	−397	−363	−34	3	2	0	−3292	−3178	−114
8	1	9	−208	−160	−48	13	1	2	−648	−679	31	3	2	−1	−2692	−2795	97
8	1	8	433	338	95	13	1	1	0	−193	193	3	2	−2	−1020	−997	−23
8	1	7	−322	−228	−94	13	1	0	−164	−5	−159	3	2	−3	6123	5805	318
8	1	6	164	257	−93	13	1	−1	−213	−326	113	3	2	−4	−671	−718	153
8	1	5	−251	−370	119	13	1	−2	358	215	143	3	2	−5	3732	3422	310
8	1	4	671	651	20	13	1	−3	−562	−550	−12	3	2	−6	−478	−506	30
8	1	3	−372	−406	35	13	1	−4	350	154	196	3	2	−7	−114	−167	53
8	1	2	203	198	5	13	1	−5	0	60	−60	3	2	−8	−716	−610	−106
8	1	1	−187	−109	−78	13	1	−6	−346	−289	−57	3	2	−9	231	109	122
8	1	0	0	−182	182	13	1	−7	353	348	5	3	2	−10	−603	−583	−20
8	1	−1	586	617	−31	14	1	2	0	−224	224	3	2	−11	−288	−218	−70
8	1	−2	−416	−407	−9	14	1	1	0	−225	225	3	2	−12	−776	−621	45
8	1	−3	653	730	−77	14	1	0	−225	−205	−20	3	2	−13	−135	−48	−87
8	1	−4	464	456	8	14	1	−1	0	−71	71	4	2	12	−167	−256	89
8	1	−5	−835	−909	74	14	1	−2	0	19	−19	4	2	11	536	556	−20
8	1	−6	172	101	71	14	1	−3	0	−25	25	4	2	10	172	148	24
8	1	−7	−1380	−1348	−32	14	1	−4	−141	−118	−23	4	2	9	1021	1024	−3
8	1	−8	−875	−935	60	14	1	−5	102	193	−91	4	2	8	−416	−435	19
8	1	−9	−151	−215	64	0	2	15	−356	−342	−14	4	2	7	191	142	49
8	1	−10	−242	−316	74	0	2	14	−708	−636	72	4	2	6	332	322	70
8	1	−11	−135	−97	−38	0	2	13	−597	−609	12	4	2	5	−1326	−1766	−160
8	1	−12	0	−16	16	0	2	12	1203	1209	−6	4	2	4	4695	4438	257
8	1	−13	0	−75	75	0	2	11	−518	−589	71	4	2	3	−3596	−3468	−128
9	1	10	174	113	61	0	2	10	671	711	−40	4	2	2	3258	3091	207
9	1	9	0	−11	11	0	2	9	450	426	24	4	2	1	−1542	−1380	−162
9	1	8	759	817	−58	0	2	8	1061	1158	−77	4	2	0	2126	1991	135
9	1	7	−689	−656	−33	0	2	7	1150	1149	1	4	2	−1	1480	1356	124
9	1	6	765	831	−66	0	2	6	551	537	14	4	2	−2	1736	1726	10
9	1	5	−376	−364	−12	0	2	5	−283	−245	−38	4	2	−3	1715	1639	76
9	1	4	391	461	−70	0	2	4	−848	−822	−26	4	2	−4	1439	1322	117
9	1	3	991	1017	−26	0	2	3	−1586	−1749	163	4	2	−5	1991	1778	213
9	1	2	−1192	−1175	−17	0	2	2	−2269	−2264	15	4	2	−6	757	774	−17
9	1	1	934	882	52	0	2	1	−106	−46	−60	4	2	−7	0	−150	150
9	1	0	0	−17	17	1	2	15	0	132	−132	4	2	−8	−384	−449	65
9	1	−1	536	592	−56	1	2	14	0	−44	44	4	2	−9	−658	−689	31
9	1	−2	965	762	203	1	2	13	0	20	−20	4	2	−10	141	109	32
9	1	−3	72	158	−86	1	2	12	489	510	−21	4	2	−11	263	242	21
9	1	−4	−132	−237	105	1	2	11	336	364	−28	4	2	−12	−88	−80	−8
9	1	−5	−1496	−1496	60	1	2	10	0	2	−2	4	2	−13	339	276	63

UM00017032
NOVARTIS EXHIBIT 1517
Novartis v. Regents, IPR2023-01347
Page 3901 of 4460

View Online

Downloaded by US Patent & Trademark Office on 19 October 2010
Published on 01 January 1964 on http://pubs.rsc.org | doi:10.1039/JR9640006036

TABLE 3—*continued.*

h	*k*	*l*	F_o	F_c	Δ	*h*	*k*	*l*	F_o	F_c	Δ	*h*	*k*	*l*	F_o	F_c	Δ
5	2	12	−1006	−954	−52	9	2	5	941	991	−50	0	3	1	−4695	−4943	248
5	2	11	−399	−361	−38	9	2	4	−1099	−1131	32	1	3	15	0	270	−270
5	2	10	−658	−738	80	9	2	3	422	415	7	1	3	14	−102	−131	29
5	2	9	−293	−376	83	9	2	2	−1425	−1340	−85	1	3	13	294	74	220
5	2	8	489	474	15	9	2	1	−306	−207	−99	1	3	12	−348	−323	−25
5	2	7	408	300	108	9	2	0	491	444	47	1	3	11	83	191	−108
5	2	6	0	−16	16	9	2	−1	261	221	40	1	3	10	−454	−478	24
5	2	5	−677	−687	10	9	2	−2	251	203	42	1	3	9	466	494	−28
5	2	4	2970	2682	288	9	2	−3	−392	−408	16	1	3	8	873	842	31
5	2	3	−819	−817	−2	9	2	−4	1749	1813	−64	1	3	−7	0	36	−36
5	2	2	2668	2499	169	9	2	−5	−804	−726	−78	1	3	6	1267	1327	−60
5	2	1	1291	1223	68	9	2	−6	2721	2786	−65	1	3	5	680	670	10
5	2	0	−2676	−2599	−77	9	2	−7	118	85	33	1	3	4	1761	1735	26
5	2	−1	286	277	9	9	2	−8	626	627	−1	1	3	3	180	171	9
5	2	−2	−1668	−1688	20	9	2	−9	−274	−294	20	1	3	2	764	919	−155
5	2	−3	−169	−143	−46	9	2	−10	0	−191	191	1	3	1	−2023	−1938	−85
5	2	−4	−836	−808	−28	9	2	−11	−496	−493	−3	1	3	0	−2462	−2338	−124
5	2	−5	1262	1180	82	10	2	10	0	−30	30	1	3	−1	−2730	−2543	−187
5	2	−6	444	361	83	10	2	9	174	109	65	1	3	−2	−727	−679	−48
5	2	−7	97	16	81	10	2	8	−278	−146	−132	1	3	−3	−854	−907	53
5	2	−8	409	379	30	10	2	7	267	275	−8	1	3	−4	501	497	4
5	2	−9	240	193	47	10	2	6	−205	−146	−59	1	3	−5	2271	2292	−21
5	2	−10	−223	−112	−111	10	2	5	0	153	−153	1	3	−6	1181	1200	−19
5	2	−11	237	199	38	10	2	4	−397	−343	−54	1	3	−7	1337	1300	37
5	2	−12	208	93	115	10	2	3	−835	−750	−85	1	3	−8	225	99	126
5	2	−13	−466	−450	−16	10	2	2	−1812	−1736	−76	1	3	−9	−362	−371	11
6	2	12	−508	−474	−34	10	2	1	−1497	−1389	−48	1	3	−10	−542	−565	23
6	2	11	−613	−611	−2	10	2	0	−1225	−1208	−17	1	3	−11	−83	−74	−9
6	2	10	−901	−889	−12	10	2	−1	−621	−673	52	1	3	−12	−182	−24	−158
6	2	9	−489	−443	−46	10	2	−2	−974	−906	−68	1	3	−13	−336	−244	−92
6	2	8	0	−79	79	10	2	−3	1010	1092	−82	1	3	−14	0	−146	146
6	2	7	316	348	−32	10	2	−4	−1350	−1424	74	1	3	−15	−213	−264	51
6	2	6	−500	−420	−80	10	2	−5	1115	1150	−35	2	3	12	0	140	−140
6	2	5	1540	1512	28	10	2	−6	0	27	−27	2	3	11	−321	−285	−36
6	2	4	−865	−731	−134	10	2	−7	0	73	−73	2	3	10	385	384	1
6	2	3	716	711	5	10	2	−8	423	394	29	2	3	9	0	125	−125
6	2	2	470	424	46	10	2	−9	213	130	83	2	3	8	1775	1759	16
6	2	1	−956	−994	38	10	2	−10	97	38	59	2	3	7	959	983	−24
6	2	0	−454	−128	−326	10	2	−11	−205	−45	−160	2	3	6	1494	1487	7
6	2	−1	497	495	2	11	2	8	307	89	218	2	3	5	−566	−522	−44
6	2	−2	1326	1145	181	11	2	7	138	50	88	2	3	4	−694	−698	4
6	2	−3	1152	1146	6	11	2	6	366	355	11	2	3	3	−263	−297	34
6	2	−4	1222	1222	0	11	2	5	−187	−288	101	2	3	2	−97	−152	55
6	2	−5	358	359	−1	11	2	4	800	932	−132	2	3	1	72	72	0
6	2	−6	528	466	62	11	2	3	−369	−406	37	2	3	0	−1769	−1648	−121
6	2	−7	0	39	−39	11	2	2	−304	−345	41	2	3	−1	−1814	−1671	−143
6	2	−8	−377	−389	12	11	2	1	−1100	−1178	78	2	3	−2	−2119	−2069	−50
6	2	−9	−816	−801	−15	11	2	0	−983	−979	−4	2	3	−3	1336	1195	141
6	2	−10	−1117	−1104	−13	11	2	−1	−529	−581	52	2	3	−4	−1198	−1173	−25
6	2	−11	−593	−646	53	11	2	−2	−242	−315	73	2	3	−5	2307	2342	−35
6	2	−12	−687	−598	−89	11	2	−3	483	509	−26	2	3	−6	−102	−115	13
6	2	−13	0	−137	137	11	2	−4	−960	−916	−44	2	3	−7	1292	1247	45
7	2	12	102	267	−165	11	2	−5	283	306	−23	2	3	−8	121	221	−100
7	2	11	−221	−183	−38	11	2	−6	0	−84	84	2	3	−9	480	479	1
7	2	10	−668	−700	32	11	2	−7	0	−26	26	2	3	−10	−258	−150	−108
7	2	9	−375	−277	−98	11	2	−8	365	460	−75	2	3	−11	245	218	27
7	2	8	−691	−705	14	11	2	−9	138	177	−39	2	3	−12	391	435	−44
7	2	7	462	471	−9	12	2	6	0	−247	247	2	3	−13	−193	−7	−186
7	2	6	−470	−423	−47	12	2	5	0	28	−28	3	3	12	0	101	−101
7	2	5	759	796	−37	12	2	4	374	325	49	3	3	11	−339	−326	−13
7	2	4	−1091	−1038	−53	12	2	3	249	217	32	3	3	10	−823	−768	−55
7	2	3	−118	−125	7	12	2	2	625	584	41	3	3	9	−704	−645	−59
7	2	2	1038	891	147	12	2	1	290	228	62	3	3	8	−1443	−1415	−28
7	2	1	593	556	37	12	2	0	−341	−399	58	3	3	7	−65	−116	51
7	2	0	299	61	238	12	2	−1	−221	−221	0	3	3	6	−237	−328	91
7	2	−1	1465	1363	102	12	2	−2	340	264	76	3	3	5	879	830	49
7	2	−2	−58	−81	23	12	2	−3	−318	−274	−44	3	3	4	−313	−307	−6
7	2	−3	1026	991	35	12	2	−4	499	525	−26	3	3	3	1086	1120	−34
7	2	−4	893	902	−9	12	2	−5	421	394	27	3	3	2	2887	2627	260
7	2	−5	566	480	86	12	2	−6	0	44	−44	3	3	1	−41	−81	40
7	2	−6	−539	−570	31	12	2	−7	392	271	121	3	3	0	4051	3994	57
7	2	−7	−741	−848	107	12	2	−8	348	296	52	3	3	−1	994	964	30
7	2	−8	−325	−349	24	12	2	−9	0	60	−60	3	3	−2	398	442	−44
7	2	−9	−1314	−1378	64	13	2	4	174	199	−25	3	3	−3	1660	1503	177
7	2	−10	153	183	−30	13	2	3	0	−18	18	3	3	−4	−476	−385	−91
7	2	−11	132	190	−58	13	2	2	481	473	8	3	3	−5	−51	−131	80
7	2	−12	138	63	75	13	2	1	−274	−214	−60	3	3	−6	−227	−184	−43
7	2	−13	563	536	27	13	2	0	−135	−210	75	3	3	−7	0	−75	75
8	2	10	341	182	159	13	2	−1	−407	−387	−20	3	3	−8	700	771	−71
8	2	9	0	−9	9	13	2	−2	−271	−329	58	3	3	−9	−862	−838	−24
8	2	8	0	168	−168	13	2	−3	93	265	−172	3	3	−10	0	105	−105
8	2	7	−193	−76	−117	13	2	−4	0	−139	139	3	3	−11	−527	−535	8
8	2	6	1170	1080	90	13	2	−5	474	518	−44	3	3	−12	−346	−462	116
8	2	5	−278	−270	−8	13	2	−6	−415	−434	19	3	3	−13	0	79	−79
8	2	4	1031	1022	9	13	2	−7	205	267	−62	4	3	12	−276	−169	−107
8	2	3	468	443	25	14	2	2	−102	−148	46	4	3	11	−370	−301	−69
8	2	2	835	865	−30	14	2	1	−97	−39	−58	4	3	10	−1007	−943	−64
8	2	1	739	677	62	14	2	0	0	−117	117	4	3	9	−1583	−1511	−72
8	2	0	−254	−7	−247	14	2	−1	200	217	−17	4	3	8	−2007	−2006	−1
8	2	−1	211	251	−40	14	2	−2	−405	−344	−61	4	3	−7	−888	−909	21
8	2	−2	−1035	−1088	53	14	2	−3	249	290	−41	4	3	6	276	279	−3
8	2	−3	−387	−339	−48	14	2	−4	0	77	−77	4	3	5	−393	−356	−35
8	2	−4	785	774	11	14	2	−5	0	114	−114	4	3	4	1135	1069	66
8	2	−5	−1524	−1467	−57	0	3	15	0	50	−50	4	3	3	−223	−142	−81
8	2	−6	1215	1177	38	0	3	14	683	653	30	4	3	2	−422	−395	−27
8	2	−7	−925	−966	41	0	3	13	−217	−226	9	4	3	1	969	876	93
8	2	−8	306	260	46	0	3	12	530	563	−33	4	3	0	−41	−35	−6
8	2	−9	−279	−219	−60	0	3	11	−348	−273	−75	4	3	−1	−388	−416	28
8	2	−10	0	9	−9	0	3	10	457	501	−44	4	3	−2	−1381	−1320	−61
8	2	−11	135	103	32	0	3	9	215	149	66	4	3	−3	674	666	8
8	2	−12	−141	−89	−52	0	3	8	710	716	−6	4	3	−4	−764	−688	−76
8	2	−13	631	562	69	0	3	7	−633	−599	−34	4	3	−5	1932	1907	25
9	2	10	0	−166	166	0	3	6	135	191	−56	4	3	−6	896	917	−21
9	2	9	−278	−223	−55	0	3	5	189	69	120	4	3	−7	−97	−173	76
9	2	8	−454	−511	57	0	3	4	1677	1768	−91	4	3	−8	1346	1364	−38
9	2	7	0	57	−57	0	3	3	328	288	40	4	3	−9	−973	−1101	128
9	2	6	−339	−301	−38	0	3	2	1539	1606	−61	4	3	−10	679	752	−73

UM00017033
NOVARTIS EXHIBIT 1517
Novartis v. Regents, IPR2023-01347
Page 3902 of 4460

View Online

Downloaded by US Patent & Trademark Office on 19 October 2010
Published on 01 January 1964 on http://pubs.rsc.org | doi:10.1039/JR9640006036

TABLE 3—*continued.*

h	*k*	*l*	F_o	F_c	Δ	*h*	*k*	*l*	F_o	F_c	Δ	*h*	*k*	*l*	F_o	F_c	Δ
4	3	−11	−467	−463	−4	9	3	2	271	269	−18	1	4	−6	1458	1539	−81
4	3	−12	−162	−102	−60	9	3	1	189	166	23	1	4	−7	−651	−719	68
4	3	−13	−296	−310	14	9	3	0	−296	−290	−6	1	4	−8	567	631	−64
5	3	12	−172	−166	−6	9	3	−1	−1112	−1121	9	1	4	−9	338	389	−51
5	3	11	231	116	113	9	3	−2	−1085	−1106	21	1	4	−10	430	505	−75
5	3	10	494	426	68	9	3	−3	−717	−714	−3	1	4	−11	196	76	120
5	3	9	208	41	167	9	3	−4	−335	−199	−136	1	4	−12	625	593	32
5	3	8	−114	−199	85	9	3	−5	256	325	−69	1	4	−13	−219	−265	46
5	3	7	132	43	89	9	3	−6	−695	−707	12	2	4	12	0	56	−56
5	3	6	−174	−66	−108	9	3	−7	148	256	−108	2	4	11	0	90	−90
5	3	5	0	20	−20	9	3	−8	−497	−476	−21	2	4	10	0	−134	134
5	3	4	1002	978	24	9	3	−9	−129	−125	−4	2	4	9	−159	−8	−151
5	3	3	376	373	3	9	3	−10	408	377	31	2	4	8	−581	−627	46
5	3	2	−983	−884	−99	9	3	−11	−198	−77	−121	2	4	7	−1905	−1901	−4
5	3	1	−296	−278	−18	10	3	8	138	101	37	2	4	6	−1927	−1985	58
5	3	0	557	539	18	10	3	7	213	116	97	2	4	5	−955	−1035	80
5	3	−1	−1916	−1878	−38	10	3	6	465	518	−53	2	4	4	−1069	−1100	11
5	3	−2	1903	1671	232	10	3	5	−312	−267	−45	2	4	3	1842	1953	−111
5	3	−3	−927	−836	−91	10	3	4	231	296	−65	2	4	2	−789	−729	−60
5	3	−4	1444	1322	122	10	3	3	225	142	83	2	4	1	596	610	−14
5	3	−5	213	226	−13	10	3	2	701	672	29	2	4	0	−180	−114	−66
5	3	−6	732	705	27	10	3	1	164	234	−70	2	4	−1	−1354	−1309	−45
5	3	−7	0	22	−22	10	3	0	470	503	−33	2	4	−2	1189	1058	131
5	3	−8	−448	−514	66	10	3	−1	0	−31	31	2	4	−3	−1040	−1125	85
5	3	−9	−430	−510	80	10	3	−2	−1760	−1793	33	2	4	−4	256	221	35
5	3	−10	−401	−410	9	10	3	−3	875	797	78	2	4	−5	−374	−358	−16
5	3	−11	−758	−814	56	10	3	−4	−1326	−1383	57	2	4	−6	329	307	22
5	3	−12	−415	−291	−124	10	3	−5	647	629	18	2	4	−7	253	297	−44
6	3	−13	97	101	−4	10	3	−6	−193	−176	−17	2	4	−8	0	55	−55
6	3	12	−174	−85	−89	10	3	−7	542	508	34	2	4	−9	302	345	−43
6	3	11	135	124	11	10	3	−8	0	26	−26	2	4	−10	−310	−274	−36
6	3	10	0	−45	45	10	3	−9	491	462	29	2	4	−11	−304	−350	46
6	3	9	196	172	24	10	3	−10	670	615	55	3	4	12	−191	−134	−57
6	3	8	−1152	−1149	−3	10	3	−11	−372	−208	−164	3	4	11	0	−61	61
6	3	7	1097	1074	23	11	3	8	−374	−315	−59	3	4	10	−743	−751	8
6	3	6	−2876	−2808	−68	11	3	7	−301	−288	−13	3	4	9	524	589	−65
6	3	5	2812	2738	74	11	3	6	0	43	−43	3	4	8	−1078	−1148	70
6	3	4	−986	−994	8	11	3	5	0	−73	73	3	4	7	458	497	−1
6	3	3	1368	1368	0	11	3	4	0	49	−49	3	4	6	−1411	−1442	31
6	3	2	696	565	131	11	3	3	−125	−180	55	3	4	5	425	465	−40
6	3	1	978	1018	−40	11	3	2	−321	−369	48	3	4	4	170	69	101
6	3	0	2083	2075	8	11	3	1	0	38	−38	3	4	3	731	808	−77
6	3	−1	1100	1139	−39	11	3	0	260	195	65	3	4	2	1084	1016	68
6	3	−2	3108	3066	42	11	3	−1	0	176	−176	3	4	1	894	922	−28
6	3	−3	−1111	−1023	−88	11	3	−2	−416	−418	2	3	4	0	118	2	116
6	3	−4	1002	961	41	11	3	−3	392	377	15	3	4	−1	470	462	8
6	3	−5	−264	−192	−72	11	3	−4	−470	−534	64	3	4	−2	1523	1518	5
6	3	−6	141	101	40	11	3	−5	761	778	−17	3	4	−3	−407	−408	1
6	3	−7	338	428	−90	11	3	−6	442	478	−36	3	4	−4	616	651	−35
6	3	−8	−177	−42	−135	11	3	−7	400	388	12	3	4	−5	0	258	−258
6	3	−9	−417	−467	50	11	3	−8	193	138	55	3	4	−6	449	512	−63
6	3	−10	−83	−119	36	11	3	−9	0	−3	3	3	4	−7	217	233	−16
6	3	−11	−369	−423	54	12	3	6	227	184	43	3	4	−8	796	836	−38
6	3	−12	0	−16	16	12	3	5	−281	−303	22	3	4	−9	−304	−406	102
6	3	−13	304	135	169	12	3	4	487	480	7	3	4	−10	−375	−378	3
7	3	10	−93	−49	−44	12	3	3	−132	−215	83	3	4	−11	−356	−322	−34
7	3	9	−331	−454	123	12	3	2	−93	−21	−72	4	4	12	279	221	58
7	3	8	121	150	−29	12	3	1	−185	−121	−64	4	4	11	0	−155	155
7	3	7	0	−161	161	12	3	0	260	345	−85	4	4	10	88	43	45
7	3	6	−537	−509	−28	12	3	−1	−758	−771	13	4	4	9	−118	−50	−68
7	3	5	656	685	−29	12	3	−2	520	518	2	4	4	8	456	463	−7
7	3	4	302	138	164	12	3	−3	−490	−445	−45	4	4	7	0	−190	190
7	3	3	430	468	−38	12	3	−4	−458	−478	20	4	4	6	718	717	1
7	3	2	264	272	−8	12	3	−5	445	443	2	4	4	5	−1237	−1240	3
7	3	1	−735	−730	−5	12	3	−6	−361	−366	5	4	4	4	−227	−178	−49
7	3	0	−1770	−1719	−51	12	3	−7	−219	−72	−147	4	4	3	97	106	−9
7	3	−1	−619	−640	21	13	3	4	97	56	41	4	4	2	233	240	−7
7	3	−2	−1430	−1443	13	13	3	3	245	149	96	4	4	1	780	716	64
7	3	−3	235	302	−67	13	3	2	221	238	−17	4	4	0	0	−163	163
7	3	−4	−1339	−1343	4	13	3	1	167	98	69	4	4	−1	185	181	4
7	3	−5	748	703	45	13	3	0	307	350	−43	4	4	−2	240	259	−19
7	3	−6	−167	−79	−88	13	3	−1	0	12	−12	4	4	−3	979	987	−8
7	3	−7	574	612	−38	13	3	−2	836	811	25	4	4	−4	1096	1135	−39
7	3	−8	1083	1101	−18	13	3	−3	−526	−496	−30	4	4	−5	138	106	32
7	3	−9	838	827	11	13	3	−4	260	304	−44	4	4	−6	451	425	26
7	3	−10	471	488	−17	13	3	−5	−263	−159	−104	4	4	−7	−65	−125	60
7	3	−11	0	219	−219	0	4	13	−296	−185	−111	4	4	−8	321	349	−28
8	3	10	138	117	21	0	4	12	−207	−206	−1	4	4	−9	447	442	5
8	3	9	93	44	49	0	4	11	375	406	−31	4	4	−10	145	132	13
8	3	8	798	809	−11	0	4	10	−114	−35	−79	4	4	−11	153	239	−86
8	3	7	−657	−672	15	0	4	9	0	−31	31	5	4	12	245	57	188
8	3	6	675	704	−29	0	4	8	0	−66	66	5	4	11	0	50	−50
8	3	5	159	0	159	0	4	7	367	361	6	5	4	10	0	37	−37
8	3	4	0	19	−19	0	4	6	989	1039	−50	5	4	9	−286	−227	−59
8	3	3	362	379	−17	0	4	5	1913	2065	−152	5	4	8	−377	−428	51
8	3	2	−312	−238	−74	0	4	4	1307	1408	−101	5	4	7	−356	−406	50
8	3	1	−2067	−2019	−48	0	4	3	678	946	−68	5	4	6	−645	−672	27
8	3	0	−1950	−1997	47	0	4	2	970	985	−15	5	4	5	0	−119	119
8	3	−1	−2000	−2137	137	0	4	1	−487	−520	33	5	4	4	−678	−658	−20
8	3	−2	−852	−855	3	1	4	12	−132	−207	75	5	4	3	1247	1232	15
8	3	−3	−872	−908	36	1	4	11	281	286	−5	5	4	2	561	580	−19
8	3	−4	895	973	−78	1	4	10	0	121	−121	5	4	1	518	577	−59
8	3	−5	−460	−430	−30	1	4	9	−1081	−1108	27	5	4	0	1052	1097	−45
8	3	−6	427	457	−30	1	4	8	−381	−404	23	5	4	−1	−1549	−1613	64
8	3	−7	233	441	−208	1	4	7	−2204	−2296	92	5	4	−2	876	810	66
8	3	−8	437	467	−30	1	4	6	−354	−433	79	5	4	−3	−1565	−1622	57
8	3	−9	0	175	−175	1	4	5	−312	−358	46	5	4	−4	562	1015	−53
8	3	−10	207	53	154	1	4	4	−785	−836	51	5	4	−5	−435	−337	−98
8	3	−11	−53	−56	3	1	4	3	1638	1789	−151	5	4	−6	−569	−601	32
9	3	10	177	142	35	1	4	2	−3103	−3038	−65	5	4	−7	570	726	−156
9	3	9	0	68	−68	1	4	1	2473	2539	−66	5	4	−8	−172	−227	55
9	3	8	316	293	83	1	4	0	−254	−274	20	5	4	−9	443	521	−78
9	3	7	−231	−672	441	1	4	−1	1373	1289	84	5	4	−10	274	373	−99
9	3	6	174	225	−51	1	4	−2	633	648	−15	5	4	−11	342	359	−17
9	3	5	208	58	110	1	4	−3	434	420	14	6	4	10	0	25	−25
9	3	4	−483	−420	−63	1	4	−4	121	139	−18	6	4	9	−177	−228	51
9	3	3	254	417	−163	1	4	−5	−191	−217	26	6	4	8	−427	−508	81

UM00017034
NOVARTIS EXHIBIT 1517
Novartis v. Regents, IPR2023-01347
Page 3903 of 4460

View Online

Downloaded by US Patent & Trademark Office on 19 October 2010
Published on 01 January 1964 on http://pubs.rsc.org | doi:10.1039/JR9640006036

TABLE 3—*continued.*

h	*k*	*l*	F_o	F_c	Δ	*h*	*k*	*l*	F_o	F_c	Δ	*h*	*k*	*l*	F_o	F_c	Δ
6	4	7	745	754	−9	11	4	−2	328	351	−23	3	5	−10	189	187	2
6	4	6	−106	−102	−4	11	4	−3	461	488	−27	3	5	−11	487	614	−127
6	4	5	422	474	−52	11	4	−4	310	251	59	4	5	10	153	29	124
6	4	4	321	368	−47	11	4	−5	0	−86	86	4	5	9	170	54	116
6	4	3	249	274	−25	11	4	−6	0	−31	31	4	5	8	240	238	2
6	4	2	−180	−135	−45	11	4	−7	0	−45	45	4	5	−7	−364	−356	−8
6	4	1	881	901	−20	12	4	4	294	337	−43	4	5	6	302	343	−41
6	4	0	−567	−603	36	12	4	3	191	215	−24	4	5	5	−1562	−537	−1025
6	4	−1	−1873	−1956	83	12	4	2	456	450	6	4	5	4	639	973	−134
6	4	−2	−2323	−2471	148	12	4	1	0	−118	118	4	5	3	−319	−311	−8
6	4	−3	−2122	−2242	120	12	4	0	729	783	−54	4	5	2	621	706	−85
6	4	−4	−2256	−2292	34	12	4	−1	−618	−706	88	4	5	1	310	290	20
6	4	−5	641	670	−29	12	4	−2	436	436	0	4	5	0	−245	−206	−39
6	4	−6	−500	−928	28	12	4	−3	−187	−257	70	4	5	−1	182	282	−100
6	4	−7	1094	1173	−79	12	4	−4	327	252	75	4	5	−2	−276	−288	12
6	4	−8	−426	−530	104	12	4	−5	0	−281	281	4	5	−3	−1796	−1893	97
6	4	−9	536	625	−89	12	4	−6	135	137	−2	4	5	−4	−1285	−1372	87
6	4	−10	307	383	−76	12	4	−7	0	57	−57	4	5	−5	−1826	−1928	102
6	4	−11	207	267	−60	13	4	2	0	92	−92	4	5	−6	−882	−914	32
7	4	10	237	383	−146	13	4	1	357	412	−55	4	5	−7	−428	−470	42
7	4	9	−207	−48	−159	13	4	0	170	237	−67	4	5	−8	72	117	−45
7	4	8	806	836	−30	13	4	−1	−449	−514	65	4	5	−9	138	123	15
7	4	7	281	277	4	13	4	−2	310	433	−123	4	5	−10	−148	−227	79
7	4	6	754	793	−39	13	4	−3	−617	−721	104	4	5	−11	273	175	98
7	4	5	279	241	38	0	5	13	138	76	62	5	5	10	346	304	42
7	4	4	582	693	−111	0	5	12	0	152	−152	5	5	9	−263	−253	−10
7	4	3	−321	−329	8	0	5	11	153	206	−53	5	5	8	−114	−29	−85
7	4	2	−302	−161	−141	0	5	10	−187	−275	88	5	5	7	325	188	137
7	4	1	522	541	−19	0	5	9	0	113	−113	5	5	6	0	−36	36
7	4	0	−836	−835	−1	0	5	8	−592	−623	31	5	5	5	874	923	−49
7	4	−1	606	621	−15	0	5	7	−273	−308	35	5	5	4	651	685	−34
7	4	−2	−1469	−1494	25	0	5	6	−844	−926	82	5	5	3	800	870	−70
7	4	−3	−884	−931	47	0	5	5	−1570	−1694	124	5	5	2	421	518	−97
7	4	−4	−876	−886	10	0	5	4	−1153	−1317	164	5	5	1	366	355	11
7	4	−5	−810	−825	15	0	5	3	−857	−1008	151	5	5	0	−170	−118	−52
7	4	−6	0	−77	−77	0	5	2	145	111	34	5	5	−1	646	683	−37
7	4	−7	0	142	−142	0	5	1	729	871	−142	5	5	−2	469	460	29
7	4	−8	−276	−485	209	1	5	13	390	399	−9	5	5	−3	0	45	−45
7	4	−9	172	181	−9	1	5	12	382	401	−19	5	5	−4	−867	−898	31
7	4	−10	−129	−185	56	1	5	11	238	212	26	5	5	−5	−551	−576	25
7	4	−11	0	−144	144	1	5	10	118	186	−68	5	5	−6	−1192	−1223	31
8	4	10	302	380	−78	1	5	9	−399	−477	78	5	5	−7	−307	−294	−13
8	4	9	−520	−587	67	1	5	8	0	185	−185	5	5	−8	0	84	−84
8	4	8	358	520	−162	1	5	7	−236	−234	−4	5	5	−9	−205	−189	−16
8	4	−7	−835	−980	145	1	5	6	312	335	−23	5	5	−10	−279	−252	−27
8	4	6	83	10	73	1	5	5	−411	−418	7	5	5	−11	0	−81	81
8	4	5	231	147	84	1	5	4	−1435	−1516	81	6	5	10	478	515	−37
8	4	4	0	80	−80	1	5	3	0	78	−78	6	5	9	364	379	−15
8	4	3	187	129	58	1	5	2	−894	−916	22	6	5	8	442	421	21
8	4	2	0	−135	135	1	5	1	412	460	−48	6	5	7	0	55	−55
8	4	1	823	844	−21	1	5	0	41	75	−34	6	5	6	260	263	−3
8	4	0	0	75	−75	1	5	−1	72	105	−33	6	5	5	−579	−622	43
8	4	−1	1715	1737	−22	1	5	−2	−919	−1091	172	6	5	4	0	−64	64
8	4	−2	756	758	−2	1	5	−3	0	−70	70	6	5	3	−271	−257	−14
8	4	−3	−180	−273	93	1	5	−4	1369	1508	−139	6	5	2	225	330	−105
8	4	−4	0	−151	151	1	5	−5	−953	−1095	142	6	5	1	−276	−271	−5
8	4	−5	−633	−702	69	1	5	−6	1636	1743	−107	6	5	0	−249	−181	−68
8	4	−6	196	81	115	1	5	−7	−235	−179	−56	6	5	−1	151	226	−75
8	4	−7	−114	−14	−100	1	5	−8	102	80	22	6	5	−2	−582	−570	−12
8	4	−8	172	170	2	1	5	−9	488	588	−100	6	5	−3	1189	1230	−41
8	4	−9	0	143	−143	1	5	−10	205	181	24	6	5	−4	−65	−49	−16
8	4	−10	−231	−89	−142	1	5	−11	−153	−110	−43	6	5	−5	299	266	33
8	4	−11	0	176	−176	1	5	−12	0	−217	217	6	5	−6	−514	−616	102
9	4	8	235	282	−47	1	5	−13	−263	−195	−68	6	5	−7	0	−72	72
9	4	−7	−849	−910	61	1	5	−14	−348	−301	−47	6	5	−8	−138	−50	−88
9	4	6	310	385	−75	2	5	10	0	−143	143	6	5	−9	170	92	78
9	4	5	−613	−638	25	2	5	9	162	163	−1	6	5	−10	325	303	22
9	4	4	302	325	−23	2	5	8	−511	−551	40	6	5	−11	391	347	44
9	4	3	0	9	−9	2	5	7	97	91	6	7	5	8	88	38	50
9	4	2	517	505	12	2	5	6	−513	−552	39	7	5	7	121	97	24
9	4	1	−633	−581	−52	2	5	5	594	514	80	7	5	6	−515	−555	40
9	4	0	−132	−76	−56	2	5	4	−217	−285	68	7	5	5	−518	−570	52
9	4	−1	−472	−540	68	2	5	3	443	413	30	7	5	4	−479	−512	33
9	4	−2	−510	−518	8	2	5	2	0	−63	63	7	5	3	0	−89	89
9	4	−3	0	−215	215	2	5	1	510	625	−115	7	5	2	−97	−164	67
9	4	−4	−795	−876	81	2	5	0	1160	1209	−49	7	5	1	805	900	−95
9	4	−5	−77	−72	−5	2	5	−1	874	916	−42	7	5	0	−254	−214	−40
9	4	−6	−376	−386	6	2	5	−2	276	332	−56	7	5	−1	244	314	−70
9	4	−7	428	442	−14	2	5	−3	1393	1552	−159	7	5	−2	0	73	−73
9	4	−8	285	266	19	2	5	−4	−114	−78	−36	7	5	−3	−562	−564	2
9	4	−9	420	485	−65	2	5	−5	997	1130	−133	7	5	−4	716	733	−17
10	4	8	−245	−294	49	2	5	−6	532	574	−42	7	5	−5	−927	−1011	84
10	4	7	193	93	100	2	5	−7	0	44	−44	7	5	−6	205	81	124
10	4	6	−162	−247	85	2	5	−8	−148	−119	−29	7	5	−7	−552	−615	63
10	4	5	0	−121	121	2	5	−9	0	69	−69	7	5	−8	118	143	−25
10	4	4	−331	−298	−33	2	5	−10	0	−164	164	7	5	−9	−177	−85	−92
10	4	3	191	171	20	2	5	−11	0	6	−6	8	5	8	167	274	−87
10	4	2	118	118	0	3	5	10	−196	−117	−79	8	5	7	−125	−133	8
10	4	1	−276	−260	−16	3	5	9	332	285	47	8	5	6	211	223	−12
10	4	0	−298	−259	−39	3	5	8	−338	−344	54	8	5	5	−203	−264	61
10	4	−1	164	12	152	3	5	7	−512	−567	55	8	5	4	211	191	20
10	4	−2	−141	−64	−77	3	5	6	397	358	39	8	5	3	−469	−455	−14
10	4	−3	0	8	−8	3	5	5	−1493	−1597	104	8	5	2	−151	−89	−62
10	4	−4	370	450	−80	3	5	4	632	796	36	8	5	1	316	342	−26
10	4	−5	−425	−383	−42	3	5	3	−1395	−1499	104	8	5	0	0	78	−78
10	4	−6	0	146	−146	3	5	2	−182	−243	61	8	5	−1	102	30	72
10	4	−7	0	92	−92	3	5	1	567	545	22	8	5	−2	−233	−325	92
10	4	−8	229	255	−26	3	5	0	177	182	−5	8	5	−3	−425	−524	99
10	4	−9	−435	−331	−104	3	5	−1	794	831	−37	8	5	−4	0	−30	30
11	4	6	0	−83	83	3	5	−2	−1280	−1375	95	8	5	−5	−354	−535	181
11	4	5	−135	−209	74	3	5	−3	532	568	−36	8	5	−6	306	375	−69
11	4	4	−206	−120	−86	3	5	−4	−2562	−2738	176	8	5	−7	−223	−260	37
11	4	3	0	94	−94	3	5	−5	854	916	−62	8	5	−8	−215	−192	−23
11	4	2	88	24	64	3	5	−6	−182	−141	−41	8	5	−9	290	253	37
11	4	1	562	531	31	3	5	−7	253	282	−29	9	5	6	0	−36	36
11	4	0	591	533	58	3	5	−8	146	243	−95	9	5	5	0	−42	42
11	4	−1	412	461	−69	3	5	−9	527	577	−50	9	5	4	−83	−13	−70

UM00017035
NOVARTIS EXHIBIT 1517
Novartis v. Regents, IPR2023-01347
Page 3904 of 4460

View Online

Downloaded by US Patent & Trademark Office on 19 October 2010
Published on 01 January 1964 on http://pubs.rsc.org | doi:10.1039/JR9640006036

TABLE 3—*continued.*

h	*k*	*l*	F_o	F_c	Δ	*h*	*k*	*l*	F_o	F_c	Δ	*h*	*k*	*l*	F_o	F_c	Δ
9	5	3	−627	−635	68	3	6	−5	555	516	41	10	6	2	−210	−28	−182
9	5	2	459	465	−26	3	6	−6	−184	−151	−33	10	6	1	−256	−254	−42
9	5	1	−745	−771	26	3	6	−7	−578	−603	25	10	6	0	0	−39	39
9	5	0	335	444	−109	3	6	−8	−516	−519	3	10	6	−1	430	368	62
9	5	−1	0	84	−84	3	6	−9	0	−134	134	10	6	−2	−166	−218	52
9	5	−2	379	381	−2	4	6	10	383	197	186	10	6	−3	506	640	66
9	5	−3	349	374	−25	4	6	9	609	504	105	10	6	−4	−323	−372	49
9	5	−4	683	655	28	4	6	8	459	386	73	10	6	−5	332	313	19
9	5	−5	141	178	−37	4	6	7	565	542	23	0	7	10	259	357	−58
9	5	−6	557	637	−80	4	6	6	100	103	−3	0	7	9	−566	−607	41
9	5	−7	−177	−161	−16	4	6	5	−91	−50	−41	0	7	8	801	828	−27
9	5	−8	68	107	−19	4	6	4	123	52	71	0	7	7	−742	−810	68
9	5	−9	−132	−49	−83	4	6	3	0	−163	163	0	7	6	180	198	−18
10	5	6	−573	−592	19	4	6	2	−219	−89	−130	0	7	5	−286	−304	18
10	5	5	0	59	−59	4	6	1	277	208	69	0	7	4	−219	−269	50
10	5	4	0	−349	349	4	6	0	1144	1077	67	0	7	3	−244	−313	69
10	5	3	0	110	−110	4	6	−1	−915	−822	−93	0	7	2	−81	−89	8
10	5	2	457	367	90	4	6	−2	1586	1484	102	0	7	1	274	448	−174
10	5	1	370	280	90	4	6	−3	−582	−424	−158	1	7	10	−116	−187	71
10	5	0	590	651	−61	4	6	−4	430	442	−12	1	7	9	197	40	157
10	5	−1	453	563	−110	4	6	−5	469	470	−1	1	7	8	407	373	34
10	5	−2	476	457	19	4	6	−6	321	325	−4	1	7	7	−174	−110	−64
10	5	−3	261	302	−21	4	6	−7	−495	−485	−10	1	7	6	160	150	10
10	5	−4	0	−140	140	4	6	−8	−153	−156	3	1	7	5	166	212	−46
10	5	−5	0	178	−178	4	6	−9	−283	−249	−34	1	7	4	0	77	−77
10	5	−6	125	95	30	5	6	8	396	317	79	1	7	3	433	377	56
10	5	−7	0	−221	221	5	6	7	838	714	124	1	7	2	586	563	23
11	5	4	0	−65	65	5	6	6	0	58	−58	1	7	1	244	256	−12
11	5	3	159	240	−81	5	6	5	0	217	−217	1	7	0	531	949	−418
11	5	2	377	407	−30	5	6	4	−367	−282	−85	1	7	−1	108	114	−6
11	5	1	469	432	37	5	6	3	−848	−790	−58	1	7	−2	739	793	−54
11	5	0	507	558	−51	5	6	2	−602	−506	−96	1	7	−3	−370	−403	33
11	5	−1	217	253	−36	5	6	1	−605	−503	−102	1	7	−4	−100	−43	−57
11	5	−2	−125	−189	64	5	6	0	479	465	14	1	7	−5	0	41	−41
11	5	−3	−298	−271	−27	5	6	−1	−459	−404	−55	1	7	−6	−180	−99	−81
11	5	−4	−376	−507	131	5	6	−2	742	711	31	1	7	−7	0	−2	2
11	5	−5	−371	−354	−17	5	6	−3	−791	−769	−22	1	7	−8	−261	−97	−164
12	5	0	187	245	−58	5	6	−4	−403	−399	−4	2	7	−9	−397	−353	−44
12	5	−1	263	293	−10	5	6	−5	−91	−45	−46	2	7	8	0	87	−87
12	5	−2	313	408	−95	5	6	−6	−197	−182	−15	2	7	7	631	575	56
12	5	−3	211	46	165	5	6	−7	−237	−149	−88	2	7	6	761	691	90
0	6	10	267	253	14	5	6	−8	0	−59	59	2	7	5	490	475	15
0	6	9	−299	−273	−26	5	6	−9	0	−134	134	2	7	4	193	67	126
0	6	8	845	793	52	6	6	6	0	−91	91	2	7	3	−237	−176	−61
0	6	7	−1063	−998	−65	6	6	7	512	456	56	2	7	2	−252	−244	−8
0	6	6	672	609	63	6	6	6	−460	−471	11	2	7	1	−741	−712	−29
0	6	5	−835	−790	−45	6	6	5	438	411	27	2	7	0	−100	−143	43
0	6	4	100	66	34	6	6	4	−352	−361	9	2	7	−1	237	235	2
0	6	3	−652	−611	−41	6	6	3	−306	−227	−79	2	7	−2	0	−6	6
0	6	2	−203	−206	3	6	6	2	0	43	−43	2	7	−3	91	123	−32
0	6	1	−452	−631	179	6	6	1	−445	−318	−127	2	7	−4	254	222	32
1	6	10	0	−3	3	6	6	0	−449	−282	−167	2	7	−5	0	159	−159
1	6	9	−108	−56	−52	6	6	−1	256	241	55	2	7	−6	277	260	17
1	6	8	383	402	−19	6	6	−2	326	340	−14	2	7	−7	613	698	−85
1	6	7	0	−131	131	6	6	−3	−346	−321	−25	2	7	−8	0	246	−246
1	6	6	−123	−191	68	6	6	−4	233	256	−23	2	7	−9	−197	−33	−164
1	6	5	−379	−407	28	6	6	−5	−244	−251	7	3	7	8	−277	−56	−219
1	6	4	−885	−817	−68	6	6	−6	0	−132	132	3	7	7	615	577	38
1	6	3	−332	−318	−14	6	6	−7	−153	−212	59	3	7	6	410	354	56
1	6	2	148	115	33	6	6	−8	197	246	−49	3	7	5	479	430	49
1	6	1	−1269	−617	−652	6	6	−9	−386	−350	−36	3	7	4	−81	−5	−76
1	6	0	0	45	−45	7	6	8	−312	−115	−197	3	7	3	71	168	−97
1	6	−1	309	301	8	7	6	7	116	33	83	3	7	2	−259	−228	−31
1	6	−2	410	438	−28	7	6	6	−309	−27	−282	3	7	1	−483	−453	−30
1	6	−3	0	−1	1	7	6	5	108	104	4	3	7	0	−180	−172	−8
1	6	−4	227	242	−15	7	6	4	0	−177	177	3	7	−1	−229	162	−67
1	6	−5	−958	−882	−76	7	6	3	292	160	132	3	7	−2	289	282	7
1	6	−6	−1075	−1029	−46	7	6	2	−170	−152	−18	3	7	−3	0	146	−146
1	6	−7	−136	−143	7	7	6	1	0	−45	45	3	7	−4	539	537	2
1	6	−8	−100	−145	45	7	6	0	0	−61	61	3	7	−5	−566	−526	−40
1	6	−9	−108	−221	113	7	6	−1	214	168	46	3	7	−6	−189	−210	21
2	6	10	339	339	0	7	6	−2	339	265	74	3	7	−7	−247	−197	−50
2	6	10	116	33	83	7	6	−3	280	262	18	3	7	−8	−410	−464	54
2	6	9	−160	−35	−125	7	6	−4	370	329	41	3	7	−9	0	1	−1
2	6	8	−359	−357	−2	7	6	−5	426	251	175	4	7	8	233	111	122
2	6	7	0	54	−54	7	6	−6	292	177	115	4	7	7	0	69	−69
2	6	6	0	−112	112	7	6	−7	449	374	75	4	7	6	292	211	81
2	6	5	0	73	−73	7	6	−8	241	200	41	4	7	5	0	33	−33
2	6	4	280	101	179	7	6	−9	219	37	182	4	7	4	203	139	64
2	6	3	510	450	60	8	6	6	493	346	147	4	7	3	329	262	67
2	6	2	547	494	53	8	6	5	−203	−284	81	4	7	2	0	20	−20
2	6	1	214	178	36	8	6	4	−280	−229	−51	4	7	1	−543	−484	−59
2	6	0	227	236	−9	8	6	3	−533	−473	−60	4	7	0	758	734	24
2	6	−1	597	915	82	8	6	2	0	−65	65	4	7	−1	−1051	−989	−62
2	6	−2	−1487	−1319	−168	8	6	1	−100	−260	160	4	7	−2	352	379	−27
2	6	−3	1662	1541	121	8	6	0	605	489	116	4	7	−3	0	−57	57
2	6	−4	−1925	−1785	−140	8	6	−1	254	90	164	4	7	−4	−81	−43	−38
2	6	−5	−492	−539	47	8	6	−2	333	370	−37	4	7	−5	−207	−222	15
2	6	−6	−1606	−1521	−85	8	6	−3	184	120	64	4	7	−6	0	−111	111
2	6	−7	−825	−804	−21	8	6	−4	569	459	110	4	7	−7	180	47	133
2	6	−8	−626	−520	−106	8	6	−5	0	−71	71	5	7	6	0	−86	86
2	6	−9	−108	−155	47	8	6	−6	−160	−37	−123	5	7	5	0	145	−145
3	6	10	123	122	1	8	6	−7	400	291	109	5	7	4	−214	−123	−91
3	6	9	116	97	19	9	6	4	−270	−225	−45	5	7	3	−203	−116	−85
3	6	8	416	329	87	9	6	3	−233	−205	−28	5	7	2	−430	−359	−71
3	6	7	−180	−253	73	9	6	2	−229	−97	−132	5	7	1	−116	−249	133
3	6	6	−752	−112	−640	9	6	1	299	236	63	5	7	0	321	305	16
3	6	5	−592	−582	0	9	6	0	465	475	−10	5	7	−1	−890	−925	35
3	6	4	623	518	105	9	6	−1	834	784	50	5	7	−2	−595	578	17
3	6	3	0	−2	2	9	6	−2	649	591	58	5	7	−3	−483	−439	−44
3	6	2	768	732	36	9	6	−3	638	633	5	5	7	−4	227	307	−80
3	6	1	108	160	−52	9	6	−4	0	50	−50	5	7	−5	259	284	−25
3	6	0	520	527	−7	9	6	−5	−237	−219	−18	5	7	−6	460	380	80
3	6	−1	61	24	37	9	6	−6	−270	−306	36	5	7	−7	148	143	5
3	6	−2	−1231	−1115	−116	9	6	−7	−439	−402	−36	6	7	6	−379	−389	10
3	6	−3	1350	1292	96	10	6	4	0	53	−53	6	7	5	265	337	−72
3	6	−4	−649	−606	−43	10	6	3	0	−174	174	6	7	4	−252	−97	−155

UM00017036
NOVARTIS EXHIBIT 1517
Novartis v. Regents, IPR2023-01347
Page 3905 of 4460

View Online

TABLE 3—*continued.*

h	*k*	*l*	F_o	F_c	Δ	*h*	*k*	*l*	F_o	F_c	Δ	*h*	*k*	*l*	F_o	F_c	Δ
6	7	3	261	235	23	0	8	5	469	464	5	3	8	-5	0	-60	60
6	7	2	-670	+793	+77	0	8	4	619	674	-55	4	8	4	91	1	90
6	7	1	633	563	50	0	8	3	389	373	16	4	8	3	244	80	164
6	7	0	-662	-687	25	0	8	2	116	207	-91	4	8	2	-160	-47	-113
6	7	-1	600	498	102	0	8	1	136	284	-148	4	8	1	-321	-285	-36
6	7	-2	651	557	94	1	8	7	+143	-66	+77	4	8	0	-321	-306	-15
6	7	-3	436	358	78	1	8	6	233	214	19	4	8	-1	-197	-107	-90
6	7	-4	312	290	22	1	8	5	274	345	+71	4	8	-2	-283	-251	-32
6	7	-5	412	358	54	1	8	4	701	648	53	4	8	-3	390	213	177
6	7	-6	0	38	-38	1	8	3	-148	-33	-115	4	8	-4	445	408	37
6	7	-7	-108	-257	149	1	8	2	493	503	-10	4	8	-5	0	250	-250
7	7	6	-237	-78	-159	1	8	1	-314	-434	120	5	8	4	-656	-503	-153
7	7	5	-363	-335	-28	1	8	0	0	-108	108	5	8	3	-247	-141	-106
7	7	4	-153	-72	-81	1	8	-1	-223	-301	78	5	8	2	-312	-307	-5
7	7	3	-180	-202	22	1	8	-2	-352	-349	-3	5	8	1	-170	-25	-145
7	7	2	-174	-280	106	1	8	-3	130	80	50	5	8	0	0	69	-69
7	7	1	197	124	73	1	8	-4	-0	70	+70	5	8	-1	-207	-194	-13
7	7	0	+721	+713	-8	1	8	-5	143	116	27	5	8	-2	193	20	173
7	7	-1	725	762	-37	1	8	-6	296	247	49	5	8	-3	283	339	-56
7	7	-2	0	-13	13	1	8	-7	-100	-46	-54	5	8	-4	465	418	47
7	7	-3	633	594	39	2	8	6	-277	-246	-31	5	8	-5	197	216	-19
7	7	-4	296	310	-14	2	8	5	0	48	-48	6	8	-2	+749	+729	+20
7	7	-5	377	432	-55	2	8	4	-160	-109	-51	6	8	1	160	245	-85
7	7	-6	-339	-210	-129	2	8	3	-229	-173	-56	6	8	0	-363	-392	29
7	7	-7	0	62	-62	2	8	2	203	173	30	6	8	-1	184	46	138
8	7	4	-622	-489	-133	2	8	1	-123	-104	-19	6	8	-2	-455	-417	-38
8	7	3	-252	-189	-63	2	8	0	0	76	-76	6	8	-3	0	54	-54
8	7	2	0	-17	17	2	8	-1	116	103	13	7	8	0	-579	-658	+79
8	7	1	-214	-178	-36	2	8	-2	-57	-48	-9	0	9	3	0	-42	+42
8	7	0	+321	+281	+40	2	8	-3	-116	-43	-73	0	9	2	0	-3	3
8	7	-1	-184	-93	-91	2	8	-4	0	-68	68	0	9	1	91	17	+74
8	7	-2	148	2	146	2	8	-5	81	97	-16	1	9	3	-219	+237	18
8	7	-3	153	23	130	3	8	6	0	+74	74	1	9	2	143	99	44
8	7	-4	449	534	-85	3	8	5	210	128	82	1	9	1	40	51	-11
8	7	-5	326	296	30	3	8	4	-148	-54	-94	1	9	0	0	-92	92
9	7	2	0	-38	38	3	8	3	440	486	-46	1	9	-1	180	241	-61
9	7	1	-306	-202	-104	3	8	2	-180	-85	-95	1	9	-2	-241	-276	35
9	7	0	0	-96	96	3	8	1	130	211	-81	1	9	-3	214	261	-47
9	7	-1	+301	-179	-122	3	8	0	-261	-272	11	2	9	2	184	170	14
9	7	-2	-430	-421	-9	3	8	-1	130	176	-46	2	9	1	0	148	-148
9	7	-3	0	38	-38	3	8	-2	0	-134	134	2	9	0	0	25	-25
0	8	7	143	136	+7	3	8	-3	-100	-10	-90	2	9	-1	40	159	-119
0	8	6	207	294	-87	3	8	-4	-116	-78	-38	3	9	0	-148	-234	86

fourteen peaks within 2·8 Å of the origin due to the salicylic acid residue [5] were resolved and identified. This gave the orientation of the molecule. It was then assumed that the molecules would be linked into dimers across centres of symmetry by hydrogen bonds of length 2·65 Å. This assumption, which proved to be justified, yielded positions for ten of the thirteen heavier atoms, and the chosen co-ordinates gave $R = 45\%$ for the 182 *h*0*l* reflexions. A Fourier synthesis with the *h*0*l* phased structure factors showed plausible positions for the three heavier atoms of the acetyl group, and this projection was then rapidly refined to $R = 15\%$ by Fourier and difference syntheses. The *y* co-ordinates could be chosen from a model of the molecule, and immediately gave satisfactory agreement for the 300 planes with $\sin\theta/\lambda < 0{\cdot}35$. The structure was then refined by a least-squares procedure which uses the block diagonal approximation. At first only the nine carbon and four oxygen atoms were included until R for the 2055 planes fell to 13·3% and $R'[= \sum w(|F_o| - |F_c|)^2 / \sum w|F_o|^2]$ to 1·33%. A three-dimensional difference map was then calculated with the 300 low-order planes and yielded positions for all eight hydrogen atoms, though the hydrogen atom involved in the hydrogen bond was a low peak showing considerable elongation towards the oxygen atoms with which it interacts. The hydrogen atoms were included in the refinement until R finally dropped to 10·6% and R' to 0·75%. Refinement was concluded when the maximum value of Δ/σ for a co-ordinate of a hydrogen atom had fallen to 0·3. By this time the heavier atoms had stopped moving completely. Constant weights were used, as we have found them more satisfactory for diffractometer intensities than a Cruickshank weighting scheme, which was devised for photographic intensities.[6] In all twenty-one three-dimensional least-squares refinement cycles were performed.

The least-squares programme necessarily refines the hydrogen atoms with anisotropic thermal factors if the heavier atoms are so refined. As might be expected, the thermal factors of the hydrogen atoms were often meaningless, merely reflecting the inadequacy of the data. Consequently a final set of structure factors was calculated with anisotropic thermal factors for the carbon and oxygen atoms, and mean isotropic thermal factors for the three different types of hydrogen atoms. The final value of R was 10·8%. The scattering factors were taken from International Tables. All

[5] H. Lipson and W. Cochran, "The Determination of Crystal Structures," 1953, G. Bell and Sons Ltd., London, p. 189.

[6] D. W. J. Cruickshank *et al.*, "Computing Methods and the Phase Problem in *X*-ray Crystal Analysis," 1961, Pergamon Press, London, p. 45.

Downloaded by US Patent & Trademark Office on 19 October 2010
Published on 01 January 1964 on http://pubs.rsc.org | doi:10.1039/JR9640006036

UM00017037
NOVARTIS EXHIBIT 1517
Novartis v. Regents, IPR2023-01347
Page 3906 of 4460

View Online

Downloaded by US Patent & Trademark Office on 19 October 2010
Published on 01 January 1964 on http://pubs.rsc.org | doi:10.1039/JR9640006036

TABLE 4.

Analysis of observed and calculated structure factors as a function of the index of the layer line. All figures are on an absolute scale.

k	$\Sigma\|F_o\|$	$\Sigma\|F_c\|$	$\Sigma\|\Delta\|$	N	R	$\Sigma\|\Delta\|/N$
0	1957·35	1959·25	142·02	182	0·073	0·780
1	2843·60	2868·88	229·90	332	0·081	0·693
2	2474·82	2400·10	221·04	328	0·089	0·674
3	1890·09	1873·04	179·53	304	0·095	0·591
4	1327·80	1405·83	165·09	269	0·124	0·614
5	921·21	988·13	154·60	231	0·168	0·669
6	711·04	649·85	132·69	181	0·187	0·733
7	418·06	407·14	91·04	140	0·218	0·650
8	163·78	157·69	48·87	73	0·298	0·670
9	15·00	20·55	8·19	15	0·546	0·546
All	12722·75	12730·46	1372·97	2055	0·108	0·668

calculations were carried out on an Elliott 803 computer with the programmes of Daly, Stephens, and Wheatley.[7]

Results.—The final atomic co-ordinates are given in Table 1, and the final thermal parameters in Table 2. Table 3 gives the observed and calculated structure factors obtained from the parameters given in Tables 1 and 2. In Table 4 an analysis is given of the structure factors in terms of the index of the layer. It will be seen that, although R increases substantially at higher equi-inclination angles, the absolute error in a structure factor remains approximately constant throughout.

TABLE 5.

Analysis of observed and calculated structure factors as a function of the magnitude of the observed structure factors. All figures are on an absolute scale.

Range of $\|F_o\|$	$\Sigma\|F_o\|$	$\Sigma\|F_c\|$	$\Sigma\|\Delta\|$	N	R	$\Sigma\|\Delta\|/N$
0	0	241·58	241·58	267	—	0·905
0·0— 5·0	2781·64	2637·72	616·60	1032	0·222	0·598
5·0— 10·0	2880·01	2885·18	212·61	405	0·074	0·525
10·0— 15·0	2021·92	2004·49	94·39	166	0·047	0·569
15·0— 20·0	1260·86	1237·35	63·31	72	0·050	0·879
20·0— 25·0	713·18	705·90	21·72	32	0·030	0·679
25·0— 30·0	969·72	938·46	37·44	35	0·039	1·070
30·0— 35·0	448·23	440·28	12·39	14	0·028	0·885
35·0— 40·0	228·22	219·30	8·92	6	0·039	1·487
40·0— 45·0	416·57	404·03	14·32	10	0·034	1·432
45·0— 50·0	188·48	189·67	6·77	4	0·036	1·693
50·0— 55·0	210·60	200·82	10·04	4	0·048	2·510
55·0— 60·0	57·02	54·94	2·08	1	0·036	2·080
60·0— 65·0	61·23	58·05	3·18	1	0·052	3·180
65·0— 70·0	67·04	68·50	1·46	1	0·022	1·460
70·0— 75·0	147·89	152·66	4·77	2	0·032	2·385
75·0— 80·0	—	—	—	—	—	—
80·0— 85·0	—	—	—	—	—	—
85·0— 90·0	175·43	183·49	8·96	2	0·051	4·480
90·0— 95·0	—	—	—	—	—	—
95·0—100·0	95·61	108·04	12·43	1	0·130	12·430

In Table 5 a similar analysis is given, but in terms of the magnitudes of the observed structure factors. R is poor for the very weak reflexions (and, of course, infinite, for those that are accidentally absent), but again, in terms of absolute errors, there is no reason to reject these weak planes. Indeed the evidence suggests that the twenty or thirty strongest planes should be down-weighted with respect to the weak planes. We feel that such satisfactory results for the weaker planes can be achieved with the diffractometer only if the size of the crystal or the counting time is so adjusted that the intensities yield structure factors that are on about absolute scale.

The bond lengths are given in Fig. 1, which also shows the labelling of the atoms. The bond angles are given in Table 6. Fig. 2 shows the structure as it appears when projected down the [b]

[7] J. J. Daly, F. S. Stephens, and P. J. Wheatley, 1963, *MRSA Final Report*, No. 52.

UM00017038
NOVARTIS EXHIBIT 1517
Novartis v. Regents, IPR2023-01347
Page 3907 of 4460

View Online

axis. The bond lengths are in fair agreement with those found in salicylic acid by Cochran,[8] though there are some very significant differences. The results for the two molecules are compared in Fig. 3. There are some very definite angular distortions within the molecule, both in the benzene ring and the carboxyl group, but, more particularly, in the acetyl group. The benzene

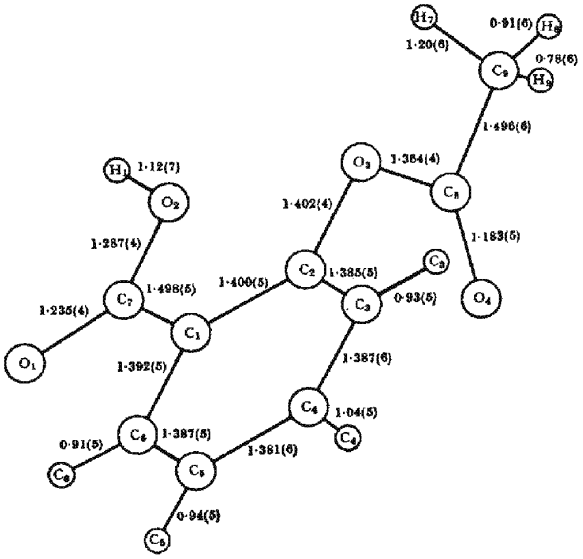


FIG. 1. Bond lengths in aspirin with their standard deviations, and the labelling of the atoms.

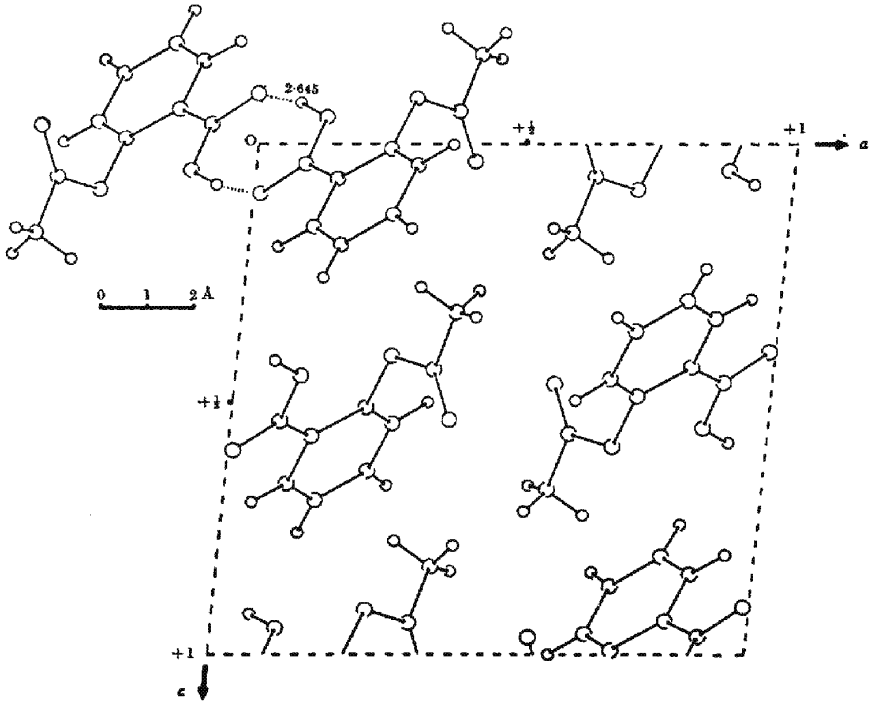


FIG. 2. The structure of aspirin as it appears in projection down [*b*].

[8] W. Cochran, *Acta Cryst.*, 1953, **6**, 260.

Downloaded by US Patent & Trademark Office on 19 October 2010
Published on 01 January 1964 on http://pubs.rsc.org | doi:10.1039/JR9640006036

UM00017039
NOVARTIS EXHIBIT 1517
Novartis v. Regents, IPR2023-01347
Page 3908 of 4460

View Online

TABLE 6.

Bond angles (°). Standard deviations are given as units in the last place.

H(1)O(2)C(7)	120·7 (37)	O(3)C(8)O(4)	122·9 (3)	C(2)C(3)C(4)	119·8 (4)
O(2)C(7)O(1)	122·9 (3)	O(3)C(8)C(9)	110·7 (3)	C(3)C(4)H(4)	121·6 (26)
O(2)C(7)C(1)	118·1 (3)	O(4)C(8)C(9)	126·4 (4)	C(5)C(4)H(4)	118·4 (26)
O(1)C(7)C(1)	119·1 (3)	C(8)C(9)H(7)	110·0 (29)	C(3)C(4)C(5)	120·0 (4)
C(7)C(1)C(2)	124·6 (3)	C(8)C(9)H(8)	119·4 (38)	C(4)C(5)H(5)	120·0 (29)
C(7)C(1)C(6)	117·7 (3)	C(8)C(9)H(9)	115·9 (44)	C(6)C(5)H(5)	120·1 (29)
C(6)C(1)C(2)	117·7 (3)	H(7)C(9)H(8)	98·7 (48)	C(4)C(5)C(6)	119·9 (4)
C(1)C(2)O(3)	121·6 (3)	H(7)C(9)H(9)	100·9 (52)	C(5)C(6)H(6)	118·5 (29)
C(3)C(2)O(3)	117·3 (3)	H(8)C(9)H(9)	108·9 (58)	C(1)C(6)H(6)	119·9 (29)
C(1)C(2)C(3)	121·0 (3)	C(2)C(3)H(3)	118·0 (29)	C(5)C(6)C(1)	121·6 (3)
C(2)O(3)C(8)	115·7 (3)	C(4)C(3)H(3)	122·2 (29)		

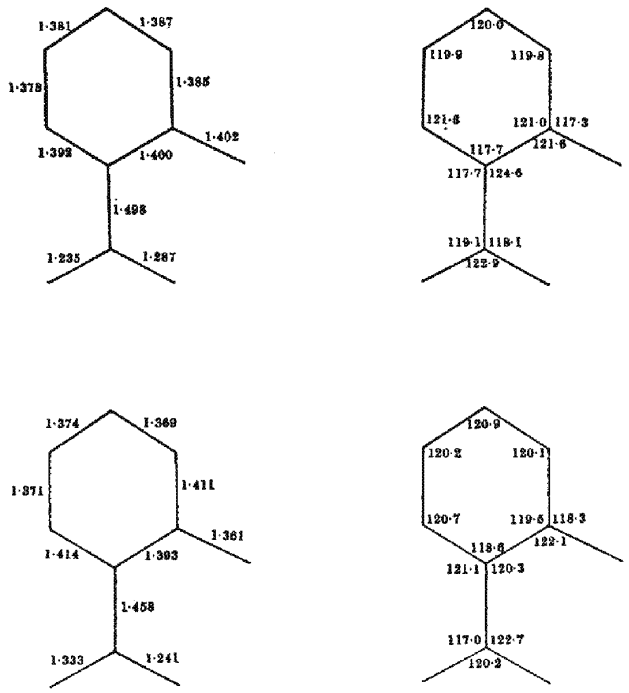


FIG. 3. Comparison of the bond lengths and angles in aspirin (above) and salicylic acid (below).

ring has the appearance of being pulled out by the carboxyl group so that the internal angles at C(2) and C(6) are greater than 120°, and that at C(1) is less. The carboxyl group is bent away from the acetyl group, possibly by repulsion between O(3) and O(2), so that there is a substantial increase in the angle C(2)C(1)C(7), and a decrease in C(6)C(1)C(7). The angle O(1)C(7)O(2) is greater than 120°, again suggesting repulsion between oxygen atoms. The angular distortions at the central atom of the acetyl group are enormous, the angles being 110·7, 122·9, and 126·4°, instead of the expected 120°. There appears to be no simple explanation for these distortions in terms of intramolecular contacts.

Except for hydrogen atoms on the methyl group, the molecule is composed of atoms lying approximately in two planes. The weighted least-squares equation for the plane of the four atoms in the acetyl group, referred to orthogonal axes a, b, and c', is

$$+0{\cdot}7512\,X + 0{\cdot}6577\,Y - 0{\cdot}0564\,Z' = 4{\cdot}3680.$$

The departures of the atoms from this plane are O(3), +0·0007; O(4), +0·0009; C(8), −0·0030; C(9), +0·0011 Å, none of which is significant. Thus, despite the large angular distortions within the plane of this group, there is no out-of-plane bending. On the other hand no satisfactory plane can be constructed through all ten of the heavier atoms of the salicylic acid residue. A number of

Downloaded by US Patent & Trademark Office on 19 October 2010
Published on 01 January 1964 on http://pubs.rsc.org | doi:10.1039/JR9640006036

UM00017040
NOVARTIS EXHIBIT 1517
Novartis v. Regents, IPR2023-01347
Page 3909 of 4460

View Online

planes were calculated, starting first with the benzene ring, and then adding one or more of the remaining four atoms. As soon as any other single atom was added, the departures from the plane increased, and these departures grew worse as more atoms were added. There seems to be no question that significant out-of-plane distortions do occur in the salicylic acid residue. It was particularly noticeable that one of the oxygen atoms of the carboxyl group always lay above the plane, and the other below, leading to the conclusion that the plane of the carboxyl group was twisted with respect to the plane of the benzene ring. In view of these various distortions it was felt that the most representative plane was the one through the six carbon atoms of the benzene ring, the equation of which is

$$+0{\cdot}5945\,X - 0{\cdot}4849\,Y + 0{\cdot}6415\,Z' = 0{\cdot}0941.$$

The departures of the atoms from this plane are given in Table 7. It will be seen that none of the carbon or hydrogen atoms of the benzene ring departs from this plane, whereas the other atoms,

TABLE 7.

Departure in Å of the atoms of the salicylic acid residue from the plane of the benzene ring.

Atom		Atom		Atom	
C(1)	−0·0031	H(1)	−0·138	O(1)	+0·1016
C(2)	+0·0050	H(3)	+0·012	O(2)	−0·0555
C(3)	−0·0026	H(4)	+0·019	O(3)	−0·0565
C(4)	−0·0016	H(5)	+0·009	C(7)	−0·0097
C(5)	+0·0034	H(6)	−0·021		
C(6)	−0·0011				

with the exception of C(7), do. The angle between the plane of the benzene ring and that of the acetyl group is 84° 45′.

The equation of the plane through the carboxyl group is

$$+0{\cdot}6091\,X - 0{\cdot}5022\,Y + 0{\cdot}6139\,Z' = 0{\cdot}0596.$$

H(1) departs from this plane by −0·064 Å, which is not significant. The angle between the plane of the benzene ring and that of the carboxyl group is 2° 2′.

Molecules of aspirin are, as expected, dimerized by hydrogen bonds across a centre of symmetry. The length of each hydrogen bond is 2·645 Å. The perpendicular distance between the two planes defined by the carboxyl groups in the dimer is 0·119 Å, which places aspirin roughly halfway down the table given by Jeffrey and Sax.[9] The weighted least-squares plane through the six heavier atoms of the eight-membered dimer ring is

$$+0{\cdot}5901\,X - 0{\cdot}5348\,Y + 0{\cdot}6084\,Z' = 0.$$

The departure of the atoms from this plane are O(1), +0·0089; O(2), +0·0077; C(7), −0·0151; H(1), −0·013 Å. Thus the eight atoms are very nearly coplanar, as would be expected from Robertson's arguments.[10]

All non-bonded intramolecular contacts were calculated in order to disclose any unusual features within the molecule. If hydrogen atoms are excluded, the two shortest intramolecular contacts are O(1)····O(2), 2·215; O(3)····O(4), 2·239 Å. Other distances of interest in connexion with the possibility of repulsion are O(2)····O(3), 2·674; O(3)····C(9), 2·354; O(4)····C(9), 2·395; C(2)····C(8), 2·342 Å. Inclusion of the hydrogen atoms results in a number of contacts of slightly less than 2 Å between hydrogen atoms on the benzene ring and next-nearest carbon atoms, and three shorter contacts between hydrogen atoms on the methyl group.

All van der Waals's contacts up to a limit of 4 Å were calculated both with and without hydrogen atoms. There is a large number of these distances, but no unusual features appear. If hydrogen atoms are excluded, the shortest contact, apart from the hydrogen bond, is 3·306 Å between two oxygen atoms. The shortest contact between hydrogen atoms is 2·50 Å.

MONSANTO RESEARCH S.A., BINZSTRASSE, 39, 8045 ZÜRICH, SWITZERLAND.

[*Received, July* 31*st*, 1964.]

[9] G. A. Jeffrey and M. Sax, *Acta Cryst.*, 1963, **16**, 430.
[10] J. H. Robertson, *Acta Cryst.*, 1964, **17**, 316.

Published on 01 January 1964 on http://pubs.rsc.org | doi:10.1039/JR9640006036
Downloaded by US Patent & Trademark Office on 19 October 2010

UM00017041
NOVARTIS EXHIBIT 1517
Novartis v. Regents, IPR2023-01347
Page 3910 of 4460

UNITED STATES PATENT AND TRADEMARK OFFICE

UNITED STATES DEPARTMENT OF COMMERCE
United States Patent and Trademark Office
Address: COMMISSIONER FOR PATENTS
P.O. Box 1450
Alexandria, Virginia 22313-1450
www.uspto.gov

APPLICATION NO.	FILING DATE	FIRST NAMED INVENTOR	ATTORNEY DOCKET NO.	CONFIRMATION NO.
12/861,203	08/23/2010	Orn Almarsson	TPI.5070XCD1	1584

23557 7590 04/13/2011

SALIWANCHIK, LLOYD & EISENSCHENK
A PROFESSIONAL ASSOCIATION
PO Box 142950
GAINESVILLE, FL 32614

EXAMINER	
BROOKS, CLINTON A	

ART UNIT	PAPER NUMBER
1621	

NOTIFICATION DATE	DELIVERY MODE
04/13/2011	ELECTRONIC

Please find below and/or attached an Office communication concerning this application or proceeding.

The time period for reply, if any, is set in the attached communication.

Notice of the Office communication was sent electronically on above-indicated "Notification Date" to the following e-mail address(es):

euspto@slepatents.com

UM00017042
NOVARTIS EXHIBIT 1517
Novartis v. Regents, IPR2023-01347
Page 3911 of 4460

Office Action Summary	Application No.	Applicant(s)	
	12/861,203	ALMARSSON ET AL.	
	Examiner	Art Unit	
	CLINTON BROOKS	1621	

-- The MAILING DATE of this communication appears on the cover sheet with the correspondence address --

Period for Reply

A SHORTENED STATUTORY PERIOD FOR REPLY IS SET TO EXPIRE 3 MONTH(S) OR THIRTY (30) DAYS, WHICHEVER IS LONGER, FROM THE MAILING DATE OF THIS COMMUNICATION.

- Extensions of time may be available under the provisions of 37 CFR 1.136(a). In no event, however, may a reply be timely filed after SIX (6) MONTHS from the mailing date of this communication.
- If NO period for reply is specified above, the maximum statutory period will apply and will expire SIX (6) MONTHS from the mailing date of this communication.
- Failure to reply within the set or extended period for reply will, by statute, cause the application to become ABANDONED (35 U.S.C. § 133). Any reply received by the Office later than three months after the mailing date of this communication, even if timely filed, may reduce any earned patent term adjustment. See 37 CFR 1.704(b).

Status

1)☒ Responsive to communication(s) filed on *26 January 2011*.

2a)☒ This action is **FINAL**. 2b)☐ This action is non-final.

3)☐ Since this application is in condition for allowance except for formal matters, prosecution as to the merits is closed in accordance with the practice under *Ex parte Quayle*, 1935 C.D. 11, 453 O.G. 213.

Disposition of Claims

4)☒ Claim(s) *1-8* is/are pending in the application.

4a) Of the above claim(s) *3 and 6* is/are withdrawn from consideration.

5)☐ Claim(s) _____ is/are allowed.

6)☒ Claim(s) *1-2, 4-5, 7-8* is/are rejected.

7)☐ Claim(s) _____ is/are objected to.

8)☐ Claim(s) _____ are subject to restriction and/or election requirement.

Application Papers

9)☐ The specification is objected to by the Examiner.

10)☐ The drawing(s) filed on _____ is/are: a)☐ accepted or b)☐ objected to by the Examiner.

Applicant may not request that any objection to the drawing(s) be held in abeyance. See 37 CFR 1.85(a).

Replacement drawing sheet(s) including the correction is required if the drawing(s) is objected to. See 37 CFR 1.121(d).

11)☐ The oath or declaration is objected to by the Examiner. Note the attached Office Action or form PTO-152.

Priority under 35 U.S.C. § 119

12)☐ Acknowledgment is made of a claim for foreign priority under 35 U.S.C. § 119(a)-(d) or (f).

a)☐ All b)☐ Some * c)☐ None of:

1.☐ Certified copies of the priority documents have been received.

2.☐ Certified copies of the priority documents have been received in Application No. _____.

3.☐ Copies of the certified copies of the priority documents have been received in this National Stage application from the International Bureau (PCT Rule 17.2(a)).

* See the attached detailed Office action for a list of the certified copies not received.

Attachment(s)

1) ☐ Notice of References Cited (PTO-892)
2) ☐ Notice of Draftsperson's Patent Drawing Review (PTO-948)
3) ☐ Information Disclosure Statement(s) (PTO/SB/08) Paper No(s)/Mail Date _____.
4) ☐ Interview Summary (PTO-413) Paper No(s)/Mail Date. _____ .
5) ☐ Notice of Informal Patent Application
6) ☐ Other: _____.

UM00017043
NOVARTIS EXHIBIT 1517
Novartis v. Regents, IPR2023-01347
Page 3912 of 4460

DETAILED ACTION

This action if **FINAL**.

Status of Claims

Claims 1-2, 4-5 are currently pending. Claims 3 and 6 stand withdrawn. Claims 7-8 are newly added.

Restriction Requirement

Applicants' election of Group I, claims 1-2, and 4-5 without traverse in the response received January 26, 2011 is acknowledged.

Response to Applicants' Arguments

In the response received January 26, 2011, Applicants requested the courtesy of an interview. An interview will gladly be granted upon formal request.. Examiner's contact information is found at the end of the action.

With respect to the 102(b) rejection in view of the Summers article, Applicants argue that "[o]nly when the Patent Office shows a sound basis for believing that the products of the applicant and the prior art are the same does applicant have the burden of showing that the products are not the same", citing In re Spada, 911 F.2d 705, 709, 15 USPQ2d 1655, 1658 (Fed. Cir. 1990). Applicants' continue stating that the claimed polymorphic form has been compared to polymorphic Form I of acetylsalicylic acid in the as-filed application. The comparison between IR spectra of Form I with the instant Form, Applicants assert is different and therefore the forms are different. In addition, Applicants argue that the DSC has an endothermic transition of 135 degrees C and a melting point of 133 degrees Celsius is outside of Applicants 135.5 and

melting point between about 128 and 130. However, this has been considered but is not persuasive... The amount of experimental error in such determinations is not mentioned with respect to IR and DSC, and in light of Applicants claim of about 128 to 130 degrees Celsius it is clear that a range of temperature can exist for a melting point. Thus, as stated in the rejection of record the burden has shifted to Applicant.

Further, Applicant states that there was only a single form of acetylsalicylic acid known prior to filing the instant application (page 7 of instant specification):

> The previously known form of acetylsalicylic acid, herein referred to as acetylsalicylic acid, Form I, or acetylsalicylic acid Form I, is commercially available by Bayer AG.

However, the Summers article suggests other forms. If Applicant is stating that the forms of the Summers article are the same form then clearly ranges in DSC traces and melting points are possible.

With respect the 102(b) rejection in view of Wheatly as evidenced by the first and second bond article, Applicants argue that the office action ignores aspects of the first Bond article. However, this is not persuasive because at least because the authors of the first Bond article state that "from the data of which the Form II structure emerged, as we have shown is possible" so from the dataset either Form I or the potential Form II could emerge.

Further, that inherency cannot be established by possibility or probability. However, according to ME 2112:

V. ONCE A REFERENCE TEACHING PRODUCT APPEARING TO BE SUBSTANTIALLY IDENTICAL IS MADE THE BASIS OF A REJECTION, AND THE EXAMINER PRESENTS EVIDENCE OR REASONING TENDING TO SHOW

INHERENCY, THE BURDEN SHIFTS TO THE APPLICANT TO SHOW AN UNOBVIOUS DIFFERENCE

"[T]he PTO can require an applicant to prove that the prior art products do not necessarily or inherently possess the characteristics of his [or her] claimed product. Whether the rejection is based on 'inherency' under 35 U.S.C. 102, on 'prima facie obviousness' under 35 U.S.C. 103, jointly or alternatively, the burden of proof is the same...[footnote omitted]." The burden of proof is similar to that required with respect to product-by-process claims. In re Fitzgerald, 619 F.2d 67, 70, 205 USPQ 594, 596 (CCPA 1980) (quoting In re Best, 562 F.2d 1252, 1255, 195 USPQ 430, 433-34 (CCPA 1977)).

The burden of proof for inherency in product-by-process claims referred to in that paragraph is found in MPEP 2113:

ONCE A PRODUCT APPEARING TO BE SUBSTANTIALLY IDENTICAL IS FOUND AND A 35 U.S.C. 102/ 103 REJECTION MADE, THE BURDEN SHIFTS TO THE APPLICANT TO SHOW AN UNOBVIOUS DIFFERENCE

"The Patent Office bears a lesser burden of proof in making out a case of prima facie obviousness for product-by-process claims because of their peculiar nature" than when a product is claimed in the conventional fashion. In re Fessmann, 489 F.2d 742, 744, 180 USPQ 324, 326 (CCPA 1974). Once the examiner provides a rationale tending to show that the claimed product appears to be the same or similar to that of the prior art, although produced by a different process, the burden shifts to applicant to come forward with evidence establishing an unobvious difference between the claimed product and the prior art product. In re Marosi, 710 F.2d 798, 802, 218 USPQ 289, 292 (Fed. Cir. 1983) (The claims were directed to a zeolite manufactured by mixing together various inorganic materials in solution and heating the resultant gel to form a crystalline metal silicate essentially free of alkali metal. The prior art described a process of making a zeolite which, after ion exchange to remove alkali metal, appeared to be "essentially free of alkali metal." The court upheld the rejection because the applicant had not come forward with any evidence that the prior art was not "essentially free of alkali metal" and therefore a different and unobvious product.).

The statement of the Bond article that "[i]ndeed, we showed that form II of aspirin as reported be derived, to the accuracy and precision reported by those workers, from experimental diffraction data collected on an aspirin crystal that was most certainly form I" suggests that the dataset encompasses the "old form" and if there is a new form, that form as well. Thus, the

dataset claimed is a broad genus and encompasses multiple species, one of which is the old form of Wheatly.

Claim Rejections – 35 USC § 102

The following is a quotation of the appropriate paragraphs of 35 U.S.C. 102 that form the basis for the rejections under this section made in this Office action:

> A person shall be entitled to a patent unless –
>
> (b) the invention was patented or described in a printed publication in this or a foreign country or in public use or on sale in this country, more than one year prior to the date of application for patent in the United States.

Claims 1-2, 4-5, 7-8 are rejected under 35 USC 102(b) as being unpatentable over the article to Summers, M.P. et al. ("the Summers article" made of record in the IDS dated August 23, 2010).

The Summers article teaches multiple forms of acetylsalicylic acid (at least Table 1). Further, the Summers article teaches a form of acetylsalicylic acid having a melting point within the range recited by Applicants. For example, the Summers article teaches Form I, the DSC melting point is 135 degrees Celsius. Further, the Summers article teaches Form I in 96% ethanol. The definition of "Form" is arbitrary, and the data teaches 135 degrees which anticipates "about 135.5".

In addition, the Summers article teaches Form II having a melting point of 128 degrees Celsius and 129 by DSC. In addition, the Summers article teaches Forms I, III, IV, V, and VI. Further, the Summers article teaches that tablets can be made "with the tabletting characteristics of various polymorphic forms" (page 615), and that the compound can be dissolved in pentanol (page 615) thus teaching compositions.

According to MPEP 2112: "[T]he PTO can require an applicant to prove that the prior art products do not necessarily or inherently possess the characteristics of his [or her] claimed product. Whether the rejection is based on inherency' under 35 U.S.C. 102, on prima facie obviousness' under 35 U.S.C. 103, jointly or alternatively, the burden of proof is the same...[footnote omitted]." The burden of proof is similar to that required with respect to product-by-process claims. In re Fitzgerald, 619 F.2d 67, 70, 205 USPQ 594, 596 (CCPA 1980) (quoting In re Best, 562 F.2d 1252, 1255, 195 USPQ 430, 433-34 (CCPA 1977)).

In this case the Summers article teaches a Form I with a melting point that is within 0.5 degrees Celsius of the claimed compound. Further, the claims recite "about 135.5" which is anticipated by 135 degrees Celsius of Form I. As stated in the initial rejection, the PTO can require an applicant to prove that the prior art products do not necessarily or inherently possess the characteristics of his [or her] claimed product. If Applicant produces evidence that proves that the forms in the Summers article are not the same as the form recited in the instant claims then this rejection will be withdrawn. Specifically, a 1.132 affidavit differentiating Form I and Form II as disclosed by Summers from the instant form would be sufficient to overcome the burden of proof required by the PTO for this rejection.

Further, with respect to the claimed range, claim 1 still reads on at least Form I of the art of record because the limitation "about 128-130 degrees C" is still met. As stated in the rejection of record, Form I, the DSC melting point is 135 degrees Celcius and the claims reads "about 135", further, Form I teaches a melting point of 133 degrees Celsius and the claim reads "about 128-130 degree C". The broadest reasonable interpretation is that the "about" is distributed between the two temperature ranges since that claim links the temperatures by a dash mark.

Claims 1-2, 4, 7-8 are rejected under 35 USC 102(b) as being unpatentable over the article to Wheatley, P.L.. ("the Wheatley article", J. Chem. Soc. 1964, 6036) as evidenced by the article to Bond et al. ("the first Bond article"), and the article to Bond et al. ("the second Bond article").

The Wheatley article teaches a polymorphic form of acetylsalicylic acid. Further, the Wheatley article teaches "…of this remarkable drug." (page 6036). Thus, the Wheatley article teaches a pharmaceutical dosage form that is effective since it must be effective to be remarkable.

The evidentiary references are brought forward for at least two reasons. First, the first Bond article provides evidence that the data set as instantly claimed "was completely superimposable on the PZ structure". Specifically, the first Bond article teaches:

> At the outset, we noted several anomalous indicators in the PZ structure: 1) The data are truncated to $2\theta = 40°$ ($Mo_{K\alpha}$); 2) The *R*-factors are unacceptably large ($R1$-$[I>2\sigma(I)] = 0.162$, $wR2$(all data) = 0.308; 3) All atoms are refined isotropically, implying that anisotropic refinement was not possible; 4) Several of the refined U_{iso} values are zero or disturbingly close to zero. Most revealingly, we noted that the unit cell reported by PZ [$a = 12.095(7)$, $b = 6.491(4)$, $c = 11.323(6)$ Å, $\beta = 111.509(9)°$, $V = 827.1(8)$ Å^3] can be transformed to the cell obtained by us for form I with the metric transformation [1 0 ½ 0 −1 0 0 0 −1]. Likewise, our experimental form I cell can be transformed to a cell having $a = 12.084$, $b = 6.552$, $c = 11.274$ Å, $\beta = 111.81°$, $V = 828.7$ Å^3. This is depicted schematically in Figure 1.
>
> We next returned to our experimental diffraction data and applied this relationship so that our data were indexed on the basis of the PZ unit cell.[8] Subsequent integration and data reduction was followed by a straightforward structure solution with direct methods,[9] using default settings in the space group $P2_1/c$ obtained automatically by the software. The result (Figure 1) was completely superimposable on the PZ structure! Isotropic refinement on data to $2\theta = 50°$ proceeded

Since the data as claimed can be refined to that of form I, the claim reads on the known polymorphic form disclosed in Wheatley.

The second Bond article provides additional evidence (page 618):

> crystal.[8] Indeed, we showed that form II of aspirin as reported by PZ may be derived, to the accuracy and precision reported by those workers, from experimental diffraction data collected on an aspirin crystal that was most certainly form I.

> Thus, we stressed that the PZ report did not establish the existence of aspirin form II to any acceptable level of scientific rigor.[1] In this report, we are able to resolve the

Thus, there is sufficient evidence that the claims read on at least "form I" which is a known form (see Wheatley).

Further, the second Bond article provides evidence that

> close packing of spheres, for example).[13] The aspirin case is apparently the first of its kind in that it exhibits two distinctly different interlayer arrangements (**A** and **B**), both of which are physically and chemically reasonable. The accidental energetic degeneracy of the two possibilities,[5,6] combined with the specific metric relation between the form I and form II lattices, is the reason for the unusual crystallographic observations, since it allows aspirin diffraction patterns to be processed in two different ways to provide two different structures, both of which are physically reasonable. The metric transformation {1 0 ½ 0 −1 0 0 0 −1} that relates the form I and form II unit cells causes all Bragg reflections *hkl* with even *l* to overlay but places the odd *l* reflections of form II halfway between those of form I.[14] Thus, the Bragg reflections arising from the two types of domain appear to a first approximation as a weighted overlay of the form I and form II diffraction patterns, with the distribution dependent

And from page 621:

> reference points. However, considering that aspirin crystals display both arrangements within a single crystal, should aspirin really be described as polymorphic? What is certain is that the PZ description of their crystal as a polymorph distinct from form I is not justifiable. The PZ crystal, like several other aspirin crystals described in this paper, is an intergrowth of two "polymorphic" domains. We emphasize that the intergrowth crystals are exactly that: they are not simply mixtures of form I and form II, and they are not twins. Each aspirin crystal is an integral whole in which the domains are intimately connected with each other, with possibly many turnovers of domain within a single crystal. Further, it seems that the ratio of the domains in aspirin crystals is likely to be constant in any particular batch prepared under the same conditions.

The evidence of the second bond article show that "[w]hat is certain is that the PZ description of their crystal as a polymorph distinct from form I is not justifiable".

Thus, in light of evidence, the claims read on form I as disclosed by Wheatley.

Conclusion

No claims are allowed.

Applicant's amendment necessitated the new ground(s) of rejection presented in this Office action. Accordingly, **THIS ACTION IS MADE FINAL**. See MPEP § 706.07(a). Applicant is reminded of the extension of time policy as set forth in 37 CFR 1.136(a).

A shortened statutory period for reply to this final action is set to expire THREE MONTHS from the mailing date of this action. In the event a first reply is filed within TWO MONTHS of the mailing date of this final action and the advisory action is not mailed until after the end of the THREE-MONTH shortened statutory period, then the shortened statutory period will expire on the date the advisory action is mailed, and any extension fee pursuant to 37

CFR 1.136(a) will be calculated from the mailing date of the advisory action. In no event, however, will the statutory period for reply expire later than SIX MONTHS from the date of this final action.

Any inquiry concerning this communication or earlier communications from the examiner should be directed to CLINTON BROOKS whose telephone number is (571)270-7682. The examiner can normally be reached on Monday-Friday 8:00 AM to 5:00 PM EST.

If attempts to reach the examiner by telephone are unsuccessful, the examiner's supervisor, DANIEL SULLIVAN can be reached on (571)272-0779. The fax phone number for the organization where this application or proceeding is assigned is 571-273-8300.

Information regarding the status of an application may be obtained from the Patent Application Information Retrieval (PAIR) system. Status information for published applications may be obtained from either Private PAIR or Public PAIR. Status information for unpublished applications is available through Private PAIR only. For more information about the PAIR system, see http://pair-direct.uspto.gov. Should you have questions on access to the Private PAIR system, contact the Electronic Business Center (EBC) at 866-217-9197 (toll-free). If you would like assistance from a USPTO Customer Service Representative or access to the automated information system, call 800-786-9199 (IN USA OR CANADA) or 571-272-1000.

Cab

/Daniel M Sullivan/
Supervisory Patent Examiner, Art Unit 1621

Electronic Acknowledgement Receipt

EFS ID:	10528788
Application Number:	10378956
International Application Number:	
Confirmation Number:	4742
Title of Invention:	Multiple-component solid phases containing at least one active pharmaceutical ingredient
First Named Inventor/Applicant Name:	Michael J. Zaworotko
Customer Number:	23557
Filer:	Glenn Ladwig/Jennifer Rogers
Filer Authorized By:	Glenn Ladwig
Attorney Docket Number:	USF.106XC1
Receipt Date:	15-JUL-2011
Filing Date:	03-MAR-2003
Time Stamp:	13:12:59
Application Type:	Utility under 35 USC 111(a)

Payment information:

Submitted with Payment	no

File Listing:

Document Number	Document Description	File Name	File Size(Bytes)/ Message Digest	Multi Part /.zip	Pages (if appl.)
1		SIDS10.pdf	434254 365e6287f1fc83cae161031e7bbab11d70368a67	yes	4

	Multipart Description/PDF files in .zip description				
	Document Description		**Start**	**End**	
	Transmittal Letter		1	2	
	Information Disclosure Statement (IDS) Form (SB08)		3	4	
Warnings:					
Information:					
2	Non Patent Literature	Bond.pdf	304384 1594a762a10d3552141ad9742b9b22be23a730b5	no	3
Warnings:					
Information:					
3	Non Patent Literature	Bond-Crystalline.pdf	528734 87fe4d66539c95170b1a7fd7a44d0969d140137d	no	5
Warnings:					
Information:					
4	Non Patent Literature	Summers.pdf	760560 a353a15580ec94882ffb9d68835657691b6b87dc	no	2
Warnings:					
Information:					
5	Non Patent Literature	Wheatly.pdf	808361 98022e97dd197d3d8ffe39f2df7dd6f328fb5987	no	13
Warnings:					
Information:					
6	Non Patent Literature	FOA04-13-2011.pdf	538380 214602408570e3d56f6053bf324a8c3dd7e1e3e0	no	12
Warnings:					
Information:					
		Total Files Size (in bytes):	3374673		

This Acknowledgement Receipt evidences receipt on the noted date by the USPTO of the indicated documents, characterized by the applicant, and including page counts, where applicable. It serves as evidence of receipt similar to a Post Card, as described in MPEP 503.

New Applications Under 35 U.S.C. 111

If a new application is being filed and the application includes the necessary components for a filing date (see 37 CFR 1.53(b)-(d) and MPEP 506), a Filing Receipt (37 CFR 1.54) will be issued in due course and the date shown on this Acknowledgement Receipt will establish the filing date of the application.

National Stage of an International Application under 35 U.S.C. 371

If a timely submission to enter the national stage of an international application is compliant with the conditions of 35 U.S.C. 371 and other applicable requirements a Form PCT/DO/EO/903 indicating acceptance of the application as a national stage submission under 35 U.S.C. 371 will be issued in addition to the Filing Receipt, in due course.

New International Application Filed with the USPTO as a Receiving Office

If a new international application is being filed and the international application includes the necessary components for an international filing date (see PCT Article 11 and MPEP 1810), a Notification of the International Application Number and of the International Filing Date (Form PCT/RO/105) will be issued in due course, subject to prescriptions concerning national security, and the date shown on this Acknowledgement Receipt will establish the international filing date of the application.

I hereby certify that this correspondence is being electronically filed in the United States Patent and Trademark Office on July 15, 2011.

Glenn P. Ladwig

Glenn P. Ladwig, Patent Attorney, Reg. # 46,853

SUPPLEMENTAL INFORMATION DISCLOSURE STATEMENT
Patent Application
Docket No. USF.106XC1
Serial No. 12/861,203

IN THE UNITED STATES PATENT AND TRADEMARK OFFICE

Examiner	:	Sahar Javanmard
Art Unit	:	1627
Applicants	:	Michael J. Zaworotko, Brian Moulton, Nair Rodriguez-Hornedo
Serial No.	:	12/861,203
Filed	:	March 3, 2003
Conf. No.	:	4742
For	:	Multiple-Component Solid Phases Containing at Least One Active Pharmaceutical Ingredient

Mail Stop Amendment
Commissioner for Patents
P.O. Box 1450
Alexandria, VA 22313

SUPPLEMENTAL INFORMATION DISCLOSURE STATEMENT
UNDER 37 C.F.R. §§ 1.97 AND 1.98

Sir:

In accordance with 37 C.F.R. § 1.56, the references listed on the attached form PTO/SB/08 are being brought to the attention of the Examiner for consideration in connection with the examination of the above-identified patent application. Copies of the cited references are enclosed. However, Applicants have not submitted a copy of the published U.S. Patent Application cited on attached Form PTO/SB/08 pursuant to 37 CFR 1.98(a)(2)(ii).

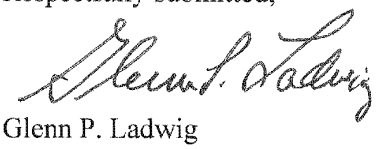
It is respectfully requested that the references cited on the attached form PTO/SB/08 be considered in the examination of the subject application and that their consideration be made of record.

J:\USF\106XC1\PTO\SIDS10.doc/jar

This information is being submitted subsequent to the filing of a Request for Continued Examination, but before the mailing of an Office Action on the merits. If any fee is required please use Deposit Account No. 19-0065.

Applicants respectfully assert that the substantive provisions of 37 C.F.R. §§ 1.97 and 1.98 are met by the foregoing statement.

Respectfully submitted,



Glenn P. Ladwig
Patent Attorney
Registration No. 46,853
Phone No.: 352-375-8100
Fax No.: 352-372-5800
Address: P.O. Box 142950
Gainesville, FL 32614-2950

GPL/jar
Attachments: Form PTO/SB/08; copies of references cited therein.

J:\USF\106XC1\PTO\SIDS10.doc/jar

Substitute for form 1449A/PTO

INFORMATION DISCLOSURE STATEMENT BY APPLICANT

(use as many sheets as necessary)

Sheet	1	of	2

Complete if Known	
Application Number	10/378,956
Filing Date	March 3, 2003
First Named Inventor	Michael J. Zaworotko
Art Unit	1627
Examiner Name	Sahar Javanmard
Attorney Docket Number	USF.106XC1

U.S. PATENT DOCUMENTS

Examiner Initials*	Cite No. [1]	Document Number Number - Kind Code[2] (if known)	Publication Date MM-DD-YYYY	Name of Patentee or Applicant of Cited Document	Pages, Columns, Lines, Where Relevant Passages or Relevant Figures Appear
	U1				
	U2				
	U3				
	U4				
	U5				
	U6				
	U7				
	U8				
	U9				

FOREIGN PATENT DOCUMENTS

Examiner Initials*	Cite No. [1]	Foreign Patent Document Country Code [3] - Number [4] - Kind Code[5] (if known)	Publication Date MM-DD-YYYY	Name of Patentee or Applicant of Cited Document	Pages, Columns, Lines, Where Relevant Passages or Relevant Figures Appear	T[6]
	F1	CA 1 101 840	05-26-1981	Sumitomo Chemical Company, Limited	All	
	F2					
	F3					
	F4					
	F5					
	F6					

Examiner Signature		Date Considered	

*EXAMINER: Initial if reference considered, whether or not citation is in conformance with MPEP 609. Draw line through citation if not in conformance and not considered. Include copy of this form with next communication to applicant. [1] Applicant's unique citation designation number (optional). [2] See Kind Codes of USPTO Patent Documents at www.uspto.gov or MPEP901.04. [3] Enter Office that issued the document, by the two-letter code (WIPO Standard T.3). [4] For Japanese patent documents, the indication of the year of the reign of the Emperor must precede the serial number of the patent document. [5] Kind of document by the appropriate symbols as indicated on the document under WIPO Standard ST. 16 if possible. [6] Applicant is to place a check mark here if English language Translation is attached.

Substitute for form 1449B/PTO

INFORMATION DISCLOSURE STATEMENT BY APPLICANT

(use as many sheets as necessary)

Sheet 2 of 2

Complete if Known	
Application Number	10/378,956
Filing Date	March 3, 2003
First Named Inventor	Michael J. Zaworotko
Group Art Unit	1627
Examiner Name	Sahar Javanmard
Attorney Docket Number	USF.106XC1

NON PATENT LITERATURE DOCUMENTS

Examiner Initials*	Cite No. [1]	Include name of the author (in CAPITAL LETTERS), title of the article, (when appropriate), title of the item (book, magazine, journal, serial, symposium, catalog, etc.), date, page(s), volume-issue number(s), publisher, city and/or country where published.	T[2]
	R1	REMENAR, J.F. *et al.* "Celecoxib sodium salt: engineering crystal forms for performance" *CrystEngComm*, 2011, 13:1081-1089.	
	R2	YADAV, A.V. *et al.* "Co-crystals: A novel approach to modify physicochemical properties of active pharmaceutical ingredients" *Indian Journal of Pharmaceutical Sciences"* 2009, 71(4):359-370.	
	R3		
	R4		
	R5		
	R6		
	R7		
	R8		
	R9		
	R10		
	R11		
	R12		
	R13		

Examiner Signature		Date Considered	

*EXAMINER: Initial if reference considered, whether or not citation is in conformance with MPEP 609. Draw line through citation if not in conformance and not considered. Include copy of this form with next communication to applicant. [1] Applicant's unique citation designation number (optional). [2] See Kind Codes of USPTO Patent Documents at www.uspto.gov or MPEP901.04. [3] Enter Office that issued the document, by the two-letter code (WIPO Standard T.3). [4] For Japanese patent documents, the indication of the year of the reign of the Emperor must precede the serial number of the patent document. [5] Kind of document by the appropriate symbols as indicated on the document under WIPO Standard ST. 16 if possible. [6] Applicant is to place a check mark here if English language Translation is attached.

UM00017060
NOVARTIS EXHIBIT 1517
Novartis v. Regents, IPR2023-01347
Page 3929 of 4460

XP009147819

CrystEngComm

www.rsc.org/crystengcomm

Volume 13 | Number 4 | 21 February 2011 | Pages 1047–1226

RSC Publishing

COVER ARTICLE
Remenar *et al.*
Celecoxib sodium salt: engineering crystal forms for performance

International Year of CHEMISTRY 2011

BNSDOCID: <XP_____9147819A__I_>

UM00017073
NOVARTIS EXHIBIT 1517
Novartis v. Regents, IPR2023-01347
Page 3930 of 4460

XP009147819

CrystEngComm

Dynamic Article Links

Cite this: *CrystEngComm*, 2011, **13**, 1081

www.rsc.org/crystengcomm

PAPER

Celecoxib sodium salt: engineering crystal forms for performance†

Julius F. Remenar,‡*[a] Mark D. Tawa,[a] Matthew L. Peterson,§[b] Örn Almarsson,[a] Magali B. Hickey[a] and Bruce M. Foxman[c]

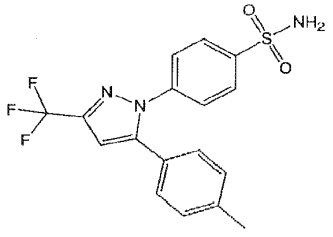
Received 31st July 2010, Accepted 14th September 2010
DOI: 10.1039/c0ce00475h

Downloaded by Technische Universiteit Delft on 03 May 2011
Published on 19 October 2010 on http://pubs.rsc.org | doi:10.1039/C0CE00475H

Crystalline hydrates and propylene glycol solvates of celecoxib sodium salt (**Cel-Na**) were prepared and characterized with the aim of improving oral drug absorption by breaking up the H-bonding interactions present in crystals of the poorly soluble marketed form of the drug (**Cel-III**). The hydrate grows rapidly from aqueous alkaline solution, forming a thick slurry of thin plates. Thicker plates for structure determination were successfully grown by adding up to 1% benzyl alcohol to the solution. The structure of the pentahydrate of the sodium salt is comprised of a bilayer motif where three waters are coordinated to sodium ions in a discrete layer, while the other two waters reside in a one-dimensional channel. At a given temperature, the hydration state changes rapidly and reversibly as a function of relative humidity (RH). The hydrated salt is physically stable in a sealed vial, but reverts rapidly to the crystalline free base if exposed to ambient CO_2 in air at 40% RH or higher. The propylene glycol (PG) solvate of **Cel-Na** exists in an anhydrous and trihydrate form. The trihydrated PG solvate of **Cel-Na** is physically stable above ~15% RH and does not react measurably with CO_2 at 66% RH over 4 days, making it the most suitable form for use in solid pharmaceutical formulations.

Introduction

Recent papers have demonstrated that the bioavailability of celecoxib (**Cel**, Scheme 1) can be enhanced by dosing forms that are transiently more soluble than the marketed crystalline form, **Cel-III**.[1–4] The low solubility of **Cel-III**, a COX-2 selective anti-inflammatory drug,[5,6] limits both the rate and the extent of absorption after dosing. Published strategies showing improvement in solubility and/or bioavailability of **Cel** have included co-crystals, salt forms, metastable polymorphs, amorphous dispersions, and solutions in organic vehicles.[1–3,7,8] Crystalline forms of the sodium salt of celecoxib (**Cel-Na**) were at an early stage of characterization at the time we published work describing their use as "springs" or high-energy forms for creating supersaturated solutions to improve drug absorption behavior.[2] It was known that the hydrated sodium salt gained and lost waters of hydration rapidly as a function of relative humidity (RH), but there was no structural basis to understand this dynamic behavior. Sodium salts of other drug molecules with variable hydration behavior are known,[9,10] and while detailed collections of physical data can be used to characterize them, the picture is incomplete without single crystal data. However, three years of work on hydrates of **Cel-Na** had yielded only very thin plates unsuitable for X-ray structure determination.



Scheme 1 Chemical structure of celecoxib (**Cel**).

Growth inhibitors were considered as a means to increase the smallest dimension of the crystalline plates. Several studies have shown "tailor-made" additives to successfully inhibit growth along specific crystal faces in order to modify habit.[11–13] A study by Davey *et al.* showed that the presence of alkanoic acids could modify the habit of the dicarboxylic acid, adipic acid. In this study, alcohols were added to crystallization media in an attempt to slow growth by inhibiting hydration of the sodium ion. In our hands, use of the additive strategy elucidated one case, benzyl

[a]*TransForm Pharmaceuticals, 29 Hartwell Ave, Lexington, MA, USA. E-mail: Julius.Remenar@alkermes.com; Fax: +1 781-609-5855; Tel: +1 781-609-6684*
[b]*TransForm Pharmaceuticals, 29 Hartwell Ave, Lexington, MA, USA. E-mail: petersom@amgen.com; Tel: +1 617-444-5267*
[c]*Brandeis University, Dept. Of Chemistry, Waltham, MA, USA. E-mail: Foxman1@brandeis.edu; Fax: +1 781-736-2516; Tel: +1 781-736-2532*
† Electronic supplementary information (ESI) available: Cif file for **Cel-NaPG(H_2O)$_5$**. CCDC reference number 787041. For ESI and crystallographic data in CIF or other electronic format see DOI: 10.1039/c0cc00475h
‡ Current Address: Alkermes, Inc. 852 Winter Street, Waltham, MA 02451, USA.
§ Current address: Amgen, Inc. 360 Binney Street, Cambridge, MA 02142, USA.

BNSDOCID: <XP_____9147819A__I_>

UM00017074
NOVARTIS EXHIBIT 1517
Novartis v. Regents, IPR2023-01347
Page 3931 of 4460

Downloaded by Technische Universiteit Delft on 03 May 2011
Published on 19 October 2010 on http://pubs.rsc.org | doi:10.1039/C0CE00475B

alcohol, where the practice proved effective and successful. Crystallization with benzyl alcohol additive enabled structural determination of celecoxib sodium pentahydrate (**Cel-Na(H_2O)$_5$**), the structure of which proved crucial to the understanding of the complex physical behavior of **Cel-Na**.

Creating supersaturated solutions of **Cel** has been shown to increase the rate and extent of drug absorption.[2] Such performance improvements offer the possibility of formulations using less drug and/or achieving faster pain relief from use of the COX-2 inhibitor. Combining a sodium salt of **Cel** with polyether surfactants was particularly effective: the duration of supersaturation increased from less than one minute for the salt alone to greater than 60 minutes for the mixtures; plasma concentrations after oral dosing were higher after 30 minutes for the mixtures than they were after even 2 hours for the marketed formulation; and total drug absorption increased from around 40% to nearly 100%.[2] Since **Cel** is a weak acid with a pK_a of 11.1,[14] its salts are neutralized rapidly in aqueous suspension at physiological pH (pH $\approx$ 1–7), and the neutral drug crystallizes rapidly. Therefore, the observed improvements are believed to require both a starting form that cannot easily revert to the thermodynamically stable form of **Cel (Cel-III)** without first dissolving, and another molecule that will solvate the dissolved **Cel** to prevent or slow down the precipitation of **Cel-III**. This contribution describes the structural findings and insights that have resulted from our effort to harness and understand the sodium salts of **Cel**.

Materials and methods

Celecoxib was obtained from Matrix Labs and used for all experiments without further purification.

Preparation of Cel-Na(H_2O)$_5$

Bulk material. Cel (3.2 g) is dissolved in 32 mL of 1.0 N NaOH with gentle heating. Solubility is reduced by adding 1.0 mL of 2.5 N NaOH followed by subsequent addition of crystalline seeds of the hydrate. Without seeding, crystals will grow slowly over time. Crystallization is allowed to occur for 30 minutes at room temperature. The sample is then cooled in an ice bath for an additional 30 minutes and the crystals are collected by suction filtration and rinsed with cold 0.02 N NaOH (2 × 8 mL). The solids are allowed to dry for 1–2 minutes under suction on the filter and then transferred to a 20 mL scintillation vial. The vial is left open and stored inside of a 53% RH humidity chamber with low CO_2 until it reaches constant weight. Thereafter, the sample remains in the controlled humidity chamber, but with a cap for further protection. The humidity chamber is prepared ahead of time and consists of a dessicator, the bottom of which is filled with a supersaturated solution of $Mg(NO_3)_2$. A 20 mL vial containing 2 mL of concentrated NaOH solution is left in the chamber to capture CO_2. The surface area of the NaOH solution is kept very small relative to the surface and volume of the salt solution so that it does not affect the humidity in the chamber.

Single crystals. Cel (1.3 g) is dissolved in 18 mL of 1.0 N NaOH and 50 μL of benzyl alcohol (0.3% v/v) are added. If a crystal for structure determination is required, it is important to avoid seeding effects. Crystallization slowly occurs over the course of up to five days. The crystals are isolated individually from the mixture. Seeding the solution will also produce high quality, thicker crystals as bulk. Adding only 10 μL of benzyl alcohol fail to slow crystallization.

Preparation of Cel-NaPG(H_2O)$_3$

Cel (1.55 g) is dissolved in 5.0 mL of 1.0 N NaOH and 0.65 mL of propylene glycol (PG) was added. A 0.90 mL aliquot of 2.5 N NaOH was added to induce precipitation. The suspension is warmed gently to re-dissolve the solids, the solution is filtered into a clean vial, seeds are added, and the suspension is sonicated for 10 seconds. On standing and cooling, the slurry becomes a thick paste over 5 minutes. The sample is cooled in an ice bath for 5 minutes, then filtered by suction filtration and rinsed with 0.02 N NaOH in water containing 5% PG (2 × 2.0 mL). The thick paste filters slowly and is left covered under vacuum for 1 hour. The paste remains damp after this treatment. The wet solids are suspended in 5 mL of *tert*-butyl methyl ether for 1 minute and suction filtered before drying in a vacuum oven at room temperature for 30 minutes with a flow of air through the oven. The drying is stopped twice to break up clumps with a spatula, ultimately yielding a dry powder.

Preparation of Cel-NaPG

A scintillation vial containing 1.5 grams of **Cel-NaPG(H_2O)$_3$** is placed in a vacuum oven at 50 °C for 2 hours and then transferred to an 80 °C oven for 1 hour. The compound melts in the 80 °C oven but crystallizes from the melt upon cooling which removes only some of the water. The residual **Cel-NaPG(H_2O)$_3$** can be removed by suspending the solid mixture in *t*-butyl methyl ether, filtering, and drying for 1.5 hours in a vacuum oven at 50 °C. Up to two suspension/vacuum drying cycles may be necessary to effectively remove all **Cel-NaPG(H_2O)$_3$**.

In addition, **Cel-NaPG** can be directly crystallized from diethyl ether in the presence of greater than one equivalent of propylene glycol by addition of one equivalent sodium ethoxide. Crystals grow immediately upon addition of base. The product is isolated by filtration and washed by additional diethyl ether to remove any excess propylene glycol.

Powder X-ray diffraction (PXRD)—Rigaku capillary transmission mode

X-Ray powder diffraction patterns are obtained using the D/Max Rapid X-ray Diffractometer equipped with a copper source (Cu/K_α 1.54056 Å), manual x–y stage, and 0.3 mm collimator. A sample is loaded into a 0.3 mm boron rich glass capillary tube by sectioning off one end of the tube and tapping the open, sectioned end into a bed of sample. The loaded capillary is mounted in a holder that is secured into the x–y stage. A diffractogram is acquired under ambient conditions at a power setting of 46 kV at 40 mA in transmission mode, while oscillating about the ω-axis from 0–5° at 1° s^{-1} and spinning about the ϕ-axis at 2° s^{-1}. The exposure time is 5 minutes unless otherwise specified. The diffractogram obtained is integrated over $2-\theta$ from 2–40° and χ (1 segment) from 0–360° at a step size of 0.02° using the *cylint* utility in the RINT Rapid display software provided with the instrument. The dark counts value is set to 8 as

 This journal is © The Royal Society of Chemistry 2011

BNSDOCID: <XP_____9147819A__I_>

UM00017075
NOVARTIS EXHIBIT 1517
Novartis v. Regents, IPR2023-01347
Page 3932 of 4460

per the system calibration; normalization is set to average; the ω offset is set to 180°; and no χ or ϕ offsets are used for the integration.

Powder X-ray diffraction (PXRD)—Bruker D8 Discover pXRD

X-Ray powder diffraction patterns are obtained using the Bruker AXS D8 Discover X-ray Diffractometer equipped with GADDS™ (General Area Diffraction Detection System), a Bruker AXS HI-STAR Area Detector at a distance of 15.05 cm as per system calibration, a copper source (Cu/K_α 1.54056 Å), automated x y z stage, and 0.5 mm collimator. A sample is compacted into pellet form and mounted on the x y z stage. A diffractogram is acquired under ambient conditions at a power setting of 40 kV and 40 mA in reflection mode while the sample remains stationary. The exposure time is 5 minutes unless otherwise specified. The diffractogram obtained undergoes a spatial remapping procedure to account for the geometrical pincushion distortion of the area detector, then is integrated along χ from −118.8 to −61.8° and $2-\theta$ 2.1–37° at a step size of 0.02° with normalization set to bin normalize. Diffraction patterns obtained on the Bruker instrument are viewed using DIFFRAC^{plus} Evaluation software.

Dynamic vapor sorption (DVS)

Moisture sorption analysis was performed using a dynamic vapor sorption apparatus (Surface Measurement Systems, Monarch Beach, CA). Each sample was placed in a clean glass crucible and equilibrated in the apparatus at a specified temperature and relative humidity (RH) level. Varying the flow rates of dry nitrogen gas and saturated wet nitrogen gas streams controlled RH; the total combined flow rate was kept constant at 200 standard cubic metres per minute. After initial temperature and RH equilibration, RH was varied and change in mass was recorded over time as an indication of moisture sorption. Mass equilibration at each humidity level was determined as a change in mass less than $\pm 2 \times 10^{-5}$ grams over a time interval of 1 minute (dm/dt of 0.002% per min). After the assay, the change in mass was mathematically converted to water molar equivalents per dry compound molar equivalent.

Scanning electron microscopy (SEM)

Crystals were analyzed using a Fenom FEI Scanning Electron Microscope. Samples were mounted onto an SEM sample holder using carbon tape and sputter-coated with a thin gold layer. Each sample was scanned at a medium level of magnification to understand the character and size distribution of the crystals. Images were captured at magnification up to 10 000×.

Proton nuclear magnetic resonance spectroscopy (^{1}H NMR)

^{1}H NMR measurements were conducted using a Varian 400 MHz spectrometer, with averaging of 128 scans. Samples were prepared as 10 mg mL^{-1} solutions of **Cel** in $CDCl_3$.

X-Ray data collection, solution, and refinement for Cel-Na(H_2O)$_5$

All operations were performed on a Bruker-Nonius Kappa Apex2 diffractometer, using graphite-monochromated MoKα radiation. All diffractometer manipulations, including data collection, integration, scaling, and absorption corrections were carried out using the Bruker Apex2 software.[15] Preliminary cell constants were obtained from three sets of 12 frames. Data collection was carried out at 150 K, using a frame time of 20 s and a detector distance of 37.5 mm. The optimized strategy used for data collection consisted of ϕ and ω scan sets, with 0.5° steps in ϕ or ω; completeness was 99.7%. A total of 1485 frames were collected. Final cell constants were obtained from the xyz centroids of 9276 reflections after integration. From the systematic absences, the observed metric constants and intensity statistics, space group $P2_1/c$ was chosen initially; subsequent solution and refinement confirmed the correctness of this choice. The structure was solved using direct methods programs in the Apex2 software.[15] The structure was refined (full-matrix-least squares) using the Oxford University *Crystals for Windows* program.[16] All non-hydrogen atoms were refined using anisotropic displacement parameters. The H atoms were initially refined with soft restraints on the bond lengths and angles to regularize their geometry (C···H in the range 0.93–0.98, N···H in the range 0.86 0.89, O···H = 0.82 Å and U_{iso} (H) in the range 1.2 1.5 times U_{eq} of the parent atom), after which the positions were refined with riding constraints. The final least-squares refinement converged to $R_1 = 0.0431$ ($I > 2\sigma(I)$, 13 607 data) and $wR_2 = 0.1163$ ($F2$, all 17 621 data, 580 parameters). The data unequivocally establish the material as a pentahydrate of the sodium salt of celecoxib (**Cel-Na(H_2O)$_5$**).

Results and discussion

As indicated in the introduction, improving the absorption of **Cel** requires a shelf-stable form of the drug that will resist conversion to the stable and poorly soluble polymorph (**Cel-III**) following dosing.[1,3,4] Our approach requires a form where the packing motifs observed in **Cel-III** have been disrupted. In the presence of polyethers, the crystallization of **Cel-III** is inhibited and results in increased *in vivo* exposure. Analysis of the packing diagram for **Cel-III**[14] reveals that the structure is comprised of head-to-tail, $R_2^2(18)$, **Cel** dimers which propagate along the a axis (Fig. 1).

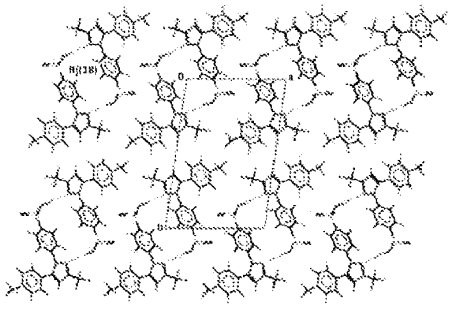


Fig. 1 View of the packing of **Cel-III** $R_2^2(18)$ dimers which propagate along the a axis in crystallographic ab plane.

Downloaded by Technische Universiteit Delft on 03 May 2011
Published on 19 October 2010 on http://pubs.rsc.org | doi:10.1039/C0CE00475H

BNSDOCID: <XP_____9147819A__I_>

UM00017076
NOVARTIS EXHIBIT 1517
Novartis v. Regents, IPR2023-01347
Page 3933 of 4460

Published on 10 October 2010 on http://pubs.rsc.org | doi:10.1039/C0CE00473H
Downloaded by Technische Universiteit Delft on 03 May 2011

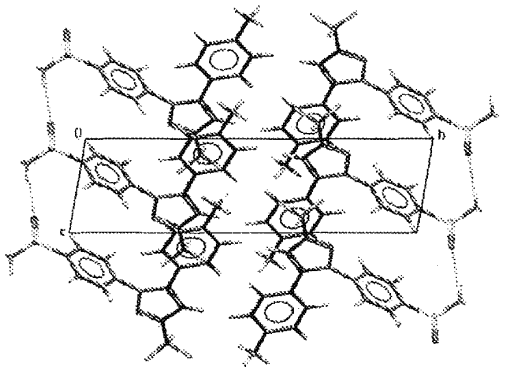


Fig. 2 View of packing of **Cel-III** chains (C4) which propagate along the *c* axis in crystallographic *bc* plane.

Additional hydrogen bonding consisting of sulfonamide chains (C4) which propagate along the *c*-axis is shown in Fig. 2.Our initial attempts were centered on salt formation with a strong base.

Crystal growth and physical characterization of sodium salt hydrates

The formation of pharmaceutically acceptable celecoxib salts is limited by the high acid dissociation constant of the sulfonamide group ($pK_a \approx 11.1$).[6] The standard guideline for salt preparation suggests choosing bases with a pK_a at least 2 units higher than the acid.[17] Since no pharmaceutically acceptable bases have a $pK_a > 13.1$, attempts to make a salt of celecoxib focused on the use of excess sodium hydroxide in aqueous solutions having pH over 12. While the aqueous solubility of celecoxib at physiological pH is <0.5 μg mL^{-1},[3] approximately 380 mg mL^{-1} concentration of celecoxib was achieved in alkaline solutions at room temperature. Evaporation of these solutions to dryness under nitrogen yielded the first crystalline materials, but it was subsequently found that allowing the solutions to stand overnight would also yield single crystals of **Cel-Na(H_2O)$_5$**. The crystallization can be accelerated and the yields improved by cooling in an ice bath or by addition of sodium chloride.

Crystallization from aqueous NaOH with or without added NaCl yielded crystalline plates that were typically less than 2 μm thick (Fig. 3A and B). While larger plates could be grown by changing temperature, sodium content, and **Cel** concentration, the thickness never increased appreciably, leaving material that was both difficult to collect and judged unsuitable for structure determination by single-crystal X-ray. Since sodium ions are generally solvated and **Cel-Na(H_2O)$_5$** has rich hydration behavior, it was reasoned that a competing OH group from an alcohol co-solvent might interfere with hydrate ordering during crystallization, thereby slowing the rapidly growing faces of the plane and allowing thicker crystals to form. Varying levels of methanol, ethanol, and benzyl alcohol were added to the crystallization from NaOH; 2-propanol and propylene glycol were not added as they were shown to form solvates with **Cel-Na** in early form screening studies. Benzyl alcohol (0.3–1%) was found to inhibit the crystallization, sometimes for several days while the remaining alcohols had little effect. The crystals grown in the presence of benzyl alcohol were larger than 10 μm in all dimensions, as shown in Fig. 3C and D.

Structure description for Cel-Na(H_2O)$_5$

The crystal structure of **Cel-Na(H_2O)$_5$** has been solved and confirms its composition as a pentahydrate. Crystallographic data for **Cel-Na(H_2O)$_5$** are shown in Table 1 with a view of the two independent celecoxib anions shown in Fig. 4. Inspection of the packing diagram indicates that the material is comprised of a bilayer-type crystal structure consisting of a hydrogen bonded sodium coordination polymer layer, which blankets two layers of celecoxib anions, all in crystallographic *bc* planes (Fig. 5).

The stoichiometry was established as a pentahydrate of the sodium salt with atom Na1 residing on a general position and coordinating to the sulfonamide anion, and atoms Na2 and Na3 which are six-coordinate, bonded only to water molecules, as shown in Fig. 6. Atoms Na2 and Na3 reside on centers of

Table 1 Crystallographic data for **Cel-Na(H_2O)$_5$**

Chemical formula	$C_{17}H_{13}F_3N_3O_2S_1Na_1 \cdot 5H_2O$
Formula weight	986.87 g mol^{-1}
Temperature	150(1) K
Wavelength	0.71073 Å
Crystal size	0.042 × 0.400 × 0.733 mm
Crystal system	Monoclinic
Space group	$P2_1/c$ (no. 14)
Unit cell dimensions	a = 25.9317(14) Å b = 9.0340(5) Å c = 19.4396(10) Å β = 100.535(2)°
Volume	4477.3(4) Å^3
Z, Z'	8, 2
Density (calculated)	1.464 Mg m^{-3}
Final R indices	Data: $I > 2.0\sigma(I)$ R_1 = 0.0431, wR_2 = 0.1065 All data: R_1 = 0.0623, wR_2 = 0.1163

Fig. 3 SEM images of **Cel-Na(H_2O)$_5$** grown from 1.0 N NaOH (A and B) and 1.0 N NaOH + 0.3% benzyl alcohol (C and D).

This journal is © The Royal Society of Chemistry 2011

BNSDOCID: <XP_____9147819A__I_>

UM00017077
NOVARTIS EXHIBIT 1517
Novartis v. Regents, IPR2023-01347
Page 3934 of 4460

Downloaded by Technische Universiteit Delft on 03 May 2011
Published on 19 October 2010 on http://pubs.rsc.org | doi:10.1039/C0CE00475H

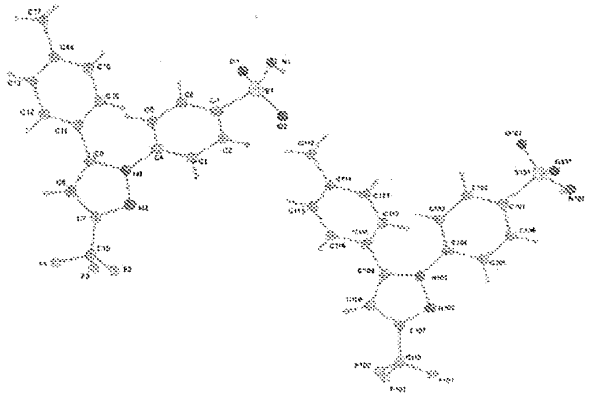


Fig. 4 A view of the two independent **Cel** anions in **Cel-Na(H_2O)$_5$**, showing labeling scheme for the **Cel** anions (50% probability ellipsoids). Na and water oxygen atoms are not shown, but are well ordered, with U_{eq} of water O at 0.03 ± 0.01 (*cf.* carboxylate O at 0.021 ± 0.006 Å^2). The molecules are conformationally similar, with the largest difference in torsion angles being that between N102–N103–C104–C105 (37.1°) and N2–N3–C4–C3 (44.9°).

symmetry at (0 0 0) and (0 ½ 0), respectively. Further analysis of the unit cell contents confirms that six of the ten water molecules are coordinated to the sodium atoms, with the remaining four molecules hydrogen bonded within a channel in the structure, also shown in Fig. 5. Atoms O7, O10, O11, and O12 are not bonded to Na while atoms O8, O9, O3, O4, O6 and O5 are coordinated to Na atoms. Specifically, the six oxygen atoms coordinated to Na have Na–O distances ranging from 2.32–2.43 Å. Of the four non-coordinated oxygen atoms, only O7 is closer than 3 Å (distance to Na2 of 2.68 Å and Na3 of 2.59 Å),

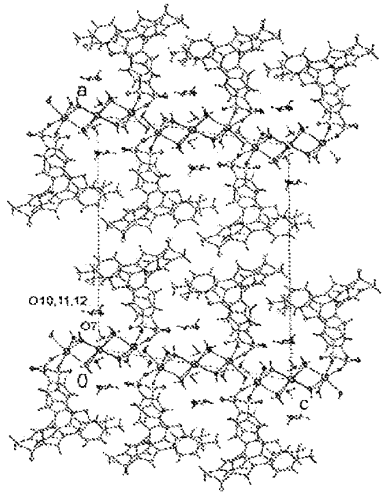


Fig. 5 A view of **Cel-Na(H_2O)$_5$** showing the packing of molecules along the *b* axis. The bilayer-type crystal structure consists of hydrogen-bonded sodium coordination polymer layers, which blanket two layers of celecoxib anions, all in crystallographic *bc* planes.

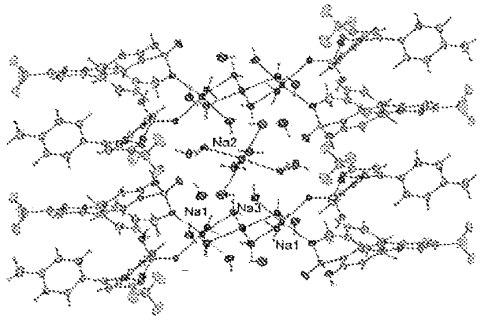


Fig. 6 A view of **Cel-Na(H_2O)$_5$** layers, emphasizing sodium ion coordination and how atoms Na2 and Na3 are six-coordinate, bonding only to water molecules. Atoms Na2 and Na3 reside on centers of symmetry at (0 0 0) and (0 ½ 0), respectively.

resulting in a significantly weaker interaction to Na. Water molecules corresponding to O10, O11, and O12 are all H bonded to each other, and O7 is H-bonded to O12. Water molecules O10, O11 and O12 are in one dimensional channels, centered at *ca.* (0.157, *y*, −0.013) and others related by symmetry. Water molecule O7 is located at the edge of the channel at (0.053, 0.744, 0.019).

Hydration states of Cel-Na(H_2O)$_x$

Despite clear assignment of **Cel-Na(H_2O)$_5$**, the molecule will be described as **Cel-Na(H_2O)$_x$**, except when specific hydration states are being discussed, since the pentahydrate exists only in the presence of bulk water or when kept cold. Indeed, understanding the behavior of the salt form before the single-crystal structure was solved was challenging in that the powder patterns seemed to change almost daily, even when powders were equilibrated in humidity chambers prior to measurement. It was only through a combination of techniques including single crystal and powder diffraction as well as dynamic vapor sorption (DVS) that a more complete understanding of the hydration behavior of **Cel-Na** could be attained.

Consistent powder patterns were obtained by two distinct methods. In the first method, powder was filled into 0.5 mm capillary tubes, equilibrated in controlled humidity chambers for 1 week, sealed with silicone grease immediately upon removal from the humidity chambers, and measured immediately with a transmission powder X-ray diffractometer. In the second method, a sample was monitored by a reflectance mode powder X-ray diffractometer fitted with a controlled humidity stage. The two methods were complementary. The capillary method provided high resolution patterns without preferred orientation effects. However, the humidity control was limited to conditions that could be achieved with standard saturated salt solutions. The controlled humidity PXRD stage showed fewer, more intense peaks, but the measurements were made in increments of 5% relative humidity, during both hydration and dehydration.

The data obtained from the transmission powder X-ray diffractometer are illustrated in Fig. 7. The overlay of the powder patterns indicates that an increase in the shift of the peak at ~3.6° $2-\theta$ is observed when the material is subjected to decreased humidity conditions. Additionally, peaks representing

BNSDOCID: <XP_____9147819A__I_>

UM00017078
NOVARTIS EXHIBIT 1517
Novartis v. Regents, IPR2023-01347
Page 3935 of 4460

Downloaded by Technische Universiteit Delft on 03 May 2011
Published on 19 October 2010 on http://pubs.rsc.org | doi:10.1039/C0CE00473H

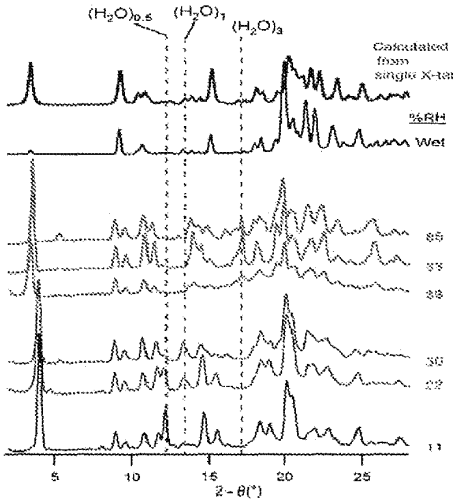


Fig. 7 PXRD patterns measured by transmission PXRD after packing samples into capillary tubes, equilibration in controlled RH chambers (saturated salt solutions), and sealing the tops with silicone grease to prevent moisture exchange during the measurement. The "wet" sample was transferred into the capillary tube directly from the crystallization slurry in aqueous NaOH without filtration, rinsing, or drying.

the different hydration states become apparent as shown in Fig. 7. A sample removed from a humidity chamber kept at ~11% RH shows a peak at 12.1° $2-\theta$ corresponding to the hemihydrate, **Cel-Na$(H_2O)_{0.5}$**. When humidity is increased (up to 30% RH) this peak begins to disappear with emergence of a new peak at 13.4° $2-\theta$, corresponding to a monohydrate, **Cel-Na$(H_2O)_1$**. Material stored between 40 and 85% RH results in the emergence of peaks at 17.2° and 25.8° $2-\theta$ for the trihydrate, **Cel-Na$(H_2O)_3$**, and the pattern remains largely unchanged when compared to a sample removed from a brine solution which is believed to correspond to the pentahydrate, **Cel-Na$(H_2O)_5$**.

Fig. 8 shows a two-dimensional plot of peak intensity *vs.* relative humidity obtained from the reflectance mode powder X-ray diffractometer fitted with a controlled humidity stage. Examination of the changes in the PXRD pattern as a function

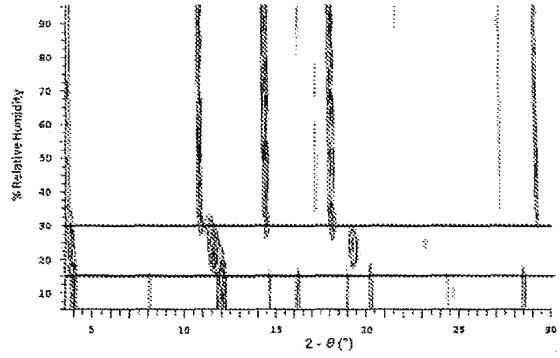


Fig. 8 PXRD pattern peak intensity map *vs.* %RH at 25 °C for a sample of **Cel-Na$(H_2O)_x$** in a controlled humidity chamber of a reflectance mode powder diffractometer.

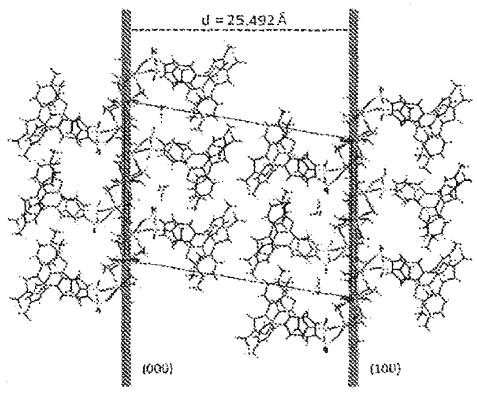


Fig. 9 View of the packing diagram for **Cel-Na$(H_2O)_5$** with the (1 0 0) family planes drawn, indicating the distance of 25.495 Å between the planes. Loss of water from the sodium coordination polymer is expected to result in a decrease in the distance between bilayers along the *a*-axis. Loss of water from the channel is not expected to result in a significant change in the crystal packing as supported by PXRD patterns taken as a function of humidity (see Fig. 7 and 8).

of decreased humidity indicates that several peaks shift to higher $2-\theta$ values. The shift is most pronounced from ~35% to ~4% RH (lowest attainable RH in the configuration at 25 °C) with minimal change at humidities above 30% RH. For example, the *d*-spacing for the peak at ~3.5° $2-\theta$, corresponding to a planar spacing at (1 0 0) decreases with lower humidity. The shift is consistent with the bilayers moving closer to one another in the direction of the longest-axis (*a*), and may be impacted most significantly by water loss from the sodium ion layer, as shown in Fig. 9. While a complete mechanistic study is required to determine the full structural impact of hydration/dehydration of **Cel-Na$(H_2O)_x$**, the PXRD data do suggest that water molecules lost from the channel will result in less significant changes to the unit cell compared to those coordinated to sodium.

The hydration of **Cel-Na** was additionally studied using dynamic vapor sorption (DVS) at 25 °C and the data are illustrated in Fig. 10. The hydration is reversible throughout the full humidity range with some hysteresis at the transition points. There are two major plateau regions in the DVS profile. The first

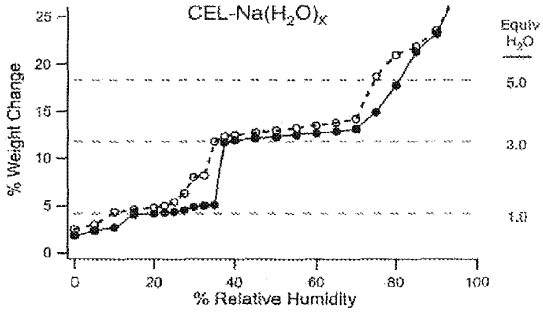


Fig. 10 DVS of **Cel-Na$(H_2O)_x$** at 25 °C. 1.8 wt% was added to all points to account for estimated residual water at 0% RH and to make weights consistent with a mono and trihydrate at the plateaus, as described in the text.

This journal is © The Royal Society of Chemistry 2011

BNSDOCID: <XP_____9147819A_I_>

UM00017079
NOVARTIS EXHIBIT 1517
Novartis v. Regents, IPR2023-01347
Page 3936 of 4460

Downloaded by Technische Universiteit Delft on 03 May 2011
Published on 19 October 2010 on http://pubs.rsc.org | doi:10.1039/C0CE00475H

plateau between 40 and 70% RH is believed to correspond to a trihydrate of **Cel-Na**. Given that the single crystal and PXRD data suggest that a trihydrate is likely to exist and that a stable trihydrate would contain 11.8% (w/w) water, a value of 1.8% weight is added to all points and is likely due to residual water at 0% RH. The smaller plateau between 15 and 30% RH is separated from the trihydrate plateau by 7.8% weight, or two water molecules, indicating the likely existence of a monohydrate. The other final unique phase region identified by VH-PXRD is between 0 and 10% RH which is consistent with a hemihydrate by DVS. The water content of **Cel-Na(H_2O)$_x$** continues to change above 70% RH, without a clear region of physical stability for the pentahydrate. In summary, the three hydration states observed by DVS at 25 °C correspond to: a hemi-hydrate below 10% RH; a monohydrate from 20–30% RH and a trihydrate from 40–70% RH. It is difficult to directly measure the amount of water remaining at 0% RH DVS or controlled humidity PXRD experiment, because opening either chamber to collect samples for techniques such as TGA or Karl-Fischer titration exposes the material to atmospheric moisture, and water uptake by **Cel-Na** is rapid.

Instability of Cel-Na(H_2O)$_x$ in air

When left exposed to the air, **Cel-III** begins to appear in samples of **Cel-Na(H_2O)$_x$**, as was initially seen by the peak at 7.9° $2-\theta$ in the PXRD patterns of samples stored in humidity chambers (see Fig. 8). The neutralization of the basic salt increases at high humidity and was shown to result from reaction with CO_2 and water in air. The behavior was first observed when using compressed air instead of nitrogen in the dynamic vapor sorption experiment, but it was also evident in samples stored open in controlled humidity chambers. The neutralization was minimized in PXRD patterns by including small vials of concentrated NaOH solution within the closed humidity chambers to adsorb CO_2 from the air. An SEM image, shown in Fig. 11, shows formation of crystalline **Cel-III** on the outside of **Cel-Na(H_2O)$_5$** crystals due to neutralization. Throughout the conversion, both the **Cel-III** and the sodium salt are clearly observed by PXRD with **Cel-III** growing in slowly over time. **Cel-III** peaks emerge without appreciable broadening of the PXRD patterns for the salt, indicating that the conversion occurs primarily at the surface rather than throughout the crystal by infiltration of CO_2 into the channels.

Fig. 11 SEM image of **Cel-Na(H_2O)$_5$** indicating the growth of **Cel-III** on the outside of the crystals. Note the appearance of needles of the latter on the surface of the plate-like crystals of the salt.

Propylene glycol (PG) solvate of Cel-Na

Alternative solvates were sought in an attempt to improve the physical stability of **Cel-Na**, both with respect to changes in mass *vs.* relative humidity, and to improve stability in air. After an initial screen yielded a hydrated 2-propanol solvate, it was rationalized that propylene glycol might have several advantages: it has two hydroxyl groups that could solvate sodium ions; it has a high boiling point (187 °C); and it is commonly used in pharmaceutical formulations. Two PG solvates were found: an anhydrous solvate (**Cel-NaPG**) and a trihydrated PG solvate (**Cel-NaPG(H_2O)$_3$**). Most importantly, **Cel-NaPG(H_2O)$_3$** was found to resist conversion to neutral **Cel** compared to **Cel-Na(H_2O)$_x$**; no detectable conversion of **Cel-NaPG(H_2O)$_3$** to **Cel-III** was observed after 4 days at 66% RH.

Cel-NaPG(H_2O)$_3$ is isolated from aqueous sodium hydroxide solutions of **Cel** containing at least one equivalent of PG. The anhydrous form, **Cel-NaPG**, is prepared from the trihydrate by removing the water of hydration in a vacuum oven at 45–55 °C and heating the dehydrated powder to 80 °C for 20–30 minutes. **Cel-NaPG** can also be crystallized from alkaline solutions of **Cel** in diethyl ether containing greater than one equivalents of PG. TGA data show that PG is retained in **Cel-NaPG** until approximately 80 °C under a flow of nitrogen. Crystals large enough for structure determination have not been grown to date.

Conversion between **Cel-NaPG** and **Cel-NaPG(H_2O)$_3$** was found to be much less facile than changes in water structure and content within **Cel-Na(H_2O)$_x$**. The dynamic vapor sorption profiles were measured starting with **Cel-NaPG** at 0% RH, and for **Cel-NaPG(H_2O)$_3$** beginning at 20% RH to avoid dehydrating it prior to the first absorption cycle. The profiles are shown in Fig. 12 alongside PXRD patterns for samples of **Cel-NaPG** stored in controlled humidity chambers for 1–2 days. The dynamic profiles differ significantly depending on the starting material, suggesting that they do not reflect equilibrium behavior. **Cel-NaPG(H_2O)$_3$** is relatively non-hygroscopic between 10 and 70% RH at 25 °C, reversibly gaining 1.2% weight. In contrast, **Cel-NaPG** shows complex behavior, gaining nearly 14% weight during adsorption and ending with a partial loss of PG after desorption. There are two major differences between the two profiles that must be explained. First, **Cel-NaPG** and **Cel-NaPG(H_2O)$_3$** both appear to be physically stable from 10–40% RH in the dynamic profile, while only one of them can be the thermodynamically stable form at a given water activity. Second, **Cel-NaPG** is already anhydrous at the beginning of the experiment, but it loses an additional 2% weight after going through the entire profile.

Samples of each form were stored in controlled humidity chambers at 25 °C and monitored for at least 1 week to determine which one is physically stable at each %RH. **Cel-NaPG(H_2O)$_3$** is formed from samples of **Cel-NaPG** when stored at 18% RH or higher, showing that the trihydrate is the more stable form over a wide humidity range. The rate of conversion to **Cel-NaPG(H_2O)$_3$** is very slow at 18% RH and increases to the point where conversion takes less than one day at 54% RH or higher. TGA shows that **Cel-NaPG** gains about 2 equiv. of water within one day when stored in a 38% RH chamber but peaks associated with **Cel-NaPG(H_2O)$_3$** only begin to appear after the second day, as indicated by PXRD. A sample of **Cel-NaPG(H_2O)$_3$** showed no

BNSDOCID: <XP_____9147819A__I_>

UM00017080
NOVARTIS EXHIBIT 1517
Novartis v. Regents, IPR2023-01347
Page 3937 of 4460

Downloaded by Technische Universiteit Delft on 03 May 2011
Published on 19 October 2010 on http://pubs.rsc.org | doi:10.1039/C0CE00475H

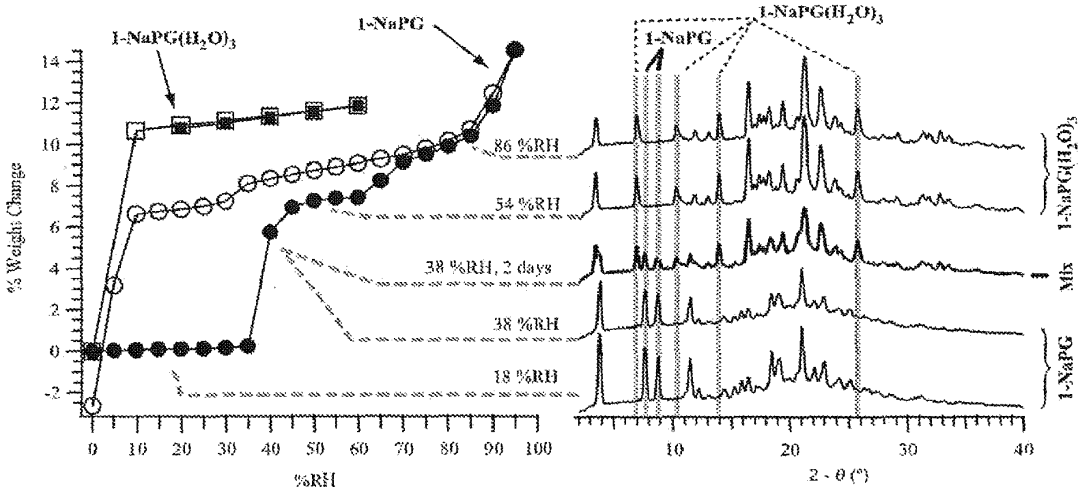


Fig. 12 DVS profiles of a sample of **Cel-NaPG** and **Cel-NaPG(H_2O)$_3$** at 25 °C (left), and PXRD patterns for samples of **Cel-NaPG** equilibrated in controlled humidity chambers for 1 or 2 days at room temperature. **Cel** is represented as **1** in the figures. Solid symbols in the DVS profile mark the adsorption cycles, hollow symbols mark the desorption cycles. The labels to the right of the PXRD patterns indicate the form assignment. The vertical grey lines and labels above highlight some characteristic peaks for each form. The %RH values given to the left of the PXRD patterns refer to the humidity of the chamber in which the samples were equilibrated.

conversion to **Cel-NaPG** after 4 days of storage over the 18% RH salt bath, indicating resistance to dehydration.

The loss of dry-weight from **Cel-NaPG** during the DVS experiment suggested that the PG could be labile, a property that could contribute to physical instability. Samples subjected to multiple humidity cycles were found to lose additional weight after each cycle, and the profiles began to look more akin to those of **Cel-Na(H_2O)$_x$**. However, no detectable loss was seen in **Cel-NaPG(H_2O)$_3$** at 20% RH after subjecting the form to a single humidity cycle. Increased lability and loss of PG during the transition from anhydrous to trihydrate was believed to be the most likely explanation for the weight loss. ^{1}H NMR was used to determine whether the PG solvate is lost continuously throughout the humidity cycle or only during change in the hydration state. **Cel-NaPG** and **Cel-NaPG(H_2O)$_3$** were exposed to 0% RH and 40% RH in the DVS and then dissolved in methanol-d_4 for NMR analysis. The **Cel** : PG ratio was stable at 1 : 1 for **Cel-NaPG(H_2O)$_3$** after treatment for either four hours at 40% RH or 18 hours at 0% RH. However, **Cel-NaPG** lost 8.2% PG equivalents over four hours at 40% RH, while remaining stable under a stream of dry nitrogen for 18 hours (0% RH) at 25 °C. Since the **Cel-NaPG(H_2O)$_3$** has a wide range of conditions supporting physical stability, conversion from the trihydrate to the anhydrous PG solvate and back to the trihydrate should be a rare event. In a closed system, such as a packaged tablet, PG should not be lost as easily as it is in the dynamic environment of the DVS where gases continuously flow over the sample and carry away any volatile components.

Conclusions

The celecoxib sodium salt forms that were previously coupled with excipients to improve oral absorption of the drug have been studied. **Cel-Na** exists as a pentahydrate when suspended in aqueous alkaline media. Addition of 0.3% benzyl alcohol facilitated the growth of crystals sufficiently large for structure determination by single X-ray diffraction. The salt crystallizes in a bilayer structure having layers of celecoxib and layers of hydrated sodium ions with channels that hold additional water. At room temperature, **Cel-Na(H_2O)$_x$** exists as a trihydrate between 40 and 70% RH, a monohydrate from 10–30% RH, and a hemi-hydrate below 10% RH; PXRD patterns containing both forms are found at humidity close to the transition between two hydration states. The exchange of moisture is rapid and samples must be protected from exposure to air during PXRD measurements to get reproducible powder patterns. **Cel-Na(H_2O)$_x$** must be protected from air in order to prevent neutralization of the salt form by carbon dioxide and water in air. Propylene glycol forms a solvate and a trihydrated solvate of **Cel-Na**. **Cel-NaPG(H_2O)$_3$** is physically stable at room temperature above ~10% RH and higher, and the form is resistant to reaction with CO_2 and water in the air. Overall, **Cel-NaPG(H_2O)$_3$** is the most shelf-stable form of **Cel-Na** discovered to date and would be the best choice for use in formulations combining excipients with a salt form to potentially enhance the rate and extent of oral absorption of celecoxib.

Notes and references

1 J. F. Remenar, *Am. Pharm. Rev.*, 2007, **10**, 84.
2 H. R. Guzman, M. Tawa, Z. Zhang, P. Ratanabanangkoon, P. Shaw, C. R. Gardner, H. Chen, J. P. Moreau, O. Almarsson and J. F. Remenar, *J. Pharm. Sci.*, 2007, **96**, 2686.
3 G. W. Lu, M. Hawley, M. Smith, B. M. Geiger and W. Pfund, *J. Pharm. Sci.*, 2005, **95**, 305.
4 M. L. Peterson, E. A. Collier, M. B. Hickey, H. R. Guzman and O. Almarsson, in *Organic Crystal Engineering: Frontiers in Crystal*

This journal is © The Royal Society of Chemistry 2011

BNSDOCID: <XP_____9147819A__I_>

UM00017081
NOVARTIS EXHIBIT 1517
Novartis v. Regents, IPR2023-01347
Page 3938 of 4460

Engineering, ed. E. R. T. Tieking, J. Vittal and M. Zaworotko, John Wiley & Sons, Ltd. 2010, ch. 3, pp. 67–99.
5 Physicians Desk Reference, electronic library version, MicroMedex (Thomson Healthcare).
6 S. K. Paulson, M. B. Vaughn, S. M. Jessen, Y. Lawal, C. J. Gresk, B. Yan, T. J. Maziasz, C. S. Cook and A. Karim, *J. Pharmacol. Exp. Ther.*, 2001, **297**, 638.
7 P. Gupta, G. Chawla and A. K. Bansal, *Mol. Pharmacol.*, 2004, **1**, 406.
8 J. F. Remenar, M. L. Peterson, P. W. Stephens, Z. Zhang, Y. Zimenkov and M. B. Hickey, *Mol. Pharmacol.*, 2007, **4**, 386.
9 L. R. Chen, V. G. Young, Jr. D. Lechuga-Ballesteros and D. J. Grant, *J. Pharm. Sci.*, 1999, **88**, 1191.
10 R. Khankari, L. Chen and D. J. Grant, *J. Pharm. Sci.*, 1998, **87**, 1052.
11 R. J. Davey, S. N. Black, D. Logan, S. J. Maginn, J. E. Fairbrother and D. J. W. Grant, *J. Chem. Soc., Faraday Trans.*, 1992, **88**, 3461.
12 C. Thompson, M. C. Davies, C. J. Roberts, S. J. B. Tendler and M. J. Wilkinson, *Int. J. Pharm.*, 2004, **280**, 137.
13 I. Weissbuch, M. Lahav and L. Leiserowitz, *Adv. Cryst. Growth Res.*, 2001, 381.
14 R. Vasu Dev, K. S. Rekha, K. Vyas, S. B. Mohanti, P. R. Kumar and G. O. Reddy, *Acta Crystallogr., Sect. C: Cryst. Struct. Commun.*, 1999, **55**, v, IUC9900161.
15 *Apex2, Version 2 User Manual, M86-E01078*, Bruker Analytical X-ray Systems, Madison, WI, June 2006.
16 P. W. Betteridge, J. R. Carruthers, R. I. Cooper, K. Prout and D. J. Watkin, *J. Appl. Crystallogr.*, 2003, **36**, 1487.
17 A. T. M. Serajuddin and M. Pudipeddi, in *Handbook of Pharmaceutical Salts*, ed. P. H. Stahl and C. G. Wermuth, Verlag Helvetica Chimica Acta, Zürich and Wiley-VCH, Weinheim, 2002, ch. 6, pp. 138–139.

Downloaded by Technische Universiteit Delft on 03 May 2011
Published on 19 October 2010 on http://pubs.rsc.org | doi:10.1039/C0CE00473H

BNSDOCID: <XP_____9147819A__I_>

UM00017082

NOVARTIS EXHIBIT 1517
Novartis v. Regents, IPR2023-01347
Page 3939 of 4460

XP-002635211

Indian Journal of Pharmaceutical Sciences

REVIEW ARTICLE
Year : 2009 | Volume : 71 | Issue : 4 | Page : 359--370

Co-crystals: A novel approach to modify physicochemical properties of active pharmaceutical ingredients

AV Yadav[1], AS Shete[2], AP Dabke[3], PV Kulkarni[4], SS Sakhare[5],
[1] Krishna Institute of Medical Scinces University and Institute of Pharmacy, Karad-415 110, India
[2] Shree Santkrupa College of Pharmacy, Ghogaon, Karad-415 111, India
[3] Goverenment College of Pharmacy, Vidyanagar, Karad-415 124, India
[4] Government College of Pharmacy, Osmanpura, Aurangabad-431 005, India
[5] Gourishankar Education Society's Institute of Pharmaceutical Sciences and Research, Limb, Satara-415 004, India

Correspondence Address:
A V Yadav
Krishna Institute of Medical Scinces University and Institute of Pharmacy, Karad-415 110
India

Abstract

Crystal form can be crucial to the performance of a dosage form. This is especially true for compounds that have intrinsic barriers to drug delivery, such as low aqueous solubility, slow dissolution in gastrointestinal media, low permeability and first-pass metabolism. The nature of the physical form and formulation tends to exhibit the greatest effect on bioavailability parameters of water insoluble compounds that need to be given orally in high doses. An alternative approach available for the enhancement of drug solubility, dissolution and bioavailability is through the application of crystal engineering of co-crystals. The physicochemical properties of the active pharmaceutical ingredients and the bulk material properties can be modified, whilst maintaining the intrinsic activity of the drug molecule. This article covers the advantages of co-crystals over salts, solvates (hydrates), solid dispersions and polymorphs, mechanism of formation of co-crystals, methods of preparation of co-crystals and application of co-crystals to modify physicochemical characteristics of active pharmaceutical ingredients along with the case studies. The intellectual property implications of creating co-crystals are also highly relevant.

How to cite this article:
Yadav AV, Shete AS, Dabke AP, Kulkarni PV, Sakhare SS. Co-crystals: A novel approach to modify physicochemical properties of active pharmaceutical ingredients.Indian J Pharm Sci 2009;71:359-370

How to cite this URL:
Yadav AV, Shete AS, Dabke AP, Kulkarni PV, Sakhare SS. Co-crystals: A novel approach to modify physicochemical properties of active pharmaceutical ingredients. Indian J Pharm Sci [serial online] 2009 [cited 2011 May 3];71:359-370
Available from: http://www.ijpsonline.com/text.asp?2009/71/4/359/57283

Full Text

Chemists and engineers in the pharmaceutical industry generally seek to deliver crystalline forms of their active compounds, mainly due to the inherent stability of crystalline materials and the well-established impact of crystallization processes on purification and isolation of chemical substances [1] . Increasing attention is now being paid to the impact of material properties on drug discovery and early development [2] as the drug substances tend to be very valuable materials. The pharmaceutical industry's mission is to rapidly advance development programs with good confidence so that formulation problems are unlikely to arise and to maximize a compounds potential as a therapeutic. This commentary seeks to raise the profile of crystal form studies and the emerging topic of crystal engineering in pharmaceutical science by discussing the state-of-the-art relating to pharmaceutical crystals and by expanding on possibilities that exist for future developments. In keeping with the common goal of making better products, faster and cheaper, we propose a paradigm of pro-active material design in pharmaceutical research. Rather than settling for the physical forms that the pure compounds intrinsically display, we should be aiming to identify the physical properties required of the target drug and make crystalline forms to meet those needs. We are not yet actively engaging in crystal engineering in the industry, and therefore we pose the question, how can we proceed toward making the crystal form that we want to use?

Pharmaceutical active ingredients (APIs) can exist in a variety of distinct solid forms, including polymorphs, solvates, hydrates, salts, co-crystals and amorphous solids. Each form displays unique physicochemical properties that can profoundly influence the bioavailability, manufacturability purification, stability and other performance characteristics of the drugs [3] .

BNSDOCID: <XP_____2635211A__I_>

UM00017083

NOVARTIS EXHIBIT 1517
Novartis v. Regents, IPR2023-01347
Page 3940 of 4460

Solid form discovery and design depends on the nature of the molecule of interest and type of physical property challenges faced in its development. The preferred solid form is generally the thermodynamically most stable crystalline form of the compound [3],[4] . However, the stable crystal form of the parent compound may exhibit inadequate solubility or dissolution rate resulting in poor oral absorption, particularly for water-insoluble compounds. In this case, alternative solid forms may be investigated. For ionizable compounds, preparation of salt forms using pharmaceutically acceptable acids and bases is a common strategy to improve bioavailability [3],[5],[6] . Like the parent compound, pharmaceutical salts may exist in several polymorphic, solvated and/or hydrated forms.

Crystal engineering is generally considered to be the design and growth of crystalline molecular solids with the aim of impacting material properties. A principal tool is the hydrogen bond, which is responsible for the majority of directed intermolecular interactions in molecular solids. Co-crystals are multi-component crystals based on hydrogen bonding interactions without the transfer of hydrogen ions to form salts; this is an important feature, since Bronsted acid-base chemistry is not a requirement for the formation of a co-crystal. Co-crystallization is a manifestation of directed self-assembly of different components. Co-crystals have been described of various organic substances over the years [7],[8] and given various names, such as addition compounds [9],[10] molecular complexes [11],[12] and heteromolecular co-crystals [13] . Regardless of naming convention, the essential meaning is that of a multi-component crystal where no covalent chemical modification of the constituents occurs as a result of the crystal formation.

Pharmaceutical co-crystals can be defined as crystalline materials comprised of an API and one or more unique co-crystal formers, which are solids at room temperature.

Co-crystals can be constructed through several types of interaction, including hydrogen bonding, p stacking, and vander Waals forces. Solvates and hydrates of the API are not considered to be co-crystals by this definition. However, co-crystals may include one or more solvent/water molecules in the crystal lattice [14] . Co-crystals often rely on hydrogen-bonded assemblies between neutral molecules of API and other component. For nonionizable compounds co-crystals enhance pharmaceutical properties by modification of chemical stability, moisture uptake, mechanical behaviour, solubility, dissolution rate and bioavailability [15].

Salts, Solvates (Hydrates), Solid Dispersions, Polymorphs and Co -Crystals

Pharmaceutical co-crystallization, which has only recently gained widespread attention as a means of modifying the physicochemical properties of APIs, has two inherent advantages over the salt form. First, because co- crystal formation may potentially be employed with all APIs, including acidic, basic and non ionisable molecules and second is a large number of potential 'counter molecules' which may be considered to be non toxic possibly increasing the scope of the pharmaceutical co- crystallization over the salt forms.

An analogy can be drawn to salt selection in which pKa arguments are used to select acid-base pairs that can be converted to salt compounds. Chemistry demonstrates that a pKa difference of at least two units (between an acid and a base) is required to form a sal that is stable in water [16] .

It is also important to remember that salt formation is generally directed at a single acidic and basic functional group. In contrast co-crystals can simultaneously address multiple functional groups in a single drug molecule. In addition space is not limited to binary combinations (acid-base pairs) since tertiary and quaternary co-crystals are realistic one [17],[18] . One very interesting thing was observed that co-crystals provide a powerful means to tailor the desired solubility and dissolution-pH dependence of APIs, even when the API is a non-ionizable molecule [19] .

The extent of polymorphism of pharmaceutical is limited to the handful of the different crystal forms. Primary difference between solvates and co-crystals is the physical state of the individual components [20] . If one component is liquid at room temperature then the crystals are designated solvates, whereas if both components are solids at room temperature then the crystals are designated as co-crystals. Solvates are commonplace because they occur as a serendipitous result of crystallization from solution [21] and have the potential to enhance drug dissolution rate, as shown for the solvated forms of spiranolactone [22] . Solvated crystals however are often unstable, leading to desolvation during storage and such solvent loss may lead to the amorphous phase crystallizing into less soluble forms. Solvent levels in solvated crystals are also often at concentrations that are not acceptable to regulatory authorities and which may also have toxicological consequences. Co-crystals, however, tend to be a product of more rational design and are more stable, particularly as the co-crystallizing agents are solids at room temperature. As with other crystalline systems, polymorphic co-crystals are not uncommon. At least 20 have been reported to date, including caffeine and glutaric acid polymorphic co-crystals [23] whilst co-crystals are defined by a single phase (miscible) multi-component system in the crystalline state, in the amorphous state they have been referred to as molecular dispersions [24],[25] with interactions between the components distinguishing them from solid dispersions. Co-crystals are not classified as solid dispersions; nevertheless solid dispersions may occur when attempting to prepare co-crystals from solution. The generic term solid dispersions refers to the dispersion of one or more active ingredients in an inert carrier in a solid state, frequently prepared by the melting (fusion) method, solvent method, or fusion solvent-method [26],[27] The solid dispersion approach to reduce particle size and therefore increase the dissolution rate and absorption of drugs was first recognized in 1961 [26] . In the preparation of solid dispersions, drugs with a poor ability to form the glassy state, and which

BNSDOCID: <XP_____2635211A__I_>

UM00017084
NOVARTIS EXHIBIT 1517
Novartis v. Regents, IPR2023-01347
Page 3941 of 4460

demonstrate notable propensity to crystallize, have generally been made amorphous by deliberately preventing crystallization. Recen additional preparation techniques have included like rapid precipitation by freeze drying [28] and spray drying [29] and using supercritical fluids [30] , often in the presence of intrinsically amorphous hydrophilic polymers and also using methods such as melt extrusion [31] . In these systems, the drug substance is either molecularly dispersed within the polymer matrix to form a solid solution or distributed as amorphous drug domains and nanoparticulates. Under appropriate conditions of temperature and humidity, amorphous materials can crystallize when sufficient molecular mobility exists. As the amorphous phase is metastable compared to the crystalline state, there is some risk that phase transformation will occur upon storage, limiting their use in pharmaceutical dosage forms. Now a question arises; are pharmaceutical co-crystals more or less prone to polymorphism than other pharmaceutical phases?

Direct answer of this question is not possible because to prove the absence of polymorphism is tantamount to the proving-the-negative. If one considers an argument that compounds have a lower degree of self - complementarity than complementarity to a rationally selected co-crystal former. Initial indications are that polymorphic substances may provide the good candidates for the co-crystals [18] . For example; carbamazepine can exist as four different well-characterized polymorphs and a dihydrate. Co-crystals of carbamazepine and saccharin showed one packing arrangement while the co-crystals along with N,N-bis(parabromophenyl) melamine-diethyl barbital demonstrated how a specific heterosynthon between the two molecules is robust, but packing of the tapes in to a crystalline arrangement can leads to two discrete polymorphs. Hence there may be opportunity to reduce the practical extent of the polymorphism of drug compounds specifically by co-crystals formation although there may be some exception [21] .

The key benefits associated with co-crystallization approach to modify properties of pharmaceutical solids are the theoretical capability of all types of drug molecules, including weakly ionizable and non-ionizable, to form co-crystals, and the existence of numerous, potential counter-molecules, including food additives, preservatives, pharmaceutical excipients as well as other APIs, for co-crystal synthesis. Major advantage is that co-crystal synthesis may offer for the pharmaceutical industry is an opportunity to address intellectual property (IP) issues by extending the life cycles of old APIs [32].

Advantages of Co-Crystals

Co-crystals having advantages like stable crystalline form (as compared to amorphous solids), no need to make or break covalent bonds, theoretical capability of all types of API molecules (weakly ionizable/non-ionizable) to form co-crystals, the existence of numerous potential counter-molecules (food additives, preservatives, pharmaceutical excipients, and other APIs), the only solid form that is designable via crystal engineering patentable expanding IP portfolios and can be produced using solid-state synthesis green technologies high yield, no solvent or by-products.

Design of Co-Crystals

The crystal engineering experiment typically involves the Cambridge Structural Database (CSD) survey followed by the experimental work. Co-crystals designed on the principal of the supramolecular synthesis; it provides a powerful approach for proactive discovery of novel pharmaceutical solid phases. Co-crystals consist of multiple components in given stoichiometric ratio, where different molecular species interact by hydrogen bonding and by non-hydrogen bonding.

The use of hydrogen bonding rules, synthons and graph sets may assist in the design and analysis of co-crystal systems. In general though, prediction of whether co-crystallization will occur is not yet possible and must, at present, be answered empirically. Co-crystal formation may be rationalised by consideration of the hydrogen bond donors and acceptors of the materials that are to be co-crystallized and how they might interact. Following the extensive examination of preferential packing preferences and hydrogen bond patterns in a number of organic crystals, Etter and co-workers proposed the guidelines to facilitate the deliberate design of hydrogen-bonded solids [33] . All good proton donors and acceptors are used in hydrogen bonding, six-membered ring intermolecular hydrogen bonds form in preference to intermolecular hydrogen bonds, the best proton donor and acceptor remaining after intermolecular hydrogen-bond formation will form intermolecular hydrogen bonds to one another (but not all acceptors will necessarily interact with donors). These observations help to address the issue of competing hydrogen bond assemblies observed when using a particular cocrystallising agent.

A detailed understanding of the supramolecular chemistry of the functional groups present in a given molecule is the prerequisite for designing the co-crystals because it facilitates the selection of the suitable co-crystal former. Supramoecular synthons that can occur in common functional group in order to design new co-crystals and certain functional groups such as carboxylic acids, amides and alcohols are particularly amenable to formation of supramolecular heterosynthon [34] . The strong hydrogen bond includes (N-H---O), (O-H---O), (-N-H---N,) and (O-H---N). The weak hydrogen bonds involves the -C-H---O and C-H---O=C [15] .

Methods of Preparation of Co -Crystals

BNSDOCID: <XP_____2635211A__I_>

UM00017085

NOVARTIS EXHIBIT 1517
Novartis v. Regents, IPR2023-01347
Page 3942 of 4460

Co-crystal formation described in the literature indicates the notoriously difficult situation these systems present with regard to preparation it has been known to take 6 months to prepare a single co-crystal of suitable quality for single X-ray diffraction analysis [35] . This is partly because such a heteromeric system will only form if the non-covalent forces between two (or more) molecules are stronger than between the molecules in the corresponding homomeric crystals. Design strategies for co-crystal formation are still being researched and the mechanism of formation is far from being understood [36] .

Co-crystals can be prepared by solvent and solid based methods. The solvent-based methods involve slurry conversion solvent evaporation, cooling crystallization and precipitation. The solid based methods involve net grinding; solvent-assisted grinding and sonication (applied to either to wet or dry solid mixtures) 80 o to 85° [37].

Solution co-crystallization:

For solution co-crystallization, the two components must have similar solubility; otherwise the least soluble component will precipitate out exclusively. However similar solubility alone will not guarantee success. It has been suggested that it may be useful to consider polymorphic compounds, which exist in more than one crystalline form as co-crystallising components. If a molecular compound exists in several polymorphic forms it has demonstrated a structural flexibility and is not locked into a single type of crystalline lattice or packing mode. Thus, the chance of bringing such a molecule into a different packing arrangement in coexistence with another molecule is increased. Clearly polymorphism alone does not guarantee the functionality of a compound to act as a co-crystallising agent, whilst the ability of a molecule to participate in intermolecular interactions obviously plays a critical role [38] .

Small-scale preparation has been described. Scale-up crystallization was performed in a 500 ml water-jacketed glass crystallization vessel. Temperature was maintained by a circulating water bath. A reflux column, digital thermometer, and overhead stirrer with a glass shaft and Teflon blade were attached to vessel ports. The drug and co-crystal former were added to a reaction vessel. The solids were dissolved in ethanol/methanol mixture and heated to 70 0 for 1 h under reflux. Temperature was decreased in 10 0 increments to induce precipitation in a stirred, unseeded system. Observe the appearance of the co-crystal. Literate to enhance solids recovery decrease the further temperature[21].

Grinding:

When preparing co-crystals, the product obtained from grinding is generally consistent with that obtained from solution. This may indicate that hydrogen-bond connectivity patterns are not idiosyncratic or determined by non-specific and unmanageable solvent effects or crystallization conditions. Nevertheless there are exceptions. Whilst many co-crystal materials can be prepared from both solution growth and solid-state grinding, some can only be obtained by solid-state grinding. An example is that in the co-crystallisatior of 2,4,6-trinitrobenzoic acid and indole-3-acetic acid, different crystal forms were obtained from solution compared with grinding. Failure to form co-crystals by grinding may be due to an inability to generate suitable co-crystal arrangements rather than due to the stability of the initial phases. When co-crystal formation has been successful from solution, but not from grinding, solvent inclusion in stabilizing the supramolecular structure may be a factor. Although co-crystal formation by solid-state grinding has been established fo some time and a late 19 th century report is often cited as the earliest reference to such a procedure, the recent technique of adding small mounts of solvent during the grinding process has been shown to enhance the kinetics and facilitate co-crystal formation and as lead to increased interest of solid-state grinding as a method for co-crystal preparation [38] .

Slurry conversion:

Slurry conversion experiments were conducted in different organic solvents and water. Solvent (100 or 200 ml) was added to the co-crystal (20 mg) and the resulting suspension was stirred at room temperature for some days. After some days, the solvent was decanted and the solid material was dried under a flow of nitrogen for 5 min. The remaining solids were then characterized using PXRD.

Antisolvent addition:

This is one of the methods for precipitation or recrystalization of the co-crystal former and active pharmaceutical ingredient. Solvents include buffers (pH) and organic solvents. For example preparation of co-crystals of aceclofenac using chitosan, in which chitosan solution was prepared by soaking chitosan in glacial acetic acid. A weighed amount of the drug was dispersed in chitosan solution by using high dispersion homogenizer. This dispersion was added to distilled water or sodium citrate solution to precipitate chitosan on drug [39] .

Influence of Process Variables on Crystal Habit

A crystalline particle is characterized by definite external and internal structures. Habit describes the external shape of a crystal,

BNSDOCID: <XP_____2635211A__I_>

UM00017086
NOVARTIS EXHIBIT 1517
Novartis v. Regents, IPR2023-01347
Page 3943 of 4460

where as polymorph state refers to the definite arrangement if molecules inside the crystal lattice [40] . Supersaturation, nucleation and crystal growth are the basic three steps in crystallization. Thermodynamic parameter like solubility, kinetical parameter like supersaturation, nucleation rate, dissolution rate, antisolvent addition rate, and evaporation rate phenomenon governs the crystallization [41] .

From the above described methods such as solution crystallization, solvent change that create supersaturation by increasing the solut concentration and decreasing the solute solubility, respectively [41] . There are process variables of crystallization like, supersaturation, rate of cooling and degree of solution agitation, nature of crystallizing solvent, temperature of crystallalizing solvent and presence of impurity having possible influence on crystal habit, crystal/dosage form performance [40],[42] .

In case of increased saturation, rate of nuclei formation is greater than crystal growth. More growth in one direction produces fine needle shaped crystals that exhibit poor folowability, while less saturation leads to platy crystals which exhibit greater dissolution rate. Cooling a supersaturated solution of drug or pouring it into crystallizing solvent maintained at low temperature immediately decreases the drug solubility and results in rapid deposition of drug molecules on the nuclei. Rapid cooling leads to formation of platy or needle shaped crystals, slow rate of cooling forms compact, symmetric or elongated prisms. The degree of solution agitation has influence on saturation level, high speed of agitation leads to elongated crystals with small particle size distribution having good folowability and less sedimentation in suspension. Slow speed of agitation or unstirred solution forms large platy crystals.

The nature of solvent has been found to have a profound effect on crystal habit of ibuprofen. Crystallization of ibuprofen from ethano and acetone having high surface tension, dielectric constant and less specific gravity were thin, platy, and neatly circular in shape, while those obtained from propylene glycol and 2-propanol were rod shaped. When pH was decreased by addition of hydrochloric acid to sodium hydroxide solution (pH-10) resulted in formation of needle shaped crystals. However, spherical agglomerates were obtained when ibuprofen was dissolved in acetonitrile because of limited miscibility with water [43] .

Low temperature of crystallizing solvent produces irregular shaped crystals while in case of high temperature nuclei formation is delayed and fine, symmetric crystals are produced. Ions, polymeric molecules, or the other substances present in solute or solvent acts as impurities for the growing crystals and modify crystal habit. Impurity is known to modify the growing crystals into a morpholog that is desirable from the viewpoint of dosage form design and performance [44] . Grinding is well known to create lattice defects anc amorphous phases, and the formation of polymorphic forms of drugs as a result of these stresses is well documented in the pharmaceutical literature. Co-crystal formation during co-grinding and storage is mediated by amorphous phase, the rate of co-crystallization is dependent on the process and storage temperature, glass transition temperatures of reactants and additives, milling time and mill type [15],[45] .

Case Studies of Pharmaceutical Co -Crystals

The earliest example of pharmaceutical co-crystals in the context of APIs relates to a series of studies conducted in the 1950s by Higuchi and Roy. They studied complex formation between macromolecules and certain pharmaceuticals. However, these would not be classified as pharmaceutical co-crystals according to the criteria applied herein [46],[47] .

Perhaps the first application of crystal engineering to the generation of pharmaceutical co-crystals was a series of studies reported by Zerkowski et al.[48] concerning the use of substituted barbituric acid, including barbital and melamine derivatives, to generate supramolecular linear tape, crinkled tape, and rosette motifs sustained by robust supramolecular synthons with three point hydrogen bonding [47]. Despite their success in cocrystal formation, the focus of these studies was not so much the physical properties of the resulting co-crystals but rather the supramolecular functionality of barbitals and their complementarities with melamine . Nevertheless, these studies illustrated very well the potential diversity of forms that can exist for a particular API as more than 60 co-crystals were structurally characterized in this series of studies. Clearly, such a diversity of forms could offer an exciting opportunity to novel and improved crystalline forms of APIs. Herein, we have chosen to focus upon several case studies that involve the formation of pharmaceutical co-crystals with altered physical properties of clinical relevance.

Pharmaceutical co-crystals of carbamazepine (Tegretol®):

Carbamazepine (CBZ) is an important antiepileptic drug that has been in use for over three decades. Oral administration of CBZ encounters multiple challenges, including low water solubility with high dosage required for therapeutic effect (i.e. >100 mg/day), dissolution-limited bioavailability and auto induction for metabolism. In contrast to its simple molecular structure, CBZ exhibits complexity in its crystal forms [20],[21]. To date, four anhydrous polymorphs, a dihydrate, an acetone solvate, and two ammonium salts of CBZ have been identified. It is noted that, in the crystal structures of all these forms, the self-complementary nature of the amide group manifests itself in a predictable manner. Therefore, CBZ has been used as an ideal candidate to demonstrate how APIs can be converted to pharmaceutical co-crystals, and how these co-crystals could offer optimized physicochemical properties over existing forms of an API [20],[43] . Two strategies have been adopted for co-crystal formation of CBZ. One crystal engineering strateg is to employ the peripheral hydrogen bonding capabilities that are not engaged in the pure form of CBZ. A second strategy for co-crystallization of CBZ involves breakage of the CBZ amide-amide dimer and formation of a supramolecular heterosynthon between CBZ

BNSDOCID: <XP_____2636211A__I_>

UM00017087

NOVARTIS EXHIBIT 1517
Novartis v. Regents, IPR2023-01347
Page 3944 of 4460

and a co-crystal former [43] . Both strategies are successful and have afforded a number of CBZ co-crystals that exhibit improved physicochemical properties. For example, the CBZ:saccharin co-crystal shows significantly improved physical stability (i.e. only one cocrystal form with equivalent chemical stability to the anhydrous polymorph has been identified after sophisticated form screening) [21] . In addition, the CBZ:saccharin cocrystal possesses favorable dissolution properties, suspension stability, and pharmacokinetics using dog models. The pharmacokinetic study reveals that the CBZ:saccharin co-crystal exhibits a higher C max and comparable T max when compared with the marketed form, Tegretol®[21] . In short, the CBZ:saccharin cocrystal appears to be superior to existing crystal forms of CBZ in the following respects: stability relative to the anhydrous polymorph of CBZ; favorable dissolution and suspension stability, favorable oral absorption profile in dogs [49] .

Pharmaceutical co-crystals of fluoxetine hydrochloride (Prozac®):

The availability and marketability of a variety of APIs as chloride salts is well recognized, and, recently, an approach to utilize such chloride salts, specifically fluoxetine hydrochloride (fluoxetine HCl), to generate co-crystals of an amine hydrochloride salt via a chloride-mediated carboxylic acid supramolecular synthon has been reported. Fluoxetine HCl is the active pharmaceutical ingredient found in the common antidepressant drug Prozac® . It is a solid under ambient conditions, only one crystalline phase is known, and it is available in the salt form. It has been demonstrated that co-crystallization of this API modifies the physical properties of fluoxetine HCl while still retaining the hydrochloride salt of the API. Fluoxetine HCl was co-crystallized with benzoic acid (1:1), succinic acid (2:1), and fumaric acid (2:1) via traditional evaporation techniques. For all three co-crystals, the carboxylic acid was found to form hydrogen bond to the chloride ion, which in turn interacted with the protonated amine, thus generating, in all three cases, amine hydrochloride salt hydrogen bonding to an additional neutral molecule. Powder dissolution experiments were carried out in water for the three novel co-crystals resulting in a spread of dissolution profiles. The fluoxetine HCl:benzoic acid cocrystal was found to have a decrease in aqueous solubility by 50%, and the fluoxetine HCl:fumaric acid cocrystal had only a slight increase in aqueous solubility. However, the fluoxetine HCl: succinic acid cocrystal exhibited an approximately twofold increase in aqueous solubility after only 5 min. The complex formed between succinic acid and fluoxetine HCl falls apart in solution to generate its pure components after about 1 h. An intriguing aspect of this study is that by simply hydrogen bonding a hydrochloride salt of an API with similar cocrystal formers, one can generate distinctively different dissolution profiles [50] .

Pharmaceutical co-crystals of itraconazole (Sporanox®):

Itraconazole is a triazole antifungal agent that is prescribed to patients with fungal infections. Itraconazole is extremely water insoluble and administered both orally and intravenously. The oral formulation of itraconazole is the amorphous form coated on the surfaces of sucrose beads, and marketed as the Sporanox® capsule. In addition, co-administration of acidified HP-ß-cyclodextrin beverages with Sporanox® capsules is required to achieve the maximal absorption of the API, even though such a co-administration can cause diarrhea [51],[52] . Interestingly, no crystalline salt of itraconazole has been reported in the patent literature, even though salt formation using itraconazole and an acidic salt former would seem to be a logical approach to improve the absorption properties of the API. In order to improve the absorption of the API and maintain the form crystallinity and stability, the pharmaceutical cocryste approach has been evaluated in the formulation of itraconazole.

Crystalline phases of itraconazole can be engineered by introduction of additional molecules to match hydrogen-bond donors and acceptors [49],[50] . A number of stable pharmaceutical co-crystals of itraconazole and 1,4-dicarboxylic acids were synthesized and crystallographically characterized [45] . Each cocrystal contains two API molecules and one acid cocrystal former, hydrogen- bonded through carboxylic acid-triazole supramolecular synthons, to form a trimeric assembly. The aqueous dissolution of itraconazole co-crystals was studied in order to assess their potential impact on bioavailability of the API. The dissolution of itraconazole co-crystals was observed to behave more akin to the Sporanox form than to the crystalline form of the pure API. In particular, it was noted that the itraconazole:L-malic acid cocrystal exhibits a similar dissolution profile to that of the marketed formulation [49] . In a further pharmacokinetic study of itraconazole co-crystals, it was revealed that cocrystal formulation of the API gives similar oral bioavailability to the Sporanox form in the animal trial using a dog model [50] . In short; this study demonstrates the use of pharmaceutical co-crystals for the improvement of solubility and bioavailability without compromising crystallinity and stability.

Pharmaceutical co-crystals of sildenafil (Viagra®) [53] :

Sildenafil is a drug used in the treatment of pulmonary arterial hypertension, congestive heart failure, atherosclerosis, conditions of reduced blood vessel potency and peripheral vascular disease, as well as male erectile dysfunction and female sexual disorders. Sildenafil selectively inhibits cyclic guanosine monophosphate (cGMP)-specific phosphodiesterase type 5 that is responsible for degradation of cGMP in the corpus cavernosum, leading to smooth muscle relaxation in the corpus cavernosum, and resulting in increased inflow of blood and an erection. Sildenafil citrate, with moderate water solubility, has been commercially developed and marketed by Pfizer and is available under the trademark Viagra® .

It has been observed that sildenafil in a pharmaceutical cocrystal form could provide an improved solubility of the API under acidic conditions. In addition, such an improvement of solubility of sildenafil could be particularly advantageous for its orally administrable formulation. Sildenafil has been successfully co-crystallized with acetylsalicylic acid (1:1 molar ratio) by slurry or under reflux conditions.

The crystal structure of the cocrystal of sildenafil and acetylsalicylic acid has been determined by single crystal X-ray diffraction, and

UM00017088
NOVARTIS EXHIBIT 1517
Novartis v. Regents, IPR2023-01347
Page 3945 of 4460

in addition, the composition of matter was confirmed by powder X-ray diffraction and infrared spectrometry. Moreover, the differential scanning calorimetry and thermo gravimetric analyses indicate that the melting point of the cocrystal is approximately 143o, and it remains thermodynamically stable up to 165o[31] . An intrinsic dissolution study in simulated gastric body fluid (pH 1.2) shows that the sildenafil: acetylsalicylic acid cocrystal exhibits an intrinsic dissolution rate (IDR) of ca. 11.75 mg/min/cm vs. 6.64 mg/min/cm for sildenafil citrate under the same conditions.

Co-crystal of melamine and cyanuric acid:

In early 2007, the FDA received complaints from owners of more than 4000 pets regarding the deaths of animals after taking food that was later recalled; it was reported that majority of those deadly incidents were caused by acute renal failure. At first, melamine, which was observed in the tainted products, was the suspected contaminant, since this particular chemical could be intentionally added to raise the apparent protein content of the food. However, melamine is considered relatively nontoxic with the acute toxicity of melamine in rats was reported with oral lethal doses 50 (LD 50) of 3100 mg/kg for the male and 3900 mg/kg for the female. Also, the quantity of melamine observed in those incidents was not at levels that would normally kill. In the course of the pet food recall investigation, cyanuric acid, another relatively nontoxic compound, was also identified in the pet food as a co contaminant. Although melamine and cyanuric acid are relatively safe individually, no data could be found in the literature that could determine the potential toxicity of melamine and cyanuric acid in combination. From the crystal engineering viewpoint, melamine and cyanuric acid (1:1 molar ratio) form an extensive two-dimensional networks in the solid-state based on the robust three-point molecular recognition and it was observed that the resulting melamine:cyanuric acid cocrystal is highly insoluble in water.

As reported by a recent investigation, the combination of melamine and cyanuric acid can result in the intra tubular precipitation of melamine:cyanuric acid co-crystals in the kidney, even though the mechanism associated with renal damage is not fully understood to date. A study conducted at the Bergh Memorial Animal Hospital in New York revealed that co-crystals blocked the tubes leading from the kidneys to the bladder in one cat, and a toxicology assessment of melamine and cyanuric acid indicated that a single oral exposure of cats to the melamine:cyanuric acid cocrystal at a concentration of 32 mg/kg body weight can result in acute renal failure. It seems clear that the formation of a low solubility cocrystal of melamine and cyanuric acid is responsible for these incidents. Perhaps this case study of melamine:cyanuric acid co-crystals are the first example showing how co-crystals can significantly alter the relevant physical properties in a negative manner [54] .

Co-crystals of theophylline:

Theophylline is useful in treatment of respiratory disease such as asthma. From the physicochemical standpoint, theophylline represents challenge to formulators in that it is known to interconvert between crystalline anhydrate and monohydrate forms as a function of relative humidity (RH). The possibility of crystalline hydrate formation complicates design of a consistent, reproducible for an API in the drug development process. Reversible hydrate formation is particularly problematic, as it indicates that neither the anhydrate nor the hydrate is fully stable across the range of common processing condition. Theophylline is structural analogue of caffeine. The co-crystals of the theophylline were prepared with oxalic acid, malonic acid, maleic acid, glutaric acid by solvent evaporation technique. The relative humidity stability comprised of the storage and subsequent PXRD analysis at four specific RH levels (0%, 43%, 75% and 98% RH) across four different time points (1 day, 3 day, 1 and 7 weeks). Over the course of 7 week study it was found that, at 75% RH and below, theophylline anhydrate converted into theophylline monohydrate. No formation of theophylline hydrate was found in any case.

The observed RH stability of theophylline co-crystal demonstrates the physical stability improvement, specifically avoidance of hydrate formation. The co-crystals formed by oxalic acid found to be more stable. This study demonstrates use of co-crystals in physical property improvement [17] .

Co-crystals of aceclofenac:

Aceclofenac is an orally effective nonsteroidal antiinflammatory drug of phenyl acetic acid group, which possesses remarkable antiinflammatory, analgesic and antipyretic properties. Aceclofenac exhibits slight solubility in water and as a consequence it exhibits low bioavailability after oral administration. Mutalic [39] prepared co-crystals of aceclofenac by simple solvent change approach by using chitosan.

Chitosan has been considered to be one of the most promising biopolymer for drug delivery purpose. Chitosan is a linear hydrophilic polysaccharide polymer of D-glucosamine. It is non-toxic natural polcationic polymer that is degraded by the microflora in the colon. I is abundant in nature and is present in the exoskeleton of crustaceans such as crabs and shrimps. Chitosan has been demonstrated to be a good vehicle for enhancing the dissolution properties and bioavailability of a number of poorly water-soluble drugs [55] .

Chitosan was precipitated on aceclofenac crystals using sodium citrate as a salting out agent. The pure drug and prepared co-crystals with different concentrations (0.05 to 0.6%) were characterized in terms of solubility, drug content, particle size, thermal behavior (differential scanning calorimetry, DSC), X-ray diffraction (X-RD), morphology, in vitro drug release, stability and phrmacokinetic study.

It was observed that particle size of co-crystals was drastically reduced during the formulation process. The DSC showed a decrease in

BNSDOCID: <XP_____2635211A_!_>

UM00017089

NOVARTIS EXHIBIT 1517
Novartis v. Regents, IPR2023-01347
Page 3946 of 4460

melting enthalpy indicating disorder in crystallinity. XRD also revealed disorder in crystallinity. The dissolution study showed that marked increase in dissolution rate in comparison to pure drug. The considerable dissolution rate of aceclofenac from optimized crystal formulation was attributed to the wetting effect of chitosan, decreased drug crystallinity, altered morphology and micronization. The optimized crystals showed excellent stability on storage at accelerated conditions. In vivo study revealed that the crystals provided a rapid pharmacological response in mice and rat; besides improve in pharmacokinetic parameters in rats [39].

Co-crystal of 5-nitrouracil:

Co-crystals of 5-nitrouracil with solvent molecules, dioxane, pyridine, DMSO, formamide and ethanol as well as with piperazine, N,N'-dimethylpiperazine, 3-aminopyridine and diazabicyclooctane obtained by deliberate inclusion, have been examined by X-ray crystallography. The tape structure found in the parent centric form of nitrouracil is retained with some modifications in the co-crystals with dioxane, piperazine, diazabicyclo-octane, N,N'-dimethylpiperazine, pyridine and DMSO, with the guest molecules forming alternate tapes. In co-crystals involving formamide, ethanol and 3-aminopyridine, the molecular tapes exhibit mixed compositions. The observed bonding patterns have been classified into six schemes. Interestingly, quadruple type hydrogen bonding patterns are seen in co-crystals containing 3-aminopyridine or ethanol and water, while a network of acyclic tetrahedral pentamers of water is found in the cocrystal containing diazabicyclo-octane and water. This case study reveals that hydrogen acceptors and donors are necessary to form cocrystal [56] .

Co-crystals of indomethacin:

Indomethacin, a non-steroidal antiinflammatory drug (NSAID), is widely prescribed for patients with arthritis. It exists as α, γ and amorphous forms, in the solid state α-form being most stable form at room temperature. Indomethacin is practically insoluble in wate (2.5-4 ˜ g/ml; it belongs to BCS class II) and poses severe challenges in the formulation development. Various cocrystal formers, including saccharin, were used in the screening for indomethacin co-crystals in a series of solvents.

Solution evaporation method was used in the screening phase. DSC, TGA, IR, Raman and PXRD techniques characterized the potential new phases. The indomethacin saccharin co-crystal (IND-SAC co-crystal) structure was determined from single crystal X-ray diffraction data. Pharmaceutically relevant properties such as the dissolution rate and dynamic vapour sorption (DVS) of the IND-SAC co-crystal were evaluated. Solid-state and solvent-drop co-grinding methods were also applied to indomethacin and saccharin.

The IND-SAC co-crystals were obtained from ethyl acetate. Physical characterization showed that the IND-SAC co-crystal is unique vis-ũ-vis thermal, spectroscopic and X-ray diffraction properties. The co-crystals were obtained in a 1:1 ratio with a carboxylic acid and imide dimer synthons. The dissolution rate of IND-SAC was considerably faster than that of the stable indomethacin α-form. DVS studies indicated that the co-crystals gained less than 0.05% in weight at 98% RH. IND-SAC co-crystals were also obtained by solid state and solvent-drop co grinding methods. The IND-SAC co-crystal was formed with a unique and interesting carboxylic acid and imide dimer synthons interconnected by weak N-H···O hydrogen bonds. The co-crystals were associated with significantly faster dissolution rate than indomethacin (α-form) in phosphate buffer pH 7.4 and were non-hygroscopic[57] .

Co-Crystals and Patents

"New" refers to anything under the sun that is made by the man, such as new composition of matter or any useful improvements. Thus a necessary condition to claim a new composition of matter is to describe clearly with precision the composition, a great challenge in the case of co-crystals [58] .

Aripiprazole co-crystals [59] , the present invention relates to co-crystals comprising aripiprazole and fumaric acid and processes for co-crystal preparation. Aripiprazole is a psychotropic drug useful for the treatment of schizophrenia and is the sixth, and most recent, of the second generation antipsychotic medications. It is available in the market under the brand name Abilify® in the form of tablets of 5, 10, 15, 20 and 30 mg strengths. Aripiprazole presents certain challenges for formulation as a rapid-onset dosage form, particularly as a rapid-onset oral dosage form. For example, aripiprazole has a very low solubility in aqueous media (being practically insoluble) and therefore is not readily dissolved and dispersed for rapid absorption in the gastrointestinal tract when administered orally, for example in tablet form. Towards this end, it has been the endeavor of pharmaceutical scientists to provide new forms of aripiprazole, more specifically, a thermodynamically stable form which would have the strengths of the crystalline forms, viz. thermodynamic stability, and those of the amorphous form, viz. enhanced solubility, rapid onset of action and an enhanced bioavailability.

Consequently, there is a need for soluble forms of aripiprazole that can be readily formulated for use in various modes of administration, including parenteral and oral administration. Co-crystal complexes of aripiprazole would add a powerful tool in the treatment of central nervous system disorders. The present invention provided co-crystals of aripiprazole and fumaric acid which are stable and are reproducible on an industrial scale.

TDFA is the co-crystal of tenofovir disoproxil hemi-fumaric Acid [60] . Tenofovir disoproxil fumarate (DF) is a nucleotide reverse

BNSDOCID: <XP_____2635211A_I_>

UM00017090
NOVARTIS EXHIBIT 1517
Novartis v. Regents, IPR2023-01347
Page 3947 of 4460

transcriptase inhibitor approved in the United States for the treatment of HIV-1 infection alone or in combination with other antiretroviral agents. Tenofovir disoproxil DF is sold under the trade name Viread (Gilead Science, Inc.) and present in combination with other antiviral agents in the Truvada and Atripla. After analysis of several commercially available products containing tenofovir DF, it was found that these contained mixtures of solid forms of tenofovir DF in varying ratios. Indications have been found by the present inventors that the solid form of tenofovir DF in commercially available products is generally a mixture of at least two forms. It has also been found that one of these forms experiences a conversion of its crystalline form into the other form when put under stress such as increased temperature and/or humidity. It is believed by the present inventors that the presence of water will induce or enhance the conversion of one form into the other. This suggests that the solid form currently used in the marketed product is not stable or at least has a reduced stability. The bulk molar ratio of tenofovir disoproxil to fumaric acid in the commercially available products is generally indicated as 1:1. The TDFA 2:1 co-crystal of the invention is more stable and is less hygroscopic than the presently known crystalline form of tenofovir.

Theophylline crystallized rapidly from a hot ethylene glycol solution forms theophylline co-crystals [61] . This technique was confirmed as being functional by testing for a known co-crystal of theophylline and p-nitrophenol. Salicylic acid, p-hydroxybenzoic acid, sorbic acid, 1-hydroxy-2-naphthoic acid, glycolic acid, and 2,5-dihydroxybenzoic acid were all tested as guest compounds and in each, a co-crystal formation had occurred. Raman spectra of the pure guest acid, theophylline, and the co-crystal were obtained and compared to confirm co-crystal formation. This invention provides information regarding a new method for co-crystallization i.e ethylene glycol based method.

As one aspect, novel co-crystals are provided. The novel co-crystals comprise one or more active agents, particularly of the salts of such active agents. Novel forms of salts of active pharmaceutical ingredients are provided. For example, the present invention provides novel co-crystals of fluoxetine HCl and benzoic acid; fluoxetine HCl and succinic acid; and fluoxetine HCl and fumaric acid. Novel forms or solid state phases of active pharmaceutical ingredients may be prepared for which there are no known polymorphs, solvates or hydrates, or where such polymorphs, solvates or hydrates were disfavored [62] . Co-crystals fulfill the criteria for patent eligibility: novelty, utility, and non obviousness.

References

1 Paul EL, Tung HH, Midler M. Organic crystallization processes. Powder Technol 2005;150:133-43.
2 Gardner CR, Walsh CT, Almarsson Φ. Drugs as materials: Valuing physical form in drug discovery. Nat Rev Drug Disc 2004;3:926-34.
3 Byrn SR, Pfeiffer RR, Stowell JG. Solid-state chemistry of drugs. West Lafayette; SSCI: 1999.
4 Brittain H, editor. Polymorphism in pharmaceutical solids. Vol. 95, New York: Marcel Dekker; 1999.
5 Berge SM, Bighley LD, Monkhouse DC. Pharmaceutical salts. J Pharm Sci 1977;66:1-19.
6 Gould PL. Salt selection for basic drugs. Int J Pharm 1986;33:201-17.
7 Kobell FV, Prakt JF. D-glucose: Sodium chloride monohydrate. Chemie 1843;28:489.
8 Wφhler F. Untersuchungen óber das Chinon Quinhydrone. Annalen 1844;51:153.
9 Buguet A. Cryoscopy of Organic Mixtures and Addition Compounds. Compt Rend 1910;149:857.
10 Grossmann H. Thiourea. Cryoscopy of organic mixtures and addition compounds. Chemiker-Zeitung 1908;31:1195.
11 Damiani A, De Santis P, Giglio E. The crystal structure of the 1:1 molecular complex between 1,3,7,9-tetramethyluric acids and pyrene. Acta Crystallogr 1965;19:340.
12 Van NJ, Saunder DH. The crystal structure of the molecular complex of 4,4'-dinitrobiphenyl with biphenyl. Acta Crystallogr 1948;1:44.
13 Pekker S, Kovats E, Oszlanyi G, Benyei G, Klupp G. Rotor-stator molecular crystals of fullerenes with cubane. Nat Materials 2005;4:764-7.
14 Matthew LP, Magali BH, Michael JZ, Almarsson Φ. Expanding the scope of crystal form evaluation in pharmaceutical science. J Pharm Pharmaceut Sci 2006;9:317-26.
15 Nair RH, Sarah J N, Adivaraha J, Swarbreek editors. Co-crystals: design, properties and formulation mechanism, in Encyclopedia of Pharmaceutical Technology, 3rd ed. Vol. 1, New York: Informa Healthcare; 2007. p. 615.
16 Serajuddin AT, Pudipeddi M, Stahl PH, Wermuth CG, editors, Handbook of pharmaceutical salts. Weinheim: Wiley-VCH; 2002. p. 138.
17 Andrew VT, Sam Motherwell WD, Jones W. Physical stability enhancement of theophylline via co crystallization. Int J Pharm 2006;320:114-23.
18 Ori A, Michael JZ. Crystal engineering of the composition of pharmaceutical phases, do pharmaceutical co-crystals represent a new path to improve medicine? Chem Comm 2004;:1889-96.
19 Koji S, Noriyuki T, Ryusuke T, Yoshiki H, Katsuhide T. Dissolution improvement and the mechanism of the improvement from co crystallization of poorly water-soluble compounds. Pharm Res 2006;23:1144-56.
20 Morrissette S, Almarsson O, Peterson M, Remenar J. High-throughput crystallisation: polymorphs, salts, co-crystals and solvates of pharmaceutical solids. Adv Drug Deliv Rev 2004;56:275-300.
21 Magali BH, Matthew LP, Lisa AS, Sherry LM, Vetter A, Hector G, *et al.* Performance comparison of a co-crystal of carbamazepine with marketed product. Eur J Pharm Biopharm 2007;67:112-9.
22 Salole EG, Al-Sarraj FA. Spiranolactone crystal forms. Drug Develop Ind Pharm 1985;11:855-64.
23 Trask AV, Motherwell WD, Jones W. Solvent-drop grinding: Green polymorph control of co-crystallization. Chem Comm 2004;890-1.

BNSDOCID: <XP_____2635211A__I_>

UM00017091

NOVARTIS EXHIBIT 1517
Novartis v. Regents, IPR2023-01347
Page 3948 of 4460

24 Taylor LS, Zografi G. Spectroscopic characterization of interactions between PVP and indomethacin in amorphous molecular dispersions. Pharm Res 1997;14:1691-8.
25 Tong P, Zografi G. A study of amorphous molecular dispersions of indomethacin and its sodium salt. J Pharm Sci 2001;90:2372-3
26 Warwick B, Dehghani F, Foster NR, Biffin JR. Pharmaceutical applications of solid dispersion systems. J Pharm Sci 1971;60:1281 302.
27 Sekiguchi K, Obi AT. Studies on absorption of eutectic mixture: I: A comparison of the behavior of eutectic mixture of sulfathiazole and that of ordinary sulfathiazole in man. Chem Pharm Bull 1961;9:866-72.
28 Emara LH, Badr RM, Elbary AA. Improving the dissolution and bioavailability of nifedipine using solid dispersions and solubilizers Drug Develop Ind Pharm 2002;28:795-807.
29 Kai T, Akiyama Y, Nomura S, Sato M. Oral absorption improvement of poorly soluble drug using solid dispersion technique. Chen Pharm Bull 1996;44:568-71.
30 Juppo AM, Boissier C, Khoo C. Evaluation of solid dispersion particles prepared by SEDS. Int J Pharm 2003;250:385-401.
31 Forster A, Hempenstall J. Rades T. Characterization of glass solutions of poorly water-soluble drugs produced by melt extrusion with hydrophilic amorphous polymers. J Pharm Pharmacol 2001;53:303-15.
32 Mirza S, Heinõmõki J, Miroshnyk I, Yliruusi J. Co-crystals: An emerging approach to improving properties of pharmaceutical solids. Eur J Pharm Sci 2008;34:S16-7.
33 Burton WK, Cabrera N, Frank FC. The growth of crystals. Phil Tran R Soc Lond A 1951;243:299-358.
34 Ning S, Michael JZ. The role of co-crystals in pharmaceutical science. Drug Discov Today 2008;13:440-6.
35 Portalone GC. First example of co-crystals of polymorphic maleic hydrazide. J Chem Crystallogr 2004;34:609-12.
36 Aakerφy CB. Beatty AM, Helfrich BA, Nieuwenhuyzen M. Do polymorphic compounds make good cocrystallising agents? A structural case study that demonstrates the importance of synthon flexibility. Cryst Growth Des 2003;3:159-65.
37 Zaworotko M. Polymorphism in co-crystals and pharmaceutical co-crystals. Florence: XX Congress of the International Union of Crystallography: 2005.
38 Blagden N, de Matas M, Gavan PT, York P. Crystal engineering of active pharmaceutical ingredients to improve solubility and dissolution rates. Adv Drug Deliv Rev 2007;59:617-30.
39 Mutalik S, Prambil A, Krishnan M, Achuta NU. Enhancement of dissolution rate and bioavailability of aceclofenac: A chitosan based solvent change approach. Int J Pharm 2008;350:279-90.
40 Tiwary AK, Swarbreek editor. Crystal habit changes and dosage form performance. Encyclopedia of Pharmaceutical Technology, 3 rd ed. Vol. 2, New York, London: Informa Healthcare; 2007. p. 820.
41 Nair RH, Ron CK, Brent DS, Jonathan MM, Swarbreek editors. Crystallization: General principles and significance on product development. Encyclopedia of Pharmaceutical Technology, 3 rd ed. Vol.2, London: Informa Healthcare; 2007. p. 834.
42 Kiang YH, Yang CY, Staples RJ, Jonan J. Crystal structure, crystal morphology, and surface properties of an investigational drug Int J Pharm 2009;368:76-82.
43 Rasenac N, Muller BW. Properties of ibuprofen crystallized under various conditions: A comparative study. Drug Develop Ind Pharm 2001;27:803-9.
44 Jingkang W, Yongli W, Ying B, Effects of solvent and impurity on crystal habit modification of 11α-hydroxy-16α,17α-epoxyprogesteron. Chin J Chem Eng 2007;15:648-53.
45 Aaltonen J, Alleso M, Mirza S, Koradia V, Gorden KC, Rantanen J. Solid form screening: A review. Eur J Pharm Biopharm 2009;71:23-37.
46 Higuchi T, Roy K. Study of possible complex formation between macromolecules and certain pharmaceuticals I. Polyvinylpyrrolidone (PVP) with sulfathiazole, procaine hydrochloride, sodium salicylate, benzylpenicillin, chloramphenicol, mandelic acid, caffeine, theophylline, and cortisone. J Am Pharm Assoc 1954;43:393-7.
47 Higuchi T, Roy K. Study of possible complex formation between macromolecules and certain pharmaceuticals II: Polyvinylpyrrolidone with p-aminobenzoic acid (PABA), aminopyrine, benzoic acid, salicylic acid, phydroxybenzoic acid, hydroxybenzoic acid, citric acid, and Phenobarbital. J Am Pharm Assoc 1954;43:398-401.
48 Zerkowski JA. Solid-state structures of 'Rosette' and 'Crinkled Tape' motifs derived from the cyanuric acid melamine lattice. J Am Chem Soc 1992;114:5473-5.
49 Fleischmann SG. Crystal engineering of the composition of pharmaceutical phases: Multiple component crystalline solids involving carbamazepine. Cryst Growth Des 2003;3:909-19.
50 Childs SL. Crystal engineering approach to forming co-crystals of amine hydrochlorides with organic acids. Molecular complexes of fluoxetine hydrochloride with benzoic, succinic, and fumaric acids. J Am Chem Soc 2004;126:13335-42.
51 Remenar JF. Crystal engineering of novel co-crystals of a Triazole drug with 1,4-dicarboxylic acids. J Am Chem Soc 2003;125:8456-7.
52 Remenar JF. Novel Crystalline forms of conazoles and methods of making and using the same. USP0070551, 2005.
53 Zegarac M. Pharmaceutically acceptable co crystalline forms of sildenafil. WO080362 A1, 2007.
54 Puschner B. Assessment of melamine and cyanuric acid toxicity in cats. J Vet Diag Invest 2007;19:616-24.
55 Portero A, Ropez R, Vila-jato JL. Effect of chitosan and chitosan glutamate on enhancing the dissolution properties of poorly water-soluble drug nifedipine. Int J Pharm 1998;175:75-84.
56 Reji T, Srinivasa RG, Kulkarni GU, Rao CNR. Hydrogen bonding patterns in the co-crystals of 5-nitrouracil with several donor anc acceptor molecules. Beilstein J Org Chem 2005;1:15.
57 Basavoju S, Bostrom D, Velaga SP. Indomethacin-saccharin co crystal: design, synthesis and preliminary pharmaceutical characterization. Pharm Res 2007;25:530-40.
58 Lara-Ochoa F, Espinosa-Perez G. Crystals and patents. Cryst Growth Des 2007;7:1213-5.
59 Devarakonda SN, Vyas K, Bommareddy SR, Padi PR, Raghupathy B. Aripiprazole co-crystals. WO/2007/092779, 2007.

BNSDOCID: <XP_____2635211A__I_>

UM00017092
NOVARTIS EXHIBIT 1517
Novartis v. Regents, IPR2023-01347
Page 3949 of 4460

60 www.faqs.org/patents/app/20090176983,Tenofovir Disoproxil Hemi-Fumaric Acid Co-Crystal, 2007 .
61 Childs S, Co-Crystallization methods WO/2007/038524, 2007.
62 Andrew V. Overview of pharmaceutical Co-crystals as intellectual property. Mol Pharmaceutics 2007;4:301-9.

Tuesday, May 03, 2011
Site Map | Home | Contact Us | Feedback | Copyright and Disclaimer

BNSDOCID: <XP_____2635211A__I_>

UM00017093

NOVARTIS EXHIBIT 1517
Novartis v. Regents, IPR2023-01347
Page 3950 of 4460

Electronic Patent Application Fee Transmittal

Application Number:	10378956
Filing Date:	03-Mar-2003
Title of Invention:	Multiple-component solid phases containing at least one active pharmaceutical ingredient
First Named Inventor/Applicant Name:	Michael J. Zaworotko
Filer:	Mark A. Buese/Jennifer Rogers
Attorney Docket Number:	USF.106XC1

Filed as Small Entity

Utility under 35 USC 111(a) Filing Fees

Description	Fee Code	Quantity	Amount	Sub-Total in USD($)
Basic Filing:				
Pages:				
Claims:				
Miscellaneous-Filing:				
Petition:				
Patent-Appeals-and-Interference:				
Post-Allowance-and-Post-Issuance:				
Extension-of-Time:				

Description	Fee Code	Quantity	Amount	Sub-Total in USD($)
Miscellaneous:				
Submission- Information Disclosure Stmt	1806	1	180	180
		Total in USD ($)		**180**

Electronic Acknowledgement Receipt	
EFS ID:	11055290
Application Number:	10378956
International Application Number:	
Confirmation Number:	4742
Title of Invention:	Multiple-component solid phases containing at least one active pharmaceutical ingredient
First Named Inventor/Applicant Name:	Michael J. Zaworotko
Customer Number:	23557
Filer:	Mark A. Buese/Jennifer Rogers
Filer Authorized By:	Mark A. Buese
Attorney Docket Number:	USF.106XC1
Receipt Date:	27-SEP-2011
Filing Date:	03-MAR-2003
Time Stamp:	10:00:28
Application Type:	Utility under 35 USC 111(a)

Payment information:

Submitted with Payment	yes
Payment Type	Credit Card
Payment was successfully received in RAM	$180
RAM confirmation Number	24629
Deposit Account	190065
Authorized User	EISENSCHENK,FRANK C.
The Director of the USPTO is hereby authorized to charge indicated fees and credit any overpayment as follows: Charge any Additional Fees required under 37 C.F.R. Section 1.16 (National application filing, search, and examination fees) Charge any Additional Fees required under 37 C.F.R. Section 1.17 (Patent application and reexamination processing fees)	

Charge any Additional Fees required under 37 C.F.R. Section 1.19 (Document supply fees) Charge any Additional Fees required under 37 C.F.R. Section 1.20 (Post Issuance fees) Charge any Additional Fees required under 37 C.F.R. Section 1.21 (Miscellaneous fees and charges)	

File Listing:

Document Number	Document Description	File Name	File Size(Bytes)/ Message Digest	Multi Part /.zip	Pages (if appl.)
1		SIDS4.pdf	434578 a7ab3dfcd6eb480b83a9b7a2996d2723b93a0920	yes	4

Multipart Description/PDF files in .zip description

Document Description	Start	End
Transmittal Letter	1	2
Information Disclosure Statement (IDS) Form (SB08)	3	4

Warnings:					
Information:					
2	Foreign Reference	CA318788.pdf	309938 dc8b8a8af2d0c831e2e8d6905d24bb9cf8bade69	no	12
Warnings:					
Information:					
3	Non Patent Literature	Remenar2011.pdf	620332 11cb83fccdc55bf69a5a1b2bc8b7767476d92781	no	10
Warnings:					
Information:					
4	Non Patent Literature	Yadav2009.pdf	299890 9da431b948ae0a666f8904ca4ac50b7308c3eb32	no	11
Warnings:					
Information:					
5	Fee Worksheet (SB06)	fee-info.pdf	30419 55701581694be1691e96b9a6cd59c70742f07fad	no	2
Warnings:					
Information:					
		Total Files Size (in bytes):	1695157		

This Acknowledgement Receipt evidences receipt on the noted date by the USPTO of the indicated documents, characterized by the applicant, and including page counts, where applicable. It serves as evidence of receipt similar to a Post Card, as described in MPEP 503.

New Applications Under 35 U.S.C. 111
If a new application is being filed and the application includes the necessary components for a filing date (see 37 CFR 1.53(b)-(d) and MPEP 506), a Filing Receipt (37 CFR 1.54) will be issued in due course and the date shown on this Acknowledgement Receipt will establish the filing date of the application.

National Stage of an International Application under 35 U.S.C. 371
If a timely submission to enter the national stage of an international application is compliant with the conditions of 35 U.S.C. 371 and other applicable requirements a Form PCT/DO/EO/903 indicating acceptance of the application as a national stage submission under 35 U.S.C. 371 will be issued in addition to the Filing Receipt, in due course.

New International Application Filed with the USPTO as a Receiving Office
If a new international application is being filed and the international application includes the necessary components for an international filing date (see PCT Article 11 and MPEP 1810), a Notification of the International Application Number and of the International Filing Date (Form PCT/RO/105) will be issued in due course, subject to prescriptions concerning national security, and the date shown on this Acknowledgement Receipt will establish the international filing date of the application.

I hereby certify that this correspondence is being electronically filed in the United States Patent and Trademark Office on September 27, 2011

Mark A. Buese, Ph.D., Patent Agent

SUPPLEMENTAL INFORMATION DISCLOSURE STATEMENT
Patent Application
Docket No. USF.106XC1
Serial No. 10/378,956

IN THE UNITED STATES PATENT AND TRADEMARK OFFICE

Examiner	:	Sahar Javanmard
Art Unit	:	1627
Applicants	:	Michael J. Zaworotko, Brian Moulton, Nair Rodriguez-Hornedo
Serial No.	:	10/378,956
Filed	:	March 3, 2003
Conf. No.	:	4742
For	:	Multiple-Component Solid Phases Containing at Least One Active Pharmaceutical Ingredient

Mail Stop Amendment
Commissioner for Patents
P.O. Box 1450
Alexandria, VA 22313

SUPPLEMENTAL INFORMATION DISCLOSURE STATEMENT
UNDER 37 C.F.R. §§ 1.97 AND 1.98

Sir:

In accordance with 37 C.F.R. § 1.56, the references listed on the attached form PTO/SB/08 are being brought to the attention of the Examiner for consideration in connection with the examination of the above-identified patent application. A copy of each cited reference is enclosed.

It is respectfully requested that the references cited on the attached form PTO/SB/08 be considered in the examination of the subject application and that their consideration be made of record.

J:\USF\106XC1\IDS\SIDS4.doc/jar

This information is being submitted subsequent to the later of three months after the filing date of the present application or the mailing of the first Office Action on the merits, but before the mailing of a final action or the notice of allowance. The fee of $180.00 has been submitted along with this filing. Please charge any additional fees to Deposit Account No. 19-0065.

If any additional fee is required, or to credit any overpayment, please use Deposit Account No. 19-0065.

Applicants respectfully assert that the substantive provisions of 37 C.F.R. §§ 1.97 and 1.98 are met by the foregoing statement.

Respectfully submitted,



Mark A. Buese, Ph.D.
Patent Agent
Registration No. 52,669
Phone No.: 352-375-8100
Fax No.: 352-372-5800
Address: P.O. Box 142950
Gainesville, FL 32614-2950

MAB/jar

Attachments: Form PTO/SB/08; copies of references cited therein.

J:\USF\106XC1\IDS\SIDS4.doc/jar

Substitute for form 1449B/PTO

INFORMATION DISCLOSURE STATEMENT BY APPLICANT

(use as many sheets as necessary)

Sheet 1 of 1

Complete if Known	
Application Number	10/378,956
Filing Date	March 3, 2003
First Named Inventor	Michael J. Zaworotko
Group Art Unit	1627
Examiner Name	Sahar Javanmard
Attorney Docket Number	USF.106XC1

NON PATENT LITERATURE DOCUMENTS

Examiner Initials*	Cite No. [1]	Include name of the author (in CAPITAL LETTERS), title of the article, (when appropriate), title of the item (book, magazine, journal, serial, symposium, catalog, etc.), date, page(s), volume-issue number(s), publisher, city and/or country where published.	T[2]
	R1	Zaworotko, Michael J., "Binary Crystals by Design," Abstracts of Papers, 23rd ACS National Meeting, Orlando, FL, United States, April 7-11, 2002, IEC-030.	
	R2	Fleischman, Scott et al. , "Crystal engineering of binary crystals that contain pharmaceutical molecules, Abstracts of Papers, 23rd ACS National Meeting, Orlando, FL, United States, April 7-11, 2002, IEC-076.	
	R3		
	R4		
	R5		
	R6		
	R7		
	R8		
	R9		
	R10		
	R11		
	R12		
	R13		

Examiner Signature		Date Considered	

*EXAMINER: Initial if reference considered, whether or not citation is in conformance with MPEP 609. Draw line through citation if not in conformance and not considered. Include copy of this form with next communication to applicant. [1] Applicant's unique citation designation number (optional). [2] See Kind Codes of USPTO Patent Documents at www.uspto.gov or MPEP901.04. [3] Enter Office that issued the document, by the two-letter code (WIPO Standard T.3). [4] For Japanese patent documents, the indication of the year of the reign of the Emperor must precede the serial number of the patent document. [5] Kind of document by the appropriate symbols as indicated on the document under WIPO Standard ST. 16 if possible. [6] Applicant is to place a check mark here if English language Translation is attached.

Crystal engineering of binary crystals that contain pharmaceutical molecules

By: Fleischman, Scott; Morales, Leslie Ann; Zaworotko, Michael J.

Abstracts of Papers, 223rd ACS National Meeting, Orlando, FL, United States, April 7-11, 2002 (2002), IEC-076

The design of binary compds. using complementary mols. represents an example of an application of crystal engineering. Pharmaceutical mols. are inherently predisposed for such crystal engineering studies since they already contain mol. recognition sites that bind selectively to biomols., and they are prone to supramol. self-assembly. Pharmaceutical mols. that we have explored and have been able to form co-crystals include ibuprofen and flurbiprofen. The co-crystals of ibuprofen/4,4'-dipyridyl, flurbiprofen/4,4'-dipyridyl and flurbiprofen/trans-1,2-bis(4-pyridyl)ethylene have been characterized by various techniques and exhibit phys. properties different from the parent compd. as a direct result of hydrogen bonding interaction. These cryst. assemblies could afford improved drug soly., dissoln. rate, stability and bioavailability.

NOVARTIS EXHIBIT 1517
Novartis v. Regents, IPR2023-01347
Page 3959 of 4460

Binary Crystals by Design

By: Zaworotko, Michael J.

Abstracts of Papers, 223rd ACS National Meeting, Orlando, FL, United States, April 7-11, 2002 (2002), IEC-030.

The design of binary cryst. compds. relies upon understanding how complementary supramol. synthons influence compn. and structure in the solid state. In this paper we shall present details concerning a range of new binary cocrystals that involve carboxylic acid, amide or ether moieties. The mol. components generate the expected stoichiometry and, in some cases, predictable crystral packing motifs. An anal. of the structure and phys. properties of the new binary cocrystals will be presented. The results will be discussed in the context of how one might exploit our results in order to generate novel pharmaceutical phases.

Electronic Acknowledgement Receipt

EFS ID:	12624133
Application Number:	10378956
International Application Number:	
Confirmation Number:	4742
Title of Invention:	Multiple-component solid phases containing at least one active pharmaceutical ingredient
First Named Inventor/Applicant Name:	Michael J. Zaworotko
Customer Number:	23557
Filer:	Mark A. Buese/Paula Shultz
Filer Authorized By:	Mark A. Buese
Attorney Docket Number:	USF.106XC1
Receipt Date:	25-APR-2012
Filing Date:	03-MAR-2003
Time Stamp:	11:46:47
Application Type:	Utility under 35 USC 111(a)

Payment information:

Submitted with Payment	no

File Listing:

Document Number	Document Description	File Name	File Size(Bytes)/ Message Digest	Multi Part /.zip	Pages (if appl.)
1		SIDS11.pdf	284318 b154ebb5aabc9e59c2cc2ebd0f71ac1fd8bf118c	yes	3

	Multipart Description/PDF files in .zip description				
	Document Description		Start	End	
	Transmittal Letter		1	2	
	Information Disclosure Statement (IDS) Form (SB08)		3	3	
Warnings:					
Information:					
2	Non Patent Literature	Fleischman-2002.pdf	56266 99f90fd45a05f55522778c38c5f8badfae3b66c5	no	1
Warnings:					
Information:					
3	Non Patent Literature	Zaworotko-2002.pdf	41534 480120004a7d03a2b4687007c65b920f4c8e365f5	no	1
Warnings:					
Information:					
		Total Files Size (in bytes):	382118		

This Acknowledgement Receipt evidences receipt on the noted date by the USPTO of the indicated documents, characterized by the applicant, and including page counts, where applicable. It serves as evidence of receipt similar to a Post Card, as described in MPEP 503.

New Applications Under 35 U.S.C. 111
If a new application is being filed and the application includes the necessary components for a filing date (see 37 CFR 1.53(b)-(d) and MPEP 506), a Filing Receipt (37 CFR 1.54) will be issued in due course and the date shown on this Acknowledgement Receipt will establish the filing date of the application.

National Stage of an International Application under 35 U.S.C. 371
If a timely submission to enter the national stage of an international application is compliant with the conditions of 35 U.S.C. 371 and other applicable requirements a Form PCT/DO/EO/903 indicating acceptance of the application as a national stage submission under 35 U.S.C. 371 will be issued in addition to the Filing Receipt, in due course.

New International Application Filed with the USPTO as a Receiving Office
If a new international application is being filed and the international application includes the necessary components for an international filing date (see PCT Article 11 and MPEP 1810), a Notification of the International Application Number and of the International Filing Date (Form PCT/RO/105) will be issued in due course, subject to prescriptions concerning national security, and the date shown on this Acknowledgement Receipt will establish the international filing date of the application.

I hereby certify that this correspondence is being electronically filed in the United States Patent and Trademark Office on April 25, 2012.

Mark A. Buese, Ph.D., Patent Agent

SUPPLEMENTAL INFORMATION DISCLOSURE STATEMENT
Patent Application
Docket No. USF.106XC1
Serial No. 10/378,956

IN THE UNITED STATES PATENT AND TRADEMARK OFFICE

Examiner	:	Sahar Javanmard
Art Unit	:	1627
Applicants	:	Michael J. Zaworotko, Brian Moulton, Nair Rodriguez-Hornedo
Serial No.	:	10/378,956
Filed	:	March 3, 2003
Conf. No.	:	4742
For	:	Multiple-Component Solid Phases Containing at Least One Active Pharmaceutical Ingredient

Mail Stop Amendment
Commissioner for Patents
P.O. Box 1450
Alexandria, VA 22313

SUPPLEMENTAL INFORMATION DISCLOSURE STATEMENT
UNDER 37 C.F.R. §§ 1.97 AND 1.98

Sir:

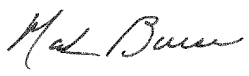
In accordance with 37 C.F.R. § 1.56, the references listed on the attached form PTO/SB/08 are being brought to the attention of the Examiner for consideration in connection with the examination of the above-identified patent application. Copies of the cited references are enclosed.

It is respectfully requested that the references cited on the attached form PTO/SB/08 be considered in the examination of the subject application and that their consideration be made of record.

J:\USF\106XC1\PTO\SIDS11.doc/ps

Applicants respectfully assert that the substantive provisions of 37 C.F.R. §§ 1.97 and 1.98 are met by the foregoing statement.

Respectfully submitted,



Mark A. Buese, Ph.D.
Patent Agent
Registration No. 52,669
Phone No.: 352-375-8100
Fax No.: 352-372-5800
Address: P.O. Box 142950
Gainesville, FL 32614-2950

MAB/ps

Attachments: Form PTO/SB/08; copies of references cited therein.

J:\USF\106XC1\PTO\SIDS11.doc/ps

I hereby certify that this correspondence is being transmitted to the United States Patent and Trademark Office on April 26, 2012.

Mark A. Buese, Ph.D. Patent Agent

REQUEST FOR REFUND
Patent Application
Docket No. USF.106XC1
Serial No. 10/378,956

IN THE UNITED STATES PATENT AND TRADEMARK OFFICE

Examiner	:	Sahar Javanmard
Art Unit	:	1627
Applicants	:	Michael J. Zaworotko, Brian Moulton, Nair Rodriguez-Hornedo
Serial No.	:	10/378,956
Filed	:	March 3, 2003
Conf. No.	:	4742
For	:	Multiple-Component Solid Phases Containing at Least One Active Pharmaceutical Ingredient

Commissioner for Patents
P.O. Box 1450
Alexandria, VA 22313-1450

REQUEST FOR REFUND

Sir:

Applicants respectfully request a refund in the above-referenced patent application for the following reason:

On October 22, 2010, Applicants filed a Request for Continued Examination in the subject application. On September 27, 2011, Applicants filed a Supplemental Information Disclosure Statement and Applicants' credit card was charged $180.00 to pay the fee for an Information Disclosure Statement. Applicants respectfully assert that the Information Disclosure Statement filed September 27, 2011 does not warrant a $180.00 charge because it was filed before receipt of an Office Action from the U.S. Patent and Trademark Office.

J:\USF\106XC1\PTO\ReqforRefund.doc/DNB/ps

Accordingly, Applicants respectfully request that a refund of $180.00 be credited to Applicants' credit card or undersigned representative's Deposit Account No. 190065.

Respectfully submitted,



Mark A. Buese, Ph.D.
Patent Agent
Registration No. 52,669
Phone No.: 352-375-8100
Fax No.: 352-372-5800
Address: Saliwanchik, Lloyd & Eisenschenk
A Professional Association
P.O. Box 142950
Gainesville, FL 32614-2950

MAB/ps

J:\USF\106XC1\PTO\ReqforRefund.doc\DNB/ps

UM00017109
NOVARTIS EXHIBIT 1517
Novartis v. Regents, IPR2023-01347
Page 3966 of 4460

Electronic Acknowledgement Receipt

EFS ID:	12636535
Application Number:	10378956
International Application Number:	
Confirmation Number:	4742
Title of Invention:	Multiple-component solid phases containing at least one active pharmaceutical ingredient
First Named Inventor/Applicant Name:	Michael J. Zaworotko
Customer Number:	23557
Filer:	Mark A. Buese/Paula Shultz
Filer Authorized By:	Mark A. Buese
Attorney Docket Number:	USF.106XC1
Receipt Date:	26-APR-2012
Filing Date:	03-MAR-2003
Time Stamp:	13:54:31
Application Type:	Utility under 35 USC 111(a)

Payment information:

Submitted with Payment	no

File Listing:

Document Number	Document Description	File Name	File Size(Bytes)/ Message Digest	Multi Part /.zip	Pages (if appl.)
1	Refund Request	ReqforRefund.pdf	100060 21e543354f570970002eeba14c0c2137169c148f	no	2

Warnings:	
Information:	

Total Files Size (in bytes):	100060

This Acknowledgement Receipt evidences receipt on the noted date by the USPTO of the indicated documents, characterized by the applicant, and including page counts, where applicable. It serves as evidence of receipt similar to a Post Card, as described in MPEP 503.

New Applications Under 35 U.S.C. 111
If a new application is being filed and the application includes the necessary components for a filing date (see 37 CFR 1.53(b)-(d) and MPEP 506), a Filing Receipt (37 CFR 1.54) will be issued in due course and the date shown on this Acknowledgement Receipt will establish the filing date of the application.

National Stage of an International Application under 35 U.S.C. 371
If a timely submission to enter the national stage of an international application is compliant with the conditions of 35 U.S.C. 371 and other applicable requirements a Form PCT/DO/EO/903 indicating acceptance of the application as a national stage submission under 35 U.S.C. 371 will be issued in addition to the Filing Receipt, in due course.

New International Application Filed with the USPTO as a Receiving Office
If a new international application is being filed and the international application includes the necessary components for an international filing date (see PCT Article 11 and MPEP 1810), a Notification of the International Application Number and of the International Filing Date (Form PCT/RO/105) will be issued in due course, subject to prescriptions concerning national security, and the date shown on this Acknowledgement Receipt will establish the international filing date of the application.

Document code: WFEE

United States Patent and Trademark Office
Sales Receipt for Accounting Date: 05/09/2012

HDENDY ADJ #00000001 Mailroom Dt: 09/27/2011
Seq No: 24629 Sales Acctg Dt: 09/27/2011 10378956
01 FC : 1806 -180.00 OP

Document code: WFEE

United States Patent and Trademark Office
Sales Receipt for Accounting Date: 05/09/2012

HDENDY RF #30110963 Mailroom Dt: 05/09/2012 10378956

Credit Card Refund Total: $180.00

American Express XXXXXXXXXXXX1003

Substitute for form 1449A/PTO

INFORMATION DISCLOSURE STATEMENT BY APPLICANT

(use as many sheets as necessary)

Sheet 1 of 2

Complete if Known	
Application Number	10/378,956
Filing Date	March 3, 2003
First Named Inventor	Michael J. Zaworotko
Art Unit	1627
Examiner Name	Sahar Javanmard
Attorney Docket Number	USF.106XC1

U.S. PATENT DOCUMENTS

Examiner Initials*	Cite No. [1]	Document Number Number - Kind Code[2] (if known)	Publication Date MM-DD-YYYY	Name of Patentee or Applicant of Cited Document	Pages, Columns, Lines, Where Relevant Passages or Relevant Figures Appear
	U1	US-5,635,535	06-03-1997	Wagstaff	All
	U2	US-6,294,186	09-25-2001	Beerse *et al.*	All
	U3	US-			
	U4	US-			
	U5	US-			
	U6	US-			
	U7	US-			
	U8	US-			
	U9	US-			

FOREIGN PATENT DOCUMENTS

Examiner Initials*	Cite No. [1]	Foreign Patent Document Country Code [3] - Number [4] - Kind Code[5] (if known)	Publication Date MM-DD-YYYY	Name of Patentee or Applicant of Cited Document	Pages, Columns, Lines, Where Relevant Passages or Relevant Figures Appear	T[6]
	F1					
	F2					
	F3					
	F4					
	F5					
	F6					
	F7					

Examiner Signature		Date Considered	

*EXAMINER: Initial if reference considered, whether or not citation is in conformance with MPEP 609. Draw line through citation if not in conformance and not considered. Include copy of this form with next communication to applicant. [1] Applicant's unique citation designation number (optional). [2] See Kind Codes of USPTO Patent Documents at www.uspto.gov or MPEP901.04. [3] Enter Office that issued the document, by the two-letter code (WIPO Standard T.3). [4] For Japanese patent documents, the indication of the year of the reign of the Emperor must precede the serial number of the patent document. [5] Kind of document by the appropriate symbols as indicated on the document under WIPO Standard ST. 16 if possible. [6] Applicant is to place a check mark here if English language Translation is attached.

This collection of information is required by 37 CFR 1.97 and 1.98. The information is required to obtain or retain a benefit by the public which is to file (and by the USPTO to process) an application. Confidentiality is governed by 35 U.S.C. 122 and 37 CFR 1.14. This collection is estimated to take 2 hours to complete, including gathering, preparing, and submitting the completed application form to the USPTO. Time will vary depending upon the individual case. Any comments on the amount of time you require to complete this form and/or suggestions for reducing this burden, should be sent to the Chief Information Officer, U.S. Patent and Trademark Office, P.O. Box 1450, Alexandria, VA 22313-1450. DO NOT SEND FEES OR COMPLETED FORMS TO THIS ADDRESS. **SEND TO: Commissioner for Patents, P.O. Box 1450, Alexandria, VA 22313-1450.**

If you need assistance in completing the form, call 1-800-PTO-9199 (1-800-786-9199) and select option 2.

Substitute for form 1449B/PTO

INFORMATION DISCLOSURE STATEMENT BY APPLICANT

(use as many sheets as necessary)

Sheet 2 of 2

Complete if Known	
Application Number	10/378,956
Filing Date	March 3, 2003
First Named Inventor	Michael J. Zaworotko
Group Art Unit	1627
Examiner Name	Sahar Javanmard
Attorney Docket Number	USF.106XC1

NON PATENT LITERATURE DOCUMENTS

Examiner Initials*	Cite No. [1]	Include name of the author (in CAPITAL LETTERS), title of the article, (when appropriate), title of the item (book, magazine, journal, serial, symposium, catalog, etc.), date, page(s), volume-issue number(s), publisher, city and/or country where published.	T[2]
	R1	CAIRA, M.R., "Molecular complexes of sulfonamides. 2. 1:1 complexes between drug molecules: sulfadimidine-acetylsalicylic acid and sulfadimidine-4-aminosalicylic acid," *Journal of Crystallographic and Spectroscopic Research*, 1992, pp. 193-200, Vol. 22, No. 2.	
	R2	CAIRA, M.R., "Molecular complexes of sulfonamides. 3. Structure of 5-methoxysulfadiazine (Form II) and its 1:1 complex with acetylsalicylic acid," *Journal of Chemical Crystallography*, 1994, pp. 695-701, Vol. 24, No. 10.	
	R3	COX, J.R. *et al.*, "Selective Crystal Growth of the Anhydrous and Monohydrate Forms of Theophylline on Self-Assembled Monolayers," *Angew. Chem. Int. Ed.*, 2007, pp. 1988-1991, Vo. 46.	
	R4	MARTINS, F.T. *et al.*, "Intermolecular Contacts Influencing the Conformational and Geometric Features of the Pharmaceutically Preferred Mebendazole Polymorph C," *Journal of Pharmaceutical Sciences*, July 2009, pp. 2336-2344, Vol. 98, No. 7.	
	R5	WHEATLEY, P.J., "The Crystal and Molecular Structure of Aspirin," *J. Chem. Soc.*, 1964, pp. 6036-6048.	
	R6		
	R7		
	R8		
	R9		
	R10		
	R11		
	R12		
	R13		
	R14		

Examiner Signature		Date Considered	

*EXAMINER: Initial if reference considered, whether or not citation is in conformance with MPEP 609. Draw line through citation if not in conformance and not considered. Include copy of this form with next communication to applicant.

[1] Applicant's unique citation designation number (optional). [2] Applicant is to place a check mark here if English language Translation is attached.

This collection of information is required by 37 CFR 1.98. The information is required to obtain or retain a benefit by the public which is to file (and by the USPTO to process) an application. Confidentiality is governed by 35 U.S.C. 122 and 37 CFR 1.14. This collection is estimated to take 2 hours to complete, including gathering, preparing, and submitting the completed application form to the USPTO. Time will vary depending upon the individual case. Any comments on the amount of time you require to complete this form and/or suggestions for reducing this burden, should be sent to the Chief Information Officer, U.S. Patent and Trademark Office, P.O. Box 1450, Alexandria, VA 22313-1450. DO NOT SEND FEES OR COMPLETED FORMS TO THIS ADDRESS. **SEND TO: Commissioner for Patents, P.O. Box 1450, Alexandria, VA 22313-1450.**

If you need assistance in completing the form, call 1-800-PTO-9199 (1-800-786-9199) and select option 2.

J:\USF\106XC1\PTO\SIDS12-form.doc/ps

Journal of Crystallographic and Spectroscopic Research, Vol. 22, No. 2, 1992

Molecular complexes of sulfonamides. 2. 1:1 complexes between drug molecules: sulfadimidine–acetylsalicylic acid and sulfadimidine–4-aminosalicylic acid

Mino R. Caira[1]

Received July 15, 1991; accepted August 5, 1991

The preparation and crystal structures of the 1 : 1 complexes sulfadimidine–acetylsalicylic acid (**I**) and sulfadimidine–4-aminosalicylic acid (**II**) are described. Each complex unit is maintained by two intermolecular hydrogen bonds, namely N—H · · · O=C and N · · · H—O, involving the N atom of the sulfonamide group and one pyrimidine N atom of the sulfonamide and the carboxylic group of the acid. Molecular parameters for protonated complexed aspirin, as found in **I**, are reported for the first time and reveal a significantly different conformation from that of the uncomplexed aspirin molecule. The structure of the 4-aminosalicylic acid molecule does not change significantly on complexation with sulfadimidine. Variation in the hydrogen bonded N · · · O distances in these complexes and their analogs is discussed.

Introduction

The first article in this series (Caira, 1991) outlined the relevance of molecular complexes of sulfonamides and reported the preparation and crystal structures of the 1 : 1 complexes between sulfadimidine [4-amino-N-(4,6-dimethyl-2-pyrimidinyl)benzenesulfonamide] and 2- and 4-aminobenzoic acids, respectively. An earlier report on the structure of the 1 : 1 sulfadimidine–salicylic acid complex (Patel *et al.*, 1988) prompted the present study in which two pharmacologically-active salicylic acid derivatives, acetylsalicylic acid (aspirin) and 4-aminosalicylic acid (PAS), were found to form analogous complexes with sulfadimidine.

The important therapeutic properties of these acids, namely analgesic, anti-inflammatory and antipyretic for aspirin, and tuberculostatic for PAS are well known. Both PAS and sulfonamides inhibit bacterial folic acid synthesis as analogues of p-aminobenzoic acid (PABA), but the binding sites for PABA on the enzyme dihydropteroate synthetase are quite specific. Thus, sulfonamides are ineffective against tubercle bacilli while PAS is ineffective against most bacteria (Jawetz, 1984; Williams and Kruk, 1981). Complex formation between different drug molecules continues to receive attention because the resultant species may display synergism and could therefore be clinically useful. Representative examples of complexes containing sulfonamides which have recently been studied in the solid state include trimethoprim-sulfamethoxazole (Nakai *et al.*, 1984), various antipyrine-sulfonamide complexes (Jeanjean *et al.*, 1985) and aminacrine-sulfadimidine (Ghose *et al.*, 1988). Although structural data for metal complexes or salts containing the anionic acetylsalicylato- and p-aminosalicylato-species have been published (e.g., Bandoli and Clemente, 1981; Greenaway *et al.*, 1984; Nishioka *et al.*, 1984; Sabirov *et al.*, 1982; Sequeira *et al.*, 1968), no crystallographic results for molecular complexes containing aspirin or PAS in their unionized forms have hitherto appeared in the literature (Cambridge Structural Database, 1991).

Experimental

Colorless single crystals of **I** grew within 2 days from a mixture of sulfadimidine and acetylsalicylic acid

[1]Department of Chemistry, Private Bag, Rondebosch 7700, South Africa.

0277-8068/92/0400-0193$06.50/0 © 1992 Plenum Publishing Corporation

BNSDOCID: <XP_____5503899A__I_>

UM00017116
NOVARTIS EXHIBIT 1517
Novartis v. Regents, IPR2023-01347
Page 3973 of 4460

in 1 : 1 molar ratio in acetonitrile. Brown prismatic crystals of **II** were obtained after 3 weeks from a mixture of sulfadimidine and *p*-aminosalicylic acid in 1 : 1 molar ratio in ethanol. Elemental analyses confirmed the 1 : 1 stoichiometry of both complexes. Preliminary unit-cell dimensions and space group data were obtained from precession photographs. Intensity data were collected at 294K in the ω-2θ mode on an Enraf–Nonius CAD4 diffractometer with Mo $K\alpha$-radiation (λ = 0.71069 Å). Accurate cell parameters were in each case determined by least-squares analysis of accurate setting angles in the range $16° \leq \theta \leq 17°$. Reflections in the range $1° \leq \theta \leq 25°$ were collected using a variable scan speed depending on I and $\sigma(I)$ with a minimum recording time of 40 s per reflection. Intensity control was performed every hour and orientation control every 200 measured reflections. Both data sets were corrected for Lp-effects and for absorption (North *et al.*, 1968) using the program EAC of the Enraf–Nonius Structure Determination Package (Frenz *et al.*, 1982). Data-collection parameters and details of structure refinements are listed in Table 1. The structures were solved by Patterson and Fourier methods. For **II**, the Patterson-derived S atom position was nearly identical to that in the 1 : 1 complex between sulfadimidine and PABA (Caira, 1991) whose unit-cell dimensions agreed with those for **II** within 2%. The nearly isomorphous relationship between the complexes allowed the atoms of the PABA complex to be successfully used as a trial model for **II**, atom O(30) of the PAS molecule being subsequently located from a difference Fourier synthesis. Refinement by full-matrix least-squares using the program SHELX76 (Sheldrick, 1976) involved minimization of $\Sigma\, w(|F_o| - |kF_c|)^2$ with anisotropic thermal parameters assigned to all nonhydrogen atoms. H-atoms were located in difference Fourier syntheses but were generally included in idealised positions (C—H = 1.00 Å). H-atoms which were refined included those of the amino, phenolic, and carboxylic groups and that attached to the N atom of the sulfonamide group. Location and refinement of H atoms in the latter two categories were deemed essential to establish unequivocally the tautomeric form of sulfadimidine present and the charged or protonated state of the complexing acid components. Complex neutral atomic scattering factors (*International Tables for X-Ray Crystallography*, 1974) were used. Other programs used were PARST (Nardelli, 1983) and PLUTO (Motherwell, 1979). Fractional atomic coordinates and equivalent isotropic thermal parameters ($U_{eq} = (\frac{1}{3})\, \Sigma_i\, \Sigma_j\, U_{ij} a_i^* a_j^* a_i \cdot a_j$) for nonhydrogen atoms are listed in Tables 2 and 3. H-atom coordinates are listed in Table 4. Structure factors, U_{ij} values, torsion angles and mean-plane data have been deposited.

Results and discussion

Perspective views of the structures of the complexes **I** and **II** are shown in Figs. 1 and 2, respectively. In each complex unit, molecular association occurs through hydrogen bonding involving the carboxylic group of the acid component and two N atoms (one pyrimidine N atom and the N atom of the sulfonamide group) of sulfadimidine. The aspirin and PAS molecules are in their unionized forms. The specific arrangement of C=O · · · H—N and O—H · · · N hydrogen bonds shown in Figs. 1 and 2 results in an eight-membered ring which occurs invariably, having now been observed in seven complexes between sulfadimidine and substituted aromatic carboxylic acids (Caira, 1991; Patel *et al.*, 1988), including p-chlorobenzoic acid and *o*-phthalic acid (Caira, 1992).

Sulfadimidine conformation

Interatomic distances and bond angles in sulfadimidine (Tables 5 and 6) are in the expected range. The sulfadimidine molecule adopts significantly different conformations in **I** and **II**. The values of the torsion angles τ_1–τ_3 (Table 7) for **I** are within a few degrees of those previously found in sulfadimidine–2-aminobenzoic acid. Those for **II** resemble closely the corresponding torsion angles in sulfadimidine–4-aminobenzoic acid, as expected for nearly isomorphous structures. The occurrence of both conformations with equal frequency in these complexes suggests that they are energetically similar, which accords with the finding (Kàlmàn *et al.*, 1981) that rotation about the S—C bond is not hindered in N-substituted aryl-sulfonamides. The conformation in which the plane of the phenyl ring approximately bisects the O—S—O angle (as in **II**, $\tau_1 \approx 160°$) is nevertheless unusual since the reported clustering range for τ_1 is 70–120°.

Aspirin and PAS structures

Because of their chemical significance, the crystal and molecular structures of both aspirin (Kim *et al.*, 1985; Wheatley, 1964) and PAS (Bertinotti *et al.*, 1954;

BNSDOCID: <XP_____55032899A__1_>

UM00017117
NOVARTIS EXHIBIT 1517
Novartis v. Regents, IPR2023-01347
Page 3974 of 4460

Table 1. Crystal data, data-collection parameters, and details of the structural analyses

	I	II
Formula	$C_{12}H_{14}N_4O_2S \cdot C_9H_8O_4$	$C_{12}H_{14}N_4O_2S \cdot C_7H_7NO_3$
M_r	458.4	431.5
Space group	$P2_1/c$	$P\bar{1}$
a/Å	7.696(1)	8.205(6)
b/Å	21.988(7)	9.449(3)
c/Å	13.432(2)	14.161(2)
α/deg	90	107.02(2)
β/deg	102.66(1)	92.29(4)
γ/deg	90	105.85(4)
V/Å^3	2218.1(8)	1001.3(9)
Z	4	2
D_x/g cm^{-3}	1.373	1.431
μ(Mo $K\alpha$)/cm^{-1}	1.82	1.94
F(000)	960	452
Crystal size/mm	0.38 × .44 × .44	0.13 × .33 × .43
Index range	−9, 9; 0, 26; 0, 16	−9, 9; −11, 11; 0, 16
Standard reflections	$\bar{6}$ 4 3, $\bar{2}$ 7 10, $\bar{1}$ 16 5	1 1 10, 6 $\bar{4}$ 2, $\bar{2}$ 7 1
Intensity variation/%	+2.4	−0.5
Scan width in ω/deg	0.85 + 0.35 tan θ	0.85 + 0.35 tan θ
Vertical aperture/mm	4	4
Aperture width/mm	1.12 + 1.05 tan θ	1.12 + 1.05 tan θ
Reflections measured	4185	3667
Unique reflections	3485	3179
R_{int}	0.013	0.021
Absorption corrections:		
min.	0.9887	0.9741
max.	1.0000	0.9997
mean	0.9959	0.9848
Observed reflections $I > 2\sigma(I)$	2933	2679
Parameters refined	316	302
R	0.040	0.051
R_w	0.040	0.055
S	2.859	1.703
w	$[\sigma^2(F_o)]^{-1}$	$[\sigma^2(F_o) + 1.545 \times 10^{-3}F_o^2]^{-1}$
Max Δ/σ for non-H atoms	0.16	0.21
$\Delta\rho$/e Å^{-3}		
min.	−0.28	−0.60
max.	0.18	0.53

BNSDOCID: <XP_____55032899A__1_>

UM00017118
NOVARTIS EXHIBIT 1517
Novartis v. Regents, IPR2023-01347
Page 3975 of 4460

Table 2. Fractional atomic coordinates ($\times 10^4$) and thermal parameters ($Å^2 \times 10^3$) with esd's in parentheses for Complex **I**

Atom	*x/a*	*y/b*	*z/c*	U_{eq}
C(1)	700(3)	2823(1)	4772(2)	40(1)
C(2)	−1005(3)	2904(1)	4940(2)	48(1)
C(3)	−2467(3)	2694(1)	4243(2)	55(1)
C(4)	−2249(3)	2395(1)	3368(2)	53(1)
C(5)	−543(4)	2307(1)	3218(2)	53(1)
C(6)	919(3)	2525(1)	3902(2)	47(1)
N(7)	−3696(4)	2173(2)	2673(2)	83(1)
S(8)	2523(1)	3097(0)	5664(0)	47(0)
O(9)	2164(2)	3040(1)	6664(1)	59(1)
O(10)	4109(2)	2831(1)	5475(1)	62(1)
N(11)	2557(3)	3837(1)	5502(2)	53(1)
C(12)	2833(3)	4133(1)	4642(2)	46(1)
N(13)	3255(3)	3802(1)	3905(2)	51(1)
C(14)	3547(3)	4111(1)	3093(2)	54(1)
C(15)	3392(4)	4740(1)	3043(2)	60(1)
C(16)	2940(3)	5043(1)	3844(2)	56(1)
N(17)	2653(3)	4742(1)	4661(2)	49(1)
C(18)	4059(4)	3746(1)	2264(2)	75(1)
C(19)	2719(4)	5725(1)	3844(3)	74(1)
C(20)	1465(3)	5505(1)	7866(2)	50(1)
C(21)	1637(3)	5271(1)	8845(2)	53(1)
C(22)	1309(4)	5622(1)	9641(2)	63(1)
C(23)	818(4)	6220(1)	9456(3)	70(1)
C(24)	666(4)	6467(1)	8498(3)	70(1)
C(25)	996(3)	6115(1)	7712(2)	58(1)
C(26)	1728(3)	5127(1)	6995(2)	54(1)
O(27)	1938(3)	5437(1)	6202(2)	69(1)
O(28)	1717(3)	4573(1)	7012(1)	74(1)
O(29)	2075(3)	4662(1)	9083(1)	60(1)
C(30)	3741(4)	4475(1)	9027(2)	57(1)
O(31)	4837(3)	4812(1)	8840(2)	68(1)
C(32)	3957(5)	3810(1)	9229(3)	82(2)

Table 3. Fractional atomic coordinates ($\times 10^4$) and thermal parameters ($Å^2 \times 10^3$) with esd's in parentheses for Complex **II**

Atom	*x/a*	*y/b*	*z/c*	U_{eq}
C(1)	2492(3)	370(3)	1502(2)	32(1)
C(2)	1377(4)	622(3)	2200(2)	40(1)
C(3)	−343(4)	−155(3)	1944(2)	41(1)
C(4)	−971(3)	−1189(3)	1002(2)	38(1)
C(5)	165(3)	−1474(3)	317(2)	40(1)
C(6)	1886(3)	−686(3)	564(2)	36(1)
N(7)	−2706(3)	−1982(3)	747(3)	49(1)
S(8)	4682(1)	1318(1)	1788(1)	33(0)
O(9)	5502(3)	407(2)	2178(2)	49(1)
O(10)	5292(2)	1718(2)	945(1)	42(1)
N(11)	4908(3)	2866(2)	2728(2)	35(1)
C(12)	4738(3)	4268(3)	2665(2)	30(1)
N(13)	3824(3)	4252(2)	1872(2)	34(1)
C(14)	3740(4)	5644(3)	1852(2)	37(1)
C(15)	4563(4)	6976(3)	2615(2)	45(1)
C(16)	5482(4)	6889(3)	3414(2)	40(1)
N(17)	5557(3)	5491(2)	3443(2)	34(1)
C(18)	2749(5)	5687(4)	961(3)	55(2)
C(19)	6447(5)	8268(4)	4266(3)	60(1)
C(20)	8759(3)	4479(3)	5981(2)	38(1)
C(21)	9685(4)	5911(3)	6637(2)	40(1)
C(22)	10733(4)	6053(4)	7458(2)	43(1)
C(23)	10898(4)	4720(3)	7646(2)	40(1)
C(24)	10002(4)	3283(4)	6995(2)	49(1)
C(25)	8950(4)	3145(3)	6168(2)	45(1)
C(26)	7625(4)	4349(3)	5126(2)	40(1)
O(27)	7491(3)	5661(3)	5053(2)	53(1)
O(28)	6822(3)	3089(3)	4511(2)	53(1)
N(29)	11924(4)	4869(4)	8475(2)	55(1)
O(30)	8125(4)	1729(3)	5567(2)	80(1)

Lin *et al.*, 1978) have been studied in some detail. Further reference to either of these compounds here cites data from the more recent structure redetermination. Crystals of both aspirin and PAS contain centrosymmetric dimers hydrogen bonded through their carboxylic groups. In aspirin, the carbonyl group of the —COOH function is *anti*-periplanar to the acetoxy group. For aspirin complexed to sulfadimidine in **I**, the relationship is *syn*-periplanar with the torsion angle O(28)—C(26)—C(20)—C(21) 16.7(4)° compared with −178.8(1)° in uncomplexed aspirin. The acetoxy groups in uncomplexed and complexed aspirin have a high degree of planarity but conform differently. In complex **I**, the acetoxy group is folded towards the carboxylic group with C(20)—C(21)—O(29)—C(30) 67.2(3)°, while in free aspirin the corresponding torsion angle is 85.2(2)°, i.e., a nearly perpendicular relationship between the phenyl ring and acetoxy group mean planes in the latter case. This conformational difference may be traced to participation by keto oxygen atom O(31) of **I** in a weak intermolecular hydrogen bond to sulfadimidine, $O(31)^{ii} \cdots H(15)—C(15)$ (Table 8). The corresponding O atom in uncomplexed aspirin is not hydrogen bonded. Distances and angles for aspirin in the two environments are generally in excellent agreement, the largest difference being that for C(26)—O(28), which is 1.218(3) Å in **I** and 1.239(2) Å in uncomplexed aspirin. Since the carboxylic acid groups are engaged in different hydrogen bonding patterns in the two cases, a difference of this magnitude is not unexpected. Accurate parameters for protonated aspirin hydrogen bonded to a molecule other than itself, as in complex **I**, have not been reported previously. Aspirin molecules included as guests in β-cyclodextrin are probably present as carboxylate anions (Nishioka *et al.*, 1984).

BNSDOCID: <XP_____55032899A__I_>

UM00017119
NOVARTIS EXHIBIT 1517
Novartis v. Regents, IPR2023-01347
Page 3976 of 4460

Table 4. Fractional atomic coordinates ($\times 10^4$ for idealised H atoms, $\times 10^3$ for refined H atoms) and isotropic thermal parameters ($Å^2 \times 10^3$) in Complexes **I** and **II** with esd's in parentheses

Atom	*x/a*	*y/b*	*z/c*	U_{iso}
Complex **I**				
H(2)	−1173	3119	5570	69(4)
H(3)	−3689	2757	4367	69(4)
H(5)	−372	2081	2600	69(4)
H(6)	2139	2468	3771	69(4)
H(71)	−371(5)	213(2)	205(3)	132(11)
H(72)	−474(5)	232(2)	277(3)	132(11)
H(11)	219(4)	404(1)	598(2)	83(11)
H(15)	3605	4968	2436	128(5)
H(181)	4221	4005	1679	128(5)
H(182)	3217	3407	2004	128(5)
H(183)	5235	3574	2617	128(5)
H(191)	3102	5888	3230	128(5)
H(192)	3477	5905	4474	128(5)
H(193)	1445	5835	3805	128(5)
H(22)	1426	5443	10338	104(5)
H(23)	569	6478	10022	104(5)
H(24)	316	6903	8373	104(5)
H(25)	897	6299	7021	104(5)
H(27)	211(5)	514(2)	565(3)	155(17)
H(321)	5234	3687	9321	104(5)
H(322)	3225	3585	8636	104(5)
H(323)	3528	3709	9860	104(5)
Complex **II**				
H(2)	1819	1363	2886	54(4)
H(3)	−1147	31	2447	54(4)
H(5)	−268	−2254	−358	54(4)
H(6)	2693	−879	64	54(4)
H(71)	−298(5)	−231(4)	13(3)	54(4)
H(72)	−323(5)	−157(4)	114(3)	54(4)
H(11)	549(4)	292(4)	327(2)	43(9)
H(15)	4491	8003	2587	110(6)
H(181)	2865	6807	1069	110(6)
H(182)	1516	5100	908	110(6)
H(183)	3211	5256	333	110(6)
H(191)	6230	9212	4171	110(6)
H(192)	7695	8380	4285	110(6)
H(193)	6063	8148	4907	110(6)
H(21)	9586	6871	6508	63(4)
H(22)	11375	7103	7924	63(4)
H(24)	10118	2327	7124	63(4)
H(27)	686(5)	557(4)	444(3)	63(4)
H(291)	1255(5)	571(5)	876(3)	63(4)
H(292)	1201(5)	406(5)	856(3)	63(4)
H(30)	747(5)	192(4)	503(3)	63(4)

Molecular dimensions for PAS in complex **II** are very similar to those in uncomplexed PAS. The only noteworthy difference is in the bond length C(25)—O(30), which is 1.329(2) Å in **II** vs 1.361(2) Å in uncomplexed PAS. In both cases, the intramolecular O—H · · · O hydrogen bond locks the phenyl and carboxy planes into near coplanarity. The least-squares planes through these sets of atoms intersect at 1.5° in PAS and 2.9(2)° in **II**. Complexation with sulfadimidine thus has no remarkable effect on the dimensions or conformation of the PAS molecule.

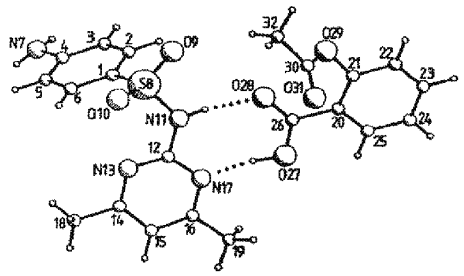


Fig. 1. Molecular structure of **I**. C atoms are labeled with numerals only. Dotted lines indicate hydrogen bonds.

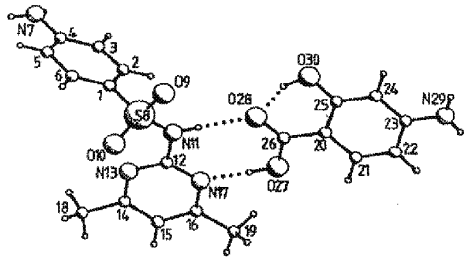


Fig. 2. Molecular structure of **II**. C atoms are labeled with numerals only. Dotted lines indicate hydrogen bonds.

Hydrogen bonding and crystal packing

Hydrogen bond data are listed in Table 8. One objective in investigating the series of 1:1 complexes between sulfadimidine and variously substituted aromatic carboxylic acids was to seek possible correlations between the N · · · O distances for the hydrogen bonds N—H · · · O and N · · · H—O and the acid p*K*a values. The former distance parameters may be taken as a measure of the strength of molecular association between sulfadimidine and the carboxylic acid and might therefore be expected to depend on acid strength. Significant variations in the distances N(11) · · · O(28) and N(17) · · · O(27) do occur in this series. The respective ranges are 2.779(3)–2.841(4) Å and 2.639(3)–2.724(4) Å for

BNSDOCID: <XP_____55032899A__I_>

UM00017120
NOVARTIS EXHIBIT 1517
Novartis v. Regents, IPR2023-01347
Page 3977 of 4460

Table 5. Bond lengths (Å) with esd's in parentheses for Complexes **I** and **II**

(a) Sulfadimidine	I	II	(b) Acetylsalicyclic acid	(I)
C(1)—C(2)	1.392(4)	1.387(4)	C(20)—C(26)	1.484(4)
C(1)—C(6)	1.382(4)	1.382(3)	C(21)—C(22)	1.386(4)
C(1)—S(8)	1.742(2)	1.745(3)	C(21)—O(29)	1.401(3)
C(2)—C(3)	1.377(3)	1.378(4)	C(22)—C(23)	1.376(3)
C(3)—C(4)	1.389(4)	1.381(3)	C(23)—C(24)	1.378(5)
C(4)—C(5)	1.385(4)	1.392(4)	C(24)—C(25)	1.377(5)
C(4)—N(7)	1.377(4)	1.392(3)	C(26)—O(27)	1.304(4)
C(5)—C(6)	1.374(3)	1.380(3)	C(26)—O(28)	1.218(3)
S(8)—O(9)	1.436(2)	1.437(3)	O(29)—C(30)	1.365(4)
S(8)—O(10)	1.425(2)	1.424(2)	C(30)—O(31)	1.189(4)
S(8)—N(11)	1.643(2)	1.624(2)	C(30)—C(32)	1.490(3)
N(11)—C(12)	1.382(4)	1.397(4)		
C(12)—N(13)	1.325(4)	1.319(4)	(c) *p*-Aminosalicyclic acid	(II)
C(12)—N(17)	1.347(3)	1.331(3)		
N(13)—C(14)	1.345(4)	1.345(4)	C(20)—C(21)	1.385(3)
C(14)—C(15)	1.389(3)	1.373(3)	C(20)—C(25)	1.408(5)
C(14)—C(18)	1.494(4)	1.491(6)	C(20)—C(26)	1.452(4)
C(15)—C(16)	1.373(4)	1.370(5)	C(21)—C(22)	1.370(4)
C(16)—N(17)	1.341(4)	1.351(4)	C(22)—C(23)	1.400(5)
C(16)—C(19)	1.509(3)	1.490(4)	C(23)—C(24)	1.379(4)
			C(23)—N(29)	1.366(4)
(b) Acetylsalicyclic acid	(I)		C(24)—C(25)	1.379(5)
			C(25)—O(30)	1.329(3)
C(20)—C(21)	1.391(4)		C(26)—O(27)	1.307(5)
C(20)—C(25)	1.393(3)		C(26)—O(28)	1.236(3)

Table 6. Bond angles (°) with esd's in parentheses for Complexes **I** and **II**

(a) Sulfadimidine	I	II	(b) Acetylsalicyclic acid	(I)
C(6)—C(1)—S(8)	121.1(2)	118.3(3)	C(21)—C(20)—C(25)	117.7(2)
C(2)—C(1)—S(8)	119.4(2)	121.6(2)	C(20)—C(21)—O(29)	122.5(2)
C(2)—C(1)—C(6)	119.5(2)	120.1(4)	C(20)—C(21)—C(22)	121.9(2)
C(1)—C(2)—C(3)	120.4(2)	119.7(3)	C(22)—C(21)—O(29)	115.6(2)
C(2)—C(3)—C(4)	120.2(2)	120.8(4)	C(21)—C(22)—C(23)	118.8(3)
C(3)—C(4)—N(7)	120.8(3)	120.8(3)	C(22)—C(23)—C(24)	120.6(3)
C(3)—C(4)—C(5)	118.9(2)	119.1(3)	C(23)—C(24)—C(25)	120.2(2)
C(5)—C(4)—N(7)	120.3(2)	120.1(3)	C(20)—C(25)—C(24)	120.9(3)
C(4)—C(5)—C(6)	121.2(3)	120.4(3)	C(20)—C(26)—O(28)	122.8(2)
C(1)—C(6)—C(5)	119.8(2)	119.9(3)	C(20)—C(26)—O(27)	114.4(2)
C(1)—S(8)—N(11)	106.6(1)	106.3(2)	O(27)—C(26)—O(28)	122.7(3)
C(1)—S(8)—O(10)	109.2(1)	108.6(2)	C(21)—O(29)—C(30)	117.2(2)
C(1)—S(8)—O(9)	108.9(1)	109.3(2)	O(29)—C(30)—C(32)	110.7(3)
O(10)—S(8)—N(11)	110.1(1)	110.7(2)	O(29)—C(30)—O(31)	122.8(3)
O(9)—S(8)—N(11)	102.9(1)	104.0(2)	O(31)—C(30)—C(32)	126.5(3)
O(9)—S(8)—O(10)	118.6(1)	117.4(3)		
S(8)—N(11)—C(12)	125.9(2)	125.3(2)		
N(11)—C(12)—N(17)	114.7(2)	113.8(3)	(c) p-Aminosalicyclic acid	(II)
N(11)—C(12)—N(13)	118.3(2)	118.6(3)		
N(13)—C(12)—N(17)	127.1(3)	127.6(3)	C(25)—C(20)—C(26)	120.8(3)
C(12)—N(13)—C(14)	116.1(2)	115.4(3)	C(21)—C(20)—C(26)	121.3(3)
N(13)—C(14)—C(18)	116.8(2)	117.3(3)	C(21)—C(20)—C(25)	117.9(3)
N(13)—C(14)—C(15)	121.0(2)	121.3(3)	C(20)—C(21)—C(22)	122.0(3)
C(15)—C(14)—C(18)	122.2(2)	121.4(3)	C(21)—C(22)—C(23)	119.7(3)
C(14)—C(15)—C(16)	118.6(2)	119.6(3)	C(22)—C(23)—N(29)	119.4(3)
C(15)—C(16)—C(19)	122.0(2)	123.6(3)	C(22)—C(23)—C(24)	119.2(3)
C(15)—C(16)—N(17)	121.1(2)	119.4(3)	C(24)—C(23)—N(29)	121.4(3)
N(17)—C(16)—C(19)	116.9(2)	117.0(3)	C(23)—C(24)—C(25)	121.0(3)
C(12)—N(17)—C(16)	116.1(2)	116.7(3)	C(20)—C(25)—C(24)	120.2(3)
			C(24)—C(25)—O(30)	118.1(3)
(b) Acetylsalicyclic acid	(I)		C(20)—C(25)—O(30)	121.6(3)
			C(20)—C(26)—O(28)	122.8(3)
C(25)—C(20)—C(26)	119.9(2)		C(20)—C(26)—O(27)	115.4(3)
C(21)—C(20)—C(26)	122.5(2)		O(27)—C(26)—O(28)	121.9(3)

BNSDOCID: <XP_____55032899A__I_>

UM00017121
NOVARTIS EXHIBIT 1517
Novartis v. Regents, IPR2023-01347
Page 3978 of 4460

Table 7. Selected torsion angles (°) with esd's in parentheses for Complexes I and II

		I	II
τ_1	C(6)—C(1)—S(8)—N(11)	104.2(2)	159.8(3)
τ_2	C(1)—S(8)—N(11)—C(12)	−64.7(3)	−82.8(4)
τ_3	S(8)—N(11)—C(12)—N(13)	−5.9(4)	23.0(5)
	C(21)—C(20)—C(26)—O(27)	−164.5(3)	−3.0(5)
	C(21)—C(20)—C(26)—O(28)	16.7(4)	177.7(4)
	C(20)—C(21)—O(29)—C(30)	67.2(3)	—
	C(21)—O(29)—C(30)—O(31)	4.0(4)	—

Table 8. Hydrogen bond data

D—H ··· A	D–H (Å)	D ··· A (Å)	H ··· A (Å)	D—H ··· A (°)
		Complex I		
N(11)—H(11) ··· O(28)	0.88(3)	2.779(3)	1.91(3)	171(3)
O(27)—H(27) ··· N(17)	1.02(4)	2.724(4)	1.72(4)	169(4)
N(7)—H(71) ··· O(10)^{i}	0.84(4)	3.065(3)	2.40(3)	137(3)
C(15)—H(15) ··· O(31)^{ii}	1.00(4)	3.276(4)	2.35(4)	154(3)
(i) = $-1+x, 0.5-y, -0.5+z$ (ii) = $1-x, 1-y, 1-z$				
		Complex II		
N(11)—H(11) ··· O(28)	0.87(4)	2.842(4)	1.97(4)	179(3)
O(27)—H(27) ··· N(17)	0.97(4)	2.664(4)	1.71(4)	172(4)
O(30)—H(30) ··· O(28)	1.00(5)	2.603(5)	1.68(5)	153(4)
N(7)—H(72) ··· O(9)^{i}	0.79(4)	3.277(4)	2.51(4)	163(4)
N(29)—H(291) ··· O(10)^{ii}	0.79(3)	3.251(4)	2.49(4)	160(4)
(i) = $-1+x, y, z$ (ii) = $2-x, 1-y, 1-z$				

seven complexes, with acid p*K*a values spanning the range 2.89–6.97. When all the available data are considered, however, no systematic change in either of the N ··· O distances with p*K*a is found. It is concluded that any subtle variations in N ··· O distance that may arise from differences in acid strength are overshadowed by the requirements of crystal packing. This was recently confirmed by the finding (Caira, 1992) that in the 1:1 complex sulfadimidine–p-chlorobenzoic acid (space group $P2_1/c$, $Z = 8$), the crystallographically independent but chemically equivalent N ··· O distances in the N—H ··· O hydrogen bonds differ by as much as 8σ, compared with a difference of 12σ for the observed distance range quoted above.

Figures 3 and 4 are stereoscopic views illustrating the molecular packing in **I** and **II**. For clarity, the hydrogen bonds indicated include only the N—H ··· O and N ··· H—O bonds referred to above, the C—H

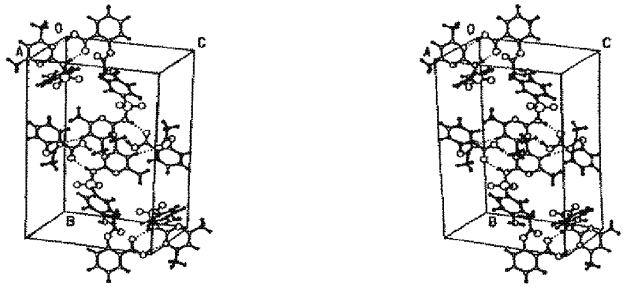


Fig. 3. Stereoview of the molecular packing and principal hydrogen bonds in I.

BNSDOCID: <XP_____55032899A__I_>

UM00017122
NOVARTIS EXHIBIT 1517
Novartis v. Regents, IPR2023-01347
Page 3979 of 4460

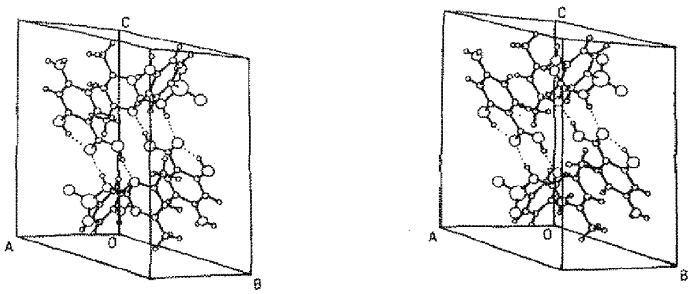


Fig. 4. Stereoview of the molecular packing and principal hydrogen bonds in **II**.

· · · O bond which stabilizes the conformation of the acetoxy group of aspirin in **I**, and the intramolecular O—H · · · O bond of PAS in **II**. There are additional weaker intermolecular N—H · · · O (sulfonyl) hydrogen bonds involving the $-NH_2$ functions in both complexes (Table 8).

Acknowledgments

Financial assistance from the FRD, Pretoria, and the University of Cape Town are gratefully acknowledged. Thanks are also due to Dr. M. L. Niven, the Computing Centre at UCT and Professor A. P. Lötter of the Research Institute for Industrial Pharmacy, PUCHO, for providing the sulfadimidine.

References

Bandoli, G., and Clemente, D. A. (1981) *J. Inorg. Nucl. Chem.* **43**, 2843–2846.
Bertinotti, F., Giacomello, G., and Liquori, A. M. (1954) *Acta Crystallogr.* **7**, 808–812.
Caira, M. R. (1991) *J. Crystallogr. Spectrosc. Res.* **21**, 641.
Caira, M. R. (1992) In preparation.
Cambridge Structural Database. (1991) Version 4.4. Cambridge Crystallographic Data Centre, University Chemical Laboratory, Cambridge.
Frenz, B. A., and Associates Inc. (1982) Structure Determination Package (College Station, Texas).
Ghose, S., Chakrabarti, C., Dattagupta, J. K., Le Page, Y., and Trotter, J. (1988) *Acta Crystallogr.* **C44**, 1810–1813.
Greenaway, F. T. Pezeshk, A., Cordes, A. W., Noble, M. C., and Sorenson, J. R. J. (1984) *Inorg. Chim. Acta* **93**, 67–71.
International Tables for X-Ray Crystallography (1974) Vol. IV (Birmingham: Kynoch Press) (Present distributor: Reidel, D., Dordrecht).
Jawetz, E. (1984) In *Basic and Clinical Pharmacology*. (second edition) B. G. Katzung (ed.) (Lange Medical Publications, Los Altos, California).
Jeanjean, B., Alberola, S., Rambaud, J., and Sabon, F. (1985) *Ann. Pharm. Fr.* **42(6)**, 561–568.
Kàlmàn, A., Czugler, M., and Argay, G. (1981) *Acta Crystallogr.* **B37**, 868–877.
Kim, Y., Machida, K., Taga, T., and Osaki, K. (1985) *Chem. Pharm. Bull.* **33(7)**, 2641–2647.
Lin, C., Siew, P., and Byrn, S. R. (1978) *J. Chem. Soc. Perkin 2*, 957–962.
Motherwell, S. (1979) *PLUTO, A program for plotting molecular and crystal structures* (University of Cambridge, England).
Nakai, H., Takasuka, M., and Shiro, M. (1984) *J. Chem. Soc. Perkin Trans* 2, **9**, 1459–1464.
Nardelli, M. (1983) *Comput. Chem.* **7(3)**, 95–98.
Nishioka, F., Nakanashi, I., Fujiwara, T., and Tomita, K. (1984) *J. Incl. Phenom.* **2**, 701–714.
North, A. C. T., Philips, D. C., and Scott Mathews, F. (1968) *Acta Crystallogr.* **A24**, 351–359.
Patel, U., Haridas, M., and Singh, T. P. (1988) *Acta Crystallogr.* **C44**, 1264–1267.
Sabirov, V. Kh., Azizov, M. A., Shabilalov, A. A., Struchkov, Yu. T., and Aleksandrov, G. G. (1982) *Koord. Khim.* **8**, 245–250.
Sequeira, A., Berkebile, C. A., and Hamilton, W. C. (1968) *J. Mol. Struct.* **1**, 283–294.
Sheldrick, G. M. (1976) *SHELX, A system of computer programs for x-ray structure determination* (University of Cambridge, England).
Wheatley, P. J. (1964) *J. Chem. Soc.* 6036–6048.
Williams, R. A. D., and Kruk, Z. L. (1981) In *The Biochemistry and Pharmacology of Antibacterial Agents*, p. 29. (Croom Helm biology in medicine series, London).

Anisotropic thermal parameters, torsion angles, weighted least-squares planes and structure factor data have been deposited with the British Library, Boston Spa, Wetherby, West Yorkshire, UK, as supplementary publication No. 63165 (45 pages).

BNSDOCID: <XP_____55032899A__I_>

UM00017123
NOVARTIS EXHIBIT 1517
Novartis v. Regents, IPR2023-01347
Page 3980 of 4460

Journal of Chemical Crystallography, Vol. 24, No. 10, 1994

Molecular complexes of sulfonamides. 3. Structure of 5-methoxysulfadiazine (Form II) and its 1:1 complex with acetylsalicylic acid

Mino R. Caira[1]

Received August 11, 1994

The X-ray structure of the biologically most active polymorph (Form II) of 5-methoxysulfadiazine (**1**) and that of the 1 : 1 complex between this sulfonamide and acetylsalicylic acid (**2**) are reported. The polymorph **1** is monoclinic, space group $P2_1/c$ with $a = 13.086(2)$ Å, $b = 5.583(1)$ Å, $c = 17.222(3)$ Å, $\beta = 99.98(1)°$, $Z = 4$ and occurs as centrosymmetric hydrogen bonded (N—H···N) dimers in the crystal. This arrangement differs from that observed in other polymorphs of the drug. Complex **2** is triclinic, $P\bar{1}$, $a = 8.102(1)$ Å, $b = 12.033(1)$ Å, $c = 12.170(2)$ Å, $\alpha = 111.67(1)°$, $\beta = 93.77(1)°$, $\gamma = 103.82(1)°$, $Z = 2$. Complexation involves linear intermolecular hydrogen bonds, N—H···O=C and N···O—H, between the amide group and pyrimidinyl N atom of the sulfonamide and the carboxylic group of the acetylsalicylic acid. On complexation to form **2**, neither molecular component undergoes any major structural change.

KEY WORDS: Key Words: Molecular complexes, sulfonamides, acetylsalicylic acid.

Introduction

In earlier parts of this series we described the structures of 1 : 1 complexes between sulfadimidine [4-amino-N-(4,6-dimethyl-2-pyrimidinyl)benzenesulfonamide] and various aromatic carboxylic acid derivatives including 2- and 4-aminobenzoic acids,[1] 4-aminosalicylic acid (p-aminosalicylic acid or PAS) and acetylsalicylic acid (aspirin).[2] These studies have been extended to an investigation of the complexing behaviour of the related drug 5-methoxysulfadiazine [4-amino-N-(5-methoxy-2-pyrimidinyl)benzeneulfonamide] (hereinafter SMD). Only one molecular complex containing SMD has been structurally characterized.[3] Various aspects of the polymorphism of this drug have also been reported during the last 25 years, including the identification of various polymorphs,[4-7] their interconversion,[8,9] and the X-ray crystal structures of two polymorphs designated Forms I and III.[10]

Reaction between SMD and aspirin produces a 1 : 1 molecular complex, analogous to that formed between sulfadimidine and aspirin. However, in our attempt to obtain a complex between SMD and PAS, large single crystals of a polymorph of SMD were obtained instead. We identified these as Form II, the biologically most active form of the sulfonamide,[8] which when prepared by the usual method involving recrystallization from ethanol by rapid cooling to −12°C, is obtained as small particles with little or no geometrical form.[5] This probably accounts for the fact that the crystal structure of this important polymorphic species has not hitherto been determined.

We report here the crystal structures of (**1**) SMD Form II and (**2**) the 1 : 1 complex between SMD and aspirin. The results allow several useful comparisons: the conformation and hydrogen bonding scheme for SMD in Form II with corresponding features in Forms I and III, the conformations of uncomplexed SMD and SMD complexed with aspirin, and finally the structures of the SMD-aspirin complex and its sulfadimidine analog. A possible reason for the crystallization of SMD Form II during the attempted preparation of a SMD-PAS complex is also discussed.

[1]Department of Chemistry, University of Cape Town, Rondebosch 7700, South Africa.

1074-1542/94/1000-0695$07.00/0 © 1994 Plenum Publishing Corporation

BNSDOCID: <XP_____55032900A__I_>

UM00017124
NOVARTIS EXHIBIT 1517
Novartis v. Regents, IPR2023-01347
Page 3981 of 4460

Experimental

Crystal preparation

SMD was purchased from Aldrich-Chemie, Steinheim. X-ray powder diffraction analysis of the unground material matched the published pattern for Form I.[5] A solution containing 0.05 g of SMD in 6 cm^3 CH_3CN was mixed with a solution containing 0.027 g PAS in 2 cm^3 CH_3CN and the mixture heated to 323K with stirring for 10 min. On evaporation, the residue consisted of unreacted PAS and several large columnar crystals. The latter were tentatively identified as SMD Form II from the resemblance between the unit cell data obtained photographically with those reported in the literature.[5] Confirmation of this assignment was obtained after the single crystal X-ray analysis had been performed, by calculating the XRD pattern and finding that it corresponded with that published for Form II.[5] A solution made by mixing 0.05 g SMD in 6 cm^3 CH_3CN and 0.032 g aspirin in 1.5 cm^3 CH_3CN and heating to 323K with stirring for ten minutes yielded, after slow evaporation, yellow prismatic crystals of (**2**) the 1 : 1 SMD-aspirin complex. Preliminary unit cell data for **2** differed from those reported for the starting materials, confirming that a compound had been formed. The 1 : 1 complex stoichiometry was confirmed by single crystal X-ray analysis.

Single crystal X-ray analyses

Analogous procedures were used for the crystal structure determinations. Preliminary unit cell dimensions and space group data were obtained from precession photographs. Intensity data were collected on an Enraf–Nonius CAD4 diffractometer with MoKα-radiation (λ = 0.71069 Å). Accurate cell parameters were determined by the least-squares analysis of accurate setting angles in the θ-range 16–17°. Reflections in the θ-range 1–25° were collected by the ω-2θ scan mode using a variable scan speed depending on I and $\sigma(I)$ with a maximum time of 40 s per reflection. A variable scan width ω of (0.85 + 0.35 tan θ)° and a variable aperture width of (1.12 + 1.05 tan θ) mm were used. Intensity control was performed every hour and orientation control every 200 measured reflections. Both data sets were corrected for Lp-effects and for absorption[11] using the program EAC of the Enraf-Nonius Structure Determination Package.[12] Data-collection parameters and details of structure refinements are listed in Table 1. Intensity statistics indicated that $P\bar{1}$ is the correct space group for the complex **2**. The structures were solved by direct methods using program SHELX86[13] and refined by full-matrix least-squares using SHELX76[14] and minimizing $\Sigma w(|F_o| - |kF_c|)^2$. All H atoms were located in difference Fourier maps. Those attached to O or N atoms were allowed to refine freely while the rest were added in idealized positions with C—H 1.00 Å. Anisotropic thermal parameters were employed for non-H atoms and common variable U_{iso} values were assigned to H atoms in different chemical groups. The latter refined in the ranges 0.046–0.090 $Å^2$ and 0.054–0.103 $Å^2$ for **1** and **2**, respectively. Complex neutral atomic scattering factors[15] were used. Program PARST[16] was used for geometrical calculations and PLUTO[17] for molecular drawings. Fractional atomic coordinates and equivalent isotropic thermal parameters (U_{eq} = (1/3)$\Sigma_i\Sigma_j U_{ij} a_i^* a_j^* a_i \cdot a_j$) for nonhydrogen atoms are listed in Tables 2 and 3. Hydrogen atom positions, U_{ij} values, torsion angles and structure factor tables have been submitted to this journal.

Table 1. Crystal data, details of data-collection and refinement

	1	**2**
Formula	$C_{11}H_{12}N_4O_3S$	$C_{11}H_{12}N_4O_3S \cdot C_9H_8O_4$
M_r/g mol^{-1}	280.3	460.5
a/Å	13.086(2)	8.102(1)
b/Å	5.583(1)	12.033(1)
c/Å	17.222(3)	12.170(2)
α/°	90.0	111.67(1)
β/°	99.98(1)	93.77(1)
γ/°	90.0	103.82(1)
V/Å^3	1239.2(4)	1055.0(3)
Z	4	2
Space group	$P2_1/c$	$P\bar{1}$
μ(MoKα)/cm^{-1}	2.59	1.94
F(000)	584	480
D_c/g cm^{-3}	1.502	1.450
Crystal size/mm	0.28 × 0.34 × 0.41	0.28 × 0.34 × 0.34
Index range	−15, 15; 0, 6; 0, 20	−9, 9; −14, 14; 0, 14
Standard intensity variation/%	+0.5	+1.4
Absorption correction factor range	0.9899, 1.0000	0.9934, 0.9992
Reflections measured	2519	3896
Unique reflections	2064	3391
R_{int}	0.015	0.033
Observed reflections, $I > 2\sigma(I)$	1905	2971
L S variables	188	315
Mean shift/error	0.01	0.01
Weighting scheme	$[\sigma^2(F_o)]^{-1}$	$[\sigma^2(F_o)]^{-1}$
R	0.041	0.037
R_w	0.041	0.038
S	3.918	2.764
Final $\Delta\rho$/e Å^{-3}, min, max	−0.42, 0.27	−0.34, 0.20

BNSDOCID: <XP_____55032900A__I_>

UM00017125
NOVARTIS EXHIBIT 1517
Novartis v. Regents, IPR2023-01347
Page 3982 of 4460

Table 2. Fractional atomic coordinates ($\times 10^4$, $\times 10^5$ for S) and equivalent isotropic thermal parameters ($Å^2 \times 10^3$) with esd's in parentheses for **1**

Atom	*x/a*	*y/b*	*z/c*	U_{eq}
S(1)	25849(5)	15494(13)	53683(4)	32(0)
O(1)	2719(1)	−309(4)	5956(1)	41(1)
O(2)	2815(1)	3961(4)	5618(1)	42(1)
O(3)	−929(2)	7023(5)	2829(2)	91(1)
N(1)	1366(2)	1251(5)	4966(1)	38(1)
N(2)	1266(2)	4468(5)	4087(1)	45(1)
N(3)	−230(2)	2321(4)	4293(1)	36(1)
N(4)	5198(2)	−813(5)	2997(2)	43(1)
C(1)	3314(2)	862(5)	4639(1)	29(1)
C(2)	3182(2)	−1305(5)	4242(2)	35(1)
C(3)	3802(2)	−1851(5)	3695(2)	36(1)
C(4)	4581(2)	−293(5)	3559(1)	33(1)
C(5)	4718(2)	1858(5)	3970(2)	35(1)
C(6)	4086(2)	2441(5)	4506(2)	33(1)
C(7)	783(2)	2775(5)	4425(2)	33(1)
C(8)	655(2)	5834(6)	3570(2)	56(1)
C(9)	−401(2)	5520(6)	3380(2)	48(1)
C(10)	−820(2)	3714(6)	3759(2)	42(1)
C(11)	−1984(2)	6628(8)	2570(2)	63(1)

Results and discussion

Bond lengths and bond angles for **1** and **2** are listed in Tables 4 and 5; hydrogen bond data appear in Table 6.

Table 3. Fractional atomic coordinates ($\times 10^4$) and equivalent isotropic thermal parameters ($Å^2 \times 10^3$) with esd's in parentheses for **2**

Atom	*x/a*	*y/b*	*z/c*	U_{eq}
S(1)	4639(1)	6152(1)	7383(1)	41(0)
O(1)	5298(2)	5604(1)	8117(2)	58(1)
O(2)	5398(2)	6082(2)	6334(2)	54(1)
O(3)	4496(2)	11363(2)	7004(2)	63(1)
O(4)	7540(2)	8323(1)	10275(2)	60(1)
O(5)	8275(2)	10339(2)	10656(2)	53(1)
O(6)	8774(2)	7613(1)	11933(1)	46(1)
O(7)	10542(2)	7135(2)	10606(2)	69(1)
N(1)	4967(2)	7608(2)	8311(2)	40(1)
N(2)	3853(2)	8292(2)	6936(2)	42(1)
N(3)	5859(2)	9694(2)	8688(2)	36(1)
N(4)	−2830(3)	3783(2)	5784(2)	55(1)
C(1)	2413(3)	5522(2)	6949(2)	37(1)
C(2)	1249(3)	5968(2)	7648(2)	43(1)
C(3)	−485(3)	5384(2)	7267(2)	47(1)
C(4)	−1096(3)	4349(2)	6181(2)	41(1)
C(5)	99(3)	3893(2)	5508(2)	44(1)
C(6)	1826(3)	4477(2)	5878(2)	43(1)
C(7)	4886(3)	8568(2)	7950(2)	34(1)

Table 3. Continued

Atom	*x/a*	*y/b*	*z/c*	U_{eq}
C(8)	3779(3)	9253(2)	6664(2)	49(1)
C(9)	4702(3)	10468(2)	7372(2)	42(1)
C(10)	5761(3)	10652(2)	8398(2)	39(1)
C(11)	5323(4)	12623(2)	7795(3)	65(1)
C(12)	9642(3)	9713(2)	11990(2)	39(1)
C(13)	9810(3)	8844(2)	12460(2)	42(1)
C(14)	10914(3)	9184(3)	13510(2)	54(1)
C(15)	11906(3)	10401(3)	14102(2)	60(1)
C(16)	11796(3)	11278(2)	13653(2)	52(1)
C(17)	10668(3)	10944(2)	12607(2)	46(1)
C(18)	8400(3)	9374(2)	10887(2)	41(1)
C(19)	9230(3)	6832(2)	10946(2)	46(1)
C(20)	7886(3)	5605(2)	10391(3)	58(1)

Table 4. Bond lengths (Å) with esd's in parentheses

	1	**2**
S(1)—O(1)	1.439(2)	1.435(3)
S(1)—O(2)	1.430(2)	1.437(3)
S(1)—N(1)	1.634(2)	1.641(2)
S(1)—C(1)	1.746(2)	1.741(2)
O(3)—C(9)	1.362(4)	1.349(4)
O(3)—C(11)	1.393(4)	1.424(3)
N(1)—C(7)	1.388(4)	1.392(4)
N(2)—C(7)	1.326(4)	1.329(3)
N(2)—C(8)	1.329(4)	1.327(4)
N(3)—C(7)	1.330(4)	1.327(3)
N(3)—C(10)	1.342(4)	1.342(4)
N(4)—C(4)	1.394(4)	1.372(3)
C(1)—C(2)	1.386(4)	1.383(4)
C(1)—C(6)	1.389(4)	1.389(3)
C(2)—C(3)	1.381(5)	1.373(3)
C(3)—C(4)	1.390(4)	1.395(3)
C(4)—C(5)	1.390(4)	1.391(4)
C(5)—C(6)	1.381(5)	1.367(3)
C(8)—C(9)	1.375(4)	1.379(3)
C(9)—C(10)	1.367(5)	1.382(4)
Acetylsalicylic acid moiety in 2		
O(4)—C(18)		1.206(2)
O(5)—C(18)		1.316(4)
O(6)—C(13)		1.394(2)
O(6)—C(19)		1.361(3)
O(7)—C(19)		1.191(3)
C(12)—C(13)		1.392(4)
C(12)—C(17)		1.399(3)
C(12)—C(18)		1.484(3)
C(13)—C(14)		1.374(3)
C(14)—C(15)		1.376(4)
C(15)—C(16)		1.373(5)
C(16)—C(17)		1.382(3)
C(19)—C(20)		1.490(3)

BNSDOCID: <XP_____55032900A__1_>

UM00017126
NOVARTIS EXHIBIT 1517
Novartis v. Regents, IPR2023-01347
Page 3983 of 4460

Table 5. Bond angles (°) with esd's in parentheses

	1	2		1	2
N(1)—S(1)—C(1)	106.7(1)	106.3(1)	O(3)—C(9)—C(8)	117.1(3)	117.6(2)
O(2)—S(1)—C(1)	108.1(1)	108.6(1)	C(8)—C(9)—C(10)	116.8(3)	116.4(2)
O(2)—S(1)—N(1)	111.3(1)	110.8(2)	O(3)—C(9)—C(10)	126.2(3)	126.1(2)
O(1)—S(1)—C(1)	109.4(1)	110.5(1)	N(3)—C(10)—C(9)	121.6(3)	121.3(2)
O(1)—S(1)—N(1)	102.5(1)	103.4(1)			
O(1)—S(1)—O(2)	118.3(1)	116.7(1)	**Acetylsalicylic acid moiety in 2**		
C(9)—O(3)—C(11)	118.7(3)	117.1(2)			
S(1)—N(1)—C(7)	127.2(2)	124.1(2)	C(13)—O(6)—C(19)	117.1(2)	
C(7)—N(2)—C(8)	115.2(3)	115.7(2)	C(17)—C(12)—C(18)	120.1(2)	
C(7)—N(3)—C(10)	116.4(3)	117.0(2)	C(13)—C(12)—C(18)	122.1(2)	
S(1)—C(1)—C(6)	118.9(2)	116.8(2)	C(13)—C(12)—C(17)	117.8(2)	
S(1)—C(1)—C(2)	120.6(2)	123.1(2)	O(6)—C(13)—C(12)	121.3(2)	
C(2)—C(1)—C(6)	120.3(2)	119.9(2)	C(12)—C(13)—C(14)	121.4(3)	
C(1)—C(2)—C(3)	119.5(3)	119.6(2)	O(6)—C(13)—C(14)	117.1(2)	
C(2)—C(3)—C(4)	120.8(3)	121.1(2)	C(13)—C(14)—C(15)	119.7(3)	
N(4)—C(4)—C(3)	121.1(2)	121.2(2)	C(14)—C(15)—C(16)	120.4(2)	
C(3)—C(4)—C(5)	119.3(2)	118.4(2)	C(15)—C(16)—C(17)	120.0(2)	
N(4)—C(4)—C(5)	119.6(2)	120.5(2)	C(12)—C(17)—C(16)	120.6(2)	
C(4)—C(5)—C(6)	120.3(3)	120.7(2)	O(5)—C(18)—C(12)	113.6(2)	
C(1)—C(6)—C(5)	119.8(3)	120.2(2)	O(4)—C(18)—C(12)	123.8(2)	
N(2)—C(7)—N(3)	126.7(3)	126.3(3)	O(4)—C(18)—O(5)	122.6(2)	
N(1)—C(7)—N(3)	114.4(3)	115.2(2)	O(6)—C(19)—O(7)	122.3(2)	
N(1)—C(7)—N(2)	118.9(3)	118.5(2)	O(7)—C(19)—C(20)	126.9(3)	
N(2)—C(8)—C(9)	123.3(3)	123.4(2)	O(6)—C(19)—C(20)	110.9(2)	

Table 6. Hydrogen bond data with esd's in parentheses

D—H···A	D—H(Å)	D···A(Å)	H···A(Å)	D—H···A(°)
Compound 1				
N(1)—H(1)···N(3)^{i}	0.86(3)	2.911(4)	2.05(3)	176(3)
N(4)—H(41)···N(4)^{ii}	0.85(4)	3.269(4)	2.48(4)	156(3)
N(4)—H(42)···O(1)^{iii}	0.92(3)	3.061(3)	2.22(3)	152(3)
(i) = $-x, -y, 1-z$; (ii) = $1-x, -1/2+y, 1/2-z$; (iii) = $1-x, -y, 1-z$				
Compound 2				
O(5)—H(51)···N(3)	0.86(3)	2.730(3)	1.87(3)	178(3)
N(1)—H(1)···O(4)	0.92(2)	2.787(3)	1.87(2)	178(2)
N(4)—H(41)···O(2)^{i}	0.91(3)	3.290(4)	2.48(3)	149(2)
N(4)—H(42)···O(2)^{ii}	0.88(3)	3.281(4)	2.72(3)	123(2)
N(4)—H(42)···N(2)^{ii}	0.88(3)	3.230(3)	2.38(2)	162(3)
(i) = $-1+x, y, z$; (ii) = $-x, 1-y, 1-z$				

Polymorphism of SMD

The nomenclature used here to designate different polymorphs of SMD is that of Bettinetti *et al.*[5] The molecular conformation adopted in **1** (SMD Form II) is shown in Fig. 1. Bond lengths and bond angles for **1** (Tables 4 and 5) are generally in excellent agreement with those reported for SMD Forms I and III.[10] The overall conformation of **1** is described by the torsion angles τ_1 C(6)—C(1)—S(1)—N(1) 130.1(2)°, τ_2 C(1)—S(1)—N(1)—C(7) — 73.5(3)°, and τ_3 S(1)—N(1)—C(7)—N(2) 11.6(4)°, which differ signif-

BNSDOCID: <XP_____55032900A__1_>

UM00017127
NOVARTIS EXHIBIT 1517
Novartis v. Regents, IPR2023-01347
Page 3984 of 4460

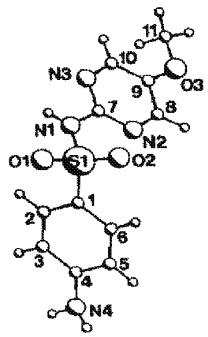


Fig. 1. Conformation of the SMD molecule in **1**, (SMD Form II).

icantly from those observed in the other known polymorphs of SMD. This is due to the different hydrogen bonding arrangements occurring in Forms I, II, and III. In each polymorph, SMD forms dimeric hydrogen bonded motifs (non-centrosymmetric in Form I, centrosymmetric in Forms II and III). These motifs, shown schematically in Fig. 2, involve different combinations of N—H···O and N—H···N hydrogen bonds. It has long been recognized that the tendency for sulfonamides to form polymorphs is due to the variety of hydrogen bonding possibilities afforded by the presence of the sulfonyl (S=O), amide (N—H) and pyrimidinyl (N) functions.[18,19] The SMD dimer reported here for **1** contains two identical N—H···N hydrogen bonds and also occurs in three solvates of SMD.[20] The crystal packing in **1** is shown in Fig. 3. A distinctive feature for this polymorph is the formation of a hydrogen bond N(4)—H···N(4′) which links the amino groups of screw-related molecules. Repetition of this interaction by the 2_1-axis (parallel to the short unit cell *b*-axis) generates an infinite chain (···N—H···N—H···) in which each N atom is both hydrogen bond donor and acceptor. There is significant pyramidization at N(4) as a result of this interaction (Fig. 1).

We have confirmed by X-ray powder diffractometry that the raw material used in our experiments is SMD Form I. We have also noted that when this form is recrystallized from acetonitrile, the same form results. However, in attempting to prepare a complex between SMD and PAS in acetonitrile, no complexation occurred and the unreacted SMD consisted of Form II, whose structure is described above. These observations do not explain the failure of SMD and PAS to complex under the conditions described, but it can be inferred that the presence of PAS induces crystallization of SMD Form II rather than Form I. A possible explanation is that the growth of nuclei of Form I are inhibited by pref-

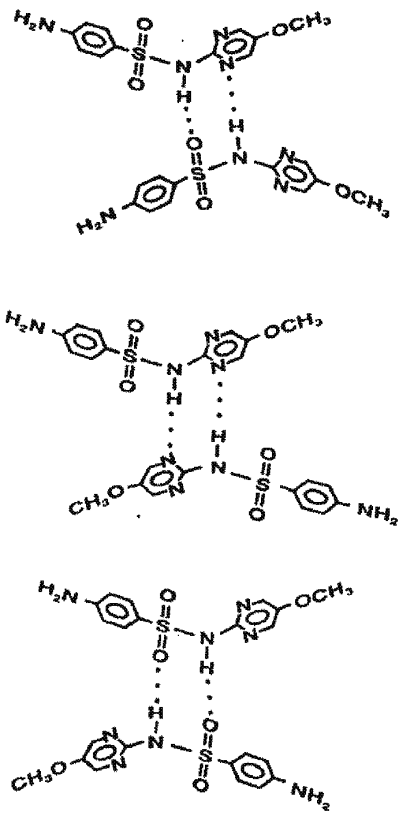


Fig. 2. Hydrogen bonded dimers in SMD polymorphs. Top: Form I[10]; Middle: Form II (present study), Bottom: Form III.[10]

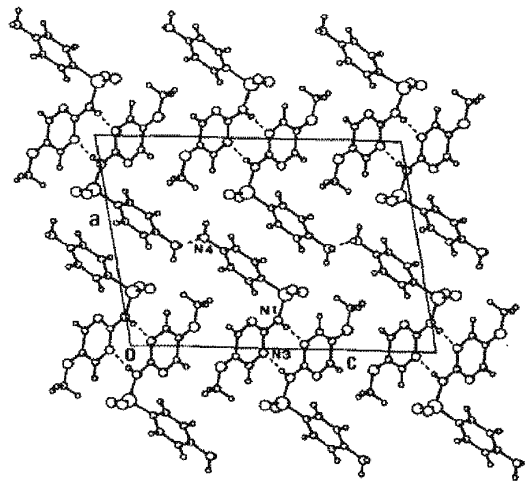


Fig. 3. [010] projection of the structure of **1** showing principal hydrogen bonds (dashed lines).

BNSDOCID: <XP_____55032900A_1_>

UM00017128
NOVARTIS EXHIBIT 1517
Novartis v. Regents, IPR2023-01347
Page 3985 of 4460

erential surface adsorption of PAS, thus favoring the crystallization of a different polymorph. Further experiments are necessary to confirm this hypothesis. Such a mechanism is likely, however, since Ebian *et al.*,[9] who studied the effect of additives on the interconversion of SMD crystal forms, have shown that molecules which are structurally related to SMD (e.g., p-aminobenzoic acid) retard the transformation of Form II to Form III in aqueous suspension by their ability to fit onto growing sites on nuclei of Form III. Attempts are being made to obtain a complex between SMD and PAS using different conditions from those described above.

Structure of the complex 2

The structure of complex **2** is shown in Fig. 4. The carboxylic acid group of the aspirin molecule engages in complementary hydrogen bonding with the SMD amide group and pyrimidinyl N atom. This mode of complexation is identical to that previously reported for complexes of the related drug sulfadimidine with substituted aromatic acids, and in particular, with acetylsalicylic acid.[2] There are no significant changes in bond lengths and bond angles in SMD upon complexation (Tables 4 and 5). The torsion angles for SMD (defined above) in the complex are τ_1 157.9(2)°, τ_2 − 78.4(2)°, and τ_3 28.9(3)°. Molecular parameters for the aspirin molecule are identical to those for aspirin in its 1 : 1 complex with sulfadimidine[2] and the carbonyl group of the —COOH function is again syn-planar to the acetoxy group. The intramolecular N—H···O and N···H—O hydrogen bonds in **2** are identical in length to those in the sulfadimidine complex but are more linear in **2**. Table 6 lists these and other hydrogen bond data for **2**.

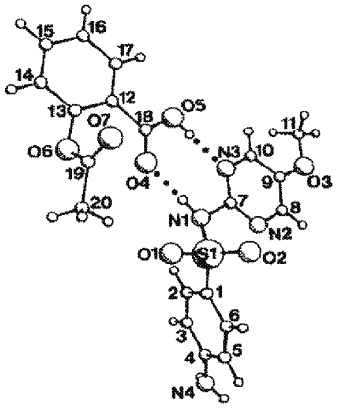


Fig. 4. Structure of the complex **2**.

Complexation by solid–solid reaction

Thus far, all of the 1 : 1 sulfonamide–aromatic carboxylic acid complexes reported in this series have been recovered from reactions occurring in solution, using either acetonitrile or ethanol as common solvent for the reacting components. However, we have recently obtained evidence for complex formation on co-grinding the solid reactants in a 1 : 1 molar ratio. These results will be published shortly.

Appendix

Hydrogen atom positions, anisotropic thermal parameters, torsion angles and structure factor tables for: **1** 5-methoxysulfadiazine (polymorphic Form II) and **2** 1 : 1 complex between 5-methoxysulfadiazine and acetylsalicylic acid.

Acknowledgments

Financial assistance from the FRD, Pretoria, and the University of Cape Town are gratefully acknowledged.

References

1. Caira, M.R. *J. Crystallogr. Spectr. Res.* **1991**, *21*, 641.
2. Caira, M.R. *J. Crystallogr. Spectr. Res.* **1992**, *22*, 193.
3. Caira, M.R.; Mohamed, R. *Acta Cryst.* **1993**, *B49*, 760.
4. Rambaud, J.; Alberola, S.; Grignon, H.; Masse, J.; Sabon, F. *Trav. Soc. Pharm. Montpellier* **1974**, *34*, 293.
5. Bettinetti, G.P.; Giordano, F.; La Manna, A.; Giuseppetti, G. *Il Farmaco-Ed.Pr.* **1974**, *29*, 493.
6. Yokoyama, T., Umeda, T., Kuroda, K., Watanabe, A. *Chem. Pharm. Bull.* **1978**, *26*, 1044.
7. Burger, A.; Ramberger, R.; Schulte, K. *Arch. Pharm. (Weinheim)* **1980**, *313*, 1020.
8. Moustafa, M.A.; Khalil, S.A.; Ebian, A.R.; Motawi, M.M. *J. Pharm. Pharmac.* **1972**, *24*, 921.
9. Ebian, A.R.; Moustafa, M.F.; Khalil, S.A.; Motawi, M.M. *J. Pharm. Pharmac.* **1973**, *25*, 13.
10. Giuseppetti, G.; Tadini, C.; Bettinetti, G.P.; Giordano, F. *Cryst. Struct. Comm.* **1977**, *6*, 263.
11. North, A.C.T.; Philips, D.C.; Scott Mathews, F. *Acta Crystallogr.* **1968**, *A24*, 351.
12. Frenz, B.A.; Associates Inc. (1982) *Structure Determination Package*, College Station: Texas.
13. Sheldrick, G.M. SHELXS86. In *Crystallographic Computing* 3,

BNSDOCID: <XP_____55032900A__I_>

UM00017129
NOVARTIS EXHIBIT 1517
Novartis v. Regents, IPR2023-01347
Page 3986 of 4460

Sheldrick, G.M., Kruger, C., and Goddard, R. Eds.; p. 175; Oxford University Press, 1985.
14. Sheldrick, G.M. SHELX, A system of computer programs for X-ray structure determination; England, University of Cambridge: 1976.
15. *International Tables for X-Ray Crystallography* Vol. IV, **1974**, Kynoch Press, Birmingham; (Present distributor: Reidel, D., Dordrecht).
16. Nardelli, M. *Comput. Chem.* **1983**, *7*, 95.
17. Motherwell, S. PLUTO, A program for plotting molecular and crystal structures; University of Cambridge: England, **1979**.
18. Byrn, S.R. *Solid-State Chemistry of Drugs*, Academic Press: London; 1982, p. 103.
19. Yang, S.S., Guillory, J.K. *J. Pharm. Sci.* **1972**, *61*, 26.
20. Caira, M.R.; Mohamed, R. *Supramolec. Chem.* **1993**, 2, 201.

BNSDOCID: <XP_____5503290OA__1_>

UM00017130
NOVARTIS EXHIBIT 1517
Novartis v. Regents, IPR2023-01347
Page 3987 of 4460

Drug Crystal Growth

DOI: 10.1002/anie.200604674

Selective Crystal Growth of the Anhydrous and Monohydrate Forms of Theophylline on Self-Assembled Monolayers

*Jason R. Cox, Marta Dabros, Jeanne A. Shaffer, and Venkat R. Thalladi**

Polymorphs and solvates of pharmaceuticals frequently exhibit differences in physicochemical properties such as bioavailability, comminution, and shelf life.[1] The control of polymorphism[2] and pseudopolymorphism[3] is, therefore, critical to pharmaceutical formulation and distribution.[4] Classical methods for the screening and selective growth of polymorphs or pseudopolymorphs involve altering conditions such as the solvent, temperature, and rate of evaporation.[5] Crystallization, however, is often mediated by heterogeneous nucleation, which can occur on the surfaces of dust particles, glass vials, or other foreign templates.[6] It has long been held that crystal growth can be influenced by the structure of the nucleating surface.[7] Accordingly, Langmuir monolayers,[8] thiol self-assembled monolayers (SAMs),[9] silane monolayers,[10] single-crystal substrates,[11] and polymer particles[12] have been used in the growth of organic and inorganic crystals.[13] Herein, we report the effect of the hydrogen-bonding ability of thiol SAMs on the crystal growth of the anhydrous and monohydrate forms of theophylline,[14] a drug widely used as a bronchodilator in asthma therapy. We show that the disparity in the number of hydrogen-bond donors and acceptors in theophylline and the geometric complementarity at the growth interface are critical to the observed selectivity in the crystal growth.

The monohydrate (space group $P2_1/n$) and anhydrous (space group $Pna2_1$) forms of theophylline crystallize concomitantly[15] from ethanol at 70% relative humidity.[16] Figures 1 and 2 show the calculated and experimental morphologies of the two forms. The thiol SAMs used in this work were fabricated on gold-coated glass slides by immersing the slides in ethanol solutions of ω-functionalized alkanethiols.[17] Hydrophobic SAMs were made from 1-dodecanethiol (**1**) and 1-hexadecanethiol (**2**), and hydrophilic SAMs from 11-mercaptoundecanol (**3**), 11-mercaptoundecanoic acid (**4**), and 16-mercaptohexadecanoic acid (**5**).

Crystallizations were carried out in ethanol solution at 20 °C and approximately 70% relative humidity.[18] A nearly saturated ethanol solution of theophylline was heated at 60 °C for 30 min to ensure complete dissolution. After cooling, the solution was transferred to vials containing SAM substrates and allowed to evaporate to yield crystals. All the experiments were performed at least five times, and the results from the repeated trials were qualitatively similar.

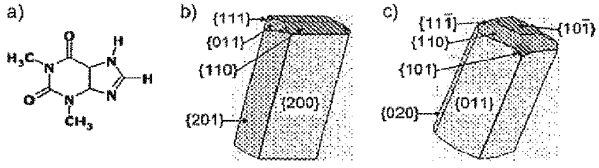


Figure 1. a) The chemical structure of theophylline. Morphologies of b) the anhydrous form and c) the monohydrate form of theophylline calculated using the Bravais–Friedel–Donnay–Harker (BFDH) theory. Symmetry-independent faces are labeled.

Substrates bearing hydrophilic SAM-**3**, SAM-**4**, or SAM-**5** selectively nucleated the anhydrous form of theophylline. Figure 2a shows the crystal growth on carboxy-terminated SAM-**4**. We found that crystals of the monohydrate form of theophylline grew on the inner surfaces of the glass vial containing SAM-**4**. Similar results were obtained with SAM-**3** and SAM-**5**. In the case of SAM-**1** and SAM-**2**, crystals of the monohydrate grew on the SAMs, as well as on the surfaces of the glass vials. We note that the conditions under which the crystal-growth experiments were performed were indistinguishable, save for the differences in the SAMs. These results suggest that SAMs with exposed hydrogen-bonding functional groups act as templates for the selective growth of anhydrous theophylline. In the absence of a SAM, under similar conditions, the crystallizations yielded both the monohydrate and the anhydrous forms, with the monohydrate being the predominant form.

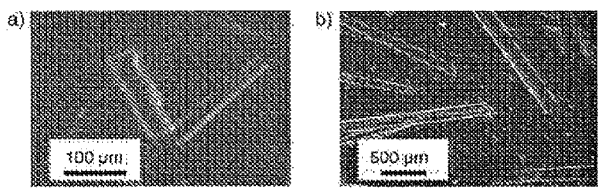


Figure 2. Optical micrographs showing a) the selective growth of the anhydrous form of theophylline on carboxy-terminated SAM-**4**, and b) the growth of the monohydrate form on methyl-terminated SAM-**2**.

[*] J. R. Cox, M. Dabros, J. A. Shaffer, Prof. V. R. Thalladi
Department of Chemistry and Biochemistry
Worcester Polytechnic Institute
Worcester, MA 01609 (USA)
Fax: (+1) 508-831-5933
E-mail: thalladi@wpi.edu

Supporting information for this article (characterization of the SAMs by contact-angle goniometry, ellipsometry, grazing-angle IR spectroscopy, and cyclic voltammetry; characterization of the crystalline forms of theophylline by ATR-IR spectroscopy, thermal methods (DSC and TGA), and powder X-ray diffraction; structural and epitaxial analysis) is available on the WWW under http://www.angewandte.org or from the author.

InterScience
© 2007 Wiley-VCH Verlag GmbH & Co. KGaA, Weinheim

BNSDOCID: <XP_____55032897A__I_>

UM00017131
NOVARTIS EXHIBIT 1517
Novartis v. Regents, IPR2023-01347
Page 3988 of 4460

Noting the influence of hydroxy and carboxy groups on the crystal growth, we evaluated the hydrogen-bonding characteristics of theophylline in both crystalline forms. Theophylline has two acidic hydrogen-bond donors (the imidazole NH and =CH groups) and three acceptors (the two-coordinate imidazole nitrogen atom and the two carbonyl oxygen atoms). Given that each carbonyl oxygen atom can act as an acceptor to two hydrogen bonds, there is a shortage of donors in the theophylline molecule. In the anhydrous crystalline form, the two donors interact with two acceptors, forming hydrogen-bonded bilayers (Figure 3). These bilayers

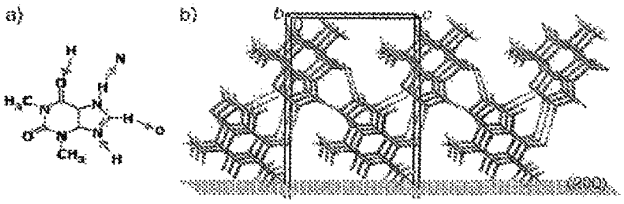


Figure 3. The crystal structure of the anhydrous form of theophylline.[16] a) The hydrogen bonds around a single molecule; the red and blue arrows indicate two distinct hydrogen bonds. b) A molecular bilayer parallel to the *bc* plane; C gray, H yellow, N blue, O red; the green dotted lines indicate hydrogen bonds. Note the presence of exposed non-hydrogen-bonded carbonyl groups at the (200) plane.

are parallel to *bc* plane and expose the third acceptor at (200). Figure 1b shows that the {200} faces are among the largest on the crystals, and Figure 2a shows that the crystals lie on the {200} faces on the SAM substrates. We surmised that hydrogen-bond donors, such as hydroxy and carboxy groups on SAMs, interact with the carbonyl acceptors exposed at the {200} faces of the crystal nuclei. These interactions lower the nucleation barrier and promote the selective crystallization of the anhydrous form, though it is thermodynamically less stable than the monohydrate form under the experimental conditions.[16] Powder X-ray diffraction analysis of the crystals showed that the intensities of the (200) and related higher-index reflections are increased compared to those of other reflections (Figure 4), indicating that SAM-**3**, SAM-**4**, and SAM-**5** nucleated the {200} faces of the anhydrous form.

To test whether the geometry (that is, the two-dimensional periodic structure) of the SAMs played any role in the crystal growth, we performed crystallizations of theophylline (under similar experimental conditions) using glass slides with exposed hydroxy groups.[19] Unlike hydrogen-bonding SAM-**3**, SAM-**4**, and SAM-**5**, the hydrophilic glass slides consistently yielded a concomitant mixture of the anhydrous and monohydrate crystalline forms. The hydroxy groups on the glass slides promoted the growth of the anhydrous form, but not as exclusively as SAM-**3**, SAM-**4**, and SAM-**5**. These results show that the geometry of the thiol SAMs enhances the selective growth of anhydrous form of theophylline.

We evaluated the geometric complementarity between the SAMs and the crystal faces of both crystalline forms of theophylline using the lattice-matching program EpiCalc.[20]

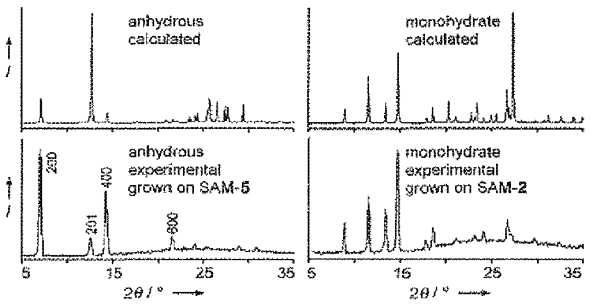


Figure 4. Top: powder X-ray diffraction patterns of the anhydrous (left) and monohydrate (right) forms of theophylline calculated from their crystal structures.[16] Bottom: experimental powder X-ray diffraction patterns of the anhydrous form grown on SAM-**5** (left) and the monohydrate form grown on SAM-**2** (right). Note the differences in the relative intensities of various peaks, particularly those labeled, in the calculated and experimental patterns of the anhydrous form.

All the SAMs used herein have the same two-dimensional lattice ($a_1 = a_2 = 4.97$ Å and $\alpha = 120°$).[21] The program determines the lattice registry by rotating an overlayer lattice (b_1, b_2, β) on a substrate lattice (a_1, a_2, α) through a series of azimuthal angles (θ; see the Supporting Information, Figure S7). For each azimuthal angle, the program calculates a dimensionless potential (V/V_o), whose value depends on the type of epitaxy between the two lattices (Table S2). Analysis of the results shows that the {200}, {201}, {111}, and {011} faces of the anhydrous form, and only the {011} and {10$\bar{1}$} faces of the monohydrate form exhibit ideal coincident epitaxy; other faces deviate from the ideal value of $V/V_o = 0.50$ (Table S3 in the Supporting Information). Of all the faces that show the ideal V/V_o value, the {200} faces of the anhydrous form have the smallest supercell area; that is, these faces exhibit the best epitaxial match with the SAM substrates.

Unlike in the anhydrous form, all the donors and acceptors in the monohydrate form of theophylline are involved in hydrogen bonding. The water molecule provides the missing hydrogen-bond donors; that is, there is no shortage of donors within the crystal structure of the monohydrate. In terms of geometric epitaxy, the {101} faces displayed the smallest supercell area (Table S3). Figure 5 shows that the molecules are arranged in a corrugated pattern at the (101) plane, such that =CH and CH_3 groups are exposed. Hydrogen-bond acceptors are not easily accessible at this plane; that is, the {101} faces are less likely to be nucleated by hydrogen-bonding SAM-**3**, SAM-**4**, and SAM-**5**. Further analysis showed that all the growth faces in the monohydrate display structural features (corrugated packing or inaccessible donors, Figure S9) that are not conducive to template-induced nucleation by the hydrophilic SAMs. The exclusive growth of the monohydrate form on hydrophobic SAM-**1** and SAM-**2** is difficult to rationalize. As noted above, the (101) and other planes expose =CH and CH_3 groups, which can interact favorably with CH_3-terminated SAMs. In addition, the growth of the anhydrous form is probably hampered in the presence of hydrophobic SAMs, leading to the enhanced growth of the monohydrate form. Powder X-ray diffraction

 © 2007 Wiley-VCH Verlag GmbH & Co. KGaA, Weinheim

BNSDOCID: <XP_____55032897A_I_>

UM00017132
NOVARTIS EXHIBIT 1517
Novartis v. Regents, IPR2023-01347
Page 3989 of 4460

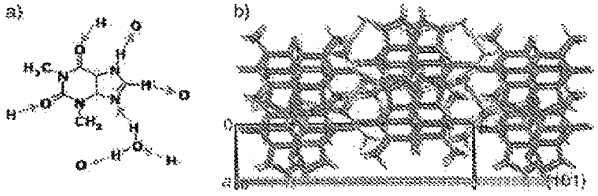


Figure 5. The crystal structure of the monohydrate form of theophylline.[16] a) The hydrogen bonds around a single molecule; the red, yellow, and blue arrows indicate three distinct hydrogen bonds. Note that all potential donors and acceptors participate in hydrogen bonding. b) The corrugated packing of the molecules; C gray, H yellow, N blue, O red; the green dotted lines indicate hydrogen bonds. Note the absence of exposed acceptors at the (101) interface. One of the hydrogen atoms of the water molecule is disordered.

analysis showed that the relative intensities of the experimental and calculated (with no preferred orientation of crystals) patterns are similar in the case of the monohydrate (Figure 4). This observation indicates that face-selective crystal growth does not occur in the case of the monohydrate. In other words, all faces of the crystals of the monohydrate form exhibit similar growth rates on hydrophobic surfaces.

We showed that hydrogen-bonding SAMs act as templates for the selective growth of the thermodynamically less stable anhydrous form of theophylline. We believe that several properties inherent to the anhydrous form led to this selectivity: an imbalance in the numbers of hydrogen-bond donors and acceptors, a layered arrangement of molecules that exposes the excess acceptors at the largest growing faces, and a serendipitous coincident epitaxy with the hydrophilic SAMs. Polymorph selection by surface templates is currently in the discovery phase. We hope that our work and the recent work by others will enable future research in this area to enter the design phase, where templates can be created for the growth of a desired polymorph. We discovered a previously unidentified or unnoted problem in the surface-induced crystallization of polymorphs: the growth of unwanted polymorphs on adventitious templates. Crystallizations are typically performed in a container, and the surface of the container is always a potential nucleation site for polymorphs. We are currently exploring several approaches to minimize or eliminate this problem of polymorph growth on surfaces other than the desired templates.

Received: November 16, 2006
Revised: December 11, 2006
Published online: February 9, 2007

Keywords: crystal growth · epitaxy · hydrogen bonds · polymorphism · self-assembled monolayers

[1] S. R. Byrn, R. R. Pfeiffer, J. G. Stowell, *Solid-State Chemistry of Drugs*, 2nd ed., SSCI, West Lafayette, **1999**; *Polymorphism in Pharmaceutical Solids* (Ed.: H. G. Brittain), Marcel Dekker, New York, **1999**; J. Bernstein, *Polymorphism in Molecular Crystals*, Oxford University Press, New York, **2002**; *Polymorphism in the Pharmaceutical Industry* (Ed.: R. Hilfiker), Wiley-VCH, Weinheim, **2006**.

[2] S. R. Chemburkar, J. Bauer, K. Deming, H. Spiwek, K. Patel, J. Morris, R. Henry, S. Spanton, W. Dziki, W. Porter, J. Quick, P. Bauer, J. Donaubauer, B. A. Narayanan, M. Soldani, D. Riley, K. McFarland, *Org. Process Res. Dev.* **2000**, *4*, 413–417.

[3] C. Näther, I. Jess, *Angew. Chem.* **2006**, *118*, 6529–6531; *Angew. Chem. Int. Ed.* **2006**, *45*, 6381–6383.

[4] For a recent discussion on the use of the terms polymorphism and pseudopolymorphism, see: G. R. Desiraju, *CrystEngComm* **2003**, *5*, 466–467; K. R. Seddon, *Cryst. Growth Des.* **2004**, *4*, 1087; G. R. Desiraju, *Cryst. Growth Des.* **2004**, *4*, 1089–1090; J. Bernstein, *Cryst. Growth Des.* **2005**, *5*, 1661–1662; A. Nangia, *Cryst. Growth Des.* **2006**, *6*, 2–4.

[5] Recently, this classical approach has been automated into a high-throughput method. See, for example: S. L. Morissette, S. Soukasene, D. Levinson, M. J. Cima, O. Almarsson, *Proc. Natl. Acad. Sci. USA* **2003**, *100*, 2180–2184.

[6] J. W. Mullin, *Crystallization*, 4th ed., Butterworth-Heinemann, New York, **2001**.

[7] M. Lahav, L. Addadi, L. Leiserowitz, *Proc. Natl. Acad. Sci. USA* **1987**, *84*, 4737–4738.

[8] E. M. Landau, M. Levanon, L. Leiserowitz, M. Lahav, J. Sagiv, *Nature* **1985**, *318*, 353–356; B. R. Heywood, S. Mann, *Adv. Mater.* **1994**, *6*, 9–20; L. M. Frostman, M. D. Ward, *Langmuir* **1997**, *13*, 330–337.

[9] L. M. Frostman, M. M. Bader, M. D. Ward, *Langmuir* **1994**, *10*, 576–582; F. C. Meldrum, J. Flath, W. Knoll, *Langmuir* **1997**, *13*, 2033–2049; J. Küther, R. Seshadri, W. Knoll, W. Tremel, *J. Mater. Chem.* **1998**, *8*, 641–650; J. Aizenberg, A. J. Black, G. M. Whitesides, *J. Am. Chem. Soc.* **1999**, *121*, 4500–4509; A. Y. Lee, A. Ulman, A. S. Myerson, *Langmuir* **2002**, *18*, 5886–5898; N. Banno, T. Nakanishi, M. Matsunaga, T. Asahi, T. Osaka, *J. Am. Chem. Soc.* **2004**, *126*, 428–429; R. Hiremath, S. W. Varney, J. A. Swift, *Chem. Commun.* **2004**, 2676–2677; R. Hiremath, J. A. Basile, S. W. Varney, J. A. Swift, *J. Am. Chem. Soc.* **2005**, *127*, 18321–18327.

[10] P. W. Carter, M. D. Ward, *J. Am. Chem. Soc.* **1994**, *116*, 769–770.

[11] C. A. Mitchell, L. Yu, M. D. Ward, *J. Am. Chem. Soc.* **2001**, *123*, 10830–10839; C. Cashell, D. Corcoran, B. K. Hodnett, *Chem. Commun.* **2003**, 374–375; L. Yu, *J. Am. Chem. Soc.* **2003**, *125*, 6380–6381.

[12] C. P. Price, A. L. Grzesiak, A. J. Matzger, *J. Am. Chem. Soc.* **2005**, *127*, 5512–5517.

[13] Other methods to control polymorphism include the use of tailor-made auxiliaries, laser-induced nucleation, and crystallization in confined spaces. See: I. Weissbuch, L. Leisorowitz, M. Lahav, *Adv. Mater.* **1994**, *6*, 952–956; R. J. Davey, N. Blagden, G. D. Potts, R. Docherty, *J. Am. Chem. Soc.* **1997**, *119*, 1767–1772; J. Zaccaro, J. Matic, A. S. Myerson, B. A. Garetz, *Cryst. Growth Des.* **2001**, *1*, 5–8; L. J. Chyall, J. M. Tower, D. A. Coates, T. L. Houston, S. L. Childs, *Cryst. Growth Des.* **2002**, *2*, 505–510; J. L. Hilden, C. E. Reyes, M. J. Kelm, J. S. Tan, J. G. Stowell, K. R. Morris, *Cryst. Growth Des.* **2003**, *3*, 921–926; J.-M. Ha, J. H. Wolf, M. A. Hillmyer, M. D. Ward, *J. Am. Chem. Soc.* **2004**, *126*, 3382–3383.

[14] D. J. Sutor, *Acta Crystallogr.* **1956**, *9*, 969–970; A. A. Naqvi, G. C. Bhattacharyya, *J. Appl. Crystallogr. J. Appl. Cryst.* **1981**, *14*, 464.

[15] J. Bernstein, R. J. Davey, J.-O. Henck, *Angew. Chem.* **1999**, *111*, 3646–3669; *Angew. Chem. Int. Ed.* **1999**, *38*, 3440–3461.

[16] N. V. Phadnis, R. Suryanarayanan, *J. Pharm. Sci.* **1997**, *86*, 1256–1263.

[17] A. Ulman, *Chem. Rev.* **1996**, *96*, 1533–1554; J. C. Love, L. A. Estroff, J. K. Kriebel, R. G. Nuzzo, G. M. Whitesides, *Chem. Rev.* **2005**, *105*, 1103–1169.

 © 2007 Wiley-VCH Verlag GmbH & Co. KGaA, Weinheim

BNSDOCID: <XP_____55032897A__I_>

UM00017133
NOVARTIS EXHIBIT 1517
Novartis v. Regents, IPR2023-01347
Page 3990 of 4460

[18] Initial results were obtained from experiments performed under the high-humidity conditions (60–80% relative humidity) that are common in the summer in Worcester. We repeated the experiments under controlled-humidity conditions to verify the reproducibility of the results. Similar results were obtained when crystallizations were carried out in 95% ethanol solutions under low-humidity conditions (25% relative humidity).
[19] Glass slides with exposed silanol (SiOH) groups were prepared by treating freshly cut slides with an air plasma (in an SPI-III plasma etcher) for 45 s. These slides are similar to SAM-**3**, SAM-**4**, and SAM-**5** in terms of their hydrophilicity and hydrogen bonding. They, however, lack the long-range two-dimensional order and periodicity that are characteristic of the SAMs.
[20] A. C. Hillier, M. D. Ward, *Phys. Rev. B* **1996**, *54*, 14037–14051; J. A. Last, D. E. Hooks, A. C. Hillier, M. D. Ward, *J. Phys. Chem. B* **1999**, *103*, 6723–6733.
[21] Thiol SAMs are known to form domains of 100–200 μm^2 that have long-range order.[17] The epitaxy calculations assume that templated nucleation occurs on these domains.

 © 2007 Wiley-VCH Verlag GmbH & Co. KGaA, Weinheim

BNSDOCID: <XP_____55032897A__I_>

UM00017134
NOVARTIS EXHIBIT 1517
Novartis v. Regents, IPR2023-01347
Page 3991 of 4460

PHARMACEUTICS, PREFORMULATION AND DRUG DELIVERY

Intermolecular Contacts Influencing the Conformational and Geometric Features of the Pharmaceutically Preferred Mebendazole Polymorph C

FELIPE T. MARTINS,[1] PERSON P. NEVES,[2] JAVIER ELLENA,[1] GERARDO E. CAMÍ,[3] ELENA V. BRUSAU,[3] GRISELDA E. NARDA[3]

[1]Physics Institute of São Carlos, University of São Paulo, CP 369, 13560-970 São Carlos, SP, Brazil

[2]Department of Exact Science, Federal University of Alfenas, 37130-000 Alfenas, MG, Brazil

[3]Química Inorgánica, Departamento de Química, Facultad de Química, Bioquímica y Farmacia, Universidad Nacional de San Luis, Chacabuco y Pedernera, 5700 San Luis, Argentina

Received 11 June 2008; revised 11 August 2008; accepted 3 September 2008

Published online 14 October 2008 in Wiley InterScience (www.interscience.wiley.com). DOI 10.1002/jps.21593

ABSTRACT: Mebendazole (MBZ) is a common benzimidazole anthelmintic that exists in three different polymorphic forms, A, B, and C. Polymorph C is the pharmaceutically preferred form due to its adequated aqueous solubility. No single crystal structure determinations depicting the nature of the crystal packing and molecular conformation and geometry have been performed on this compound. The crystal structure of mebendazole form C is resolved for the first time. Mebendazole form C crystallizes in the triclinic centrosymmetric space group and this drug is practically planar, since the least-squares methyl benzimidazolylcarbamate plane is much fitted on the forming atoms. However, the benzoyl group is twisted by 31(1)° from the benzimidazole ring, likewise the torsional angle between the benzene and carbonyl moieties is 27(1)°. The formerly described bends and other interesting intramolecular geometry features were viewed as consequence of the intermolecular contacts occurring within mebendazole C structure. Among these features, a conjugation decreasing through the imine nitrogen atom of the benzimidazole core and a further resonance path crossing the carbamate one were described. At last, the X-ray powder diffractogram of a form C rich mebendazole mixture was overlaid to the calculated one with the mebendazole crystal structure. © 2008 Wiley-Liss, Inc. and the American Pharmacists Association J Pharm Sci 98:2336–2344, 2009

Keywords: crystallography; crystal structure; polymorphism; crystallization; X-ray powder diffractometry; mebendazole; polymorph C; benzimidazole derivative; anthelmintic drugs

INTRODUCTION

Mebendazole [(5-benzoyl-1*H*-benzimidazole-2-yl)-carbamic acid methyl ester, MBZ] is a potent, orally active, broad-spectrum anthelmintic which is intensively used in the treatment of ascariasis, uncinariasis, oxyuriasis, and trichuriasis. As with

Correspondence to: Felipe T. Martins (Telephone: 1633739333; Fax: 163372-2218; E-mail: felipetmartins@yahoo.com.br)

Journal of Pharmaceutical Sciences, Vol. 98, 2336–2344 (2009)
© 2008 Wiley-Liss, Inc. and the American Pharmacists Association

WILEY InterScience® DISCOVER SOMETHING GREAT

BNSDOCID: <XP_____55032898A__I_>

UM00017135
NOVARTIS EXHIBIT 1517
Novartis v. Regents, IPR2023-01347
Page 3992 of 4460

other benzimidazole anthelmintics, MBZ primary mechanism of action is consistent with tubulin binding.

MBZ belongs to class II of the biopharmaceutics classification systems (BCS), polymorphism studies being then essential for this compound. Several authors have investigated the polymorphism and physical stability of MBZ solid phases.[1–3] Three polymorphic forms (A, B, and C) displaying significantly different solubilities and therapeutic effects have been identified and characterized.[4,5] Diverse techniques have been applied to feature particular polymorphic forms in samples, infrared spectroscopy being the most commonly used method in the literature to identify MBZ solid state phases, whereas X-ray powder diffraction is preferred to quantify MBZ polymorphic mixtures and references.[3,6,7]

Even though some discrepancies are reported in the literature concerning the relative solubility of forms B and C, all the authors agree that form A is the most abundant and stable and then the least soluble one.[1,5] Thus, form C is pharmaceutically preferred since its solubility is enough to ensure optimal bioavailability without exhibiting the toxicity associated to form B.[5,8,9] Furthermore, it was determined that at least 30% of form A in the formulation is enough to suppress the desirable pharmacological activity,[10,11] thus indicating the high polymorphism dependence of the anthelmintic efficacy of MBZ.

Regarding physical properties, the three polymorphs have been mainly studied in relation to their thermal stability and dissolution behavior in several solvents. In addition, some MBZ solvates determined by single crystal X-ray diffraction have been reported. Mebendazole hydrobromide was found to crystallize in a monoclinic space group, $P2_1/c$,[12] whereas recrystallization of MBZ in propionic acid yields a 1:1 molecular complex crystallizing in the noncentrosymmetric triclinic space group, $P1$.[13]

Complete crystal structure data of MBZ polymorphs are not found in the literature because single crystals seem to be hard to obtain. In an attempt to obtain adequate crystals for single crystal X-ray diffraction we have recently reported a new stable salt, mebendazole hydrochloride which was also fully characterized by structural, vibrational and thermal analysis.[14]

In the present work we report the crystal structure solved by single crystal X-ray diffraction of MBZ C, which was obtained by recrystallization of the commercially available corresponding polymorph. Finally, the elucidation of the crystal structure of MBZ form C can contribute to approach the crystal structures of forms A and B, that still remain unknown, and the structure–property relationships of MBZ will be stated.

EXPERIMENTAL

Materials and Preparation of MBZ Polymorph C

Polymorph C single crystals were obtained by recrystallization of microcrystalline MBZ C from methanol at 15°C. The methanolic solution (20 mg MBZ C in 100 mL) was let to stand in the dark for about 15 days until extremely thin, colorless prismatic crystals suitable for single crystal X-ray analysis were obtained. However, the crystals seem to be twinned by optical microscopy, due to the individual thin plates growing nearly. After the crystal structure solving, this mebendazole C behavior was related to its characteristic crystal packing. The mebendazole polymorph A was prepared from a glacial acetic acid solution according to a recrystallization protocol described in the literature.[3] All used chemicals were of analytical grade. Concerning the X-ray powder diffraction analyses, the used samples, a raw material which is an MBZ form C rich mixture and a polymorph A sample, were obtained from the Instituto Nacional de Controle de Qualidade em Saúde, Fundação Oswaldo Cruz (FIOCRUZ, Manguinhos, Rio de Janeiro, Brazil), and from the Fundação Ezequiel Dias (FUNED, Gameleira, Belo Horizonte, Brazil), respectively. Both MBZ materials are certified as reference standard chemicals by the drug manufacturers. Nevertheless, the X-ray powder diffractograms of these samples were previously compared to that reported in the literature for the different MBZ polymorphs in order to ensure the expected contents.

Single Crystal X-Ray Diffraction Experiment

Recrystallizations of raw mebendazole (MBZ) in methanolic solution yielded a crystalline material, from which a well-shaped clear single crystal was selected for the X-ray diffraction experiment. Intensity data were collected at low temperature (150(2) K) kept by a cryogenic device (Oxford Cryosystem) and with graphite monochromated Mo Kα radiation ($\lambda = 0.71073$ Å), using the *Enraf-Nonius Kappa-CCD* diffractometer. The cell refinements were performed using the software

BNSDOCID: <XP_____55032898A__I_>

UM00017136
NOVARTIS EXHIBIT 1517
Novartis v. Regents, IPR2023-01347
Page 3993 of 4460

Collect[15] and Scalepack,[16] and the final cell parameters were obtained on all reflections. Data for MBZ were measured up to 50.90° in 2θ, totaling 4498 Bragg reflections. Data reduction was carried out using the software Denzo-SMN and Scalepack[15] and XdisplayF for visual representation of data. A negligible absorption coefficient of 0.103 mm^{-1} was observed. Although the International Union of Crystallography (IUCr) states that there is no need of absorption correction if the product μx, where μ is the absorption coefficient value (0.103 mm^{-1}) and x is the medial crystal size (0.10 mm for the measured MBZ crystal, Tab. 1), is below 0.1,[17] trial refinements were employed considering this procedure. However, significant statistical improvements were not obtained and we have preferred to comply with IUCr recommendations, ruling out the absorption correction since the product μx was 0.0103 for the experimented mebendazole C crystal.

The structure was solved using SHELXS-97[18] and refined using SHELXL-97 software.[19] The C, N, and O atoms were clearly solved and full-matrix least-squares refinement of these atoms with anisotropic thermal parameters was carried out. The C–H hydrogen atoms were positioned stereochemically and were refined with fixed individual displacement parameters [$U_{iso}(H) = 1.2U_{eq}(C^2_{sp})$ or $1.5U_{eq}(C^3_{sp})$] using a riding model with aromatic C–H bond length of 0.95 Å and methyl C–H one of 0.98 Å. The amine H atoms were located by difference Fourier analysis and were set as isotropic ($U_{iso}(H) = 1.2U_{eq}(N)$). Wherefore, the positional parameters of these H atoms were not constrained during refinements. An attempt was made to consider the twinning with the ROTAX procedure, which is able to identify possible twin laws using trends in the indices of the poorly agreeing data group wherein the observed structure factor values are quite greater than the calculated ones.[20] The twin orientation matrix and the refined twin ratio (defined as the fractional contribution of each twin component) allowing the structure solving are found to be (1 0 0, 1,−1,0, 1,0,−1) and 0.17, respectively.

Table 1 presents a summary of data and structure refinement that was prepared with WinGX (version 1.70.01).[21] ORTEP-322 and MERCURY23 were also used in order to prepare the crystal data for publication, as well as the MOGUL,[22] a useful program to check the molecular conformation and geometry. This last tool performs substructure searches for chemicals

Table 1. Crystal Data and Structure Refinement for Mebendazole (MBZ)

Empirical formula	$C_{16}H_{13}N_3O_3$
Formula weight	295.29
Temperature (K)	150(2)
Wavelength (Å)	0.71073
Crystal system	Triclinic
Space group	$P-1$
Unit cell dimensions	$a = 5.1480(9)$ Å, $b = 7.8779(15)$ Å, $c = 17.907(3)$ Å, $\alpha = 82.425(6)°$, $\beta = 82.743(7)°$, $\gamma = 71.091(13)°$
Volume (Å^3)	678.3(2)
Z	2
Density (calculated) (Mg/m^3)	1.446
Absorption coefficient (mm^{-1})	0.103
$F(0\,0\,0)$	308
Crystal size (mm)	0.25 × 0.10 × 0.05
θ-Range for data acquisition (°)	4.20–25.45
Index ranges	$-6 \le h \le 5$, $-9 \le k \le 9$, $-21 \le l \le 21$
Reflections collected	4498
Independent reflections	2434 [R(int) = 0.1502]
Completeness to $\theta = 25.45°$	96.7%
Refinement method	Full-matrix least-squares on F^2
Data/restraints/parameters	2434/0/207
Goodness-of-fit on F^2	1.348
Final R for $I > 2\sigma(I)$	$R1 = 0.1325$
R for all data	$wR2 = 0.4089$
Largest diff. peak and hole (e.Å^{-3})	0.281 and −0.373

DOI 10.1002/jps

BNSDOCID: <XP_____55032898A__1_>

UM00017137
NOVARTIS EXHIBIT 1517
Novartis v. Regents, IPR2023-01347
Page 3994 of 4460

deposited at Cambridge Crystallographic Data Centre (CCDC)[23] that are composed of moieties similar to those of the query compound inputted either manually or by another computer software via an instruction-file interface.

The crystallographic information file (CIF) loading the data sets (excluding the structure factors) for MBZ form C has been deposited with the Cambridge Structural Data Base under deposit code CCDC 690724 (copies of these data may be obtained free of charge from The Director, CCDC, 12 Union Road, Cambridge CB2 1EZ, UK, fax: +44-123-336-033; e-mail: deposit@ccdc.cam.ac.uk or http:www.ccdc.cam.ac.uk).

X-Ray Powder Diffraction (XRPD) Matching

The X-ray patterns of the mebendazole raw material, a form C rich mixture of polymorphs A and C, and form A were recorded at room temperature (293 K) on a Rigaku Denki diffractometer using Cu Kα radiation ($\lambda = 1.5418$ Å), 50 kV and 400 mA generator settings, RINT2000 wide angle goniometer and continuous scan mode. The samples were finely ground, mounted on a grooved glass slide employed as sample holder and exposed to the X-ray beam with scan speed 1.000 °/min, sampling width 0.020°, scan axis $\theta - 2\theta$, 2θ range 3–40°. It is key to highlight that polymorphic transformations surely did not occur due to grinding procedure and that significant particle-size effects were not observed in the powder diffraction patterns; the measured diffractograms of a form A sample and raw material are in good agreement with those reported in the literature.[3] Furthermore, there is a need of a simple care not to introduce a preferred orientation of MBZ crystals.[3]

The experimental X-ray powder diffraction (XRPD) patterns of mebendazole raw material and polymorph A were indexed with the data base PDF-2 Release 2006 (International Center for Diffraction Data®-ICDD), entries number 00-039-1606, 00-037-1627, and 00-034-1570 utilizing the program MATCH! a software for phase identification from X-ray powder diffraction data.[24]

The theoretical XRPD peak positions were simulated with MERCURY[25] inputting the MBZ CIF file created after the structure refinement has been finalized. The unit cell parameters from the single crystal structure were slightly adjusted with the use of PowderCell software,[26] in an attempt to avoid bias due to the temperature discrepancy between the experimental powder analysis (room temperature) and single crystal measurements (150 K). Afterwards, the subtly shifted X-ray diffraction peak positions from the crystal structure were then used for comparisons with the experimental X-ray powder diffractograms, which were also performed with PowderCell.[26]

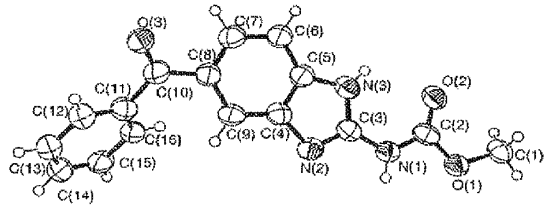


Figure 1. The ORTEP view of MBZ. Ellipsoids represent 50% probability level and an atom labeling scheme is arbitrarily adopted. The hydrogen atoms are shown as spheres of arbitrary radii.

RESULTS AND DISCUSSION

The asymmetric unit of MBZ is depicted in Figure 1, an ORTEP-3 view.[27] Among all the likely taumeric forms illustrated in Figure 2 for MBZ, it was concluded by XRD analysis that tautomer MBZ1 is predominant in the crystalline state. Such specific tautomer plays a decisive role in the crystal packing due to its intermolecular hydrogen bond pattern. As it can be seen in Table 2, where the details of the classical and nonclassical hydrogen-bond contacts in the network of MBZ are presented, and Figure 3 exhibiting the solid-state packing representation of MBZ onto the plane (1 2 3), a strong intermolecular hydrogen bond involving the atoms N(1)–H(1)···N(2) contacts two inversely related molecules in the lattice to form a dimer in which the nitrogen atom of the carbamate moiety is the hydrogen donor and the imine nitrogen one of the benzimidazole group is the acceptor. Into this same plane, the dimers are bonded to each other by a weak nonclassical hydrogen bond involving the atoms C(6)–H(6)···O(2), which gives rise to the infinite one-dimensional chains along the [2,−1,−3] direction (Tab. 2). These chains form stacked plane layers that explain the crystal morphology in aggregated thin plates and the tendency for the lattice twinning. Furthermore, the crystal structure solving and the final R factors of the refinement were just possible if a twinned structure model is taken, as it was described in the Experimental part. The previous

BNSDOCID: <XP_____55032898A__I_>

UM00017138
NOVARTIS EXHIBIT 1517
Novartis v. Regents, IPR2023-01347
Page 3995 of 4460

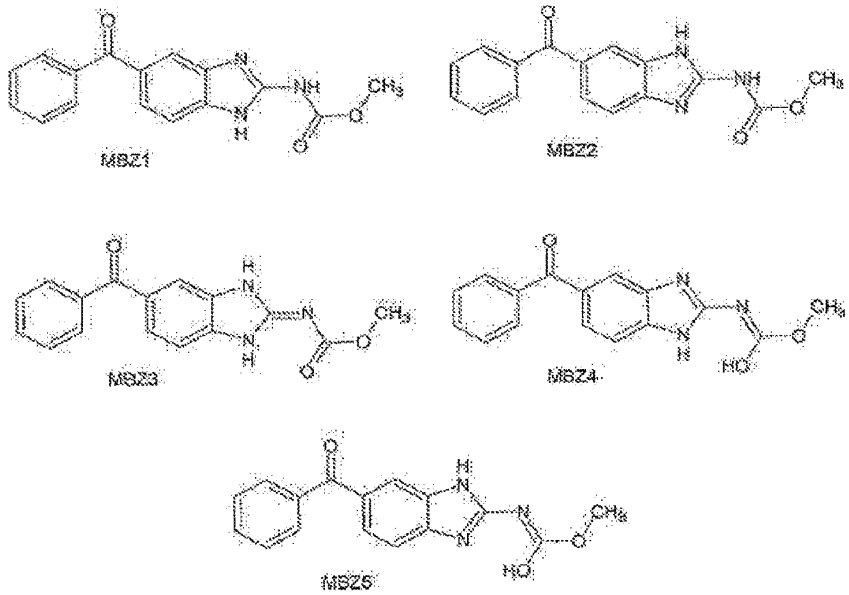


Figure 2. Tautomers of MBZ. The XRD structural determination has proved to be the tautomeric form MBZ1 present in the polymorph C crystal.

contact is shown in Figure 4, together with the nonclassical C(1)–H(1C)···O(3) H-bond connecting the 3.5 Å distanced parallel layers (Fig. 5). Another important interaction between two molecules of adjacent layers is the charge transfer from electron-rich C(6) carbon atom of the benzimidazolyl group to the electronically depleted C(2) one of the carbamate moiety. A key observation provides evidence for this contact and its importance for crystal packing: the geometry of the sp^2-hybridized C(6) carbon atom is partially tetrahedral as result of the intermolecular bond formation between C(2) and C(6), which can be affirmed accounting the marked contraction of the valence angle C(5)–C(6)–C(7) (115.4(7)°). An expected corresponding value for a perfect trigonal geometry is 120(2)°, as it was found by MOGUL analysis of 1160 hits in CSD.

The O(2) oxygen atom also acts as an intramolecular hydrogen acceptor from the amine N(3)–H(3) group present in the benzimidazole core (Tab. 2, Fig. 3). The classical moderate N(3)–H(3)···O(2) hydrogen bond closes a chelating six-membered system composed by O(2)–C(2)–N(1)–C(3)–N(3)–H(3) atoms. The highest deviation from the least-squares plane passing through the six cyclic atoms above mentioned is 0.11(3) Å for H(3) (root mean square deviation (r.m.s.d.) of fitted atoms is 0.0636 Å), showing that such system is appreciably planar. However, since the

Table 2. Hydrogen-Bonding Geometry (Å, °) for MBZ

D–H···A	D–H	H···A	D···A	D–H···A
N(3)–H(3)···O(2)	0.82(9)	2.31(7)	2.720(9)	112(6)
N(1)–H(1)···N(2)[a]	0.81(7)	2.09(7)	2.877(9)	165(6)
C(6)–H(6)···O(2)[b]	0.95	2.51	3.35(1)	147
C(1)–H(1C)···O(3)[c]	0.98	2.70	3.56(1)	147

The symbols "D" and "A" mean hydrogen donor and acceptor, respectively.
[a]Symmetry: $-x, 1-y, -z$.
[b]Symmetry: $2-x, -y, -z$.
[c]Symmetry: $1-x, -y, -z$.

DOI 10.1002/jps

BNSDOCID: <XP_____55032898A__I_>

UM00017139
NOVARTIS EXHIBIT 1517
Novartis v. Regents, IPR2023-01347
Page 3996 of 4460

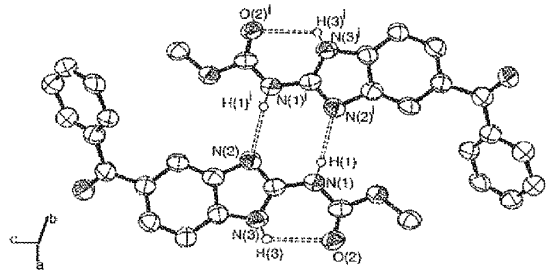


Figure 3. MBZ dimer projected onto the plane (1 2 3) showing the strong intermolecular N(1)–H(1)···N(2) hydrogen bond connecting the molecules, likewise the moderate intramolecular N(3)–H(3)···O(2) interaction can be evidenced. Double dotted lines illustrate the hydrogen bonds. The H-atoms involved in the hydrogen bonds are shown as spheres of arbitrary radii. Symmetry code: (i) $-x$; $1-y$; $-z$.

noncovalent interaction between the amine and carbonyl groups is not strong (N(3)···O(2) separation and the N(3)–H(3)···O(2) angle are 2.720(9) Å and 112(6)°, respectively), a planarity decrease was already expected in a chelating ring wherein an amine sp^3-hybridized nitrogen atom, the N(3), is present. The highest deviation from the least-squares plane fitted on this cycle for H(3) hydrogen atom reveals that the geometry of the nitrogen atom bonded to it, N(3), lies between trigonal-planar and trigonal-pyramidal, distorting slightly the planarity of the intramolecularly hydrogen bonded system. Furthermore, this chelating system is also weakened because the intermolecular C(6)–H(6)···O(2) hydrogen bonding contributes to take the carbonyl O(2) oxygen atom away from the six-membered moiety.

The carbonyl group of the benzoyl moiety is twisted from the benzimidazole plane, which can be noted by looking at the C(7)–C(8)–C(10)–O(3) torsional angle value, 31(1)°, a value that is significantly greater than expected for a perfectly conjugated π-system, about 0°. Similarly, the carbonyl group is noncoplanar with the phenyl ring, since the dihedral angle C(12)–C(11)–C(10)–O(3) measures 27(1)° instead 0°, an approximate value that is required to consider them as coplanar. Strengthening the statement concerning the absence of planarity between the carbonyl bridge and the two cyclic systems bonded to it, the O(3) oxygen atom deviates 0.60(1) and 0.61(1) Å from the least-squares benzimidazole and phenyl planes, respectively. Therefore, there are no resonance effects between the C(10)=O(3) carbonyl and benzimidazolyl groups, likewise this carbonyl motif is not conjugated with the phenyl one. A cause for these interesting conformational features is in the occurrence of the intermolecular C(1)–H(1C)···O(3) hydrogen bonding that bends the O(3) oxygen atom to accept the donated hydrogen by the side chain methyl group of a adjacent molecule packed along the layer overlapping direction [1 2 3]. Indeed, the C(10)=O(3) carbonyl twisting is a consequence of the C(1)–H(1C) hydrogen donor pulling the O(3) oxygen atom to optimize the hydrogen bond orientation.

The determined intramolecular geometry of compound MBZ was analyzed using MOGUL,[22] and all bond angles and distances are in agreement with what is expected for good structural solving and refinement. However, the MOGUL evaluation showed some notable deviations from the expected values for intramolecular bond distances that can be rationalized taking in

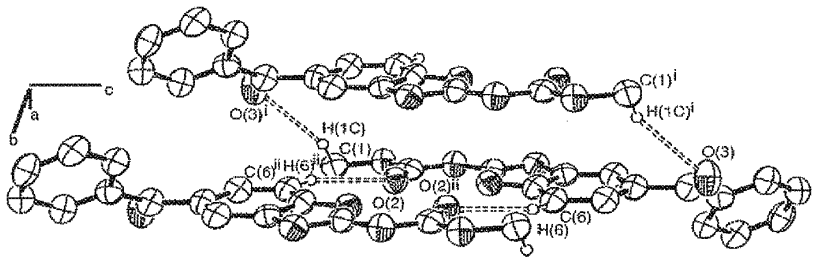


Figure 4. Weak nonclassical hydrogen bonds contributing to MBZ crystal packing along the directions [1 2 3] (symmetry operator: (i) $1-x$; $-y$; $-z$) and [2,−1,−3] (symmetry operator: (ii) $2-x$; $-y$; $-z$). Double dotted lines represent the intermolecular hydrogen bonds. The H-atoms involved in the hydrogen bonds are shown as spheres of arbitrary radii.

BNSDOCID: <XP_____55032898A_1_>

UM00017140
NOVARTIS EXHIBIT 1517
Novartis v. Regents, IPR2023-01347
Page 3997 of 4460

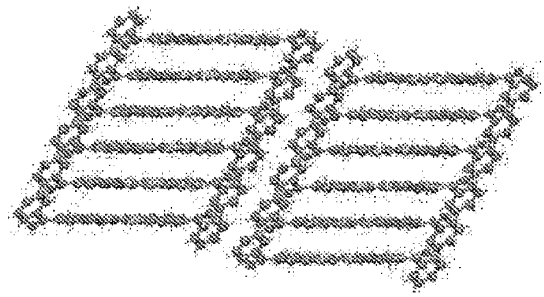


Figure 5. Mebendazole layers separated by 3.5 Å in the polymorph C crystal packing.

account the influence of the intermolecular contacts on the MBZ electronic properties. The N(2) nitrogen atom accepting hydrogen in the strong intermolecular N(1)–H(1)···N(2) interaction has its free electron pair hindered to be donated to the C(4) carbon atom in a resonance path passing through the benzimidazole ring, once these two electrons are directly implicated in the hydrogen acceptance from the amide N(1)–H(1) group. So, the conjugation is decreased through the N(2) nitrogen and carbon atoms bonded to it, C(3) and C(4). The detached double bond character of the N(2)=C(3) binding (1.30(1) Å) and the N(2)–C(4) one (1.42(1) Å) with an enhanced single bond feature have allowed us to get this insight, since the N(2)=C(3) distance is markedly shorter than the average value in query, 1.33(2), and the single bond N(2)–C(4) is longer than the measurement 1.39(2) Å averaged on 1266 MBZ-like compounds returned by MOGUL surveys in the Cambridge Structural Database (CSD).[23] In Figure 6, a MOGUL histogram exhibits the comparison of the N(2)–C(4) single bond distance with equivalent N–C bond lengths of MBZ-like structures deposited in the CSD. In an opposed behavior, the mono-substituted amide N(1) nitrogen has a tendency to conjugate the free electrons since this atom is a hydrogen donor in the N(1)–H(1)···N(2) intermolecular interaction. In this way, a further conjugated system occurs through the carbamate moiety, which was revealed by the double bond feature of the single N(1)–C(2) bond that is shortened in MBZ (1.33(1) Å compared to a MOGUL mean value of 1.37(2) Å).

Regarding the polymorphism of MBZ, at least three true polymorphs are known to exist, that is, crystalline forms A, B, and C.[4,7] In this context, we have analyzed samples of purified form A and polymorph C rich mixture by X-ray powder diffraction (XRPD) at room temperature to

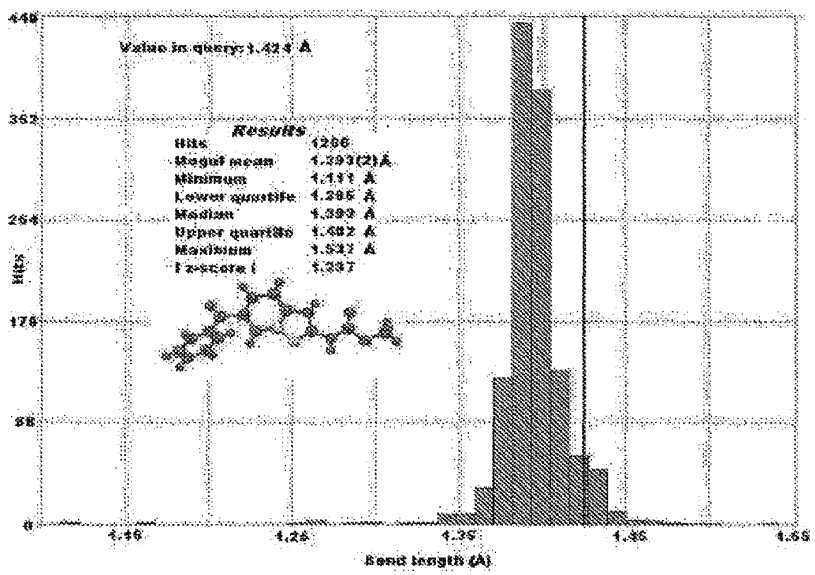


Figure 6. Histogram comparing the N(2)–C(4) bond length of MBZ with the equivalent distances of resembled compounds found in CSD.

 DOI 10.1002/jps

BNSDOCID: <XP_____55032898A__1_>

UM00017141
NOVARTIS EXHIBIT 1517
Novartis v. Regents, IPR2023-01347
Page 3998 of 4460

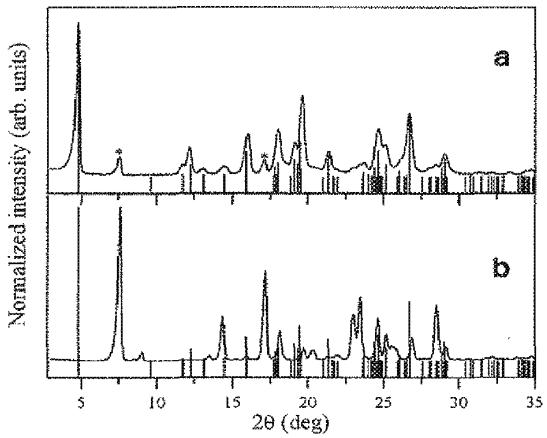


Figure 7. Comparison among the X-ray powder peak positions from MBZ single crystal structure (vertical bars) and diffractograms (full line) of a form C rich mixture containing the mebendazole polymorphs A and C (a) and raw mebendazole polymorph A (b). The asterisks represent the most intense Bragg reflections of phase A that appear in the form C rich mixture.

identify which one was determined using single crystal X-ray diffraction. After the structure refinement end, an MBZ CIF file was then generated. From this file, the theoretical XRPD peak positions were simulated with MERCURY.[23] They were compared with the experimental diffractograms of: (a) a mixture of MBZ forms A and C containing the polymorph C in higher proportion (Fig. 7a), and (b) a pure polymorph A sample (Fig. 7b). All simulated diffraction peaks were overlaid to those of the form C rich mixture diffractogram. Just two Bragg reflections detected in the mixture XRPD profile were absent in the theoretical diffractogram. These diffraction peaks are the most intense ones of phase A (asterisk marked). It is important to emphasize that MBZ crystal transformations do not occur at low temperatures[3] and therefore the calculated XRPD peak positions have been fitted with PowderCell program[26] by adjusting the crystallographic unit cell parameters. With this procedure, peak position discrepancies potentially caused by temperature differences (crystal structure diffractogram is at 150 K and the experimental measurements are at 293 K) are avoided. Concluding, the XRPD profile matching has assigned the MBZ single crystal structure determined here to be the pharmaceutically preferred form C.

CONCLUSIONS

The crystal structure of mebendazole polymorph C was determined for the first time in this work, resulting in a complete characterization of intra- and inter-molecular geometries. In the solid state of mebendazole form C, the featured tautomer shows an intermolecular contact pattern with nonclassical and classical hydrogen bonds, including a strong hydrogen bond involving the amide and imine groups of the carbamate and benzimidazole moieties, respectively. Such intermolecular interaction connects two inversely related molecules to form dimers that are repeated infinitely into layers hydrogen bonded by the methyl group and carbonyl one of the benzoyl portion. Furthermore, the supramolecular assembly noncovalent bonds have influenced the mebendazole C electronic properties and structure conformation. The availability of this full crystallographic analysis let us to go deeper into the vibrational–structural relationship of MBZ C. Additionally, a more reliable assignment of the IR and Raman spectra is currently on progress.

ACKNOWLEDGMENTS

The authors thank CNPq (CNPQ), FAPESP (F.T.M.) and FAPEMIG (P.P.N.) for research fellowships, the CONICET: PID 6246/05 and UNSL (Argentina) for financial support. G.E.N. is member of the CONICET.

REFERENCES

1. Swanepoel E, Liebenberg W, de Villiers MM. 2003. Quality evaluation of generic drugs by dissolution test: Changing the USP dissolution medium to distinguish between active and non-active mebendazole polymorphs. Eur J Pharm Biopharm 55:345–349.
2. Swanepoel E, Liebenberg W, Devarakonda B, de Villiers MM. 2003. Developing a discriminating dissolution test for three mebendazole polymorphs based on solubility differences. Pharmazie 58:117–121.
3. de Villiers MM, Terblanche RJ, Liebenberg W, Swanepoel E, Dekker TG, Song M. 2005. Variable-temperature X-ray powder diffraction analysis of the crystal transformation of the pharmaceutically preferred polymorph C of mebendazole. J Pharm Biomed Anal 38:435–441.

BNSDOCID: <XP_____55032898A__1_>

UM00017142
NOVARTIS EXHIBIT 1517
Novartis v. Regents, IPR2023-01347
Page 3999 of 4460

4. Himmelreich M, Rawson BJ, Watson TR. 1977. Polymorphic forms of mebendazole. Aust J Pharm Sci 6:123–125.
5. Rodriguez-Caabeiro F, Criado-Fornelio A, Jimenez-Gonzalez A, Guzmán L, Igual A, Pérez A, Pujol M. 1987. Experimental chemotherapy and toxicity in mice of three mebendazole polymorphic forms. Chemotherapy 33:266–271.
6. Aboul-Enein HY, Bunaciu AA, Fleschin S. 2002. Analysis of mebendazole polymorphs by Fourier Transform IR spectrometry using chemometric methods. Biopol Biospectrosc 67:56–60.
7. Liebenberg W, Dekker TG, Lotter AP, de Villiers MM. 1998. Identification of Mebendazole polymorphic form present in raw materials and tablets available in South Africa. Drug Dev Ind Pharm 24:485–488.
8. Charoenlarp P, Waikagul J, Muennoo C, Srinophakun S, Kitayaporn D. 1993. Efficacy of single-dose mebendazole, polymorphic forms A and C, in the treatment of hookworm and *Trichuris infections*. Southeast Asian J Trop Med Public Health 24:712–716.
9. Costa J, Fresno M, Guzmán L, Igual A, Oliva J, Vidal P, Pérez A, Pujol M. 1991. Polymorphic forms of mebendazole: Analytical aspects and toxicity. Circ Farm 49:415–424.
10. Evans AC, Fincham JE, Dhansay MA, Liebenberg W. 1999. Anthelmintic efficacy of mebendazole depends on the molecular polymorph. S Afr Med J 89:1118.
11. Ren H, Cheng B, Ma J, Hua D. 1987. Comparative effectiveness of mebendazole with different polymorphic forms against nippostrongylus braziliensis. Yiyao Gongye 18:356–3359.
12. Blaton NM, Peeters OM, De Ranter CJ. 1980. (5-benzoyl-1H-benzimidazol-2-yl)-carbamic acid methyl ester hydrobromide (Mebendazole.HBr), $C_{16}H_{14}BrN_3O_3$. Cryst Struct Comm 9:181–186.
13. Caira MR, Dekker TG, Liebenberg W. 1998. Structure of a 1:1 complex between the anthelmintic drug mebendazole and propionic acid. J Chem Crystallogr 28:11–15.
14. Brusau EV, Camí GE, Narda GE, Cuffini S, Ayala AP, Ellena J. 2008. Synthesis and characterization of a new mebendazole salt: Mebendazole hydrochloride. J Pharm Sci 97:542–552.
15. Enraf-Nonius 1997–2000. COLLECT Nonius BV, Delft, The Netherlands.
16. Otwinowski Z, Minor W. 1997. Processing of X-ray diffraction data collected in oscillation mode. HKL Denzo and Scalepack. Methods in Enzymology 276:307–326. In: Carter CW Jr., Sweet RM, editors. Macromolecular Crystallography, Part A. New York: Academic Press.
17. International Union of Crystallography. 2008. Notes for Authors. Acta Crystallogr. Sect C 64: e2–e9.
18. Sheldrick GM. 1997. SHELXS97 Program for Crystal Structure Resolution, University of Göttingen, Germany.
19. Sheldrick GM. 1997. SHELXL97 Program for Crystal Structures Analysis, University of Göttingen, Germany.
20. Cooper RI, Gould RO, Parsons S, Watkin DJ. 2002. The derivation of non-merohedral twin laws during refinement by analysis of poorly fitting intensity data and the refinement of non-merohedrally twinned crystal structures in the program CRYSTALS. J Appl Crystallogr 35:168–174.
21. Farrugia LJ. 1999. WinGX suite for small-molecule single-crystal crystallography. J Appl Crystallogr 32:837–838.
22. Bruno IJ, Cole JC, Kessler M, Luo J, Motherwell WDS, Purkis LH, Smith BR, Taylor R, Cooper RI, Harris SE, Orpen AG. 2004. Retrieval of crystallographically-derived molecular geometry information. J Chem Inf Comput Sci 44:2133–2144.
23. Allen FH. 2002. The Cambridge Structural Database: A quarter of a million crystal structures and rising. Acta Crystallogr Sect B 58:380–388.
24. Brandenburg K, Putz H. MATCH!, version 1.8, Crystal Impact, Bonn, Germany.
25. Bruno IJ, Cole JC, Edgington PR, Kessler MK, Macrae CF, McCabe P, Pearson J, Taylor R. 2002. New software for searching the Cambridge Structural Database and visualizing crystal structures. Acta Crystallogr Sect B 58:389–397.
26. Kraus W, Nolze G. PowderCell for Windows, version 2.3, Federal Institute for Materials Research and Testing, Berlin, Germany.
27. Farrugia LJ. 1997. ORTEP-3 for Windows—A version of ORTEP-III with a Graphical User Interface (GUI). J Appl Crystallogr 30:565.

BNSDOCID: <XP_____55032898A__1_>

UM00017143
NOVARTIS EXHIBIT 1517
Novartis v. Regents, IPR2023-01347
Page 4000 of 4460

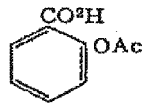
XP009085424

1163. *The Crystal and Molecular Structure of Aspirin.*

By P. J. Wheatley.

The crystal structure of aspirin (acetylsalicylic acid) has been determined by three-dimensional *X*-ray diffraction methods. The crystals are monoclinic, space group $P2_1/c$, with $a = 11{\cdot}446$, $b = 6{\cdot}596$, $c = 11{\cdot}388$ Å, $\beta = 95°\ 33'$. The final parameters were obtained by a least-squares refinement of 2055 intensities collected with a Hilger–Watts linear diffractometer. The eight hydrogen atoms were located from a three-dimensional difference synthesis and included in the refinement. The final *R* factor, including 267 planes of zero intensity, was 10·8%.

The crystal structure of aspirin (I) has not previously been determined, although it is known that a number of attempts have been made.[1] This investigation was undertaken to provide



(I)

adequate structural knowledge which might form a basis for an interpretation of the mode of operation of this remarkable drug.

Experimental.—$C_9H_8O_4$. $M = 180{\cdot}2$. Monoclinic. $a = 11{\cdot}446 \pm 0{\cdot}013$, $b = 6{\cdot}596 \pm 0{\cdot}006$, $c = 11{\cdot}388 \pm 0{\cdot}009$ Å, $\beta = 95°\ 33' \pm 2'$. $U = 855{\cdot}7$ Å^3. $D_m = 1{\cdot}40$. $Z = 4$. $D_c = 1{\cdot}398$. $F(000) = 376$. Space group $P2_1/c$ (C_{2h}^5, No. 14).

Excellent crystals (m. p. 143°) can be obtained from many common organic solvents with [*b*] as the axis of elongation. Those used in the present analysis were grown from benzene. The cell dimensions, obtained from oscillation photographs (Cu-K_α, $\lambda = 1{\cdot}5418$ Å), yield the axial ratio: $a:b:c :: 1{\cdot}7533 : 1 : 1{\cdot}7265$, $\beta = 95°\ 33'$. They may be compared with the optical results of Niini:[2] $a:b:c :: 1{\cdot}7322 : 1 : 1{\cdot}7322$, $\beta = 96°\ 42{\cdot}5'$, and with those of Nitta and Watanabe obtained by *X*-rays:[3] $a = 11{\cdot}37$, $b = 6{\cdot}54$, $c = 11{\cdot}37$ kX, $a:b:c :: 1{\cdot}7385 : 1 : 1{\cdot}7385$, $\beta = 95°\ 27'$.

The intensities were collected round [*b*] with Mo-K_α radiation on a Hilger–Watts linear diffracto-

[1] Private communication from Dr. J. H. Robertson.
[2] R. Niini, *Z. Krist.*, 1931, **79**, 532.
[3] I. Nitta and T. Watanabe, *Sci. Papers Inst. Phys. Chem. Res.* (*Tokyo*), 1937, **31**, 125.

BNSDOCID: <XP_____9085424A__I_>

UM00017144
NOVARTIS EXHIBIT 1517
Novartis v. Regents, IPR2023-01347
Page 4001 of 4460

XP009085424

meter equipped with SrO–ZrO_2 balanced filters.[4] On the *h*0*l*–*h*2*l* layers, each reflexion was measured three times, and on *h*3*l*–*h*9*l* five times, with each filter. The *h*0*l*–*h*5*l* intensities were collected with a 3°, and the *h*6*l*–*h*9*l* with a 4° oscillation angle. About thirty reflexions had to be hand-measured. For these, a 4° oscillation was used. The maximum recording angle was $\theta = 30°$. A half-minute motor was used. The scale of the intensities so obtained was such that, when corrected for Lorentz and polarization factors, the resulting observed structure factors were on a scale slightly greater than absolute. In these circumstances it was felt justified to include all planes with the actual corrected count obtained, except when such a count was negative, in which case the reflexion was allotted zero intensity. In this manner 2055 independent reflexions (excluding 0*k*0) were obtained, of which 267 (13%) were zero. The analysis is based on these 2055 planes, and all values of R and R' include the zero reflexions.

The structure was solved from a sharpened three-dimensional Patterson synthesis. The

TABLE 1.

Final atomic co-ordinates in Å. Standard deviations are given as units in the last place.

Atom	*X*	*Y*	*Z*
O(1)	0·1209 (27)	1·2377 (28)	1·1004 (28)
O(2)	1·3764 (26)	0·9148 (28)	−0·5786 (27)
O(3)	3·2639 (23)	2·7176 (26)	−1·0070 (23)
O(4)	4·6127 (29)	1·4508 (33)	0·3906 (27)
C(1)	1·7513 (31)	2·8796 (34)	0·7679 (33)
C(2)	2·8180 (33)	3·8762 (34)	0·1047 (33)
C(3)	3·4249 (36)	4·5825 (39)	0·4774 (40)
C(4)	2·9845 (39)	5·3062 (40)	1·5338 (43)
C(5)	1·9428 (39)	4·8260 (40)	2·2077 (40)
C(6)	1·3357 (34)	3·6315 (37)	1·8242 (36)
C(7)	1·0279 (32)	1·5944 (34)	0·4241 (33)
C(8)	4·1795 (33)	1·7226 (39)	−0·7189 (36)
C(9)	4·5424 (45)	1·0675 (52)	−1·9791 (42)
H(1)	0·8160 (690)	−0·0133 (794)	−0·9209 (687)
H(3)	4·1336 (446)	4·8674 (491)	0·0168 (447)
H(4)	3·4349 (446)	6·1985 (501)	1·8538 (446)
H(5)	1·6477 (446)	5·3156 (498)	2·9276 (446)
H(6)	0·6357 (444)	3·3448 (494)	2·2671 (443)
H(7)	3·5432 (572)	0·7956 (657)	−2·6885 (574)
H(8)	4·9306 (572)	0·2440 (646)	−1·9332 (573)
H(9)	4·9193 (566)	1·6189 (643)	−2·4623 (573)

TABLE 2.

Thermal parameters in Å². Standard deviations are given as units in the last place.

Atom	U_{11}	U_{22}	U_{33}	$2U_{13}$	$2U_{23}$	$2U_{12}$
O(1)	0·0501 (15)	0·0458 (15)	0·0562 (16)	−0·0372 (25)	−0·0190 (26)	0·0416 (25)
O(2)	0·0465 (14)	0·0480 (15)	0·0518 (15)	−0·0169 (25)	−0·0285 (26)	0·0253 (24)
O(3)	0·0392 (12)	0·0416 (13)	0·0359 (12)	0·0016 (21)	0·0094 (21)	0·0136 (19)
O(4)	0·0589 (17)	0·0729 (21)	0·0413 (14)	0·0562 (32)	0·0125 (29)	0·0040 (25)
C(1)	0·0292 (15)	0·0332 (16)	0·0384 (16)	0·0005 (25)	0·0082 (27)	0·0032 (25)
C(2)	0·0366 (16)	0·0322 (16)	0·0375 (17)	0·0127 (27)	0·0084 (27)	0·0020 (26)
C(3)	0·0398 (18)	0·0394 (19)	0·0547 (22)	−0·0131 (31)	0·0127 (34)	0·0119 (32)
C(4)	0·0471 (20)	0·0380 (19)	0·0609 (24)	−0·0040 (33)	−0·0036 (36)	0·0058 (35)
C(5)	0·0483 (21)	0·0403 (19)	0·0510 (21)	0·0080 (33)	−0·0164 (34)	0·0124 (33)
C(6)	0·0341 (16)	0·0396 (18)	0·0436 (18)	−0·0022 (29)	−0·0030 (30)	0·0128 (28)
C(7)	0·0335 (16)	0·0339 (16)	0·0366 (16)	0·0057 (26)	0·0078 (27)	0·0027 (26)
C(8)	0·0309 (16)	0·0476 (20)	0·0431 (19)	−0·0029 (30)	0·0057 (32)	0·0112 (27)
C(9)	0·0582 (25)	0·0721 (30)	0·0481 (22)	0·0157 (45)	−0·0199 (43)	0·0236 (38)
H(1)	0·12 (6)	0·12 (7)	0·12 (6)	0·0 (1)	0·0 (1)	0·023 (99)
H(3)	0·04 (3)	0·04 (3)	0·04 (3)	0·0 (5)	0·0 (5)	0·008 (50)
H(4)	0·04 (3)	0·04 (3)	0·04 (3)	0·0 (5)	0·0 (5)	0·008 (50)
H(5)	0·04 (3)	0·04 (3)	0·04 (3)	0·0 (5)	0·0 (5)	0·008 (50)
H(6)	0·04 (3)	0·04 (3)	0·04 (3)	0·0 (5)	0·0 (5)	0·008 (50)
H(7)	0·08 (5)	0·08 (5)	0·08 (5)	0·0 (8)	0·0 (8)	0·015 (75)
H(8)	0·08 (5)	0·08 (5)	0·08 (5)	0·0 (8)	0·0 (8)	0·015 (75)
H(9)	0·08 (5)	0·08 (5)	0·08 (5)	0·0 (8)	0·0 (8)	0·015 (75)

[4] U. Arndt and D. C. Phillips, *Acta Cryst.*, 1961, **14**, 807.

BNSDOCID: <XP_____9085424A_I_>

UM00017145

NOVARTIS EXHIBIT 1517
Novartis v. Regents, IPR2023-01347
Page 4002 of 4460

XP009085424

TABLE 3.

h	*k*	*l*	F_o	F_c	Δ	*h*	*k*	*l*	F_o	F_c	Δ	*h*	*k*	*l*	F_o	F_c	Δ
5	0	12	−285	−259	−26	0	0	10	−375	−295	−84	1	1	−2	−1306	−1270	−38
5	0	12	125	66	59	8	0	8	0	11	−11	1	1	−3	2502	2438	64
5	0	10	−753	−721	−32	8	0	6	−469	−490	21	1	1	−4	467	495	−34
5	0	8	−2592	−2585	−7	8	0	4	−1237	−1308	71	1	1	−5	−2371	−2362	11
5	0	6	−597	−627	30	8	0	2	−749	777	−28	1	1	−6	1114	988	126
5	0	4	−324	−141	−183	8	0	0	3109	3003	106	1	1	−7	−2904	−2738	−166
5	0	2	9561	10804	−1243	8	0	−2	2222	2091	131	1	1	−8	185	172	13
5	0	14	249	156	93	8	0	−4	387	362	25	1	1	−9	0	−61	61
5	0	12	−354	−218	−136	8	0	−6	859	842	17	1	1	−10	−110	−153	43
5	0	10	−1096	−1135	39	8	0	−8	0	50	−50	1	1	−11	170	168	2
5	0	8	−2566	−2470	−96	8	0	−10	−318	−88	−230	1	1	−12	−203	−160	−43
5	0	6	−2578	−2519	−59	6	0	−12	0	109	−109	1	1	−13	−191	−118	−73
5	0	4	−319	−297	−22	8	0	−14	−153	−299	146	1	1	−14	225	261	−36
5	0	2	−1661	−1621	−40	9	0	12	−219	−49	−170	1	1	−15	0	49	−49
5	0	0	3917	3828	89	9	0	10	0	68	−68	1	1	14	0	−43	43
5	0	−2	3242	3151	91	9	0	8	977	1035	−58	1	1	13	135	119	16
5	0	−4	−3037	−3164	131	9	0	6	1451	1595	−144	1	1	12	0	65	−65
5	0	−6	−279	−237	−42	9	0	4	1059	1061	−2	1	1	11	174	189	−15
5	0	−8	1921	1991	−70	9	0	2	−1187	−1226	39	1	1	10	114	77	37
5	0	−10	1457	1428	29	9	0	0	−894	−909	15	1	1	9	132	284	−152
5	0	−12	88	204	−116	9	0	−2	554	545	9	1	1	8	−299	−355	56
5	0	−14	−172	−98	−74	9	0	−4	−1033	−1100	67	1	1	7	151	75	76
6	0	12	0	−145	145	9	0	−6	−1545	−1538	−7	1	1	6	530	576	−46
6	0	10	1224	1263	−39	9	0	−8	−403	−392	−11	1	1	5	805	714	91
6	0	8	611	666	−55	9	0	−10	−625	−670	47	1	1	4	−3263	−3120	−143
6	0	6	0	142	−142	10	0	8	0	8	−8	1	1	3	5361	5374	−13
6	0	4	2654	2508	146	10	0	6	398	493	−95	1	1	2	−8846	−9211	365
6	0	2	−6704	−6850	146	10	0	4	1385	−280	105	1	1	1	7444	7653	−209
6	0	0	−4631	−4609	−22	10	0	2	−141	−27	−114	1	1	0	2834	2841	−7
6	0	−2	4023	3913	110	10	0	0	979	1046	−67	1	1	−1	2975	2840	135
6	0	−4	−3897	−3723	−174	10	0	−2	746	965	−19	1	1	−2	2753	2655	98
6	0	−6	−1000	−942	−58	10	0	−4	−114	−70	−44	1	1	−3	−1494	−1510	16
6	0	−8	−1183	−1218	35	10	0	−6	−619	−793	26	1	1	−4	2628	2539	89
6	0	−10	−1940	−1942	2	10	0	−8	−804	−894	10	1	1	−5	−2422	−2257	−165
6	0	−12	−301	−377	76	10	0	−10	−761	−663	−98	1	1	−6	1322	1305	17
6	0	−14	−225	−256	31	11	0	9	−288	−361	73	1	1	−7	−1186	−1367	181
7	0	12	−266	−168	−98	11	0	7	191	−160	−111	1	1	−8	−742	−780	38
7	0	10	325	317	8	11	0	5	0	−32	32	1	1	−9	592	541	49
7	0	8	875	667	208	11	0	3	747	683	64	1	1	−10	813	969	−156
7	0	6	−1883	−1727	−156	11	0	1	628	659	−31	1	1	−11	1264	1294	−30
7	0	4	−3222	−3172	−50	11	0	−1	−437	−411	−26	1	1	−12	777	831	−54
7	0	2	2934	2908	26	11	0	−3	−1026	−1026	0	1	1	−13	429	438	−9
7	0	0	2644	2573	71	11	0	−5	−1177	−1170	−7	1	1	−14	405	353	52
7	0	−2	2671	2566	105	11	0	−7	0	167	−167	1	1	−15	0	150	−150
7	0	−4	−203	−41	−162	11	0	−9	603	599	4	1	1	−16	365	342	23
7	0	−6	−1892	−1834	−58	12	0	8	102	172	−70	1	1	11	−620	−600	−20
7	0	−8	189	178	11	12	0	6	−767	−892	−125	1	1	10	964	933	31
7	0	−10	700	728	−28	12	0	4	1260	1324	−64	1	1	9	−792	−835	43
7	0	−12	646	635	11	12	0	2	129	60	69	1	1	8	1208	1223	−15
7	0	−14	321	202	119	12	0	0	0	93	−93	1	1	7	312	286	26
8	0	12	271	445	−174	12	0	−2	0	−24	24	1	1	6	−515	−569	54
8	0	10	1144	1194	−50	12	0	−4	−677	−812	135	1	1	5	−499	−566	67
8	0	8	1371	1413	−42	12	0	−6	0	−272	272	1	1	4	0	−133	133
8	0	6	−233	−345	112	12	0	−8	632	543	89	1	1	3	554	437	117
8	0	4	−859	−780	−79	13	0	5	−517	−552	35	1	1	2	−5101	−4913	−188
8	0	2	0	−218	218	13	0	3	−362	−348	−14	1	1	1	4017	3970	47
8	0	0	−4148	−4057	−91	13	0	1	−390	−403	13	1	1	0	−8607	−9138	531
8	0	−2	−1731	−1694	−37	13	0	−1	233	250	−17	1	1	−1	−2927	−2884	−43
8	0	−4	−4293	−4058	−235	13	0	−3	1241	1335	−94	1	1	−2	−3931	−3899	−32
8	0	−6	−1822	−1807	−15	13	0	−5	1116	1205	−89	1	1	−3	−3749	−3590	−159
8	0	−8	4096	4185	−89	13	0	−7	0	95	−95	1	1	−4	−2866	−2685	−181
8	0	−10	2862	2759	103	14	0	4	−540	−674	134	1	1	−5	1008	980	28
8	0	−12	640	543	97	14	0	2	177	48	129	1	1	−6	−1084	−1070	−14
8	0	−14	339	229	110	14	0	0	−141	−34	−107	1	1	−7	211	246	−35
9	0	12	156	74	122	14	0	−2	570	610	−40	1	1	−8	492	505	−13
9	0	10	−121	−121	0	14	0	−4	499	316	183	1	1	−9	503	486	17
9	0	8	−653	−724	71	14	0	−6	−422	−448	10	1	1	−10	1459	1461	−2
9	0	6	332	308	24	15	0	3	−495	−617	122	1	1	−11	933	903	30
9	0	4	−1215	−1196	−17	15	0	1	−215	−273	58	1	1	−12	1464	1411	53
9	0	2	−1959	−1885	−104	15	0	−1	−281	−375	94	1	1	−13	235	321	−14
9	0	0	−1114	−1045	−69	15	0	−3	−350	−306	−44	1	1	−14	0	59	−59
9	0	−2	−1051	−996	−55	16	0	2	354	239	115	1	1	−15	0	75	−75
9	0	−4	1896	1780	116	16	0	0	0	−29	29	1	1	−16	386	250	136
9	0	−6	901	820	81	16	0	−2	0	119	−119	2	1	9	198	236	−38
9	0	−8	1114	1115	−1	0	1	15	403	535	−132	2	1	8	997	972	25
9	0	−10	1876	1887	−11	1	1	14	−261	−180	−81	2	1	7	507	446	61
9	0	−12	162	173	−11	1	1	13	−267	−294	27	2	1	6	−769	−696	−73
9	0	−14	−273	−200	−73	1	1	12	−765	−716	−49	2	1	5	−1302	−1160	−142
10	0	12	−334	−277	−57	1	1	11	−530	−502	−28	2	1	4	1080	1005	−75
10	0	10	0	115	−115	1	1	10	−682	−726	44	2	1	3	−4040	−4159	−161
10	0	8	0	114	−114	1	1	9	−1076	−1105	29	2	1	2	−288	−447	159
10	0	6	−1813	−1600	−113	1	1	8	−129	−212	83	2	1	1	−2524	−2899	375
10	0	4	−2459	−2514	55	1	1	7	185	57	128	2	1	0	−77	−134	57
10	0	2	−1605	−1450	−155	1	1	6	267	261	6	2	1	−1	−459	−531	72
10	0	0	−1734	−1784	50	1	1	5	490	538	−48	2	1	−2	2848	2670	178
10	0	−2	−2625	−2719	94	1	1	4	132	84	48	2	1	−3	−1090	−1116	26
10	0	−4	340	536	−196	1	1	3	−2752	−2696	−56	2	1	−4	263	290	−27
10	0	−6	−2358	−2330	−28	1	1	2	−1059	−1069	10	2	1	−5	−1148	−983	−165
10	0	−8	−2262	−2200	−62	1	1	1	4627	4977	−150	2	1	−6	1116	1155	−39
11	0	10	1009	999	10	1	1	0	−3028	−3119	91	2	1	−7	−632	−518	−114
11	0	12	702	720	−18	1	1	−1	0	−80	80	2	1	−8	−662	−705	43
11	0	14	406	413	−7	1	1	−2	0	8	−8	2	1	−9	−1142	−1132	−10
11	0	12	310	355	−45	1	1	−3	−256	−332	76	2	1	−10	−1929	−1930	1
11	0	10	939	956	−17	1	1	−4	−182	−213	31	2	1	−11	−446	−451	5
11	0	8	385	547	−162	1	1	−5	−244	−313	69	2	1	−12	−244	−231	−13
11	0	6	−1325	−1376	51	1	1	−6	687	869	−182	2	1	−13	93	276	−183
11	0	4	−1309	−1300	−9	1	1	−7	−1135	−1037	−98	2	1	−14	−278	−58	−220
11	0	2	404	292	112	1	1	−8	2478	2134	344	3	1	11	850	863	−13
11	0	0	4343	4261	82	1	1	−9	−1295	−1305	10	3	1	10	−677	−723	46
11	0	−2	1695	1775	−116	1	1	−10	2837	2768	69	3	1	9	266	325	−59
11	0	−4	−1308	−1206	−102	1	1	−11	−723	−711	−12	3	1	8	0	−127	127
11	0	−6	−1513	−1491	−22	1	1	−12	−1837	−1991	154	3	1	7	−167	−73	−94
11	0	−8	−1622	−1660	38	1	1	−13	2269	2159	110	3	1	6	−514	−456	−58
11	0	−10	−787	−774	−13	1	1	−14	−7345	−7613	268	3	1	5	−359	−282	−77
12	0	12	193	249	−56	1	1	−15	1573	1650	−77	3	1	4	−3338	−3317	−19
12	0	10	−511	−506	−5	1	1	−16	−2693	−2684	−29	3	1	3	−3157	−3155	−2
12	0	8	523	534	−11	1	1	−17	−1092	−1097	5	3	1	2	−1092	−969	−124

BNSDOCID: <XP_____9085424A__I_>

UM00017146
NOVARTIS EXHIBIT 1517
Novartis v. Regents, IPR2023-01347
Page 4003 of 4460

XP009085424

TABLE 3—*continued.*

h	*k*	*l*	F_o	F_c	Δ
5	1	1	0	54	−54
5	1	0	514	540	−26
5	1	−1	3358	3296	62
5	1	−2	4136	3995	141
5	1	−3	685	584	104
5	1	−4	3274	3158	116
5	1	−5	−505	−362	−143
5	1	−6	−491	−411	−80
5	1	−7	0	−125	125
5	1	−8	−435	−430	−5
5	1	−9	−516	−561	45
5	1	−10	−485	−501	16
5	1	−11	0	40	−40
5	1	−12	0	−67	67
5	1	−13	196	49	147
6	1	−12	285	316	−31
6	1	11	481	502	−101
6	1	10	801	750	11
6	1	9	83	165	−82
6	1	8	875	887	−12
6	1	7	−235	−250	15
6	1	6	1434	1376	58
6	1	5	0	−151	151
6	1	4	516	580	−64
6	1	3	−156	−41	−115
6	1	2	−976	−1020	44
6	1	1	−148	−211	63
6	1	0	−1379	−1389	10
6	1	−1	461	475	−14
6	1	−2	1225	1038	187
6	1	−3	1027	952	75
6	1	−4	0	−193	193
6	1	−5	850	809	41
6	1	−6	−2891	−2952	61
6	1	−7	1802	1758	44
6	1	−8	−1068	−1058	−10
6	1	−9	1498	1436	62
6	1	−10	−322	−246	−76
6	1	−11	0	209	−209
6	1	−12	0	−113	113
6	1	−13	−198	−136	−62
7	1	12	−207	−193	−14
7	1	11	−198	−117	−81
7	1	10	−162	−51	−111
7	1	9	0	−74	74
7	1	8	−574	−581	7
7	1	7	200	143	57
7	1	6	585	582	3
7	1	5	1043	1001	42
7	1	4	1057	1051	6
7	1	3	0	−53	53
7	1	2	1560	1559	1
7	1	1	−1469	−1470	1
7	1	0	2447	2438	9
7	1	−1	−223	−134	−89
7	1	−2	1197	1192	5
7	1	−3	412	377	35
7	1	−4	2313	2292	21
7	1	−5	319	264	55
7	1	−6	180	16	164
7	1	−7	1120	1174	−54
7	1	−8	−2092	−2088	−4
7	1	−9	450	401	49
7	1	−10	−793	−804	11
7	1	−11	−330	−394	58
7	1	−12	−718	−600	−118
7	1	−13	0	25	−25
8	1	10	−219	−316	97
8	1	9	−208	−160	−48
8	1	8	433	338	95
8	1	7	−322	−228	−94
8	1	6	164	257	−93
8	1	5	−291	−370	119
8	1	4	671	651	20
8	1	3	−372	−408	36
8	1	2	203	198	5
8	1	1	−187	−109	−78
8	1	0	0	−182	182
8	1	−1	586	617	−31
8	1	−2	−416	−407	−9
8	1	−3	653	730	−77
8	1	−4	464	456	8
8	1	−5	−835	−909	74
8	1	−6	172	101	71
8	1	−7	−1360	−1348	−12
8	1	−8	−1875	−1935	60
8	1	−9	−151	−215	64
8	1	−10	−242	−316	74
8	1	−11	−135	−97	−38
8	1	−12	0	−16	16
8	1	−13	0	−75	75
9	1	10	174	113	61
9	1	9	0	−11	11
9	1	8	759	817	−58
9	1	7	−689	−656	−33
9	1	6	785	871	−86
9	1	5	−376	−364	−12
9	1	4	391	461	−70
9	1	3	991	1017	−26
9	1	2	−1132	−1175	43
9	1	1	934	882	52
9	1	0	0	−17	17
9	1	−1	516	552	−36
9	1	−2	965	762	203
9	1	−3	72	150	−78
9	1	−4	−132	−237	105
9	1	−5	−1496	−1436	−60
9	1	−6	582	540	42
9	1	−7	−1439	−1448	9
9	1	−8	−174	−54	−120
9	1	−9	0	178	−178
9	1	−10	−162	−253	91
9	1	−11	196	222	−26
10	1	10	−435	−482	47
10	1	9	0	94	−94
10	1	8	−193	−305	112
10	1	7	0	124	−124
10	1	6	−342	−311	−31
10	1	5	376	383	−7
10	1	4	−310	−296	−14
10	1	3	1090	1079	11
10	1	2	0	−11	11
10	1	1	1061	1068	−7
10	1	0	−290	−258	−32
10	1	−1	240	112	128
10	1	−2	564	651	−87
10	1	−3	0	−13	13
10	1	−4	509	523	−14
10	1	−5	325	243	82
10	1	−6	−227	−178	−49
10	1	−7	−281	−382	101
10	1	−8	−156	−140	−16
10	1	−9	0	−111	111
10	1	−10	196	189	7
10	1	−11	227	319	−92
11	1	8	0	−159	159
11	1	7	342	−392	50
11	1	6	0	44	−44
11	1	5	−407	−424	17
11	1	4	407	322	85
11	1	3	−321	−398	77
11	1	2	276	291	−15
11	1	1	0	66	−66
11	1	0	−804	−893	89
11	1	−1	−170	−82	−88
11	1	−2	−118	−164	46
11	1	−3	473	494	−21
11	1	−4	409	343	66
11	1	−5	526	651	−125
11	1	−6	180	78	102
11	1	−7	−360	−316	−44
11	1	−8	213	227	−14
11	1	−9	−407	−365	−42
11	1	−10	0	−178	178
11	1	−11	0	123	−123
12	1	6	0	−167	167
12	1	5	−529	−574	45
12	1	4	−1122	−1217	95
12	1	3	−674	−788	114
12	1	2	−999	−1060	61
12	1	1	−288	−259	−31
12	1	0	−180	−138	−42
12	1	−1	221	145	76
12	1	−2	200	262	−62
12	1	−3	0	−171	171
12	1	−4	1323	1381	−58
12	1	−5	0	−131	131
12	1	−6	1209	1258	−49
12	1	−7	−167	−171	4
12	1	−8	360	325	35
12	1	−9	−423	−323	−100
13	1	8	0	−184	184
13	1	5	229	114	115
13	1	4	−378	−565	187
13	1	3	−357	−163	−34
13	1	2	−648	−679	31
13	1	1	0	−193	193
13	1	0	−164	−5	−159
13	1	−1	−213	−326	113
13	1	−2	358	215	143
13	1	−3	−562	−550	−12
13	1	−4	350	154	196
13	1	−5	0	−60	60
13	1	−6	−346	−289	−57
13	1	−7	353	348	5
14	1	−2	0	−224	224
14	1	−3	0	−225	225
14	1	−4	−225	−205	−20
14	1	−5	0	+71	71
14	1	−6	0	19	−19
14	1	−7	−141	−116	−25
14	1	−8	102	193	−91
0	2	15	−356	−342	−14
0	2	14	−708	−636	−72
0	2	13	−597	−609	12
0	2	12	1203	1209	−6
0	2	11	−518	−589	71
0	2	10	671	−711	−40
0	2	9	450	426	24
0	2	8	1051	1158	−77
0	2	7	1150	1149	1
0	2	6	551	537	14
0	2	5	−283	−245	−38
0	2	4	−848	−822	−26
0	2	3	−1586	−1749	163
0	2	2	−2269	−2284	15
0	2	1	−106	−46	−60
1	2	15	0	132	−132
1	2	14	0	−44	44
1	2	13	0	20	−20
1	2	12	489	510	−21
1	2	11	336	364	−28
1	2	10	0	2	−2
2	2	9	983	1012	−29
2	2	8	−237	−245	8
2	2	7	114	156	−42
2	2	6	1339	1324	15
2	2	5	0	−22	22
2	2	4	1229	1128	101
2	2	3	187	201	−14
2	2	2	2104	2081	23
2	2	1	−2258	−2248	−10
2	2	0	1541	1436	105
2	2	−1	781	822	−41
2	2	−2	−656	−577	−79
2	2	−3	−2359	−2387	28
2	2	−4	630	404	226
2	2	−5	−5702	−5494	−208
2	2	−6	534	533	1
2	2	−7	−1295	−1243	−52
2	2	−8	−617	−560	−57
2	2	−9	261	369	−108
2	2	−10	−1429	−1475	46
2	2	−11	524	539	−15
2	2	−12	−437	−342	−95
3	2	10	859	801	58
3	2	9	286	326	−40
3	2	8	370	264	106
3	2	7	−327	−262	−65
3	2	6	138	156	−18
3	2	5	−294	−260	−34
3	2	4	233	70	163
3	2	3	−634	−679	45
3	2	2	−352	−376	24
3	2	1	720	765	−45
3	2	0	817	756	61
3	2	−1	632	670	−38
3	2	−2	1706	1675	31
3	2	−3	−1942	−1893	−49
3	2	−4	114	162	−48
3	2	−5	−4210	−3811	−399
3	2	−6	−1524	−1459	−65
3	2	−7	−2716	−2535	−181
3	2	−8	−924	−764	−160
3	2	−9	−2766	−2680	−86
4	2	11	97	24	73
4	2	10	586	555	31
4	2	9	0	21	−21
4	2	8	507	521	−14
4	2	7	−110	−103	−7
4	2	6	256	311	−55
4	2	5	322	369	−47
4	2	4	−474	−535	61
4	2	3	227	200	27
4	2	2	−697	−772	75
4	2	1	−215	−215	0
4	2	0	0	1	−1
4	2	−1	0	19	−19
4	2	−2	414	474	−60
4	2	−3	−253	−30	−223
4	2	−4	1641	1641	0
4	2	−5	784	738	46
4	2	−6	1060	1082	−22
4	2	−7	208	307	−99
5	2	6	1993	1963	30
5	2	5	−1956	−1942	−14
5	2	4	2031	1949	82
5	2	3	−2619	−2641	178
5	2	2	−5253	−4796	−457
5	2	1	−5345	−4939	−346
5	2	0	−3292	−3178	−114
5	2	−1	−2892	−2795	−97
5	2	−2	−1020	−997	−23
5	2	−3	6123	5805	318
5	2	−4	−671	−718	153
5	2	−5	3732	3422	310
5	2	−6	−476	−506	30
5	2	−7	−114	−167	53
6	2	5	−716	−610	−106
6	2	4	231	109	122
6	2	3	−603	−563	−20
6	2	2	−288	−218	−70
6	2	1	−776	−821	45
6	2	0	−135	−46	−67
6	2	−1	−167	−256	89
6	2	−2	536	556	−20
6	2	−3	148	124	24
6	2	−4	1021	1024	−3
6	2	−5	−416	−435	19
6	2	−6	151	162	−11
7	2	4	292	222	70
7	2	3	−1926	−1766	−160
7	2	2	4695	4438	257
7	2	1	−3596	−3468	−128
7	2	0	3298	3091	207
7	2	−1	−1542	−1380	−162
7	2	−2	2126	1991	135
7	2	−3	1480	1356	124
7	2	−4	1736	1726	10
7	2	−5	1715	1639	76
8	2	3	1439	1322	117
8	2	2	1591	1378	213
8	2	1	757	774	−17
8	2	0	0	158	−158
8	2	−1	−384	−449	65
8	2	−2	−658	−689	31
8	2	−3	141	109	32
8	2	−4	263	242	21
8	2	−5	−88	−80	−8
9	2	2	339	276	63

BNSDOCID: <XP_____9085424A___I_>

UM00017147
NOVARTIS EXHIBIT 1517
Novartis v. Regents, IPR2023-01347
Page 4004 of 4460

XP009085424

TABLE 3—*continued.*

h	*k*	*l*	F_o	F_c	Δ
5	5	12	−1006	−954	−52
5	5	11	−399	−361	−38
5	5	10	−658	−738	80
5	5	9	−293	−376	83
5	5	8	489	474	15
5	5	7	408	300	108
5	5	6	0	−16	16
5	5	5	−677	−687	10
5	5	4	2970	2682	288
5	5	3	−819	−817	−2
5	5	2	2668	2499	169
5	5	1	1291	1223	68
5	5	0	−2676	−2599	−77
5	5	−1	286	277	9
5	5	−2	−1668	−1688	20
5	5	−3	−169	−143	−26
5	5	−4	−826	−868	42
5	5	−5	1252	1180	82
5	5	−6	444	361	83
5	5	−7	97	15	81
5	5	−8	409	379	30
5	5	−9	240	193	47
5	5	−10	−223	−112	−111
5	5	−11	237	199	38
5	5	−12	208	93	115
6	6	13	−466	−450	−16
6	6	12	−508	−474	−34
6	6	11	−613	−611	−2
6	6	10	−901	−889	−12
6	6	9	−489	−443	−46
6	6	8	0	−79	79
6	6	7	316	348	−32
6	6	6	−500	−420	−80
6	6	5	1540	1512	28
6	6	4	−865	−731	−134
6	6	3	−716	−711	−5
6	6	2	470	424	46
6	6	1	−956	−994	38
6	6	0	−454	−128	−326
6	6	−1	497	495	2
6	6	−2	1326	1145	181
6	6	−3	1152	1146	6
6	6	−4	1222	1222	0
6	6	−5	358	359	−1
6	6	−6	528	466	62
6	6	−7	0	39	−39
6	6	−8	−377	−389	12
6	6	−9	−816	−801	−15
6	6	−10	−1117	−1104	−13
6	6	−11	−593	−646	53
6	6	−12	−687	−598	−89
7	7	13	0	−137	137
7	7	12	102	267	−165
7	7	11	−221	−183	−38
7	7	10	−668	−700	32
7	7	9	−375	−277	−98
7	7	8	−691	−705	14
7	7	7	462	471	−9
7	7	6	−470	−423	−47
7	7	5	−759	−796	37
7	7	4	−1091	−1038	−53
7	7	3	−118	−125	7
7	7	2	1038	891	147
7	7	1	593	556	37
7	7	0	299	61	238
7	7	−1	1465	1363	102
7	7	−2	−58	−81	23
7	7	−3	1026	991	35
7	7	−4	895	902	−7
7	7	−5	566	480	86
7	7	−6	−539	−570	31
7	7	−7	−741	−848	107
7	7	−8	−325	−349	24
7	7	−9	−1314	−1378	64
7	7	−10	153	183	−30
7	7	−11	132	190	−58
7	7	−12	136	61	75
7	7	−13	563	536	27
8	8	10	341	182	159
8	8	9	0	−9	9
8	8	8	0	168	−168
8	8	7	−193	−76	−117
8	8	6	1170	1060	90
8	8	5	−278	−270	−8
8	8	4	1031	1022	9
8	8	3	468	443	25
8	8	2	835	865	−30
8	8	1	739	677	62
8	8	0	−254	−7	−247
8	8	−1	211	251	−40
8	8	−2	−1035	−1088	53
8	8	−3	−387	−339	−48
8	8	−4	785	774	11
8	8	−5	1524	1467	57
8	8	−6	1215	1177	38
8	8	−7	−925	−966	41
8	8	−8	305	260	45
8	8	−9	−279	−219	−60
8	8	−10	0	9	−9
9	9	11	135	103	32
9	9	10	−141	−89	−52
9	9	9	631	562	69
9	9	8	0	−166	166
9	9	7	−278	−223	−55
9	9	6	−454	−511	57
9	9	5	57	57	0
9	9	4	−339	−301	−38
9	9	3	941	991	−50
9	9	2	−1039	−1131	92
9	9	1	422	415	7
9	9	0	−1425	−1340	−85
9	9	−1	−306	−207	−99
9	9	−2	491	444	47
9	9	−3	261	221	40
9	9	−4	251	209	42
9	9	−5	−392	−408	16
9	9	−6	1749	1813	−64
9	9	−7	−804	−726	−78
9	9	−8	2721	2786	−65
9	9	−9	118	25	93
9	9	−10	626	627	−1
9	9	−11	−274	−294	20
10	10	10	0	191	191
10	10	9	−496	−493	−3
10	10	8	0	−30	30
10	10	7	174	109	65
10	10	6	−278	−146	−132
10	10	5	267	275	−8
10	10	4	−205	−146	−59
10	10	3	0	153	−153
10	10	2	−397	−243	−154
10	10	1	−835	−750	−85
10	10	0	−1812	−1736	−76
10	10	−1	−1437	−1389	−48
10	10	−2	−1225	−1208	−17
10	10	−3	−621	−573	−52
10	10	−4	−974	−906	−68
10	10	−5	1010	1092	−82
10	10	−6	−1350	−1424	74
10	10	−7	1115	1150	−35
10	10	−8	0	27	−27
10	10	−9	0	−73	73
10	10	−10	423	394	29
10	10	−11	213	130	83
11	11	9	−205	−45	−160
11	11	8	307	89	218
11	11	7	138	50	88
11	11	6	306	355	−49
11	11	5	−187	−288	101
11	11	4	600	932	−132
11	11	3	−369	−406	37
11	11	2	−304	−345	41
11	11	1	−1100	−1178	78
11	11	0	−983	−979	−4
11	11	−1	−529	−581	52
11	11	−2	−242	−315	73
11	11	−3	483	509	−26
11	11	−4	−960	−816	−144
11	11	−5	283	306	−23
11	11	−6	0	−84	84
11	11	−7	0	−26	26
11	11	−8	385	460	−75
11	11	−9	138	177	−39
12	12	8	0	−247	247
12	12	5	0	−28	28
12	12	4	374	325	49
12	12	3	249	217	32
12	12	2	625	584	41
12	12	1	290	228	62
12	12	0	−341	−399	58
12	12	−1	−221	−221	0
12	12	−2	340	264	76
12	12	−3	−318	−274	−44
12	12	−4	499	525	−26
12	12	−5	421	394	27
12	12	−6	0	44	−44
12	12	−7	392	271	121
12	12	−8	348	296	52
13	13	9	0	60	−60
13	13	4	174	199	−25
13	13	3	0	−18	18
13	13	2	481	473	8
13	13	1	−274	−214	−60
13	13	0	−135	−210	75
13	13	−1	−407	−387	−20
13	13	−2	−271	−329	58
13	13	−3	93	265	−172
13	13	−4	0	−139	139
13	13	−5	474	518	−44
13	13	−6	−415	−434	19
13	13	−7	205	267	−62
14	14	2	−102	−148	46
14	14	1	−97	−39	−58
14	14	0	0	−117	117
14	14	−1	200	217	−17
14	14	−2	−405	−344	−61
14	14	−3	249	290	−41
14	14	−4	0	−77	77
14	14	−5	0	114	−114
15	15	0	0	−30	30
15	15	−1	683	653	30
15	15	−2	−217	−226	9
15	15	−3	530	563	−33
15	15	−4	−348	−273	−75
16	16	0	457	501	−44
16	16	−1	215	149	66
16	16	−2	−710	−715	5
16	16	−3	−633	−559	−74
16	16	−4	135	191	−56
16	16	−5	189	69	120
16	16	−6	1677	1768	−91
16	16	−7	328	288	40
16	16	−8	1539	1600	−61
0	3	1	−4895	−4940	245
1	3	15	0	270	−270
1	3	14	−102	−131	29
1	3	13	294	74	220
1	3	12	−348	−323	−25
1	3	11	83	191	−108
1	3	10	−454	−478	24
1	3	9	466	494	−28
1	3	8	673	842	−31
1	3	7	0	36	−36
1	3	6	1267	1127	140
1	3	5	689	670	10
1	3	4	1761	1735	26
1	3	3	180	171	9
1	3	2	−764	−919	155
1	3	1	−2023	−1938	−85
1	3	0	−2462	−2338	−124
1	3	−1	−2730	−2543	−187
1	3	−2	−727	−679	−48
1	3	−3	−854	−907	53
1	3	−4	501	497	4
1	3	−5	2271	2292	−21
1	3	−6	1181	1200	−19
1	3	−7	1337	1300	37
1	3	−8	225	99	126
1	3	−9	−362	−371	11
1	3	−10	−542	−565	23
1	3	−11	−83	−74	−9
1	3	−12	−182	−24	−158
1	3	−13	−336	−244	−92
1	3	−14	0	−146	146
1	3	−15	−213	−264	51
2	2	12	0	140	−140
2	2	11	−321	−285	−36
2	2	10	385	384	1
2	2	9	0	125	−125
2	2	8	1775	1759	16
2	2	7	559	563	−4
2	2	6	1494	1487	7
2	2	5	−566	−522	−44
2	2	4	−894	−898	4
2	2	3	−263	−297	34
2	2	2	−97	−152	55
2	2	1	72	72	0
2	2	0	−1769	−1648	−121
2	2	−1	−1814	−1671	−143
2	2	−2	−2119	−2069	−50
2	2	−3	1336	1195	141
2	2	−4	−1198	−1173	−25
2	2	−5	2307	2342	−35
2	2	−6	102	115	−13
2	2	−7	1292	1247	45
2	2	−8	121	221	−100
2	2	−9	480	479	1
2	2	−10	−258	−150	−108
2	2	−11	245	218	27
2	2	−12	391	435	−44
2	2	−13	−193	−7	−186
3	3	12	0	101	−101
3	3	11	−339	−326	−13
3	3	10	−823	−768	−55
3	3	9	−704	−645	−59
3	3	8	−1443	−1415	−28
3	3	7	−65	−116	51
3	3	6	−237	−328	91
3	3	5	879	830	49
3	3	4	−313	−307	−6
3	3	3	1086	1120	−34
3	3	2	2887	2627	260
3	3	1	−41	−81	40
3	3	0	4051	3994	57
3	3	−1	994	964	30
3	3	−2	398	442	−44
3	3	−3	1660	1503	157
3	3	−4	1476	−385	−91
3	3	−5	−51	−131	80
3	3	−6	−227	−184	−43
3	3	−7	0	−75	75
3	3	−8	−700	−771	71
3	3	−9	−862	−838	−24
3	3	−10	0	105	−105
3	3	−11	−527	−535	8
3	3	−12	−346	−462	116
3	3	−13	0	−79	−79
4	4	12	−276	−169	−107
4	4	11	−370	−301	−69
4	4	10	−1007	−943	−64
4	4	9	−1583	−1511	−72
4	4	8	−2007	−2006	−1
4	4	7	−888	−909	21
4	4	6	276	279	−3
4	4	5	−393	−358	−35
4	4	4	−1135	−1069	−66
4	4	3	−1223	−1142	−81
4	4	2	−1422	−1395	−27
4	4	1	969	876	93
4	4	0	−41	−25	−16
4	4	−1	−388	−416	28
4	4	−2	−1381	−1320	−61
4	4	−3	674	666	8
4	4	−4	−764	−688	−76
4	4	−5	1932	1907	25
4	4	−6	896	917	−21
4	4	−7	−97	−173	76
4	4	−8	1046	1364	−318
4	4	−9	−973	−1101	128
4	4	−10	679	752	−73

BNSDOCID: <XP_____9085424A__I_>

UM00017148
NOVARTIS EXHIBIT 1517
Novartis v. Regents, IPR2023-01347
Page 4005 of 4460

XP009085424

TABLE 3—*continued.*

h	k	l	F_o	F_c	Δ	h	k	l	F_o	F_c	Δ	h	k	l	F_o	F_c	Δ
4	3	−11	−487	−463	−14	9	3	2	271	259	+18	1	4	6	1458	1539	−91
4	3	−12	−162	−102	−60	9	3	1	189	+166	23	1	4	7	−651	+719	68
4	3	−13	−296	−310	14	9	3	0	−296	−230	−6	1	4	8	567	631	+64
5	3	12	−172	−166	−6	9	3	−10	−1112	−1121	9	2	4	9	338	389	−51
5	3	11	231	116	113	9	3	−2	−1085	−1106	21	2	4	−10	430	505	+75
5	3	10	454	426	65	9	3	−3	−717	−714	−3	2	4	−11	196	76	120
5	3	9	208	41	167	9	3	−4	−335	−159	−136	2	4	−12	625	593	32
5	3	−8	−114	−199	85	9	3	−5	256	325	−69	2	4	−13	−215	−265	46
5	3	−7	132	63	69	9	3	−6	−695	−707	12	3	4	12	0	56	−56
5	3	−6	−174	−66	−108	9	3	−7	148	256	−108	3	4	11	0	50	−50
5	3	5	0	20	−20	9	3	−8	−497	−476	−21	3	4	10	0	−134	134
5	3	4	1002	978	24	9	3	−9	−129	−125	−4	3	4	9	−159	−8	−151
5	3	3	376	373	3	9	3	−10	408	377	31	4	4	8	−581	−627	46
5	3	−2	−883	−884	−99	9	3	−11	−198	−77	−121	4	4	7	−1905	−1901	−4
5	3	−1	−296	−278	−18	10	3	8	130	101	97	4	4	6	−1927	−1985	58
5	3	0	557	539	18	10	3	7	213	116	97	4	4	5	−955	−1035	80
5	3	1	−1916	−1878	238	10	3	6	465	518	−53	4	4	4	−1089	−1100	11
5	3	2	1903	1671	232	10	3	5	−312	−267	−45	4	4	3	1842	1959	−111
5	3	3	−927	−836	−91	10	3	4	231	296	−65	4	4	2	−789	−729	−60
5	3	4	1444	1322	122	10	3	3	225	142	83	4	4	1	596	610	−14
5	3	5	213	225	−10	10	3	2	701	672	29	4	4	0	−180	−114	−66
5	3	6	732	705	27	10	3	1	164	234	−70	4	4	−1	−1354	−1309	−45
5	3	7	0	22	−22	10	3	0	470	503	−33	4	4	−2	1169	1058	131
6	3	−11	−448	−514	66	10	3	−1	0	−31	31	4	4	−3	−1040	−1125	85
6	3	−10	−430	−510	80	10	3	−2	−1760	−1793	33	4	4	−4	256	221	35
6	3	−9	−401	−410	9	10	3	−3	875	797	78	4	4	−5	−374	−358	−16
6	3	−8	−758	−814	56	10	3	−4	−1326	−1393	67	4	4	−6	329	307	22
6	3	−7	−415	−291	−124	10	3	−5	647	629	18	4	4	−7	253	297	−44
6	3	−6	−97	101	−14	10	3	−6	−193	−176	−17	4	4	−8	0	55	−55
6	3	−5	−174	−85	−89	10	3	−7	542	508	34	4	4	−9	302	345	−43
6	3	−4	135	124	11	10	3	−8	0	26	−26	4	4	−10	−310	−274	−36
6	3	−3	0	−45	45	10	3	−9	491	462	29	4	4	−11	−304	−350	46
6	3	−2	196	172	24	10	3	−10	670	615	55	4	4	−12	−191	−134	−57
6	3	−1	−1152	−1145	−7	10	3	−11	−372	−208	−164	4	4	−11	0	−61	61
6	3	0	1097	1074	23	11	3	8	−374	−315	−59	4	4	−10	−743	−751	8
6	3	1	−2876	−2808	−68	11	3	7	−301	−288	−13	4	4	−9	524	589	−65
6	3	2	2812	2738	74	11	3	6	0	43	−43	4	4	−8	−1078	−1148	70
6	3	3	−986	−994	6	11	3	5	0	−73	73	4	4	−7	498	497	1
6	3	4	1368	1368	0	11	3	4	0	49	−49	4	4	−6	−1411	−1442	31
6	3	5	696	565	131	11	3	3	−125	−180	55	4	4	−5	425	465	−40
6	3	6	978	1018	−40	11	3	2	−321	−369	48	4	4	−4	170	69	101
6	3	7	2083	2075	8	11	3	1	0	38	−38	4	4	−3	731	808	−77
6	3	8	1100	1139	−39	11	3	0	260	195	65	4	4	−2	1084	1016	68
6	3	9	3108	3066	42	11	3	−1	0	176	−176	4	4	−1	894	922	−28
6	3	10	−1111	−1023	−88	11	3	−2	−416	−418	2	4	4	0	118	2	116
6	3	11	1002	961	41	11	3	−3	392	377	15	4	4	−1	470	462	8
6	3	−12	−264	−192	−72	11	3	−4	−470	−534	64	4	4	−2	1523	1518	5
6	3	−11	141	101	40	11	3	−5	761	778	−17	4	4	−3	−407	−406	−1
6	3	−10	338	428	−90	11	3	−6	442	478	−36	4	4	−4	615	651	−35
6	3	−9	−177	−42	−135	11	3	−7	400	388	12	4	4	−5	0	258	−258
6	3	−8	−417	−467	50	11	3	−8	193	138	55	4	4	−6	449	512	−63
6	3	−7	−83	−119	36	11	3	−9	0	−3	3	4	4	−7	217	233	−16
6	3	−6	−369	−423	54	12	3	6	287	184	43	4	4	−8	798	836	−38
6	3	−5	0	−16	16	12	3	5	−281	−303	22	4	4	−9	−304	−406	102
6	3	−4	304	135	169	12	3	4	487	480	7	4	4	−10	−375	−378	3
6	3	−3	−93	−49	−44	12	3	3	−132	−215	83	4	4	−11	−256	−322	34
6	3	−2	−331	−454	123	12	3	2	−93	−21	−72	4	4	−12	279	221	58
6	3	−1	121	150	−29	12	3	1	−185	−121	−64	4	4	−11	0	−155	155
6	3	0	0	−161	161	12	3	0	260	345	−85	4	4	−10	88	43	45
6	3	1	−537	−509	−28	12	3	−1	−758	−771	13	4	4	−9	−118	−50	−68
6	3	2	656	685	−29	12	3	−2	520	518	2	4	4	−8	456	463	−7
6	3	3	302	138	164	12	3	−3	−490	−445	−45	4	4	−7	0	−190	190
6	3	4	420	468	−48	12	3	−4	−458	−478	20	4	4	−6	718	717	1
6	3	5	264	272	−8	12	3	−5	445	449	−4	4	4	−5	−1237	−1240	3
6	3	6	−1735	−1730	−5	12	3	−6	−361	−366	5	4	4	−4	−227	−178	−49
6	3	7	−1770	−1719	−51	12	3	−7	−219	−72	−147	4	4	−3	97	106	−9
6	3	8	−619	−640	21	13	3	4	97	56	41	4	4	−2	233	240	−7
6	3	9	−1430	−1443	13	13	3	3	221	238	−17	4	4	−1	780	716	64
6	3	10	235	302	−67	13	3	2	245	149	96	4	4	0	0	−163	163
6	3	11	−1339	−1343	4	13	3	1	167	98	69	4	4	−1	105	101	4
6	3	−12	−748	−703	−45	13	3	0	307	350	−43	4	4	−2	240	259	−19
6	3	−11	−167	−79	−88	13	3	−1	0	12	−12	4	4	−3	979	987	−8
6	3	−10	574	612	−38	13	3	−2	836	811	25	4	4	−4	1096	1135	−39
6	3	−9	1083	1101	−18	13	3	−3	−526	−496	−30	4	4	−5	138	106	32
6	3	−8	838	827	11	13	3	−4	260	304	−44	4	4	−6	451	425	26
6	3	−7	471	488	−17	13	3	−5	−263	−159	−104	4	4	−7	−65	−125	60
6	3	−6	0	219	−219	13	3	−6	−296	−185	−111	4	4	−8	321	349	−28
6	3	−5	138	117	21	13	3	−7	−207	−206	−1	4	4	−9	447	442	5
6	3	−4	93	44	49	14	3	3	375	406	−31	4	4	−10	146	132	14
6	3	−3	798	809	−11	14	3	2	−114	−35	−79	4	4	−11	153	239	−86
6	3	−2	−657	−672	15	14	3	1	0	−51	51	4	4	−12	245	57	188
6	3	−1	675	704	−29	14	3	0	0	−66	66	4	4	−11	0	50	−50
6	3	0	159	0	159	14	3	−1	367	361	6	4	4	−10	0	37	−37
6	3	1	0	119	−119	14	3	−2	989	1039	−50	4	4	−9	−286	−227	−59
6	3	2	362	379	−17	15	3	1	1913	2065	−152	4	4	−8	−377	−428	51
6	3	3	−312	−238	−74	15	3	−1	1307	1408	−101	4	4	−7	−356	−406	50
6	3	4	−2067	−2019	−48	16	3	0	878	946	−68	4	4	−6	645	672	−27
6	3	5	−1950	−1997	47	16	3	−1	970	985	−15	4	4	−5	0	−119	119
6	3	6	−2000	−2137	137	17	3	0	−467	−520	53	4	4	−4	678	658	20
6	3	7	−852	−855	3	17	3	−1	−132	−207	75	4	4	−3	1247	1232	15
6	3	8	−872	−508	−36	18	3	0	281	286	−5	4	4	−2	561	580	−19
6	3	9	895	973	−78	18	3	−1	0	121	−121	4	4	−1	518	577	−59
6	3	10	−460	−430	−30	19	3	0	−1081	−1108	27	4	4	0	1052	1097	−45
6	3	11	427	457	−30	19	3	−1	−381	−404	23	4	4	−1	−1549	−1613	64
6	3	−12	233	441	−208	20	3	1	−2204	−2296	92	4	4	−2	876	810	66
6	3	−11	437	467	−30	21	3	0	−354	−433	79	4	4	−3	−1565	−1622	57
6	3	−10	0	175	−175	21	3	−1	−312	−358	45	4	4	−4	962	1015	−53
6	3	−9	207	53	154	22	3	0	−785	−836	51	4	4	−5	−435	−337	−98
6	3	−8	−93	−56	−37	22	3	−1	1638	1788	−151	4	4	−6	−569	−601	32
6	3	−7	177	142	35	23	3	0	−3103	−3038	−65	4	4	−7	570	726	−156
6	3	−6	0	68	−68	23	3	−1	2473	2539	−66	4	4	−8	−172	−227	55
6	3	−5	316	253	63	24	3	0	−254	−274	20	4	4	−9	443	521	−78
6	3	−4	−231	−672	441	25	3	−1	1373	1289	84	4	4	−10	274	373	−99
6	3	−3	174	225	−51	26	3	0	633	648	−15	4	4	−11	342	359	−17
6	3	−2	208	98	110	27	3	−1	434	480	−34	4	4	−10	0	−25	25
6	3	−1	−483	−420	−63	28	3	0	121	139	−18	4	4	−9	−177	−228	51
6	3	0	254	417	−163	29	3	−1	−151	−217	26	6	4	6	−427	−508	81

BNSDOCID: <XP_____9085424A__1_>

UM00017149
NOVARTIS EXHIBIT 1517
Novartis v. Regents, IPR2023-01347
Page 4006 of 4460

XP009085424

TABLE 3—*continued*.

h	*k*	*l*	F_o	F_c	Δ	*h*	*k*	*l*	F_o	F_c	Δ	*h*	*k*	*l*	F_o	F_c	Δ
6	4	7	745	754	−9	11	4	−2	328	351	−23	3	5	−10	189	187	2
6	4	6	−106	−102	−4	11	4	−3	461	488	−27	3	5	−11	487	614	−127
6	4	5	422	474	−52	11	4	−4	310	251	59	4	5	10	153	29	124
6	4	4	321	368	−47	11	4	−5	0	−66	66	4	5	9	170	54	116
6	4	3	249	274	−25	11	4	−6	0	−31	31	4	5	8	240	238	2
6	4	2	−180	−135	−45	11	4	−7	0	−45	45	4	5	−7	−364	−356	−8
6	4	1	861	901	−20	12	4	4	294	337	−43	4	5	−8	302	343	−41
6	4	0	−567	−603	35	12	4	3	191	215	−24	4	5	−9	−1562	−537	−1025
6	4	−1	−1873	−1556	83	12	4	2	456	450	6	4	5	−10	599	573	1134
6	4	−2	−2323	−2471	148	12	4	1	0	−118	118	4	5	−11	319	311	8
6	4	−3	−2122	−2242	120	12	4	0	729	783	−54	4	5	−12	621	706	−85
6	4	−4	−2258	−2292	34	12	4	−1	−618	−706	88	4	5	−13	310	290	20
6	4	−5	641	670	−29	12	4	−2	436	436	0	4	5	−14	−245	−206	−39
6	4	−6	−500	−928	28	12	4	−3	−187	−257	70	4	5	−15	182	282	−100
6	4	−7	1094	1173	−79	12	4	−4	327	252	75	4	5	−16	−276	−288	12
6	4	−8	−426	−530	104	12	4	−5	0	−281	281	4	5	−17	−1756	−1093	−57
6	4	−9	536	625	−89	12	4	−6	135	137	−2	4	5	−18	−1265	−1172	−87
6	4	−10	307	383	−76	12	4	−7	0	−57	57	4	5	−19	−1826	−1928	102
6	4	−11	207	267	−60	13	4	2	0	−92	92	4	5	−20	−862	−914	52
7	4	10	237	383	−146	13	4	1	397	412	−15	4	5	−21	−428	−470	42
7	4	9	−207	−48	−159	13	4	0	170	237	−67	4	5	−22	−72	117	−185
7	4	8	806	836	−30	13	4	−1	−449	−514	65	4	5	−23	138	123	15
7	4	7	281	277	4	13	4	−2	310	433	−123	4	5	−24	−148	−227	79
7	4	6	754	793	−39	13	4	−3	−617	−721	104	4	5	−25	273	175	98
7	4	5	279	241	38	0	5	13	138	76	62	5	5	10	346	304	42
7	4	4	582	693	−111	0	5	12	0	152	−152	5	5	9	−263	−253	−10
7	4	3	−321	−389	68	0	5	11	153	206	−53	5	5	8	−1114	−1229	115
7	4	2	−302	−161	−141	0	5	10	−187	−275	88	5	5	−7	325	188	137
7	4	1	522	541	−19	0	5	9	0	113	−113	5	5	−8	0	−36	36
7	4	0	−836	−825	−11	0	5	8	−592	−623	31	5	5	−9	874	923	−49
7	4	−1	606	621	−15	0	5	7	−273	−308	35	5	5	−10	651	685	−34
7	4	−2	−1469	−1434	25	0	5	6	−844	−926	82	5	5	−11	600	870	−270
7	4	−3	−884	−931	47	0	5	5	−1570	−1694	124	5	5	−12	421	518	−97
7	4	−4	−876	−886	10	0	5	4	−1153	−1317	164	5	5	−13	366	365	1
7	4	−5	−810	−825	15	0	5	3	−857	−1008	151	5	5	−14	−170	−118	−52
7	4	−6	0	−77	77	0	5	2	145	111	34	5	5	−15	646	683	−37
7	4	−7	0	142	−142	0	5	1	729	871	−142	5	5	−16	469	460	9
7	4	−8	−276	−485	209	1	5	13	398	399	−1	5	5	−17	0	45	−45
7	4	−9	172	161	−9	1	5	12	382	401	−19	5	5	−18	−867	−898	31
7	4	−10	−129	−185	56	1	5	11	238	212	26	5	5	−19	−551	−576	25
7	4	−11	0	−144	144	1	5	10	118	186	−68	5	5	−20	−1192	−1223	31
8	4	10	302	380	−78	1	5	9	−359	−477	118	5	5	−21	−307	−294	−13
8	4	9	−520	−587	67	1	5	8	0	185	−185	5	5	−22	0	84	−84
8	4	8	358	520	−162	1	5	7	−238	−234	−4	5	5	−23	−205	−169	−116
8	4	7	−635	−580	145	1	5	6	312	335	−23	5	5	−24	279	252	27
8	4	6	63	10	73	1	5	5	−411	−418	7	5	5	−25	0	−81	81
8	4	5	231	147	84	1	5	4	−1435	−1516	81	6	6	10	478	515	−37
8	4	4	0	80	−80	1	5	3	0	78	−78	6	6	9	364	329	35
8	4	3	187	129	58	1	5	2	−894	−916	22	6	6	8	442	421	21
8	4	2	0	−135	135	1	5	1	412	468	−56	6	6	−7	0	55	−55
8	4	1	823	844	−21	1	5	0	41	75	−34	6	6	−8	260	263	−3
8	4	0	0	75	−75	1	5	−1	72	105	−33	6	6	−9	578	622	−43
8	4	−1	1715	1737	−22	1	5	−2	−919	−1091	172	6	6	−10	0	−64	64
8	4	−2	−756	−758	2	1	5	−3	0	−70	70	6	6	−11	−271	−257	−14
8	4	−3	−180	−273	93	1	5	−4	1369	1508	−139	6	6	−12	225	330	−105
8	4	−4	0	−151	151	1	5	−5	−953	−1095	142	6	6	−13	−276	−271	−5
8	4	−5	−633	−702	69	1	5	−6	1636	1743	−107	6	6	−14	−249	−181	−68
8	4	−6	198	81	115	1	5	−7	−235	−179	−56	6	6	−15	151	226	−75
8	4	−7	−114	−14	−100	1	5	−8	102	82	20	6	6	−16	−582	−570	−12
8	4	−8	172	170	2	1	5	−9	488	588	−100	6	6	−17	1189	1230	−41
8	4	−9	0	143	−143	1	5	−10	205	181	24	6	6	−18	−665	−649	−16
8	4	−10	−231	−89	−142	1	5	−11	−153	−110	−43	6	6	−19	299	266	33
8	4	−11	0	176	−176	1	5	−12	0	−217	217	6	6	−20	−514	−616	102
9	4	9	235	202	33	1	5	−13	−263	−195	−68	6	6	−21	0	−72	72
9	4	8	−849	−910	61	1	5	−14	−348	−301	−47	6	6	−22	−138	−50	−88
9	4	7	−310	−305	−5	1	5	−15	0	−143	143	6	6	−23	170	92	78
9	4	6	−613	−838	225	2	5	9	162	163	−1	6	6	−24	325	303	22
9	4	5	302	385	−83	2	5	8	−511	−551	40	6	6	−25	391	347	44
9	4	4	0	99	−99	2	5	7	97	91	6	7	7	8	88	38	50
9	4	3	517	505	12	2	5	6	−513	−552	39	7	7	−7	121	97	24
9	4	2	−633	−581	−52	2	5	5	594	514	80	7	7	−8	−515	−555	40
9	4	1	−132	−176	44	2	5	4	−217	−285	68	7	7	−9	−518	−570	52
9	4	0	−472	−540	68	2	5	3	443	413	30	7	7	−10	−479	−512	33
9	4	−1	−510	−518	8	2	5	2	0	−63	63	7	7	−11	0	−89	89
9	4	−2	0	−215	215	2	5	1	510	625	−115	7	7	−12	−57	−164	67
9	4	−3	−795	−876	81	2	5	0	1160	1209	−49	7	7	−13	805	900	−95
9	4	−4	−77	−122	45	2	5	−1	874	916	−42	7	7	−14	−254	−214	−40
9	4	−5	−376	−366	−10	2	5	−2	276	332	−56	7	7	−15	244	314	−70
9	4	−6	428	442	−14	2	5	−3	1393	1552	−159	7	7	−16	0	−73	73
9	4	−7	285	266	19	2	5	−4	−114	−78	−36	7	7	−17	−562	−564	2
9	4	−8	420	485	−65	2	5	−5	997	1130	−133	7	7	−18	716	733	−17
9	4	−9	−245	−294	49	2	5	−6	532	574	−42	7	7	−19	−927	−1011	84
9	4	−10	193	93	100	2	5	−7	0	44	−44	7	7	−20	205	81	124
9	4	−11	−162	−247	85	2	5	−8	−148	−119	−29	7	7	−21	−552	−615	63
10	4	10	0	−121	121	2	5	−9	0	69	−69	7	7	−22	118	143	−25
10	4	9	−331	−298	−33	2	5	−10	0	−164	164	7	7	−23	−177	−36	−141
10	4	8	191	171	20	2	5	−11	0	−6	6	8	8	7	167	274	−107
10	4	7	118	118	0	3	5	10	−196	−117	−79	8	8	−7	−125	−133	8
10	4	6	−276	−260	−16	3	5	9	332	285	47	8	8	−8	211	223	−12
10	4	5	−298	−259	−39	3	5	8	−398	−344	−54	8	8	−9	−203	−264	61
10	4	4	164	12	152	3	5	7	−512	−567	55	8	8	−10	211	191	20
10	4	3	−141	−64	−77	3	5	6	397	458	−61	8	8	−11	−469	−455	−14
10	4	2	0	8	−8	3	5	5	−1493	−1597	104	8	8	−12	151	89	62
10	4	1	370	450	−80	3	5	4	832	796	36	8	8	−13	316	342	−26
10	4	0	−425	−363	−62	3	5	3	−1395	−1499	104	8	8	−14	0	78	−78
10	4	−1	0	146	−146	3	5	2	−182	−243	61	8	8	−15	102	30	72
10	4	−2	92	92	0	3	5	1	567	545	22	8	8	−16	−233	−325	92
10	4	−3	229	285	−56	3	5	0	177	182	−5	8	8	−17	−425	−524	99
10	4	−4	−435	−331	−104	3	5	−1	794	831	−37	8	8	−18	0	−30	30
10	4	−5	0	183	−183	3	5	−2	−1280	−1375	95	8	8	−19	−354	−535	181
11	4	9	−135	−203	74	3	5	−3	532	566	−34	8	8	−20	306	375	−69
11	4	8	−206	−120	−86	3	5	−4	−2562	−2738	176	8	8	−21	−223	−260	37
11	4	7	0	94	−94	3	5	−5	854	916	−62	8	8	−22	−215	−192	−23
11	4	6	88	24	64	3	5	−6	−182	−141	−41	9	9	6	293	255	37
11	4	5	562	531	31	3	5	−7	253	262	−9	9	9	5	0	−36	36
11	4	4	591	533	58	3	5	−8	148	243	−95	9	9	4	0	−42	42
11	4	−1	412	461	−49	3	5	−9	527	577	−50	9	9	4	−83	−13	−70

BNSDOCID: <XP_____9085424A__I_>

UM00017150
NOVARTIS EXHIBIT 1517
Novartis v. Regents, IPR2023-01347
Page 4007 of 4460

XP009085424

TABLE 3—*continued.*

h	k	l	F_o	F_c	Δ	h	k	l	F_o	F_c	Δ	h	k	l	F_o	F_c	Δ
0	0	3	627	−635	62	3	6	−5	565	516	41	10	6	2	−210	−28	−182
0	0	2	485	465	20	3	6	−6	−184	−151	−33	10	6	1	−296	−254	−42
0	0	1	−745	−771	26	3	6	−7	−578	−603	25	10	6	0	0	−39	39
0	0	0	335	444	−109	3	6	−8	−516	−519	3	10	6	−1	430	368	62
1	0	4	0	84	−84	4	6	−9	0	−174	174	10	6	−2	−166	−218	52
1	0	3	329	381	−52	4	6	10	383	197	186	10	6	−3	908	840	68
1	0	2	389	374	15	4	6	9	609	504	105	10	6	−4	−323	−372	49
1	0	1	603	655	−52	4	6	8	459	386	73	10	6	−5	332	313	19
1	0	0	141	178	−37	4	6	−7	565	542	23	0	7	10	259	357	−98
2	0	5	557	637	−80	4	6	6	100	103	−3	0	7	9	−566	−607	41
2	0	4	−177	−161	−16	4	6	5	−91	−50	−41	0	7	8	801	828	−27
2	0	3	68	107	−39	4	6	4	123	52	71	0	7	7	2742	2810	68
2	0	2	−132	−49	−83	4	6	3	0	−163	163	0	7	6	180	198	−18
2	0	1	573	592	−19	4	6	2	−219	−69	−150	0	7	5	−286	−304	18
2	0	0	0	59	−59	4	6	1	277	208	69	0	7	4	−219	−269	50
3	0	4	0	−349	349	4	6	0	1144	1077	67	0	7	3	−244	−313	69
3	0	3	0	110	−110	4	6	−1	−915	−822	−93	0	7	2	−81	−89	8
3	0	2	457	267	190	4	6	−2	1586	1484	102	0	7	1	274	448	−174
3	0	1	370	280	90	4	6	−3	−582	−424	−158	1	7	10	−116	−187	71
3	0	0	590	651	−61	4	6	−4	430	442	−12	1	7	9	197	40	157
4	0	5	453	563	−110	4	6	−5	469	470	−1	1	7	8	407	373	34
4	0	4	476	457	19	4	6	−6	321	325	−4	1	7	7	−174	−110	−64
4	0	3	281	302	−21	4	6	−7	−495	−485	−10	1	7	6	160	150	10
4	0	2	0	140	−140	4	6	−8	−153	−156	3	1	7	5	166	212	−46
4	0	1	0	178	−178	4	6	−9	−283	−249	−34	1	7	4	0	77	−77
4	0	0	125	95	30	5	6	9	396	317	79	1	7	3	433	377	56
5	0	7	0	−221	221	5	6	−7	838	714	124	1	7	2	586	563	23
5	0	6	0	−165	165	5	6	6	0	56	−56	1	7	1	244	256	−12
5	0	5	159	240	−81	5	6	5	0	217	−217	1	7	0	531	949	−418
5	0	4	377	407	−30	6	6	4	−367	−282	−85	1	7	−1	108	114	−6
5	0	3	469	432	37	6	6	3	−848	−790	−58	1	7	−2	−735	−793	54
5	0	2	507	558	−51	6	6	2	−602	−506	−96	1	7	−3	−370	−403	33
5	0	1	217	253	−36	6	6	1	−605	−503	−102	1	7	−4	−100	−43	−57
5	0	0	−125	−149	64	6	6	0	476	465	14	1	7	−5	0	41	−41
6	0	3	−298	−271	−27	6	6	−1	−459	−404	−55	1	7	−6	−180	−99	−81
6	0	2	−376	−507	131	6	6	−2	−742	−711	−31	1	7	−7	0	−2	2
6	0	1	−371	−354	−17	6	6	−3	−791	−769	−22	1	7	−8	−261	−97	−164
6	0	0	187	245	−58	6	6	−4	−403	−399	−4	1	7	−9	−397	−753	144
7	0	3	283	293	−10	6	6	−5	−191	−45	−146	2	7	8	0	87	−87
7	0	2	315	408	−93	6	6	−6	−197	−182	−15	2	7	7	631	575	56
7	0	1	211	46	165	6	6	−7	237	−149	−88	2	7	6	781	691	90
7	0	0	267	253	14	6	6	−8	0	−59	59	2	7	5	490	475	15
8	0	3	−299	−273	−26	6	6	−9	0	−134	134	2	7	4	193	67	126
8	0	2	845	−793	−52	7	6	8	0	−91	91	2	7	3	−237	−176	−61
8	0	1	−1083	−998	−85	7	6	7	512	456	56	2	7	2	−252	−244	−8
8	0	0	672	609	63	7	6	6	−460	−471	11	2	7	1	−741	−712	−29
9	0	3	−835	−790	−45	7	6	5	438	411	27	2	7	0	−108	−149	42
9	0	2	100	66	34	7	6	4	−352	−361	9	2	7	−1	237	235	2
9	0	1	−692	−611	−81	7	6	3	306	−227	−79	2	7	−2	0	−6	6
10	0	2	−203	−206	3	7	6	2	0	−43	−43	2	7	−3	91	123	−32
10	0	1	452	−631	179	8	6	1	−445	−378	−127	2	7	−4	254	222	32
10	0	0	0	−3	3	8	6	0	−449	−282	−167	2	7	−5	0	156	−156
0	1	9	−108	−56	−52	8	6	−1	256	241	15	2	7	−6	277	260	17
0	1	8	383	402	−19	8	6	−2	326	340	−14	2	7	−7	613	698	−85
0	1	7	0	−131	131	8	6	−3	−346	−321	−25	2	7	−8	0	246	−246
0	1	6	−123	−191	68	8	6	−4	233	256	−23	2	7	−9	−197	−33	−164
0	1	5	−379	−407	28	8	6	−5	−244	−251	7	3	7	8	−277	−58	−219
0	1	4	−885	−817	−68	9	6	−6	0	−132	132	3	7	7	615	577	38
0	1	3	−332	−318	−14	9	6	−7	−153	−212	59	3	7	6	410	354	56
0	1	2	148	115	33	9	6	−8	197	246	−49	3	7	5	479	430	49
0	1	1	−1269	−617	−652	9	6	−9	−386	−350	−36	3	7	4	−81	−5	−76
0	1	0	0	45	−45	10	6	8	−312	−115	−197	3	7	3	−71	168	−237
1	1	9	309	301	8	10	6	−7	116	33	83	3	7	2	−259	−228	−31
1	1	8	410	438	−28	10	6	6	−309	−27	−282	3	7	1	−493	−463	−30
1	1	7	0	−1	1	10	6	5	108	104	4	3	7	0	−108	−172	64
1	1	6	227	242	−15	10	6	4	0	−177	177	3	7	−1	−229	162	−67
1	1	5	−958	−882	−76	10	6	3	292	160	132	3	7	−2	269	262	7
1	1	4	−1075	−1029	−46	10	6	2	−170	−152	−18	3	7	−3	0	146	−146
1	1	3	−136	−143	7	10	6	1	0	−45	45	3	7	−4	539	537	2
1	1	2	−100	−145	45	10	6	0	0	−61	61	3	7	−5	−566	−526	−40
1	1	1	−108	−221	113	0	7	11	214	168	46	3	7	−6	−189	−210	21
1	1	0	339	339	0	0	7	10	319	265	74	3	7	−7	−247	−197	−50
2	1	9	116	33	83	0	7	9	280	262	18	3	7	−8	−410	−464	54
2	1	8	−160	−35	−125	0	7	8	310	329	−19	3	7	−9	0	1	−1
2	1	7	−359	−357	−2	0	7	7	426	251	175	4	7	8	−233	−111	−122
2	1	6	0	54	−54	0	7	6	252	177	115	4	7	7	0	−69	69
2	1	5	0	−112	112	0	7	5	449	374	75	4	7	6	292	211	81
2	1	4	0	−73	−73	0	7	4	241	200	41	4	7	5	0	33	−33
2	1	3	280	101	179	0	7	3	219	37	182	4	7	4	203	139	64
2	1	2	510	450	60	0	7	2	493	346	147	4	7	3	329	262	67
2	1	1	547	494	53	0	7	1	−203	−264	61	4	7	2	0	20	−20
2	1	0	214	178	36	1	7	10	−260	−229	−31	4	7	1	−543	−484	−59
3	1	9	227	236	−9	1	7	9	−533	−473	−60	4	7	0	−758	−734	−24
3	1	8	997	915	82	1	7	8	0	−65	65	4	7	−1	−1051	−989	−62
3	1	7	−1487	−1319	−168	1	7	7	−100	−260	160	5	7	7	352	379	−27
3	1	6	1662	1541	121	1	7	6	605	489	116	5	7	6	0	−57	57
3	1	5	−1925	−1785	−140	2	7	11	254	90	164	5	7	5	−81	−43	−38
3	1	4	−492	−539	47	2	7	10	333	370	−37	5	7	4	−207	−222	15
3	1	3	−1606	−1521	−85	2	7	9	194	129	64	5	7	3	0	−111	111
3	1	2	−625	−504	−121	2	7	8	569	459	110	5	7	2	180	47	133
3	1	1	−626	−520	−106	2	7	7	0	−71	71	5	7	1	0	−86	86
3	1	0	1108	−1155	47	2	7	6	−160	−37	−123	5	7	0	0	145	−145
4	1	9	123	122	1	3	7	7	400	291	109	5	7	−1	−214	−123	−91
4	1	8	116	97	19	3	7	6	−1270	−825	−45	5	7	−2	−203	−116	−87
4	1	7	416	329	87	3	7	5	−1233	−1205	−28	5	7	−3	−430	−359	−71
4	1	6	−1180	−1253	73	3	7	4	−1225	−1087	−138	5	7	−4	−116	−249	133
4	1	5	−752	−1112	640	3	7	3	299	236	63	5	7	−5	327	305	22
4	1	4	1552	−1582	0	3	7	2	465	475	−10	5	7	−6	−650	−525	−125
4	1	3	623	518	105	3	7	1	814	764	50	5	7	−7	595	578	17
4	1	2	0	−12	12	3	7	0	649	591	58	5	7	−8	−483	−439	−44
4	1	1	768	732	36	3	7	−1	638	633	5	5	7	−9	227	307	−80
4	1	0	108	160	−52	4	7	10	0	50	−50	6	7	6	259	284	−25
5	1	9	520	527	−7	4	7	9	−237	−219	−18	6	7	5	460	380	80
5	1	8	61	24	37	4	7	8	−270	−306	36	6	7	4	148	143	5
5	1	7	−1231	−1115	−116	4	7	7	−430	−402	−28	6	7	3	−379	−369	−10
5	1	6	1390	1292	98	5	7	11	0	53	−53	6	7	2	265	337	−72
5	1	5	−649	−606	−43	10	6	3	0	−174	174	6	7	1	−252	−97	−155

BNSDOCID: <XP_____9085424A__1_>

UM00017151
NOVARTIS EXHIBIT 1517
Novartis v. Regents, IPR2023-01347
Page 4008 of 4460

XP009085424

TABLE 3—*continued.*

h	k	l	F_o	F_c	Δ	h	k	l	F_o	F_c	Δ	h	k	l	F_o	F_c	Δ
6	7	3	261	238	23	0	8	5	462	464	5	3	8	5	0	−60	60
6	7	2	−670	−723	−77	0	8	4	619	674	−55	4	8	4	91	1	90
6	7	1	633	583	50	0	8	3	389	373	16	4	8	3	244	80	164
6	7	0	−662	−687	25	0	8	2	116	207	−91	4	8	2	−160	−47	−113
6	7	−1	600	498	102	0	8	1	136	284	−148	4	8	1	−321	−285	−36
6	7	−2	651	557	94	1	8	7	−143	−66	−77	4	8	0	−321	−306	−15
6	7	−3	436	358	78	1	8	6	233	214	19	4	8	−1	−197	−107	−90
6	7	−4	312	290	22	1	8	5	274	345	−71	4	8	−2	−283	−251	−32
6	7	−5	412	358	54	1	8	4	701	648	53	4	8	−3	390	213	177
6	7	−6	0	38	−38	1	8	3	−148	−33	−115	4	8	−4	445	408	37
6	7	−7	−108	−257	149	1	8	2	493	503	−10	4	8	−5	0	250	−250
7	7	6	−237	−78	−159	1	8	1	−314	−434	120	5	8	4	−656	−503	−153
7	7	5	−363	−335	−28	1	8	0	0	−108	108	5	8	3	−247	−141	−106
7	7	4	−153	−72	−81	1	8	−1	−223	−301	78	5	8	2	−312	−307	−5
7	7	3	−160	−202	22	1	8	−2	−352	−349	−3	5	8	1	−170	−25	−145
7	7	2	−174	−280	106	1	8	−3	130	80	50	5	8	0	0	69	−69
7	7	1	197	124	73	1	8	−4	−0	70	−70	5	8	−1	−207	−194	−13
7	7	0	−721	−713	−8	1	8	−5	143	116	27	5	8	−2	193	20	173
7	7	−1	725	762	−37	1	8	−6	295	247	49	5	8	−3	283	339	−56
7	7	−2	0	−13	13	1	8	−7	−100	−46	−54	5	8	−4	465	418	47
7	7	−3	633	594	39	2	8	6	−277	−246	−31	5	8	−5	197	216	−19
7	7	−4	296	310	−14	2	8	5	0	48	−48	6	8	2	−749	−729	−20
7	7	−5	377	402	−25	2	8	4	−160	−109	−51	6	8	1	160	245	−85
7	7	−6	−339	−210	−129	2	8	3	−229	−173	−56	6	8	0	−363	−392	29
7	7	−7	0	62	−62	2	8	2	203	173	30	6	8	−1	184	46	138
8	7	4	−622	−489	−133	2	8	1	−123	−104	−19	6	8	−2	−455	−417	−38
8	7	3	−252	−189	−63	2	8	0	0	176	−176	6	8	−3	0	54	−54
8	7	2	0	−17	17	2	8	−1	116	103	13	7	8	0	−579	−658	79
8	7	1	−214	−178	−36	2	8	−2	−57	−48	−9	0	9	3	0	42	−42
8	7	0	−321	−281	−40	2	8	−3	−116	−43	−73	0	9	2	0	−3	3
8	7	−1	−184	−53	−131	2	8	−4	0	−68	68	0	9	1	91	17	74
8	7	−2	148	2	146	2	8	−5	81	97	−16	1	9	3	−219	−237	18
8	7	−3	153	23	130	3	8	6	0	−74	74	1	9	2	143	99	44
8	7	−4	449	534	−85	3	8	5	210	128	82	1	9	1	40	51	−11
8	7	−5	326	296	30	3	8	4	−148	−54	−94	1	9	0	0	−92	92
8	7	−6	0	−38	38	3	8	3	440	486	−46	1	9	−1	186	241	−61
9	7	4	−306	−202	−104	3	8	2	−180	−85	−95	1	9	−2	−241	−276	35
9	7	3	0	−96	96	3	8	1	130	211	−81	1	9	−3	214	261	−47
9	7	−1	−301	−179	−122	3	8	0	−261	−272	11	2	9	2	184	170	14
9	7	−2	−430	−421	−9	3	8	−1	130	176	−46	2	9	1	0	148	−148
9	7	−3	0	38	−38	3	8	−2	0	−134	134	2	9	0	0	25	−25
0	8	7	143	136	7	3	8	−3	−100	−10	−90	2	9	−1	40	159	−119
0	8	6	207	294	−87	3	8	−4	−116	−78	−38	3	9	0	−148	−234	86

fourteen peaks within 2·8 Å of the origin due to the salicylic acid residue[5] were resolved and identified. This gave the orientation of the molecule. It was then assumed that the molecules would be linked into dimers across centres of symmetry by hydrogen bonds of length 2·65 Å. This assumption, which proved to be justified, yielded positions for ten of the thirteen heavier atoms, and the chosen co-ordinates gave $R = 45\%$ for the 182 $h0l$ reflexions. A Fourier synthesis with the $h0l$ phased structure factors showed plausible positions for the three heavier atoms of the acetyl group, and this projection was then rapidly refined to $R = 15\%$ by Fourier and difference syntheses. The y co-ordinates could be chosen from a model of the molecule, and immediately gave satisfactory agreement for the 300 planes with $\sin\theta/\lambda < 0{\cdot}35$. The structure was then refined by a least-squares procedure which uses the block diagonal approximation. At first only the nine carbon and four oxygen atoms were included until R for the 2055 planes fell to 13·3% and $R'[= \sum w(|F_o| - |F_c|)^2 / \sum w|F_o|^2]$ to 1·33%. A three-dimensional difference map was then calculated with the 300 low-order planes and yielded positions for all eight hydrogen atoms, though the hydrogen atom involved in the hydrogen bond was a low peak showing considerable elongation towards the oxygen atoms with which it interacts. The hydrogen atoms were included in the refinement until R finally dropped to 10·6% and R' to 0·75%. Refinement was concluded when the maximum value of Δ/σ for a co-ordinate of a hydrogen atom had fallen to 0·3. By this time the heavier atoms had stopped moving completely. Constant weights were used, as we have found them more satisfactory for diffractometer intensities than a Cruickshank weighting scheme, which was devised for photographic intensities.[6] In all twenty-one three-dimensional least-squares refinement cycles were performed.

The least-squares programme necessarily refines the hydrogen atoms with anisotropic thermal factors if the heavier atoms are so refined. As might be expected, the thermal factors of the hydrogen atoms were often meaningless, merely reflecting the inadequacy of the data. Consequently a final set of structure factors was calculated with anisotropic thermal factors for the carbon and oxygen atoms, and mean isotropic thermal factors for the three different types of hydrogen atoms. The final value of R was 10·8%. The scattering factors were taken from International Tables. All

[5] H. Lipson and W. Cochran, "The Determination of Crystal Structures," 1953, G. Bell and Sons Ltd., London, p. 189.

[6] D. W. J. Cruickshank *et al.*, "Computing Methods and the Phase Problem in X-ray Crystal Analysis," 1961, Pergamon Press, London, p. 45.

BNSDOCID: <XP_____9085424A__I_>

UM00017152
NOVARTIS EXHIBIT 1517
Novartis v. Regents, IPR2023-01347
Page 4009 of 4460

XP009085424

TABLE 4.

Analysis of observed and calculated structure factors as a function of the index of the layer line. All figures are on an absolute scale.

h	$\Sigma\|F_o\|$	$\Sigma\|F_c\|$	$\Sigma\|\Delta\|$	N	R	$\Sigma\|\Delta\|/N$
0	1957·35	1959·25	142·02	182	0·073	0·780
1	2843·60	2868·88	229·90	332	0·081	0·693
2	2474·82	2400·10	221·04	328	0·089	0·674
3	1890·09	1873·04	179·53	304	0·095	0·591
4	1327·80	1405·83	165·09	269	0·124	0·614
5	921·21	988·13	154·60	231	0·168	0·669
6	711·04	649·85	132·69	181	0·187	0·733
7	418·06	407·14	91·04	140	0·218	0·650
8	163·78	157·69	48·87	73	0·298	0·670
9	15·00	20·55	8·19	15	0·546	0·546
All	12722·75	12730·46	1372·97	2055	0·108	0·668

calculations were carried out on an Elliott 803 computer with the programmes of Daly, Stephens, and Wheatley.[7]

Results.—The final atomic co-ordinates are given in Table 1, and the final thermal parameters in Table 2. Table 3 gives the observed and calculated structure factors obtained from the parameters given in Tables 1 and 2. In Table 4 an analysis is given of the structure factors in terms of the index of the layer. It will be seen that, although R increases substantially at higher equi-inclination angles, the absolute error in a structure factor remains approximately constant throughout.

TABLE 5.

Analysis of observed and calculated structure factors as a function of the magnitude of the observed structure factors. All figures are on an absolute scale.

Range of $\|F_o\|$	$\Sigma\|F_o\|$	$\Sigma\|F_c\|$	$\Sigma\|\Delta\|$	N	R	$\Sigma\|\Delta\|/N$
0	0	241·58	241·58	267	—	0·905
0·0— 5·0	2781·64	2637·72	616·60	1032	0·222	0·598
5·0— 10·0	2880·01	2885·18	212·61	405	0·074	0·525
10·0— 15·0	2021·92	2004·49	94·39	166	0·047	0·569
15·0— 20·0	1260·86	1237·35	63·31	72	0·050	0·879
20·0— 25·0	713·18	705·90	21·72	32	0·030	0·679
25·0— 30·0	969·72	938·46	37·44	35	0·039	1·070
30·0— 35·0	448·23	440·28	12·39	14	0·028	0·885
35·0— 40·0	228·22	219·30	8·92	6	0·039	1·487
40·0— 45·0	416·57	404·03	14·32	10	0·034	1·432
45·0— 50·0	188·48	189·67	6·77	4	0·036	1·693
50·0— 55·0	210·60	200·82	10·04	4	0·048	2·510
55·0— 60·0	57·02	54·94	2·08	1	0·036	2·080
60·0— 65·0	61·23	58·05	3·18	1	0·052	3·180
65·0— 70·0	67·04	68·50	1·46	1	0·022	1·460
70·0— 75·0	147·89	152·66	4·77	2	0·032	2·385
75·0— 80·0	—	—	—	—	—	—
80·0— 85·0	—	—	—	—	—	—
85·0— 90·0	175·43	183·49	8·96	2	0·051	4·480
90·0— 95·0	—	—	—	—	—	—
95·0—100·0	95·61	108·04	12·43	1	0·130	12·430

In Table 5 a similar analysis is given, but in terms of the magnitudes of the observed structure factors. R is poor for the very weak reflexions (and, of course, infinite, for those that are accidentally absent), but again, in terms of absolute errors, there is no reason to reject these weak planes. Indeed the evidence suggests that the twenty or thirty strongest planes should be down-weighted with respect to the weak planes. We feel that such satisfactory results for the weaker planes can be achieved with the diffractometer only if the size of the crystal or the counting time is so adjusted that the intensities yield structure factors that are on about absolute scale.

The bond lengths are given in Fig. 1, which also shows the labelling of the atoms. The bond angles are given in Table 6. Fig. 2 shows the structure as it appears when projected down the [*b*]

[7] J. J. Daly, F. S. Stephens, and P. J. Wheatley, 1963, *MRSA Final Report*, No. 52.

BNSDOCID: <XP_____9085424A__I_>

UM00017153
NOVARTIS EXHIBIT 1517
Novartis v. Regents, IPR2023-01347
Page 4010 of 4460

XP009085424

axis. The bond lengths are in fair agreement with those found in salicylic acid by Cochran,[8] though there are some very significant differences. The results for the two molecules are compared in Fig. 3. There are some very definite angular distortions within the molecule, both in the benzene ring and the carboxyl group, but, more particularly, in the acetyl group. The benzene

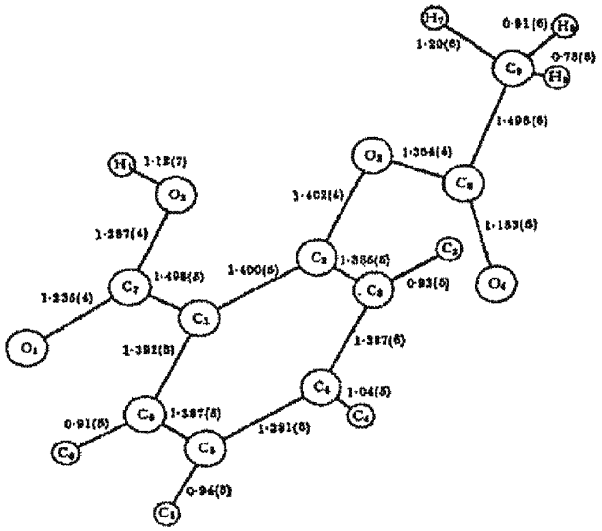


FIG. 1. Bond lengths in aspirin with their standard deviations, and the labelling of the atoms.

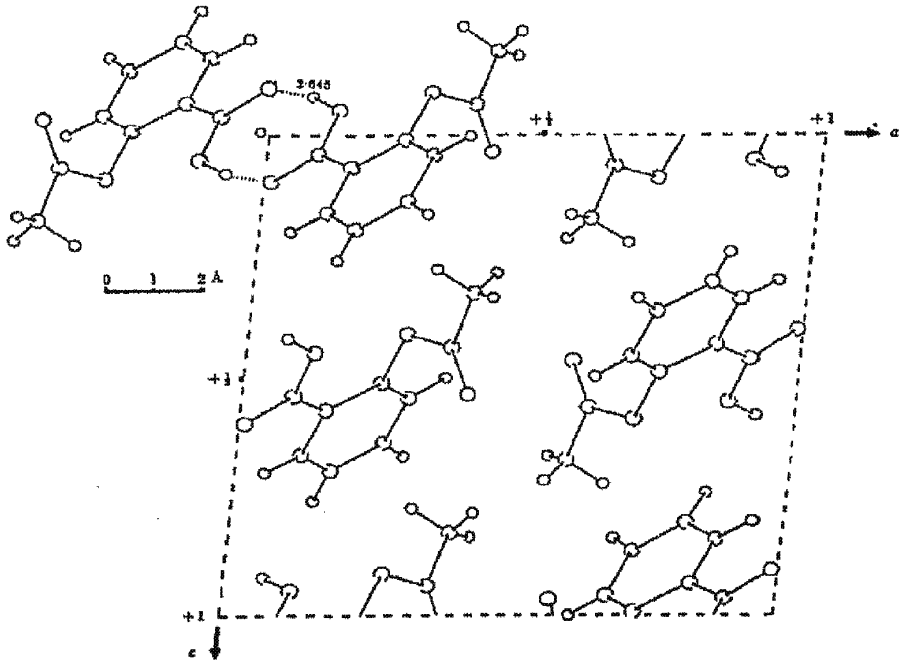


FIG. 2. The structure of aspirin as it appears in projection down [*b*].

[8] W. Cochran, *Acta Cryst.*, 1953, **6**, 260.

BNSDOCID: <XP_____9085424A__1_>

UM00017154
NOVARTIS EXHIBIT 1517
Novartis v. Regents, IPR2023-01347
Page 4011 of 4460

TABLE 6.

Bond angles (°). Standard deviations are given as units in the last place.

H(1)O(2)C(7)	120·7 (37)	O(3)C(8)O(4)	122·9 (3)	C(2)C(3)C(4)	119·8 (4)
O(2)C(7)O(1)	122·9 (3)	O(3)C(8)C(9)	110·7 (3)	C(3)C(4)H(4)	121·6 (26)
O(2)C(7)C(1)	118·1 (3)	O(4)C(8)C(9)	126·4 (4)	C(5)C(4)H(4)	118·4 (26)
O(1)C(7)C(1)	119·1 (3)	C(8)C(9)H(7)	110·0 (29)	C(3)C(4)C(5)	120·0 (4)
C(7)C(1)C(2)	124·6 (3)	C(8)C(9)H(8)	119·4 (38)	C(4)C(5)H(5)	120·0 (29)
C(7)C(1)C(6)	117·7 (3)	C(8)C(9)H(9)	115·9 (44)	C(6)C(5)H(5)	120·1 (29)
C(6)C(1)C(2)	117·7 (3)	H(7)C(9)H(8)	98·7 (48)	C(4)C(5)C(6)	119·9 (4)
C(1)C(2)O(3)	121·6 (3)	H(7)C(9)H(9)	100·9 (52)	C(5)C(6)H(6)	118·5 (29)
C(3)C(2)O(3)	117·3 (3)	H(8)C(9)H(9)	108·9 (58)	C(1)C(6)H(6)	119·9 (29)
C(1)C(2)C(3)	121·0 (3)	C(2)C(3)H(3)	118·0 (29)	C(5)C(6)C(1)	121·6 (3)
C(2)O(3)C(8)	115·7 (3)	C(4)C(3)H(3)	122·2 (29)		

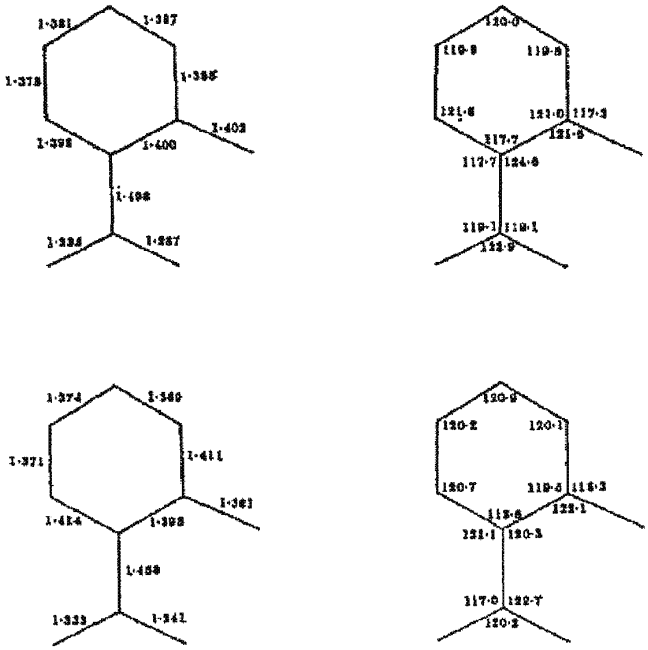


FIG. 3. Comparison of the bond lengths and angles in aspirin (above) and salicylic acid (below).

ring has the appearance of being pulled out by the carboxyl group so that the internal angles at C(2) and C(6) are greater than 120°, and that at C(1) is less. The carboxyl group is bent away from the acetyl group, possibly by repulsion between O(3) and O(2), so that there is a substantial increase in the angle C(2)C(1)C(7), and a decrease in C(6)C(1)C(7). The angle O(1)C(7)O(2) is greater than 120°, again suggesting repulsion between oxygen atoms. The angular distortions at the central atom of the acetyl group are enormous, the angles being 110·7, 122·9, and 126·4°, instead of the expected 120°. There appears to be no simple explanation for these distortions in terms of intramolecular contacts.

Except for hydrogen atoms on the methyl group, the molecule is composed of atoms lying approximately in two planes. The weighted least-squares equation for the plane of the four atoms in the acetyl group, referred to orthogonal axes a, b, and c', is

$$+0{\cdot}7512\,X + 0{\cdot}6577\,Y - 0{\cdot}0564\,Z' = 4{\cdot}3680.$$

The departures of the atoms from this plane are O(3), +0·0007; O(4), +0·0009; C(8), −0·0030; C(9), +0·0011 Å, none of which is significant. Thus, despite the large angular distortions within the plane of this group, there is no out-of-plane bending. On the other hand no satisfactory plane can be constructed through all ten of the heavier atoms of the salicylic acid residue. A number of

BNSDOCID: <XP 9085424A >

UM00017155
NOVARTIS EXHIBIT 1517
Novartis v. Regents, IPR2023-01347
Page 4012 of 4460

XP009085424

planes were calculated, starting first with the benzene ring, and then adding one or more of the remaining four atoms. As soon as any other single atom was added, the departures from the plane increased, and these departures grew worse as more atoms were added. There seems to be no question that significant out-of-plane distortions do occur in the salicylic acid residue. It was particularly noticeable that one of the oxygen atoms of the carboxyl group always lay above the plane, and the other below, leading to the conclusion that the plane of the carboxyl group was twisted with respect to the plane of the benzene ring. In view of these various distortions it was felt that the most representative plane was the one through the six carbon atoms of the benzene ring, the equation of which is

$$+0{\cdot}5945\,X - 0{\cdot}4849\,Y + 0{\cdot}6415\,Z' = 0{\cdot}0941.$$

The departures of the atoms from this plane are given in Table 7. It will be seen that none of the carbon or hydrogen atoms of the benzene ring departs from this plane, whereas the other atoms,

TABLE 7.

Departure in Å of the atoms of the salicylic acid residue from the plane of the benzene ring.

Atom		Atom		Atom	
C(1)	−0·0031	H(1)	−0·138	O(1)	+0·1016
C(2)	+0·0050	H(3)	+0·012	O(2)	−0·0555
C(3)	−0·0026	H(4)	+0·019	O(3)	−0·0565
C(4)	−0·0016	H(5)	+0·009	C(7)	−0·0097
C(5)	+0·0034	H(6)	−0·021		
C(6)	−0·0011				

with the exception of C(7), do. The angle between the plane of the benzene ring and that of the acetyl group is 84° 45′.

The equation of the plane through the carboxyl group is

$$+0{\cdot}6091\,X - 0{\cdot}5022\,Y + 0{\cdot}6139\,Z' = 0{\cdot}0596.$$

H(1) departs from this plane by −0·064 Å, which is not significant. The angle between the plane of the benzene ring and that of the carboxyl group is 2° 2′.

Molecules of aspirin are, as expected, dimerized by hydrogen bonds across a centre of symmetry. The length of each hydrogen bond is 2·645 Å. The perpendicular distance between the two planes defined by the carboxyl groups in the dimer is 0·119 Å, which places aspirin roughly halfway down the table given by Jeffrey and Sax.[9] The weighted least-squares plane through the six heavier atoms of the eight-membered dimer ring is

$$+0{\cdot}5901\,X - 0{\cdot}5348\,Y + 0{\cdot}6084\,Z' = 0.$$

The departure of the atoms from this plane are O(1), +0·0089; O(2), +0·0077; C(7), −0·0151; H(1), −0·013 Å. Thus the eight atoms are very nearly coplanar, as would be expected from Robertson's arguments.[10]

All non-bonded intramolecular contacts were calculated in order to disclose any unusual features within the molecule. If hydrogen atoms are excluded, the two shortest intramolecular contacts are O(1)···O(2), 2·215; O(3)···O(4), 2·239 Å. Other distances of interest in connexion with the possibility of repulsion are O(2)···O(3), 2·674; O(3)···C(9), 2·354; O(4)···C(9), 2·395; C(2)···C(8), 2·342 Å. Inclusion of the hydrogen atoms results in a number of contacts of slightly less than 2 Å between hydrogen atoms on the benzene ring and next-nearest carbon atoms, and three shorter contacts between hydrogen atoms on the methyl group.

All van der Waals's contacts up to a limit of 4 Å were calculated both with and without hydrogen atoms. There is a large number of these distances, but no unusual features appear. If hydrogen atoms are excluded, the shortest contact, apart from the hydrogen bond, is 3·306 Å between two oxygen atoms. The shortest contact between hydrogen atoms is 2·50 Å.

MONSANTO RESEARCH S.A., BINZSTRASSE, 39, 8045 ZÜRICH, SWITZERLAND.

[*Received, July 31st*, 1964.]

[9] G. A. Jeffrey and M. Sax, *Acta Cryst.*, 1963, **16**, 430.
[10] J. H. Robertson, *Acta Cryst.*, 1964, **17**, 316.

BNSDOCID: <XP_____9085424A__i_>

UM00017156
NOVARTIS EXHIBIT 1517
Novartis v. Regents, IPR2023-01347
Page 4013 of 4460